Proceedings
of the
5th American
Water Jet Conference

Compte rendu
de la
5e Conférence américaine
sur les jets d'eau

August / août 29 — 31, 1989

Toronto, Canada

Edited by / Sous la direction de
M.M. VIJAY, National Research Council of Canada
G.A. SAVANICK, U.S. Bureau of Mines

Proceedings
of the
5th American Water Jet Conference

August 29 — 31, 1989
Toronto, Canada

Edited by
M.M. Vijay, National Research Council of Canada
G.A. Savanick, U.S. Bureau of Mines

Sponsored by

National Research Council of Canada
U.S. Water Jet Technology Association

Compte rendu
de la
5e Conférence américaine sur les jets d'eau

29 — 31 août 1989
Toronto, Canada

Sous la direction de
M.M. Vijay, Conseil national de recherches du Canada
G.A. Savanick, U.S. Bureau of Mines

Parrainé par

Conseil national de recherches du Canada
U.S. Water Jet Technology Association

Printed in Canada / Imprimé au Canada

ISBN no. 0-660-55089-8
NRCC no. 30547
DSS no. MR 15-40/1989

Copies obtainable from:

Conference Services Office
National Research Council of Canada
Ottawa, Ontario K1A 0R6
Canada
or
U. S. Water Jet Technology Association
Suite 918
818 Olive St.
St. Louis, MO 63101
USA
Price : $75. (payable in advance)

ISBN nº 0-660-55089-8
CNRC nº 30547
MAS nº MR 15-40/1989

On peut obtenir des exemplaires
en s'addressant à :

Service des conférences
Conseil national de recherches
Ottawa (Ontario) K1A 0R6
Canada
ou
La U.S. Water Jet Technology Association
Suite 918
818 Olive St.
St. Louis, MO 63101
USA
Prix : 75 $ (payable à l'avance)

PREFACE

"A learned man is like a branch of a fruit bearing tree; the more fruit it bears, the more it bows".

Ancient Scripts

Since the FIRST INTERNATIONAL SYMPOSIUM on JET CUTTING TECHNOLOGY in 1972, the uses of water jets have spread, almost worldwide, from simple cleaning to decommissioning of nuclear installations and promising novel medical applications. This is largely due to the hard work of dedicated workers who have disseminated and continue to disseminate their new and unusual findings in SYMPOSIA and CONFERENCES on Water Jet Technology, inspiring others to follow. Each successive conference or symposium since 1972 has seen not only well-known faces in the field, but increasing number of novices eager to learn and widen the spectrum of applications. It is sincerely hoped that the same spirit which pervaded the 5th American Water Jet Conference, held on this occasion in Canada, will continue to encourage *international collaboration* which is so important for peace and progress, achievable through sharing of knowledge.

The Canadian Organising Committee sincerely thanks the U.S. Water Jet Technology Association for the privilege of holding the 5th Conference in Canada, and the Division of Mechanical Engineering of the National Research Council of Canada (NRC) for readily agreeing to co-sponsor the Conference.

On a more personal note, I am very thankful to all the members of the Organising Committees, particularly to Dr. G.A. Savanick for valuable discussions on the phone, to Prof. T. Labus for organising the Water Jet Course, and to Mr. A.D. Hink for arranging the technical tours. Encouragement to hold the Conference in Canada came from the SUPPORTERS and this is gratefully acknowledged. Special thanks go to the prestigious international advisors for giving wide publicity to the Conference in their countries, and to the reviewers for painstakingly reviewing the abstracts submitted to the Conference. My sincere thanks to the authors, who complied with all the instructions and submitted the papers in time for printing, and to the session chairmen for the smooth running of the sessions. The firms which took part in the exhibitions and technical demonstrations of their equipment enhanced the value of the Conference. This is gratefully acknowledged.

It would be very difficult to state in a few words the immense help received from the staff of the Conference Services at NRC. I am particularly indebted to Mr. K. Charbonneau, Mrs. H. Lacoste and Mrs. R. King for assisting me in all aspects of the Conference. Thanks are also due to Mr. D. Hewitt-White and his staff of the Duplication Services, Mr. D. Getz & Mr. M. Acres of the Photography Section who have made impressive contributions to the art-work and printing of all the materials pertaining to the Conference, and to Mr. N. Paquette for assisting in the audio-visual aids.

It is with great pleasure that I acknowledge Mr. E. Dudgeon, Vice-President Engineering, Mr. J. Ploeg, Director, Division of Mechanical Engineering, and Dr. R.G. Williamson, Head, Gas Dynamics Laboratory for their moral support and encouragement, and Mr. G. McGregor, General Manager, Manufacturing Technology Centre, NRC, for producing, with water jets, the beautiful souvenirs, a replica of which appears on the front cover of this proceedings.

I thank, on behalf of the Organising Committees, Staff of the Four Seasons' Inn on the Park for all the arrangements, Ace International Entertainment Agency for the exciting entertainment at the banquet, Office of the Premier of Ontario for co-sponsoring the reception, and the Office of the Mayor, City of Toronto, for opening the Conference.

This PREFACE would be incomplete without expressing my gratitude to my wife, Dr. Hari Vijay, from whom I have learnt the art of listening in the pursuit of new knowledge and to my daughters, Sangeeta & Sheela, who have always volunteered to help, with smiling faces, whenever I needed it.

M.M VIJAY
Editor & Conference Co-Chairperson

PRÉFACE

"A learned man is like a branch of a fruit bearing tree; the more fruit it bears, the more it bows".

Écritures anciennes

Depuis le PREMIER COLLOQUE INTERNATIONAL sur LA TECHNOLOGIE DES JETS D'EAU, tenu en 1972, l'utilisation des jets d'eau s'est répandue, presque à l'échelle du globe, ses applications passant du simple nettoyage jusqu'au déclassement d'installations nucléaires et à des applications nouvelles et pleines de promesses en médecine. Cela est attribuable en grande partie aux efforts ardus de travailleurs motivés qui ont diffusé et qui continuent de diffuser les résultats nouveaux et exceptionnels de leurs recherches dans le cadre de COLLOQUES et de CONFÉRENCES sur la technologie des jets d'eau, inspirant d'autres à suivre leurs traces. Chaque conférence ou colloque successif tenu depuis 1972 a vu non seulement des visages bien connus dans le domaine, mais aussi un nombre croissant de débutants désireux d'apprendre et d'élargir le spectre des applications des jets d'eau, Nous espérons sincèrement retrouver ce même esprit à l'occasion de la 5e Conférence américaine sur les jets d'eau, tenue cette fois au Canada afin d'encourager la **collaboration internationale,** laquelle est si importante pour la paix et le progrès que le partage des connaissances permet de réaliser.

Le Comité organisateur canadien désire remercier chaleureusement la U.S. Water Jet Technology Association de lui avoir concédé le privilège de tenir la 5e conférence au Canada, ainsi que la Division de génie mécanique du Conseil national de recherches du Canada (CNRC) d'avoir accepté avec empressement de coparrainer la conférence.

Sur une note plus personnelle, je désire exprimer ma reconnaissance envers tous les membres des Comités organisateurs, spécialement le Dr. G.A. Savanick pour de précieuses discussions au téléphone, le professeur T. Labus, qui a organisé le Cours abrégé sur la technologie des jets d'eau, ainsi que M. A.D. Hink, qui s'est chargé des excursions techniques. C'est grâce à l'appui et à l'encouragement des COMMANDITAIRES que la conférence a eu lieu au Canada, et nous le reconnaissons avec gratitude. J'offre mes sincères remerciements aux conseillers internationaux éminents qui ont fait beaucoup de publicité pour la conférence dans leurs pays, et aux examinateurs qui ont examiné assidûment les résumés soumis pour la conférence. Mes vifs remerciements aux auteurs, qui ont observé toutes les instructions données et qui ont soumis leurs communications à temps pour la publication, de même qu'aux présidents de séances qui ont assuré le bon fonctionnement des séances. Les sociétés qui ont participé à l'exposition et aux démonstrations techniques de leur équipement ont rehaussé la valeur de la conférence. Je tiens donc à leur témoigner ma reconnaissance.

Il serait très difficile de décrire en quelques mots l'aide immense que nous avons reçue du personnel des Services de conférence du CNRC. Je suis particulièrement redevable à M. K. Charbonneau, à Mmes H. Lacoste et R. King de leur assistance relativement à tous les aspects de la conférence. Je présente également mes sincères remerciements à M. D. Hewitt-White et son personnel au sein du Service de reprographie et également à MM. D. Getz et M. Acres de la Section de photographie pour leurs excellentes contributions aux travaux d'arts graphiques et de publication de tous les documents se rapportant à la conférence, de même qu'à M. N. Paquette pour son aide en matière d'audiovisuel.

C'est avec grand plaisir que j'offre mes remerciements à M. E. Dudgeon, vice-président, Génie, à M. J. Ploeg, directeur de la Division de génie mécanique, et au Dr. R.G. Williamson, chef du Laboratoire de la dynamique des gaz, pour leur appui moral et leur encouragement. Il ne faut pas oublier M. G. McGregor, directeur général du Centre de technologie en production industrielle, CNRC, qui a produit, à l'aide de jets d'eau, de superbes souvenirs de la conférence. La couverture du présent compte rendu est une copie exacte de l'oeuvre de M. McGregor.

Au nom des Comités organisateurs, je tiens à remercier le personnel du Four Seasons' Inn de tous les arrangements faits, l'Ace International Entertainment Agency du spectacle saisissant présenté au banquet, le Bureau du Premier ministre de l'Ontario d'avoir coparrainé la réception et le Bureau du maire de la ville de Toronto d'avoir inauguré la conférence.

Cette PRÉFACE ne serait pas complète si je n'exprimais pas ma gratitude envers mon épouse, le Dr Hari Vijay, de qui j'ai appris l'art de bien écouter dans ma quête de connaissances nouvelles, de même qu'envers mes filles, Sangeeta et Sheela, qui m'ont toujours aidé de bon coeur, le sourire aux lèvres, lorsque j'ai eu besoin d'elles.

Le codirecteur du compte rendu
et coprésident de la conférence

M.M. VIJAY

FOREWORD

It is with pride and pleasure that the U.S. Water Jet Technology Association herewith presents the Proceedings of the Fifth American Water Jet Conference. The previous conferences, sponsored by the Association, were held in Golden, Colorado, in 1981, Rolla Missouri, in 1983, Pittsburgh, Pennsylvania, in 1985, and Berkeley, California, in 1987. These four were titled "U.S. Water Jet Conferences." The fifth in the series, chronicled in this volume, is called the "Fifth American Water Jet Conference" in recognition of the Canadian venue and the major role played by Canadians in the organization and presentation of the meeting. The U.S. Water Jet Technology Association thanks the National Research Council of Canada for cosponsoring the conference and the members of the organizing committee, especially Dr. Mohan Vijay, the Canadian chairman.

Industrial acceptance of water-jet cutting is growing rapidly. Abrasive jet machining and water-jet robots have attracted much attention. These subjects and much more are included in the following pages. Read on and become informed about the cutting edge of this exciting new technology.

GEORGE A. SAVANICK

Editor & Conference Co-Chairperson
and President of the
U.S. Water Jet Technology Association

AVANT-PROPOS

C'est avec fierté et plaisir que la U.S. Water Jet Association présente le compte rendu de la Cinquième conférence américaine sur les jets d'eau. Les conférences antérieures, parrainées par l'Association, se sont tenues à Golden, au Colorado, en 1981, à Rolla, au Missouri, en 1983, à Pittsburg, en Pennsylvania, en 1985, et à Berkeley, en Calfornie, en 1987. Ces quatre conférences s'intitulaient "U.S. Water Jet Conferences". La cinquième de cette série, dont la chronique est faite dans le présent volume, s'appelle la "Cinquième conférence américaine sur les jets d'eau", en reconnaissance du fait qu'elle s'est tenue au Canada et du rôle important qu'ont joué les Canadiens dans son organisation et sa tenue. La U.S. Water Jet Technology Association tient à remercier le Conseil national de recherches du Canada d'avoir coparrainé la conférence, ainsi que les membres du comité organisateur, et plus particulièrement le Dr Mohan Vijay, président canadien.

L'acceptation du découpage au jet d'eau par l'industrie accroît rapidement. L'usinage à l'aide de jets contenant un abrasif et les robots utilisant des jets d'eau ont attiré beaucoup d'attention à la conférence. Ces sujets, et bien d'autres encore, sont abordés dans les pages qui suivent. Poursuivez votre lecture et renseignez-vous sur le côté tranchant de cette technologie nouvelle des plus excitantes.

Le codirecteur du compte rendu,
coprésident de la conférence
et président de la
U.S. Water Jet Technology
Association

GEORGE A. SAVANICK

ORGANISING COMMITTEE / COMITÉ ORGANISATEUR

CANADA

Dr. M.M. Vijay (Chairperson / Président)
National Research Council of Canada
Ottawa, Ontario

Dr. D.J. Burns, University of Waterloo
Waterloo, Ontario

Dr. N.C. Franz, Professor Emeritus
Vancouver B.C.

Mr. H.P. Hayne
Ceda Reactor Ltd.
Sherwood Park, Alberta

Mr. A.D. Hink
Atomic Energy of Canada Ltd.
Mississauga, Ontario

Ms. Lucie Legris, ISOCAB Inc.
Montréal, Quebec

Mr. J. Macneil
Mac & Mac Industrial Services Ltd.
Surrey, B.C.

Dr. R.J. Puchala
Indescor Hydrodynamics Inc.
Concord, Ontario

Dr. I.H. Rowe
Spar Aerospace Ltd.
Weston, Ontario

Dr. S. Tavoularis
University of Ottawa
Ottawa, Ontario

M. K. Charbonneau
Conseil national de recherches du Canada
Ottawa, Ontario

USA / É-U

Dr. G. A. Savanick (Chairperson / Président)
Bureau of Mines
Minneapolis, Minnesota

Dr. J.L. Evers
Southern Illinois University
Carbondale, Illinois

Dr. M. Hashish
Flow Research Inc.
Kent, Washington

Mr. T. Labus
University of Wisconsin-Parkside
Kenosha, Wisconsin

Mr. D. Schroter
Ingersol-Rand
Baxter Springs, Kansas

Mr. F. Shook
NLB Corporation
Wixom, Michigan

Ms. E. Steele
Supreme Technology Inc.
Lebanon, Ohio

Dr. D.A. Summers
University of Missouri-Rolla
Rolla, Missouri

Dr. F.D. Wang
Colorado School of Mines
Golden, Colorado

Mr. J.E. Wolgamott
Stone Age
Durango, Colardo

Mr. M. Woodward
Weatherford Water Jetting Systems
Houston, Texas

INTERNATIONAL ADVISORS / CONSEILLERS INTERNATIONAUX

Australia / Australie	Mr. B. Hare, Gardner Bros. Pty. Ltd. , Altona
Austria / Autriche	Mr. F. Trieb, Boehler, Kapfenberg
Brazil / Brésil	Dr. J. Sielawa, Instituto de Pesquisas Especials, Sao Paulo
China / Chine	Dr. Cheng Dazhong, China University of Mining & Technology, Xuzhou
Czechoslovakia / Czechoslovakie	Dr. J. Noskievic, Technical University Ostrava, Ostrava
France	Dr. J.F. Raffoux, CERCHAR, Verneuil-en-Halatte
Germany / Allemagne	Dr. H. Louis, Universität Hannover, Hannover
Hungary / Hongrie	Dr. S. Toth, University of Debrecen, Debrecen
India / Inde	Mr. J.A. Shah, GOMA Engineering Pvt. Ltd., Bombay
Italy / Italie	Dr. A. Bortolussi, Centro Studi Ceominerarie e Mineralurgici del C.N.R., Cagliari
Japan / Japon	Dr. R. Kobayashi, Tohoku University, Sendai
New Zeland / Nouvelle - Zélande	Mr. M.J. Simpson, Department of Scientific & Instructional Research, Christchurch
Poland / Pologne	Dr. S. Kukialka, University of Mining & Metallurgy, Krakow
Sweden / Suède	Mr. B. Grinndal, Aquabrasive AB, Stockholm
United Kingdom / Royaume-Uni	Dr. P. Wood, Warren Spring Laboratory, UK Dept.. of Trade and Industry
Yugoslavia / Yugoslavie	Dr. Ivancic Ivan, Nikola Tesla, Zagreb

TABLE OF CONTENTS / TABLE DES MATIÈRES

INDUSTRIAL INVESTIGATIONS – 1 ÉTUDES INDUSTRIELLES – 1

COAL AND SOIL CUTTING INVESTIGATIONS ÉTUDES SUR LE DÉCOUPAGE DU CHARBON ET DES SOLS

Pages

POSTER SESSION **SESSION D'AFFICHAGE**

SAFETY CONSIDERATIONS **QUESTIONS DE SÉCURITÉ**

Pages

SUPPORTERS / COMMANDITAIRES

Aquablast Corp., Scarborough, Ontario, Canada
Aqua-Dyne Jetting Inc., Mississauga, Ontario, Canada
Atomic Energy of Canada Limited, Mississauga, Ontario, Canada
Autoclave Engineers Inc., Erie, Pennsylvania, USA
Ceda-Reactor Ltd., Sherwood Park, Alberta, Canada
C-I-L Inc., McMasterville, Québec, Canada
Flow Systems Inc., Kent, Washington, USA
Hydrokinetics / Jet Edge, Minneapolis, Minnesota, USA
Ingersol-Rand Canada Inc., Mississauga, Ontario, Canada
Jet-Blast Hydro Demolition Canada Inc., Mississauga, Ontario, Canada
Mac & Mac Industrial Services Limited, Surrey, British Columbia, Canada
Nandiroyce International Limited, Toronto, Ontario, Canada
NLB Corporation, Wixom, Michigan, USA
Ontario Hydro, Toronto, Ontario, Canada
Spar Aerospace Limited, Weston, Ontario, Canada
Teledyne Canada, Mining Products, Thornbury, Ontario, Canada
University of Waterloo, Waterloo, Ontario, Canada
V-Tech Industries Inc., Mississauga, Ontario, Canada
Water Jet Specialties Inc., Burlington, Ontario, Canada

and / et

Government of Ontario / le Gouvernement de l'Ontario
(co-sponsor of the reception / coparraineur de la réception)

5th American Water Jet Conference
August 29 - 31, 1989: Toronto, Canada

Paper / Communication 1

EVALUATION OF WATER DELIVERY SYSTEMS FOR WATER-JET-ASSISTED CUTTING

P.D. Kovscek
Boeing Services International

C.D. Taylor AND E.D. Thimons
Pittsburgh Research Center, Bureau of Mines
Pittsburgh, Pennsylvania 15236, USA

ABSTRACT: Use of high-pressure solid streams of water, known as water jets, have been proposed as a way to improve the cutting performance of metal drag bits currently used on longwall shearer mining machines. A specially designed nozzle is used to direct the water jet so that it strikes the rock surface within 2 mm of the bit tip. To be effective the fluid energy supplied by the water jets must reach the rock surface. Reducing the water pressure loss that occurs between the nozzle and rock surface can have a great effect on the amount of fluid energy available for water-jet-assisted cutting.
Studies were conducted to evaluate how the flow upstream of the nozzle and the nozzle design affects the water pressure that is delivered to the rock. Use of straight smooth tubing, placed just upstream of the nozzle, decreased flow turbulence and increased water pressure up to 35 pct. Stainless steel and tungsten carbide nozzles provided coherent water jets for the range of operating conditions expected during underground mining.

RÉSUMÉ : L'utilisation d'écoulements continus d'eau à haute pression, appelés jets d'eau, a été proposée comme moyen pour améliorer l'efficacité de coupe des taillants de métal dont sont actuellement dotées les ravageuses de longue taille. Une buse spéciale sert à diriger le jet d'eau de façon qu'il frappe la surface rocheuse en deçà de 2 mm du taillant. Pour être efficace, l'énergie hydraulique fournie par le jet d'eau doit être communiquée à la surface rocheuse. La réduction de la perte de charge de l'eau entre la buse et la surface rocheuse peut influer considérablement sur la quantité d'énergie hydraulique utilisable pour la coupe assistée par jet d'eau.
Des études sont menées pour évaluer comment l'écoulement en amont de la buse et la conception de la buse influent sur la pression de l'eau exercée sur la roche. L'utilisation de tuyaux droits lisses, placés juste en amont de la buse, diminue la turbulence de l'écoulement et augmente la pression de l'eau de 35 % dans certains cas. Les buses en acier inoxydable et en carbure de tungstène produisent des jets d'eau cohérents dans la fourchette des conditions de fonctionnement prévues pendant l'exploitation souterraine.

Organized and Sponsored by the National Research Council of Canada and the U.S. Water Jet Technology Association.

1.0 INTRODUCTION

1.1 Background

Water-jet-assisted cutting is a rock fragmentation method that uses a drag bit and high-pressure stream of water to cut rock. The combined use of fluid and mechanical energy has the potential to increase productivity in mines where harder rock must be mined, and cutting with mechanical bits alone is inefficient. Prior laboratory tests, performed with a single-bit linear cutting apparatus, showed that cutting forces on the bit can be reduced as much as 45 pct when the energy delivered to the rock surface exceeds a minimum threshold energy (energy per unit length of cut) (Hood, 1976). The energy delivered per length of rock cut was a function of the water pressure, water flow rate, and the cutting speed. During the laboratory tests the pressure supplied to the water jet nozzle was 50 MPa and the cutting speed was .254 m/s.

A longwall shearer was equipped to provide water-jet-assisted cutting at pressures up to 41 MPa (Kovscek, P. D., 1986). Cutting speed was 3.3 m/s. The high-pressure water was directed through the cutting drum to water jet nozzles that were mounted in front of each bit block. Each nozzle was positioned so that the water jet struck the rock within 3 mm of the bit tip (fig. 1). During initial testing the shearer cut a simulated coal face while using either low-pressure conventional type sprays or high-pressure water jets.

The electrical energy supplied to the shearer cutting and tram motors was continuously monitored while cutting with low- and high-pressure water. An improvement in cutting efficiency with water jet assist would be indicated by a decrease in the electrical energy required to cut an equivalent quantity of rock with low-pressure water. For the conditions tested there was no significant change in electrical energy when the water jets were used.

The energy level, per length of cut, was 40 to 60 times greater during the single-bit laboratory tests than during the shearer tests. Therefore, one explanation for the failure to improve cutting efficiency during the shearer tests was that the minimum threshold energy was not provided.

It would be difficult to increase the fluid energy provided for water-jet-assisted cutting on the shearer. High-pressure water was supplied continuously to all 32 nozzles on the cutting drum. The maximum pressure was limited by the capacity of the pump and the size and strength of the hose used to carry the water to the shearer. The cutting speed could not be reduced without greatly modifying the structure of the shearer.

1.2 Objective

There were several locations within the water delivery system on the shearer that were identified as sites where large pressure losses could occur. These included the rotary coupling, and piping inside the drum. The objective of this work was to identify where the major losses occurred, and, if they were large, determine how to reduce them.

2.0 WATER DELIVERY SYSTEM-PRESSURE LOSSES

2.1 Pressure Losses in Cutting Drum

On the shearer, the high-pressure water is directed into the cutting drum (fig. 2). Inside the drum the water passes through a rotary union. The water is carried through tubing from the union outlet to the bit blocks, which are located on the surface of the cutting drum. As the water passes through the drum, pressure losses can occur in the rotary union or tubing.

Operating water pressure at the union inlet and outlet was measured with transducers, and the pressure drop across the union calculated. Similarly, the operating pressures were measured at the union outlet and the inlet to the bit block. The calculated total pressure loss within the drum (union plus tubing) was about 7 pct of the pressure entering the drum. That is, when the supply pressure to the drum was 41 MPa, the pressure reaching the bit block was 38 MPa. The magnitude of this loss was not considered to be significant in relation to the supply pressure.

2.2 Pressure Loss Between Nozzle Inlet and Rock Surface

Large pressure losses in the water delivery system, that could be attributed to friction head losses, were not identified within the cutting drum. Another potential cause of pressure loss was investigated.

Pressure at the nozzle must be transferred to the rock surface if water-jet-assisted cutting is to be used effectively. The pressure of the water at the impact location is defined as the stagnation pressure. Prior research has shown that the stagnation pressure delivered by a high-pressure jet decreases with distance from the nozzle (Leach, S. J., 1966). This loss is primarily due to the breakup of the solid water stream into droplets that rapidly lose their velocity as they

travel through the air. The total pressure loss that occurs between the time the water leaves the nozzle and impacts the rock is difficult to determine because there is no way to directly measure the water pressure at the rock surface.

A test apparatus that allowed the simultaneous monitoring of pressure at the nozzle and stagnation pressure at the impact location was built (fig. 3). To measure the stagnation pressure, the water jet was directed at a target that consisted of a 0.34-mm tungsten carbide orifice installed in a flat plate. A strain-gauge pressure transducer, installed beneath the orifice, monitored the pressure striking the plate. Before making the measurements, each nozzle was visually aligned with the target hole. The initial alignment of the water stream with the target hole was performed at a water pressure of .48 MPa. Using a lower water pressure allowed better visual alignment of the jet with the target hole.

After the jet was aligned, the water pressure was raised to 41 MPa. The jet stream was traversed across the target hole in orthogonal directions to obtain a pressure profile (fig. 4). The fluid stagnation pressure was determined by noting the maximum sustained pressure on the pressure profile. Periodically duplicate tests were conducted to assure that the results were reproducible.

Stainless steel nozzles with an internal Leach and Walker configuration were used for all the tests (Leach, S. J., 1966). Orifice diameter was 0.6 mm. The supply pressure was the pressure measured at the nozzle. The difference in pressures at the nozzle and target location indicated how effective the water delivery system and nozzle would be for delivering the fluid energy to the rock surface. In practice the measurement could not be made at the nozzle location because the transducer's size and shape interfered with the water flow. The transducer was placed at a location upstream of the nozzle. The difference in pressure between the upstream location and the nozzle was measured and found to be negligible.

To simulate water flow conditions on a shearer, a bit block was installed on the tests apparatus. To provide operating conditions typical of water-jet-assisted cutting on a longwall shearer, supply pressure at the nozzle was set at 41 MPa with a nozzle-to-target distance of 10-cm. For these operating conditions the stagnation pressure was approximately 20 MPa, or 50 pct of the supply pressure.

3.0 REDUCING NOZZLE TO TARGET PRESSURE LOSSES

3.1 Factors

The pressure loss that occurs between the nozzle and rock surface is significantly greater than the combined loss in the rotary coupling and cutting drum, and therefore, has the greatest impact on the stagnation water pressure delivered during water-jet-assisted cutting. A fluid delivery system that minimizes the amount of solid stream breakup and maintains a more coherent flow stream should increase the stagnation pressure. Two of the factors that affect fluid stream coherence are upstream flow turbulence and nozzle design.

3.2 Flow Turbulence

Water flow turbulence is a function of the internal geometry of the flow path. On the shearer, the water enters the nozzle from a water channel that is drilled in the bit block. One shearer bit block was milled to expose the water channel (fig. 5). The straight flow channel upstream of the nozzle is about 11-cm long. However, the channel diameter is not uniform and a close physical examination indicates that the drilling process and the accumulation of rust caused the inner surface to be rough. It can be assumed that the flow channels in all bit blocks on the shearer were similar.

The rough irregular surface of the flow channel in the bit block increased the flow turbulence. To reduce turbulence resulting from flow through the bit block would require that the channel diameters be made more uniform and inner surfaces smoother. Due to the shape of flow channels inside the solid bit block, modifications could not be made easily.

The effects of a modified flow path were simulated by using a straight piece of tubing in place of the bit block (fig. 6). The length of the tubing (10 cm) was about the same as the water channel in the bit block. The inner surface of the tubing was smooth and had a uniform diameter that was equal to the nozzle inlet diameter (4 mm). Stagnation pressures were measured at nozzle to target distances between 2.54 and 12.7 cm. Stagnation pressure readings were also made while using the bit block and the same operating parameters.

Figure 7 compares the average stagnation pressures measured while using the 10 cm long tubing and the bit block. For both configurations the stagnation pressure decreased with standoff distance. However, at each standoff distance, the stagnation pressure was less when the nozzle was used in the bit block. The average stagnation pressure, for all standoff distances, was 35 pct greater when the nozzle was used with the straight tubing.

3.3 Nozzle Design

Several different nozzle types are available for water-jet-assisted cutting. Nozzle performance, for water-jet-assisted cutting, was determined by comparing the stagnation water pressures delivered using three nozzle types. Each nozzle was designed to deliver a solid stream of high-pressure water. All nozzles tested were suitable for use on a longwall shearer. Eleven sapphire, nine tungsten carbide, and ten stainless steel nozzles were used during the testing program. The sapphire and tungsten carbide orifices were installed in stainless steel bodies.

Stainless steel-

The stainless steel nozzles had a solid one-piece construction and were similar to the nozzles used during the shearer tests described above (fig. 8A). Orifice and inlet cone was machined directly into the nozzle body.

Tungsten carbide -

Tungsten carbide nozzles were purchased with integral lead-in cones, similar to the Leach and Walker design, and installed in stainless steel bodies (fig. 8B).

Sapphire -

Sapphire nozzles, as purchased, were mounted in a threaded fitting (fig. 8C). Stainless steel bodies were drilled and tapped and the sapphire orifice fitting inserted. Because of the fitting design the orifice could be installed only with the tapered cone directed out. Therefore the water entered through the sharp-edged side of the orifice. Nozzles with sapphire orifices are typically used with ultra high pressure applications where precise and fine cutting is required and nozzle wear can occur more rapidly. They can also be used with moderately high-pressure water-jet cutting.

To simulate operation on a longwall shearer, the nozzle test supply pressure was maintained at 41 MPa and standoff distances varied from 2.5 to 12.7 cm. Each test was conducted with a 10-cm long piece of tubing placed upstream of the nozzle. The effect of straight flow length on stagnation pressure was similar for each of the three nozzle types tested.

Flow rate must also be considered when comparing nozzle performance. For a constant supply pressure, flow rate varies with area of the nozzle orifice. Because the fluid energy delivered to the rock surface is a function of pressure and flow rate, stagnation pressures should be compared for nozzles having the same supply pressure and flow rates.

Three different size orifices were selected for each nozzle type. The range of orifice sizes provided a range of flow rates that would be acceptable on a longwall shearer. However, orifice size alone is not a good indicator of relative flow rate. Internal nozzle design, which was different for each of the nozzle types tested, also affects flow rate.

To categorize nozzles according to flow rate, the flow through each nozzle, at a pressure of 41 MPa, was measured using a graduated cylinder. Nozzles having similar flow rates were placed in one of the four categories shown in Table 1. Nozzle performance was compared with other nozzles in the same category.

Each nozzle in a category provided approximately the same flow rate at equal supply pressures. The stagnation water pressure measured at the target location was an indicator of how effectively the nozzle would deliver high pressure water to the rock surface.

The results showing stagnation pressure versus standoff distance are given in figures 9 to 12. In each of the four categories the stagnation pressure delivered by the three nozzle types decreased as the standoff distance increased. The amount of this decrease does not vary significantly between the nozzles in category 1. However the stagnation pressure loss was greater for the sapphire nozzles in categories 2, 3, and 4. Comparing the performance of the same nozzles in different categories, the tungsten carbide orifices in category 1 had greater stagnation pressure losses than the tungsten carbide orifices in categories 3 and 4. Tungsten carbide and stainless steel nozzles supplied stagnation pressures greater than 50 pct of the pump pressure at 10-cm nozzle-to-target distance.

For flow rates of 75 to 215 ml/s (categories 2, 3 and 4), the tungsten carbide and stainless steel nozzles delivered approximately the same stagnation pressure at equal standoff distances, while the stagnation pressure delivered by the sapphire nozzles was much less.

4.0 DISCUSSION

4.1 Effect of tubing length -

A straight piece of smooth tubing placed upstream of each of the nozzle types tested reduced flow turbulence and increased stagnation pressure. A test was conducted to determine what effect changing the tubing length would have on stagnation pressure. To study the relative effects of the

tube length on stagnation pressure, 5-, 10-, and 15.2-cm long pieces of straight tubing were used with a stainless steel nozzle. At a nozzle supply pressure of 41 MPa and a standoff distance of 10 cm, the average stagnation pressure increased with increasing tube length, although the pressure increase above 10 cm was small (fig. 13). For the type nozzles used in this study, a 10-cm long straight flow length was adequate to reduce flow turbulence.

4.2 Effect of nozzle wear

For this study, testing periods were short and the amount of nozzle wear was too little to affect nozzle performance. The amount of wear will increase with time and will occur more rapidly at higher pressures. Although one advantage of stainless steel nozzle construction is ease of manufacturing, nozzles with tungsten carbide or sapphire orifices are more durable and less subject to wear.

A wear test was conducted to determine what effects prolonged use would have on the performance of a stainless steel nozzle. One stainless steel nozzle with a 0.6 mm nozzle was operated at 41 MPa for a total of 280 hours. Periodically during the tests, the stagnation pressure was measured and plotted vs. the number of hours of operation. Figure 14 shows that stagnation pressure, at a 10-cm standoff distance, remained relatively constant for the entire test period.

4.3 Effect of nozzle profile

If a larger orifice size is used while keeping the pressure constant, flow rate and the amount of fluid energy will increase. Increasing the orifice size also increases the diameter of the flow stream. The stagnation pressure profiles for two tungsten carbide nozzles having two different size orifices (.8 and 1.0 mm) are shown in figure 15. The stagnation pressure delivered by the two nozzles was approximately the same. The major difference between the two nozzle profiles was the profile width. The advantages of a wider profile, for water-jet-assisted cutting are not known, but, when maintaining the same supply pressure, the wider profile indicates a higher flow rate. It is reasonable to assume that for some cutting conditions a wider pattern will remove more material from around the bit tip. The larger orifice nozzle does not provide a higher stagnation pressure, but higher pressures are delivered a greater distance from the nozzle centerline.

5.0 CONCLUSIONS

The test apparatus used simulated flow conditions on a longwall shearer equipped for water-jet-assisted cutting. The results show that the stagnation water pressure can be increased without increasing the supply pressure or moving the nozzle closer to the bit tip. The greatest loss in pressure occurred between the nozzle and the rock surface. Reducing the flow turbulence at the nozzle inlet increased the stagnation pressure 35 percent.

6.0 REFERENCES

1. Hood, M.: "Cutting Strong Rock with a Drag Bit Assisted by High-Pressure Water Jets." J. Of the South African Inst. of Min. and Met., Nov. 1976, pp. 79-90.

2. Kovscek, P. D., C. D. Taylor, H. Handewith, and E. D. Thimons: "Longwall Shearer Performance Using Water-Jet-Assisted Cutting." U.S. Bureau of Mines Rpt. of Investigation No. 9046, 1986, 15 pp.

3. Leach, S. J., and G. L. Walker: "The Application of High-Speed Liquid Jets to Cutting; Some Aspects of Rock Cutting by High Speed Water Jets." Proc. R. Soc. London, Phil Trans. A, v. 260, 1966, pp. 295-308.

TABLE 1. Nozzles Used for Testing

Category	Range of Flow rates, ml/s	No. of Nozzles Tested*	Average Orifice Diameter, mm
1	50 to 63	1 SA, 3 TC	0.5
2	75 to 88	4 SA, 4 SS	0.6
3	110 to 145	3 SA, 5 TC, 3 SS	0.7
4	185 to 215	3 SA, 1 TC, 3 SS	0.9

* SA : Sapphire, TC : Tungsten Carbide, SS : Stainless Steel

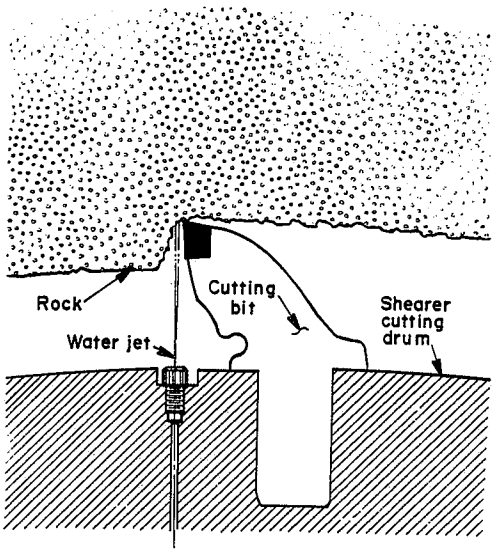

FIG. 1 WATER-JET-ASSISTED CUTTING BIT

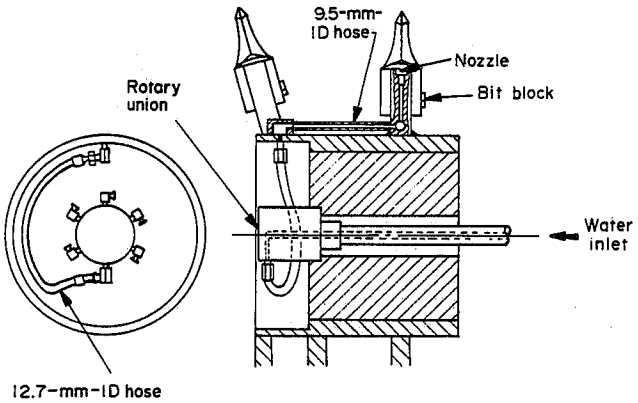

FIG. 2 WATER PASSAGE THROUGH ROTARY UNION AND CUTTING DRUM

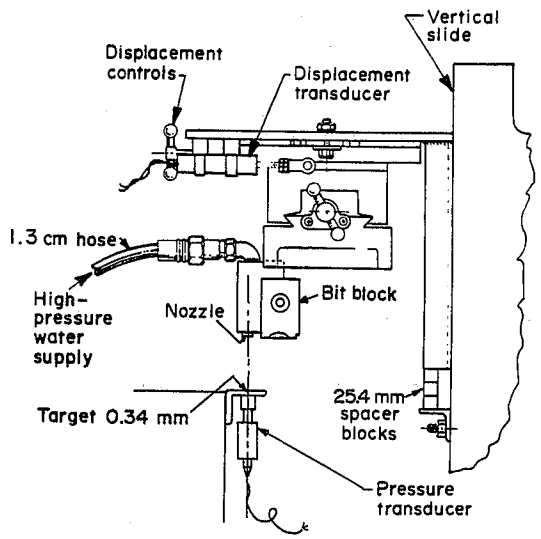

FIG. 3 TEST APPARATUS WITH BIT BLOCK

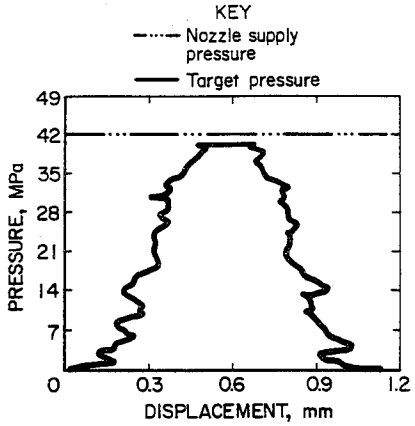

FIG. 4 EXAMPLE OF STAGNATION PRESSURE PROFILE

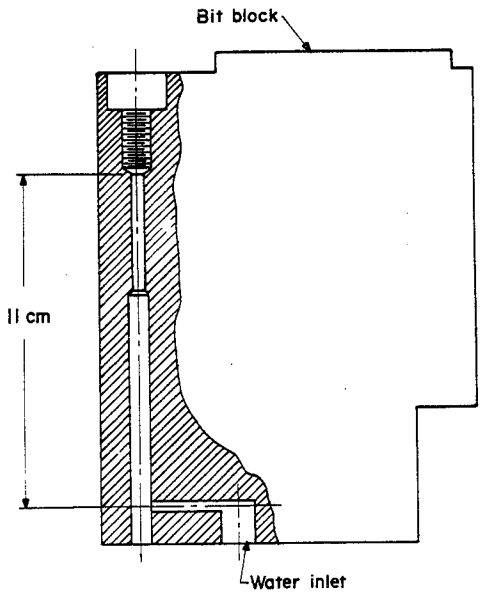

FIG. 5 BIT BLOCK WATER CHANNEL

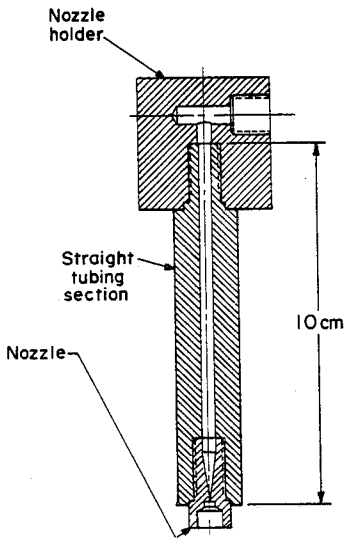

FIG. 6 NOZZLE WITH STRAIGHT TUBING

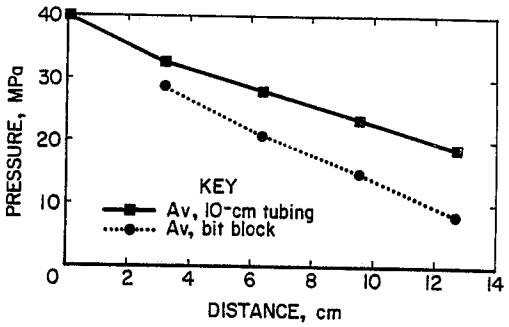

FIG. 7 STAGNATION PRESSURE, BIT BLOCK AND 10-CM TUBING

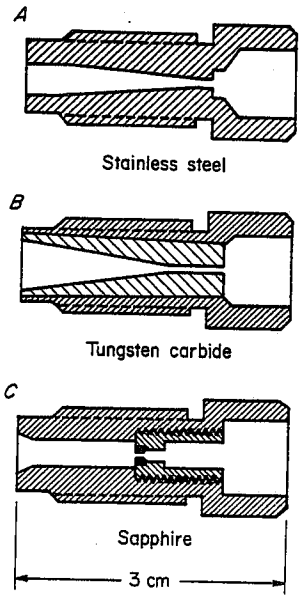

FIG. 8 COMPARISON OF NOZZLE TYPES

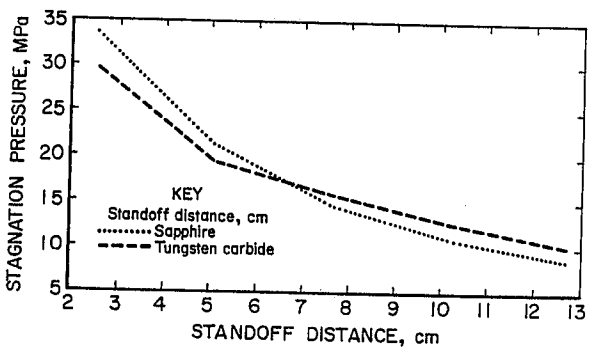

FIG. 9 STANDOFF DISTANCE VERSUS STAGNATION PRESSURE (CATEGORY 1)

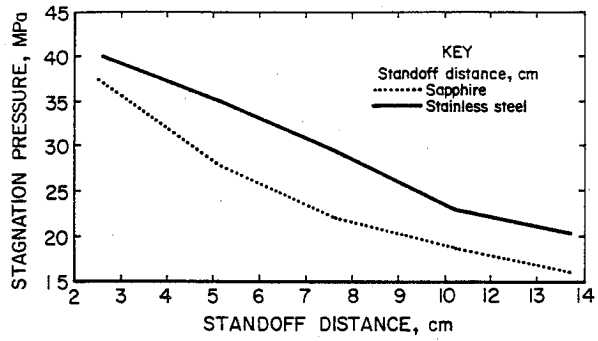

FIG. 10 STANDOFF DISTANCE VERSUS STAGNATION PRESSURE (CATEGORY 2)

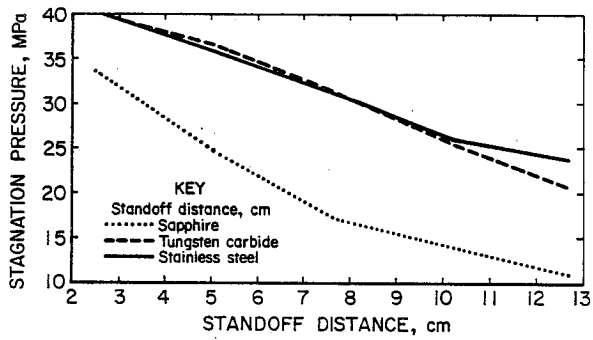

FIG. 11 STANDOFF DISTANCE VERSUS STAGNATION PRESSURE (CATEGORY 3)

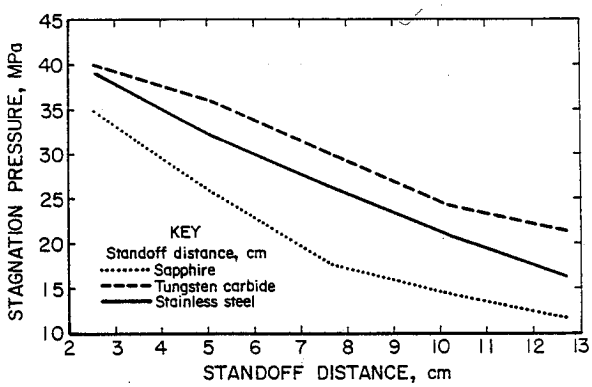

FIG. 12 STANDOFF DISTANCE VERSUS STAGNATION PRESSURE (CATEGORY 4)

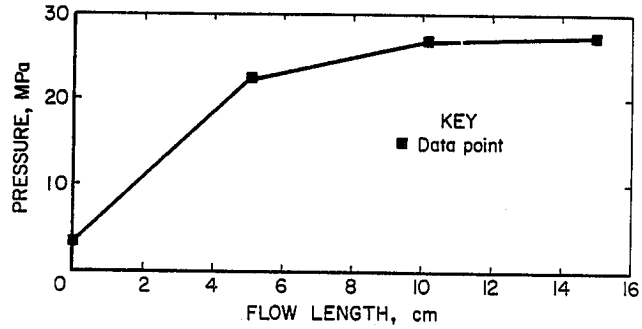

FIG. 13 EFFECT OF STRAIGHT TUBING LENGTH ON STAGNATION PRESSURE

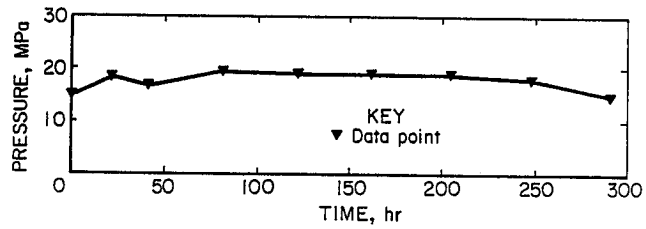

FIG. 14 STAGNATION PRESSURE VERSUS OPERATING TIME FOR STAINLESS STEEL NOZZLES

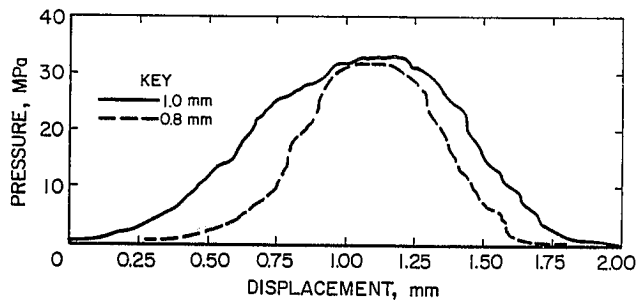

FIG. 15 STAGNATION PRESSURE PROFILES FOR 0.8 and 1.0-MM NOZZLES

5th American Water Jet Conference
August 29 - 31, 1989: Toronto, Canada

Paper
Communication 2

WATER-JET-ASSIST OIL SHALE BOOM-MINER DEVELOPMENT

W.J. Kogelmann
Alpine Equipment Corporation, State College
Pennsylvania 16804, USA

E.D. Thimons
U.S. Bureau of Mines
Pittsburgh, Pennsylvania 15236, USA

J. E. Virgona
U.S. Department of Energy
Grand Junction, Colorado 81502, USA

L.A. Weakly
Exxon Company
Grand Junction, Colorado 81502, USA

ABSTRACT: The U.S. Department of Energy's Grand Junction Projects Office (DOE) is participating in a $1.5 million Cooperative Agreement with Alpine Equipment Corporation/Astro International Corporation (Alpine) of State College, Pennsylvania, to evaluate the water-jet-assisted (WJA) mechanical cutting of oil shale under actual mining conditions. The cost of the 24-month, three-phase Technology Development Project, started in February 1988, is shared equally between Alpine and the Department of Energy. Alpine has designed, is assembling, and will test two WJA mining machines. A 20-ton WJA roadheader will commence WJA oil shale cutting tests in the spring of 1989. Based on the results of these tests a novel WJA cutting system will be designed for a commercial-sized boom-type mining machine.
Field testing of the machine will be conducted at the Exxon Company, USA, Colony Pilot Oil Shale Mine located in the Piceance Basin of western Colorado. Additional support will be provided by the U.S. Bureau of Mines (USBM) Pittsburgh Research Center and oil shale companies, through the Colorado Mining Association (CMA).
The physical characteristics of oil shale (a dolomitic limestone containing kerogen) make conventional mechanized production mining methods impractical by causing excessive machine vibration, high bit-wear rates, and excessive dust generation. Current mechanical excavation methods for oil shale are less efficient and more costly than the traditional drill-and-blast methods. However, conventional drill-and-blast methods have limitations imposed by excessive rock damage and regulatory considerations. By improving mechanical excavation technologies, oil shale could be more competitive with other energy sources. The WJA cutting technology currently being developed is expected to be applicable to oil shale deposits to ore and coal mining and for tunnel drivage at civil engineering projects.
An evaluation under actual mining conditions will provide field data that can be utilized by the private sector to develop and commercialize WJA mechanized equipment to mine oil shale. The successful application of high-pressure water-jet technology in conjunction with mechanical mining could favorably impact the mining of oil shale by reducing capital and operating costs, improving safety, and increasing the extraction ratio of oil shale mined. The WJA roadheader field tests on coal have shown that high-pressure water-jets increase cutter life and reduce ventilation costs by cooling the cutting head, removing already mined rock from the cutting surface, and reducing dust production.

RÉSUMÉ : Le Grand Junction Projects Office du U.S. Department of Energy (DOE) participe à un accord de collaboration de 1,5 million $ avec Alpine Equipment Corporation/Astro International Corporation (Alpine) du State College de la Pennsylvanie sur l'évaluation de la coupe mécanique assistée par jet d'eau (AJE) de schistes bitumineux dans des conditions réelles d'exploitation minière. Le coût du Projet de développement de la technologie en trois phases qui a duré 24 mois à compter de février 1988 est partagé également entre Alpine et le DOE. Alpine a conçu, assemble et mettra à l'essai deux machines minières AJE. Une abatteuse de front de taille AJE de 20 tonnes sera utilisée dans les premiers essais de coupe AJE de schistes bitumineux au printemps de 1989. Selon les résultats de ces essais, un nouveau système de coupe AJE sera conçu pour une machine minière à fiche de taille commerciale.
Les essais sur le terrain de la machine seront menées à la mine pilote de schistes bitumineux Colony de la société Exxon USA, dans le bassin Piceance dans l'ouest du Colorado. Une aide additionnelle sera fournie par le Centre de recherches de Pittsburgh du US Bureau of Mines (USBM) et des sociétés de schistes bitumineux par l'entremise de la Colorado Mining Association (CMA).
Les caractéristiques physiques des schistes bitumineux (calcaire dolomitique contenant du kérogène) rendent les méthodes mécanisées classiques de production minières inutilisables à cause des vibrations excessives des machines, de la vitesse d'usure élevée des outils et de la production excessive de poussière. Les méthodes actuelles d'excavation mécanique des schistes bitumineux sont moins efficaces et plus coûteuses que les méthodes classiques d'abattage à l'explosif. Ces dernières ont toutefois des limites qui tiennent à l'endommagement excessif par la roche et aux exigences de la réglementation. En améliorant les techniques d'excavation mécanique, on pourrait rendre les schistes bitumineux plus concurrentiels par rapport à d'autres sources d'énergie. La technologie de la coupe AJE qui est en voie de développement devrait être applicable à l'exploitation des gisements de schistes bitumineux, des minerais et des charbons, et au creusement de tunnels dans des projets de génie civil.
Une évaluation dans des conditions d'exploitation minière réelles fournira des données de terrain qui pourront servir au secteur privé à mettre au point et à commercialiser du matériel mécanisé AJE pour l'exploitation des schistes bitumineux. L'application avec succès de la technologie des jets d'eau à haute pression à l'exploitation mécanique pourrait améliorer l'exploitation des schistes bitumineux en diminuant les frais d'immobilisation et d'exploitation, en améliorant la sécurité et en augmentant le taux d'extraction. Les essais effectués sur le charbon à l'abatteuse de front de taille AJE ont montré que les jets d'eau à haute pression augmentent la durée des taillants et diminuent les coûts de ventilation en refroidissant l'outil de coupe, en dégageant la roche déjà abattue du front de taille et en diminuant la production de poussière.

Organized and Sponsored by the National Research Council of Canada and the U.S. Water Jet Technology Association.

1.0 INTRODUCTION

1.1 Background

The U.S. Department of Energy (DOE) Oil Shale Program is directed to the development of advanced technologies for extracting shale oil from the large U.S. oil shale resources. The overall goal of the DOE Oil Shale Program is to foster development of an economically competitive and environmentally acceptable oil shale industry whose products can compete in the marketplace. The program has two primary objectives:

1. To produce an engineering and scientific information base for industry use in designing and developing oil shale processes with reduced costs and enhanced environmental acceptability and to foster the development of novel oil shale processes.

2. To develop a comprehensive data base on pollutant generation and the steps required to mitigate the impacts in a cost-effective manner.

In the pursuit of these objectives, the DOE has expanded its rock fragmentation research to encompass the study of advanced extraction (mining) methods. The Idaho National Engineering Laboratory (INEL), through the DOE Idaho Operations Office (DOE/ID), was included in the Oil Shale Program by the U.S. Congress in 1987 and was funded to conduct extraction research. The DOE/ID three-part mining research program comprises: assessment of state-of-the art oil shale mining, research of advanced mining concepts, and demonstration of continuous mining techniques.

The DOE/ID WJA Project, managed by the DOE/ID Grand Junction, Colorado, Projects Office (GJPO), is a U.S. $1.5 million Cooperative Agreement to evaluate WJA mechanical cutting of oil shale under actual mining conditions and to address the potential for applying this technology to the extraction of both eastern and western oil shale resources (Virgona et al., 1988). The project's objectives are:

1. To provide a technological basis, through evaluation of water-jet-assist enhancing oil shale extraction on a sufficient scale and in an actual underground mine environment, that will enable realistic testing to identify environmental and economic constraints to commercialization.

2. To obtain the data sets requisite to development of a production machine specifically designed for operation in oil shale mining operations for dissemination to the private sector.

Some advantages of a WJA machine to achieve cost-effective oil shale extraction include improving safety and health conditions in underground mines with enhanced ground-control conditions.

Most oil shale mining operations have been planned with blasting as the primary rock removal mechanism, but this method presents potential problems. The load-carrying capacity of the oil shale pillars remaining after conventional blasting is much less than the capacity obtained when using mechanical mining. Blasting also produces major instantaneous releases of blasting gases and dust, with possible large releases of methane in gassy formations. Mechanical mining can achieve a significant increase in resource recovery and continual savings in operating costs due to the reductions in required pillar size and/or increases in span dimensions.

Mechanical excavation of oil shale offers major safety, health, and productivity advantages as compared with blasting. However, the physical characteristics of oil shale make it somewhat difficult to cut mechanically. During tests with a conventional roadheader in a western Colorado oil shale mine, bit wear was relatively high and dust generation was a problem.

Although mechanized excavation might be feasible for development mining of oil shale due to the smaller volumes of rock that are cut, it is not currently practical for production mining of oil shale. The addition of water-jet-assist to mechanical cutting machines used for production purposes in oil shale mines could make the operation more cost effective because machine productivity and cutter life are expected to improve.

The WJA cutting uses a mechanical cutting tool in combination with a high-pressure (> 138 bar, 2,000 psi) stream of water directed just in front of the tool. Recent laboratory and underground studies of WJA cutting in coal indicate that the addition of the water-jet-assist to the cutting tool significantly reduces respirable dust and cutting-tool wear,

decreases the probability of frictional sparking, increases product size, and improves cutting in harder materials.

All these potential benefits could be used to an advantage in the mining of oil shale, but research is needed to ascertain the extent of applicability to oil shale and of associated problems.

1.2 Water-Jet-Assisted Cutting In Coal

Significant laboratory and underground research has been conducted on the application of water-jet-assist to roadheaders and longwall shearers for coal mining applications. A cooperative research effort of the USBM and British Coal showed that there were benefits in using WJA cutting on roadheaders operating in coal mines, especially when cutting rock as part of the coal extraction process. WJA cutting at pressures above about 138 bar (2,000 psi) resulted in dust reductions of at least 50 percent when compared with conventional-pressure water sprays for dust control. Marked reductions in frictional sparking and bit-wear rates were also noted with the water-jet-assist. In some cases where hard rock was being cut, bit life was extended by as much as 200 percent. Using water-jet-assist did not result in any meaningful reduction in roadheader power consumption when coal was being cut. However, there were improvements in cutting when harder rock was encountered, probably due to reduction in bit wear.

The first WJA roadheader, supplied by Alpine, was tested in 1975 in the BOM Safety Research Coal Mine at Bruceton, Pennsylvania. A light-weight (10 ton) roadheader with a transverse (ripper) cutter head (33 kW, 44 hp cutter motor) was augmented with high-pressure water at a rate of 80 l/min (21 gal/min). The nonrotating, nonphased water-jets were aimed ahead of conical point-attack bits of the transverse cutter head (see Figure 1). This early WJA cutting system doubled the roadheader's rate of coal production and achieved a 70 percent reduction in respirable dust levels (McNary et al., 1976).

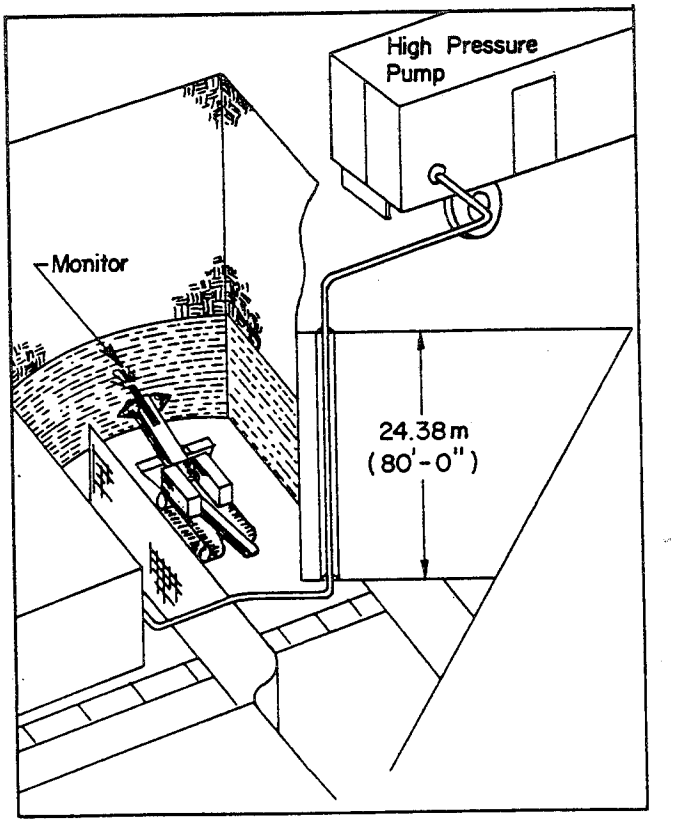

Figure 1. World's first WJA miner: Alpine roadheader at Bruceton, Pennsylvania Coal Mine of the U.S. Bureau of Mines.

Full scale laboratory and underground testing of WJA longwall shearers produced results similar to those obtained with the roadheaders. The USBM used a WJA shearer to cut a simulated coal block consisting of coal, fly ash, and cement. The coal block had a compressive strength similar to coal.

In 1984, the USBM funded a contract for the design and in-mine testing of a high-pressure (up to 700 bar, 10,000 psi) WJA longwall shearer (USBM Contract, 1984). Two of the authors of this report (W.J. Kogelmann and E.D. Thimons) had key roles in this pioneering WJA cutting project. Under that contract, the world's first WJA shearer (Eickhoff EW-200/170-L) with a high-pressure water-phasing system (see Figure 2) was in-mine tested at the Auguste Victoria Coal Mine in Marl, West Germany for a sustained period. The WJA shearer ran at a peripheral bit-tip speed of 2.14 m/s (423 ft/min). Formerly, practically all WJA cutting tests were conducted in laboratories at unrealistic mining machine cutting speeds (less than 0.5 m/s, 100 ft/min) that were not applicable to actual minig machines.

Alpine is using the findings of the USBM WJA shearer project for the development of the WJA oil shale miner. Both the laboratory and underground test programs shows that use of high-pressure water did little to reduce the shearer motor energy required to maintain a given cutting rate. However, several other major benefits were achieved with the use of WJA cutting (Kogelmann et al., 1986).

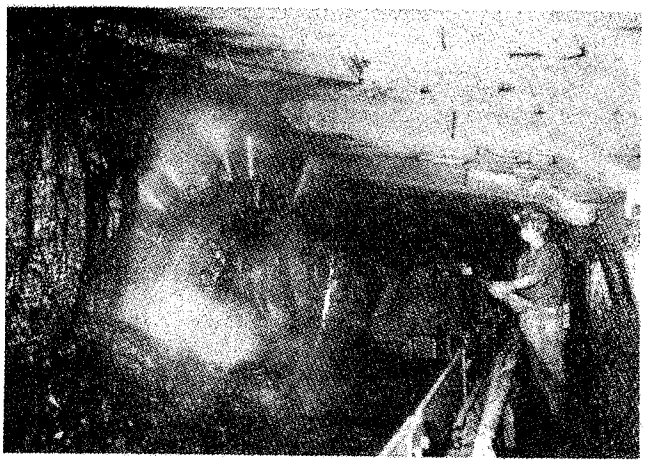

Figure 2. Water-jet-assisted longwall shearer cutting in coal.

Water pressures of between 138 to 207 bar (2,000 to 3,000 psi) reduced respirable dust in the air by about 80 percent, as compared with the use of conventional water sprays operating at pressures below 20.7 bar (300 psi). Increasing the WJA pressure above about 207 bar (3,000 psi) resulted in no additional dust reduction.

The use of water-jet-assist on a longwall shearer also contributed to a reduction in coal product fines. A pressure of 138 bar (2,000 psi) decreased product fines approximately 10 percent, with major cost savings to the coal industry due to reduced cleaning plant costs and increased product recovery.

No controlled measurement of bit wear was possible in the laboratory tests due to the limited amount of cutting and the absence of rock in the simulated coal block. Bit wear as a function of water-jet pressure could not be ascertained in the underground testing because of the constantly changing conditions on the longwall face. If the entire test program is considered, with varying water-jet pressures of 138 to 690 bar (2,000 to 10,000 psi), the use of water-jet-assist doubled the average bit life.

Similar results have been reported in tests of WJA roadheaders and longwall shearers in a number of other coal mining countries. More than 60 WJA roadheaders have been purchased worldwide by the coal mining industry and several WJA shearers are operating in England and West Germany. The first WJA longwall shearer designed and manufactured under USBM Contract No. J0145039, equipped with a phased water-jetting system (Kogelmann et al., 1986) will be installed in Kerr-McGee Corporation's Galatia coal mine in Illinois in the spring of 1989.

2.0 PROGRAM PLAN

The 24-month Technology Development Project is divided into three phases.
Phase I (4 months): conceptual engineering
Phase II (10 months): detail engineering and construction of prototype machine
Phase III (10 months): in-mine testing of WJA machine

During the 10-month Phase III actual cutting tests will be conducted at the Colony Pilot Oil Shale Mine (see Table 1 for mine details). The cutting tests will include a series of short-term tests to evaluate machine performance under various water pressures, flow rates, and other critical parameters. Once the optimal cutting parameters (water pressure and flow rate) are ascertained from the short-term tests, a continuous extended test will be conducted at these optimum conditions.

Throughout the extended testing period, water pressure and flow rates will be varied to evaluate their effect upon rotational torque, revolutions per minute, thrust, and total machine power consumption. Data on machine power consumption, cutter wear, average and range of product size, noise, vibration, and respirable dust data will be collected throughout the test program as a function of both pressure and flow. This data will allow a cost comparison between conventional mechanical cutting and WJA cutting of oil shale.

TABLE 1. Exxon's Colony Pilot Oil Shale Mine

Parameter	Data
Mining Method	Room-and-pillar (Panel-and-main)
Mineral	Dolomitic limestone containing varying amounts of kerogen comparable to the Mahogany Zone of the Green River Formation
Grade	125 to 158 l/metric ton (30 to 38 gal/ton)
Density (in situ)	2.03 to 2.15 g/cm^3 (127 to 134 lb/ft^3)
Uniaxial (unconfined) Compressive Strength	85.52 to 109.66 MPa (12,400 to 15,900 psi) Average 89.66 MPa (13,000 psi)
Tensile Strength	Average 11.03 MPa (1,600 psi)

2.1 Phase I Conceptual Design

The experience gained by Alpine from earlier research for the USBM on WJA roadheaders and shearers, both in the laboratory and in the field, was thoroughly utilized for the development of this system. A basic standard Alpine 330 Roadheader (Figure 3) will be modified to accept the WJA system (Figure 4). A summary of the design and reasons for the design selections follow.

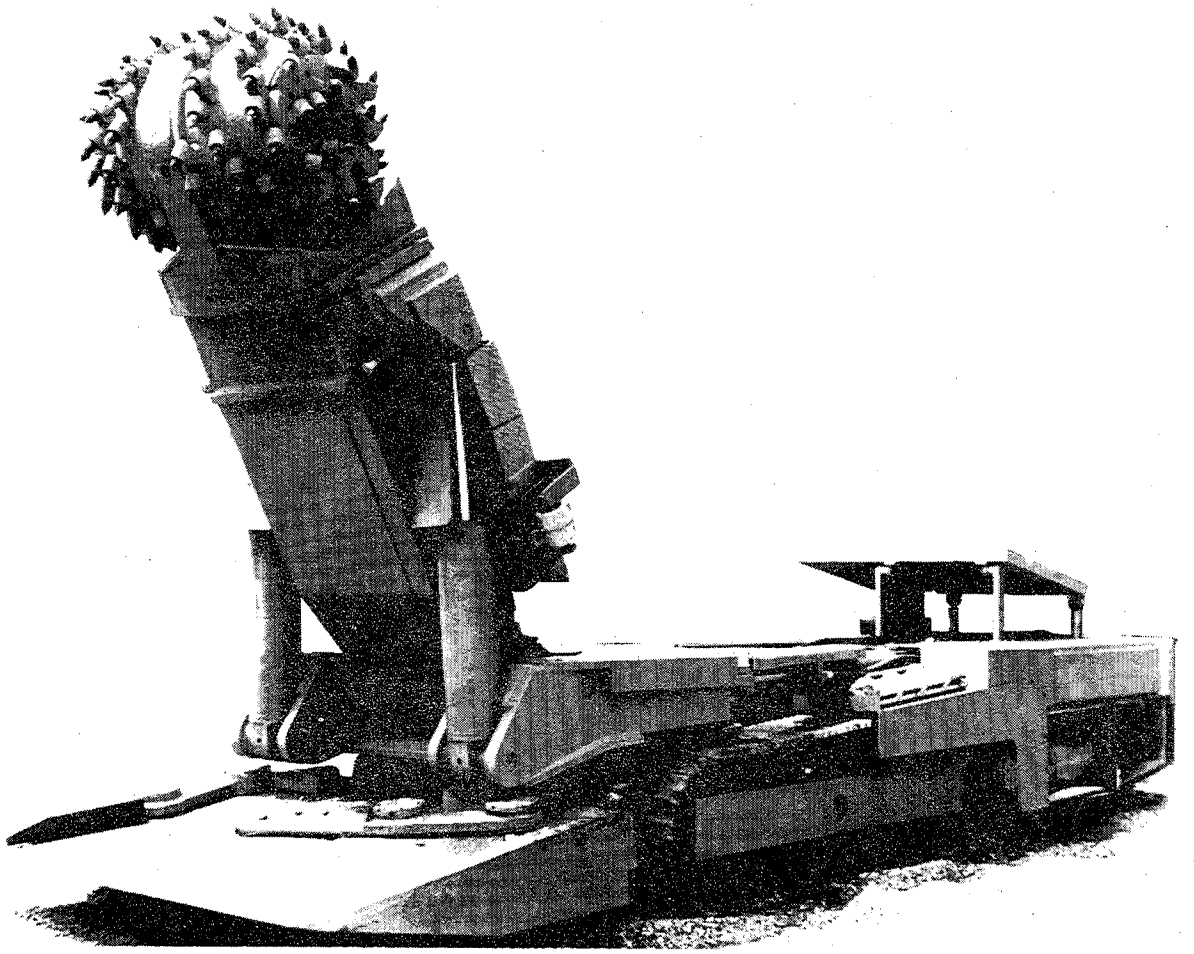

Figure 3. Alpine Equipment Corporation Roadheader to be equipped with water-jet-assisted cutting system.

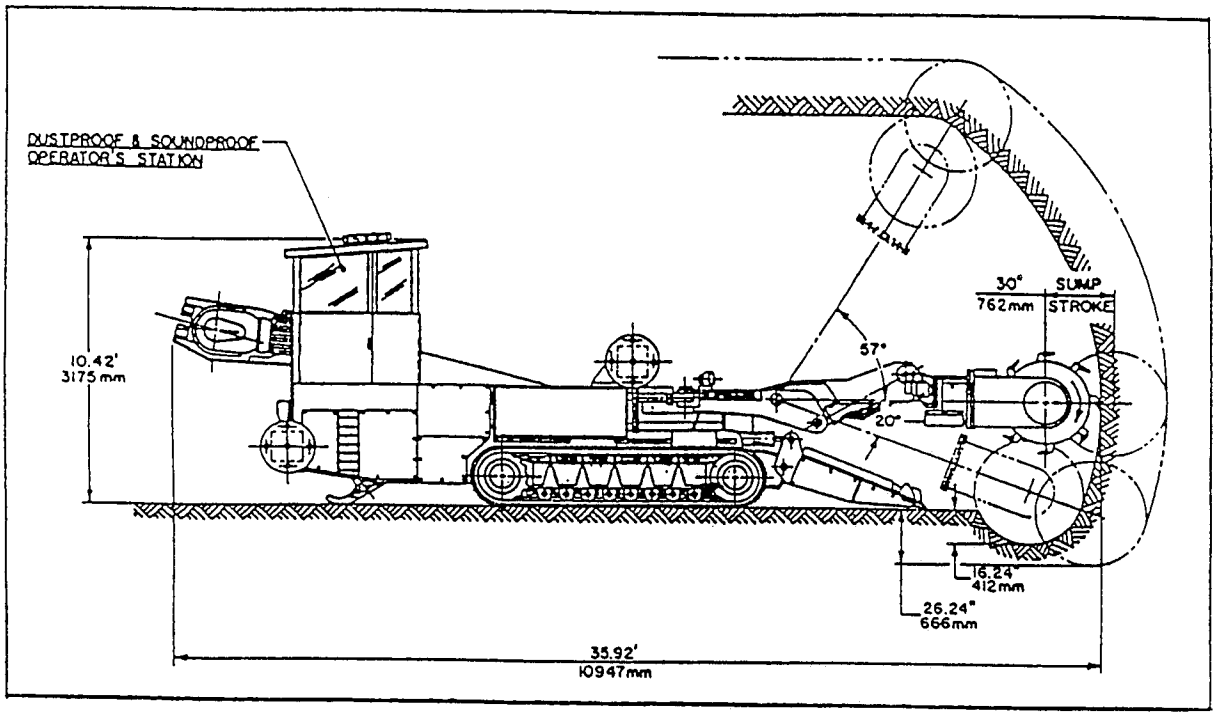

Figure 4. Alpine Equipment Corporation's conceptual design of the water-jet-assisted oil shale miner with transverse (ripper) cutter head.

2.1.1 Cutter Boom Design And Stiffness

Stiff cutter booms are required for energy-efficient cutting at a low bit cost, especially when cutting hard rock with heavy-duty roadheaders (Morris et al., 1983). All new roadheader models introduced in the 1980's (such as the AM65 Alpine Miner, Dosco LH1300, Eickhoff ET-100, Eimco TM100, Salzgitter STM 300, and Westfalia WAV130) utilize stiff box-type cutter booms supported by forward-mounted cylinders. Long-cantilever soft-rock booms, with the cutter motor as a load-carrying member of the boom, are no longer used on modern roadheaders. Figure 5 shows a comparison of cutter boom designs.

Alpine designed a hard-rock boom (HRB) to cut the oil shale with a minimum of vibration and bounce. Cutter-boom vibration causes the bits to "chatter" on the rock and shatter the tungsten-carbide inserts, resulting in excessive tool consumption (Schenck, 1982).

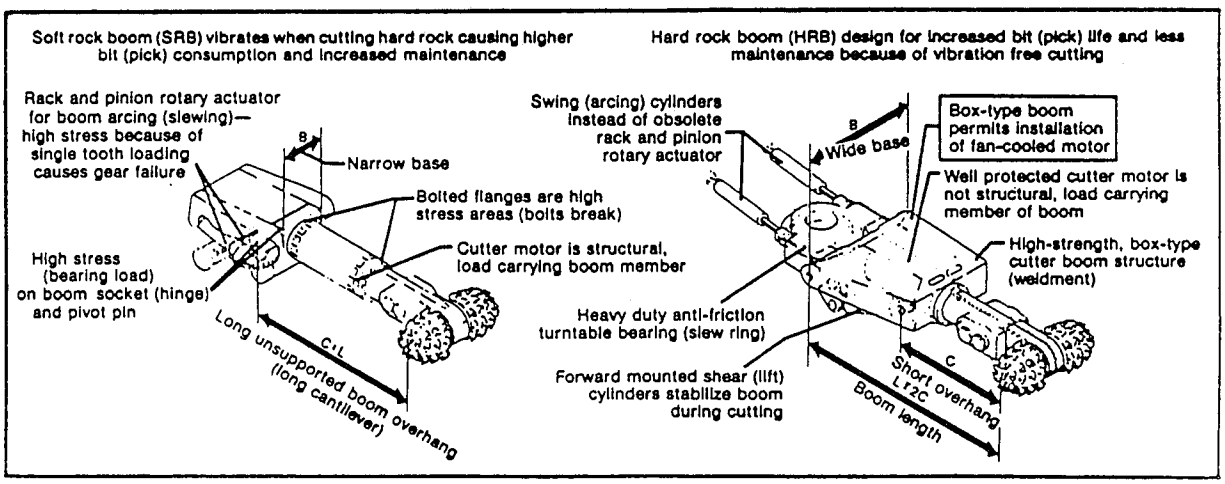

Figure 5. Comparison of cutter boom designs. A "stiff" HRB boom was selected for the WJA oil shale miner.

2.1.2 Cutter Head Styles

The cutter head's design and tooling are extremely important and can directly determine this project's success. The two primary types of cutter heads are in-line (milling) and transverse (ripper). For equivalent cutter motor capacity (i.e., rock production), ripper-type machines can be significantly lighter weight than milling-type machines (Frenyo, 1974). Field experience and actual findings of independent experts (Mertens, 1985) and roadheader owners (Morris, et al., 1983) follow.

Roadheaders with transverse heads are more suitable for varying rock conditions and operate better in difficult-to-cut rock because boom-slewing (arcing) speed and, thus, bit spacing are variable. Machines with in-line heads achieve high production rates in easy-to-cut rock.

Figure 6. Various bit (pick) types will be tested on transverse (ripper) cutter head.

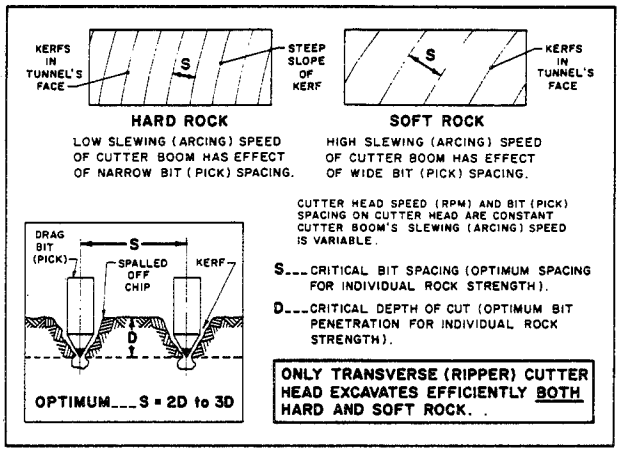

Since bit penetration and spacing are determined by rock strength, only one rock strength value can be cut by an in-line (milling) cutter head under optimum conditions. However, a transverse (ripper) head can be optimally matched to any rock strength by simply varying the boom's slewing speed (see Figure 6). This project will "reverse" the aforementioned process because the oil shale is of fairly constant strength throughout the test horizon with an average 89.7 MPa (13,000 psi) uniaxial compressive strength (see Table 1), and the cutting head parameters will be varied. The optimum bit style and lacing will be determined by varying the parameters of cutting speed, torque, normal force, and bit geometry.

Contrary to an in-line (milling) head, all bits on a transverse (ripper) head operate at approximately same peripheral bit tip speed and cutting force (see Figure 7). This permits exact measurement of operating conditions resulting in an optimum bit design and cutter head lacing. This characteristic of the "ripper" head is of great importance in the development of novel PDC "diamond" cutter bits for which no prior testing in oil shale has been done.

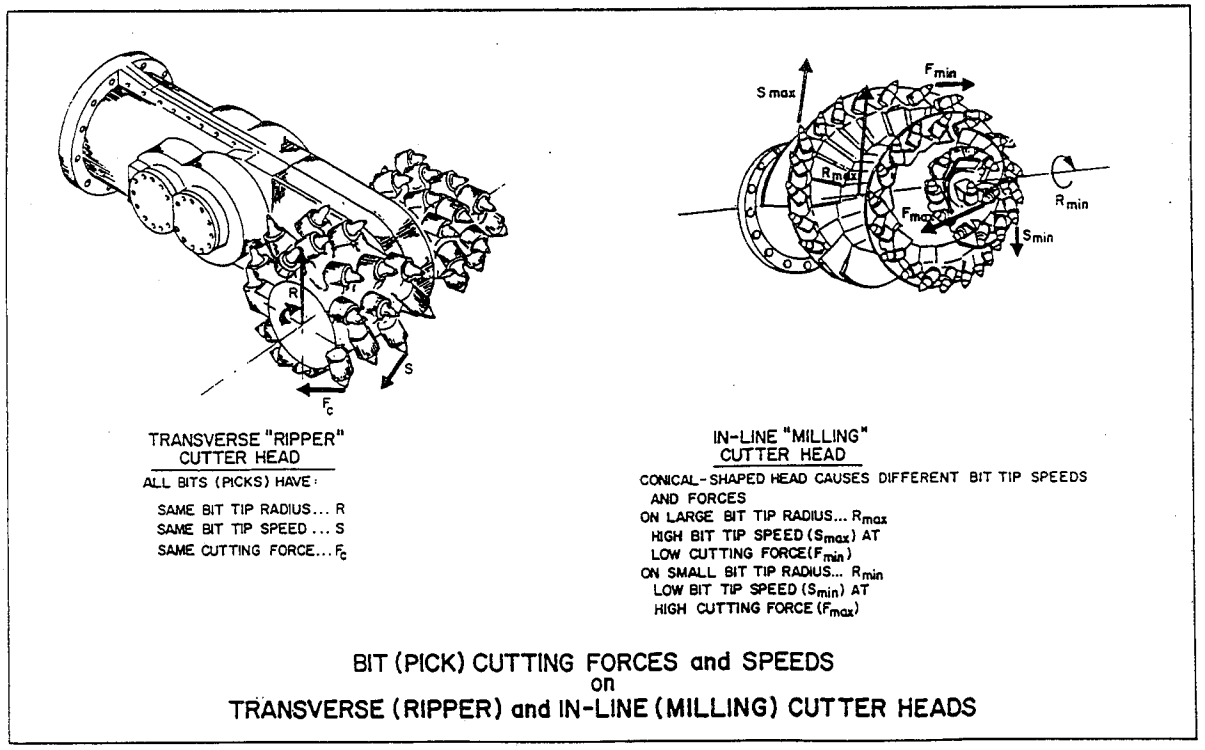

Figure 7. Tests will be made with transverse (ripper) cutter head because it provides for all bits (picks) to have approximately same bit tip speed and cutting force.

2.1.3 Roadheader Stabilization

Roadheaders with in-line (milling) heads must be braced (stelled) against the tunnel's rib (walls). If an in-line (milling) roadheader is not braced (stelled) against the rib, it slews away from the cutting action even in relatively soft rock (Wilcox et al., 1988). This bracing requirement makes a "milling" roadheader impractical for work in an oil shale mine where drifts are up to 18.30 m (60 ft.) wide.

At comparable weights "ripper" type roadheaders are more stable because their main cutting forces are directed perpendicular to the floor and, therefore, no bracing (stelling) of the machine is required (Pearse, 1988). The superior machine stability was one of the main reasons for Alpine selecting a transverse (ripper) head for WJA oil shale cutting tests with novel bits.

2.2 Cutting Tools

A roadheader is only as good as the bits used to cut the rock. Cutter bits are the most costly consumable machine components, especially when cutting hard and tough oil shale. Therefore, Alpine's main effort will be to increase tool life, which will have the greatest impact on lowering the cost of mechanized oil shale extraction. The two basic types of cutting tools evaluated for this project were roller disc cutters and drag bits.

2.2.1 Roller Disc Cutter

Roller disc cutters initially attack the rock by crushing (i.e., the disc has to overcome the uniaxial compressive strength of the oil shale). Alpine chose not to use roller discs because the uniaxial compressive strength of rock at the Colony mine is eight times higher than its tensile strength (see Table 1 and Figure 8). Additionally, roller discs are energy inefficient and have a high tool cost when used on a slewing (traversing) cutter boom rather than on a conventional boring head (Farmer, 1986).

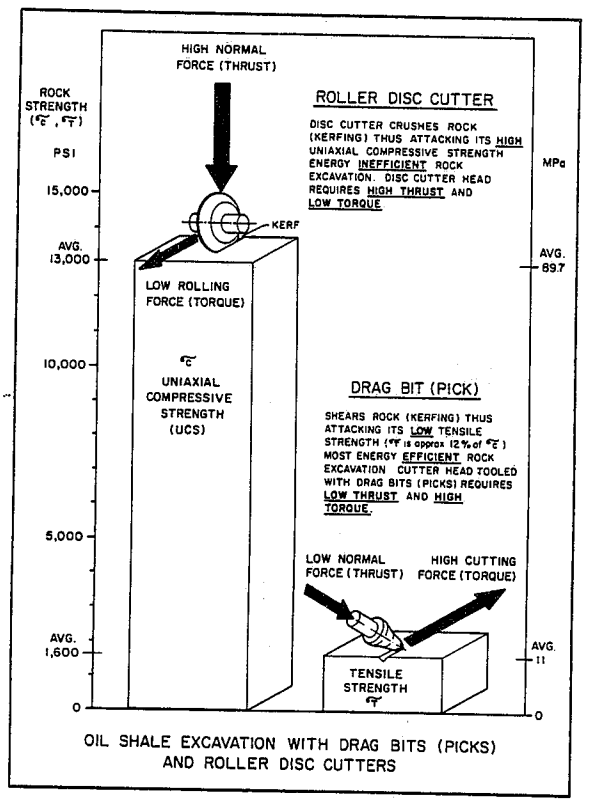

Figure 8. Drag bits (picks) will be used for oil shale test mining because they are more energy efficient and require lower thrust than disc cutters.

2.2.2 Drag Bits

Cutter heads tooled with drag bits require low thrust and high torque because drag bits shear rock (kerfing) by attacking its low tensile strength. Alpine selected drag bits for the WJA oil shale mining machine because drag bits are the most energy-efficient tool for the excavation of oil shale (Crookston et al., 1983). Roadheaders can use both rotating and non-rotating drag bits. The in-mine tests will include rotating conical "point-attack" bits and radial, polycrystalline diamond composite (PDC) bits.

Alpine plans to test a new conical, rotating bit with a demonstrated lifetime that is 10-times longer than a standard bit, according to data from numerous rock heading operations of a major European mining company.

During Alpine's initial investigations it was learned that some mining companies achieved high rates of penetration (ROP) at excellent bit life when drilling oil shale with rotary PDC "diamond" bits.

At Unocal's Energy Mining Division near Parachute, Colorado, a 89 mm (3.5 in.) diameter PDC bit drilled 27,614 m (90,600 ft.) and is still in use (E&MJ, 1989). In comparison, conventional rotary tungsten-carbide tipped drill bits lasted only some 60 m (200 ft.) in the same oil shale formation. The PDC tool had more than 450 times longer lifetime than the conventional carbide bit.

Cutting tests by the U.S. Bureau of Mines showed a potential for 10 to 20 times longer life for PDC bits over conventional carbide drag bits (Plis et al., 1988).

Based on the aforementioned tests both in laboratories and under actual underground mining conditions, it was decided that water-jet-assisted PDC drag bits have a great potential for cost-effective, high-production mining of oil shale. It was, therefore, decided to compare modern rotating "point-attack" bits (Sandvik System 35) with newly developed radial PDC bits on a WJA roadheader.

3.0 WATER-JET-ASSISTED PDC "DIAMOND" DRAG BITS

The introduction of polycrystalline diamond composites (also called "compounds"), commonly abbreviated PDC, has opened up new possibilities for cost-effective mechanized excavation of hard and abrasive rocks and minerals which could not have been cut economically with conventional carbide tools.

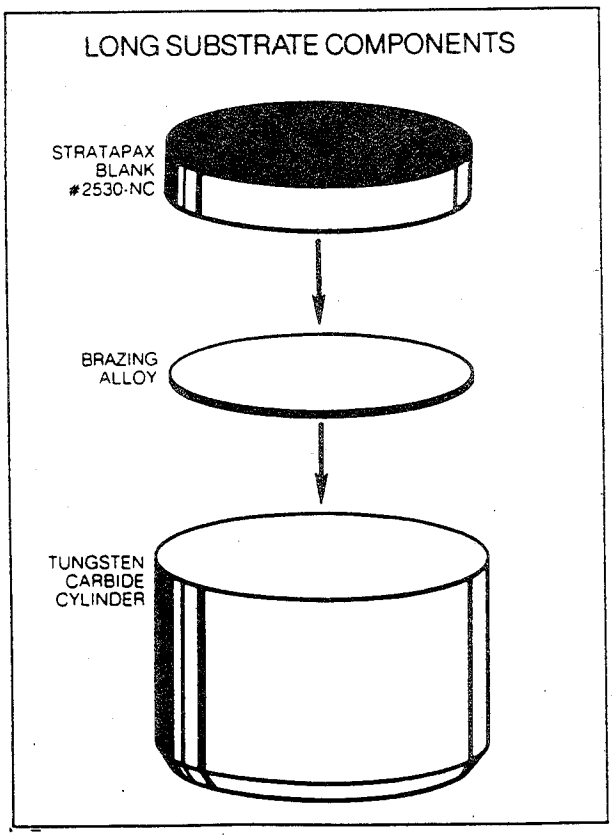

Figure 9. PDC blank and tungsten carbide stud.

3.1 Cutting Mode

Ideally, PDC cutters should shear the rock thus attacking its low tensile strength. For example, at Exxon's Colony mine the uniaxial compressive strength of the oil shale is avg. 89.7 MPa (13,000 psi); nearly 8 times higher than its tensile strength (11 MPa; 1,600 psi).

3.2 Thermal Stability

The thin PDC "diamond" layer which is only 0.3 to 1 mm (0.01 to 0.04 in.) thick is very sensitive to high temperatures (Clark, 1988).

The high thermal sensitivity of the PDC blanks might be one of the main reasons why PDC bits have mainly been used in drill and slurry-wall cutting applications where the tools are always submerged and cooled in water or in bentonite slurry. Alpine expects that water-jet-assist will dramatically increase the lifetime of PDC cutter bits.

3.3 Comparison Of Conventional Carbide Tools With PDC "Diamond" Cutter Bits (Picks)

The relationship of PDC and conventional tungsten-carbide tools with an "ideal" cutter bit are shown in Figure 10. An "ideal" bit is a theoretical tool which can cut rock of any strength at high production rates and unlimited lifetime. This "ideal" bit is used to compare the characteristics of various bit types.

A water-jet-assisted PDC cutter bit has the potential to approach the performance of the "ideal" bit.

Alpine's WJA cutting tests on both artificial face and in the Colony oil shale mine will show how close modern PDC cutting technology will get to this ambitious goal.

Drag bits using PDC inserts are designed to cut rock by a shearing action. Although some crushing of the rock will inevitably be involved as the bit advances through the rock, shearing is the primary mode of rock removal. This can be an extremely fast and efficient process, particularly with PDC, as it remains sharp. Thus, the shearing action can continue efficiently throughout virtually the entire life of the tool and results in the high rates of production associated with PDC cutter bits.

Tungsten-carbide drag bits are also designed to shear the rock but they become blunt, which severely reduces their efficiency. "Worn-in", heavy-duty conventional radial and tangential carbide bits require much higher cutting and normal forces than small and sharp carbide bits.

Alpine will investigate how much lower these forces will be for PDc bits, in both "dry" and WJA cutting modes.

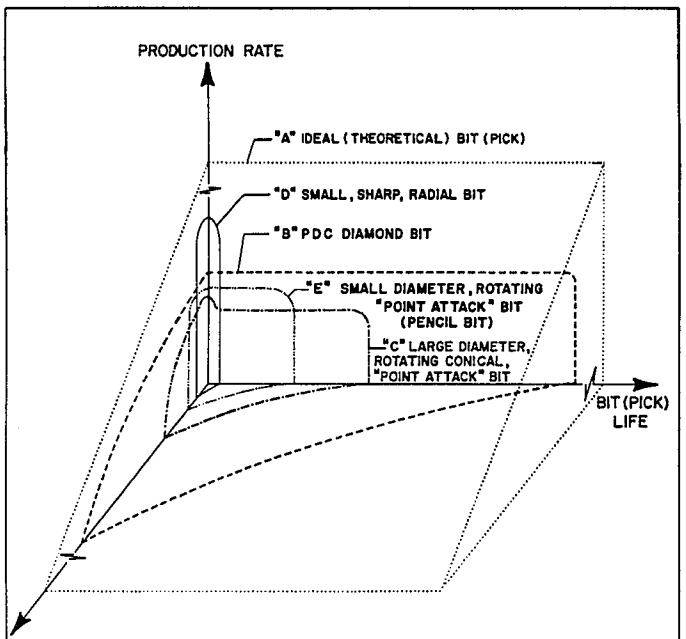

RELATIONSHIP BETWEEN ROCK STRENGTH, PRODUCTION RATE, AND BIT LIFE for VARIOUS DRAG BIT TYPES

Figure 10.

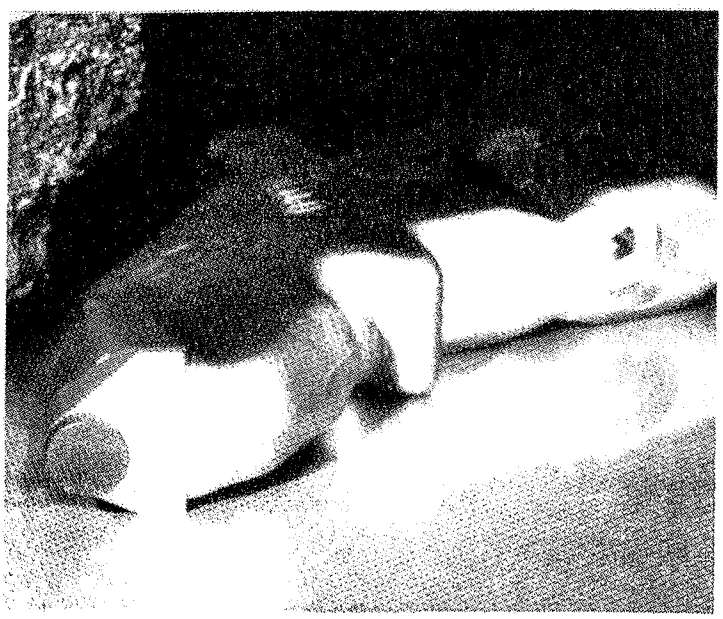

Fig. 11. Radial drag bit with "diamond" cutter blank

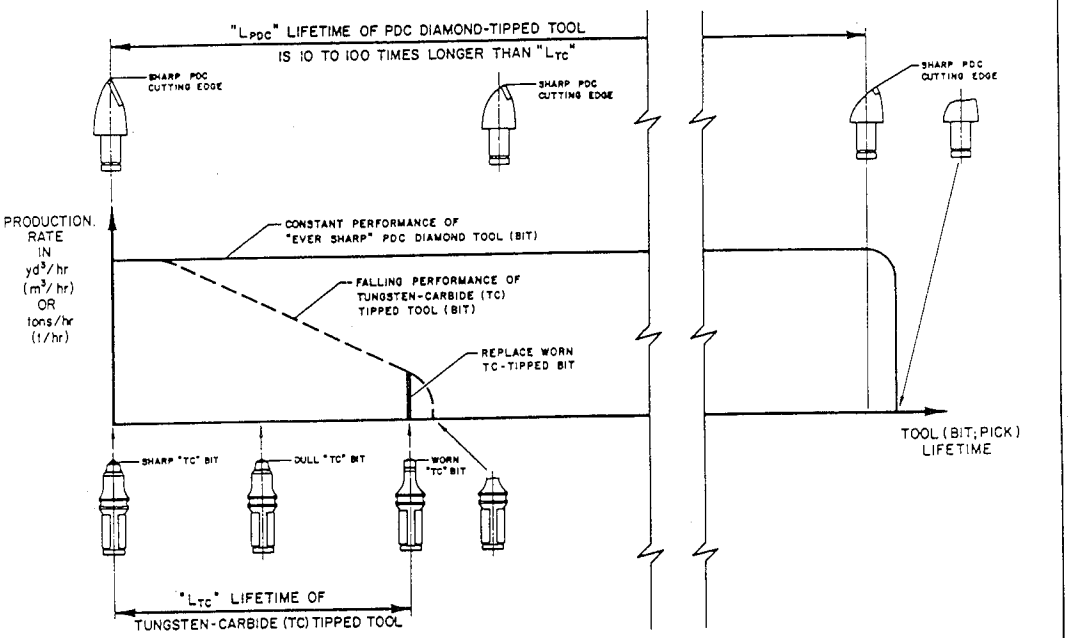

COMPARISON OF LIFETIME AND PERFORMANCE OF TUNGSTEN-CARBIDE AND PDC DIAMOND CUTTER BITS(PICKS)

Figure 12.

4.0 FACTORY CUTTING TESTS

Investigations in Phase I of the project indicated that water-jet-assisted PDC "diamond" bits have a large potential for success. Because practically no information on design and operating parameters were available on WJA "diamond" drag bits, it was decided to conduct oil shale cutting tests on a smaller size roadheader at Alpine's plant.

4.1 Test Stand And Artificial Face

Eighteen metric tons (20 short tons) of oil shale boulders were shipped from Exxon's Colony mine to Alpine's plant. These boulders were cast into lean concrete. The artificial face and the WJA roadheader are depicted in Figure 13.

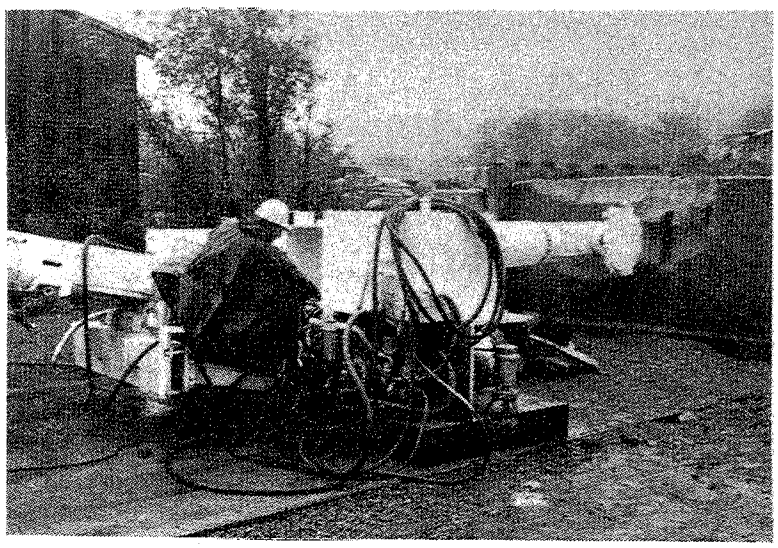

Figure 13. WJA roadheader at artificial oil shale face.

4.2 WJA Roadheader For Factory Cutting Tests

A standard size Alpine roadheader was modified to serve as a test bed and tool carrier for WJA cutting tests. The test roadheader was especially designed for changing of all parameters required for design of a new, high-production WJA cutting system.

4.2.1 Hydraulic Cutter Head Drive

The cutter head is driven via a speed reducer by a hydraulic motor. The hydraulic motor is powered by an axial-piston pump with variable flow volume and pressure. With this design cutter head, rotation (i.e. peripheral bit tip speed) and cutting force can be varied over a large range.

4.2.2 Cutter Boom

The telescoping "sumping" cutter boom is hydraulically actuated in order to vary the WJA cutter head's penetration force and speed. Furthermore, the slewing (arcing) and shearing speed and force of the boom can be changed via a variable-volume, pressure-adjusted hydraulic pump.

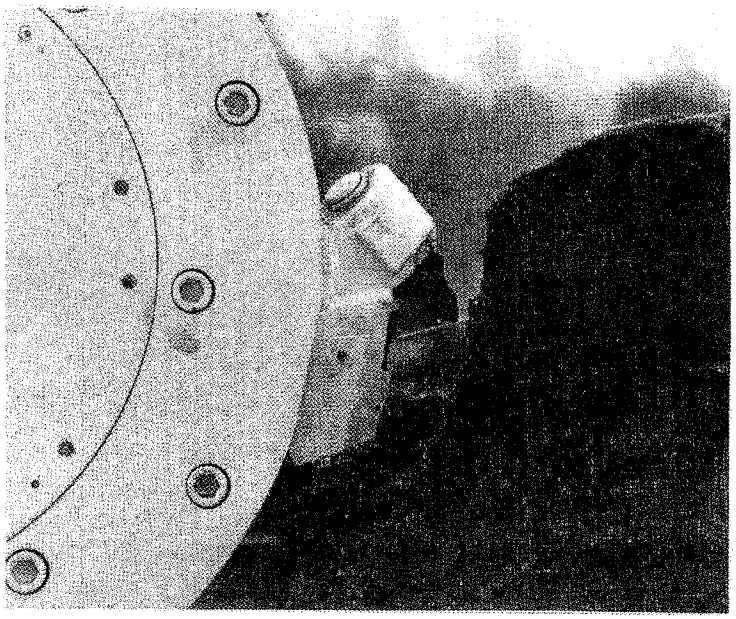

Figure 14. WJA bit (pick) cutting oil shale.

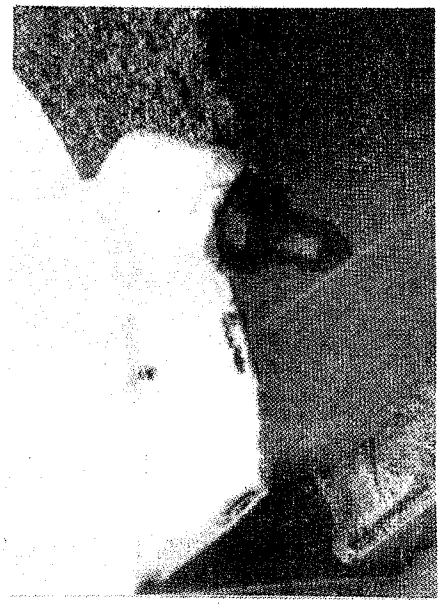

Figure 15. Cutter bit (pick) with water-jet.

4.3 High Pressure Water (HPW) System

The HPW system consists of the following components:

4.3.1 Pump

A triplex plunger pump will supply the WJA test miner. The pump has a flow volume of 227 l/min. (60 GPM) at a pressure of 414 bar (6,000 psi). By equipping the pump with smaller (ø 19 mm; 3/4") diameter pistons, its pressure can be raised to 1379 bar (20,000 psi) at a flow rate of 37.85 l/min. (10 GPM).

4.3.2 Nozzles

Alpine will use nozzles with different diameters suitable for water pressures ranging from 207 to 1,380 bar (3,000 to 20,000 psi). Depending on the water pressure the nozzles will consist of tungsten-carbide and artificial sapphire. Their diameters will range from 0.4 mm (0.0158") to 1.0 mm (0.0394").

4.3.3 Water Phasing System

The WJA roadheader for cutting tests on the artificial oil shale face has a non-phased rotary union. The second roadheader for in-mine testing at the Colony shale oil project will be equipped with a water-phasing-system to reduce fluid energy consumption and provide a safe working area. Only the tools that are actually in contact with the rock will be augmented with a high-pressure-water jet.

5.0 WATER-JET-ASSISTED (WJA) CUTTING versus HYDRO-DEMOLITION (WATER JETTING)

Fragmentation of rock, minerals, and concrete with water jetting (hydro-demolition) is (1) energy inefficient and (2) expensive ($/m^3) when compared to mechanical cutting. For example, a European-made, high-pressure (1,000 bar; 14,500 psi) hydro-demolition machine (Woma, 1989) has a concrete removal rate of up to 1m^3/h (1.3 yd^3/h).

A transverse "ripper" roadheader-type cutter boom (Parr, 1985), powered by a 123 kW (165 hp) motor, excavated concrete of avg. 38 MPa (5,500 psi) uniaxial compressive strength (UCS) at an average rate of 9.62 m^3/h (12.5 yd^3/h) and a specific energy consumption of 12.8 kW.h/m^3 (13.2 hp.h/yd^3). The following data are from 26 hydro-demolition projects (Aquajet, 1989).

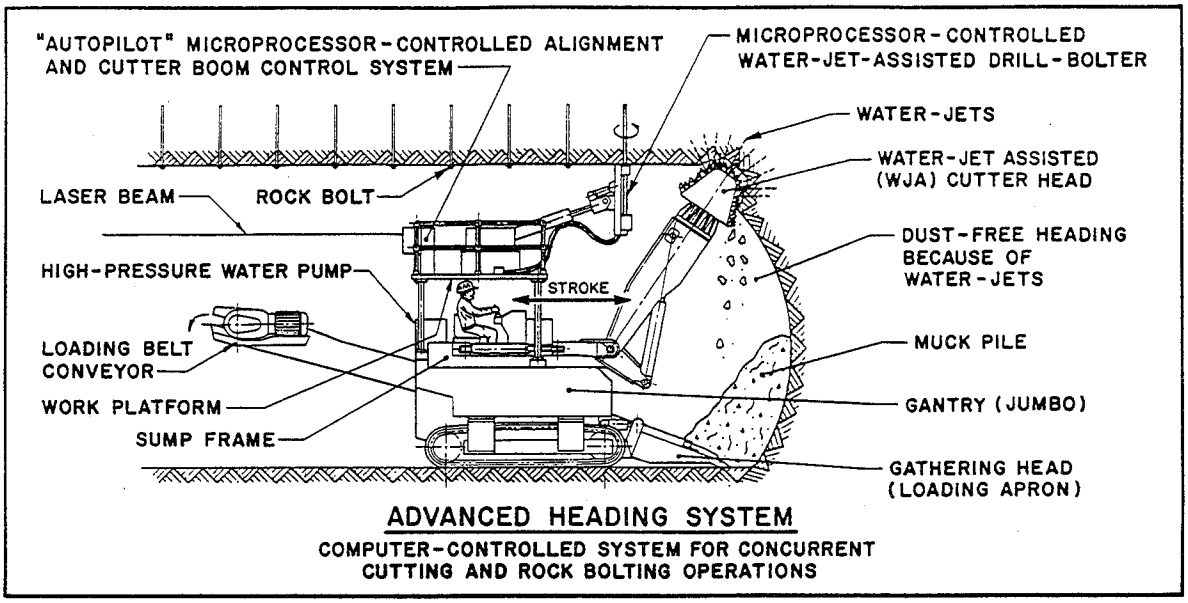

Figure 16. Oil shale mining machine of the future: Alpine Equipment Corporation's advanced, water-jet-assisted heading system incorporating computer-control for concurrent cutting and rock bolting for single-pass excavation of large cross-section entries and rooms.

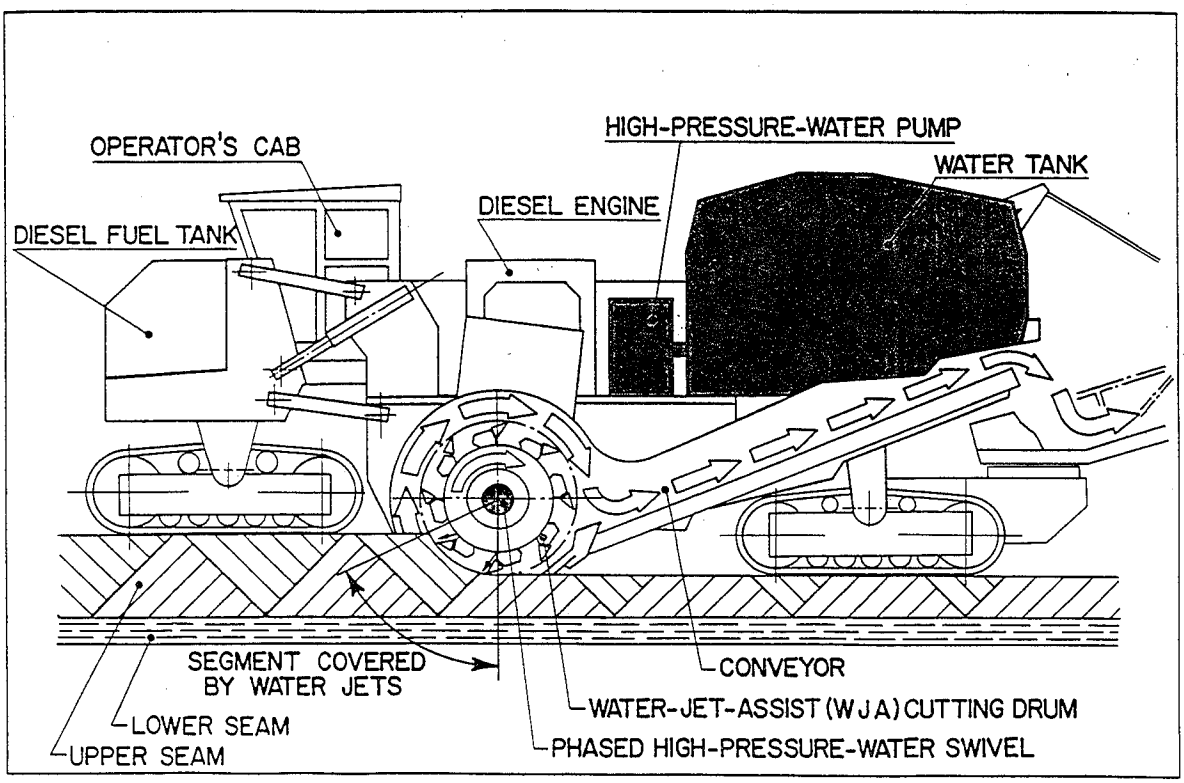

Figure 17. Conceptual layout of WJA surface miner for automated, selective mining of two different seams.

A hydro-demolisher powered by a much larger 325 kW (450 hp) engine averaged 0.62 m^3/h (0.81 yd^3/h) of concrete removal at a specific energy consumption of 540 kW.h/m^3 (557 hp.h/yd^3).

This comparison shows that mechanical cutting is about 42 times as energy efficient as water jetting. This is the reason why water jetting (hydro-demolition) is not used for high production applications such as mining and road milling (planing). Water jetting is only employed for "dental work" such as removal of deteriorated concrete underneath rebar as found on many bridge deck rehabilitation projects.

6.0 FUTURE PLANS

Based on the findings of the factory cutting tests, Alpine will design and manufacture the optimum WJA cutting system for in-mine tests in Phase III of the project.

Data from the underground WJA cutting tests in Phase III will be recorded and evaluated. This field data will be used for development and commercialization of the WJA machines for mining and construction applications.

We envision the following progressions and applications for this new WJA cutting system.

* Development of innovative cutting tools, most likely water-jet-assisted PDC bits, of the radial (flat) style, for the most energy-efficient cutting at minimum dust levels with the lowest possible water flow and pressure.

* Optimization of rock size for retorting purposes.

* Testing of novel WJA tools, that are not presently available, for mining of harder rock.

* Development and in-mine testing of a WJA cutting boom for future incorporation in a gantry-type mining machine for single-pass or twin-pass excavation of large cross-sectional 18.3 m x 7.6 m (60 ft. x 25 ft.) entries in oil shale.

* Using the miner's HPW system to augment a WJA drill bolter.

* Using the test data for design of a fully automated, microprocessor-controlled WJA machine for concurrent cutting and rock bolting (see Figure 16). Computer systems for roadheader control are already available from several manufacturers (Weber et al., 1985). Such controls for selective excavation are already employed in potash mines and in longwall installations in coal mines (Kogelmann et al., 1986).

* The potential exists to equip a surface miner or a road milling machine with a WJA cutting system.

This project's goal is to decrease the cost of oil shale mining and lower the overall cost of synthetic fuel derived from oil shale. The potential exists for synthetic fuel costs to be competitive with petroleum-based products by using WJA mining machines to decrease the cost of extraction, in combination with lower retorting and refining cost.

7.0 REFERENCES

1. Virgona, J. E. and Thimons, E. D.,"DOE/USBM Will Study Water-Jet-Assist for Mechanized Mining of Oil Shale," Engineering & Mining Journal, September 1988, pp. 70-71.

2. McNary, R.P., Blair, J.R., Novak, D.D., and Johnson, D.L., "Augmentation of a Mining Machine with a High-Pressure Jet," Proceedings of Third International Symposium on Jet Cutting Technology," Chicago, Illinois, May 11-13, 1976, pp. D2-13 through D2-20.

3. Kogelmann, W.J. and Thimons, E.D., "Safer and More Productive Mining with a Computer-Controlled Water-Jet-Assisted Longwall Shearer," Proceedings of the Second International Conference on Innovative Mining Systems, The Pennsylvania State University, State College, Pennsylvania, October 27-29, 1986, pp. 56-68.

4. Morris, A.H., Collins, R.D., Swoboda, and Kleinert," Round Table Discussion B, Boom Headers," Proceedings of Symposium on Roadway Drivage Techniques in the Coal Mines of the European Community, Luxembourg, November 9-10, 1983, pp. 336-338.

5. Chadwick, J.R., "Continuous Miners Mine More Than Coal," World Mining, September 1983, p. 42.

6. Schenck, G.H.K., "Boom-Type Miners and Roadheaders," Underground Mining Methods Handbook (W.A. Hustrulid, Editor), Chapter 14, New York, New York, 1982, pp. 1160-1168.

7. Frenyo, P., "Erfahrungen mit Teilschnitt-Vortriebsmaschinen," Glückauf, June 20, 1974, pp. 465-470.

8. Mertens, V., "Stand und Entwicklung des Maschinellen Streckenvortriebs im Steinkohlenbergbau," Glückauf, August 22, 1985, pp. 1199-1212.

9. Wilcox, J.C. and Lehman, R.D., "Inter-Seam Slope Construction at The Florence Mining Company," Paper presented at 1988 Joint Meeting -- PCMIA/SME Pittsburgh Section, November 4, 1988, p. 2.

10. Pearse, G., "Cutter Boom Tunnelling Machines," World Tunnelling, March 1988, pp. 81-91.

11. Farmer, I., "Mechanical Excavation of Rock," Report to Construction Industry Research and Information Association, London, England, 1986.

12. Crookston, R.D., Weiss, D.A., and Weakly, L.A., "Mechanical and Conventional Excavating Experience in Oil Shale Shafts and Tunnels," Proceedings of 1983 RETC, pp. 817-833, 1983.

13. "Record Drill Bit Footage in Colorado Oil Shales," Engineering & Mining Journal (E&MJ), March 1989, p. 77.

14. Plis, M.N., Wingquist, C.F., and Roepke, W.W., "Preliminary Evaluation of the Relationship of Bit Wear to Cutting Distance, Forces and Dust Using Selected Commercial and Experimental Coal - and Rock-Cutting Tools," Report of Investigation No. R19193, U.S. Bureau of Mines, 1988, pp. 1-63.

15. Clark, I.D., "PCD Drill Bits and Their Applications in the Mining Industry," Indiaqua, No. 51/3, 1988, pp. 123-128.

16. "Concrete Rehabilitation with High Pressure Water," International Construction, January 1989, p. 63.

17. Parr, W.E., "Mining Tool Adapted to Concrete Removal for Lock Wall Rehabilitation Project," The REMR Bulletin, Vol. 2, No. 1, March 1985, p. 3.

18. "Project Summary," Aquajet Systems AB, Sweden, April 1989.

19. Weber, K.H., and Kogelmann, W.J., "Monitoring and Control of Boom-Type Roadheaders," German Mining, No. 3, 1985, pp. 166-172.

5th American Water Jet Conference
August 29 - 31, 1989: Toronto, Canada

Paper / Communication 3

DEVELOPMENT OF WATER JETTING EQUIPMENT FOR EXCAVATING LARGE-DIAMETER BOREHOLES IN GRANITE

R.J. Puchala AND B.M. Hawrylewicz
Indescor Hydrodynamics Inc., Concord, Ontario, Canada

B.H. Kjartanson AND M.N. Gray
Atomic Energy of Canada Limited, Pinawa, Manitoba, Canada

ABSTRACT: Experiments pertinent to the Canadian nuclear fuel waste disposal concept are to be carried out in situ in granitic rock at Atomic Energy of Canada Limited's Underground Research Laboratory (URL). Two of these experiments require 1240-mm-diameter, 5-m-deep boreholes to be excavated in the floors of rooms in the URL. For this purpose, a coring tehcnique using high-pressure rotary water jet rock slotting was developed.
The coring rig incorporates a rotary, double water jet nozzle to cut a vertical, circular slot, the outside diameter of which equals the required borehole diameter. The nozzle, which operates at a water pressure of 135 MPa and a water flow rate of 50 L/min, is mounted on coring sections rotating in the vertical slot.
The stages of development of the coring rig have involved nozzle testing and optimization, shop tests in large granite blocks and field trials at the URL. This work has shown that coring production rates vary significantly from 190 to 250 mm/h for granite blocks and surface outcrops to 30 to 58 mm/h for boreholes drilled in the floor of an underground room. The major factor influencing rates is believed to be the in situ stresses and confinement of the granite; mineralogy and fabric are thought to play a secondary role. The development of drilling procedures to excavate a large-diameter borehole to a depth of 5 m includes the use of an overlapping 96-mm-diameter sump hole to collect and remove the cuttings and the staged removal of core as the hole is advanced. The present development of the technology should allow completion of a borehole at depth in the URL in about twenty to thirty 12-h shifts.

RÉSUMÉ : Des expériences sur la méthode canadienne d'élimination des résidus de combustible nucléaire seront menées sur place dans la roche granitique au Laboratoire de recherche souterrain (LRS) de l'Energie atomique du Canada Limitée. Deux de ces expériences nécessitent l'excavation de trous de sonde de 1 240 mm de diamètre et de 5 m de profondeur dans les planchers des salles du LRS. A cette fin, une technique de carottage reposant sur le découpage de la roche au moyen de jets d'eau rotatifs à haute pression a été mise au point.
L'installation de carottage comprend une buse rotative à deux jets d'eau pour faire des coupes circulaires à la verticale de diamètre extérieur égal au diamètre requis du trou de sonde. La buse qui admet des pressions d'eau de 135 MPa et des débits d'eau de 50 L/min est montée sur des sections de carottage tournant dans le trait vertical.
Les étapes de mise au point de l'installation de carottage sont au nombre de trois : essai et optimisation de la buse, essais en atelier sur de gros blocs de granit et essais sur le terrain au LRS. Ce travail a révélé que les taux de production par carottage varient considérablement entre 190 à 250 mm/h dans les blocs de granit et les affleurements et 30 à 58 mm/h dans les trous de sonde forés dans le plancher d'une salle souterraine. Le facteur déterminant pour les taux serait l'ensemble des contraintes sur place et le confinement du granit; la minéralogie et la fabrique joueraient un rôle secondaire. L'élaboration de méthodes de forage pour excaver un trou de sonde de grand diamètre à une profondeur de 5 m comprennent l'aménagement d'un trou à boue coïncidant de 96 mm de diamètre pour recueillir et évacuer les déblais, et l'enlèvement par étapes de la carotte à mesure que le trou s'approfondit. L'état actuel de la technologie devrait permettre la réalisation d'un trou de sonde en profondeur dans le LRS après vingt à trente quarts de 12 h environ.

Organized and Sponsored by the National Research Council of Canada and the U.S. Water Jet Technology Association.

1.0 INTRODUCTION

The Canadian concept for nuclear fuel waste disposal proposes that the waste be emplaced in a vault located at a depth of 500 to 1000 m in stable plutonic rock of the Canadian Shield. The general configuration of the reference vault is illustrated in Figure 1. The expected radionuclide release mechanism is for groundwater to penetrate the waste containers, leach out the radionuclides and slowly transport them back to the surface. The potential groundwater flow paths from the containers to the biosphere include the excavations (rooms, tunnels and shafts), or, when these are satisfactorily backfilled and sealed, excavation-disturbed zones surrounding the excavations. Therefore, excavation methods that limit damage to the rock are preferred.

Two experiments related to the Canadian nuclear fuel waste disposal concept require full scale emplacement boreholes (1240-mm-diameter by 5-m-deep) to be excavated in the floors of rooms in Atomic Energy of Canada Limited's Underground Research Laboratory (URL) (Kjartanson, B.H. and Gray, M.N., 1987). Besides being able to blind drill relatively large diameter boreholes, the drilling equipment had to conform to the URL operating conditions, particularly in terms of size and mass limitations.

After a review of potential shaft drilling, drilling/reaming and coring techniques, a coring technique that is an extension of high-pressure rotary water jet rock slotting (Hawrylewicz, B.M. et al., 1988) was selected for development. Apparent advantages of the water jet technique over the other methods include: the water jet cutting nozzles are longer lived and much less expensive to replace than conventional cutting tools and bits, the equipment is relatively light and readily transportable, and high thrust forces are not required for the water jet cutting nozzles. Moreover, the transient high-pressure water forces should cause less disturbance to the surrounding rock than blasting, and perhaps even less disturbance than the vibrations and abrasive forces of conventional drilling machines. Also important was the potential longer-term benefit of developing a new rock cutting technology with possible applications to other URL experiments.

Deep slotting in Stanstead granite has been successfully carried out on a semi-industrial scale using a double water jet rotary nozzle (Hawrylewicz, B.M. et. al., 1988). In this case, the prototype rock cutter was able to cut a straight, 5-m-long, 3.4-m-deep and about 44-mm-wide slot, with an effective exposure rate of 1.13 m^2/h at 135 MPa water pressure and 55 L/min water flow. These results indicated that a rotary double water jet nozzle could cut the vertical, circular slot needed for drilling the large-diameter emplacement boreholes in Lac du Bonnet granite. Incorporation of a horizontal notching or undercutting jet would facilitate core breakage. The properties of the Lac du Bonnet granite are shown in Table 1.

A coring rig using high-pressure water jets has been designed and built. Laboratory, surface and underground tests have been carried out in the course of the technology development. The laboratory and surface drilling trials are described by Kjartanson, B.H. et al. (1989).

This paper describes the development of the nozzles and the coring rig hardware. The results of underground drilling trials are presented, and compared with those from surface and laboratory tests.

2.0 NOZZLE DEVELOPMENT

The nozzle development program involved laboratory slotting tests on small samples of Lac du Bonnet granite.

The tests allowed

1. Selection of the nozzle designs;
2. Selection of the range of cutting parameters that yield the required slot width and the undercut depth; and
3. Estimation of coring and undercutting productivity.

The slotting tests were carried out with an experimental rock cutter described by Hawrylewicz et al. (1988). The cutter operated at a water pressure of 125 to 135 MPa and a water flow rate up to 43 L/min. The rock cutter allowed traversing along a straight line, downward incrementing and rotating motions of the tested nozzle.

The following types of nozzles were tested:

1. Slotting nozzles: abrasive rotary double jet (AD6) and water rotary double jet (WD7 and WD8) (see Figure 2a).

2. Undercutting nozzles: abrasive (A1, A2) and water single jet (W3) (see Figure 2b).

The jet equivalent diameter for the tested nozzles is given in Tables 2 and 3, while the positions of the tungsten carbide jet orifices relative to the axis of the nozzle are shown in Figure 2. The abrasive jet nozzles were constructed with water jet orifices located in the steel nozzle body and secondary carbide orifices positioned so that the water jet is mixed with abrasives, focussed in the secondary orifices and ejected at the angles shown in Figure 2.

The undercutting, non-rotary nozzles were traversed along a rock sample at a constant stand-off distance of about 5 mm. Single and multiple passes were performed. The rotary slotting nozzles were traversed along the rock samples and incremented down at about 5 to 7 mm after each pass. Multiple passes were performed in a vertical plane.

The Lac du Bonnet granite test samples comprised blocks (B) from the surface or cores (C) from different underground locations. Block samples B1 and B2 were positioned on the concrete floor and cut by the jets either from the top or from the side. Core samples C1, C4 and C5 were cast into a concrete block. Three cores in one concrete block were cut at a time. Results of the tests with the corresponding nozzle and sample data specifications are shown in Table 2 (undercutting tests) and Table 3 (slotting tests).

The undercutting tests showed that the abrasive jet can cut a slot 100 to 120 mm deep without the nozzle being inserted into the slot. The shape of the slot is, however, irregular along the cutting plane. The cross-section of the slot tapers. The required depth of the undercut, 100- 120 mm, was achieved by traversing the nozzle with the speed of 700 mm/min approximately 12 to 16 times. The water jet was not able to cut a slot deeper than 90 mm. Thus the undercutting abrasive jet, with superior performance in these tests, was the preferred choice for cutting undercut slots in the core.

Both the abrasive and the water rotary double jet nozzles could cut slots in the Lac du Bonnet granite to the required 40- to 50-mm width. Under the same test conditions water jet nozzles WD7 and WD8 produced similar newly opened surface area and slot width. The water rotary jets were able to slot the Lac du Bonnet granite four to five times faster than the abrasive rotary jet. Several deficiencies in the abrasive delivery systems, which influenced the cutting rate were noticed. It was concluded that the abrasive rotary slotting technique was not sufficiently well developed and therefore preference was given to the rotary water jets for use in the coring operation.

The fabric and mineralogy of the test samples affected the rotary water jet slotting rate and slot geometry. For example, the width and depth of slots cut in core sample C1, which contained quartz inclusions, were smaller than slots cut in samples C4 and C5 using essentially the same cutting parameters. The presence of pegmatite veins in the block samples did not significantly influence the width and depth of the cut, but the cuttings were coarser grained.

Three types of nozzles, rotary double water jet coring, rotary double abrasive jet coring and abrasive undercutting were designed for use and further evaluation on the coring rig. The tests with nozzles WD7 and WD8 showed no influence of orifice angle on the cutting rate. Moreover, there was no apparent advantage in having the orifices asymmetrical, which makes nozzle fabrication more difficult and tends to unbalance the nozzle. Thus nozzle WC10 (Figure 3) was designed with symmetrical water jet orifices at an angle of 25° from the nozzle axis. This nozzle was supplemented by a similar type nozzle WC11 (Figure 3) with wider angled orifices. The shape and operational design of the abrasive slotting and undercutting nozzles have been guided by geometric considerations and the cutting parameters required to be used on the coring rig. Nozzles AC5 and AU3 (Figure 3) have thus evolved from the test nozzles AD6 and A1, respectively. The angle of the abrasive undercutting nozzle orifice has no influence on cutting rate but rather is selected to give a dipping slot to facilitate the emplacement of expanding cement grout. The rotary abrasive jet coring nozzle AC5 was to serve as a backup and was only to be used if considered necessary.

3.0 CORING RIG DEVELOPMENT

The design of the drilling system required the selection or development of a high-pressure pump unit, coring rig, hydraulic power pack and core removal equipment.

The high-pressure pump unit selected consisted of a triplex plunger pump powered by a 250-HP electric motor, low-pressure water filters, a hydraulic water accumulator and electrical controls. The pump is capable of delivering up to 56 L/min of water at a maximum pressure of 140 MPa.

The coring rig, shown schematically in Figure 4, consists of a three-piece static frame, a carriage with a rotating drum and coring sections. The frame can be anchored to rock or a concrete floor. Attached to each coring section are two rotary slotting lances, two non-rotating undercutting lances and a suction pipe for cuttings removal. The rotary slotting lances consist of a high-pressure rotary coupling rotated by a pneumatic motor, high-pressure water pipe sections coupled together, and a double water jet, or double abrasive jet nozzle. The undercutting lance ends in a single non-rotary abrasive jet nozzle. The rotary and undercutting lances are connected to the high-pressure rotary joint with high-pressure flexible hoses. The supply of water to the lances is controlled by manual on-off valves. Only one slotting nozzle or two undercutting nozzles can work at one time. The suction pipe is joined to a pneumatic diaphragm suction pump mounted on the drum. Abrasives are stored in the hopper installed inside the drum. The abrasives can be delivered to any of the abrasive jet nozzles through hoses and on-off valves.

The coring sections are bolted to the drum and are successively bolted together (to a maximum of four) as the borehole is advanced, so that the rotary motion of the drum is transfered directly to the coring sections. The drum is rotated in relation to the carriage by a hydraulic motor and chain drive. The carriage can be moved vertically by power screws driven by a directly coupled hydraulic motor. During the coring mode, the step-down motion is executed by power screws driven through the gear drive by the second hydraulic motor. Both power screws are connected by a chain drive at the top of the frame. The carriage is guided by four lineal bearings mounted to the side frames. All high-pressure pipes and the suction pipe run through the coring sections to the nozzles fixed at the bottom end. The vertical carriage motion and drum rotation can be adjusted by the hydraulic controls installed on the coring rig; the configuration is shown on the hydraulic schematic (see Figure 5).

The rotation rate of the rotary lances, and the suction pump speed can be regulated by pneumatic controls installed inside the drum. The supply of abrasives to the nozzles is induced by a vacuum created in an abrasive nozzle. A pneumatic vibrator installed on the hopper stimulates the smooth flow of abrasives to the nozzles.

4.0 EQUIPMENT TESTING

The following stages of equipment testing have been carried out:

- Laboratory coring and undercutting tests on large granite blocks,
- Surface trials at the URL, and
- Underground trials at the URL.

4.1 Laboratory Tests and Surface Trials

The laboratory tests were carried out on two samples of medium- to coarse-grained, pink porphyritic Lac du Bonnet granite containing pegmatite veins. Both samples were 1.5 m wide, 2 m long, and 0.6 m high. With the coring rig anchored to each sample, water and abrasive jet rotary nozzles were tested by coring through the samples. Two abrasive undercutting nozzles were used to cut a slot in each core.

The surface trials were carried out on an outcrop at the URL site. The rock was generally a pink, coarse-grained porphyritic granite, with discontinuous granitic pegmatite zones, 0.2 to 0.4 m thick. Sporadic quartz veins, generally less than 15 mm thick, were associated with these pegmatites. Coring was performed using the same water jet rotary nozzle used in the laboratory tests. These laboratory tests and surface trials are described in more detail by Kjartanson, B.H. et al. (1989).

The laboratory tests and surface trials indicated that 1240-mm-diameter boreholes can be cored at a rate of about 190 to 250 mm/h (see Table 4). This rate was achieved using double rotary water jets operating at 135 MPa water pressure and 50 L/min water flow. Because of field operational delays and difficulties with cuttings removal and occasional jamming of the coring sections in the slot, the actual advance rates of the boreholes were much slower than the coring rates would indicate. In 8 days the first hole was advanced to a depth of 1.74 m whereas the second hole was drilled to a depth of 2.57 m. The increase in the rate of advancement of the second hole reflects the effects of increasing experience with the drilling equipment and modifications, particularly in terms of cuttings removal, to improve the rate of borehole advance.

To overcome the difficulty of removing gravel-sized cuttings, which the original system could not handle, a revised cuttings removal system was developed to core the second borehole. The rig was positioned so that the slot would overlap a 6-m-deep, 96-mm-diameter pilot hole used to define the rock lithology, hydrogeology and fractures in the large-diameter borehole location. The cuttings removal system comprised a 50-mm-diameter, 5.5-m-long pipe down the pilot (sump) hole, which was connected to a sand and gravel trap, in turn connected to a 50-mm suction diaphragm pump. This system performed well.

Experience from the surface trials indicated that it was preferable to remove the core in stages as the hole is advanced rather than to attempt to slot the entire 5 m before removing the core. This option not only allows access to the base of the slot as the hole is proceeding, even at depth, but also minimizes potential problems with cuttings removal and jamming of the coring sections. The preferred drilling sequence is illustrated in Figure 6.

The laboratory and surface trials also indicated that an 80- to 100-mm deep undercut slot can be cut in the core in about 35 min by two abrasive jets at 135 MPa water pressure and 50 L/min water flow with a garnet abrasive feed rate of about 3 kg/min. Moreover, an 80-mm-deep and 8-mm-wide undercut slot, when filled with expanding cement grout, will permit core breakage.

4.2 Underground Trials

The last stage of development of the emplacement borehole drilling equipment was performed at the URL in a test room located 240 m underground. Between 0.3 and 0.5 m of concrete was placed on the uneven rock floor to provide a level working base. The equipment configuration and locations of the boreholes in the test room are shown in Figure 7.

Two 96-mm-diameter, 6-m-deep holes were previously drilled in the floor of the test room to define rock lithology, hydrogeology and fractures in the large-diameter borehole locations. The rock type encountered in both holes was generally homogeneous, medium-grained, slightly pink porphyroblastic granite. Pegmatitic leucocratic zones were encountered below 3.4 m in EPH1 (closest to the end of the room) and 4.0 m in EPH2. The top 0.2 to 0.5 m of rock was blast-fractured. As on the surface, each 96-mm-diameter hole was used as a sump for the removal of cuttings.

The underground trials involved drilling one large-diameter borehole to a depth of 5.1 m and another to a depth of 2.4 m. The drilling technique and sequence for UG1, closest to the end of the room, largely followed experience gained in the surface trials. After setting up, levelling and anchoring the coring rig to the concrete floor so that the slot would overlap the 96-mm- diameter sump hole, the cuttings removal system was installed and the concrete floor was cored. After removal of the concrete plug, coring to a depth of 1.33 m below the floor surface was carried out. To break out the granite core, an undercut slot was cut at the base of the core stub and expanding cement grout emplaced. When this technique failed to break the core, a revised technique involving the placement of expanding cement grout into an array of 32-mm-diameter holes drilled vertically into the core stub was used. This technique successfully broke the core into small and manageable pieces overnight (within 18 hours). The core pieces were then lifted from the hole using an air-powered winch and a block mounted in the roof of the room directly above the hole. This technique allowed the coring rig to remain in place while removing the core. Removal of the core and preparation for further slotting usually took about 4 hours. The borehole was advanced to a depth of 5.1 m, with the core being removed about every one metre. Undercut slots were not required to break the core when using the vertical array of holes. The second hole, UG2, was drilled to a depth of 2.4 m using techniques developed in the first hole. During the underground test, only rotary water jets were used for coring.

Unlike the surface test, underground coring could not be carried out continuously. For UG1, the slot had to be reamed every 30 to 40 mm, even at a very slow coring rate. Both the width of the slot and the stand-off distance between the nozzle and the bottom of the slot were

reduced, thus inhibiting downward advancement of the coring lance. For UG2, even though the coring rate could not be increased above that used for UG1, much less reaming was required, with unimpeded coring runs of 100 to 170 mm being common. The cutting parameters used and coring rates achieved for the underground trials are compiled in Table 4.

The first hole was drilled to a depth of 5.1 m in 53 days, while the second hole was advanced to a depth of 2.4 m in 14 days. The relatively long duration to drill the first hole included underground operational delays, equipment debugging and the development of coring and core removal techologies. The rate of advancement of the second hole is more reflective of the expected production rate of the system as developed to date. Moreover, as noted above, much more slot reaming was required for the first hole than the second. This is further discussed in the next section.

The average life of the water jet slotting nozzles was about 25 to 35 h. The use of tungsten carbide inserts in these nozzles has increased the nozzle life by about five to six times.

During the underground trials, only one undercut slot was cut in the granite core, as the revised core breaking procedure with vertically drilled holes did not require undercut slots. An average undercut slot depth of about 120 mm and width of about 8 mm was achieved after 16 passes of two abrasive jets around the core. About 1 m/min traverse velocity of the jets and about 3 kg/min of garnet abrasives were used for cutting this slot.

5.0 DISCUSSION

Whilst the effects of mineralogy and fabric of the granite may partly account for the faster coring rate achieved in the surface trials than underground, a major effect is believed to be the influence of rock stresses and confinement of the underground granite. The in situ stresses vary with depth and location within the batholith and the position of the holes in the underground test room. The coring rate for the underground trials was four to eight times slower than the rate for the surface trials. Moreover, the coring rate at the different borehole locations in the underground room was probably affected by different stress distributions in the floor close to the end of the room (UG1) and away from end effects (UG2). In addition, the increased rate of penetration in the second hole could be attributed to the higher jet power and differences in the geometry of nozzles WC10 and WC11.

Further indication of the influence of in situ stresses and confinement was found in cutting trials conducted on granite core samples taken from the large-diameter boreholes (Onagi et al., 1989). The samples were set up beneath the coring rig and cut with the rotary double water jet nozzle. Cutting rates five to six times higher were achieved in the same rock in an unconfined state than in place.

Based on the results of these trials, a mechanism through which water jets cut crystalline rocks, such as granite, may be hypothesized. Near the ground surface and in unconfined blocks, the grain structure may be more open than in the confined, stressed state. Moreover, and probably more importantly, the destressed rock would contain microcracks. It appears necessary for a water jet to be able to penetrate microcracks or the grain structure to effectively cut slots in granite. In confined granite, particularly in areas of high stress concentrations, the cutting action might be a much more surficial, localized process, without significant penetration into the grain structure. Thus, slower productivity could be expected in areas where in situ stresses and stress concentration effects are more severe.

The water jet nozzles, bottom part of the high-pressure rotating pipe and the bottom pipe support were exposed to the abrasive action of the rock cuttings and water during coring. Deterioration of the tungsten carbide orifices also occurred because of impurities in the high-pressure water supply. This abrasion and wear required replacement of the rotary nozzle and bushing in the bottom pipe support every 25 to 35 h of cutting; three to four nozzles were needed to finish one 5-m-deep borehole.

The coring sections were originally designed to cut a 5-m-deep slot without removing the core. The underground trials have shown that removing the core in stages as the borehole is advanced is preferred. This allows for the coring sections to be redesigned, which helps eliminate jamming during coring and also reduces the need to ream the slot. A possible redesign would involve a simplified lance support structure, about one metre long, connected to the end of a segmented hollow structural member. The segmented structural member would, in turn, connect to the drum. The lance could be stabilized along the length of the hollow structural member with cantilevered horizontal supports with bushings.

6.0 CONCLUSIONS

The underground trials proved that 1240-mm-diameter boreholes can be blind drilled in granite using water jet coring technology. The following conclusions can be made at the current stage of development:

1. Water jets can be used to core 1240-mm-diameter, 5-m-deep holes underground in the URL at an average coring rate of 30 to 58 mm/h when using double rotary water jets operating at a water pressure of 135 MPa and a flow rate of up to 56 L/min. This productivity rate should allow completion of a borehole at depth in the URL in about twenty to thirty, 12-h shifts.

2. The preferred drilling sequence is to remove the core in stages as the borehole is advanced. Core can be broken every 1 to 1.3 m by emplacing expanding cement grout into a pattern of 32-mm-diameter holes drilled vertically into the core.

3. Coring productivity could be enhanced by redesigning the coring sections to limit jamming and reduce the need for reaming the slot. With the exception of further optimizing the angle between the orifices, the rotary double water jet nozzle has been pushed to its limit of productivity with the existing water pressures and flows. In view of the difficulties in cutting stressed rock with water jets, there may be merit in pursuing the development of abrasive jets.

4. The coring rig and associated equipment selection allows for fast and easy adjustment of coring parameters, such as nozzle speed and advance rate, and a fast nozzle replacement procedure. The rotary nozzle configuration should be reviewed to assess if abrasive wear of the nozzle body, orifices and the pipe supports and bushings can be reduced.

5. The penetration rate of rotary double water jets appears to be sensitive to in situ rock stresses and confinement of the granite. Higher cutting rates were achieved in granite at the ground surface and in unconfined blocks of granite than in confined, stressed granite at depth. Mineralogy and fabric also appear to influence the cutting rate, but to a lesser extent.

ACKNOWLEDGEMENTS

The assistance provided by Messrs. D. Onagi, C. Kohle, and D. Winchester of AECL and Mr. A. Hampton of J.S. Redpath Ltd. during the URL field trials is gratefully acknowledged.

REFERENCES

1. Kjartanson, B.H. and Gray, M.N.: "Buffer/Container Experiments in the Underground Research Laboratory." In: Proceedings of the 40th Canadian Geotechnical Conference. Regina, Saskatchewan, Canada, October 1987, p. 275-283.

2. Hawrylewicz, B., Vijay, M.M., Remisz, J. and Paquette, N.: "Design and Testing of a Rock Slotter for Mining and Quarrying Applications." In: Proceedings of the 9th Int. Symp. on Jet Cutting Technology, Sendai, Japan 4-6 Oct. 1988 BHRA, England.

3. Katsube, T.J. and Hume, J.P.: "Geotechnical Studies at Whiteshell Research Area (RA-3)." CANMET. Mining Research Divisional Report MRL 87-52, 1987.

4. Kjartanson, B.H., Gray, M.N. Puchala, R.J., and Hawrylewicz, B.M.: "Excavating Large-Diameter Boreholes in Granite with High Pressure Water Jetting." In: Proceedings IMM Shaft Engineering Conference, Harrogate, England, June 5-7, 1989.

5. Onagi, D., Kjartanson, B.H., Hampton, A. and Winchester, R.: "Underground Water Jet Drilling Trials at the URL." Atomic Energy of Canada Limited Technical Record, in progress.

Table 1. Mineralogy and Mechanical Properties of Lac du Bonnet Granite (after Katsube and Hume, 1987)

Average Mineralogy	quartz - 31% ± 4% plagioclase - 38% ± 6% microline - 27% ± 7% muscovite - 0.5% ± 0.3% biotite - - 3.5% ± 1.5% others - 0.5% ± 0.5%	
Bulk Density (Mg/m^3)	2.63 ± 0.05	
Compressive Strength* (MPa)		
	Pink (to ~ 260-m depth)	
	range	134-248
	mean	200
	Grey (below ~ 260-m depth)	
	range	147-198
	mean	167

* Values representative of Undergrounnd Research Laboratory site

Table 2. Undercutting Test Results

#	Nozzle Type	Jet Equiv Dia.	Water Pressure	Water Flow	Jet Power	Abrasive Nozzle Diameter	Traverse Velocity	No. of Passes	Avg. Depth Per Pass	Average Width	Newly Open Surface	Removal Rate	Specific Energy
		mm	MPa	L/min	kW	mm	cm/min		mm	mm	m^2/h	cm^3/min	kJ/cm^3
B1/1.1	A2	1.07	125.000	23.48	49.01	3.00	71.12	4.00	14.75	6.00	0.63	63.07	46.63
B1/1.2	A2	1.07	138.000	24.67	54.11	3.00	71.12	8.00	11.25	6.00	0.48	48.10	67.49
B1/1.3	A2	1.07	125.000	23.48	49.01	3.00	71.12	12.00	8.75	6.00	0.37	37.41	78.60
B1/1.4	A2	1.07	120.000	23.00	47.05	3.00	71.12	16.00	7.19	6.00	0.31	30.73	91.86
B1/2.1	A2	1.07	115.000	22.52	45.09	3.10	71.12	16.00	5.63	6.00	0.24	24.05	112.48
B1/3.1	A2	1.07	137.500	24.62	53.91	3.10	137.00	10.00	5.50	5.00	0.45	37.75	85.68
B1/3.2	A2	1.07	137.500	24.62	53.91	3.10	137.00	20.00	4.00	5.00	0.33	27.45	117.82
B1/3.3	A2	1.07	137.500	24.62	53.91	3.10	137.00	30.00	2.83	5.00	0.23	19.45	166.33
B1/4.1	A1	1.10	120.000	24.31	47.05	3.20	71.00	2.00	5.00	12.00	0.21	42.69	66.13
B1/5.1	A1	1.10	120.000	24.31	47.05	3.20	71.00	4.00	2.50	14.00	0.11	24.90	113.37
B1/6.0	W3	1.05	137.500	23.71	54.05		35.50	6.00	14.67	12.50	0.31	65.21	50.09
B1/7.1	W3	1.05	137.500	23.71	54.45		71.12	10.00	4.80	18.00	0.20	61.57	53.06
B1/7.2	W3	1.05	137.500	23.71	54.45		71.12	20.00	4.25	18.00	0.18	54.52	59.92
B1/7.3	W3	1.05	137.500	23.71	54.45		71.12	30.00	3.00	18.00	0.13	38.48	84.89

Table 3. Slotting Test Results

#	Nozzle Type	Jet Equiv Dia	Water Flow	Jet Power	Abrasive Nozzle Diameter	Rotational Velocity	Traverse Velocity	No. of Passes	Avg. Depth Per Pass	Average Width	Newly Open Surface	Removal Rate	Specific Energy
		mm	L/min	kW	mm	rpm	cm/min		mm	mm	m^2/h	cm^3/min	kJ/cm^3
C1/1.1	WD7	1.36	39.42	88.86		355.00	305.00	19.00	5.16	45.00	0.94	709.34	7.52
C1/2.1	WD7	1.36	39.42	88.86		355.00	457.00	26.00	5.15	40.00	1.41	944.01	5.65
C5/1.1	WD7	1.36	39.42	88.86		355.00	305.00	19.00	6.26	70.00	1.15	1339.86	3.98
C5/2.1	WD7	1.36	39.42	88.86		355.00	457.00	26.00	6.00	59.00	1.65	1621.02	3.29
C4/1.1	WD7	1.36	39.42	88.86		355.00	305.00	19.00	6.11	55.00	1.12	1026.21	5.20
C4/2.1	WD7	1.36	39.42	88.86		355.00	457.00	26.00	5.65	48.00	1.55	1242.71	4.29
C1/3.1	WD8	1.36	39.42	88.86		355.00	457.00	26.00	5.04	39.50	1.38	911.34	5.85
C1/4.1	WD8	1.36	39.42	88.86		355.00	610.00	26.00	4.88	39.00	1.79	1164.37	4.58
C5/3.1	WD8	1.36	39.42	88.86		355.00	457.00	26.00	6.00	68.50	1.65	1882.03	2.83
C5/4.1	WD8	1.36	39.42	88.86		355.00	610.00	26.00	5.81	60.00	2.13	2129.87	2.50
C4/3.1	WD8	1.36	39.42	88.86		355.00	457.00	26.00	5.62	53.00	1.54	1362.82	3.91
C4/4.1	WD8	1.36	39.42	88.86		355.00	610.00	26.00	5.27	50.00	1.93	1610.33	3.31
C1/5.1	AD6	1.41	42.37	95.52	2 x 3.0	42.00	71.00	2.00	5.00	50.00	0.21	177.86	32.22
C1.5.2	AD6	1.41	42.37	95.52	2 x 3.0	100.00	71.00	6.00	5.00	48.00	0.21	170.74	33.57
C1/5.3	AD6	1.41	42.37	95.52	2 x 3.0	150.00	71.00	20.00	3.75	40.00	0.16	106.71	53.71
C1/5.4	AD6	1.41	42.37	95.52	2 x 3.0	150.00	71.00	36.00	4.72	40.00	0.20	134.38	42.65
C5/5.1	AD6	1.41	42.37	95.52	2 x 3.0	42.00	71.00	2.00	10.00	50.00	0.43	355.71	16.11
C5/5.2	AD6	1.41	42.37	95.52	2 x 3.0	100.00	71.00	6.00	9.17	50.00	0.39	326.07	17.58
C5/5.3	AD6	1.41	42.37	95.52	2 x 3.0	150.00	71.00	20.00	5.25	75.00	0.22	280.12	20.46
C5/5.4	AD6	1.41	42.37	95.52	2 x 3.0	150.00	71.00	36.00	5.83	75.00	0.25	311.25	18.41
C4/5.1	AD6	1.41	42.37	95.52	2 x 3.0	42.00	71.00	2.00	10.00	50.00	0.43	355.71	16.11
C4/5.2	AD6	1.41	42.37	95.52	2 x 3.0	100.00	71.00	6.00	7.50	53.00	0.32	282.79	20.27
C4/5.3	AD6	1.41	42.37	95.52	2 x 3.0	150.00	71.00	20.00	5.25	60.00	0.22	224.10	25.57
C4/5.4	AD6	1.41	42.37	95.52	2 x 3.0	150.00	71.00	36.00	5.83	75.00	0.25	311.25	18.41
B2/6.1	AD6	1.41	42.37	95.52	2 x 3.0	150.00	71.00	11.00	5.00	42.00	0.21	149.40	38.36
B2/7.1	WD8	1.36	39.42	88.86		150.00	71.00	8.00	6.88	50.00	0.29	244.55	21.80
B2/8.1	WD8	1.36	39.42	88.86		300.00	71.00	8.00	6.25	52.50	0.27	233.43	22.84
B2/9.1	WD8	1.36	39.42	88.86		300.00	305.00	8.00	5.25	40.00	0.96	641.78	8.31
B2/9.2	WD8	1.36	39.42	88.86		300.00	305.00	19.00	5.26	39.50	0.96	635.35	8.39
B2/10	WD8	1.36	39.42	88.86		200.00	305.00	27.00	5.74	39.50	1.05	684.23	7.79
B2/11	WD8	1.36	39.42	88.86		200.00	254.00	30.00	5.67	43.00	0.86	620.15	8.60
B2/12	WD8	1.36	39.42	88.86		200.00	254.00	30.00	7.00	40.00	1.07	712.62	7.48

Table 4. Comparative Laboratory, Surface and Underground Test Results

#	Test Description	Average Size of Cuttings	Nozzle Type — Avg. Flow at 135 MPa	Nozzle Rotation	Traverse Velocity	Avg. Depth Per Pass	Avg. Width Per Pass	Avg. Coring Rate
		mm	L/min	rpm	m/min	mm	mm	mm/h
1	Laboratory Test Sample #1	3 to 10	WD1/50	177	2.23 / 2.55	7.7 / 5.7	47	232 to 274
2	Laboratory Test Sample # 2	3 to 10	WD1/50	210	2.50	6.3	45	252
3	Surface Test Hole #1	2 to 10	WD1/40	200	2.43	5.6 to 6.4	45	220 to 250
4	Surface Test Hole # 2	2 to 10	WD1/40	200	2.43	4.9 to 6.4	45	190 to 250
5	Underground Test Hole #1	1 to 3	WD1/40	190	2.05 to 2.43* / 2.43**	1.5 to 2.0* / 2.0 to 4.0**	25* / 43**	30 to 46
6	Underground Test Hole # 2	2 to 4	WD2/55	190	2.43	1.0 to 1.5	43	40 to 58

* initial slot cutting
** slot reaming

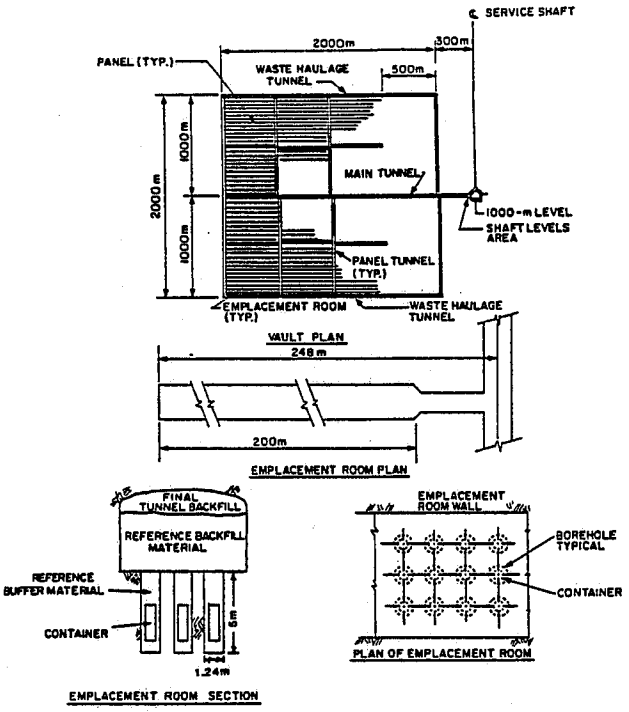

Fig. 1. Schematic diagram of nuclear fuel waste disposal vault.

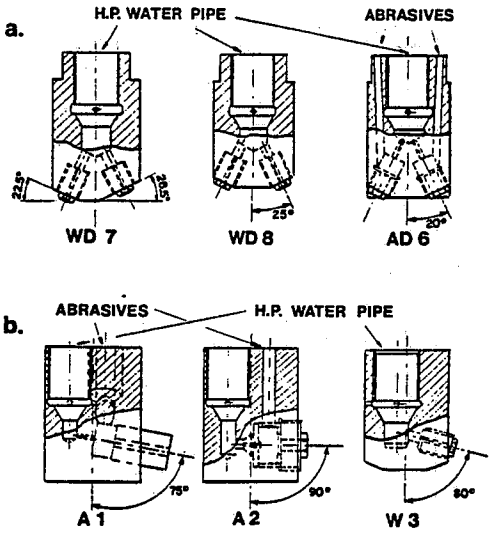

Fig. 2. Development phase nozzles:
(a) slotting nozzles WD7, WD8 and AD6;
(b) undercutting nozzles A1, A2 and W3.

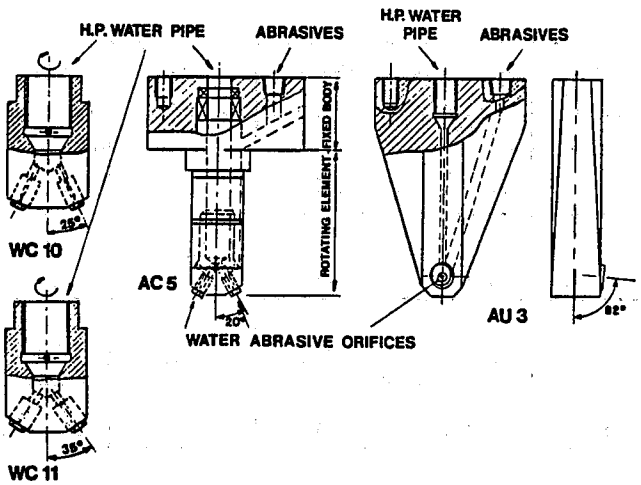

Fig. 3. Coring and undercutting nozzles:
(a) water jet coring nozzles WC10 and WC11;
(b) abrasive jet coring nozzle AC5;
(c) abrasive undercutting nozzle AU3.

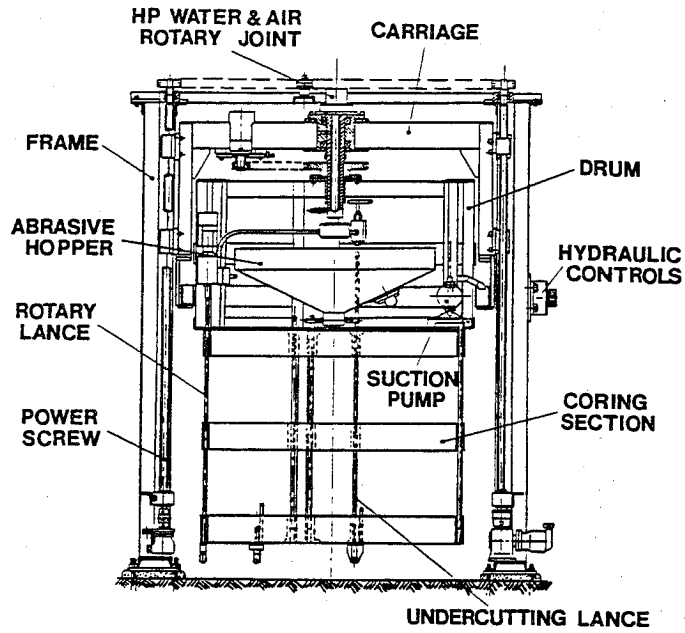

Fig. 4. Coring rig.

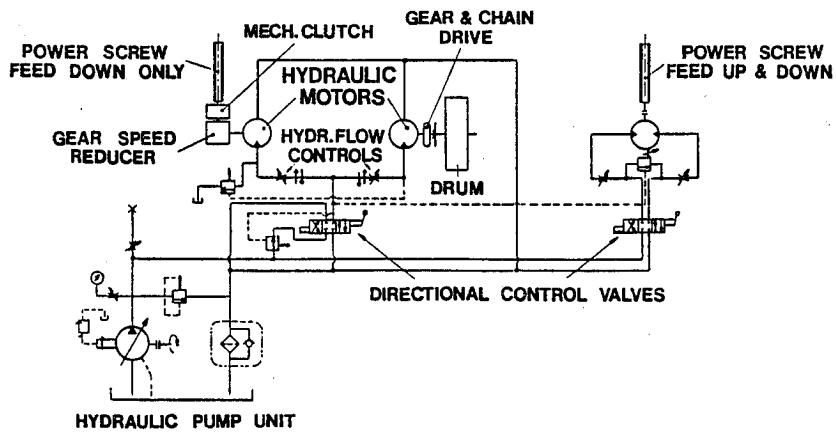

Fig. 5. Hydraulic schematic.

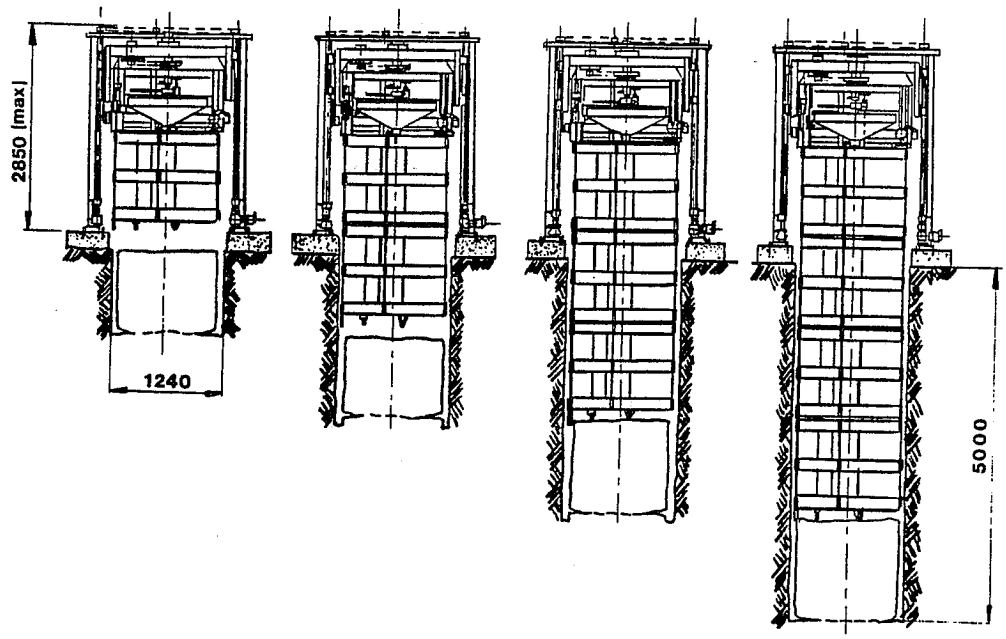

Fig. 6. Drilling sequences.

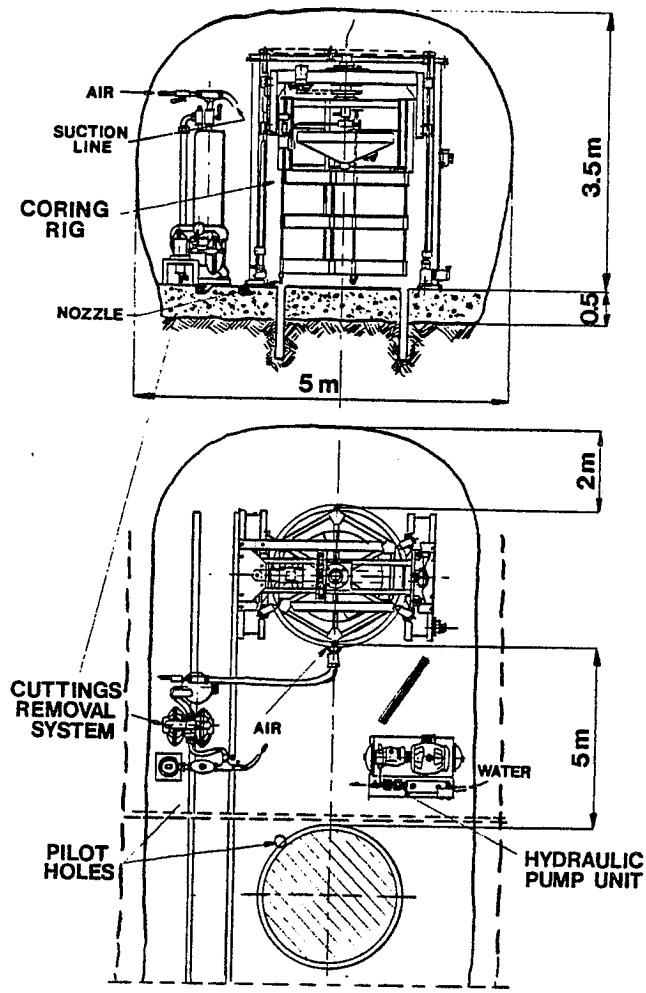

Fig. 7. Configuration of the underground testing equipment.

5th American Water Jet Conference
August 29 - 31, 1989: Toronto, Canada

Paper / Communication 4

LINEAR CUTTING APPARATUS FOR EVALUATING MINING APPLICATIONS OF WATER-JET-ASSISTED CUTTING

P.D. Kovscek
Boeing Services International

AND

C.D. Taylor AND E.D. Thimons
Pittsburgh Research Center, Bureau of Mines
Pittsburgh, Pennsylvania 15236, USA

ABSTRACT: Studies have been conducted by the Bureau of Mines to evaluate the effect of water-jet-assisted cutting on shearer cutting efficiency. Two longwall shearers were equipped for water-jet-assisted cutting, and tests showed that the mechanical energy required for mining was not reduced when the high-pressure water, up to 69 MPa, was used. Although several prior laboratory studies had shown that mechanical bit cutting forces should be reduced when using water jet-assisted-cutting, none of those studies were conducted using cutting conditions that simulated mining conditions on a longwall shearer.
To provide a testing tool that simulated shearer cutting conditions, a single bit linear cutting test apparatus was built at the Bureau of Mines' test facility. During cutting tests, the amount of mechanical cutting energy required was measured while the fluid energy supplied by the water jet was varied. Using the test apparatus and a range of fluid energies between 5 and 25 joules/mm, there were no significant reductions in the levels of mechanical cutting energy. The water-jet was also traversed over the rock surface without the cutting bit. Increasing the fluid energy increased the depth of the kerf cut in the rock, but there appears to be no significant relationship between the measured kerf depths and reduced mechanical cutting energies as measured during the cutting tests.

RÉSUMÉ : Des études ont été menées par le Bureau of Mines pour évaluer comment la coupe assistée par jet d'eau influe sur l'efficacité de coupe des ravageuses. Deux ravageuses de longue taille ont été équipées pour la coupe assistée par jet d'eau, et les essais ont montré que l'énergie mécanique requise pour l'abattage n'est pas réduite lorsque la pression de l'eau est portée jusqu'à 69 MPa. Même si plusieurs études de laboratoires antérieures avaient révélé que les forces de coupe des taillants mécaniques devraient être réduites lorsque la coupe est assistée par un jet d'eau, aucune de ces études n'a été menée dans des conditions de coupe simulant des conditions d'abattage à la ravageuse de longue taille.
Pour réaliser un outil d'essai simulant les conditions de coupe à la ravageuse, on a construit un appareil expérimental de coupe droite à un taillant au centre d'essais du Bureau of Mines. Au cours des essais de coupe, la quantité d'énergie mécanique de coupe requise a été mesurée et on a fait varier l'énergie hydraulique fournie par le jet d'eau. Avec l'appareil d'essai et pour des énergies hydrauliques variant entre 5 et 25 joules/mm, les niveaux d'énergie mécanique de coupe ne diminuent pas sensiblement. Le jet d'eau a aussi été projeté sur la surface rocheuse sans l'utilisation d'un taillant. Une augmentation de l'énergie hydraulique se traduit par une entaille plus profonde dans la roche, mais il ne semble y avoir aucune relation importante entre les profondeurs d'entailles mesurées et les valeurs réduites de l'énergie mécanique de coupe telles que mesurées au cours des essais de coupe.

Organized and Sponsored by the National Research Council of Canada and the U.S. Water Jet Technology Association.

1.0 INTRODUCTION

1.1 Background

Water-jet-assisted cutting is a mining technique that uses high-pressure water jets to assist the mechanical cutting performed by rock bits. The water jet, supplied at pressures from 20.7 to 69 MPa, is directed to strike the rock just in front and within 3 mm of the bit tip. Broken and crushed rock is cleared from around the bit tip by the high-pressure jet. Removing this material allows the bit tip to directly contact the unbroken rock and should increase cutting efficiency. A minimum or threshold level of energy must be supplied before water-jets can clear the broken material. This threshold level can be defined as the fluid energy level required to achieve a reduction in bit cutting force (Geier, J. E., 1987).

Several studies were conducted to identify the effects of water-jet-assist on cutting forces which have shown that bit forces can be reduced when fluid energy is supplied at energy levels between 20 and 30 joules/mm (Geier, J. E., 1987). Most of these results were obtained with single bit cutting machines that were operated at a cutting depth less than 1.3 cm and speeds less than 25 cm/s.

The Bureau of Mines equipped two longwall shearers, one underground and the other at a surface test facility, for water-jet-assisted cutting (Thimons, E. D. 1988). Maximum fluid energy that could be supplied was limited by the water flow rate and pressure that could be delivered to the shearer, and the rotational speed of the cutting drums. The joules of energy delivered per length of rock surface cut increases with water flow rate and pressure, and decreases with bit velocity. The fluid energy supplied by each water nozzle on the shearer cutting drums varied from 1 to 3 joules/mm. While maintaining the same cutting rate, the electrical energy supplied to the shearer cutting and tramming motors for mechanical cutting was measured during operation with and without water jet-assist. The results indicated that there was no significant reduction in the amount of mechanical energy used while operating with water-jet-assisted cutting; thus the bit cutting forces were not reduced.

1.2 Objective

The objective of the current study was to determine what threshold fluid energy level was required to reduce bit cutting energy during normal mining conditions. A test apparatus was constructed to simulate the cutting conditions of a bit operating on a longwall shearer drum.

2.0 TEST PROCEDURE

2.1 Test Apparatus

The linear-cutter apparatus built for these tests used a single bit to make linear, constant depth cuts in a test rock (figure 1). The four basic components of this linear cutter apparatus are the:

- counterbalance carriage,
- cutter bit carriage,
- rock holding (pedestal) fixture and,
- high-pressure pump.

Counterbalance and cutter bit carriages

The cutting bit is fixed to the bit carriage. The counterbalance and bit carriages move vertically on adjacent tracks, and are connected by steel cables. The bit carriage is lifted to the desired height by a winch. A clamp holds the winch to the carriage cable until it is released, by remote control, and the carriage drops. The bit velocity, when it strikes the rock, is determined by gravity and the amount of weight placed on the counterbalance carriage. After the bit contacts the rock, the carriage speed decreases depending on the resistance of the rock to bit movement.

A Kistler piezoelectric triaxial force dynamometer was mounted on the bit carriage to monitor bit forces. The dynamometer measured forces in the three component orthogonal directions. Only the cutting force measurements are discussed in this paper.

Bit cutting speed and vertical location were monitored with a velocity position transducer (0-254 cm displacement, 0-380 cm/s velocity) that was actuated by a cable that rotated a potentiometer and tachometer generator. One end of the cable was attached to the bit carriage and the other end to the transducer, which was mounted on the base of the test fixture.

Rock holding fixture

The rock holding fixture held a 46-cm high by 61-cm wide piece of rock. The maximum length of cut was 46 cm. A hydraulic ram on the fixture moved the rock toward the bit to obtain a cutting depth of either 1.3 or 2.5 cm. After setting the rock for the desired depth, the sample was clamped in place.

To move the rock horizontally to a new cutting track, an hydraulically-powered screw mechanism was used. The distance between cutting tracks was 2.54 cm and as many as 22 cuts could be made for each complete pass across a rock face. For each pass across the rock face, the depth of cut was maintained constant. The horizontal distance between cuts was set manually by measuring the distance between adjacent bit positions. The distance between cuts was also measured with a position transducer. The bit position, recorded with the other test data, was used to identify specific test runs.

High-pressure pump

A triplex 3-piston positive-displacement pump (capacity of 42 lpm at 69 MPa) was used to supply the high-pressure water. The water pressure was monitored with a 0 - 69 MPa pressure transducer installed in the high pressure supply line at the pump outlet. Nine meters of 1.3 cm ID high pressure flexible hose connected the pump to the bit carriage. The nozzle was mounted beneath the cutting bit in the end of a 10-cm straight piece of stainless steel tubing. The stainless steel tubing reduced water flow turbulence and increased the stagnation pressure delivered by the nozzle (Kovscek, P. D., 1988).

A tungsten carbide nozzle with a 1.0-mm diameter orifice (Coefficient of discharge = .88) was used for all tests. Located below the bit, the nozzle was positioned so that the water jet stream passed in front of the cutter bit, less than 1 mm from the cutting edge. The standoff distance between the nozzle and the bit tip was 5 cm. The water pressure was maintained at 62 MPa, with a flow rate of 14 lpm, for all water-jet tests.

2.2 Rock types

Berea sandstone and Indiana limestone were selected for lab testing because both have well documented cutting properties and can be obtained in homogeneous samples that are dimensionally stable. Both rocks are typical of the types of rock that would be cut during continuous mining operations. The following properties are given for each rock (Krech, W. W., 1974):

Berea sandstone:
- Density: 2.11 g/cc
- Unconfined compressive strength: 46 MN/m^2
- Tensile strength: 1.07 MN/m^2
- Porosity: 19.1 pct

Indiana limestone:
- Density: 2.34 g/cc
- Unconfined compressive strength: 44 MN/m^2
- Tensile strength: 5.23 MN/m^2
- Porosity: 12.5 pct

2.3 Cutting tests

A Kennametal K-107 radial attack bit was used for all cutting tests. The shank of the bit was modified to fit in the dynamometer. Before the first cut was made, the rock was mounted in the test fixture and the rock face was "squared" by taking 1.3 cm deep cuts, 2.54 cm apart. For each cut, during the same pass, the cutting depth was maintained constant at either 1.3 or 2.5 cm. The bit force, in the cutting direction was continuously monitored. Water pressure was maintained at 62 MPa for the water jet tests, or 0.5 MPa or less for the non-water jet tests. The cutting rate for the tests was varied from 12.7 to 267 cm/s to achieve fluid energy levels between 5 and 25 joules/mm.

Signal conditioning for the pressure, position, and velocity transducers was accomplished with Honeywell 218 Accudata bridge amplifiers. Power and signal conditioning for the force dynamometer was provided by a Kistler type 5004 dual mode amplifier.

All signals were scaled to an analogous 0- 10 volt DC signal. The signals were digitized and recorded on a Honeywell HTM 3000 computer and data acquisition system. The data was recorded at a sample rate of 1,000 samples/s and stored on a hard disk for subsequent data processing.

Data acquisition was triggered prior to cutter contact with the rock, thereby capturing the data both before bit entry and after the bit exited the rock. However, the initial contact of the bit

with the rock produced higher than normal bit forces, while during the breakout from the rock, forces were lower than normal. The data was only analyzed from 2.54 cm below the top of the rock to 2.54 cm above the bottom of the rock. Thus, data from each cutting test was analyzed for the middle 41 cm of each pass across the rock. The cutter velocity, water pressure and cutter bit force data were averaged from the time wave form. The average values from each cut were used to compare and contrast the bit forces.

3.0 RESULTS AND DISCUSSION

3.1 Cutting tests

Knowing the cutting speed, the mechanical energy supplied per length of cut (joules/mm) was calculated. This calculated energy per length of cut is subsequently referred to in this paper as the "mechanical cutting energy." Mechanical cutting energy versus cutting speed with and without water jet assist is plotted for both rock types in figures 2 and 3. Reductions or changes in mechanical cutting energy while using water-jet assist can be compared at the 1.3 and 2.5 cm depths of cut for the range of cutting speeds. The amount of mechanical cutting energy required for cutting in the limestone was higher than for cutting in the sandstone. The average percent reduction in mechanical cutting energy resulting from use of water-jet assist is given in Table 1.

The data plotted in figures and 2 and 3 indicates that the depth of cut has a much greater effect on cutting forces than the use of water-jet-assisted cutting. With the limestone rock, cutting speed also appears to have some effect on mechanical cutting energy, but speed had little if any effect on mechanical cutting energy in sandstone. To evaluate the combined effect of water pressure, depth of cut, and cutting speed on mechanical cutting energy, multiple regression techniques were used. For each rock type a multiple regression was performed using water pressure, depth of cut, and cutting speed, to predict mechanical cutting energy. The regression equation for each rock type is given below:

Multiple Regression Equations for:

Berea sandstone:

$$Y = 1.06*X_1 - 0.0001*X_2 - 0.003*X_3 + 0.54$$

Indiana limestone:

$$Y = 2.01*X_1 + 0.009*X_2 - .007*X_3 - 1.11$$

Where:

X_1 - Depth of cut, cm
X_2 - Traverse speed, cm/s
X_3 - Water pressure, MPa
Y - Mechanical cutting energy in joules/mm

The lines of best fit are shown in figures 4 and 5. Except for cutting speed in Berea sandstone, all three variables had a significant effect (90 percent confidence level) on the lines of best fit. The coefficients in the regression equations indicate that the relative contribution of the depth of cut to the bit cutting forces is much greater than the contribution due to water pressure or cutting speed.

Fluid energy per length of cut by the water jet was calculated in joules/mm. This energy quantity is subsequently referred to as "fluid energy." In figures 6 and 7, fluid energy supplied by the water jet and mechanical cutting energy supplied by the bit has been plotted versus cutting speed. At a cutting speed of approximately 50 cm/s, the fluid energy is about 12 times greater than the mechanical cutting energy. At cutting speeds approaching 270 cm/s, the fluid energy is about twice as great as the mechanical cutting energy. Also in figures 6 and 7 it can be seen that, for the range of cutting speeds tested, there are only minimal reductions in mechanical cutting energy due to changes in fluid energy supplied by the water jet. Therefore, at fluid energy levels from 2 to 12 times higher than the mechanical cutting energies being supplied, only minor mechanical cutting energy reductions are achieved.

3.2 Kerfing tests

The bit carriage, without the bit installed, but with the water jet operating, was dropped past the test rock. The impact of the water jet on the rock surface created a linear kerf or slot (figure 8). The same water pressure (62 MPa), standoff distance (5 cm), and traverse speeds (12.7 to 280 cm/s), were used during the cutting and kerfing tests. The depth of the kerf produced by the traversing jet was measured with a vernier caliper, and the average depth recorded for each pass.

The traverse speed the jet passed over the rock surface is plotted versus kerf depth in figure 9. The results indicate that rock type and speed are important factors affecting kerf depth. Increasing the fluid energy per length of cut by reducing the cutting speed increased the kerf depth for both rock types within the range of variables tested. Although the level of fluid energy supplied had a direct effect on kerf depth, there appears to be no significant relationship between these increased kerf depths and the reductions in mechanical cutting energies seen in the cutting tests.

4.0 CONCLUSIONS

A Bureau study evaluated the effect water-jet-assisted cutting has on mechanical cutting energy. The range of fluid energy levels was 5 to 25 joules/mm. To reduce the mechanical cutting energy an average of 3 to 11 percent, the water jet fluid energy level had to be 2 to 12 times higher than the mechanical cutting energy. As the fluid energy was increased there was little significant change in the cutting forces. Therefore the fluid energy threshold level could not be identified for the range of test conditions in these experiments.

Earlier test results with longwall shearers equipped for water-jet- assisted cutting had not shown any reductions in shearer mechanical cutting energy when high-pressure water was used. During those tests the maximum fluid energy that could be supplied by each nozzle was 3 joules/mm. Based on the current test results, the fluid energy level would have to be almost doubled in order to achieve small reductions in mechanical cutting energy. Considering the size of the anticipated reductions (2 to 11 percent) in mechanical cutting energy it does not appear that the additional expenditure of fluid energy is warranted.

Even if larger reductions in mechanical cutting energy were possible with water-jet-assisted cutting, it does not appear practical to supply the needed water pressures and/or flow rates with current mining technology. However, Bureau of Mines research has shown that there are other benefits that may be realized by using water jet assisted cutting at moderately high-pressure. At water pressures between 14 and 21 MPa, use of water jets reduced dust, product fines and bit wear (Kovscek, P. D., 1986).

5.0 REFERENCES

1. Geier, J. E., M. Hood, and E. D. Thimons: "Water-Jet-Assisted Drag Bit Cutting in Medium-Strength Rock." U.S. Bureau of Mines Inf. Circular No. 9164, U.S. Dept. of the Interior, 1987, 10 pp.

2. Thimons, E. D., P. D. Kovscek, K. Neinhaus, and C. D. Taylor: "Evaluation of Water-Jet-Assisted Cutting on Longwall Shearers." Proceedings of the 8th International Conference on Coal Research, Oct. 16-20, 1988, Tokyo, Japan, 16 pp.

3. Kovscek, P. D., C. D. Taylor, and E. D. Thimons: "Techniques to Increase Water Pressure for Improved Water-Jet-Assisted Cutting." U.S. Bureau of Mines Rpt. of Investigation No. 9201, U.S. Dept of the Interior, 1988, 10 pp.

4. Krech, W. W, F. A. Henderson, and K. E. Hjelmsted: "A Standard Rock Suite for Rapid Excavation Research." U.S. Bureau of Mines Rpt. of Investigation No. 7865, U.S. Dept. of the Interior, 1974, 29 pp.

5. Kovscek, P. D., C. D. Taylor, H. Handewith, and E. D. Thimons: "Longwall Shearer Performance Using Water-Jet-Assisted Cutting." U. S. Bureau of Mines Rpt of Investigation No. 9046, U. S. Dept of the Interior, 1986, 15 pp.

Table 1. Average Percent Reduction in Cutting Energy

Depth of Cut	Berea Sandstone	Indiana Limestone
1.3 cm	13	10
2.5 cm	3	9

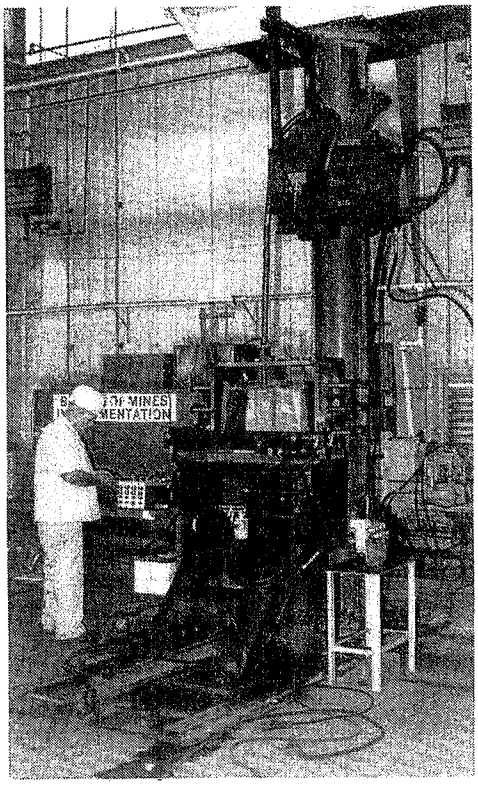

FIG. 1 TEST APPARATUS SHOWING BIT CARRIAGE AND ROCK HOLDING FIXTURE

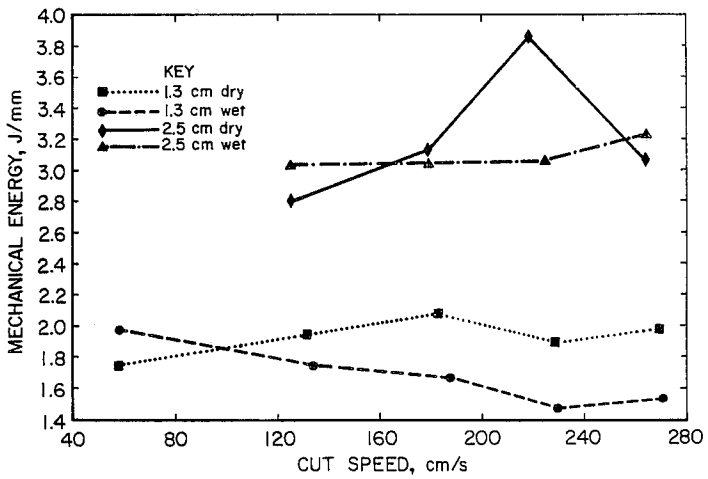

FIG. 2 CUTTING SPEED VERSUS MECHANICAL CUTTING ENERGY FOR BEREA SANDSTONE

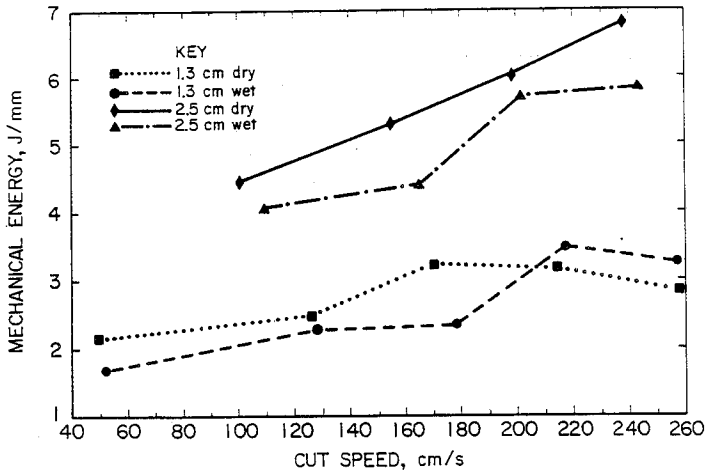

FIG. 3 CUTTING SPEED VERSUS MECHANICAL ENERGY FOR INDIANA LIMESTONE

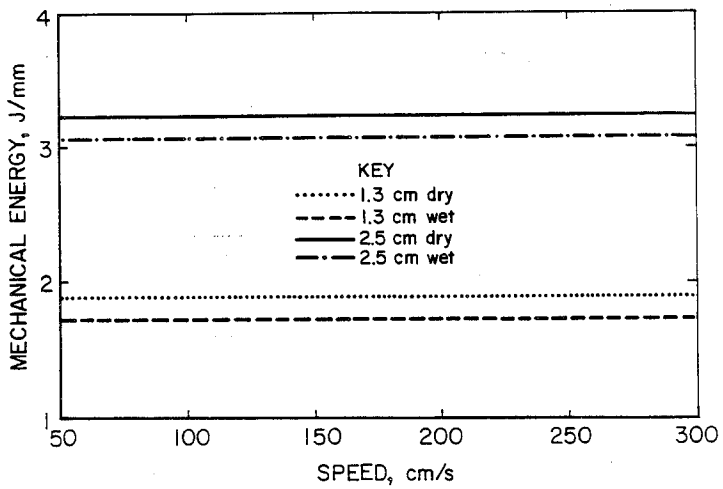

FIG. 4 MULTIPLE REGRESSION FOR SANDSTONE MECHANICAL CUTTING ENERGY DATA

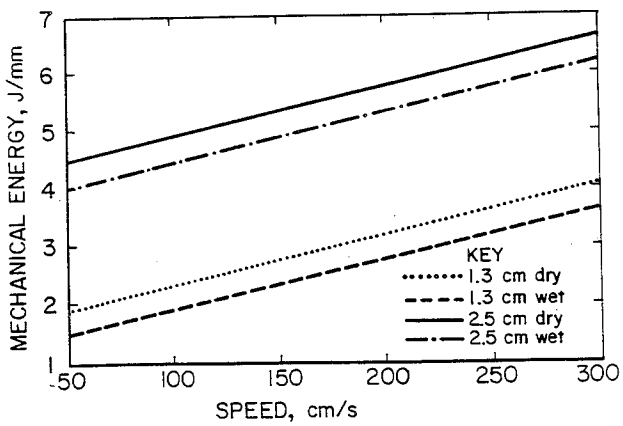

FIG. 5 MULTIPLE REGRESSION FOR LIMESTONE MECHANICAL CUTTING ENERGY DATA

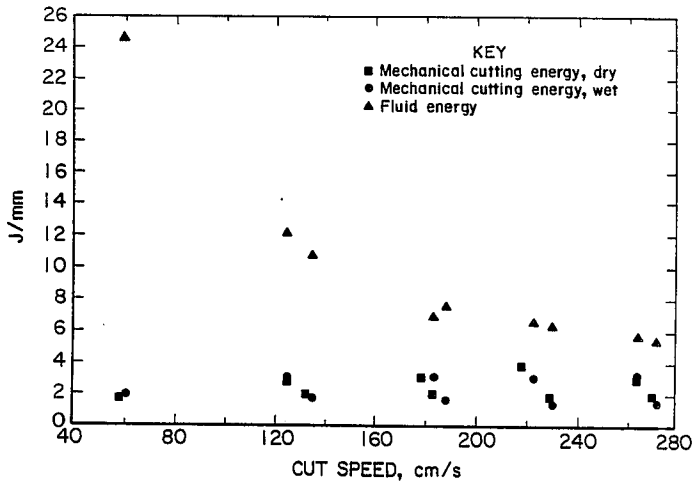

FIG. 6 COMPARISON OF FLUID AND MECHANICAL CUTTING ENERGY LEVELS SUPPLIED DURING CUTTING OF BEREA SANDSTONE

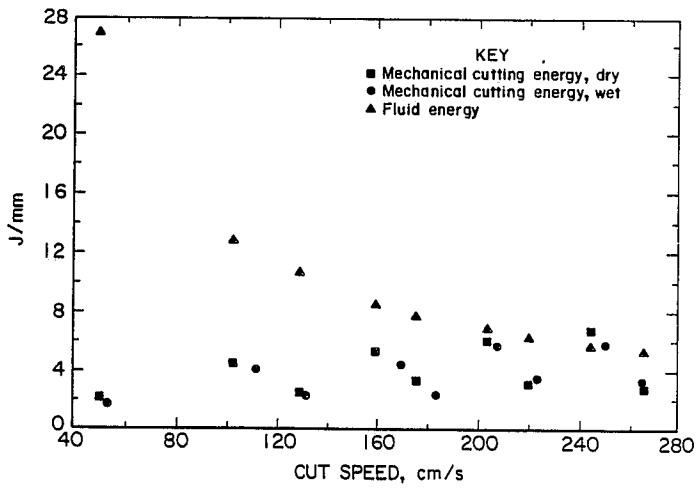

FIG. 7 COMPARISON OF FLUID AND MECHANICAL CUTTING ENERGY LEVELS SUPPLIED DURING CUTTING OF INDIANA LIMESTONE

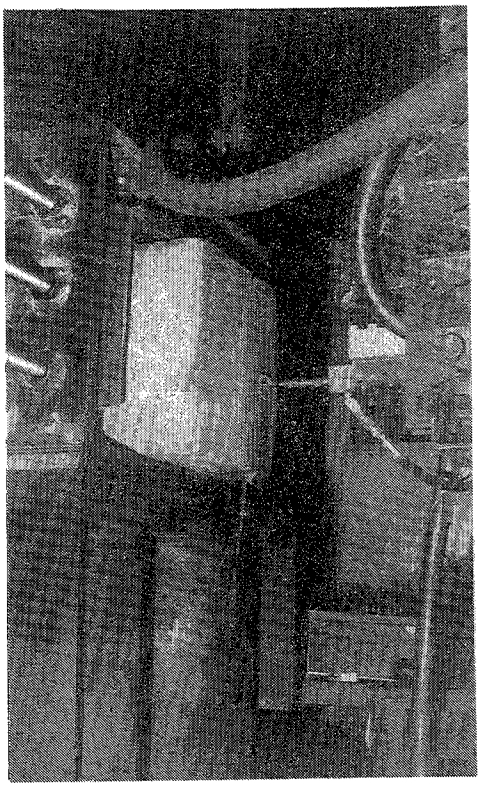

FIG. 8 KERF CUTTING USING THE TEST APPARATUS

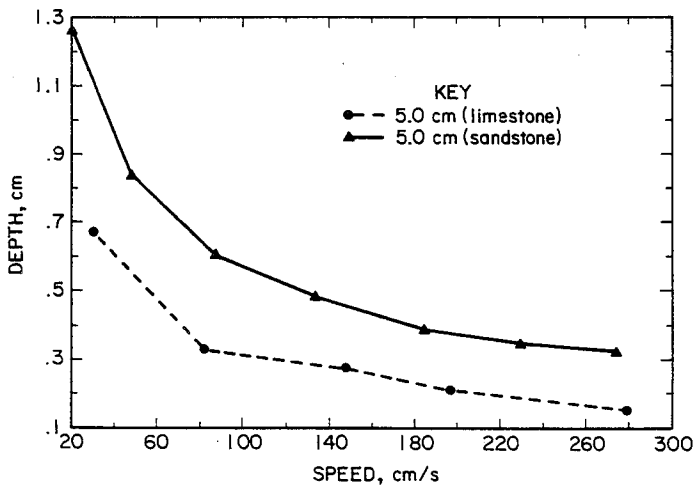

FIG. 9 KERF DEPTH VERSUS TRAVERSE SPEED

5th American Water Jet Conference
August 29 - 31, 1989: Toronto, Canada

Paper / Communication 5

GRANITE QUARRYING WITH WATER JETS: A VIABLE TECHNIQUE?

A. Bortolussi, R. Ciccu, P.P. Manca AND G. Massacci
Dipartimento di Ingegneria Mineraria e Mineralurgica
Centro Studi del CNR
Universita' degli Studi di Cagliari
Cagliari, Italy

ABSTRACT: After a comprehensive outline of the results hitherto obtained in cutting granite with different methods, the paper deals with the experience so far gained using waterjets. The attention is focussed on the operational problems related to the technique, which can be applied either as the integral quarrying method or in suitable combination with other available techniques like explosive splitting, diamond wire sawing and wedge shearing, depending on the results of technical performance.
Surface smoothness is also taken into consideration as the prospects of successful application of waterjet technique lie in its ability to make precision cuts, resulting a considerably higher pay volume than less expensive but ruder techniques.

RÉSUMÉ : Après une description détaillée des résultats obtenus jusqu'ici avec différentes coupes du granite, la communication traite de l'expérience acquise jusqu'à maintenant sur les jets d'eau. L'attention est portée sur les problèmes opérationnels que présente la technique, laquelle peut être appliquée comme méthode d'exploitation intégrale ou en combinaison judicieuse avec d'autres techniques disponibles comme le fendage à l'explosif, le sciage du diamant au fil hélicoïdal et le cisaillement en coins, selon les résultats de performance technique.
L'uniformité de la surface est aussi prise en compte car le succès d'une technique par jet d'eau réside dans sa capacité de réaliser des coupes précises, produisant ainsi un volume utile beaucoup plus grand qu'avec des techniques moins coûteuses, mais plus grossières.

Organized and Sponsored by the National Research Council of Canada and the U.S. Water Jet Technology Association.

1.0 FOREWORD

Today dimensional stone for ornamental uses and for construction engineering is quarried using different techniques. The most common of these, at least as far as experience in Europe is concerned, are, in order of decreasing popularity (Bortolussi et al., 1978):

- Dynamic splitting. Rock is sheared by blasting with detonating fuse or decoupled linear charges of slower explosives loaded into closely spaced holes. Satisfactory productivity can be achieved with flexible bench design, easily adaptable to different quarry configurations. Capital costs are moderate provided that simple machinery is employed, but grow rapidly for mechanized operations. Despite heavy drill-steel wear, running costs are relatively low especially for primary cuts of larger area.

  However the technique is somewhat destructive in that a certain amount of rock is wasted or not paid, because of unwanted bank fracturation, block face irregularities and some induced damage, either real or simply inferred, at a depth of few centimetres from the cut surface (commercial allowance).The overall loss may be of the order of 10 to 20 % of the expected block volume, according to the extent of the block face area obtained with the explosive technique; such incidence becomes progressively higher for smaller blocks. (Fig. 1)

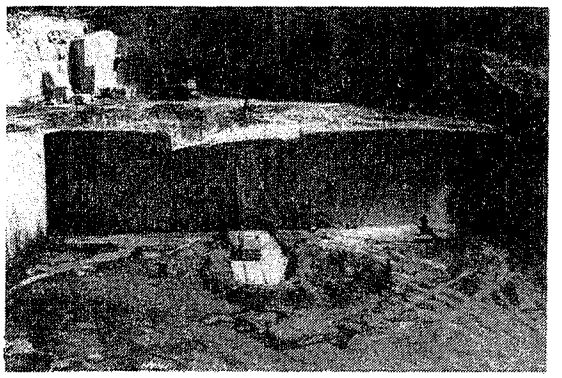

FIG. 1. Primary explosive splitting cut in a granite quarry (Sardinia)

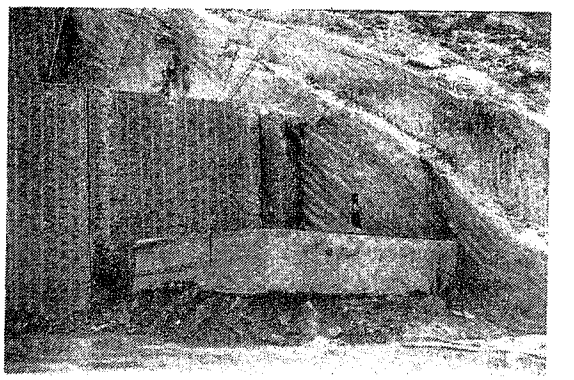

FIG. 2. Bench opening cut with flame torching

- Flame torching. Bench opening free faces, up to 6-8 m deep and several m long can be obtained by firing the rock with a high temperature flame directed toward the slot bottom by means of a hand-driven thermal lance. Operating costs are dependent upon the ever-rising price of fuel oil whose incidence is over 60 % including the production of the burning-supporter compressed air. The technique was initially favoured by its ability to pierce the rock in any direction, without the need for preliminary operations. However the interest in flame torching is inevitably declining due to excessive noise, heat and dangerous dust which cause a severe impact on the environment even at some km away from the site. Moreover a considerable proportion of pay volume is lost due to material damage and face roughness, amounting to even 40 % for 10 m^3 blocks, should all the faces be cut with the flame.

- Diamond wire sawing. After the outstanding improvements obtained during a decade of industrial application in marble quarrying, this technique has recently been proposed also for cutting granite and akin rocks using a wear-resistant modified tool. Modern equipment, powered with either a directly-coupled electric motor or a Diesel engine, is automatically controlled for optimum performance under ever-changing working conditions (shape and length of the cut profile).

  Despite the efforts to improve tool life, wear accounts for at least 70 % of sawing cost for granite, including hole drilling for wire loop encompassing around the perimeter of the face to be cut. The great advantage stands in the surface smoothness and in the absence of any material damage, resulting in a considerable increase of stone recovery, especially in the case of whole-diamond quarrying operation. An important technological restriction is related to the cut area which is suggested should not exceed 100 m^2 (owing to cooling and optimum control problems) or be smaller than 10 m^2 (to avoid fatigue stress and excessive bead load due to pronounced curvature). For block shaping purposes the wire can be driven by large diameter pulleys mounted on suitable headframes.

  On the basis of the industrial results so far obtained, diamond wire is being increasingly applied for sawing granite in the range of 30 - 100 m^2 cut area, thus covering the requirements of narrow bench quarrying.

- Continuous drilling. Rock can be split by drilling a row of adjacent holes and subsequently destroying the thin ribs between them. Hole parallelism and complanarity must be strictly ensured by resorting to suitable drilling equipment. Moreover, since the hole length should be limited for alignment control, a low-bench design becomes preferable which however is not the best

FIG. 3. Bench opening cuts with diamond wire

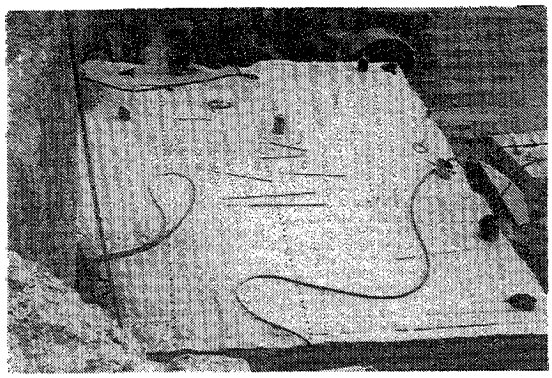

FIG. 4. Wedge shearing for block shaping

solution in cases where selective quarrying is required.

- Wedge shearing. The presence of roughly orthogonal planes of easier splittability makes the granite amenable to shearing by hammering wedges or feather-plug devices into closely spaced holes or by using hydraulic splitting tools. The technique is generally applied for block squaring and shaping. The material is not damaged but the face roughness is not negligible, being of the order of some centimetres, leading to considerable volume penalization given the size of the blocks (generally between 5 and 12 m^3) and the amount of surface area split with this technique.

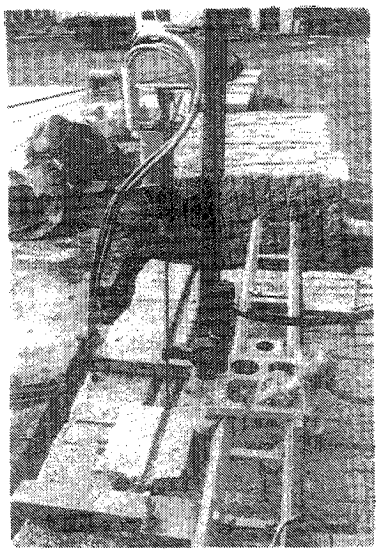

FIG. 5. Rotating twin-jet equipment used for the cutting tests on Sardinian granites.

Waterjet has some prominent advantages such as cut precision, face smoothness, relatively low impact on the environment, safer and less harmful working conditions (noise, dust, vibrations).

However it is still rather expensive and not yet fully reliable; it also appears to be more sensitive than diamond wire and the drilling-based methods to localized variations of the rock features like for instance crossing quartz veins. Further research is therefore needed in order to overcome these drawbacks. Abrasive waterjet can be foreseen as the winning solution for the future, especially as far as block working operations are concerned.

Besides kerfing, waterjet can be used for drilling parallel holes for explosive or wedge splitting exploiting the advantage of a more precise drilling direction, it being less sensitive than percussion methods to changes in rock features. To this end further improvements should be expected after the development of reliable abrasive jets systems which look particularly promising for long small-diameter holes (Vijay, 1982).

2.0 LABORATORY INVESTIGATION

A great deal of research has been carried out universally on the fundamentals of high velocity jets of different kinds and features and their action on a variety of materials from soft to hard, including rocks. Most results have been reported in the technical literature and are well known to most waterjet experts (Summers, 1985; Hilaris, 1980). For the sake of conciseness only the results of the Italian experience are briefly described here (Ciccu, 1986 and references cited therein).

The pumping unit used in the experiments recently carried out by the research team of the University of Cagliari consisted of a booster stage followed by three intensifiers powered by a 97 kW Diesel engine. The lance, connected via a swivel and flexible piping, was fitted with a head with two diverging 0.584 mm corundum orifices angled at 45 degrees. The experimental set up is illustrated in Figure 5.

The maximum operating pressure was 280 MPa at the pump outlet and 250 MPa the head due to

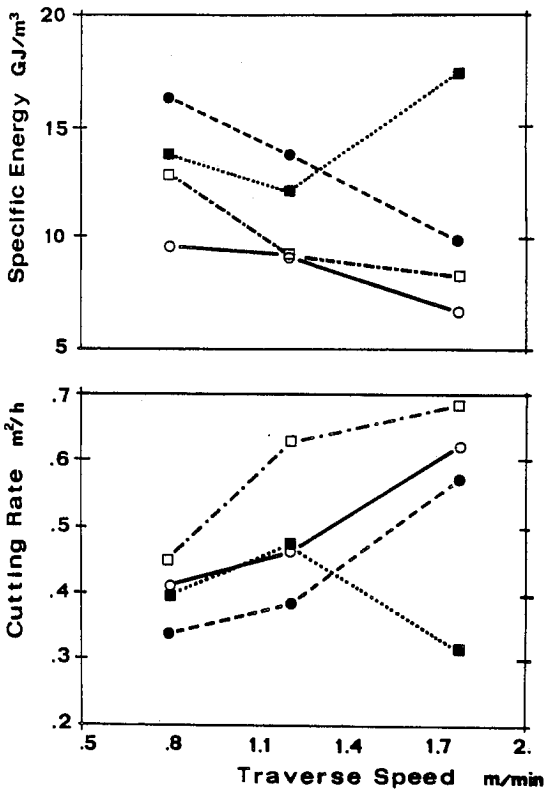

FIG. 6. Experimental results of waterjet cutting of "Ghiandone L." granite.

friction losses. The lance penetration movement was assured by a hydraulically driven feed chain; the traverse displacement by a distinct hydraulic motor acting through a rack-pinion coupling on the lance supporting beam.

Systematic tests have been conducted on blocks of granite samples of different origin, mostly from Sardinia, with the aim of studying the effect of the operating variables with particular consideration to pressure, lance spinning and traverse velocity. For each test at a given setting of control variables kerf depth per pass was measured every 3 cm along the cutting direction and averaged. Stand-off distance was maintained around 1 cm (Bortolussi, 1985).

Cutting rates for the different experimental conditions are reported in the graphs of figure 6 and the best results resumed in table 1.

Generally no peak values were observed, suggesting that better performance could be obtained at higher traverse velocities than 1.8 m/min allowed by the system at hand. Maybe a further increase in pressure and water rate should also have proven beneficial in reducing the specific energy on account of the relatively coarse grain size of the tested materials.

The minimum experimental specific energy was then assumed for conservative extrapolations to higher cutting rates achievable by increasing the hydraulic power of the system and in particular the water flow (Labus, 1976 and 1984).

Table 1 - Experimental Cutting Rates for Various Italian Granite Samples

Type of granite	Compr. str. MPa	Freez. test MPa	Impact Str. cm	Grain size	Cutting rate m^2/h
- Ghiandone L.	190	194	58	Coarse	0.69
- Rosa G.	192	190	61	Medium	0.69
- Grigio S.	-	-	-	Medium	0.86
- Bianco M.	234	224	70	Fine	1.19

3.0 FIELD EXPERIENCE

Four meaningful examples of waterjet granite kerfing in the field are so far available, all in North America.

In Colorado (USA) a fine grained red granite is quarried by employing the oscillating waterjet system powered with about 30 kW. The operating pressure at the pump outlet is above 310 MPa with a water rate of 5 l/min flowing through a 0.36 mm single nozzle. Despite the very limited power involved, a net cutting rate of 0.6 m^2/h is claimed as the result of a translation velocity of 4.2 m/min and a penetration step of 5 mm per cycle. The unit is able to cut along both the horizontal and vertical directions (Fig. 7) (Bortolussi, 1987).

In Georgia (USA) experiments have been made at an Elberton granite quarry, using the rotating jet solution. Cutting at a pressure of approximately 100 MPa with a flow rate of 60 l/min across two nozzles, the excavation rate varied between 1.2 and 2.5 m^2/h. The lance was moved at a traverse velocity of 3 m/min and penetrated 6 to 14 mm per pass. The slot was 6 m long and 1 m deep. The tests allowed to study the optimum jet angle (around 45 degrees) producing a slot wide enough for lance penetration.

A similar system was tested also in a South Dakota granite quarry (USA) where production plan required primary kerfs 20 m long and 4 m deep. The pumping system with a total installed power of 115 kW supplied an overall water rate of 41 l/min through a twin-nozzle head (1.19 mm orifice diameter) under a pressure of 100 MPa. The rock, characterized by a compressive strength of 175 MPa, was cut at a rate of 1.5 m^2/h as the result of a translation speed of 3 m/min and an increase in depth of 8 mm per pass; spinning speed was around 360 rpm (Reather, 1983).

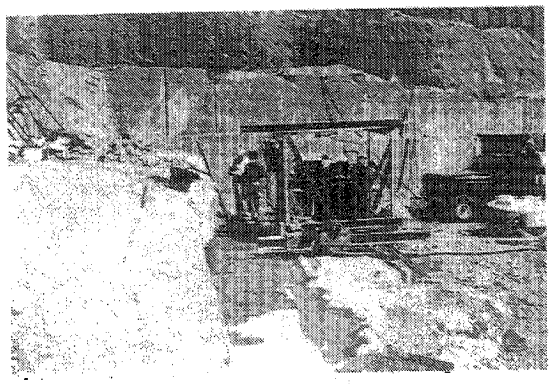

FIG. 7. Waterjet quarrying in Colorado with the oscillating lance equipment.

The last instance is that in course at a Quebec quarry (Canada) using a Diesel powered pumping unit supplying 76 l/min of water under a pressure of 138 MPa. The overall results indicate that the rock can be cut at an exposure rate of 1.7 m^2/h (pure cutting time) with an effective performance of 1.15 m^2/h (taking into account also the idle time). The typical cut is 5 m long and 3.4 m deep (Hawrylewicz, 1988).

In France waterjet is being currently applied as the integral method in a sandstone quarry. The equipment consists of the high pressure pumping unit, the connecting pipes and the lance fitted with the unique multi-nozzle head, swinging inside a sector-shaped steel encasement. The rock is excavated by the sweeping action of the jets as the lance is traversed along the slot. Although not proven with long-run industrial application, the system, powered with 230 - 330 kW (45 - 80 l/min of water under a pressure of 120 - 190 MPa) is alleged to cut granite at an exposure rate up to 6 m^2/h according to the kind of rock.

4.0 INDUSTRIAL PROSPECTS

The results of laboratory investigation and field trials lead to conclude that waterjet kerfing is viable and safe compared with flame torching, at least for cuts shallower than 3 - 4 m, with additional advantages in terms of automation and impact on the working environment. It is also claimed that waterjet is still superior to explosive splitting due to higher stone saving. Actually this may be true for smaller volumes like those worked in low bench operations or in the block shaping phases. It is not so for primary cuts of larger area for blasting huge volumes, greater than 1,000 - 2,000 m^2, now customary in the Italian operations, for which the relative amount of stone lost is much less significant.

In particular, the feasibility of waterjet technology in granite quarrying implies its technical and economic competitiveness with the other alternative methods available for the various operations, i.e., for a typical quarry organized according to a high-bench design with three subdivision stages:

- lateral bench opening cuts (suitable techniques: flame, diamond wire and sometimes explosive);
- vertical primary cuts (suitable techniques: explosive and diamond wire, to a much lesser extent: flame and wedge shearing);
- horizontal primary cuts (suitable technique: explosive in simultaneous blasting with the corresponding vertical cut, exceptionally: flame)
- bench slicing secondary cuts (suitable techniques: explosive, diamond wire and wedge shearing);
- block squaring (suitable technique: wedge shearing).

In the near future, waterjet and diamond wire will probably be the winning choice sharing the common feature of precision and smooth cutting.

Due to its technical features waterjet technology could be theoretically applied for all the above operations. Actually there are some technical restrictions which waterjet systems developed so far have not yet overcome.

The first is related to the bench geometry and in particular to the height of the face. When the occurrence of defects of different kinds (flaws, veins, staining minarals, fractures, grain heterogeneity, and so on) is relatively important, the rock must be quarried by adopting subsequent division procedures in order to maximize overall recovery; this condition is met by resorting to a high-bench design allowing a sufficiently large slice area to be available for optimizing the selective block extraction devoid of objectionable defects. For this purpose, faces higher than 8 m may be necessary. Cuts of such a depth can be easily done with drillhole-based metods or with

diamond wire, much less so with waterjet for which kerf depth is limited due to the difficulty of controlling the lance vibration and the wear against the slot walls.

The second drawback is related to the sensitiveness of plain jets to the rock features (grain size, mineral composition, textural and structural properties) and in particular to the presence of difficult-to-cut crossing quartz veins . The consequences are a slowing down or even stoppage of the cutting action with corresponding cost increase and considerable surface roughness with possible nozzle-holder jamming. Although the use of carbide tipped lance heads could be somewhat helpful (Vijay, 1982), the problems still remain, thus steering the choice towards ruder but simpler and more reliable solutions.

Better chances for waterjet application as the integral quarrying method can be reasonably predicted in the case of homogeneous rocks characterized by very low defect frequency and thus giving higher stone recovery dispensing with the need for adopting block selection procedures. In fact under these favourable conditions the low-bench option becomes advisable offering better opportunities for mechanization, easier production scheduling and improved safety. In this case shallow kerfs are required, thus minimizing the problems encountered at depth. (Summers, 1985)

5.0 ECONOMIC EVALUATION

The problem of the optimum choice among different quarrying methods based on either single technologies or suitable combinations can be thereof solved by resorting to suitable computer algorithms that evidence the influence of the various technical, economic, geometrical and operating variables.

A computer program of general application has been set up on the basis of available data of equipment performance and tool productivity for the various instances. Given the quarry situation (rock features, site conditions, fracture spacing, defect frequency and thence quarry recovery and block size distribution) together with the set of external conditions (price and efficiency of productive factors, stone value, restrictions on block face quality) the optimum solution allowing maximum margin of contribution can be devised (kind and size of the equipment, bench geometry). As modern quarrying is organized on a modular basis with little incidence of overhead expenses and fixed burdens, the economic results referred to the product unit are little sensitive to production level and to the size of the operation, provided that manpower, machinery and facilities are exploited at satisfactory efficiency levels. (Berry, 1989)
As regards the application of waterjet technology two different hypotheses are examined here:

1. Integral waterjet quarrying of a granite rock exploitable with a low-bench design (Fig. 8 B) compared with the alternatives consisting of either explosive splitting and wedge shearing (flame for opening cuts only) (Fig. 8 A) or of a combination of explosive splitting (for primary cuts) and diamond wire (for opening and secondary cuts), again resorting to wedging for final block shaping.

2. Combination of diamond wire and waterjet for a high-bench granite quarrying operation (Fig. 7 C) compared with the same methods of point 1.

As shown by figure 8 B, the bench to be worked out with waterjet is first undercut for a suitable length; the main vertical slot, parallel to the face, is then completed and individual blocks are subsequently isolated in ordered sequence by means of orthogonal cuts. All the block faces are cut with a rotating jet lance connected by flexible pipings to separate pumping units.

For the case of high-bench quarrying, the method involving advanced techniques is sketched in Fig. 8 C. First the two concealed vertical faces of the bench are cut with diamond wire, in sequence or simultaneously; then the under-hand slot is opened with waterjet at the base of each slice which is subsequently isolated with the wire and toppled to the floor; the slice is finally inspected for defects, traced out and divided into blocks again with waterjet. The jet lance driving device can be mounted on the articulated arm of a back-hoe excavator for fast installation and ready availability.

The computer simulation results look quite interesting demonstrating that waterjet, alone or in combination with diamond wire, can be competitive on condition that stone worth or quarry recovery or both are sufficiently high.

5.1 Low-bench, whole waterjet quarrying

As regards the first case of integral waterjet quarrying, the new technique can be competitive with explosive splitting provided that a suitable cutting rate is obtained with a sufficiently powerful system.

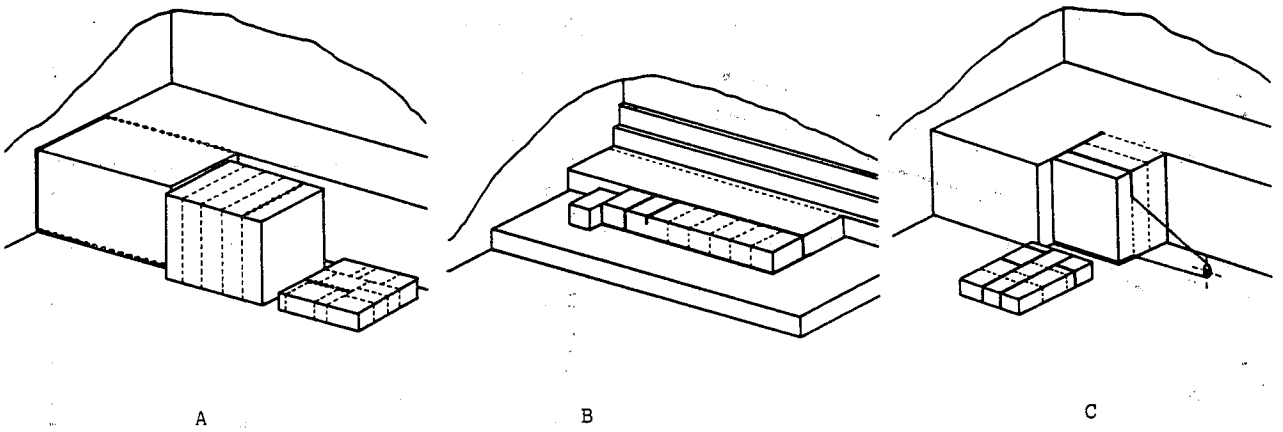

Fig. 8 - Schematic diagram of the quarry operations for the technical options:

A - Base solution (flame for side opening, explosive splitting for primary and secondary cuts, wedge shearing for block squaring and shaping).
B - Integral waterjet quarrying according to low-bench design.
C - Combined innovative technologies (diamond wire for all vertical primary and secondary cuts, waterjet for base slot and all block working cuts).

As shown by the curves of Fig. 9, the economic feasibility of the waterjet solution depends mainly on the cutting rate which in turn is a function of the hydraulic power. Assuming a stone worth 535 US$/m^3, the break-even point is obtained with a 260 kW unit for a stone recovery around 65 %, whereas less power is required in the case of increasing recovery (220 kW at 80 %). With the operating pressure of 250 MPa the jet power of 185/220 kW allows a cutting rate of 2.0/2.5 m^2/h to be obtained, water flow being about 45/53 l/min, across two 1.0/1.1 mm nozzles. These parameters have been calculated starting from the experimental data of 8.3 GJ/m^3 for the specific energy.

Waterjet appears preferable, although at higher quarry recoveries, also to the improved solution where secondary cuts are made with diamond wire.

Of course, for a given equipment break-even points shift towards lower/higher recovery levels for more/less valuable materials. If stone worth falls below 350 US$/m^3, the traditional quarrying method remains unrivalled over the full recovery range, since stone losses (real or due to commercial allowance) are offset by the lower production cost per unit block volume.

5.2. High-bench quarrying with combined innovative techniques

For the case of high bench quarrying involving advanced techniques, the computer simulation results are reported in figure 10 where the economic profit is plotted against the quarry recovery at different stone worth levels.

For diamond wire a cutting rate of 4.2 m^2/h and a wire productivity of 6 m^2/m have been assumed as the input data , while the waterjet exposure rate was taken around 2.5 m^2/h, attainable with a hydraulic jet power of about 220 kW.
The camparison between the available options results as follows:

- At 535 US$/m^3 stone worth, the (WJ + DW) alternative is better than the (FT + ES + WS) basic solution, starting from 35 % quarry recovery, whereas the (ES + DW + WS) intermediate option is left behind from 70 % recovery onwards.

- At 350 US$/m^3, the break-even point of the fully innovative (DW + WJ) alternative against the traditional (FT + ES + WS) solution is found at 65 % recovery whereas the other option is dominated over the full recovery range.

The effect of face smoothness and cut precision is clearly highlighted by the curves. In fact as either stone worth or quarry recovery or both increase, so too does the advantage of using waterjet to the extent that it overtakes the traditional methods which are less expensive but produce more waste and lower pay volume.

It seems interesting to point out that for block cutting operations abrasive waterjet may be a

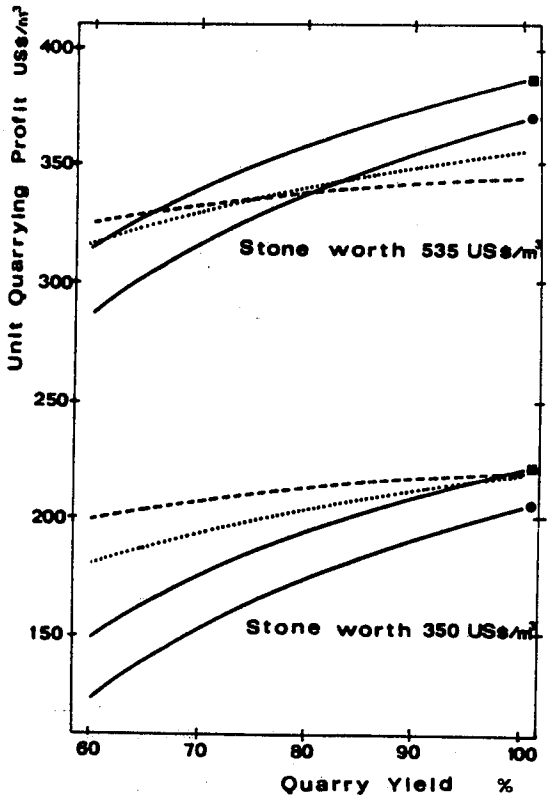

FIG. 9. Economic results of low-bench waterjet quarrying compared with the alternative solutions for stones of different market value:
- classic solution (Explosive Splitting + Wedge Shearing, broken lines);
- improved solution (Explosive Splitting + Diamond Wire sawing + Wedge Shearing, dotted lines)
- integral waterjet quarrying (full lines) with 220 kW (●) or 260 kW (■) units;

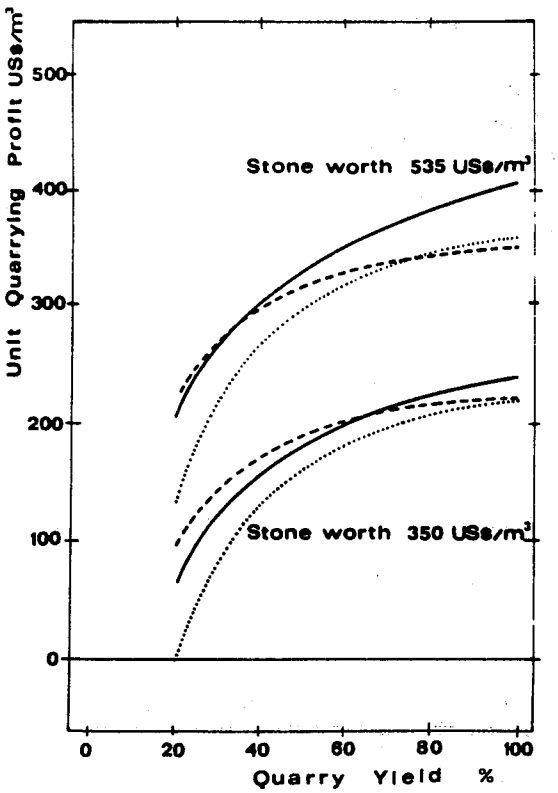

FIG. 10 Economic results of high-bench quarrying for stones of different market value:
- classic solution (Flame Torching + Explosive Splitting + Wedge Shearing, broken lines);
- improved solution (Explosive Splitting + Diamond Wire sawing + Wedge Shearing, dotted lines);
- advanced solution with combined Diamond Wire sawing and Waterjet Kerfing (full lines).

even better solution, being faster than plain jet and consequently less expensive; the problems faced for large area cuts are here less important also because of the presence of lateral free faces providing easy escape for the pulp, thus avoiding any clogging problem.

All the above calculations have been made at the quarrying stage since blocks are sold at the site, loaded onto trucks. However there are additional advantages on the customer's side, deserving some consideration according to the particular instances. They are related to the fact that of the overall block volume only part is recovered in the form of finished slabs or other shaped manufacts at the processing plant, whereas the remaining is rejected at the sawing and trimming stages. The incidence of the lost material increases as long as block shape differ from the ideal parallelepiped with smooth faces. Production costs also rise accordingly.

Firstly freight charges are proportionally affected, the more for farther destinations (stone is marketed all-over-the-world). Secondly sawing cost per unit slab area may considerably increase due to a productivity deterioration related to the unexploited gangsaw room, as well as on account of the larger area to be sawn exceeding the limits of the inscribed rectangle (Actually the overall cost of sawing a given gangsaw load substantially depends on the "whole-rock" block heigth, practically irrespective of the overall slab area to be sawn). Finally higher polishing costs are incurred, for this operation is done before the final trimming.

All this can be avoided should blocks conform to the ideal shape which can be approached by using accurate quarrying techniques like waterjet.

6.0 CONCLUSIONS

The possibility of kerfing hard rocks with high velocity waterjets has been demonstrated both in the laboratory and in the field although its economic competitiveness has not yet been sufficiently proven with continuous industrial application.

In fact whereas the use of plain jets requires the supply of relatively high hydraulic power for adequate cutting rates to be achieved, thus involving considerable capital expenditure for the pump and the equipment, the development of a reliable system based on the use of abrasive jets is still slow to get off the ground. Moreover deep kerfing is still a particularly difficult task due to the presence of increasing lance vibration and the possibility of nozzle-holder jamming due to the slot asperities.

However, for more valuable materials and in the case of high enough quarry yield, waterjet becomes competitive, alone or in combination with diamond wire, compared with explosive splitting and wedging for block squaring due to increasing stone savings which offset the higher cutting cost, thus confirming the principle that ruder techniques are more convenient for cheaper materials recovered from low-yield quarries only, whereas advanced and more sophisticated techniques, although more expensive, are to be recommended for the most favourable situations. For this purpose diamond wire should be used for larger cuts and waterjet for smaller and shallower cuts where it performs with higher reliability and economic competitiveness.

7.0 REFERENCES

1. Bortolussi, A., Ciccu, R., Manca, P.P., Massacci, G.: "Improved technology and planning in modern stone quarries". In: Mine Planning and Equipment Selection, Proc. Int. Symp.,Calgary, Canada, Nov. 1988, pp 107-119.

2. Bortolussi, A., Ciccu, R., Manca, P.P., Massacci, G.: "Prospects of waterjet technology in granite quarrying." In: Proc. 13th Word Mining Congr., Stockholm, Sweden, June 1987, pp 149-159, and references quoted therein.

3. Vijay, M.M., Grattan-Bellew, P.E., Brierley, W.H.: "Drilling of rock with rotating high pressure water jets: influence of rock properties." In: Proc. 6th Int. Symp. on Jet Cutting Technology, USA, 1982, E1 pp 179-198.

4. Summers, D.A.: "A review of water jet excavation research." In: Proc. 26th U.S. Symp. on Rock Mechanics, Rapid City, USA, 1985, pp 895-903.

5. Hilaris, J.A., Bortz, S.A.: "Quarrying granite and marble using high pressure water jet." In: Proc. 5th Int. Symp.on Jet Cutting Tecnology. Hanover, FRG, 1980, pp 229-236.

6. Ciccu, R., Pinzari, M.: "Nuove tecnologie nella coltivazione di rocce ornamentali: il taglio con l'acqua in pressione." In Proc. Int. Convention Quarrying in the year 2000, Carrara, Italy, 1986..

7. Bortolussi, A., Ciccu, R., Manca, P.P., Massacci, G.: "Innovazione tecnologica delle cave di granito in Sardegna: La tecnologia 'Water jet'". In Resoc.Ass.Min.Sarda. 110(2)..

8. Labus, T.J.:" Energy requirements for rock penetration by water jets." In: Proc. 3th Int. Symp. on Jet Cutting Technology, Chicago, USA, 1976, E3 pp 29-40.

9. Labus, T.J.: "Material excavation using rotation water jets." In Proc. 7th Int. Symp. on Jet Cutting Technology, Ottawa, Canada, June 1984, P3 pp 504-516.

10. Raether, R.J., Robison, R.G., Summers, D.A.: "Use of high pressure water jet for cutting granite." In: Proc. 2nd U.S. Water Jet Conf., Rolla, USA, 1983, pp 203-207.

11. Hawrylewicz, B.M., Vijay, M.M., Remisz, J., Paquette, N.: "Design and testing of a rock slotter for mining and quarrying applications." In: Proc. 9th Int. Symp. on Jet Cutting Technology, Sendai, Japan, October 1988, G4 pp 377-386.

12. Summers, D.A., Mazurkiewicz, M.: "Technical and Technological Considerations in the Carving of Granite Prism by High Pressure Water Jets." Proc. 3rd U.S. Jet Conf., May 1985, pp 272-287.

13. Berry, P., Bortolussi, A., Ciccu, R., Manca, P.P:, Massacci, G., Pinzari, M.: "Optimum use of Diamond Wire Equipment in Stone Quarrying" In: Proc. 21st APCOM Int. Symp., Las Vegas, USA,

1989, pp 351-365.
14. Vijay, M.M., Remisz, J., Hawrylewicz, B.M., Puchala, R.J.: " Considerations in the Use of High Speed Water Jets for Deep Slotting of Granite." In: Proc. 4th U.S. Water Jet Conf, Berkeley, USA, April 1987, pp 121-128.

5th American Water Jet Conference
August 29 - 31, 1989: Toronto, Canada

Paper / Communication 6

WATER JET NOZZLE GEOMETRY AND ITS EFFECT ON EROSION PROCESS OF METALLIC MATERIAL

R. Kobayashi, T. Arai AND Y. Masuki,
Faculty of Engineering, Tohoku University
Sendai, Japan

ABSTRACT: The present paper is concerned with experimental studies of nozzle geometry of conically contracting type and orifice type in relation to the water jet structure and the damage process of metallic material caused by impinging of water jet in air. The experiment was made under the condition of 50MPa in injection pressure and a nozzle inner diameter of d = 1mm. Aluminum alloy was used as test metallic material. The contraction angle α, the cylindrical length ℓ and the exit diverging angle θ were independently varied. The results showed that there was little difference between the mass loss of aluminum specimen by using the contraction nozzle and that by the orifice nozzle, while the standoff distance where the maximum mass loss could be taken was remarkably shorter for the orifice nozzle than that for the contraction nozzle. Suitable conditions of the nozzle configuration were recommended to be α = 13° and $\ell = 4d$ for the contraction nozzle and $\ell \geq 2d$ for the orifice nozzle. The exit diverging angle θ larger than 30° did not influence to formation of the water jet.

RÉSUMÉ : La présente communication traite d'études expérimentales sur la géométrie de buses à contraction conique et à orifice et son effet sur la structure du jet d'eau et les dommages causés à un métal par le jet d'eau dans l'air. L'expérience a été réalisée à une pression d'injection de 50 MPa avec une buse de diamètre intérieur d = 1 mm. Un alliage d'aluminium a été utilisé comme métal d'essai. L'angle de contraction α, la longueur cylindrique ℓ et l'angle divergent de sortie θ ont été modifiés tour à tour. Les résultats ont montré qu'il y a peu de différence entre la perte de masse de l'éprouvette d'aluminium avec la buse à contraction et celle avec la buse à orifice, tandis que la distance de projection à laquelle la perte de masse est maximale est beaucoup plus courte pour la buse à orifice que pour la buse à contraction. Les géométrie suivantes ont été recommandées pour les buses: α = 13° et ℓ = 4 d pour la buse à contraction, et $\ell \geq$ 2d pour la buse à orifice. Les angles divergents de sortie θ supérieurs à 30° n'influent pas sur la forme du jet d'eau.

Organized and Sponsored by the National Research Council of Canada and the U.S. Water Jet Technology Association.

1.0 INTRODUCTION

The water jet nozzle plays an important role in the water jet technology. Several ideas were previously presented for constructions of the nozzle with use of center body or vanes. Yanaida (Ref.1) compared the characteristics of water jet issuing from some typical nozzles. Nozzles with different conical contraction angles and straight cylindrical lengthes were also tested (Refs.2 and 3). Shavlovsky (Ref.2) gave attention to a continuous core length of water jet in air in relation to the nozzle configuration. Louis et al.(Ref.3) tried to find suitable conditions of the conical nozzle configuration by using aluminium specimens in submerged water jet accompaning cavitation. The present paper describes experimental studies of the nozzle configuration of conical and orifice types in relation to the water jet structure and the damage process of metallic material which was caused by impinging of water jet in air, and discusses suitable conditions of the nozzle configuration for the water jet technology.

2.0 EXPERIMENTAL APPARATUS AND PROCEDURE

Figure 1 shows a schematic diagram of the experimental apparatus. Tap water, as working fluid, was pressurized in the range of 30MPa to 90MPa by a three-throw plunger pump and injected horizontally from a test nozzle into still air. The injection pressure was measured by a pressure transducer at the inlet of the nozzle. The test specimen adopted in the present investigation was aluminium alloy of 50mm square and 10mm thickness. Relative position of the test specimen to the nozzle exit could be set up optionally by use of a three-dimensional traverse apparatus. The mass loss M of each specimen due to damage was measured using a chemical balance.

Figure 2 shows a schematic geometry of the water jet nozzle tested. The contraction angle α, the cylindrical length ℓ and the exit diverging angle θ were independently varied. Table 1 gives main dimensions of eight contraction nozzles and six orifice nozzles (α = 180°). The ratio of the cylindrical length ℓ to the nozzle exit diameter d was varied from 0 to 8. The contraction angle α was varied between 10° and 20° for the contraction nozzle, while the exit diverging angle θ was between 30° and 180° for the orifice nozzle. The test nozzles were made of carbon steel (S45C) and the nozzle exit was d = 1mm in diameter. The inner surface was finished smoothly by reaming. The structure of the water jet was observed by a method of shadow photography using a stroboscope with a flashing time of 0.8μs.

3.0 RESULTS AND DISCUSSIONS

3.1 Mass Loss

Figure 3 shows the mass loss curves representing the relation between the mass loss M caused by impinging of the water jet and the standoff distance x from the nozzle exit to the test specimen for the exposure time t = 60s and the injection pressure P = 50MPa. As the previous paper (Ref.4) made clear, there exist two peaks on the mass loss curve. We call them the first peak (near the nozzle) and the second peak (far from the nozzle). It was confirmed that the other nozzles tested had also two peaks on their mass loss curves. It can be seen in Fig.3 that the location of the peak for the orifice nozzle (0418) is different from that for the contraction nozzle (C418).. It shows that the location of the peaks on the mass loss curve is strongly affected by the geometry of the nozzle.

Figure 4 gives effect of the cylindrical length ℓ/d on the mass loss M at the first and the second peak locations for both the cases of the contraction nozzle (α = 13°) and the orifice nozzle. The magnitudes of the mass loss at both the peak locations increase with decreasing the cylindrical length ℓ/d for the contraction nozzle , while, for the orifice nozzle, there is no effect of ℓ/d on the mass loss at the second peak location.

Figure 5 is the standoff distances x/d corresponding to Fig.4. It can be clearly seen that the standoff distance x/d for the second peak of the contraction nozzle (α = 13°) increases from about 400 to 800 as the cylindrecal length ℓ/d increases from 0 to 8. The second peak location (x/d = 400) for the orifice nozzle and the first peak locations (x/d = 30 and 100) for the nozzles of both types do not change for variations of the cylindrical length ℓ/d. Therefore, for the contraction nozzle the cylindrical length ℓ/d = 4 is recommendable, and a larger length ($\ell/d \geq 4$) brings no desirable contribution. It should be also remarked in field applications that the location of the first and the second peaks is quite different between the contraction nozzle and the orifice nozzle.

Figures 6 and 7 represent effects of the contraction angle α on the mass loss and the standoff distance at the two peak locations. There exists an optimum angle $\alpha = 13°$ for the maximum mass loss. The present results are well coincide with a previous result by Shavlovsky (Ref.2), who gave the optimum condition of $\alpha = 10°$ to $14°$ and $\ell/d = 4$, though his optimum condition was defined as the maximum length of "constant velocity core in continuous water jet". It can be, therefore, concluded that the combination of $\alpha = 13°$ and $\ell/d = 4$ is the most suitable as the geometry of the contraction nozzle.

Figures 8 and 9 show effects of the exit diverging angle θ for the orifice nozzle ($\ell/d = 4$) on the mass loss M and the standoff distance x/d at the first and the second peak locations, respectively. It is seen that erosion performance of the orifice nozzle is improved little by adding the exit diverging cone.

3.2 Damage Pattern of Specimen

Figure 10 represents damaged surfaces of aluminium for the three nozzles (C013, C413 and 0218) at various standoff distances x/d under the conditions of the injection pressure P = 50MPa and the exposure time t = 60s. The damaged surfaces could be classified into three patterns. The first is a petal-like pattern which is seen in a region from the nozzle exit to the first peak location on the mass loss curve shown in Fig.3. The second is a circular pattern which has rather small damaged area and can be seen in a range near to the first peak. The third is a cone-shape pattern which appears in a region near to the second peak.

Figure 11 shows structures of the water jets over a range from the nozzle exit to the breakup region for three nozzles of Fig.10. The structure of tha water jets could be roughly divided into the following three parts (Ref.5). The first is a region near the nozzle, where the water jet is continuous and cylindrical and there are small droplets around the jet. The damage pattern corresponding to this region makes the petal-like pattern as shown in Fig.10. In the second part, there exist large deformations of the water jet and the deformations are grown up downstream. This part corresponds to a range from the first peak location to the second peak location on the mass loss curve. In the third part, the deformation reaches the jet center, where the water jet breaks up into water lumps and droplets. This part corresponds to a range near to the second peak location on the mass loss curve and also corresponds to the third region where the damage surface shows the cone-shape pattern. Consequently, It is clear from the experiment mentioned above that the erosion patterns and the magnitude of the mass loss of the material have a close correlation with the structure of the water jet.

It was confirmed by a detailed observation that the air-water interface of the water jet just downstream from the nozzle exit was smoother for the orifice nozzle (0218) than that for the other two contraction nozzles. The breakup length is, however, shorter for the orifice nozzle, where the breakup length represents a length from the nozzle exit to a location of the water jet breakup. Therefore, it is considered that the magnitude of the initial surface disturbance has not a direct effect on the breakup length and thus the second peak location on the mass loss curve.

3.3 Sharpness of Damage

Figure 12 shows the ratio H/D of a damage depth H to an equivalent diameter $\bar{D}$ of the damage zone. The ratio H/D is considered to be one of the important parameters related to the precision of the cutting processing. It is seen from Fig.12 that the ratio H/D takes peak values of about 0.6 at x/d = 150 and 400 for the contraction nozzle and at x/d = 50 for the orifice nozzle. It is clear from the comparison between Figs.5 and 12 that these locations are just downstream of the first peak on the mass loss curve for both cases. Figure 12 also indicates that the value of H/D is smaller for the orifice nozzle than that for the contraction nozzle in a region far from the nozzle. It can be, therefore, suggested that a short standoff distance near the first peak will be suitable for the purpose of precision processing.

It was found that the peak value of H/D receives little effect of the cylindrecal length ℓ/d and the contraction angle α for the contraction nozzle and also no effect of ℓ/d and the exit diverging angle θ for the orifice nozzle.

4.0 CONCLUSION

The present results are summarized as follows :

(1) There was little difference between the mass loss of aluminium specimen by using the contraction nozzle and that by the orifice nozzle. However, the standoff distance, where the maximum mass loss can be taken, is remarkably shorter for the orifice nozzle than that for the contraction nozzle.

(2) It can be recommended as suitable conditions of the nozzle configuration that the contraction nozzle is of the converging angle $\alpha = 13°$ and the cylindrical length $\ell/d = 4$, while the orifice nozzle of $\ell/d \geq 2$. The exit diverging angle θ larger than 30° gives no influence on the formation of the water jet.

(3) The ratio H/D of the depth to the effective diameter of the damage area becomes the maximum value just downstream of the first peak location. The maximum mass loss can be obtained at the second peak location.

5.0 REFERENCES

1. Yanaida, K. : "Flow Characteristics of Water Jets." In: Proc. 2nd Int. Symp. on Jet Cutting Technology, Cambridge, England, April 1974, pp. A2/19-32.

2. Shavlovsky, D.S.: "Hydrodynamics of High Pressure Fine Continuous Jets." In : Proc. 1st Int. Symp. on Jet Cutting Technology, Conventry, England, April 1972, pp. A6/81-92.

3. Erdmann-Jesnitzer, F., Hassan, A.M. and Louis, H.: " A Study of the Effect of Nozzle Configuration on the Performance of Submerged Water Jets." In: Proc. 4th Int. Symp. on Jet Cutting Technology, Canterbury, England, April 1978, pp. A2/21-38.

4. Kobayashi, R., Arai, T. and Yanada, H. : "Structure of a High-Speed Water Jet and the Damage Process of Metals in Jet Cutting Technology." In: Japan Soc. Mech. Engrs. Int. J., Ser. 2, Vol. 31, No.1, February 1988, pp. 53-57.

5. Kobayashi, R. and Arai, T.: "Local Structure of Water Jet and Related Erosion Process of Metallic Materials." In: Proc. 9th Int. Symp. on Jet Cutting Technology, Sendai, Japan, October 1988, pp. D1/155-164.

TABLE 1. MAIN DIMENSIONS OF WATER JET NOZZLES TESTED

1. *CONTRACTION NOZZLE* (θ=180°, d=1mm)

α \ ℓ/d	0	2	4	6	8
10°					C810
13°	C013	C213	C413	C613	C813
16°					C816
20°					C820

2. *ORIFICE NOZZLE* (α=180°, d=1mm)

θ \ ℓ/d	2	4	8
30°		O403	
60°		O406	
120°		O412	
180°	O218	O418	O818

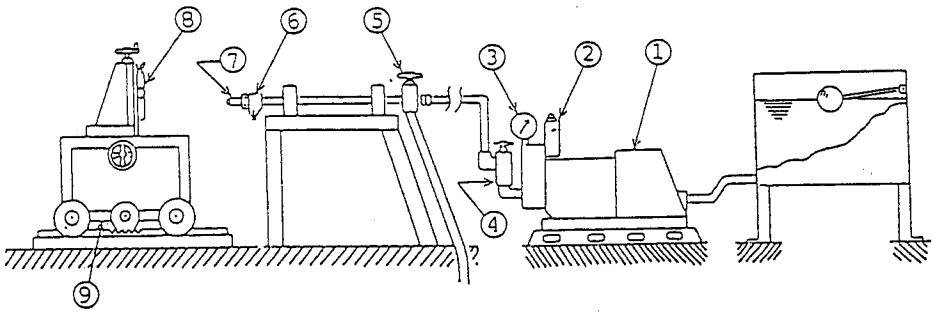

① Pump ② Pressure Control Valve ③ Pressure Gauge
④ Release Valve ⑤ Control Valve ⑥ Pressure Transducer
⑦ Nozzle ⑧ Specimen Holder ⑨ Traverse Unit

FIG. 1 EXPERIMENTAL APPARATUS

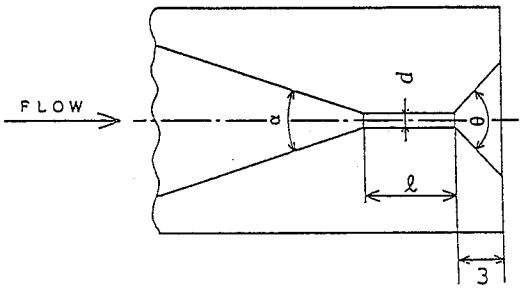

FIG. 2 SCHEMATIC GEOMETRY OF WATER JET NOZZLES TESTED

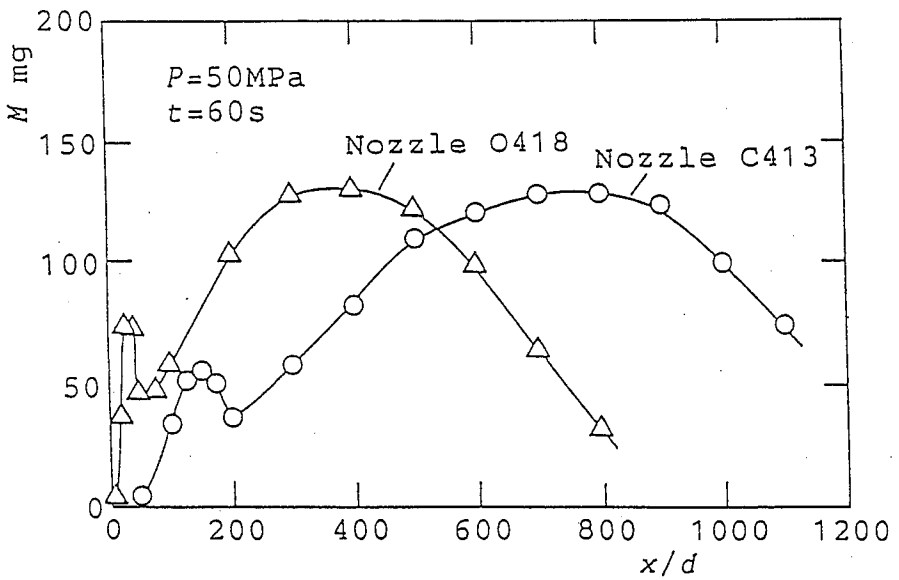

FIG. 3 MASS LOSS CURVES FOR CONTRACTION NOZZLE(C413) AND ORIFICE NOZZLE (O418)

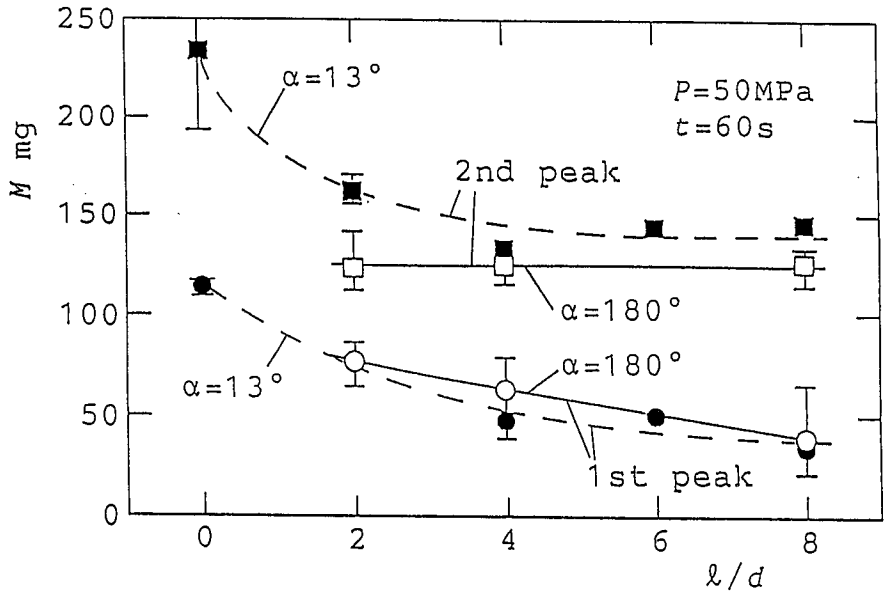

FIG.4 PEAK MASS LOSS M IN RELATION TO CYLINDRICAL LENGTH ℓ/d FOR CONTRACTION NOZZLES(α=13°) AND ORIFICE NOZZLES(α=180°)

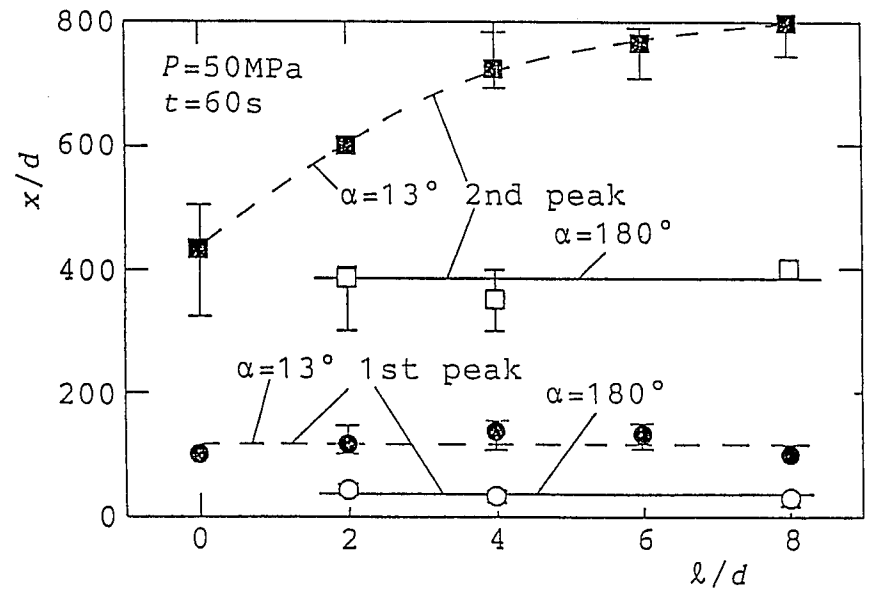

FIG. 5 STANDOFF DISTANCE OF PEAK LOCATIONS CORRESPONDING TO FIG.4

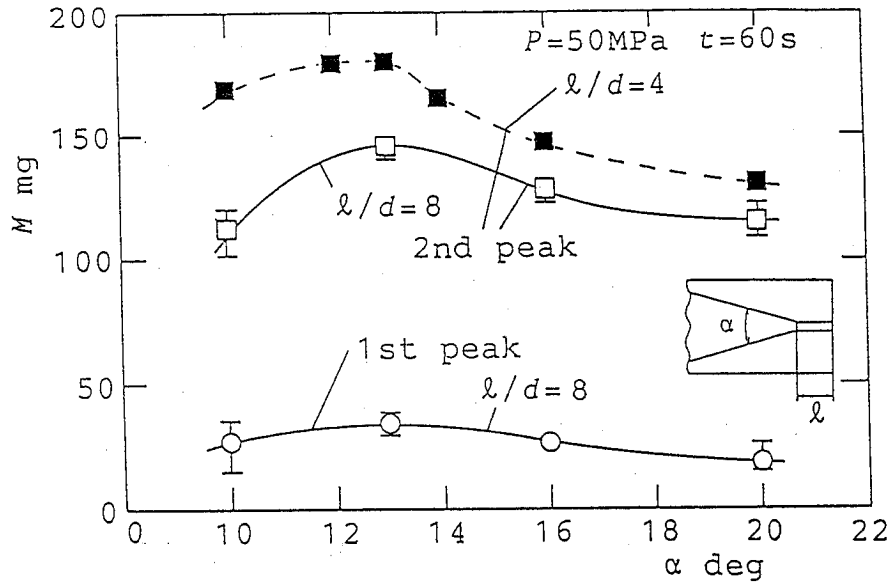

FIG. 6 PEAK MASS LOSS M IN RELATION TO CONVERGING ANGLE α FOR CONTRACTION NOZZLE

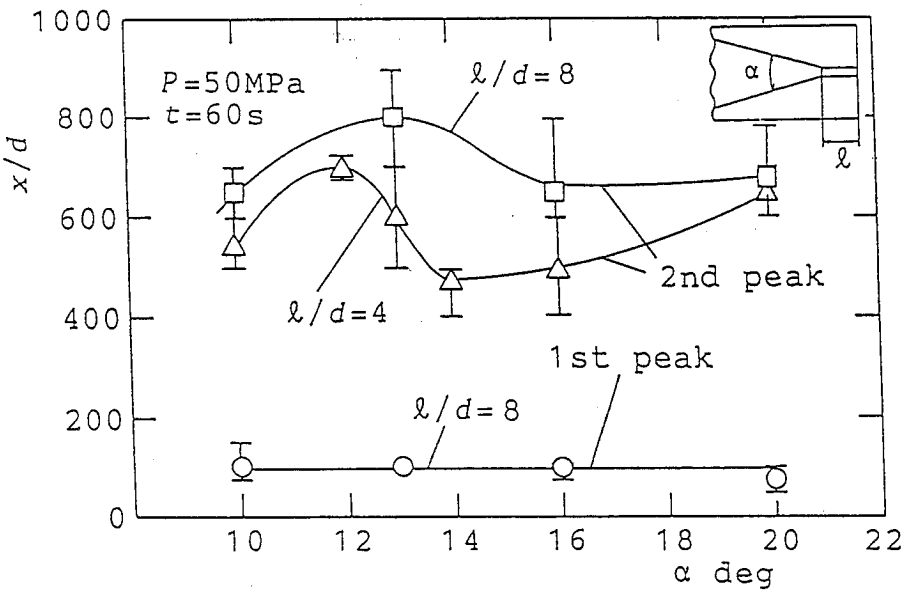

FIG. 7 STANDOFF DISTANCE OF PEAK LOCATIONS CORRESPONDING TO FIG.6

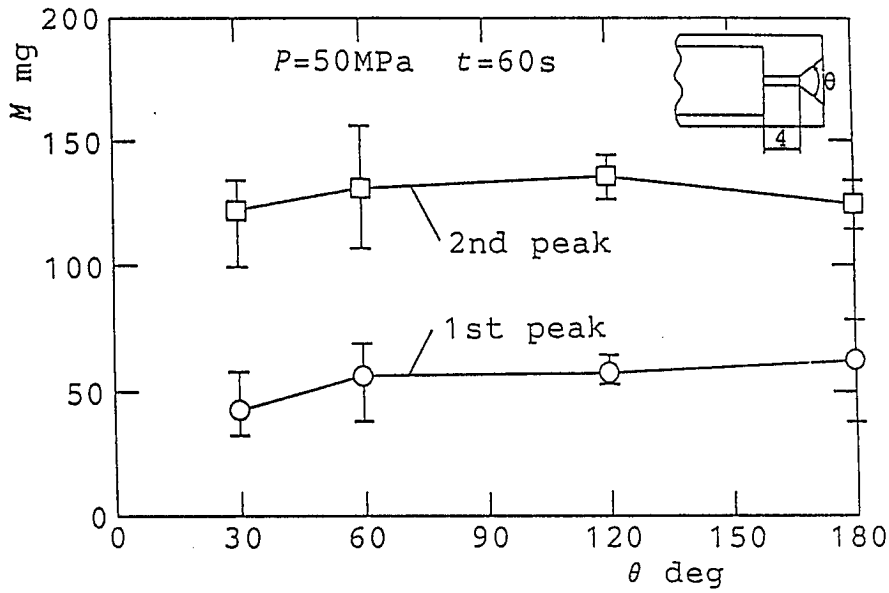

FIG. 8 PEAK MASS LOSS M IN RELATION TO EXIT DIVERGING ANGLE θ FOR ORIFICE NOZZLES

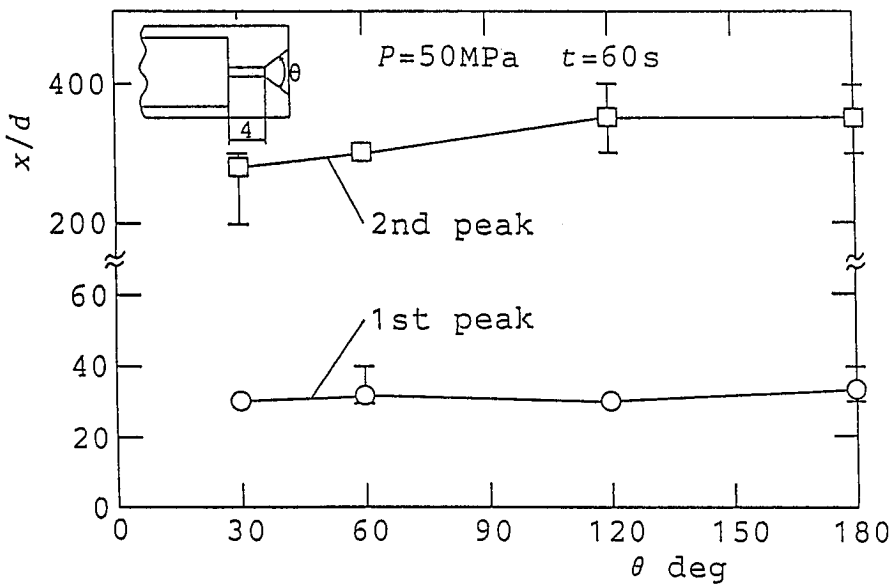

FIG. 9 STANDOFF DISTANCE OF PEAK LOCATIONS CORRESPONDING TO FIG. 8

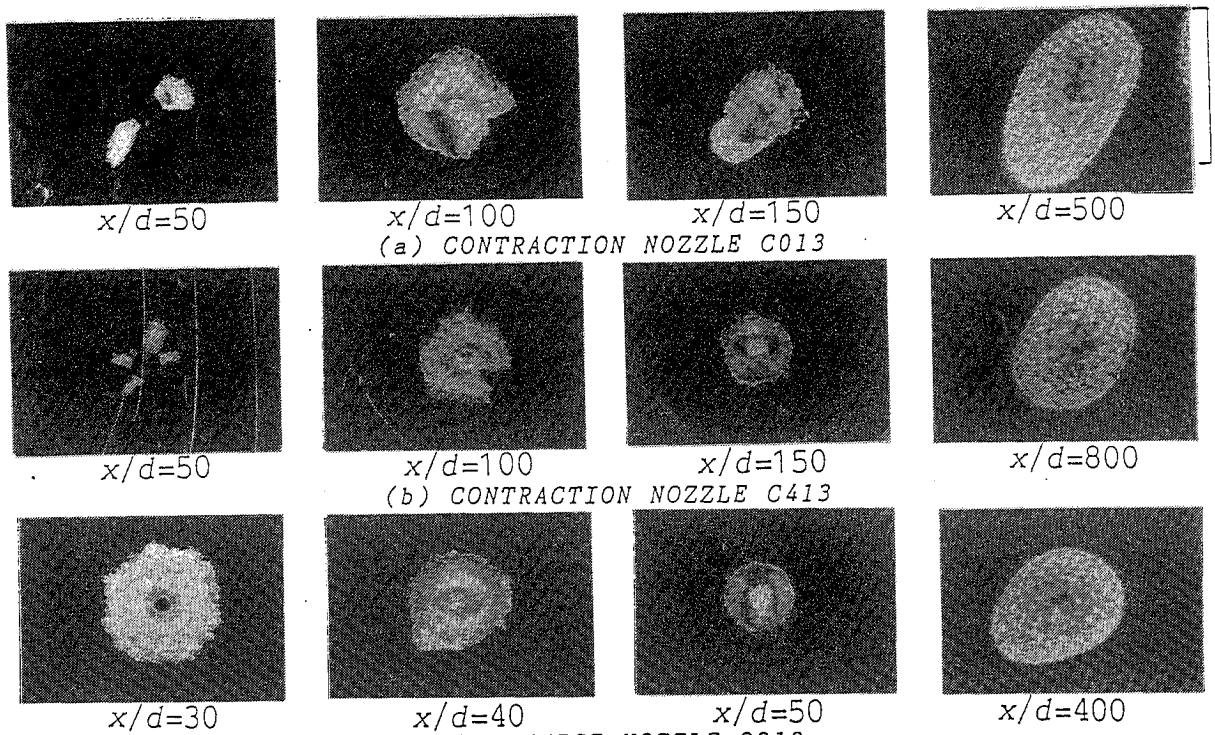

FIG. 10 CHANGE OF DAMAGED SURFACE WITH STANDOFF DISTANCE
(A1 , P=50MPa , t=60s)

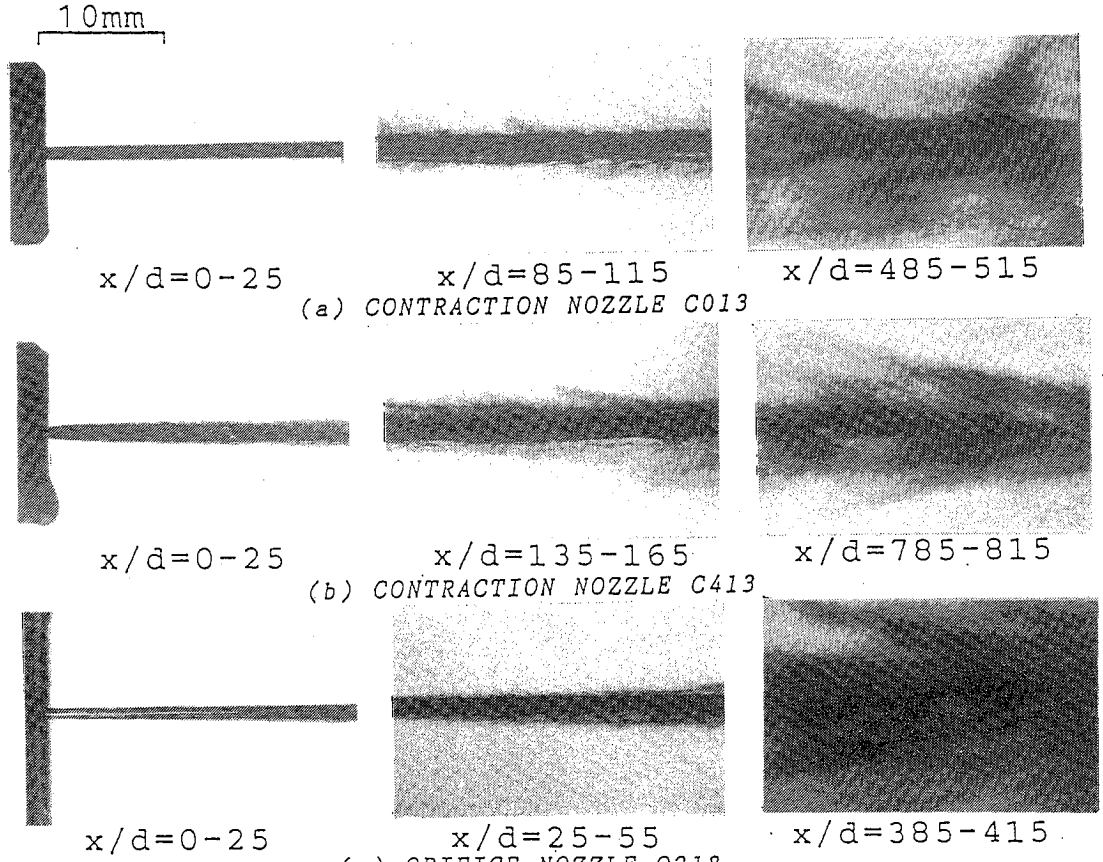

FIG. 11 STRUCTURE OF WATER JET (P=50MPa)

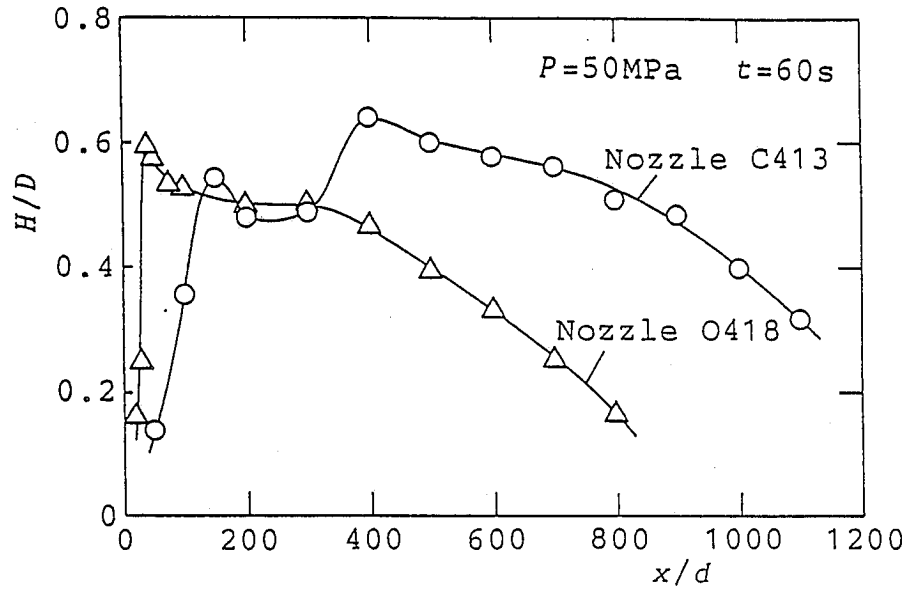

FIG. 12 SHARPNESS OF DAMAGE FOR CONTRACTION NOZZLE (C413) AND ORIFICE NOZZLE (O418)

5th American Water Jet Conference
August 29 - 31, 1989: Toronto, Canada

Paper / Communication 7

INVESTIGATION OF FORCES EXERTED BY AN ABRASIVE WATER JET ON A WORKPIECE

H.Y. Li, E.S. Geskin AND W.L. Chen
New Jersey Institute of Technology
Newark, NJ 07102, USA

ABSTRACT: This study is concerned with the development of a practical procedure for the measurement of forces exerted on a workpiece in the impingment zone. Two piezoelectric transducers of Kistler Co. measuring three components of the force were used to construct an experimental setup. The output of the transducers through an amplifier is connected to readout devices. This set up enables us to investigate the dynamics of the force development. In order to validate the designed procedure, the forces are measured simultaneously by the transducer and strain gauge. The difference between two measurements does not exceed 5 %. Monitoring forces developed by a water jet containing and not containing abrasive particles reveal some peculiarities of jet behavior.

RÉSUMÉ: Cette étude porte sur la mise au point d'une méthode pratique de mesure des forces exercées sur une éprouvette dans la zone d'impact. Deux transducteurs piézoélectriques de Kistler Co. mesurant les trois composantes de force ont été utilisés pour construire un montage expérimental. La sortie des transducteurs a été amplifiée et reliée à des dispositifs d'affichage. Pour valider la méthode, on mesure les forces simultanément au moyen des transducteurs et d'un extensomètre. La différence entre les deux mesures ne dépasse pas 5 %. La surveillance des forces exercées par un jet d'eau exempts d'abrasif révèle quelques particularités du comportement des jets.

Organized and Sponsored by the National Research Council of Canada and the U.S. Water Jet Technology Association.

1.0 INTRODUCTION

The forces developed in the impingment zone provide substantial information about the process of water jet cutting. For examples, the effects of operational conditions on these forces enable us to estimate the optimal range of process variables. The information about the forces developed in the course of the jet- work piece interaction can be used for the design of cutting facilities and the control of water jet cutting. The study of the forces generated in water jet cutting was carried by Kim[1978], Hashish[1982] and Kesavan[1985]. However, those studies do not contain the details of the relationship between operational variables and forces. The determination of such a relationship is the objective of the presented paper. This paper is concerned with the development and verification of a new measurement procedure as well as estimating the effect of the process variables on the forces.

2.0 EXPERIMENTAL APPARATUS

The measuring system used in this study(Fig. 1) includes two piezoelectric force transducers, a charge amplifier and read-out devices. The jet emanating from the sapphire nozzle or carbide tube exerted force on the work-piece. Proper setting of each component of this measurement system can assure a sufficient measuring range and the accurate magnitude of the forces.

A steel plate with six holes, which are used to attach this steel plate and an insulating wood plate to the transducers, constitutes a work-piece. The diameter of the hole is 0.0375 inch. The selected design minimizes heating and vibration of the transducer.

Two Kistler three-component force measurement platforms (model 9257A) are used in this study[1971]. The interaction between the jet and workpiece results in the generation of electric current by transducers. This current is transmitted to the charge amplifier, where the signal is converted to voltage, proportional to the force acting on the workpiece. The voltage is measured by read-out devices.

A digital multi-meter(Fluck model 8010A) and a multi-channel pen recorder are used as read-out devices. A Nicolet digital oscilloscope connected to computer will be used as read-out devices in the future.

This experiment was carried out in the Ingersoll Rand robotic workcell. The jet was generated by the use of Ingersoll rand nozzle for the abrasive water jet.

3.0 EXPERIMENT PROCEDURE

The first stage of this experiment involved validation of the measurement procedures. The force was measured in different locations on the work-piece. The results of this measurement(Fig. 2 and 3) show that the position of the impingment did not affect reading. The validity of the presented technique was also estimated by comparing the results of the force measurements produced by the developed system(Fig. 1) and Lebow strain gauge (model 3168). This result(Fig. 4) validated the developed measurement technique. The calibration of the measuring system was carried out by loading a transducer of known weight.

In the course of the experiment, the value of forces was measured at different magnitudes of process variables.(Table 1 and 2) The coaxiality of the carbide tube and sapphire nozzle was checked to assure the consistency of experiment conditions. The effect of the destruction of the work-piece in the impingment zone was eliminated by changing the impinging position on the work-piece. This assured the stability of the stand-off distance.

4.0 RESULTS AND DISCUSSION

4.1 Pure water jet

In this study, we determined the effects of the different stand-off distances, sapphire nozzles, and carbide tube exit areas on the forces developed at the impingment zone. The experiment results are given in Fig. 5 and 10.

The effect of the sapphire exit area is shown in Fig. 5. As followed from the depicted charts, this area is the principal variable in determining the jet force which is directly proportional to the exit area. The effect of other process variables is much smaller than the effect of the sapphire diameter.

In Fig 6 the relationship between the force and stand-off distance at different carbide exit areas is given. These graphs show that the force always has the maximum value at the stand-off distance ranging from 12.7 mm to 25.4 mm. At a comparatively small distance between the nozzle and the workpiece ,closed contact between the reflected and direct flow causes an extensive energy dissipation in the jet. Increasing this distance reduces and then totally eliminates losses due to the flow reflection from the workpiece surface but increases the energy dissipation in the direct jet. The total change of the jet force due to the change in the stand-off distance does not exceed 10-15 %. This demonstrates

that the jet preserves a strong penetrative ability along the distance of the 100 diameter of the carbide tube. As demonstrated by Fig. 6, increasing the carbide tube diameter increases the force due to reduction of the friction losses in the tube, but the overall effect of this variable is not significant in practical operation.

4.2 Abrasive water jet

The effect of the sapphire diameter on the jet force are shown in Fig. 7. As followed from the constructed graph, the sapphire diameter is also the principal variable determining the value of the force.

A curve representing the effect of the stand-off distance on the force has a maximum at the distance of 10-25 mm shown in Fig. 8. Force extremity for the abrasive water jet, as well as pure water jet, probably is due to the excessive energy dissipation at the impingment zone at a small stand-off distance and energy dissipation in the water flow at a large stand-off distance..

The abrasive flow rate has a comparatively complex effect on the jet forces.(Fig. 9) At a small diameter of sapphire(0.004, 0.005, 0.007 inch diameter), the increase in the flow rate reduces the force in the impingement zone, while at the large sapphire diameter(Fig. 10) the increase in the flow rate elevates the force. The effect of carbide tube exit area on the jet momentum is similar to that of a pure water jet.

5.0 CONCLUSIONS

This performed experiment enables us to determine some important phenomena occurring in the course of water jet cutting. It was found that at a constant stagnation pressure the momentum of the jet and the forces developed in the impingment zone are practically determined by the water flow rate. The relationship between the forces and stand-off distance has a maximum. However, the variation of the change of the forces caused by different stand-off distance, not exceeding 10-15 %, is not significant.

The carbide tube diameter, flow rate and size of the abrasive have a secondary effect on the flow momentum. However, at some conditions, these variables can substantially change the flow development.

6.0 ACKNOWLEDGEMENT

This work was partially supported by the NSF grant DMC8810659.

7.0 REFERENCES

[1] D.C. Hunt, T.J. Kim, J.G. Sylvia. *A Parametric Study of Abrasive Water Jet By Piercing Experiment.* Sept. 1978

[2] M. Hashish. *High-Pressure Water Jet Cutting Techniques* Jet Cutting Technology, Apr. 1982

[3] S.K. Kesavan, N.P. Reddy. *Measurement of Dynamic Impact Trust Exerted By High Frequency Liquid Jet.* Experiment Technical, Sept. 1985.

[4] G. H. Gautschi. *Cutting Forces in Machining and The Routine Measurement with Multico mponent Piezoelectric Force Transducer.* Proceeding of the 12th International Machine Tool Design and Resear ch Conference. 1971

THE RANGE OF PROCESS VARIABLES IN THE COURSE OF EXPERIMENT

VARIABLES	NOTATION	VALUE	UNIT
STAND-OFF DISTANCE	Z	2.54, 12.7, 25.4, 50.8, 76.2	mm
SAPPHIRE NOZZLE DIAMETER	N	4, 5, 7, 10, 14	0.001 inch
CARBIDE TUBE DIAMETER	C	30, 43, 63	0.001 inch
ABRASIVE SIZE	S	50, 80, 120, 220	MESH
ABRASIVE FLOW RATE	m	0, 5, 10	SET POINT ON THE CONTROLLER

ABRASIVE FLOW RATE 0 IS PURE WATER JET.

ABRASIVE FLOW RATE IN g/min FOR DIFFERENT ABRASIVE SIZE ARE GIVEN IN TABLE 2.

TABLE 1.

ABRASIVE FEED CALIBRATION(g/min)

ABRASIVE SIZE/SET POINT	50 MESH	80 MESH	120 MESH	220 MESH
0	0	0	0	0
5	150	109	118.5	64
10	540.75	447	498.5	318.5

TABLE 2.

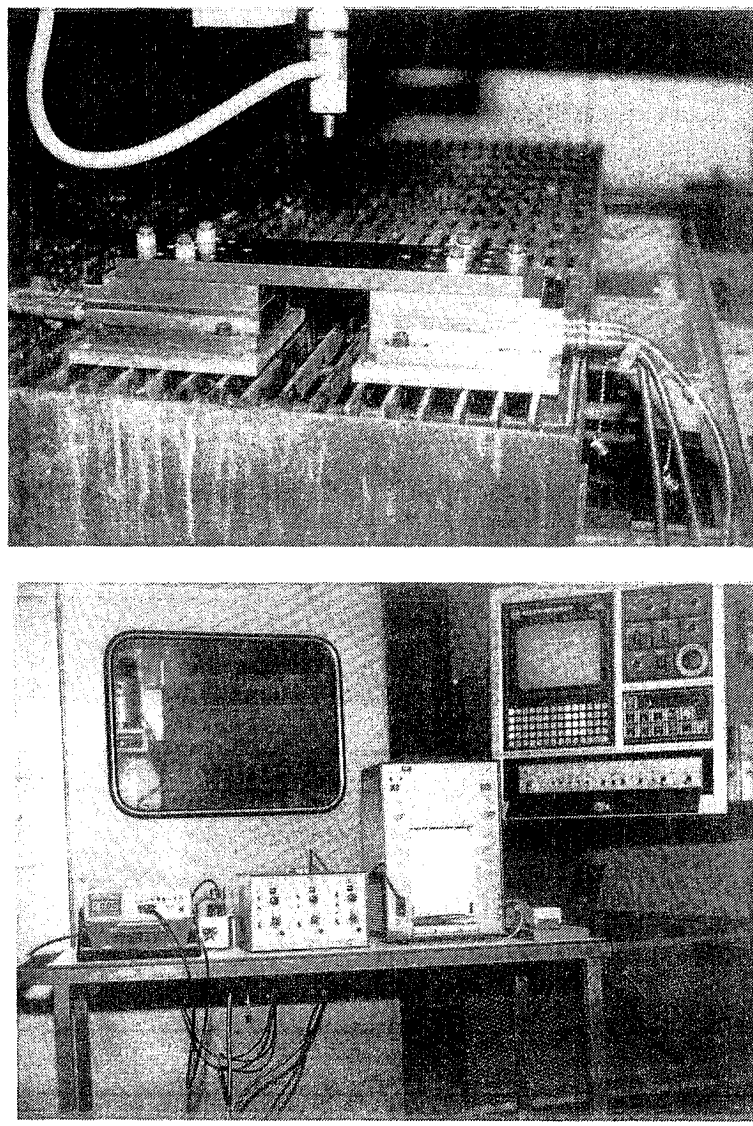

Fig. 1: Experimental setup.
(a)Work piece and transducer.
(b)Amplifier and read out devices.

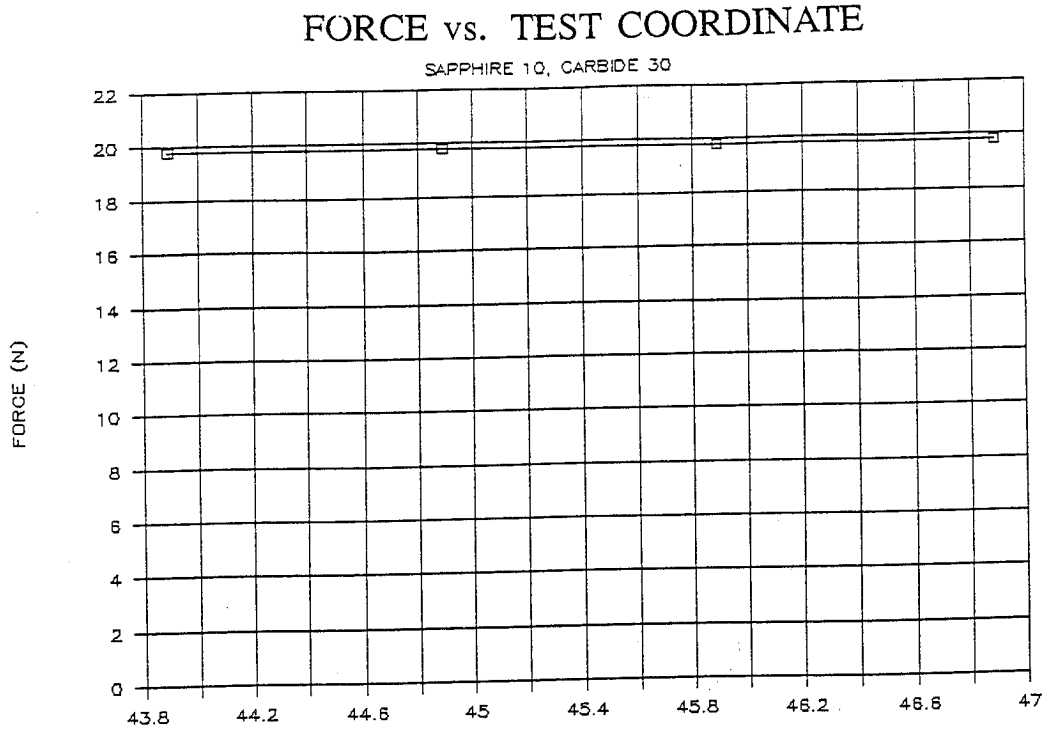

Fig. 2: Effect of the position (X direction) of the impingment zone on the force of a pure water jet.
Notice the zero correlation between the jet position and the force.

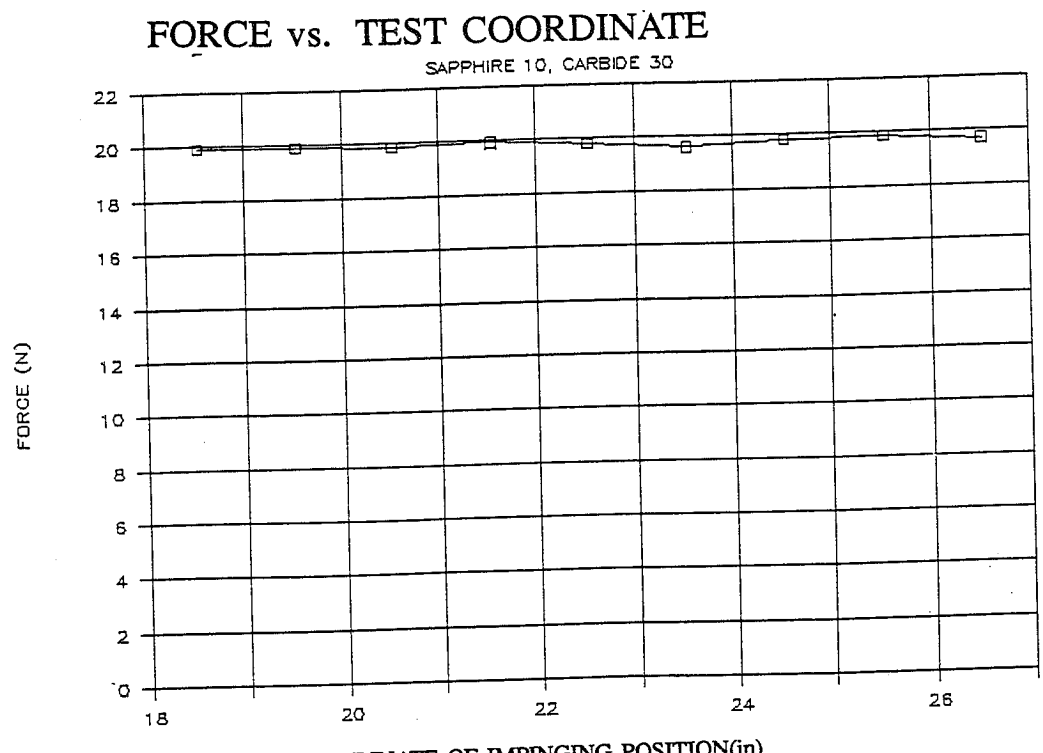

Fig. 3: Effect of the position (Y direction) of the impingment zone on the force of a pure water jet.
Notice the zero correlation between the jet position and the force.

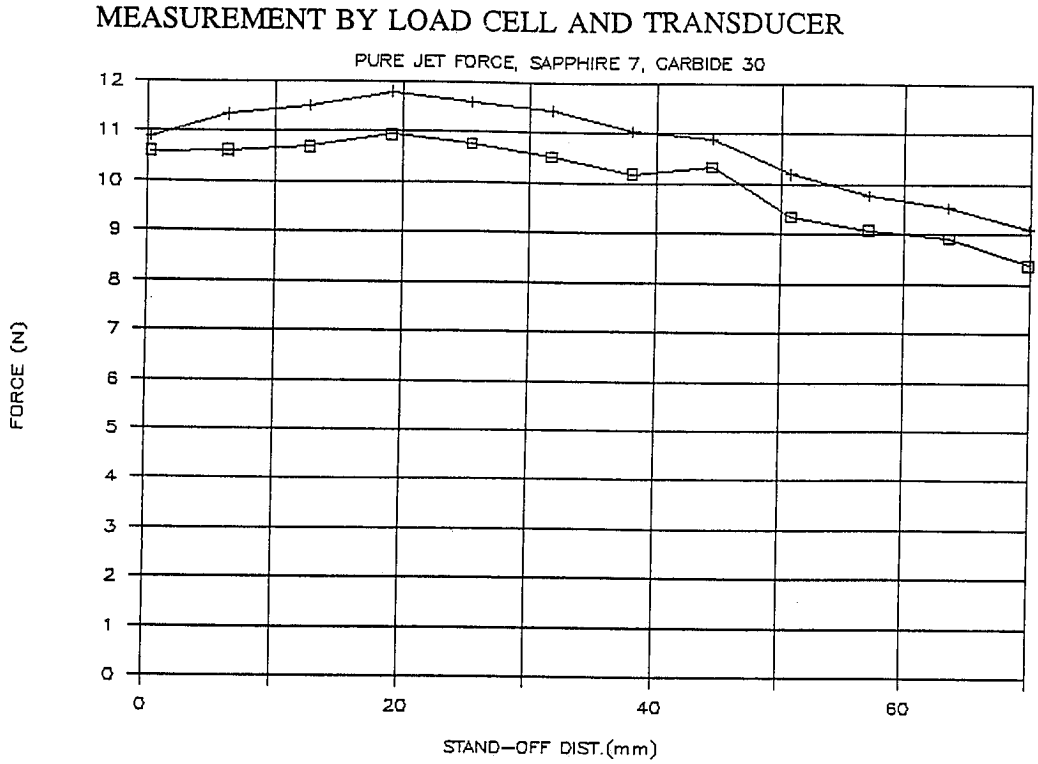

Fig. 4: Measurement of the force by the Kistler transducer and the Lebow load cell.
Notice the strong correlation between the results of the measurement by two devices.

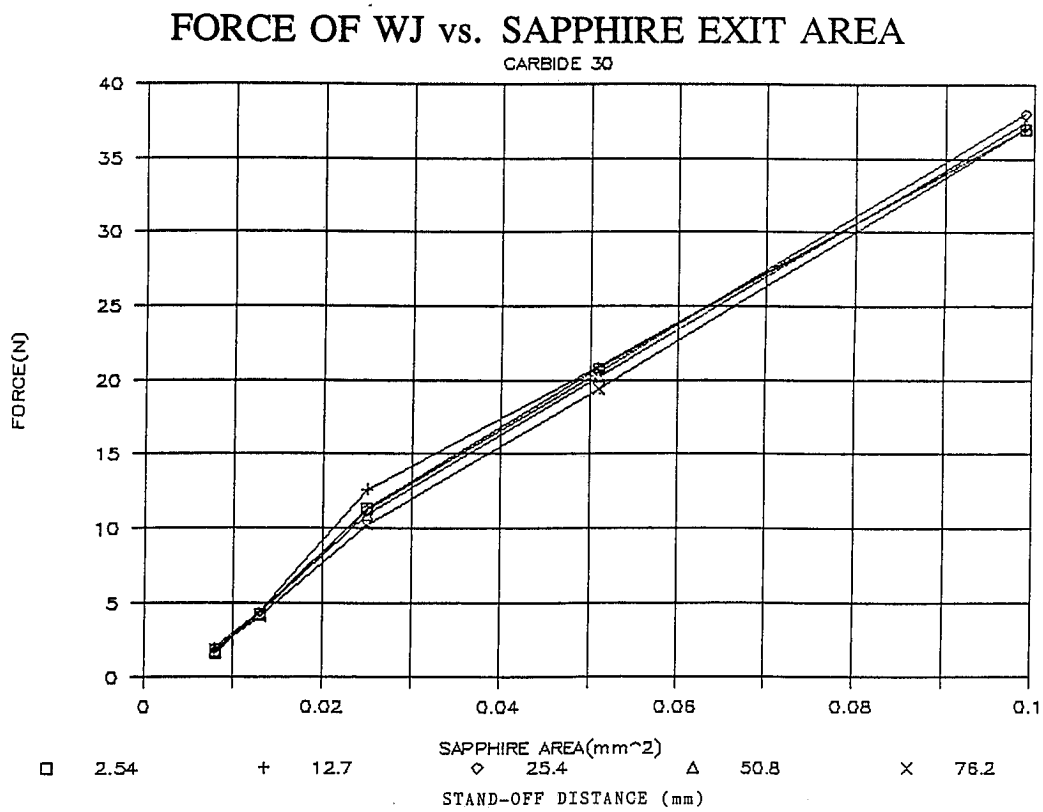

Fig. 5: Effect of the sapphire exit area on the force for a pure water jet.
Notice the proportionality between the area and the force and compara tively low effect of other factors.

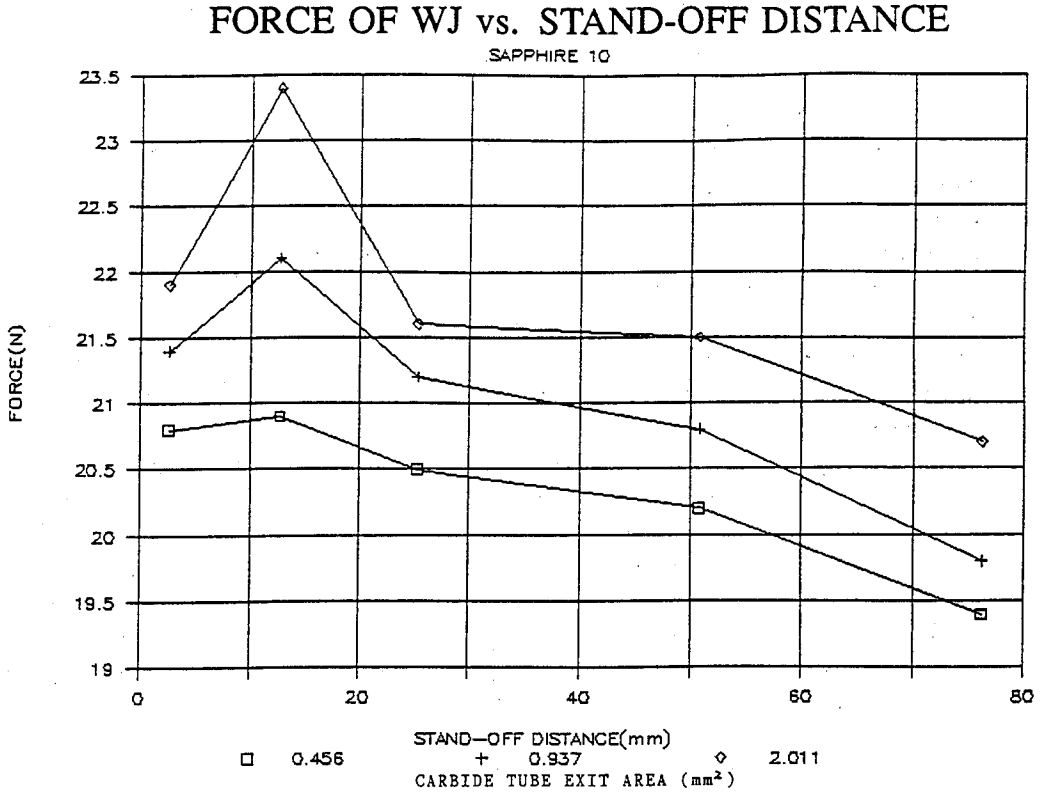

Fig. 6: Effect of the stand-off distance and carbide tube exit area on the force for the abrasive water jet.
Notice the existence of the extremum at this relationship.

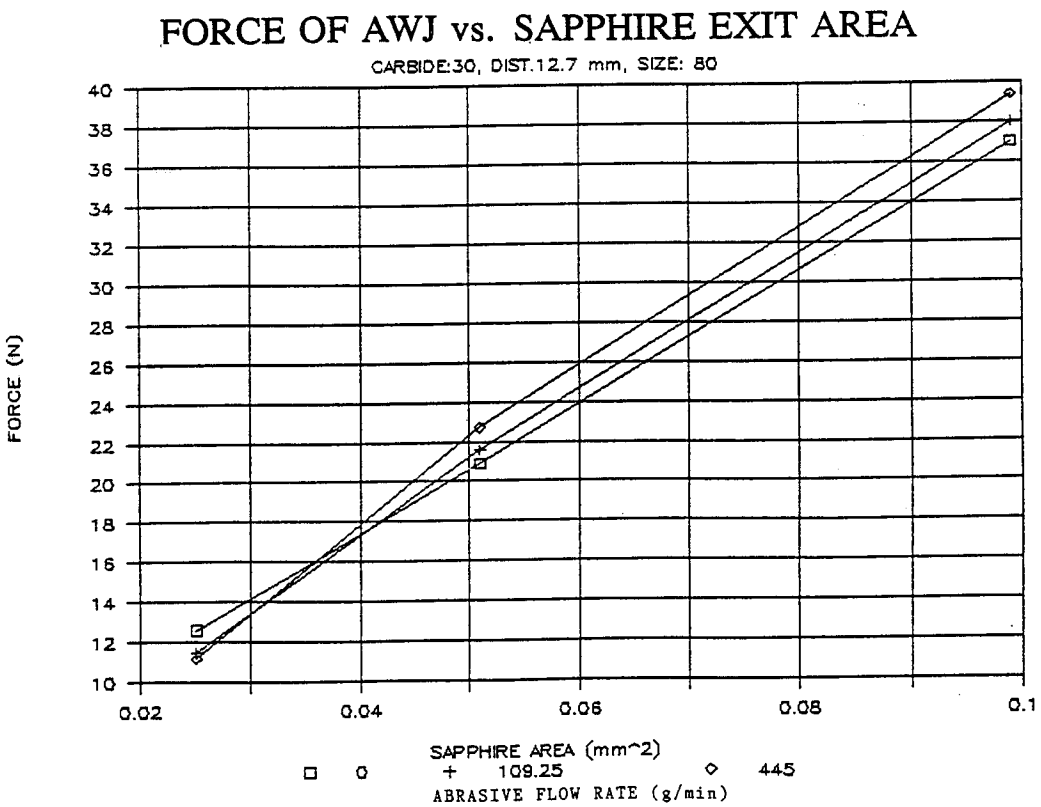

Fig. 7: Effect of the the sapphire exit area on the force of the abrasive water jet.
Notice the proportionality between the exit area and the force and comparatively loe effect of other variables.

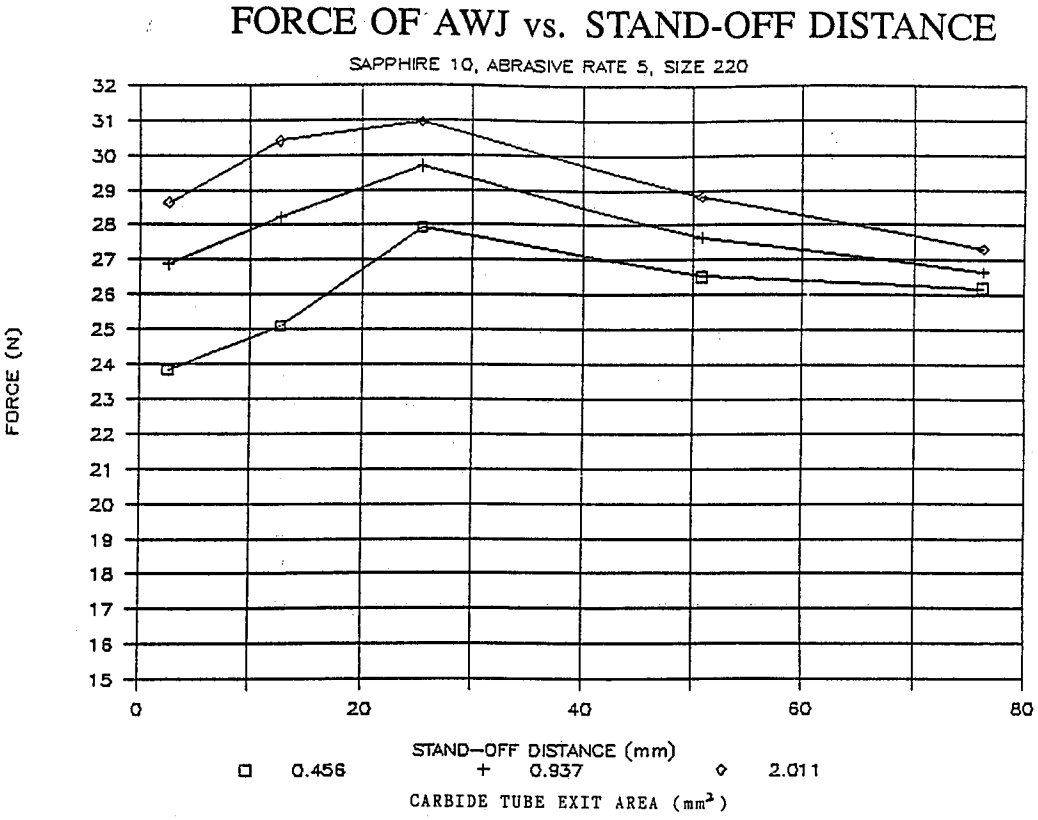

Fig. 8: Effect of the stand-off distance and carbide tube exit area on the force for the abrasive water jet.
Notice the existence of the extremum in the correlation chart and the effect of the diameter of the carbide tube on the force.

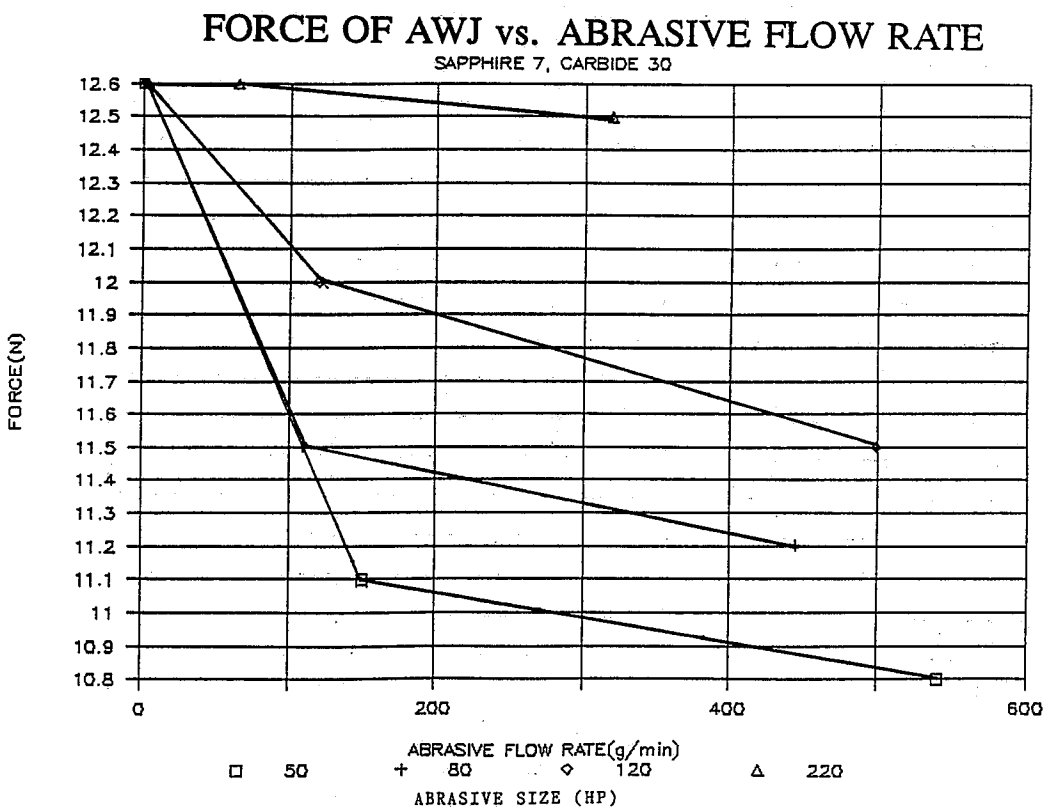

Fig. 9: Effect of the abrasive flow rate and abrasive particle size on the force for the abrasive water jet.

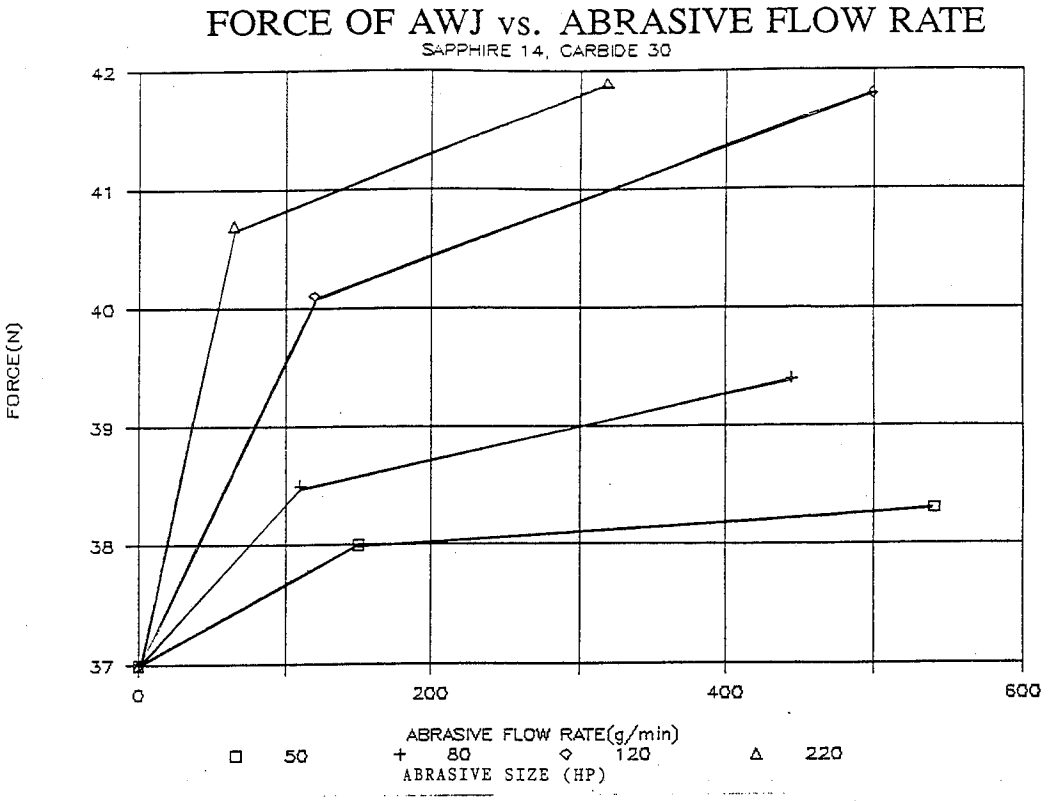

Fig. 10: Effect of the abrasive flow rate and abrasive particle size on the force for the abrasive water jet.
Notice the difference with Fig. 9.

5th American Water Jet Conference
August 29 - 31, 1989: Toronto, Canada

Paper / Communication 8

THEORETICAL ANALYSIS AND PRELIMINARY EXPERIMENTAL RESULTS FOR AN ABRASIVE WATER JET CUTTING HEAD

M. ABUDAKA AND P.S.J. CROFTON
Mechanical Engineering Dept., Imperial College
London SW7, UK

SUMMARY: Introducing abrasive materials to a high speed water jet has the potential of becoming the ultimate tool for cutting composites and laminated materials as well as tough metals such as armour plate. Mixing abrasive with the fast moving water jet is a troublesome operation, since the penetration of low energy abrasive particles into the high kinetic energy, water jet is not easily accomplished in the mixing chamber. For an efficient cutting process the transfer of energy from the water to the abrasive particles must be optimised. Factors which affect the mixing process such as the shape of the mixing chamber and the length and bore of the focusing tube are discussed analytically and preliminary experimental results are presented.

RÉSUMÉ : Les jets d'eau à haute vitesse contenant des abrasifs pourraient devenir l'outil ultime pour la coupe des matériaux composites et laminés ainsi que des métaux durs comme les plaques de blindage. L'admixtion de l'abrasif dans le jet d'eau rapide est une opération délicate car il est difficile de faire pénétrer des particules abrasives de faible énergie dans le jet d'eau qui possède beaucoup d'énergie cinétique, dans la chambre de mélange. Pour que la coupe soit efficace, il faut optimiser le transfert d'énergie entre l'eau et les particules abrasives. Les facteurs influant sur le mélange comme la forme de la chambre de mélange et la longueur et l'alésage du tube de mise au point sont analysés, et les résultats expérimentaux préliminaires sont présentés.

Organized and Sponsored by the National Research Council of Canada and the U.S. Water Jet Technology Association.

Nomenclature

F_w	Drag force
A	Projected area of particle
C_d	Drag coefficient
s	Distance along the flow
ρ_w	Density of the water jet
u	Speed of jet
v	Speed of particle
v_i	Initial speed of particle
n	Any positive real number
K	Constant
m_a	Mass of particle
z	= u - v

1- Introduction

Effective cutting by abrasion of material requires a high speed particles to strike the cut surface at a certain angle of attack. Particles are accelerated by fast water jet (usually about 3 times the speed of sound in air). Ideally, the acceleration of the particles is uniform and the particles are only subjected to the fluid (water) flow drag law (as illustrated later). Due to the high speed of the water and surface tension the particles tend to bounce on the jet surface and particle penetration of the jet is not achieved. The internal shape of the mixing chamber is found to be critical to the flow of abrasive and to the mixing process.
However, the spread of the water jet due to air friction and entrainment is an important factor in designing the cutting head. Air entrainment contributes to undesirable jet spread which makes the jet less focused and increases wear in the focusing tube. Conversely, a coherent jet renders the penetration of the water jet by the abrasive particles still more difficult to achieve.
Tests show that the speed of cut and the quality of the cut are largely influenced by the the cutting head design. It is also found that the design of the cutting head influences the wear of the focusing tube.

2-Cutting head mixing chamber.

The incorporation of a mixing chamber in the cutting head is found to be essential since a partial vacuum is generated in the chamber as a result of the venturi effect. This low pressure area draws abrasive particles from the abrasive tank, which are then directed into the centre of the water jet. The abrasive particles are mixed with air to ease the flow of abrasive in the pipes leading to the mixing chamber (Figure 1). The speed of abrasive input is increased as the pressure difference between the inside of the chamber and atmospheric pressure is increased. Also particle speed is increased when the air flow rate is increased since increasing the air flow rate eases abrasive flow and reduces the internal friction inside the feed pipe.
However air flow with abrasive contributes to the jet spread, tests show that a substantial increase in jet diameter occurs at the outlet of focusing tube when unrestricted air is allowed to enter the mixing chamber (Photo. 1, 2).
Increasing the speed of the abrasive particles is beneficial, since high speed particles result in improved mixing of abrasive with the jet. Experiments show feeding abrasive at right angle to the jet not only it makes it easy to fabricate the cutting head but also improves the mixing process in two ways. Firstly, it results in a shorter length mixing chamber which results in less jet spread. Secondly, particles impacting the water jet normally results in deeper penetration of the jet. However, theoretical analysis shows that the larger the difference between the speed of jet and the particles the larger is the drag on the particles (section 3.1).
Internal shape of the chamber has no effect on the pressure generated in the chamber, but the pressure is found to be a function of water mass flow rate (or sapphire orifice diameter) (1), and the speed of the jet which is a function of pump pressure and the focusing tube bore (Figure 2). Conical shaped chambers result in improved mixing, while square section chambers produce poor mixing and cause frequent abrasive feed pipe blockages.

3- Focusing tube

Experiments show that the speed of the abrasive particles increases inside the focusing tube with the increase peaking at a critical tube length. It is also observed that the increase in particles speed is a function of the bore of the focusing tube. Generally, large bore focusing tubes create a less focused jet of water and abrasive which results in a wide cut in the material and produce a kerfed cut surface.
The focusing tube restricts the jet spread and more importantly, unmixed abrasive is accelerated in the tube. These unmixed abrasive particles are mainly found on the periphery of the expanding jet. Since few particles are considered to be able to penetrate the jet, the length of focusing tube is critical. Using small tube lengths of < 20 mm results in a relatively slow cutting time and at very small lengths (<10 mm) abrasive particles are clearly observed falling freely around the periphery of the jet at the cut material surface. Tube lengths of about 30 mm are observed to give the maximum cutting speed.
The following theoretical analysis was developed to predict the length of tube required to achieve particle speed approaching the water jet speed.

3.1- Approximate analytical solution for the velocity of a single solid abrasive particle injected in a water jet.

If the effect of gravity forces on the motion of the water jet and on the injected abrasive particle are considered negligible, and if the flow parameters (including the velocity) are constant across any cross-section of the flow then the force on any abrasive particle in the jet is given by

$$F_w = \frac{1}{2} A . C_d(s) . \rho_w(s) \left(u(s) - v(s) \right)^n \text{ ---------- (1)}$$

Where C_d, ρ_w, u and v are functions of s the distance along the flow of water. Assuming C_d and ρ_w are constants along the jet.
This reduces to

$F_w = K (u - v)^n$ where K is a constant,

hence,

$$m_a . \frac{ds^2}{dt^2} = K (u - v)^n \text{ ---------- (2)}$$

In general, u is a function of time or, alternatively, of distance from the point of injection, since the jet slows down due to air friction and air entrainment. Thus to solve for the velocity of an abrasive particle another relationship is needed to describe the variations of u with time of distance s. If, however, u can be assumed roughly constant (i.e. the same average values are used) then such an additional relationship becomes unnecessary and the abrasive velocity can be found by solving the equation

$$\frac{d^2s}{dt^2} = \frac{K}{m_a} \left(u - \frac{ds}{dt} \right)^n \text{ ---------- (3)}$$

(assuming u is constant)
This non-linear ordinary differential equation has no general analytic solution for any n. However, by making the substitution v=ds/dt, the equation can be rewritten as.

$$\frac{d}{dt}(v) = \frac{dv}{ds} . \frac{ds}{dt} = v . \frac{dv}{ds} = \frac{K}{m_a} \left(u - v \right)^n \text{ ---------- (4)}$$

from which it is possible to find (in implicit form) an analytical solution for v for any value of n. This can be conveniently done by introducing the substitution (u-v) = z from which -dv/ds = dz/ds.
Equation (4) becomes

$$-(u - z) \frac{dz}{ds} = \frac{K}{m_a} . z^n \text{ ---------- (5)}$$

hence

$$\frac{z - u}{z^n} . \frac{dz}{ds} = \frac{K}{m_a} \text{ ---------- (6)}$$

Integrating (6) yields

$$\int z^{1-n} . dz - u \int z^{-n} . dz = \frac{K}{m_a} . s + C \text{ ---------- (7)}$$

The integration is standard but n = 2 and n = 1 are special cases :

1 n = 1 ; Equation (7) yields

$$z - u \ln z = \frac{K}{m_a} . s + C$$

but when s = 0 , i.e. at the point of injection of the abrasive

$$(u - v_i) - u \ln (u - v_i) = C$$

hence

$$z - u \ln z = \frac{K}{m_a} . s + (u - v_i) - u \ln(u - v_i) \quad \text{---------} (8)$$

2 n = 2 ; Equation (7) yields

$$\ln z + \frac{u}{z} = \frac{K}{m_a} . s + C$$

when s = 0

$$\ln (u - v_i) + \frac{u}{(u - v_i)} = C$$

hence

$$\ln z + \frac{u}{z} = \frac{K}{m_a} . s + \ln (u - v_i) + \frac{u}{(u - v_i)} \quad \text{---------} (9)$$

3 n > 2 This include any real value of n > 2, e.g. 2.1, 2.8 and so on .
Equation (7) yields;

$$\frac{z^{2-n}}{(2-n)} - u . \frac{z^{1-n}}{(1-n)} = \frac{K}{m_a} . s + C$$

or

$$\frac{z^{1-n}[z (1-n) - u (2-n)]}{(2-n)(1-n)} = \frac{K}{m_a} . s + C$$

when s = 0

$$\frac{(u - v_i)^{1-n} [(u - v_i)(1-n) - u (2-n)]}{(2-n)(1-n)} = \frac{(u - v_i)^{1-n} (-v_i (1-n) - u)}{(2-n)(1-n)} = C$$

hence

$$\frac{z^{(1-n)} [z (1-n) - u (2 - n)]}{(2-n)(1-n)} = \frac{K}{m_a} . s + \frac{(u - v_i)^{1-n} (- v_i (1-n) - u)}{(2-n)(1-n)} \quad \text{----} (10)$$

For each of the above three cases equations (8), (9) and (10) the value of v at any distance (tube length) s may be found, or more appropriate 's' can be found at which the particle achieves the same speed as the jet medium. The variations of 's' against the v are shown (Figures 3, 4).
For the above analysis to be valid for a stream of particles in the jet, kinetic energy must be conserved i.e. energy loss due to impact and friction between particles in the jet is ignored. However, as the speed of the water jet increases and the jet spreads the water density ρ_w is decreased and also the drag coefficient C_d is decreased. At large Re (turbulent flow) the coefficient C_d becomes very small (C_d= 0.01 at Re= 10^7) and with a random variation in magnitude (2).
For the flow conditions described above the relationship between drag and speed difference is non-linear and it is assumed that n ≥ 2. The analysis show for such conditions that the length of the tube is insignificant for the acceleration of the particles, assuming good mixing has occurred and that the particle has penetrated the jet stream. In consequence, the tube acts mainly to focus the spreading jet and accelerate the abrasive particles which do **not** penetrate the jet stream.

3.2-Wear of the focusing tube

It is found that the wear of the internal surface of the tube is dependent on the mechanical properties of the hard materials used to make the tube. Both tungsten carbide and hard ceramic tubes exhibit the same wear rate (3) but the wear of the tungsten is linearly distributed along the internal surface (Figure 5 a) of the tube, whereas ceramic tubes hardly show any wear at the inlet of the tube and relatively large wear at the outlet (figure 5 b). The cross sectional of the internal surface of a used ceramic tube is distinctly curved.
Wear at the inside of the focusing tube differs according to the material used to make the tube, since brittle ceramic materials are more resistant to sliding wear than impact wear (4). The increase in wear at the outlet of ceramic focusing tubes indicates that abrasive particle strike the tube more at the outlet than at the inlet.
Generally, shorter mixing chambers result in lower wear rate of focusing tube due to the fact that the jet spread is less and hence the friction between the mixed jet and the inside surface of the

focusing tube is minimum. Reducing the air flow for the same flow of abrasive particles to the mixing chamber also results in less tube wear.Further tests are required to produce quantitative results for the optimum cutting head design (3).

4-Conclusion

From the tests described above it may be concluded that:

- The design of the mixing chamber plays an important part in mixing abrasive particles with the high speed water jet.
- Air flow into the mixing chamber also influences the mixing process and the jet spread
- An optimum length of focusing tube is required and any increase over this length is unnecessary expense.
- The main functions of the focusing tube are; to restrict the jet spread and to accelerate the unmixed abrasive particles on the periphery of the jet.
- Focusing tube wear is largely confined to the outlet of the tube.

5-Acknowledgements

This research project is financed by UHDE, Werk Hagen, W. Germany. The authors would like to thank N. Tailor and A. Noorbhai of the high pressure laboratory, Imperial College for fabrication of the cutting heads.

6-References

1 M. Abudaka, P. S. Crofton
Abrasive water jets for controlled demolition and dismantling
Presented to the 1st International Conference on Decommissioning, 22 - 24 March 1988, UMIST, Manchester, Sponsored by the New Civil Engineer, Offshore Engineer, U.K.

2 G. N. Abramovich
The theory of turbulent jets
MIT Press Cambridge, Mass. (1963)

3 M. Abudaka
Development of a high pressure abrasive water jet cutting system
PhD thesis 1989, London University, U.K.

4 J. G. Bitter
A study of erosion phenomena
Part I, Wear, 6 (1963), 5 - 21, and Part II, 169 - 190.

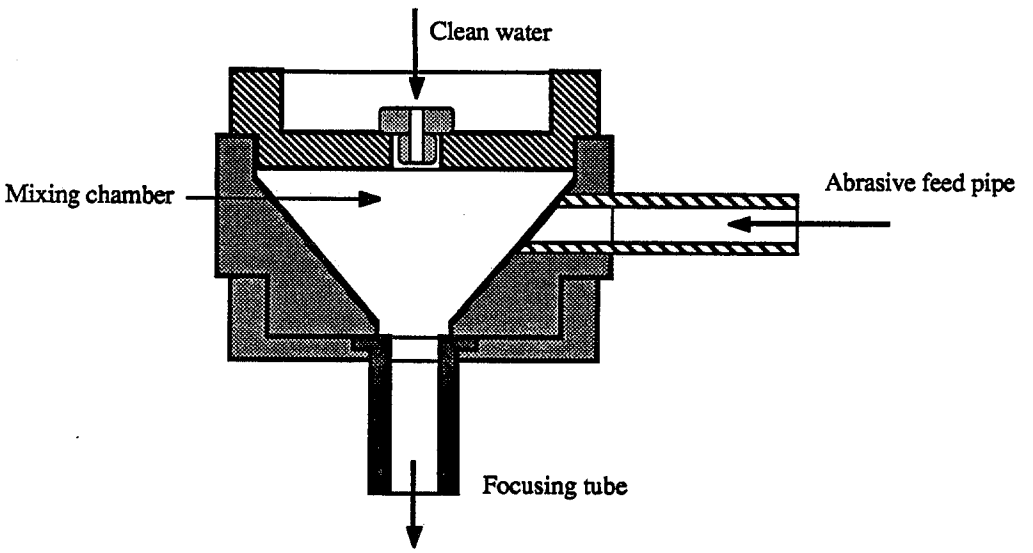

Figure 1, Abrasive cutting head

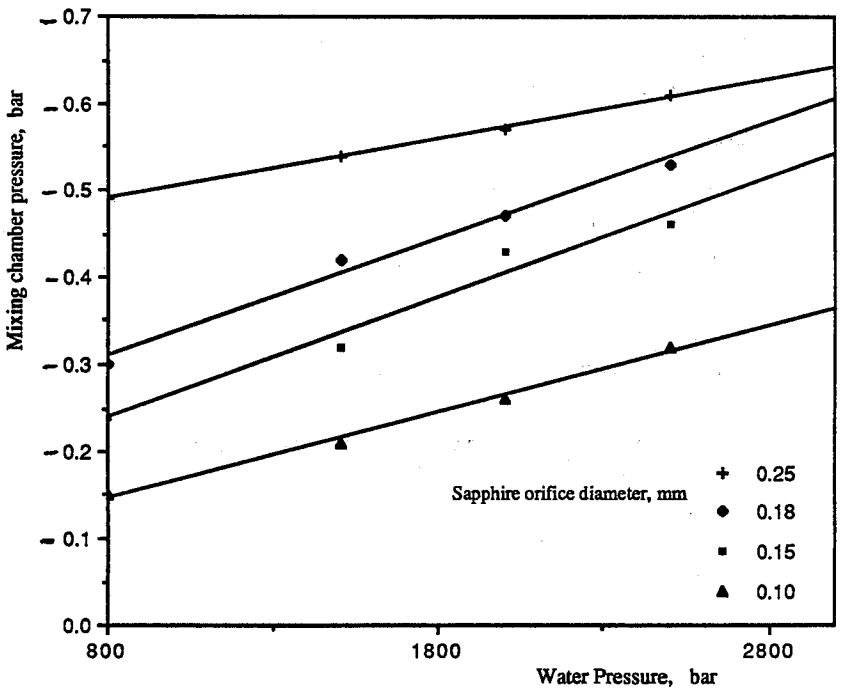

Figure 2. Pressure inside mixing chamber

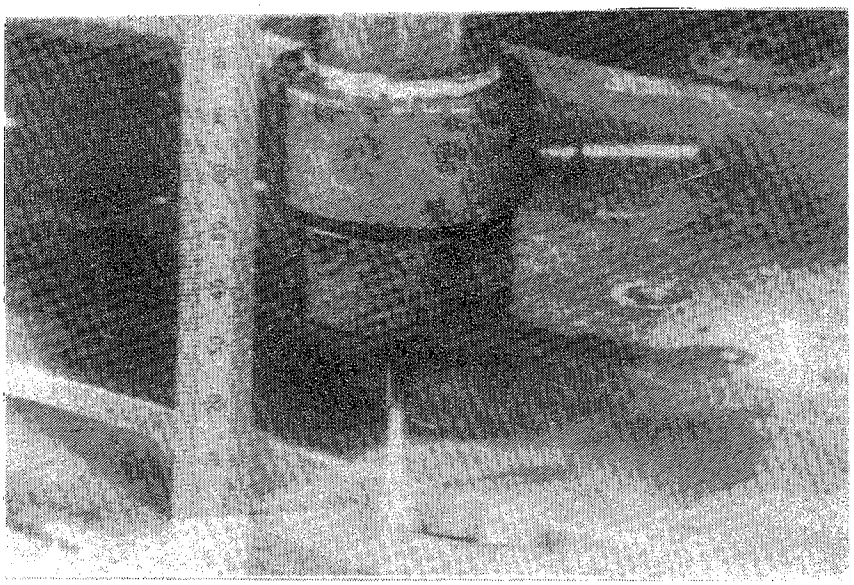

Photo.1, Free flow of air into the abrasive mixing chamber

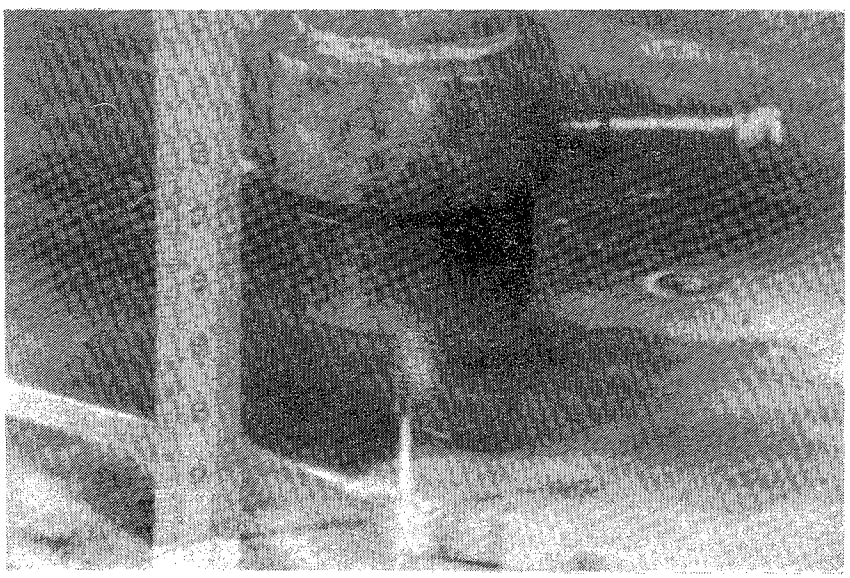

Photo.2, No air flow into the abrasive chamber

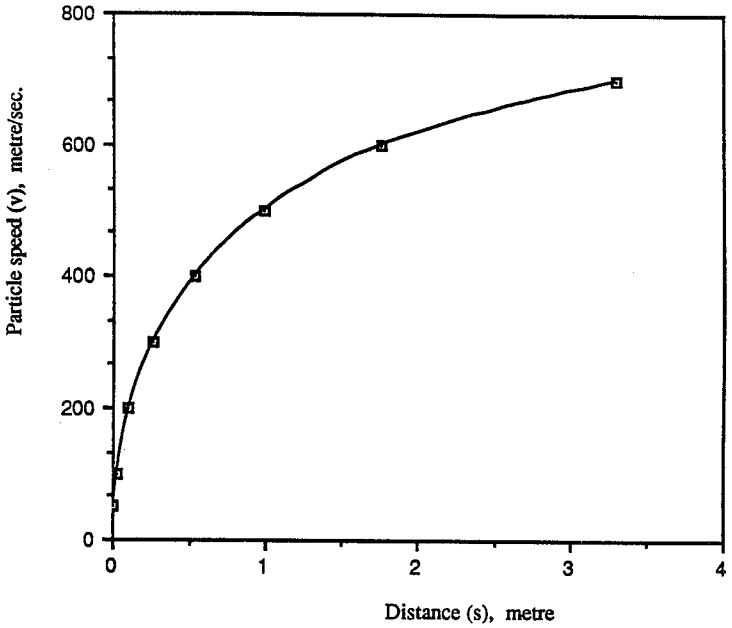

Figure 3, Particle speed along the jet when n=1

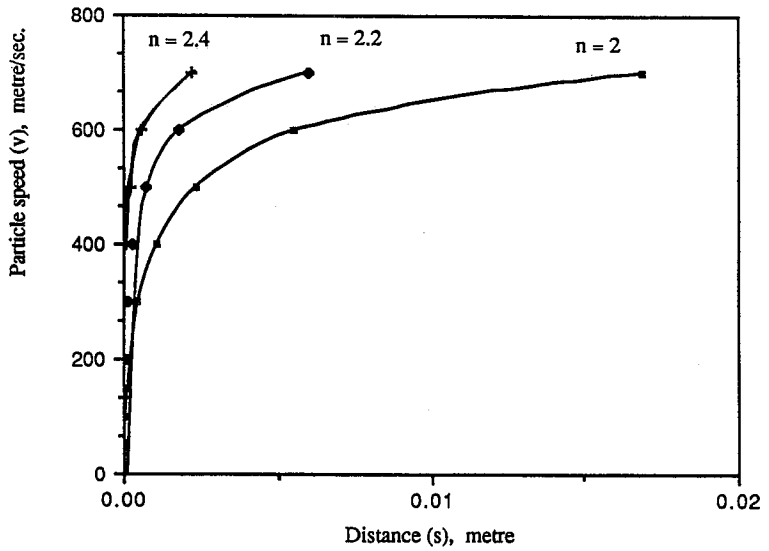

Figure 4, Particle speed along turbulent jet

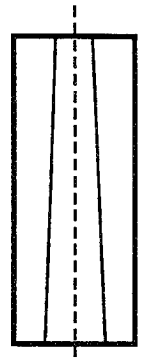

Figure 5 a , A worn out tungsten carbide tube

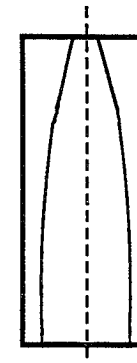

Figure 5 b , A worn out ceramic tube

5th American Water Jet Conference
August 29 - 31, 1989: Toronto, Canada

Paper / Communication 9

STRUCTURE OF WATER JET AND EROSION OF MATERIALS

H. Murai AND S. Nishi
Hirosima Institute of Technology
Hirosima, Japan

ABSTRACT: The general aspect of the structure of water jet and its variation with increasing the distance from the nozzle exit, its mechanism and their relations to the erosion of materials were presented. The new advantages for the processing technology by water jet were also discussed.

RÉSUMÉ : La communication traite des grandes lignes de la structure et du mécanisme des jets d'eau, de leurs variations en fonction de la distance à la sortie de la buse et de leurs rôles dans l'érosion des matériaux. Les nouveaux avantages que présente la technologie des jets d'eau dans le traitement sont aussi analysés.

Organized and Sponsored by the National Research Council of Canada and the U.S. Water Jet Technology Association.

1.INTRODUCTION

As for the researches concerning the structure of high speed water jet and its relations to the shock pressure, the state and mechanism of erosion of solid materials, and the correlation between the two matters, though being scarce compared with the researches on applications of a water jet technology to various fields, the following researches can be found as far as the authors are aware. M.Yokota and N.Yamakado investigated the structure of jet through observations of the state of the eroded surface of metals and rock [1]. K.Yanaida and A.Ohashi measured the distribution of the dynamic pressure in the jet by using a Pitot tube [2]. A.J.Watson et.al. investigated the relation between the structure of the single-loaded water jet and shock pressure [3]. Recently R.Kobayashi et.al. presented the research on the relations between the structure of jet and the process of erosion of metallic materials. However, the structure of water jet has not been made clear yet, and its relation to the process of erosion of materials leaves some problems unknown either.

The present research has attemted to make the structure and velocity of water jet visible and measurable, and correlate the structure, dimension and velocity as well as their variations with the distance from the nozzle exit with the process of erosion and the dimensions of the eroded pits as well as their variations with the stand off distance to contribute for the processing technology by water jet to exhibit more efficiency and accuracy.

NOMENCLATURE

c:velocity of sound in water, m/s
d_1:diameter of eroded pit at entrance, mm
l:depth of eroded pit, mm
N50:nozzle of nominal diameter 0.5 mm
T:exposure time, sec
v:jet velocity, m/s
ρ:density of specimen material, kg/mm^3
D:nozzle diameter, mm
d_2:diameter of eroded pit at bottom, mm
N15:nozzle of nominal diameter 0.15 mm
p:spouting pressure, kgf/cm^2
UT:ultimate strain energy, kgf-m/m^3
w:weight loss, mg

2.Experimental Apparatus and Method

Fig.1 shows the experimental setup. The two nozzles were presented with diameters of 0.51 mm (nominal diameter 0.5 mm, N50) and 0.18 mm (nominal diameter 0.15 mm, N15), and the different sectional forms as are shown in Fig.2. Tap water was used as a working liquid.

The spouting pressure upstream the nozzle inlet was set up at 1000 and 1500 kgf/cm^2 for the

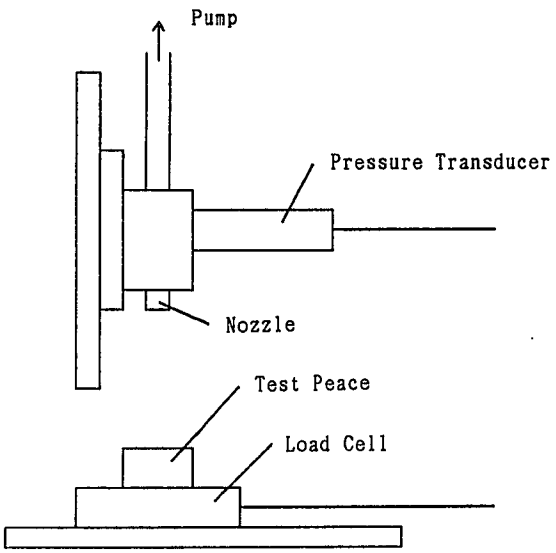

Fig.1 Experimental Setup

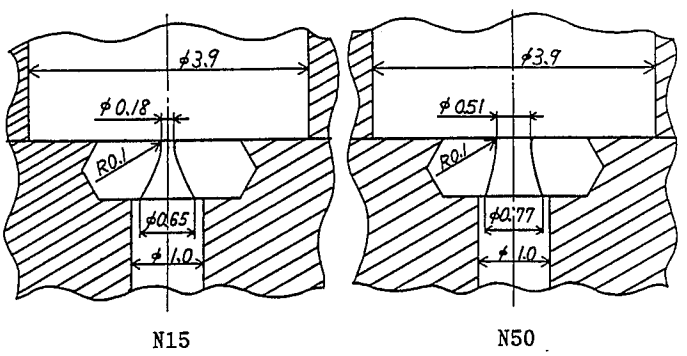

Fig.2 Nozzles

nozzle N50, and 500,1000,1500 and 2000 kgf/cm^2 for the nozzle N15 as the time-averaged value, which was measured by using a pressure transducer of strain gage type.

The test piece was made of Aluminium alloy, and was hexagonally shaped with an opposite height of breadth of 23 mm and 13 mm. It was equipped on a load cell of strain gage type for measuring the strength of impact force on it by a water jet. The impact force measuring system was equipped on the table movable horizontally in two perpendicular directions, and the nozzle was equipped on the axis movable vertically.

An erosion intensity was estimated by an amount of weight loss measured by a dial scale of 1/10 mg, and an average maximum diameter and a maximum depth of an eroded pit were measured. An eroded surface was observed by using a scanning electron microscope.

In order to investigate the structure of a jet, a shadowgraph was taken with an exposure time of about 30ns, by using a giant pulse ruby laser. Drops from a jet was recorded on a high speed photograph of streak mode with 1.2 mm/μs by using a high speed movie camera Cordin 330A.

3.EXPERIMENTAL RESULTS AND DISCUSSION

3.1 Variation of Weight Loss with Stand Off Distance

Dependence on the exposure time, T sec, of the variations of weight loss, w mg, with the variations of stand off distance, x mm, at a spouting pressure, p= 1500 kgf/cm^2 for example, and dependence on p of the same variations for the two nozzles are shown in Figs.3 and 4, respectively. All curves in these Figures have two maximums, first and second peaks in order of x, and one minimum, respectively, similarly to those in reference [1,4]. But the maximum values at the first peaks are larger than those at the second peaks for the nozzle N15, and the formers are comparable with, though smaller than, the latters for the nozzle N50, which tendencies differ from the tendency in references [1,4]. x at the first peak decreases just slightly, while that at the second peak increases gradually with the increase of T and p. x's at the first peaks for N50 and N15, being about 18 and 27 at T= 15 respectively, have a large difference between the two nozzles.

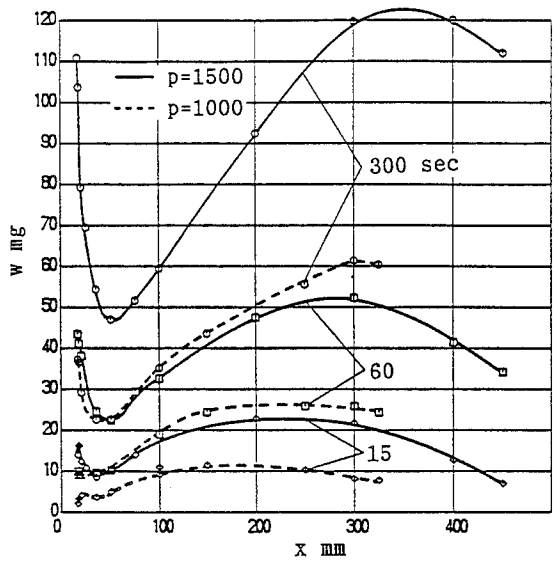

Fig.3 Weight Loss of Aluminium, N50

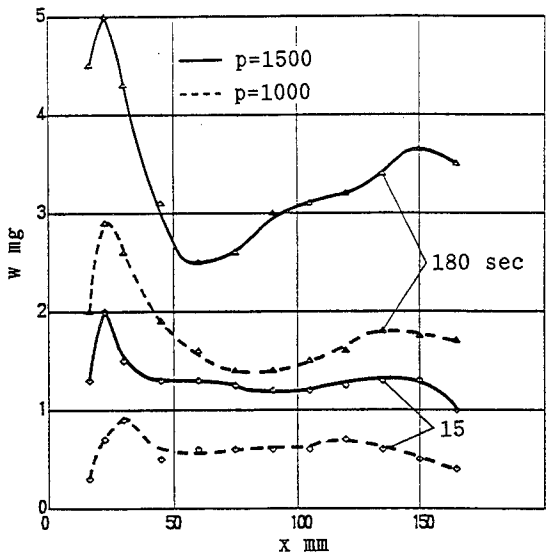

Fig.4 Weight Loss of Aluminium, N15

In order to investigate the causes of the variations of w with x and the difference of the aspects of variations between the two nozzles, a cross sections of an eroded pit was observed and the diameters at the specimen surface, d_1, and the bottom, d_2, and the depth, l, of it were measured. Damaged surfaces were observed also, by using a scanning electron micrometer as occasion calls. The result may be useful also for applications of a water jet technology to the drilling, slotting or cutting. The result of the measurements and examples of photographs of

cross sections are shown in Fig.5 through 8, corresponding to Figs.3 and 4. These Figures, together with Figs.3 and 4, indicate that w around the first peak (Region I) is caused by a different mechanism from one at x larger than one at the minimum weight loss (Region II), as was pointed out already [1,4].

3.2 Structure of Jet and Its Variation with Travelling Distance,Velocity in Jet

In order to investigate the structure of jet and its variation with the travelling distance, x, shadowgraphs of jet with the $3*10^{-3}$ second exposure time were taken, considering the jet velocity. Examples are shown in Fig.9 and 10 for N50 and N15, respectively.

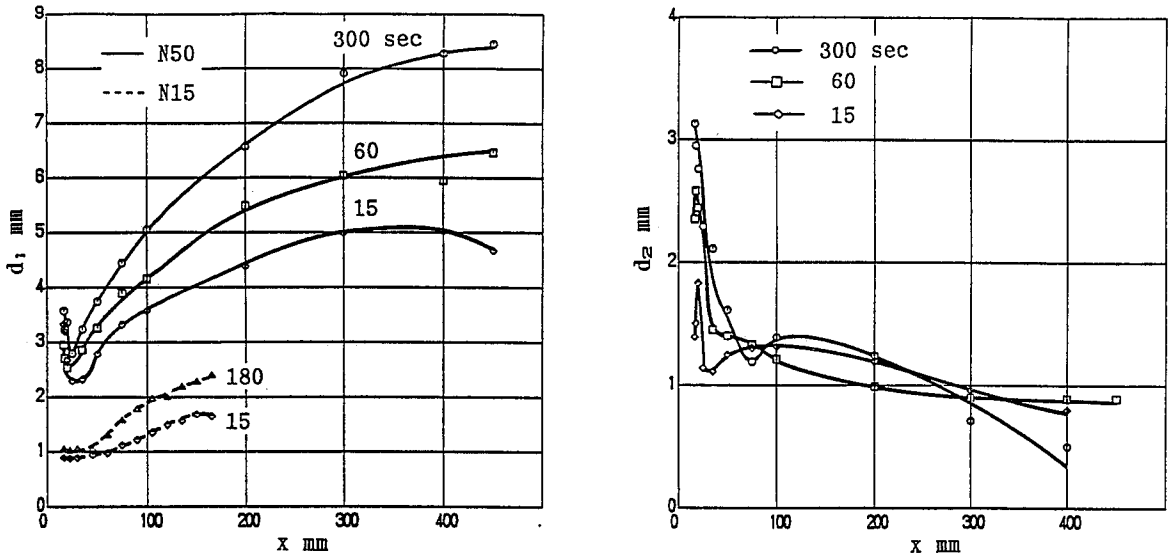

Fig.5 Eroded pit, Diameter, p=1500

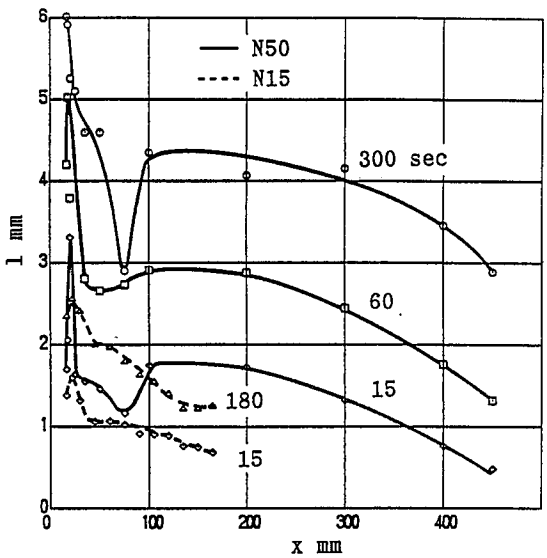

Fig.6 Eroded pit, Deepth, p=1500

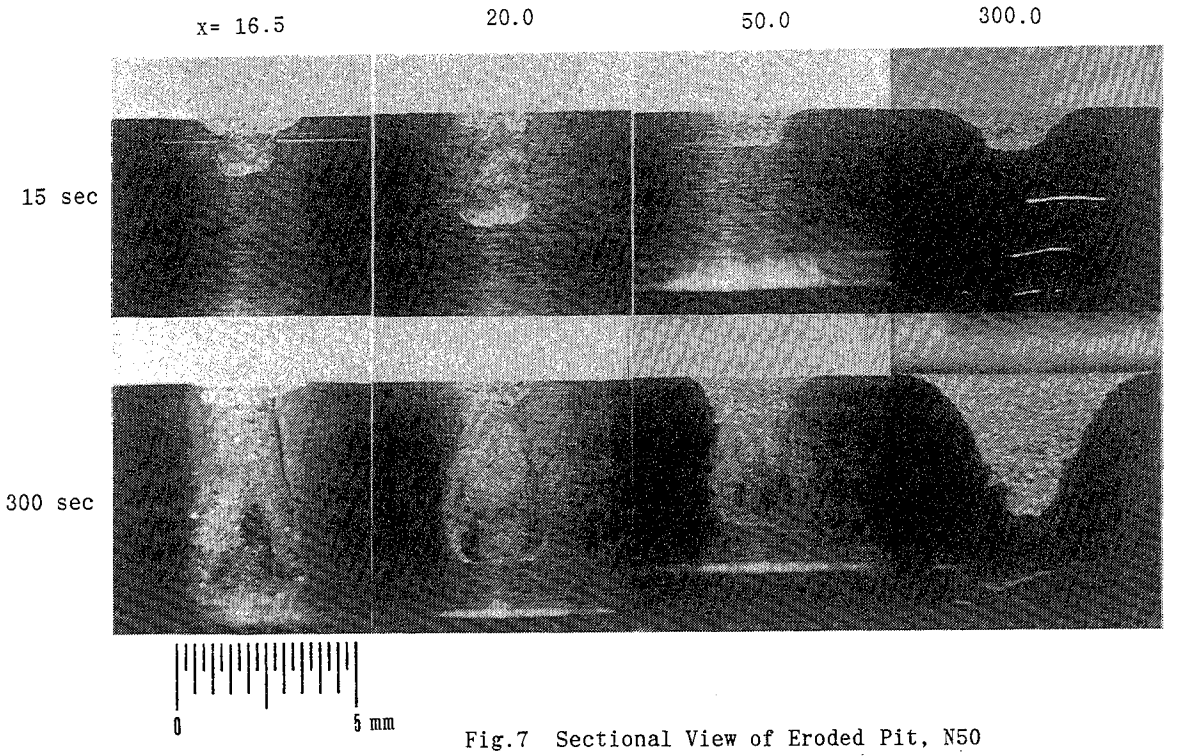

Fig.7 Sectional View of Eroded Pit, N50

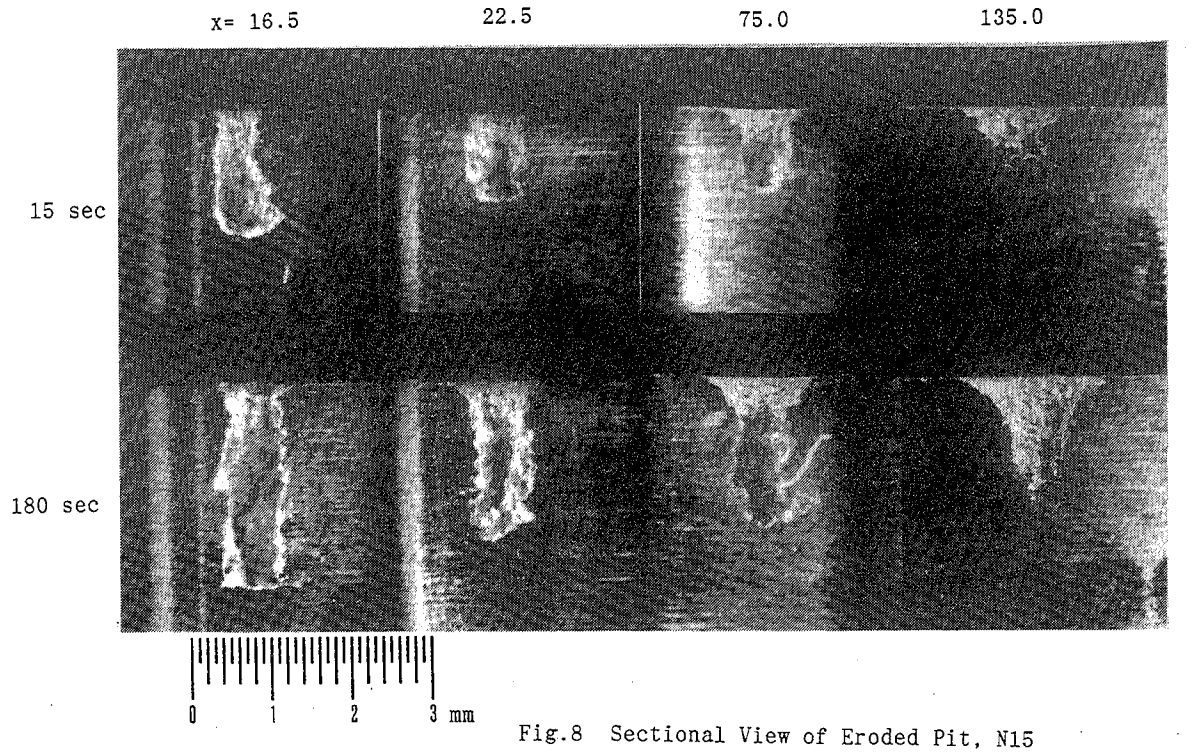

Fig.8 Sectional View of Eroded Pit, N15

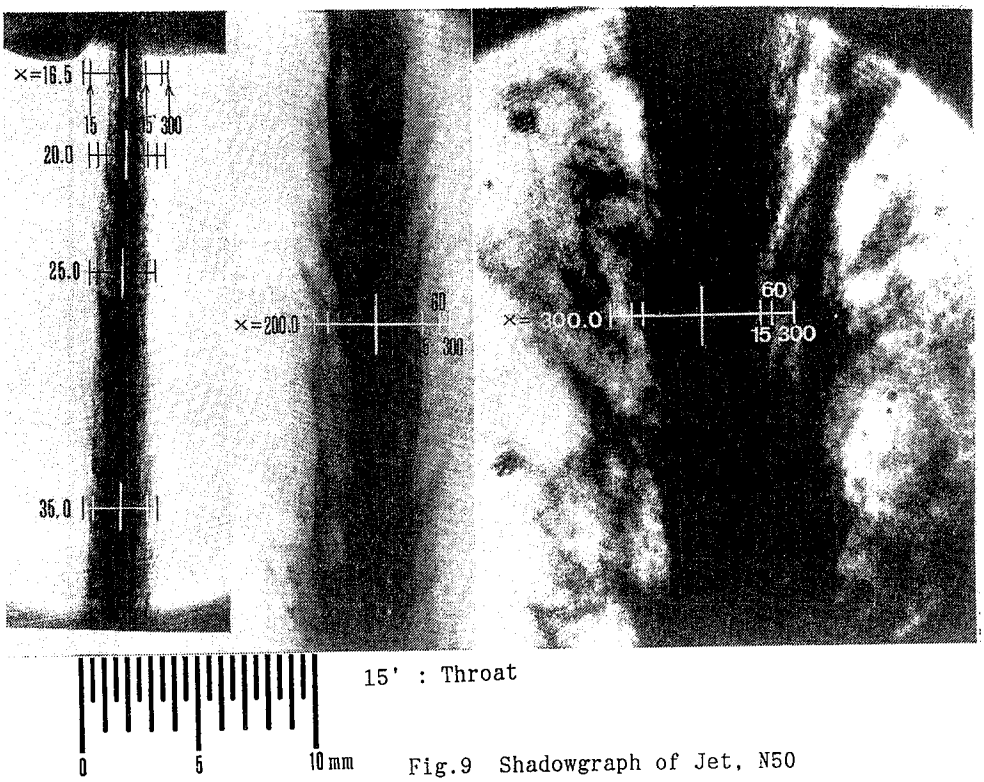

Fig.9 Shadowgraph of Jet, N50

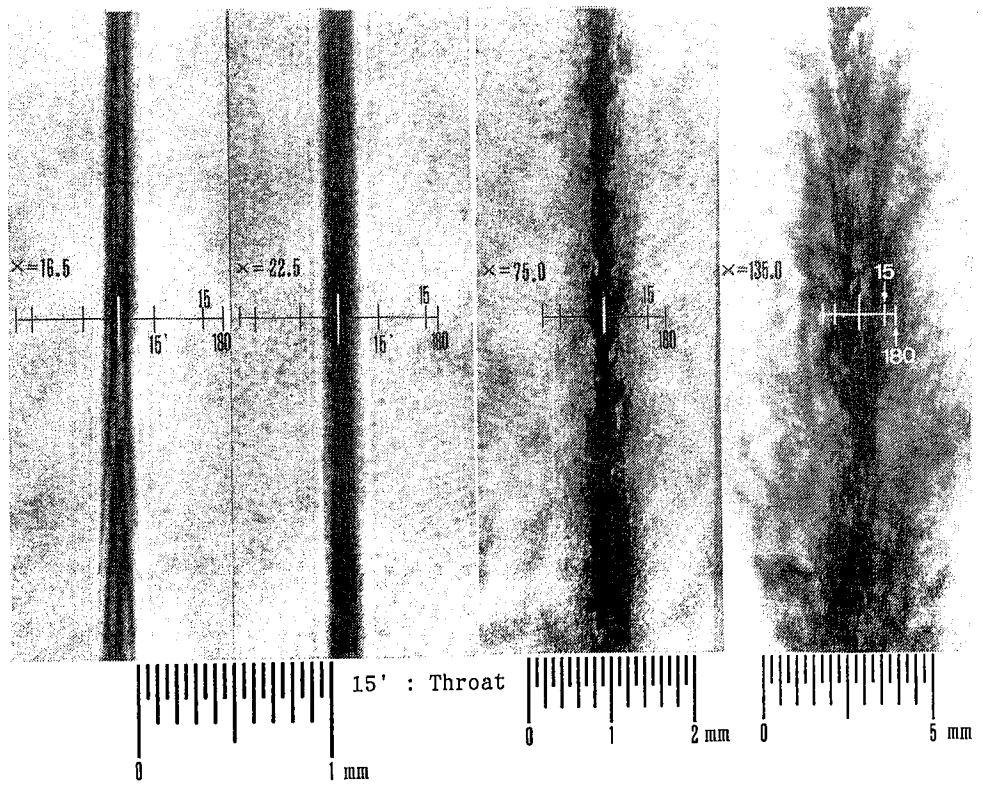

Fig.10 Shadowgraph of Jet, N15

3.3 Generation Mechanism and Aspect of First Peak

The small lumps and drops in the surface layer of jet can be considered to erode materials through the water hammer effect and cut into the specimen surface. The comprehensive diameter of the jet from N50 was about 1.6, 1.9 and 2.4 mm at x= 17, 20 and 26 mm, respectively.

The cross sectional forms and the inside surface of the eroded pit at T= 15 and p= 1500 for N50 shown in Figs.5 and 7 indicate that in the Region I at the proper x(20) the core of jet penetrated into the specimen as deep as to make the stagnation pressure in the pit high enough to fracture the circumference and bottom of the pit for making cracks or small caves, while at an x smaller than that, say 17, the jet core could not penetrate so deep and splashed with as large momentum as to tear off the circumference of the pit near the specimen surface to make d_1 larger, although small cracks could be found also in the pit. Similar breaking or crushing actions in concrete and rock were reported [5] d_1's at x= 17, 20 and 26 were, as can be seen in Fig.7, about 3.3, 2.7 and 2.3 mm, respectively, and fairly larger than the respective comprehensive jet diameter except at x= 26. The reason was written above, but the diameters of eroded pits at the throats were about the same with the jet diameters in both cases of x= 17 and 20. At a larger x beyond 20, the jet could not penetrate so deep nor splash so strongly to make smaller l and d_1 owing to the decay of velocity by the disruption of jet, and d_1 corresponded roughly with the comprehensive jet diameter at x= 20.

With the increase of T, the jet core became to penetrate into the specimen deeper and the stagnation pressure in the eroded pit became more effective to fracture the circumference and bottom of the hole, and l became the deeper, the smaller x was until a proper value of it corresponding to T (Fig.7), because the stagnation pressure was the larger, the smaller x was and the ability of cutting into the specimen surface of the jet surface was considered to grow with increasing x until the disruption of the jet core stated before became striking.

In the case of p= 1000, as compared with the case of p= 1500, the first peak w appeared at x= 17, though indications were found when T was smaller than 60. Contrary to that l had the same tendency with w at the first peak, d_1 had the peak even when T= 15. And the inner surface of the deeply eroded pits around the first peak at T= 300 were very similar to those in the case of p= 1500. From the facts also, it can be deduced that appearance of the first peak is deeply connected to the penetration of the jet core into the specimen and the fracture of the circumference and bottom of the eroded pit by the stagnation pressure of the jet core.

In the case of N15, the first peak appeared at x= 27 which was lager than x= 18 at the first peak in the case of N50, and the maximum value of w at the first peak was larger than that at the second peak which was contrary to their relation in the case of N50. The former fact can be explained by that the jet surface from N15 needed larger x compared with that from N50 for entraining surrounding air and developing the mixed phase flow layer containing small lumps or drops of water to enough degree for giving w of the first peak (Fig.10), because the radii of curvatures up- and downstreams the nozzle throats were almost the same for the two nozzle (Fig.2), whereas what controlled the flow pattern through the nozzle was their ratios to the respective diameter. The comprehensive diameter of the jet at x= 27 was 0.22 mm, while the diameter of the eroded pit at its throat was 0.24 mm, which corresponded well to the jet diameter.

The cause of the fact that w at p= 1500 per unit area of the nozzle throat at the first peak for N15 is almost the same with that for N50, as can be seen in Fig.12, and l/d for N15 is much larger than that for N50, can be considered as follows: The thickness of the mixed phase flow layer on the jet surface, which plays an important part in cutting into the specimen surface, is similar to each other for the two nozzles, and the part of the area of the layer in the cross sectional area of jet, which is closely related to the intensity of penetration into the specimen of the jet, is the larger, the smaller the jet diameter is.

The eroded pits in the SS41 specimen behaved similarly in general trend to the Aluminium specimens although l and d's were smaller (as can be sew in the photographs shown bellows).

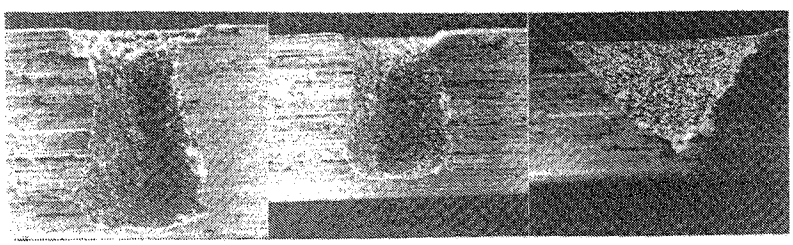

N50
p= 1500
T= 300
x= 18.5, 35, 300

Figs.9 and 10, Fig.9 more clearly, show that at the distance from the nozzle exit, x, near the first peak, the longitudinal street of vortex formed on the surface of jet had entrained surrounding air to generate tiny drops and/or lumps of water and form the shear layer of mixed phase flow around the jet surface, and made the surface of the core of jet wavy longitudinally. With increasing x, the mixed phase flow layer grew and became to generate black longitudinal strips (Fig.9 x= 40 ~ 50), which were short at first and then grew to be longer cylindrical bars extending obliquely backwards and outwards. The cylindrical bars seemed to be vortices generated in the shear layer, and they promoted the further radial diffusion of jet and the irregularity of the jet core.

With further increasing x, the vortices grew further in intensity and number to make the radial disruption of the jet core become striking and to make the thickness irregularity develop to be the longitudinal segmentation of the jet core, other than making the radial diffusion of the jet develop further. Especially in the jet from N15, which had the smaller diameter, the thickness irregularity approached to the central part of core, and the longitudinal segmentation became striking at so small x that the radial disruption of the jet core and the radial diffusion of jet had not yet progressed enough.

Fig.11 shows an example of streak mode shadowgraphs of jet. Oblique lines were loci of water drops or small lumps diffused from the jet core. The jet ran perpendicularly to the film, and the velocity of drops could be calculated by using the slopes of loci in the film, and shown in Table 1. The corresponding water hammer pressure are also shown in the Table. Two or three values of velocity at the same x indicates the spread depending on the radial position, which could not be measured in this experiment. The difference between 480 of N50 at x= 50 and 510 of N15 at x= 75 is considered to be caused by an error of measurement, because if the difference is caused by the difference of growth of the surface shear layer, the value v= 480 of N50 at x= 250 must be too large, although some difference due to the difference of the nozzle geometry may be able to exist. The decay of velocity in N15 during x increases from 105 to 135 was much larger than the velocity decay in N50 during x decreases from 250 to 300, which must be caused by the difference of the structure of jet between the two nozzles stated above. Accordingly, the values of water hammer pressure exceeded the tensile strength of the specimen of Aluminium alloy 40.9 kgf/mm^2, until x= 300 for N50, but was almost equal or inferior to it at x= 135 for N15, which corresponded the variations of w and d_1 with increasing x as would be written bellow.

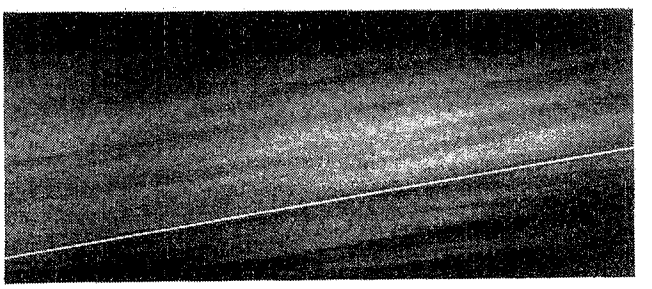

Fig.11 Streak Mode Shadowgraphs of Jet
N15, p= 1500, x= 135

Table 1. Velocity of Drop in Jet

Nozzle	N15						N50			
x (mm)	75	105		135			50	250	300	
v (m/sec)	512	497	523	140	239	300	484	476	418	441
ρcv (Kg/mm^2)	77.3	75.2	79.0	21.1	36.1	45.3	73.1	72.0	63.1	66.6

3.4 Generation Mechanism and Aspect of Second Peak

The difference of the manner of break down of the jet core between N50 and N15 written before brought the differences of the radial diffusion of jet, the velocity decay (Table 1), and the variations of erosion pattern and w with increasing x, as were shown in Fig.3 through 8.

The variations of d_2 and l show some indication about the scale and the velocity of the central part of jet. By the N50 jet, d_2 remained almost constant, though reduced slightly, in the Region II until a certain x depending on T, beyond which diminished very soon. While by the N15 jet, d_2 had diminished at the beginning of the region II. l reduced very slightly while d_2 remained almost constant with increasing x, but began reducing with the higher rate at x where d_2 diminished by the N50 jet, and from the beginning of the Region II by the N15 nozzle, at almost the same rate with each other.

d_1 can be estimated as the radial distance where a small lump or a drop of water can reach with the velocity which can erode the specimen surface. d_1 increased with increasing x with a constant rate common to the two nozzles at the initial stage of the Region II, but the rate began reducing with the further increase of x to make the maximums of d_1 with x.

As a result of above mentioned processes the variations of w with increasing x at given p and T were brought and the second peaks appeared. That the second peaks were lower than the first peaks for N15 are considered to have been caused by the variation of the structure of jet as written above.

It had been shown that the w/D^2p verus x curves for different pressures coincide with each other during rising towards right in the Region II [6], however, that did not realized in the present experiment.

Table 2. Impact Force to Specimen

Nozzle	N15			N50		
x (mm)	22.5	75.0	135.0	17.5	35.0	300
I.F. (Kg)	0.57	0.63	0.45	5.8	5.4	4.8

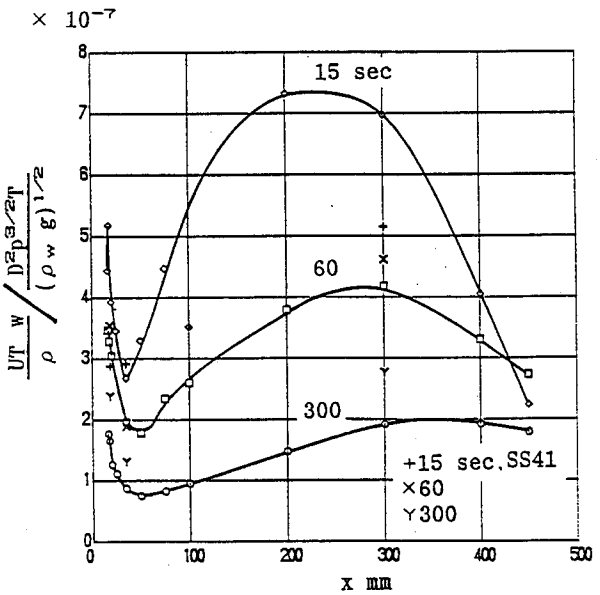

Fig.12 Work Done Rate, p=1500

Table 2 shows the load measured at the bottom of specimen by using a load cell of strain gage type. The table shows that the mean load exceeded the total pressure at the nozzle multiplied by the nozzle area, and reduced with increasing x.

Fig.12 shows the variations of the ratio of the work done to the input work versus x. The ultimate strain energies were obtained by the tension test of the materials presented for the experiment, the aluminium alloy and the steel SS41 and were 22.836×10^4 and 64.651×10^4 kgf-m/m^3, respectively. In the Figure the results for the SS41 specimens are plotted to show the poor coincidence with the Aluminium alloy.

4.CONCLUDING REMARKS

From the results obtained in the present research, it can be concluded as follows:

1. The general aspects of the structure and velocity of water jet and their variations with increasing the distance from the nozzle exit and its mechanism and their relations to the erosion of materials were presented and discussed. The difference of the variation of the jet structure with the travelling distance due to the nozzle diameter was also discussed.

2. The relations between the structure and velocity of jet and their variation with the travelling distance, and the processes of erosion and their variation with the stand off distance were discussed.

3. The first peak of weight loss is generated through fracture of the circumference and/or the bottom of the penetrated pit by the stagnation pressure of the jet core.

4. The weight loss at the first peak can be larger than that at the second peak, when a nozzle diameter is so small that the jet core breaks down by longitudinal segmentation before the jet has diffused radially enough.

5. There is a possibility of drilling or slotting deeper, or cutting a thicker plate by choosing a stand off distance at the first peak rather than the second peak, provided cracks or pits on the circumference and/or at the bottom of the penetrated pit or on the section are of no hindrance.

6. There is the same possibility as the above with a smaller diameter or less loss of breadth and without cracks or pits by choosing a stand off distance far smaller than the second peak.

ACKNOWLEDGEMENT

The experimental apparatus were arranged by the subsidy for private universities of Ministry of Education of Japan and the subsidy of Hirosima Institute of Technology. The pump used for experiment was offered by Dengyosha Mf.Co.Ltd. The ultimate strain energies of the two materials presented to the research were obtained by the aid of Mr. Kido, Associate Professor of Hirosima Institute of Technology and the staff of his laboratory. The observations of eroded surfaces by using the scanning electron microscope were made by the aid of Mr. M.Konishi, Lecturer of the same Institute and the staff of his laboratory. And the experiments, were carried out by the aid of Mr. M.Sakurai, Technical Associate, Mr. K.Nakamura and Mr. Y.Murakami, the post graduate students, and Mr. D.Suzuki the student of the same Institute. The authors would like to express their gratitude to them.

5th American Water Jet Conference
August 29 - 31, 1989: Toronto, Canada

Paper / Communication 10

HISTORY, THEORY AND PRACTICE OF HYDRODEMOLITION

R. Medeot
Fip Industriale
I - 35030 - Selvazzano - Italy

ABSTRACT: By hydrodemolition we mean a process of selective removal of concrete by means of one or more high-speed water jets.
This new technique was developed in Italy towards the end of the 1970's, when it was realized that the problem of removing large areas of deteriorated concrete was becoming increasingly urgent. This paper describes the theoretical basis of this method as well as its practical applications. It also traces its evolution since the first positive results and points out new possibilities of expansion to other fields.

RÉSUMÉ : L'hydrodémolition s'entend d'un procédé d'enlèvement sélectif du béton au moyen d'un ou plusieurs jets d'eau à haute vitesse.
Cette nouvelle technique a été mise au point en Italie vers la fin des années 1970, lorsqu'il est apparu de plus en plus urgent de résoudre le problème de l'enlèvement de grandes surfaces de béton détérioré. Cette communication décrit la base théorique de cette méthode ainsi que ses applications pratiques. Elle trace aussi son évolution depuis les premiers résultats positifs et souligne de nouvelles possibilités d'expansion dans d'autres domaines.

Organized and Sponsored by the National Research Council of Canada and the U.S. Water Jet Technology Association.

1.0 INTRODUCTION

Hydrodemolition is a new word that, borrowing two terms from ancient Greek and Latin, has been created to describe a process as old as the earth itself: the destruction of rock and materials harder than concrete by the relentless force of falling and surging water.

The wearing force of water is well known. Over aeons of geological time the Colorado River carved the Grand Canyon, and the Niagara River, the famous falls.

In practice, the hydraulic power of a waterfall of about 10,000 meters, 150 to 300 litres/min, has been harnessed to produce equipment to remove concrete.

Hydrodemolition technology, in essence, compresses time from centuries to seconds by speeding water flow to realtime cutting force, to demolish the bonds uniting concrete aggregate.

But let us pause here, to give a history on the discovery and development of hydrodemolition.

In the later 1970s it was realized that the problem of removing large areas of deteriorated concrete (for example, bridge decks) was becoming increasingly urgent.

Apart from the specific repair techniques to be adopted, any restoration work first involves removal of deteriorated concrete. This delicate and often difficult task requires:

a) total removal of all traces of deteriorated concrete;
b) avoidance of any damage to sound concrete and reinforcing steel;
c) good bonding, e.g., a good support surface between existing concrete and restoration materials.

Traditional methods, based essentially on the use of pneumatic hammers, did not guarantee satisfactory results.

In particular, the greatest problem was operator difficulty in differentiating between poor-quality and good-quality concrete, which led to either incomplete removal of poor concrete or excess removal of good concrete.

Serious research on possible alternative methods revealed that several studies had been carried out on this subject thus confirming its importance. However, no practical results had been achieved, although we may quote, for the sake of curiosity, heat treatment methods (all based on producing rapid heating of the damaged area, e.g., by using flamethrowers, plasma beams, or even lasers); abrasive processes (based on the use of rotating discs coated with industrial diamonds in a metal matrix or carbonium bound with bakelite); electrical and chemical processes (only applicable in special situations) and - the most curious new method in the group - the use of microwaves.

Research revealed that, although pressurized water could demolish concrete, no successful attempt had been made. In spite of this, we believed that water jets represented the most promising path and, in spring 1979, we decided to start a research program aiming at producing equipment for removing concrete by means of high-speed water jets.

The most important discovery made during this research was the following:
"Removing a layer of concrete is a process which differs radically from boring and cutting". To use a familiar example, it is like the difference between sawing and planing a piece of wood: the tools are different, and so are the ways of using them.

The failure of attempts all over the world was due essentially to having used techniques which were more suitable for boring or cutting.

Strong in this knowledge, we needed a few months to prepare a prototype which was successfully used on the Viadotto del Lago in November 1979 in conjuction with the Italian Road Authorities. The first commercial equipment was ready by spring 1980.

After a series of improvements to perfect the system, hydrodemolition technology was introduced into other countries.
The first was Sweden where, in the summer of 1984, the equipment was used on many bridges and was tested by the Swedish Road Authorities (Vägverket), with very flattering results.
In spring 1984 it was presented at the World of Concrete in Washington D.C. In the autumn of the same year it began working in Toronto in the Manulife Parking Garage. In 1985 hydrodemolition equipment was successfully used in the U.S.A. on the Memorial Bridge Rehabilitation Project.
Today hydrodemolition is unanimously accepted as the best process for concrete removal. It has become popular in many countries and the new rehabilitation projects specify this technique at least as an alternative to the traditional methods.

2.0 HYDRODEMOLITION

By "hydrodemolition" we mean the process of selective removal of concrete by means of one or more high-speed water jets.

Although the term "demolition" may recall its synonym, "destruction", it should be clarified at once that our technique deals with the selective removal of deteriorated parts, aiming at static restoration of the structure and not at its total destruction.

2.1 Hydrodemolition Mechanism

Concrete is an unhomogeneous material made up of aggregates (sand and gravel) and bonding agent (cement), with gaseous inclusions which make up the so-called porosity. Porosity is generally undesirable, since it alone is an effective weakening agent, through which degradation takes place.

The water jet accomplishes its destructive action by means of three separate mechanisms, i.e.:
- direct impact, pressurization of cracks and cavitation.

These three processes reach their maximum efficiency when the water jet strikes the bonding agent. The nozzle is thus played rapidly and continually over the area to be removed and excess water allowed to drain away. However, jet efficiency is maximum when the jet itself is stable, and stability is influenced by shape and configuration of feeding pipe and nozzle, exit speed of water, distance from point of impact, etc.

The conclusion is that an efficient and therefore economic removal process by hydrodemolition may be obtained by carefully combining fluido-dynamic, geometric and kinetic parameters, as a function of existing situation (strength of concrete, presence of reinforcing steel, cracks, etc) and the type of work required.

Obviously, satisfactory work requires highly qualified and experienced personnel, capable of optimizing the equipment and skills necessary for each single case.

The equipment must be sufficiently powerful, but sophisticated movements and electronic control systems are also necessary, since without them one of the most important advantages of hydrodemolition is lost - i.e., selective removal.

2.2 Selective Removal

Clearly, operative conditions being equal, removal involves a greater depth of degraded or generally weaker concrete than it does in the case of sound and resistant concrete, but this is not selective removal.

Referring to hydrodemolition equipment, selective removal is defined as the capacity to remove completely all and only the deteriorated concrete, independently of the depth to which the damage has penetrated.

Deterioration in bridge decks or parking areas may involve thicknesses which vary from point to point - in practice, from zero to the whole thickness (Fig. 1).

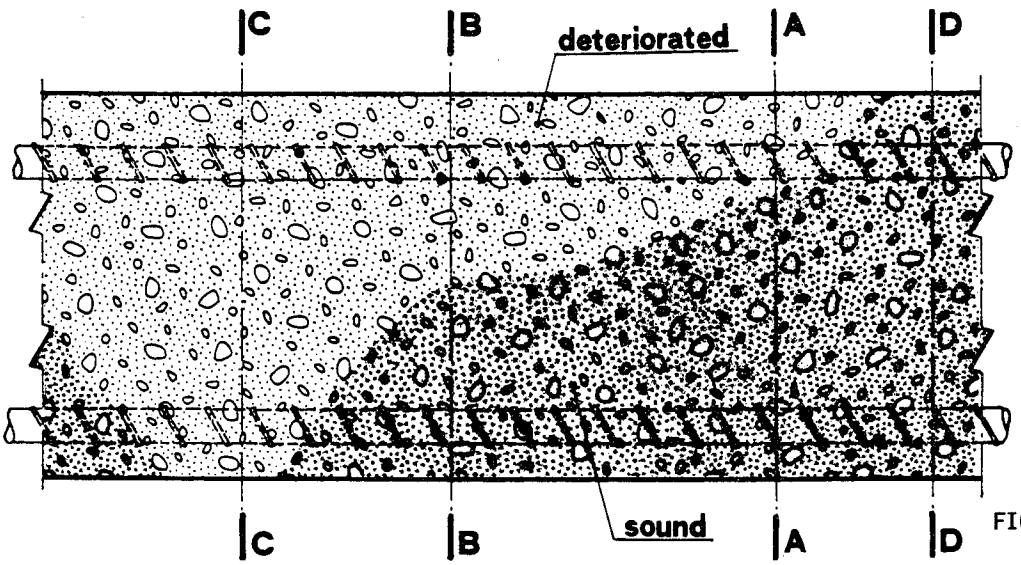

FIG. 1

However, selective removal may also be defined as the capacity to remove only concrete with strength of less than a certain pre-established value, avoiding removal of concrete which has been considered as acceptable by the engineer.

As we shall see later, the term "strength" (commonly understood as compression cubic strength) is incorrect in identifying the type of concrete to be removed.

In order to understand the phenomenon of selective removal, we must - albeit briefly - go back to theory.

If gradually increasing force, e.g. compression, is exerted on a material, the latter is deformed according to a curve called stress-strain characteristic, up to breaking-point (Fig. 2).

By using specific units, we have: $E_r = \int_0^{\varepsilon_1} \sigma \, d\varepsilon$

where E_r is specific breaking energy (KJ/m3), and ε_r is breaking strain.

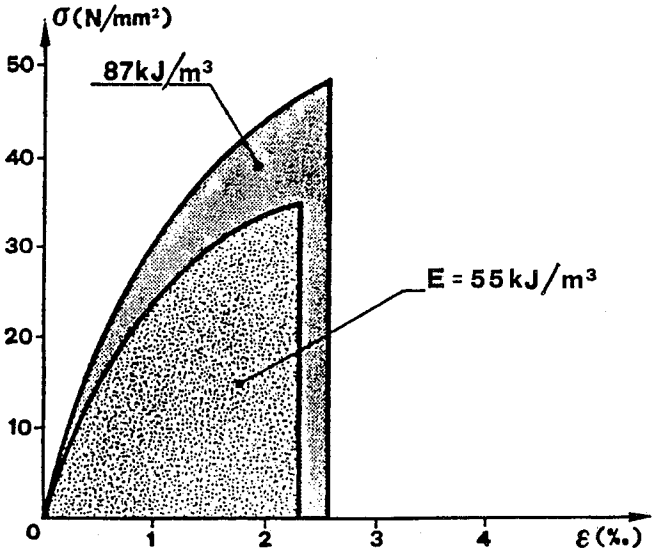

FIG. 2

Obviously, if breaking stress is not reached or if the material receives energy less than breaking energy, it will remain intact.
Clearly, materials at higher strength require greater energy, so that there is a law of proportionality between the two parameters. We may thus conclude that:
- all materials have a threshold energy value at breaking-point;
- there is a law of proportionality between the above threshold energy value and the strength of the same material.

Therefore, if we plot the trend of the strength of concrete as a function of depth, as shown for example in section A-A in Fig. 1, the same diagram may also represent the energy required to break the specimen, on a suitable scale (Fig. 3).

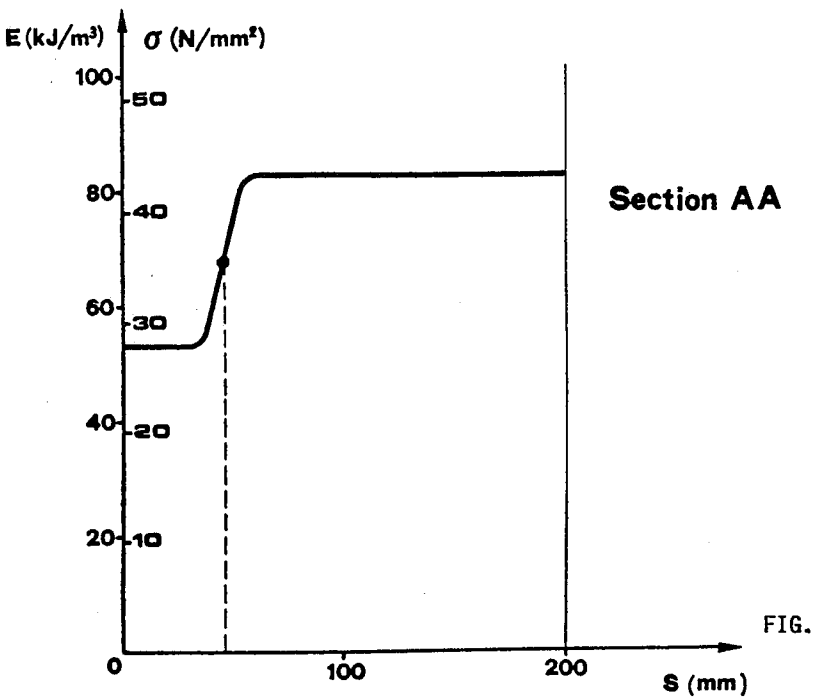

FIG. 3

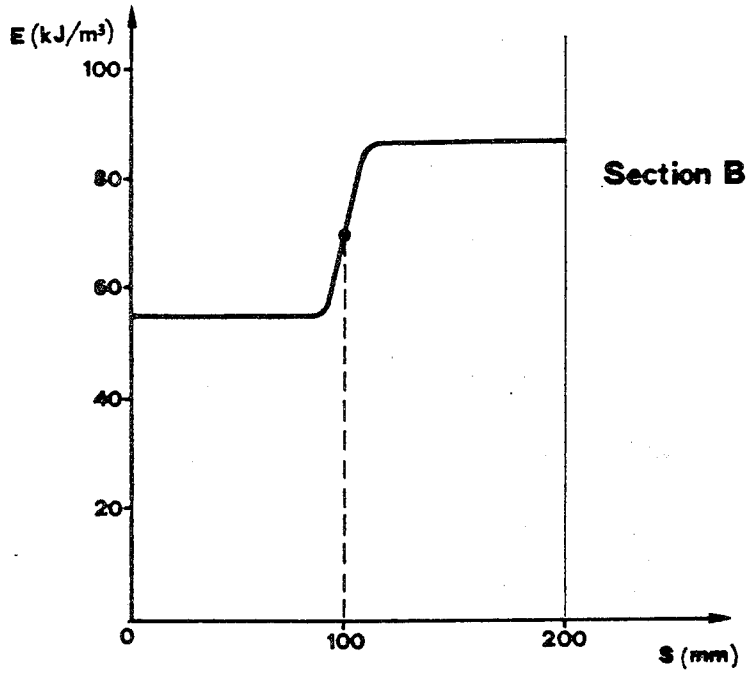

FIG. 4

If we want to represent the trend of the strength (or breaking energy) in a section in which deterioration extends to a greater depth, as in section B-B, the trend is that shown in Fig. 4.

The power of a water jet of flow rate q (m^3/sec) and velocity v (m/sec) is given by the equation:

$$W = \frac{1}{2} \rho q v^2 \text{ (Watt)}$$

where ρ is the specific weight of water.

The energy developed by time interval t is:

$$E = W \cdot t \text{ (Joule)}$$

Let us now presume that the operational parameters of the hydrodemolition equipment (pressure or water velocity, flow rate, and the other geometric and kinetic parameters) have been fixed.

We have thus established the amount of energy which may be distributed over one surface unit. Let us now define the trend of energy available in the jet per unit of volume of concrete in increasingly deeper sections (Fig. 5).

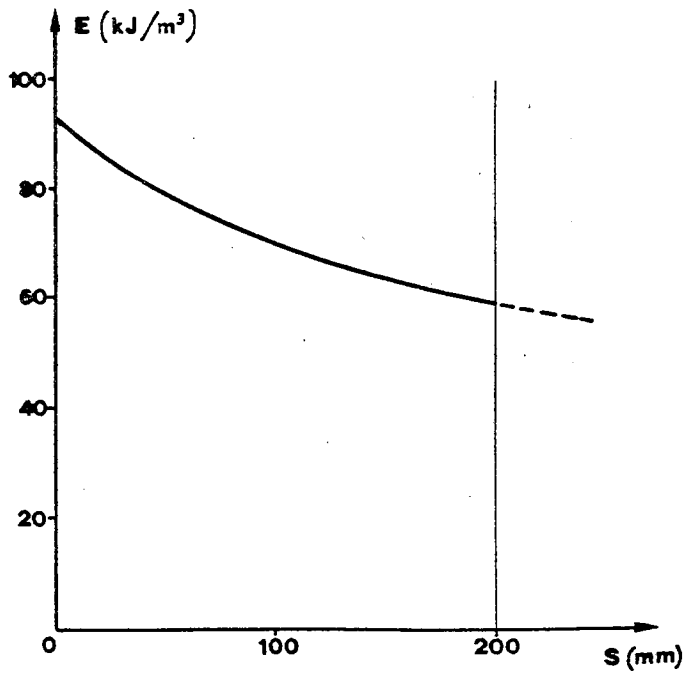

FIG. 5

It should be noted that the power of the jet decreases with distance from the nozzle, not only due to dissipation in the concrete and water, but also and above all due to the instability of the jet itself, since it produces small drops which rapidly lose their energy even in the air.

If we superimpose the two curves (energy necessary to break the concrete and energy available in the water jet), we see that their cross point defines the thickness of concrete which will be removed (Fig. 6).

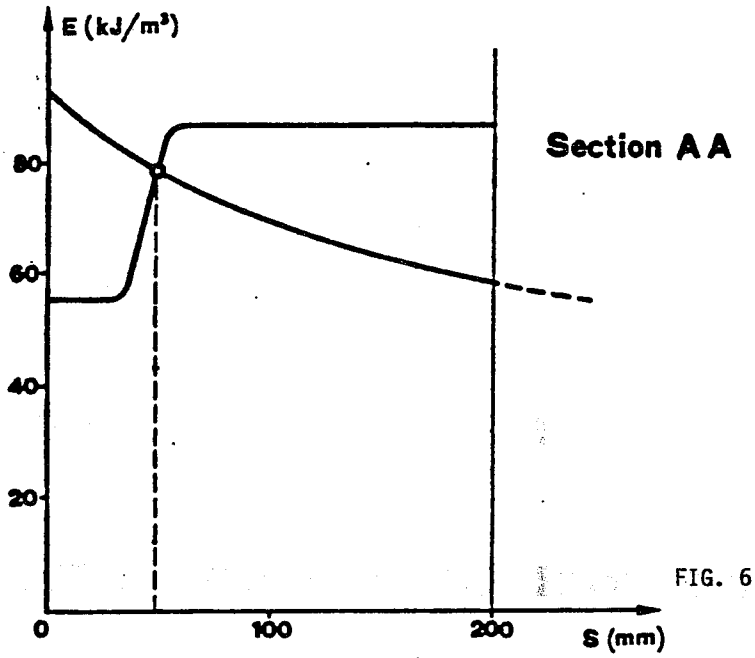

FIG. 6

If deterioration in another part of the deck had reached a deeper level (for example section B-B of Fig. 1), deeper removal would automatically be obtained (Fig. 7).

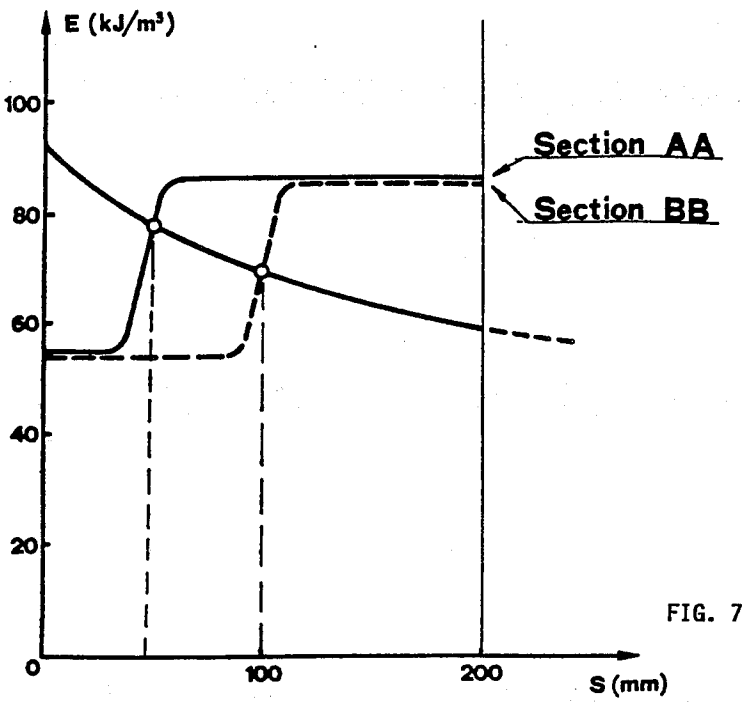

FIG. 7

Naturally, with sound concrete, a constant thickness may be removed by using a sufficiently powerful jet (Fig. 8).

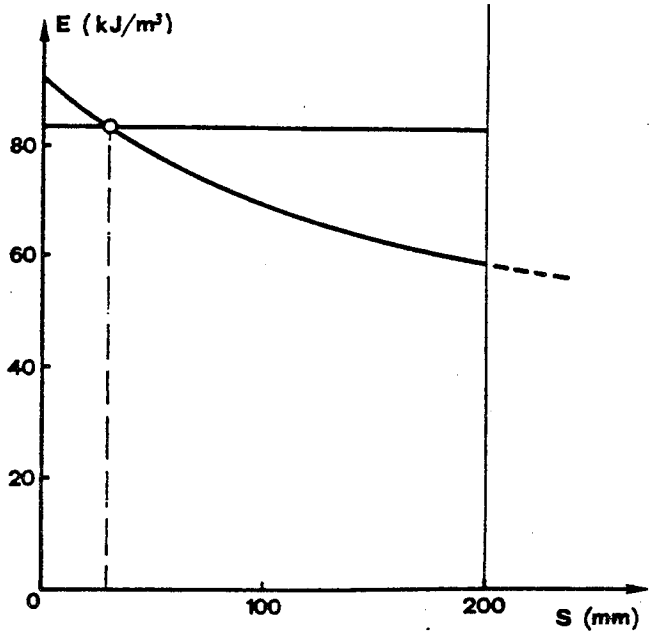

FIG. 8

As already explained, in order to change the curve of available energy at the jet, various parameters may be changed: $E = Wt = \frac{1}{2} \rho q v t$

However, the simplest method is that of varying time t by changing kinematic and geometric parameters of the movement. According to the above, it seems that selective removal is an intrinsic characteristic of hydrodemolition, and it may be achieved with any equipment capable of controlling a water jet. This is not entirely accurate. In effect, selectivity may be achieved only with equipment supplied with a nozzle-moving system and electronic control for guaranteed constancy of selected parameters in time; moreover the water jets must be highly stable and powerful.

The trend of an instable jet versus position is shown in Fig. 9.

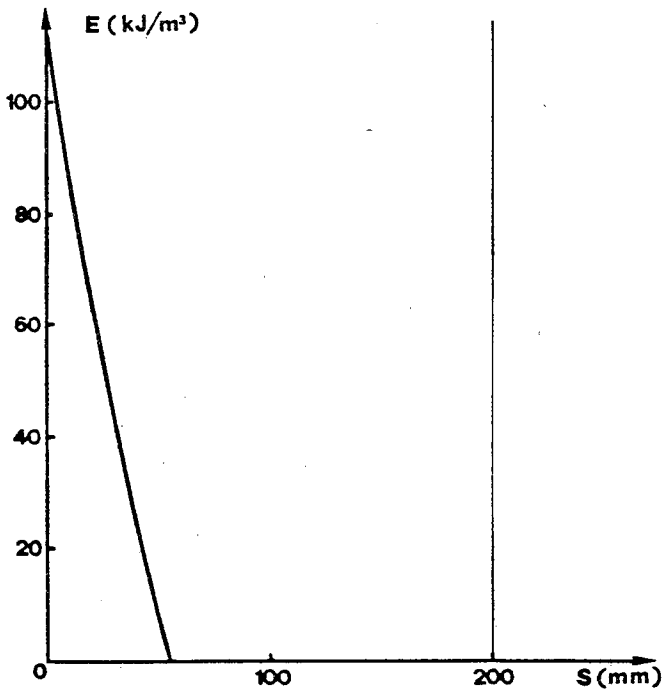

FIG. 9

By overlapping Figs 3, 4 and 9, we see that about the same thickness is removed in each case and that this thickness does not even change to any great extent if the area in question has sound concrete (Fig. 10).

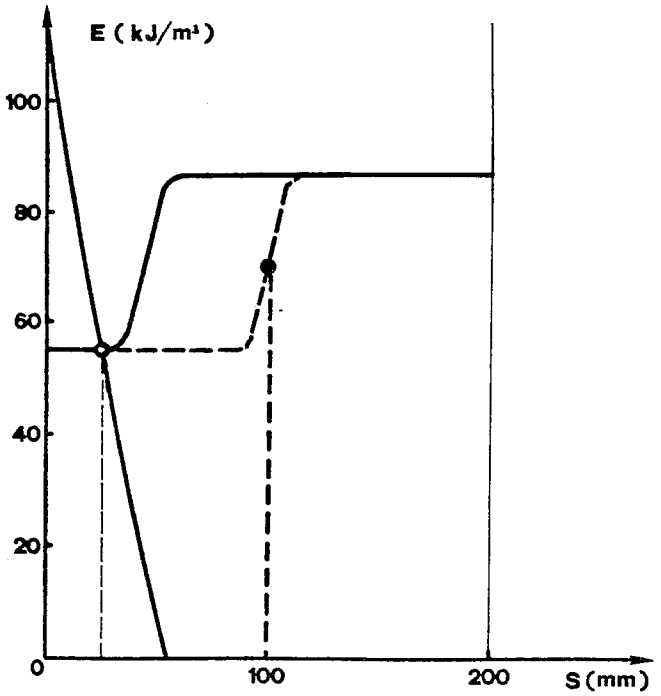

FIG. 10

The experimental evidence of the capacity for selective removal of our equipment was shown by two series of tests carried out by the Swedish Road Administration (Vägverket) in collaboration with the Royal Concrete Institute of Stockholm.

Concrete slabs with indentations of regular geometry (squares and rectangles) and varying depths were prepared (Fig. 11). After emplacement of re-bars, concrete of lesser strength was pouered over the slabs, in order to simulate deteriorated concrete.
Hydrodemolition was carried out after curing. It was noted that only the "deteriorated" concrete was removed, leaving the sound concrete practically intact, both in original geometry and depth of the indentations (Fig. 12).

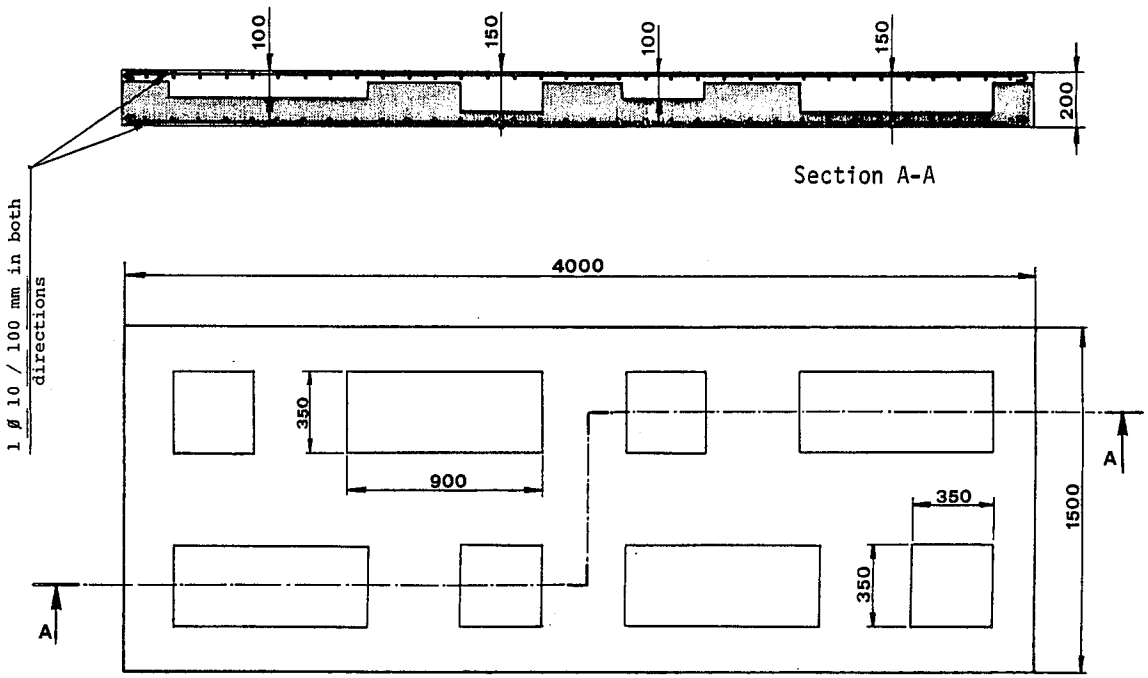

FIG. 11

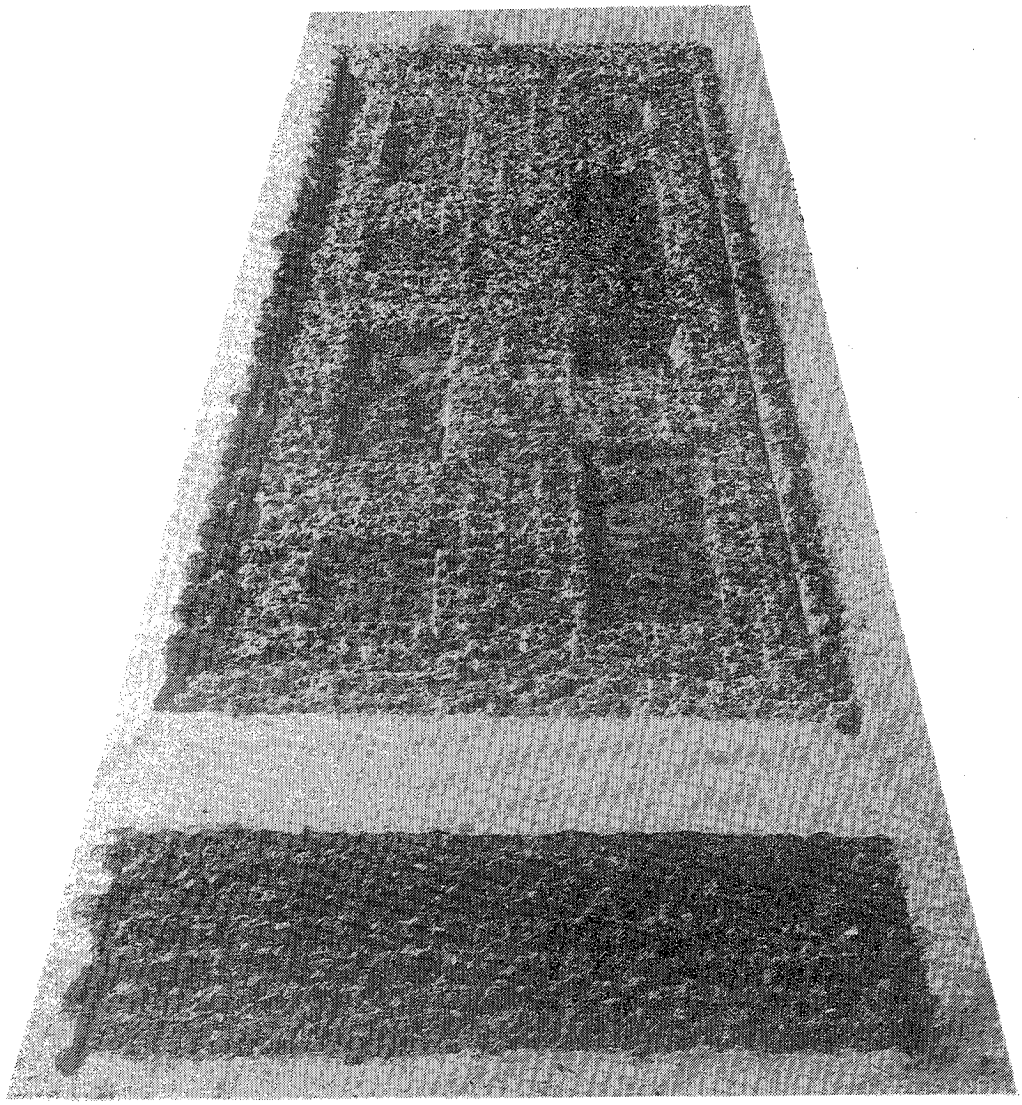

FIG. 12.- Results of selective removal tests.

2.3 Modes of operation

The above shows that hydrodemolition with selective removal does not require detailed testing of the bridge deck in order to identify deteriorated areas and their depth - operations which are expensive and far from precise with existing methods - but it is sufficient to calibrate the equipment carefully and proceed to removal.

Within this apparent simplicity, there are various modes of operation suiting many different situations.

Two of the main ones are described below.

The first case deals with quite wide-spread deterioration in terms of surface area, with depths varying from zero to the whole thickness and with potential involvement of re-bars.

Once the minimum thickness to which the repair material can be applied (e.g. 50 mm) has been established, a few square meters of sound concrete are identified. As a first step the strength of the concrete is determined on samples or, more simply, in situ using non-destructive methods or pullout tests. Working parameters are then fixed with the help of diagrams and tables, obtained from previous tests carried out on slab of predetermined strength.

An initial attempt is made on about 1 square meter and, if necessary, the parameters are redefined.

The equipment is then moved to the area of worst deterioration (the ideal situation would be an area where deterioration involves the entire thickness of the deck).

Testing is considered successful if, with the same parameters as before, all the deteriorated concrete is removed.
If there is reason to suppose that the concrete is not homogeneous over the entire deck, the minimum thickness of removed concrete should be checked periodically.
Sometimes all the re-bars must be exposed and all the deteriorated concrete removed at the same time.
The mode of operation is in any case the same.
The second case often encountered is that of decks of relatively good condition but with insufficient cover, leading to delamination.
In this case hydroscarification (5 to 10 mm) of the entire surface is recommended.
In this way the upper part, possibly contaminated, is removed and, at the same time, excellent roughness is ensured for good bonding of repair materials.
Hydroscarification also shows up possible areas which have undergone some degree of deterioration, but where delamination has not yet occurred.
The bound areas of the deteriorated areas are marked with regular geometrical shapes, if possible grouping several adjacent zones into a single patch. Deep removal is then carried out.
It should be noted, however, that patching is never recommended. It is done, for reasons, of economy, only if the deteriorated areas do not exceed 15-20% of the whole deck.

3.0 ADVANTAGES OF HYDRODEMOLITION

Understood as a new process in the field of removing concrete, hydrodemolition generally offers many advantages over traditional methods.
Of course, additional advantages also derive from the kind of equipment used, its power, manoeuvrability, control system, etc., which all influence removal speed (or productivity) and quality of work - in other words, the economic result.
From the technical viewpoint, the advantages of hydrodemolition are the following:
- constant, repeatable results, once operating characteristics have been established;
- guaranteed total removal of deteriorated concrete (see paragraph on selective removal);
- no damage caused to sound parts of concrete;
- possibility of working even in presence of re-bars, which are not damaged: on the contrary, they are given a thorough cleaning and any trace of corrosion is removed from even their lower parts, usually not reached by other processes such as sand blasting;
- creation of a very rough surface ensuring excellent bonding to repair materials, much higher than the case of jacking or chipping hammers;
- no impacts of vibrations, thus on one hand avoiding damage to reinforcement and on the other ensuring that noise is kept to an acceptable level.
  Moreover, some simultaneous and otherwise impossible operations, such as casting in immediately adjacent areas, may be carried out.
- No dust of fumes (until now an inevitable accompaniment to concrete removal works).
  It should also be noted that work may be done even in poor weather conditions and sub-freezing temperatures.

4.0 THE EQUIPMENT

As already noted, historically hydrodemolition came into being to solve the problems of bridge deck restoration.
However, it has also been extended to other similar applications, such as repair work on parking garages, airport runways, concrete roads, etc.
All these applications refer to horizontal or almost horizontal surfaces.
For even vertical surfaces and soffitts, a new demolition unit has been designed and manufactured, using very complex mechanical and oleodynamic systems requiring computerized control.
Fig. 13 shows a real robot with a demolition head on the end of an articulated arm supported by a 360° swivelling tower. It may be remote-controlled for work even in inaccessible areas (e.g. "hot" areas of nuclear power plants during decomissioning).
For removal of concrete cladding in tunnels, a special truck-mounted piece of equipment has been designed (Fig 14.)
Many accessories have been developed to fulfill special requirements.
For areas where access is very difficult, special manual equipment has been designed - the "Bazooka".
This is a kind of thrust-compensated gun allowing removal of concrete underneath bridge decks and girders (Fig. 15).

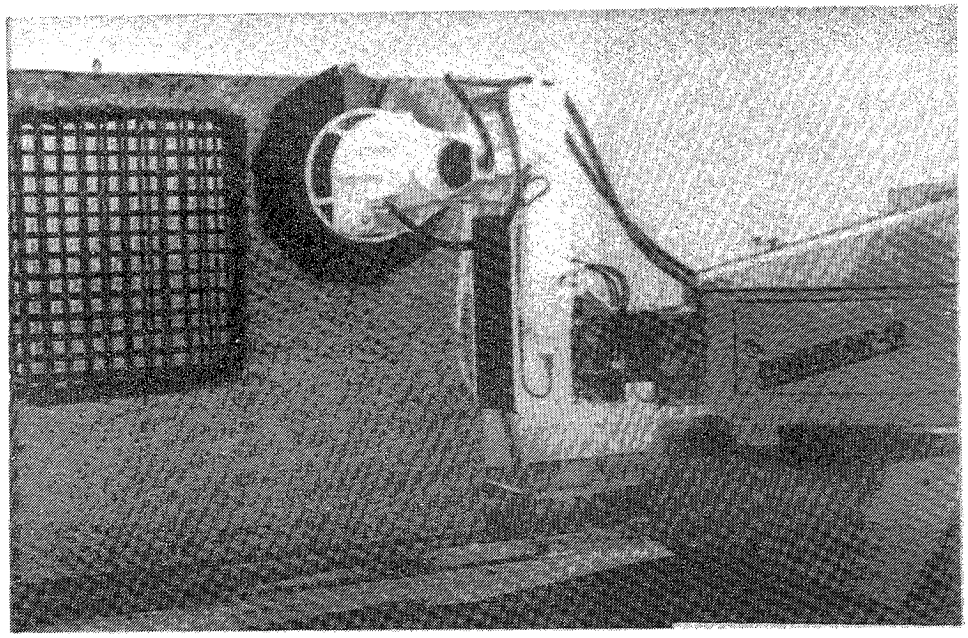

FIG. 13.-

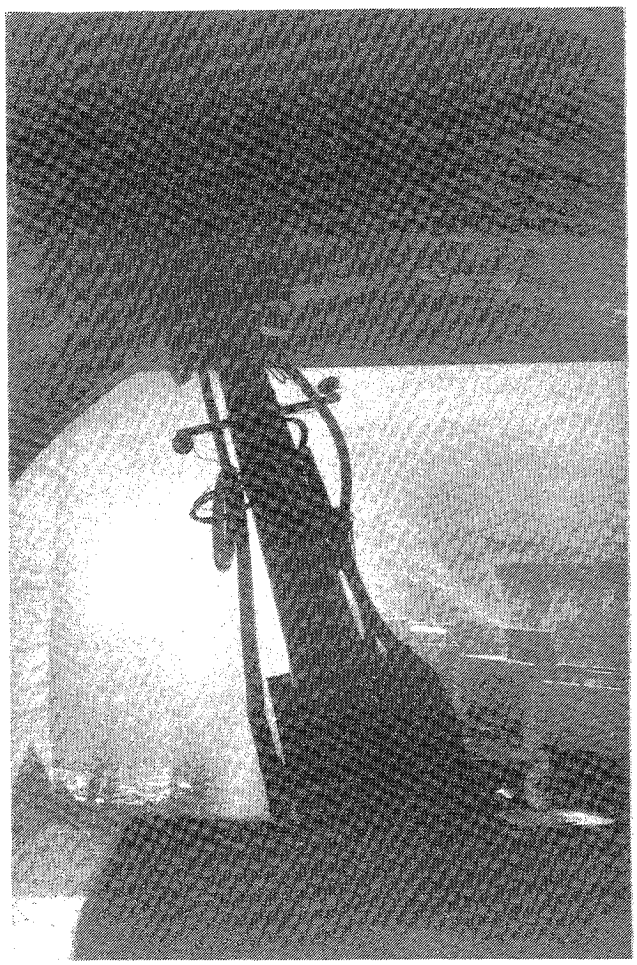

FIG. 14.-

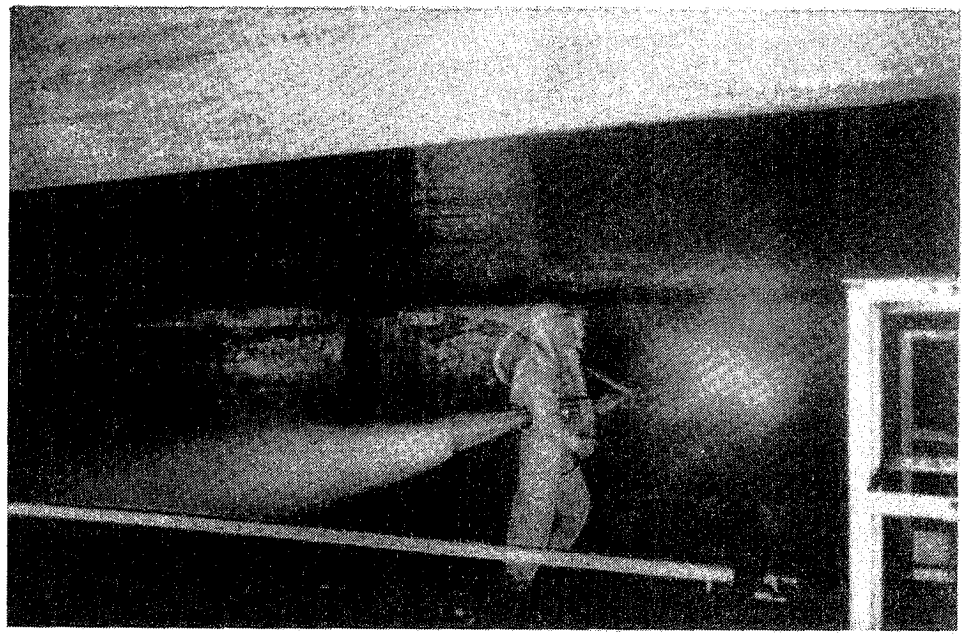

FIG. 15.-

5.0 CONCLUSIONS

Experience world wide has shown that hydrodemolition reperesents a revolutionary, but mature technique in concrete removal.
It is not only a great improvement over conventional systems, but operations which were once impossible may easily be carried out. Structures may be restored even in cases of advanced deterioration.
It is firm belief that to date only a few applications have been explored. Therefore new R&D is to be carried out, aimed at improving reliability and efficiency of existing machinery as well as at designing new equipment.

5th American Water Jet Conference
August 29 - 31, 1989: Toronto, Canada

Paper / Communication 11

RECENT DEVELOPMENTS AND APPLICATIONS USING WATER JETTING FOR TIEBACK ANCHORS AND HILLSIDE DEWATERING

R.D. Mahony AND C.A. Carville
Soil Engineering Construction, Inc.
San Diego, California, USA

ABSTRACT: Two new major areas for the use of water jet technology have recently been introduced in California. The success of the recently developed water jet tools for application to civil and foundation engineering problems has brought about an entirely new area of exploration and development for the water jet. Many applications of the water jet have been developed, tested, and successfully implemented in the geotechnical construction activities of Soil Engineering Construction, Inc. Two of the most important areas are the application of water jetting to tieback anchors and hillside dewatering.

RÉSUMÉ : Deux nouveaux domaines importants d'utilisation de la technologie des jets d'eau ont été récemment découverts en Californie. Le succès des récents outils mis au point pour résoudre des problèmes de génie civil et de construction de fondations a ouvert un tout nouveau champ d'exploration et de développement en matière de jets d'eau. Un grand nombre d'applications des jets d'eau ont été mises au point, vérifiées et utilisées avec succès dans des travaux géotechniques de construction de la Soil Engineering Construction, Inc. Deux des plus importants domaines sont l'application des jets d'eau aux ancres de tirants et à l'assèchement des flancs de colline.

Organized and Sponsored by the National Research Council of Canada and the U.S. Water Jet Technology Association.

1.0 INTRODUCTION

Developers and builders in California are very quickly using up flat, stable, and easily accessible land. They have been and will continue to invade the foothills, terraces, steep hillsides, and mountainous terrain that surround and flank the large valleys, basins, and plains of the towns and cities throughout the state. As this development of steeper or questionable terrain has taken place, marginal or failing hillsides, cliffs, and slopes have been encroached upon and unstable geotechnical situations have arisen.

Landslides have occurred or are eminent; collapsing or endangering one or hundreds of homes.

Mud flows have stripped hillsides bare and encroached upon or collapsed homes and businesses.

Buildings have settled differentially due to cut-fill development on slopes.

Homes have moved laterally or separated due to fill or colluvial soil creep on competent material.

Ocean front property has slid into or is left overhanging steep bluffs due to beach erosion and cliff instability.

Stream front homes are washed away or are left severely damaged due to flooding caused by new developments upstream.

When these situations occur, conventional restoration and rehabilitation techniques may not be enough to rebuild or save the property. Soil Engineering Construction, Inc. was founded nearly 20 years ago to deal with these foundation and geotechnical specialization problems both from engineering design as well as construction. When these foundation specialty situations arise we design or assist in the design and construct the solution.

Many remedies are available to solve the problem, i.e. soldier beam and retaining walls, caisson and pipe pile underpinning, compaction and injection grouting, sea walls and gabions, and gunite or shotcrete surfaces. To design and install one or more of these remedies, different tools and approaches are available, both conventional and contemporary.

The subject of this paper is two unique techniques, used successfully by Soil Engineering Construction, Inc. in the past several years, which involves water jet technology. The first application will be water jetted holes in hillsides and cliffs for installation of high tension tiebacks to withstand lateral earth pressures imposed on gunite or shotcrete faces and on soldier beam, caisson or conventional retaining walls. The water jet in the second application has most recently been used to install overhead hydraugers from within a tunnel to drain water from an active landslide.

FIG 1 MULTI-MILLION DOLLAR HOME ON FAILING CLIFF FACE OVERLOOKING THE PACIFIC OCEAN BEFORE SLOPE STABILIZATION USING WATER JET TECHNOLOGY

2.0 TIEBACKS

The application of water jet drilling for high tension tiebacks or soil nailing was initiated several years ago. Conventional drilling equipment could not be used economically on the steep cliffs and slopes where gunite blanketing was required to stabilize the homes and land above. Water jet drilling proved to be not only economical but much faster than conventional auger or percussion drilling in the extremely difficult locations.

The first water jet drill used was hand held and weighed about 30 pounds. It required a man to be suspended from the cliff face in mountain climbing gear which proved successful in most instances. It was limited in depth (five to 20 feet [1.5 to 6 meters]) and hardness of material since the drill's weight and torque had to be resisted by one man.

FIG 2 HAND HELD WATER JET DRILL

Another application of the hand held water jet drill has been in extremely narrow passage ways. By using drill stems two to three feet (60cm to 90cm) long; holes up to 40 feet (12 meters) deep and four inches (10cm) in diameter have been drilled in a hallway 36 inches (91cm) wide for caisson tiebacks. The material was sandstone and the spoils were contained at the mouth of the hole and pumped to a nearby storm drain. The water jet drilled holes were cleaned with compressed air, and a one inch (2.5cm) high strength steel Dywidag bar grouted in the 40 foot (12 meters) deep horizontal hole. The grouted bar was post tensioned to 85 kips and anchored to the concrete caisson with a steel beam.

The second version of the water jet drill was a light weight track, eight foot (2.4 meters) long with five foot (1.5 meters) sections and drill stem, anchored to the hillside with pins and cables.

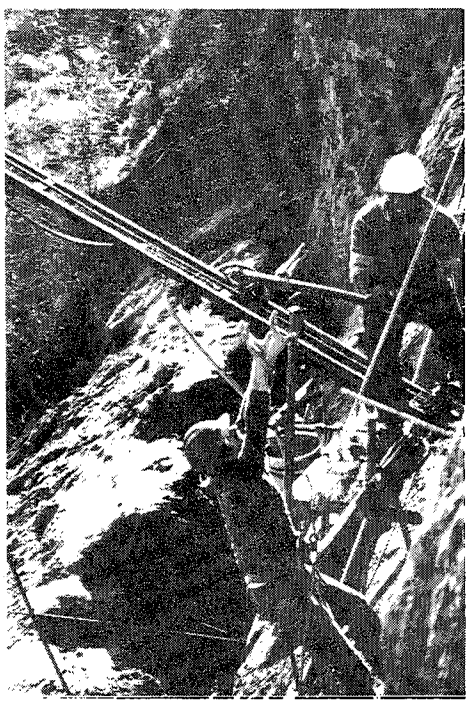

FIG 3A WATER JET DRILLING ON CLIFF FACE

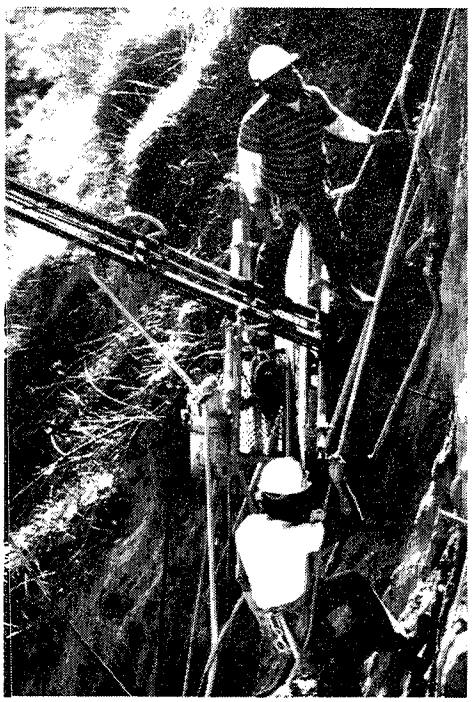

FIG 3B WATER JET DRILL TRACK SUSPENDED FROM CLIFF FACE

The air powered rotation motor on the drill track was advanced with a hand crank by a man suspended from ropes. The method proved extremely successful for three to four inch (7.5 to 10cm) diameter holes up to 60 foot (18 meters) depths in sandstone, siltstone and clay stones. Cobbles or loose sand proved difficult but using casing and/or starter augers helped in some installations.

In addition to suspending a man and the drill rack over a cliff with ropes, the water jet drill has been anchored in crane suspended platforms and lifted up the slope from below in man lifts. On a man lift platform the eight foot (2.4 meters) drill rack is clamped to the platform's top railing and the articulation of the man lift allows the drill to be positioned in a horizontal or tilted position at any height along the cliff face.

FIG 3C WATER JET DRILL ON CLIFF OVERHANGING AMERICAN RIVER

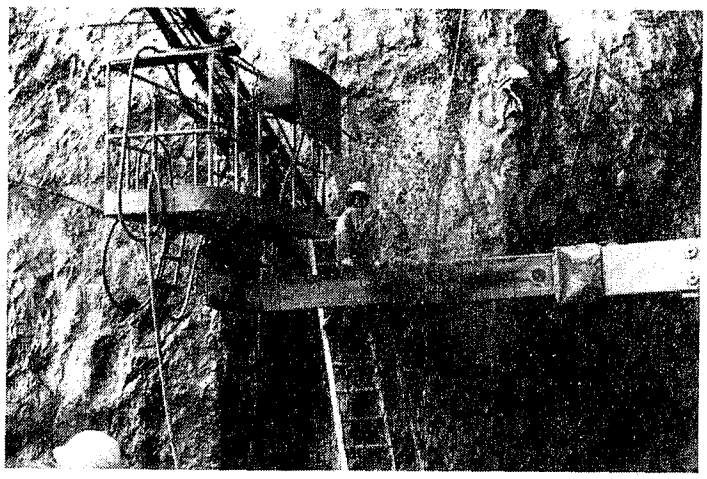

FIG 4 WATER JET DRILL MOUNTED ON MAN LIFT PLATFORM

The man lift also is used for the insertion and grouting of the steel tieback bars, installing of the steel rebar mesh between drill holes and for shooting of the gunite on the slope face. The results of cliff stabilization using water jetted tiebacks are permanent and aesthetic.

FIG 5 MAN LIFT PLATFORM WITH WATER JET DRILL ON FACE

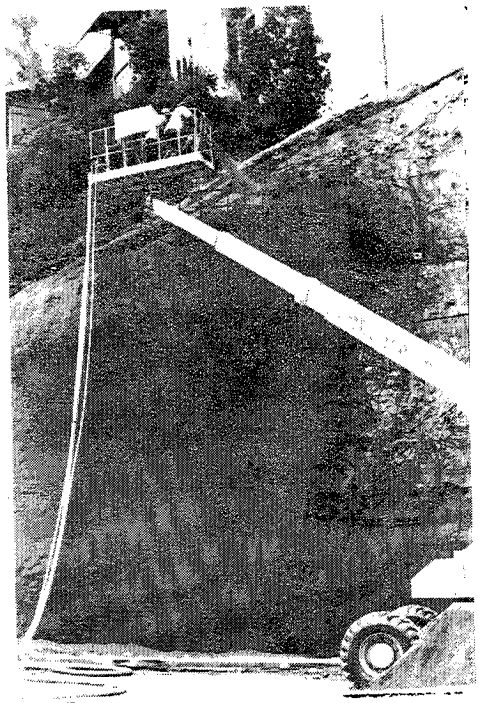

FIG 6 GUNITE BEING APPLIED OVER TIEBACKS FOR CLIFF STABILITY

FIG 7 COMPLETED CLIFF STABILIZATION USING WATER JET DRILLING TECHNIQUES SEVERAL YEARS AFTER COMPLETION

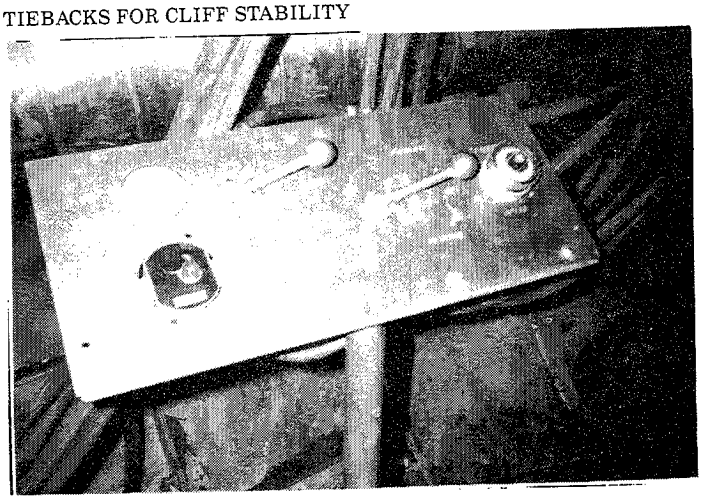

FIG 8 CONTROL PANEL FOR WATER JET DRILL

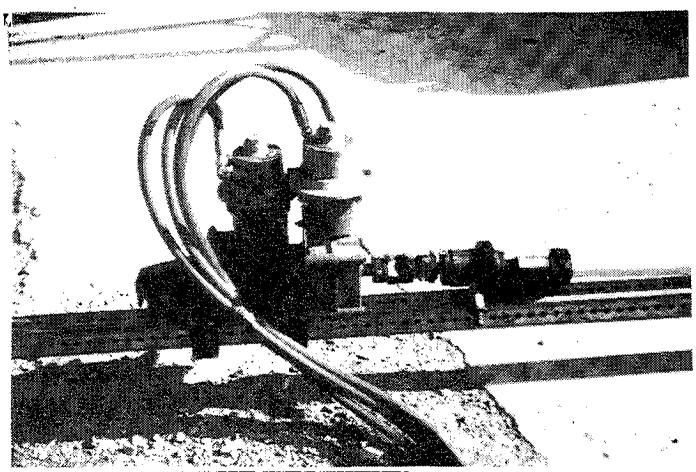

FIG 9 AIR OPERATED MOTOR TO CONTROL ROTATION AND ADVANCE OF WATER JET SWIVEL

The latest version of the water jet drill is a drill rack 25 feet (7.5 meters) long using 10 foot (3 meters) and 20 foot (6 meters) drill rods for holes up to 6 inches (15cm) in diameter at horizontal or inclined positions. The drill is completely automated and operated from a control panel at a close up or remote location.

The water jet drill rotation (forward and reverse) is operated by a variable air motor. A second air motor powers the drill up and down the drill rack at variable speeds and torques depending on the hardness of the material being drilled.

This new drill rack can be suspended from the side of a cliff with ropes, a crane line, lifted by man lift, or simply pinned into a hillside slope at a prescribed angle and the drill stem advanced. The water jet drill is normally powered by a 10,000 p.s.i. hydro blaster pump.

The three to six inch (7.5 to 15 cm) drill bit normally has three water jet holes for water jetting and steel carbide blades for reaming the hole clean. The cuttings are removed from the hole with the normal water jet volume of water which ranges from five to 20 gallons per minute depending on nozzle diameter and output of the pump. Final cleaning of the hole is performed with a compressed air tube down the hole before installation of the tieback bar and grout.

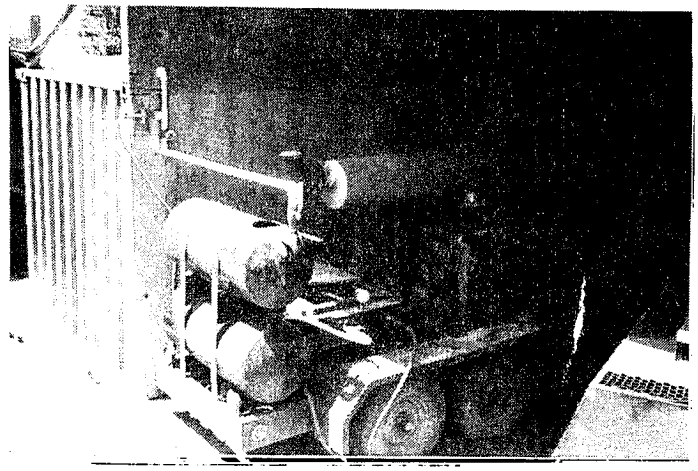

FIG 10 10,000 PSI HYDRO BLASTER PUMP

Belling drill bits are also used to increase the diameter of the hole up to two feet (.6 meters) for increased tieback capacity.

Some disadvantages exist in the water jet drilling system such as disposal of the soil and water. In most cases a stream or storm drain is nearby or separators can be used to remove the soil particles from the water. Not all loose or cobbly soils or extremely hard rock can be drilled using the water jet but our success rate has been well over 90 per cent.

FIG 11 DRILL CUTTING AND WATER BEING REMOVED FROM TIEBACK HOLE WITH COMPRESSED AIR

3.0 HYDRAUGERS

The most recent success in water jetting has come in the installation of hydraugers.

Traditionally, hydraugers are horizontally drilled holes two to six inches (5 to 15cm) in diameter, cased with PVC or steel pipe and left open to drain water from a hillside or slope by gravity. The removal of ground water increases the stability of the slope or soil and rock mass and in many instances deactivates or slows down the progress of an occurring or eminent landslide or slope failure. Hydraugers are drilled at the face of the slope or hillside and have been installed up to 1100 feet (330 meters) into formational soils at horizontal and slightly inclined angles of one to five degrees.

Within the past year a landslide situation in Oceanside, California has arisen where hydraugers, a tunnel, and water jet technology have been combined in an attempt to stop a landslide and save over 200 homes on the slope above.

The landslide began moving in the early to mid 1970's and 11 homes were destroyed. Geotechnical investigations have resulted in several design solutions to stabilize the hillside and the remaining homes. The solutions have ranged from a huge buttress fill whereby dozens of homes would have to be temporarily relocated to move several 100,000 yards of soil to dozens of seven foot diameter concrete and steel shear pin caissons to depths approaching 100 feet (30 meters) in depth. The solution selected however was one where disturbances to the home and life styles of the homeowners would be minimal, yet effective to increase the factor of safety at the landslide.

Dames & Moore, Los Angeles, CA, the selected geotechnical engineer designed a seven foot (2.1 meters) tunnel 1,100 feet (330 meters) long, under and into the landslide to provide access to install hydraugers into the entire length and width of the landslide rather than only at the face of the slide. The tunnel was successfully excavated by hand digging using a hydraulic advanced shield and lining the excavation with steel liner plates. Access holes were left in the crown of the lined tunnel for drilling the hydraugers. The engineers required overhead PVC cased holes to drain the water from above in the slide mass into the tunnel and by gravity out of the tunnel to a flood control channel nearby.

Drilling the overhead hydraugers in the seven foot (2.1 meters) diameter enclosure using conventional auger or percussion drilling equipment was considered to be extremely time consuming and costly, therefore Soil Engineering Construction, Inc. selected the water jet drill to perform the work. The 25 foot (7.5 meters) water jet tieback drill rock was modified into a 100 foot (30 meters) long drill track mounted on wheels to travel on the tunnel invert in a horizontal position.

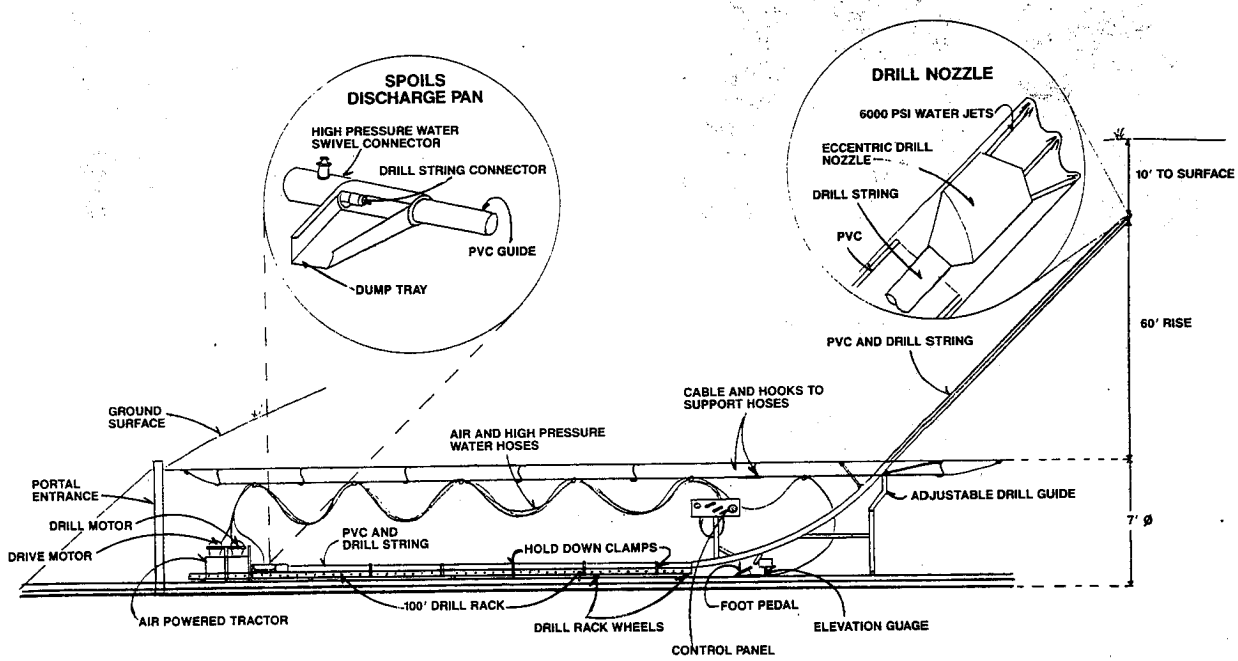

FIG 12 SCHEMATIC DIAGRAM OF WATER JET DRILL IN TUNNEL

A 20 foot (6 meters) long "sweep" was attached to the front of the drill track at a 45 degree angle to the horizontal to propel the water jet drill rod into the landslide foundation above. The drill string travels down the drill track using an air operated motor controlled at a panel mounted on the sweep pipe.

FIG 13 SEVEN FOOT (2.1 meters) DIAMETER TUNNEL LINED WITH STEEL LINER PLATE

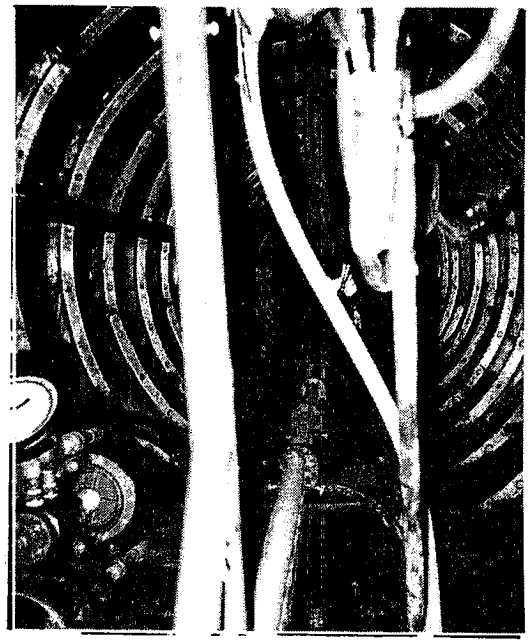

FIG 14 WATER JET DRILL STRING

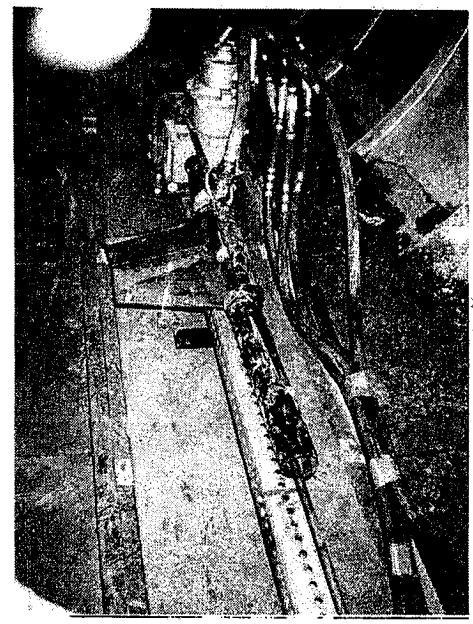

FIG 15 WATER JET DRILL

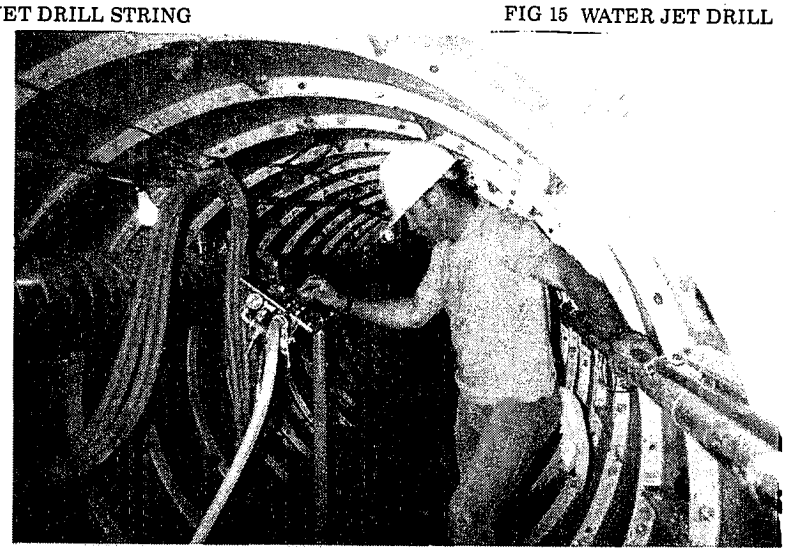

FIG 16 CONTROLS FOR WATER JET DRILL

Rotation of the drill string is achieved using a second air motor. Both motors are variable and reversible. High pressure water (4,000 to 10,000 p.s.i.) is introduced through a swivel attached between motors and the drill string and controlled by a foot pedal.

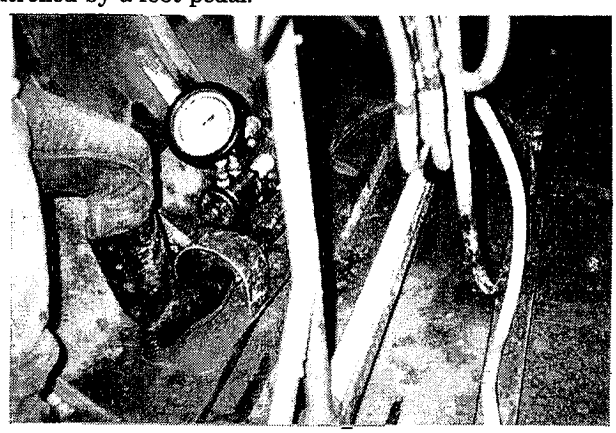

FIG 17 WATER JET FOOT CONTROL

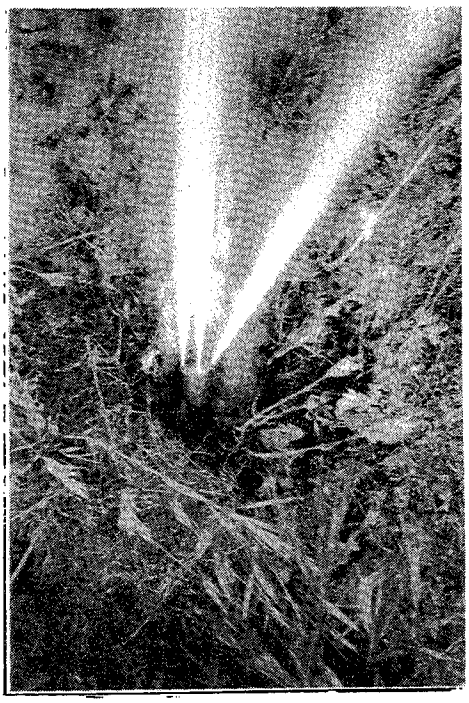

FIG 18 WATER JET DRILL BIT EXITING ON
GROUND SURFACE FROM TUNNEL 60 FEET BELOW

Water jetting of the formational soils above is achieved using a specially designed eccentrically rotating drill bit with three jets in the tip.

The tip holes' diameters can be varied using inserts depending on the hardness of material being drilled, the volume of water desired for removing the drill cuttings in the holes and the operating pressure of the hydroblaster.

The holes can be drilled uncased and slotted PVC pipe inserted at the completion of drilling or PVC casing can be advanced with the drill bit and string to prevent caving or squeezing of the hole. The drill string and bit can be advanced in the formations above or into the sides of the tunnel at any angle from the horizontal to the 45 degree position by repositioning of the sweep.

The drill rack can also be used in a conventional manner outside of a tunnel on the face of the slope by shortening the drill rack and/or mounting or suspending it from man lifts, cranes, or even backhoes for added mobility in moving from hole to hole.

4.0 SUMMARY

An ever expanding frontier is before the geotechnical and foundation engineer and contractor in using water jet technology provided research and development is continued. Many other solutions to unique or extremely difficult foundation problems are under consideration due to the light weight, economy and mobility of the water jet drills. Conventional auger, rotary, or percussion drills will never be replaced by the water jet drill but in the near future the water jet drill will take its place along side the conventional tools as a reliable and economical means to construct holes and cavities into soil and rocks.

5.0 ACKNOWLEDGEMENTS

The authors wish to thank John Wolgamott and Jerry Zink at Stoneage in Durango, Colorado for their assistance and support in the last five years to help develop and construct the water jet technology and tools that have led to our success in water jet drilling. Additionally we wish to thank and congratulate the entire staff of Soil Engineering Construction, Inc. that have contributed to the advancement of water jetting and especially Al Rock for his recent re-designs of the hydrauger water jet for successful completion of a major project and to Sherry Ross for compiling, drafting, and typing this manuscript.

5th American Water Jet Conference
August 29 - 31, 1989: Toronto, Canada

Paper / Communication 12

CONCRETE CUTTING USING ROTARY WATER JETS

H. Yoshida, K. Nishi AND T. Isobe
Kajima Institute of Construction Technology
2-19-1, Tobitakyu, Chofu City, Tokyo 182, Japan

ABSTRACT: Recently, the abrasive water jet has been drawing attention as a concrete cutting technology with which low noise and low vibration cutting is possible. However, due to its expense, the problem of slurry disposal, and a decline in cutting efficiency when making deep cuts, the application of this method has not become common. As a new concrete cutting technology which can replace the abrasive jet system, we have developed a device using rotary jets. For the development of the device, a high-pressure nozzle was designed making use of appropriate materials. Aiming at reducing size and weight, a new high-pressure swivel was developed. Based on the results of cutting tests, the cutting capability was examined in terms of the effects of a variety of factors and also energy efficiency. As a result, it was found that the higher the nozzle traverse rate is, the better the cutting capability becomes and that the rate of nozzle rotation is not especially influential. Also determined was that with a conical entry nozzle roughly doubled cutting capability is attained compared with that attained with a straight entry nozzle, that cutting deeply with a constant capability is possible if the nozzle is inserted, that the cutting capability is in proportion to the jet energy when the pressure is set at 147 Mpa or above, and that the rotary water jet method assures a higher cutting capability than that obtained by the abrasive water jet method for cutting at depths deeper than a particular level.

RÉSUMÉ : Le jet d'eau abrasif a récemment attiré l'attention comme technique pour réaliser dans le béton des coupes avec peu de bruit et de vibrations. Cependant, à cause de son coût, du problème de l'élimination des boues et du rendement décroissant en fonction de la profondeur des coupes, l'application de cette méthode n'est pas devenue répandue. Comme nouveau moyen de coupe du béton qui peut remplacer les jets abrasifs, nous avons mis au point un dispositif à jets rotatifs. Pour construire le dispositif, nous avons conçu une buse à haute pression à partir de matériaux appropriés. Dans le but de réduire les dimensions et le poids du dispositif, nous avons mis au point un nouveau pivot à haute pression. A partir des résultats des essais de coupe, nous avons examiné la capacité de coupe en termes des effets d'une variété de facteurs et aussi du rendement énergétique. Nous avons constaté que plus la vitesse de déplacement de la buse est élevée, plus la capacité de coupe augmente et que la vitesse de rotation de la buse n'a aucun effet particulier. Nous avons aussi trouvé que la capacité de coupe d'une buse à entrée conique est environ le double de celle d'une buse à entrée droite, que les coupes profondes sont possibles avec une capacité constante si la buse est insérée, que la capacité de coupe est proportionnelle à l'énergie du jet lorsque la pression est réglée à 147 MPa ou plus, et que le jet rotatif a une capacité de coupe supérieure à celle du jet abrasif pour les coupes d'une profondeur dépassant une valeur donnée.

Organized and Sponsored by the National Research Council of Canada and the U.S. Water Jet Technology Association.

1.0 INTRODUCTION

Recently, the use of the abrasive water jet has spread rapidly in the construction industry, being a new cutting technology for working with reinforced concrete structures. The abrasive water jet system has many merits such as low noise, low vibration, and low amounts of dust, and is suitable for a remote control operation. The abrasive water jet may be promising basic technology when the application of automatic, low noise and low-polluting systems for the dismantlement of existing structures is required. However, factors limiting its popularity include its higher cost than other cutting methods and its decline in cutting capability when applied to deep cuts. Its application is limited to particular situations including the remodeling of residential structures and the dismantling of biological shield of nuclear reactor buildings.

The rotary water jet is proposed as a technology which can improve on the factors of cost and cutting capability. This cutting technology has been studied mainly in regards to the drilling and cutting of hard rocks.[1),2)] This method is characterized by nozzle rotation, which can widen the width of the cut, and the insertion of the nozzle into the kerf as the cutting proceeds. A merit of this system is that it can maintain a given cutting capability even for deep cuts.

We expected this merit is applicable for concrete cutting and we have conducted basic research to clarify the rotary water jet's cutting and drilling capabilities for concrete. As regards concrete dismantlement, it is expected that high pressures and high flow rates are required in order to crush aggregate. Therefore, a new system was developed so that swivels and nozzles can withstand such high pressures and high flow rates. This report outlines the development of a high-pressure swivel and presents the results of cutting tests using this system on concrete.

2.0 DEVELOPMENT OF HIGH-PRESSURE SWIVEL

2.1 Outline of High-Pressure Swivel

As shown in Fig. 1, there are two sealing methods--one employing a packing seal and another making use of a mechanical seal -- which are used for rotary water jet systems. Both types encounter problems concerning the durability of the actual sealing surfaces and the size of the whole system including a power unit for rotation. Friction on seal surfaces results in heat generation, wear, and resistance to rotation when used under pressures of 100 Mpa or larger and at high speeds for long periods of time.

Therefore, a new type of swivel was developed, which is shown in Fig. 2. This swivel's seal is generally called a non-contact seal. In this system there is a gap at the seal surfaces from which a particular volume of fluid is leaked. This system has advantages in terms of greater durability and lower rotation resistance. Such seals have been applied previously in low-pressure equipment and hydraulic equipment. During the design of the seal, the clearance between the two cylinders and the seal length L are determined so as to maintain the volume of water leak below a given amount. In addition, it is important to select appropriate materials taking into consideration potential deformation under high pressure. The deformation is estimated using the axial- symmetry, two-dimensional finite-element method.

2.2 Performance Tests

Table 1 compares the performance of the swivel using a non-contact seal, which was obtained from the verification test, with that of a swivel using a conventional mechanical seal. As the table definitely shows, the rotation resistance load with the non-contact system is far smaller (about 1/20 at 196 Mpa) than that with the taper type, and also the leakage flow rate is less than 0.1% of the maximum flow rate of 50 l/min tested. As regards durability, the rate of wear is extremely low because the surfaces are not in contact. Measurements after 50-hours of use revealed that the clearance change due to wear was 0.1 μm or less. No problems have occurred over more than 200 hours' operation.

3.0 CONCRETE CUTTING TEST

3.1 Test Apparatus and Specimens

Table 2 shows the main specifications of the test apparatus. The concrete specimens produced for testing had an unconfined compressive strength of 34.3 Mpa and a maximum aggregate size of 20 mm. Photo 1 shows the rotary nozzle unit and a test specimen. Three types of nozzle bodies, which are shown in Fig. 3, were used in the tests. A difference of (c) from both (a) and (b) is the presence of a conical taper of the nozzle's inside wall. Unit (a) was designed as a shape for which a diamond nozzle is applicable. Such a nozzle was used for the abrasive water jet and pure water jet studies. Units (b) and (c) were newly designed so that the insertion of the nozzle into the kerf was made possible. The selection of nozzle materials for high-pressure water jets (100 Mpa or more) is problematic, considering the eroding effect of high-speed fluids. Therefore, unit (b) was designed so that a sapphire nozzle can be used adopting a nozzle mount which had actually been used as high-pressure nozzle. As for (c), since there is no product with a conical inlet on the market, a specimen was manufactured using particular ceramics which were selected according to material test results.

3.2 Test Methods

For cutting using a rotary water jet, conditions of nozzle placement (nozzle angles, and the distance from the central axis) are important test factors because they greatly affect the cutting capability and the shape of the kerf. In addition, the shape of the nozzle also affects the cutting capability, as reported by Dr. Vijay[1]. Therefore, this factor has to be evaluated as well. Also, water jet parameters such as pressure P, water nozzle diameter d, and operation parameters such as nozzle traverse rate T, rotational speed of the nozzle R, and the method of inserting the nozzle influence cutting characteristics.

Concerning these factors, tests were conducted for five different cases as shown in Table 3, and the cutting depth, the cut volume and the cutting width were measured for each case. Cutting depth for a 300 mm distance (the length of cutting being 400 mm) was measured at intervals of 10 mm using a measuring rod with a diameter of 3 mm. The measured values were then averaged. The cutting volume was measured according to the volume of fine sand (grain diameter of 0.5 mm) required to fill the kerf for a 300 mm length. The cutting width was measured at intervals of 50 mm along the cutting length at depth intervals of 30 mm using an inside caliper. The average width was then calculated.

Pressure was measured by a strain type pressure gauge which was fixed on the joint block of the nozzle unit. The flow rate was measured by a positive displacement flowmeter which was fixed on the water supply side of the pump.

3.3 Test Results

In this study, nozzle body design was evaluated through tests and the test results were evaluated according to the effects of various factors using the cutting depth as the characteristic value.

(1) Design of Nozzle Body

It can be expected that the surface width of the kerf depends on the rotation radius at the specimen surface as shown in Fig. 4, and the shape of the kerf depends on the degree of dispersion of the water jet, quantified as the angle θ. (See Fig. 4.) Figs. 5 and 6 show the shapes of the kerfs and the specific energies as related to the nozzle angle for cases where r is almost unchanged.

The cutting width is standardized with r in Fig. 5. The specific energy shown in Fig. 6 is presented as an indicator which shows cutting capability, details of which are given in section 3.3 (5). Fig. 5 suggests that the surface width of the kerf is proportional to r (approximately 2.5 r). In addition, the width of kerf becomes narrower at at great depths when θ is 0. When $\theta=4^{\circ}$ or 8.5°, the kerf width is larger than the surface width at least up to cutting depth H = 8 cm.

As regards cutting capability, a slightly better result was obtained at $\theta = 4^{\circ}$. However, there is no considerable difference from the viewpoint of practical application. Thus these results show that there are no considerable differences in the cutting width and cutting capability for cases where θ is between 4° and 8.5°.

On the other hand, nozzle placement is determined based on the following reasons in addition to the findings from the results presented above. As regards concrete cutting, it is more effective to free the coarse aggregate from the matrix rather than crush it. For that purpose, the cutting width should at least be larger than the maximum coarse aggregate size (20 mm). Thus the cutting width was determined to be 40 mm, two times the maximum aggregate size. When the outside diameter of the nozzle to be inserted is 27 mm, e=8.5 mm and $\theta=8.5^{\circ}$ are the maximum design values, and clearance between the cutting kerf and the nozzle body becomes 6.5 mm on one side. To assure the cutting width of 40 mm, r should be 15 mm or above (see Fig. 5). The standoff distance S.D. is 147 mm for $\theta=4^{\circ}$ and 57 mm for $\theta=8.5^{\circ}$.

Generally, the larger the S.D. is, the smaller the cutting capability of the water jet becomes, so a better angle for a nozzle body to be inserted would be $\theta = 8.5^{\circ}$. For these reasons, e = 8.5 mm and $\theta = 8.5^{\circ}$ were chosen for nozzle body insertion.

(2) Comparison of Nozzle Shapes

According the the inside shape of the water nozzle, the structure of the water jet varies, affecting the cutting capability. In order to confirm this effect, cutting capabilities were compared using nozzles (b) and (c) which are shown in Fig. 3. The results are shown in Fig. 7. It was proved that the cutting depth can be about doubled by using a conical water nozzle.

(3) Effects of Nozzle Insertion

Fig. 8 shows the relationship between the number of passes N and and the cutting depth H for the case in which the nozzle is not inserted (S.D. = 10 mm). Fig. 9 shows the relationship between N, H, and S.D., when the nozzle is inserted, for each N/T = 0.125 sec/mm.

According to Fig. 8, the deeper the cutting depth is, the smaller the incremental increase of the cutting depth when the S.D. is fixed.

On the other hand, as shown in Fig. 9, the cutting depth increased at almost the same rate as the rate of increase of N when the nozzle is inserted.

In order to examine the change in the increase of kerf depth ΔH, as related to the relative distance R.D. between the nozzle and the cutting surface (See Fig. 4), the relationship between R.D and ΔH (N/T=0.125) is given in Fig. 10. According to Fig. 10, it was found that ΔH decreases linearly with an increase of R.D. Accordingly, with the method in which the nozzles is inserted, the best efficiency is attained if the distance between the nozzle and cutting surface is minimized (at the distance required to maintain r). Also, the cutting capability does not decrease even when the cut becomes deeper.

(4) Effects of Jet Parameters and Operational Parameters

Fig. 11 relates the nozzle rotation speed and the cutting depth, with the traverse rate T and the nozzle diameter d as variable parameters. This figure suggests that the nozzle rotation speed does not really affect the cutting depth.

Figs. 12, 13 and 14 show the relationship of the cutting depth to the traverse rate, nozzle diameter, and pressure, respectively.

The relationship between the traverse rate and the cutting depth for the water jet can be approximated by the use of an exponent. Therefore, the results which were approximated by the least squares method are given in Fig. 12. The exponent for the approximation equations vary slightly according to the nozzle diameter, within the range between -0.3 and -0.4.

In the case of the abrasive water jet, the value of the exponent is -0.59.[3] The difference in the values suggest that the effect of the traverse rate is smaller for the rotary water jet as compared to the abrasive water jet. The relationships of the cutting depth to nozzle diameter and jet pressure are almost linear.

(5) Relationship between Input Energy and Cutting Depth

When discussing the effects of various factors on the performance of the rotating water jet, if the energy required for cutting to a particular depth is quantified, this value can serve as a useful guide to estimating cutting capability, as well as being basic data for engineering purposes. Therefore the results presented in parts (2) and (4) have been revised to show the relationship between the cutting depth and the specific energy. The specific energy S_E is defined by the following equation.

$$S_E = 166.8 \times (P \cdot Q \cdot N)/(T \cdot H) \quad (Joule/cm^2) \qquad (1)$$

The units for the variables on the right are different: Mpa for P, liter/min for Q, pass for N, mm/sec for T and cm for H. These are justified with the constant on the right side. As the above equation clearly shows, S_E is the input energy quantity related to the area cut (length x depth) per unit time. If this is related to the depth at which cutting takes place, it can serve as an indicator to evaluate the energy efficiency (the ratio of the energy expended to the work done) for a particular depth of cut.

Fig. 15 shows the results of such an evaluation on the effect of the traverse rate for different nozzle diameters. According to the figure, the energy required for a particular depth of cut becomes smaller with an increase of the traverse rate (almost the same at T=4 mm/sec and 8 mm/sec), and there are almost no effects resulting from variation of the nozzle diameter.

Fig. 16 shows the results of an evaluation of jet pressure. This figure suggests that efficiency is extremely low at P=98 Mpa, while there is no considerable difference in cutting efficiency among jet pressures of 147 Mpa or above. According to the above results it was found that if the jet pressure is set at 147 Mpa, the cutting capability is proportional to the jet energy, i.e. pressure and flow rate.

As has been described above, a merit of the rotating water jet is that cutting at a consistent efficiency is possible even for a large cutting depth. On the other hand, the cutting capability falls when cutting deeply by abrasive water jet. Fig. 17 compares both methods in terms of the relationship between the cutting depth and the specific energy. As represented by the figure, the cutting capability is higher with the rotating jet than with the abrasive water jet beyond a given depth, about 20 cm with silica sand abrasive and about 40 cm with garnet abrasive.

4.0. CONCLUDING REMARKS

The following findings were obtained by the study.

1) Among the operation parameters of the rotating water jet, the effect of the traverse rate is large, while nozzle rotation speed has almost no effect. The higher the traverse speed is, the better the cutting capability becomes.

2) As regards nozzle shapes, roughly doubled cutting capability is attained with a conical entry nozzle compared with a straight nozzle.

3) By means of inserting the nozzle, a constant cutting capability is obtained for deep cutting.

4) When the pressure is set 147 Mpa or over, the cutting capability is in proportion to the jet energy regardless of variations of pressure and nozzle diameter.

5) When compared with the abrasive water jet method, cutting deeper than a particular depth, i.e. 20 cm for silica sand abrasive and 40 cm for garnet abrasive, a higher cutting capability is attained by the rotary water jet method.

It is considered that the rotary water jet method possesses great potential as a new concrete cutting technology which could replace the abrasive water jet method. Therefore we are planning to develop new engineering methods using this technology.

5.0 References

1) Vijay, M. M., W. H. Brierley and P. E. Grattan-Bellew: "Drilling of Rocks with Rotating High Pressure Water Jets: Influence of Rock Properties", Proceeding, 6th International Symposium on Jet Cutting Technology , April 1982.

2) Hillaris J. A. and S. A. Bortz: "Quarrying granite and Marble Using High Pressure Water Jet", Proceeding, 5th International Symposium on Jet Cutting Technology, June 1980.

3) Isobe, Takahisa: "A Fundamental Study on the Cutting Characteristics of Abrasive Jets (PART 2)", Annual Report of Kajima Institute of Construction Technology, Vol. 35, June 1987.

Table 1 Comparison between a Mechanical Seal and Non-Contact Seal

	Mechanical seal		Non-Contact seal	
Pressure (Mpa)	Resistance torque (kg·cm)	Leakage flow rate (cc/min)	Resistance torque (kg·cm)	Leakage flow rate (cc/min)
0	68.25	measurement impossible	1.62	0
98	94.33		2.67	6.70
147	119.25		3.87	19.55
196	122.30		5.80	51.40

Table 2 Specification of Test Equipments

High pressure triplex plnger pump

Operation pressure: 200 Mpa
Maximum flow rate : 64 litter/min
Maximum power : 250 kw

Nozzle support and traverse equipment

Speed range : 0.5 - 120 mm/sec (horizontal)
1 - 5 mm/sec (vertical)

Pressure gauge

Maximum measurable pressure: 196 Mpa
Non-linearity : 0.2 % F.S

Flowmeter

Measurable range : 10 - 100 litter/min

Table 3 List of Testing Factors and Conditions

Test number	1	2	3	4	5
Water pressure P[Mpa]	196	137	196	196	98, 147, 196
Nozzle diameter d[mm]	1.6, 1.0, 0.7	1.6	1.6, 1.0, 0.7	0.8x2 / 0.7x2 1.0x2	0.7x2
Nozzle shape	Straight entry	Straight entry	Straight entry	Straight / Conical	Conical entry
Rotation speed R[r.p.m]	300, 150, 75	300	300, 150, 75	150	300, 150, 75
Traverse rate T[mm/sec]	2, 4, 8, 16	4	2, 4, 8, 16	8, 16	8 / 16
Number of pass(maximum) N	4, 8, 16, 32	8	4, 8, 16, 32	up to H=20cm	8 / 16
Nozzle angle θ[degree]	0	0, 4	4	8.5	8.5
Distance from central axis e[mm]	10	10, 15	10	8.5	8.5
Remark	S.D.= 10 mm	S.D.= 10 mm	S.D.= 10 mm	Insertion Initial S.D.=50 mm	Insertion Initial S.D.=50 mm

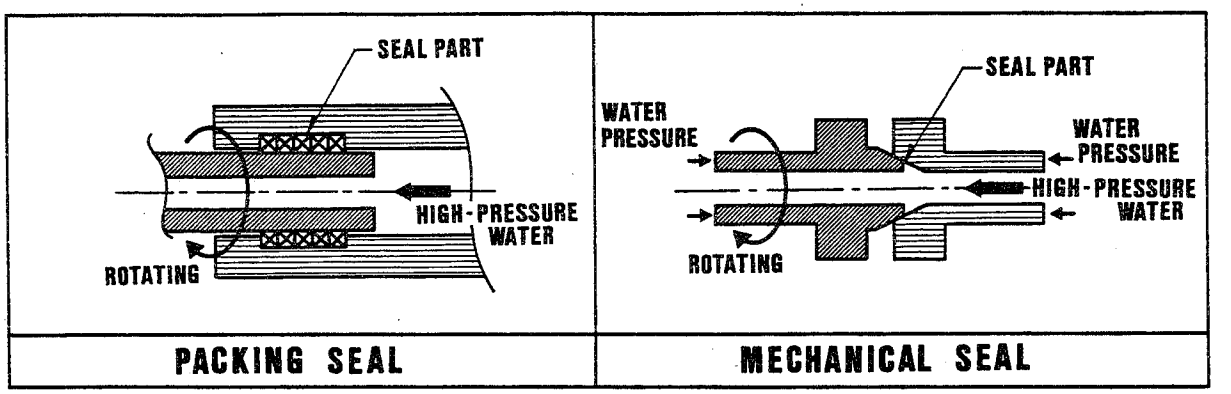

Fig. 1 Sealing Method

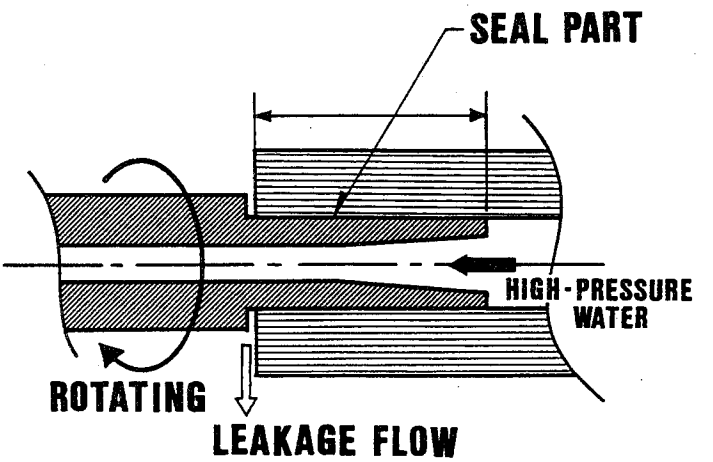

Fig. 2 Non-Contact Sealing Method

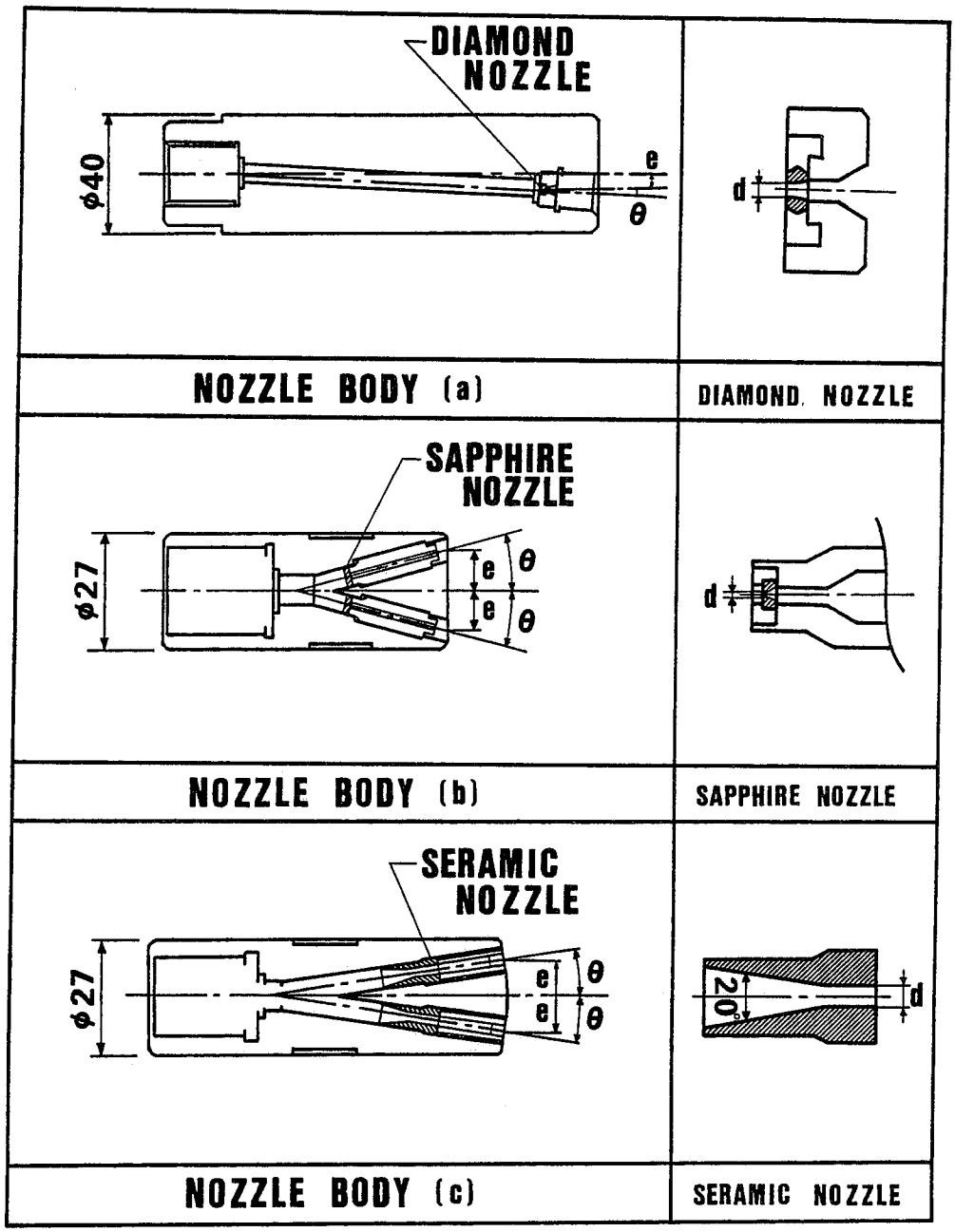

Fig. 3 Rotary Jet Nozzles and Nozzle Bodies

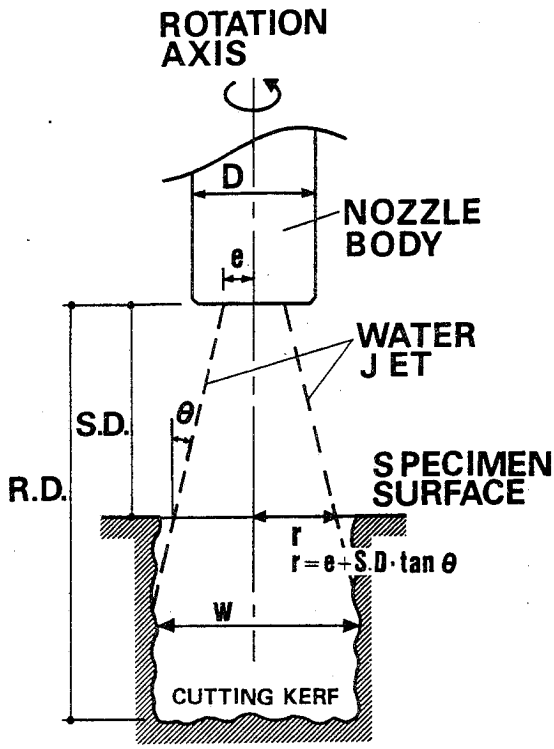

Fig. 4 A Sketch Illustrating the Positions of Nozzle and Kerf

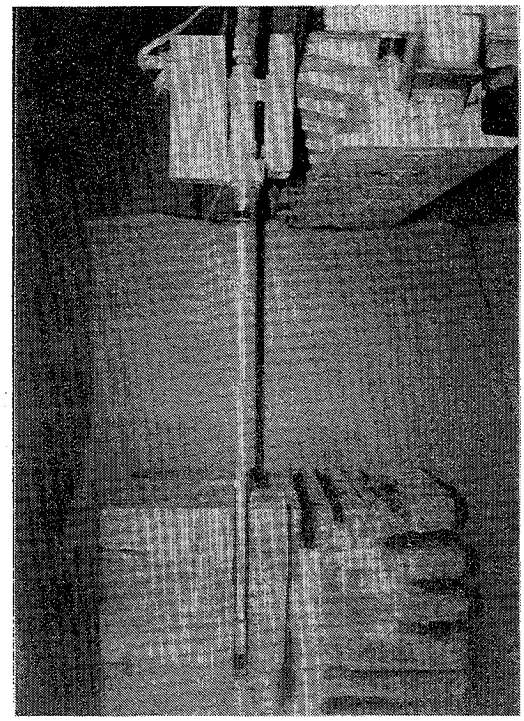

Photo 1 Rotary Jet Unit and Test Piece for Cutting

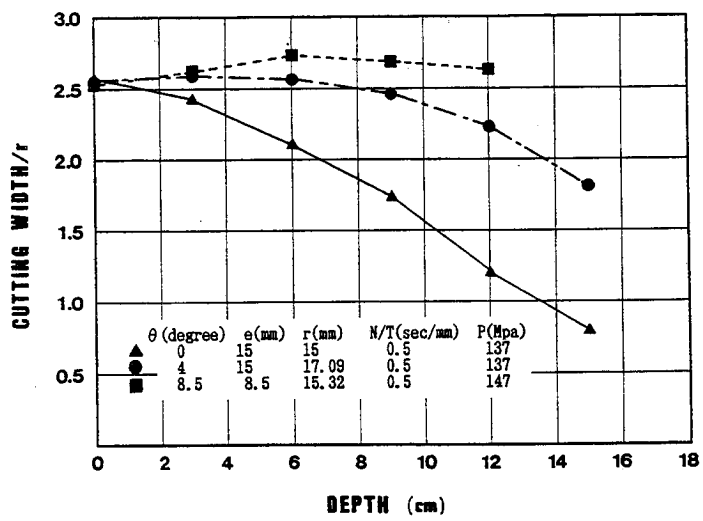

Fig. 5 The Shapes of Kerf at Variable Nozzle Angles

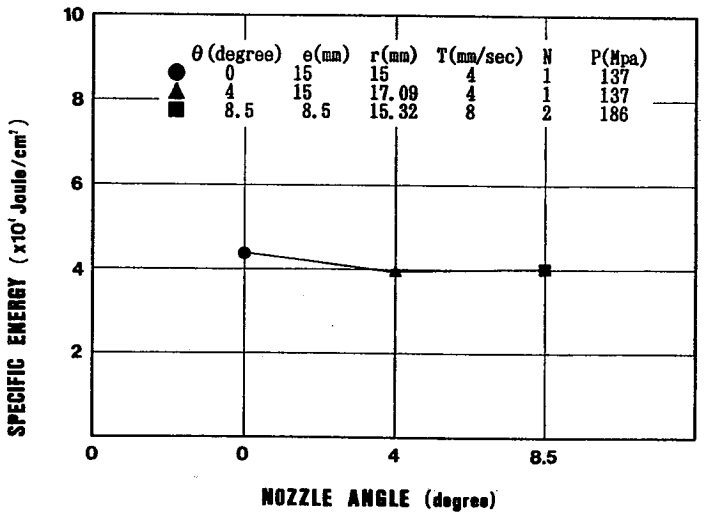

Fig. 6 Comparison of the Cutting Ability of Different Nozzle Angles

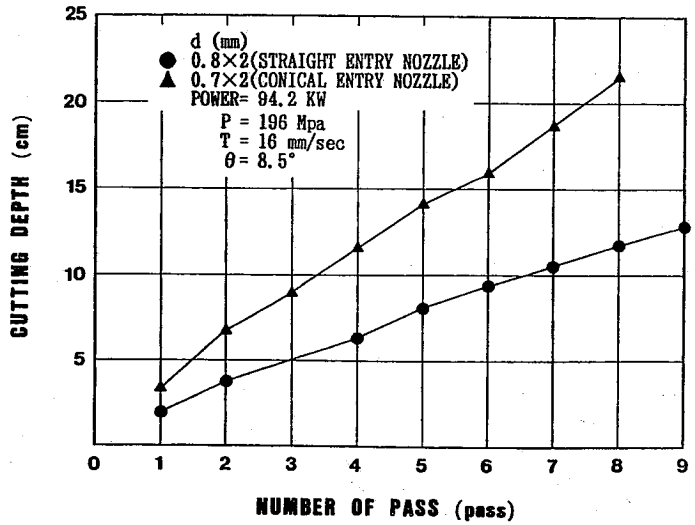

Fig. 7 Comparison of Nozzle Shape

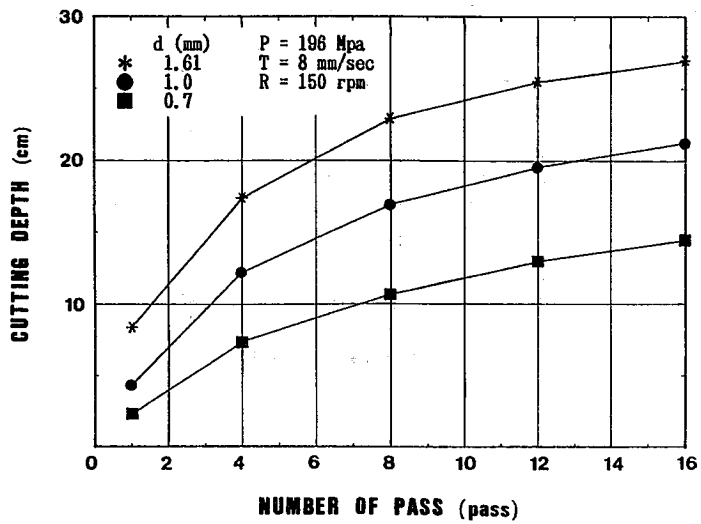

Fig. 8 Relationship between Pass Number and Depth

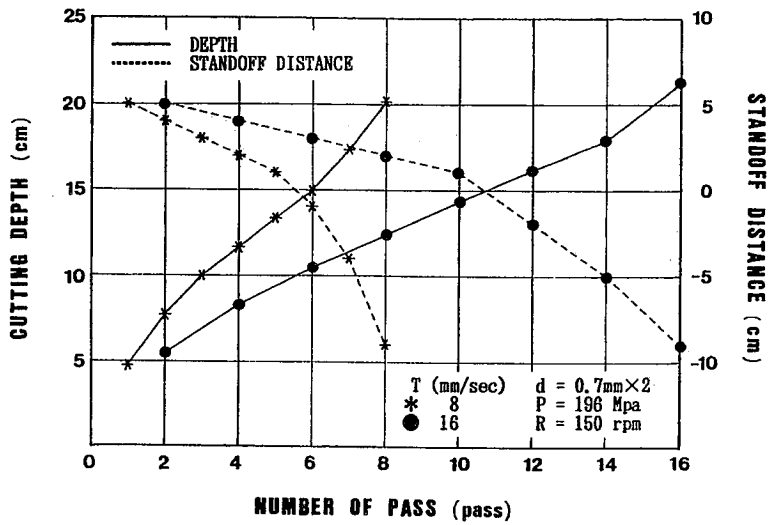

Fig. 9 Relation between Pass Number and Depth

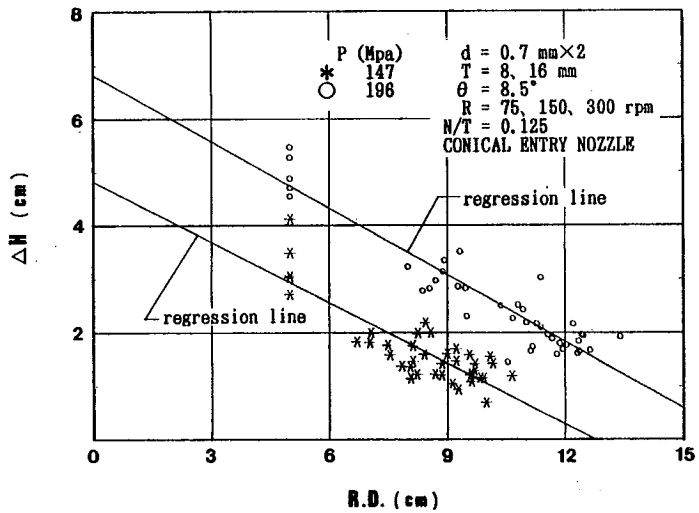

Fig. 10 Relation between R.D and ΔH

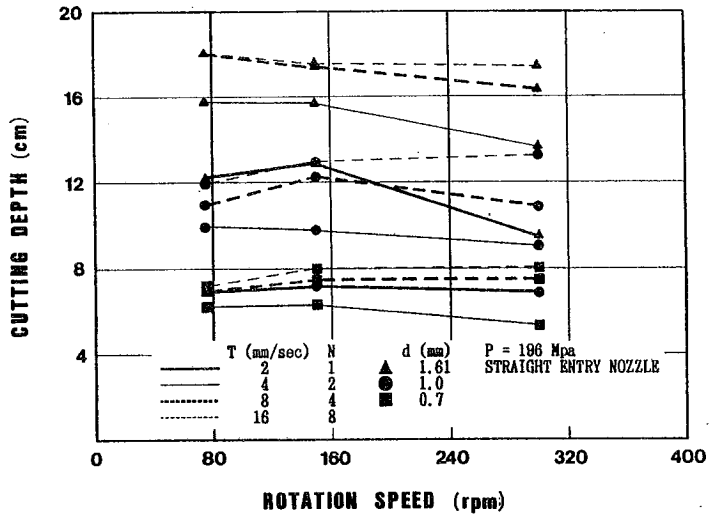

Fig. 11 Relation between Rotation Speed and Depth

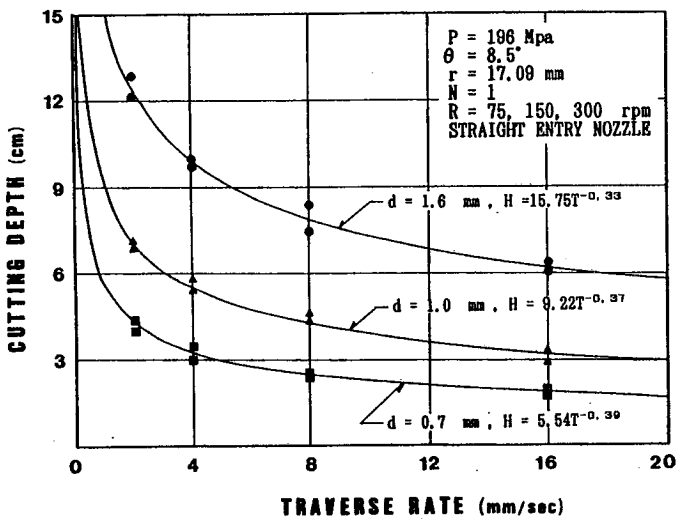

Fig. 12 Relation between Traverse Rate and Depth

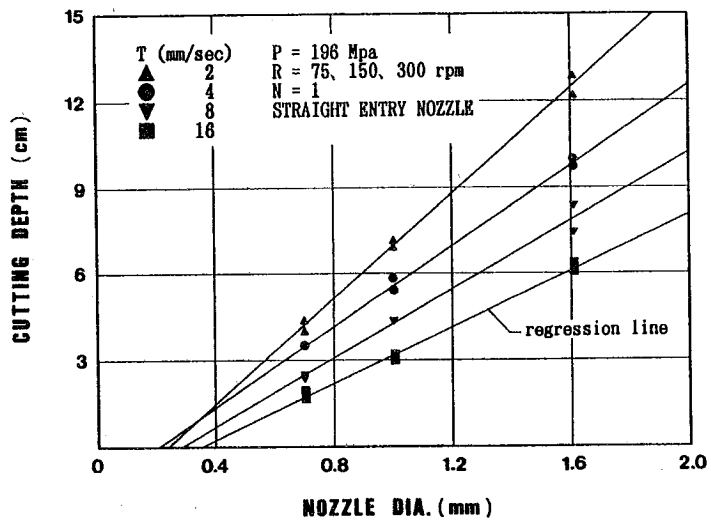

Fig. 13 Relation between Nozzle Diameter and Depth

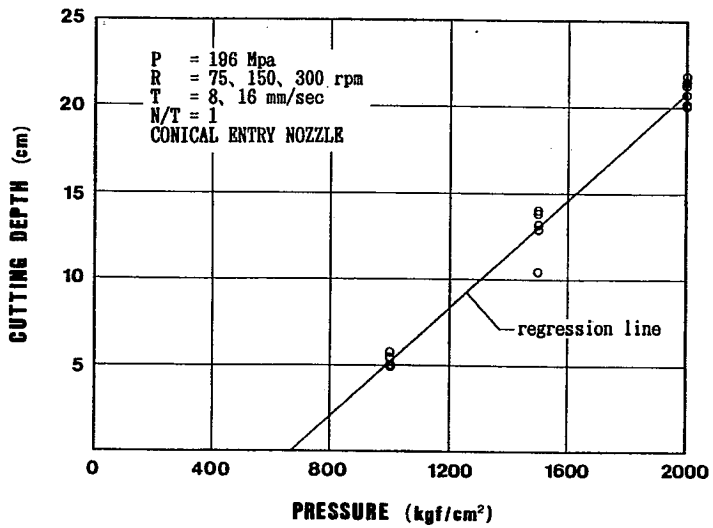

Fig. 14 Relation between Pressure and Depth

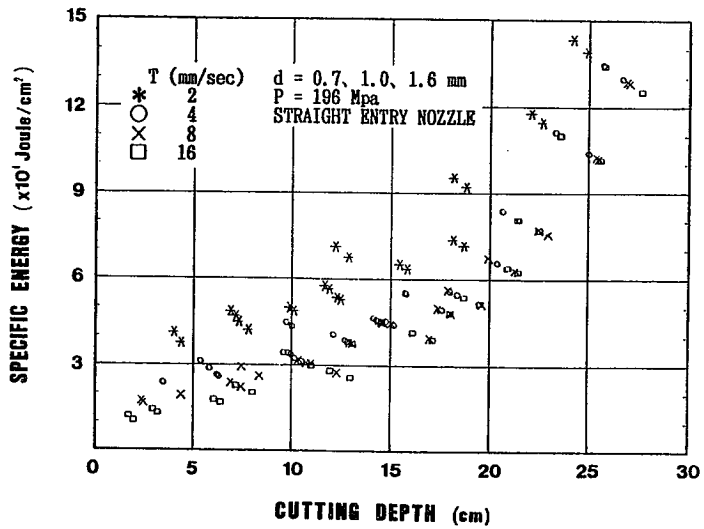

Fig. 15 Relation between Specific Energy and Cutting Depth

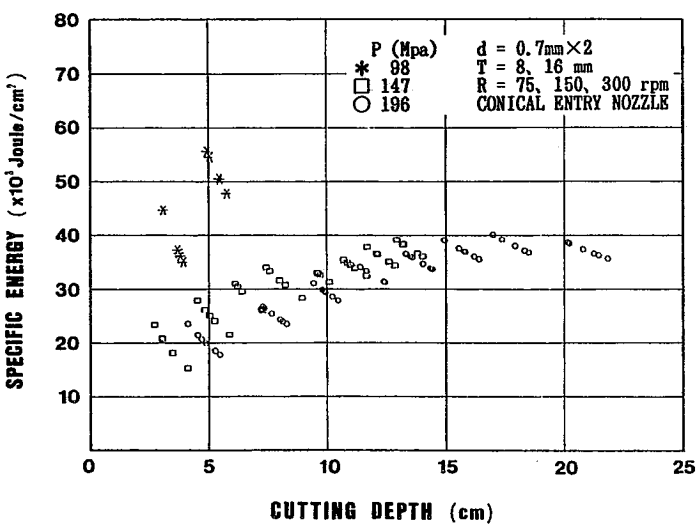

Fig. 16 Relation between Specific Energy and Cutting Depth

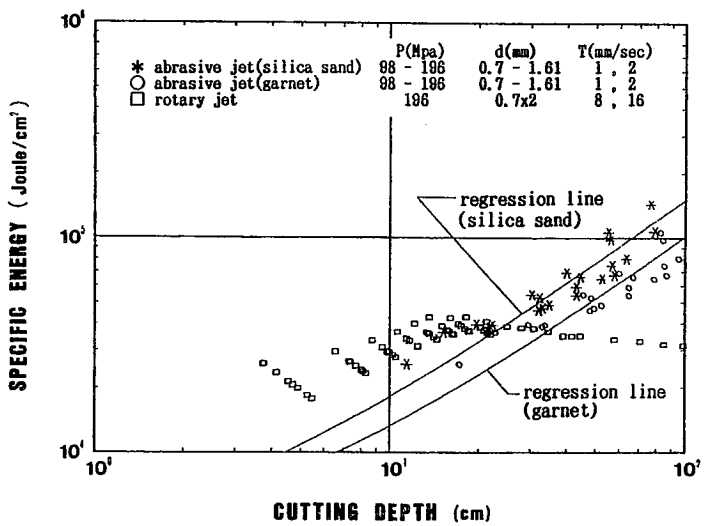

Fig. 17 Comparison between Abrasive Jets and Rotary Jets

5th American Water Jet Conference
August 29 - 31, 1989: Toronto, Canada

Paper / Communication 13

ASBESTOS REMOVAL WITH SELF-RESONATING WATER JETS

A.F. Conn
Conn Consulting, Inc.
Baltimore, Maryland 21209, USA

ABSTRACT: A new, safe, and economical method for removing asbestos from existing buildings has been developed. In field trials, self-resonating, impulsive water jets rapidly removed the tightly adhered, sprayed-on asbestos fire-retardant layer from steel and concrete surfaces.Cleaning rates of 250 to 300 sq. ft (23 to 28 sq. m) per man-hour are now being achieved with a single water jet tool, on surfaces that were previously cleaned at only 3 to 4 sq. ft (0.3 to 0.4 sq. m) per man-hour, using hand-held metal scrapers and small brushes. The SERVOJET self-resonating impulsive water jet tool that was developed for this application delivered about 2 gpm (7.6 l/m) at 10,000 psi (69 MPa). This new procedure should greatly reduce the time required to remove this hazardous and ubiquitous material.

RÉSUMÉ : Une nouvelle méthode sûre et économique pour l'enlèvement de l'amiante dans les bâtiments existants a été mise au point. Dans des essais sur le terrain, on a réussi à enlever, au moyen de jets d'eau pulsés auto-résonants, la couche d'amiante ignifuge pulvérisée qui adhérait solidement à des surfaces d'acier et de béton. On atteint maintenant des vitesses de décapage de 23 à 28 m^2 par heure-personne avec un outil à un seul jet d'eau sur des surfaces qui étaient préalablement décapées à la main à raison de seulement 0,3 à 0,4 m^2 par heure-personne au moyen de grattoirs de métal et de petites brosses. Le SERVOJET à jets d'eau pulsés auto-résonants qui a été mis au point à cette fin a débité environ 7,6 L/min à 69 MPa. Cette nouvelle méthode devrait diminuer grandement le temps nécessaire pour enlever cette matière dangereuse très répandue.

Organized and Sponsored by the National Research Council of Canada and the U.S. Water Jet Technology Association.

1.0 INTRODUCTION

1.1 Background

Since ancient times asbestos has been used for insulating and fire-proofing. This natural, mineral-derived fiber is also an effective material for sound-deadening applications. Unfortunately, the same properties of this complex fiber which allowed its usefulness, have now been discovered to be capable of irritating the lung wall, and initiating cancer in many people. Thus, a new industry has been spawned, to either remove or encapsulate this hazardous material, in order to keep it from entering the lungs of homeowners, students, and workers. In the U.S.A., asbestos abatement is already a multi-billion-dollar-a-year industry, with only a small percentage of the fibers as yet removed or enclosed in a plastic sealant.

In multi-story office or residential buildings, it was very common to apply asbestos, in a suitable sprayable and adhering binder, onto the steel decking that supported the floor above, in order to prevent a fire from spreading from one floor to the next. The standard procedure now used to remove this layer of asbestos from ceilings is to first spray on water containing a wetting agent, to presoak the fibers, and thus minimize the amount of released, airborne fibers during the removal process. Removal is then begun with hand-held metal scrapers, to take off the main bulk of the layer, which might be anywhere from less than 1 in. to as much as 5 to 6 in. thick, or more (25 mm, to 130 to 150 mm). Final cleaning could involve small, hand-held brushes, rags, or low pressure water sprays. It should be noted that prior to initiating the removal process, the work area must be entirely enclosed in an air-tight plastic housing, complete with a multi-stage air lock for the egress of personnel and equipment; fans and filters to insure a negative air-pressure at all times within the work area so that no asbestos fibers can escape; and a network of automated air-monitors, inside and outside the work area, and on each person that enters the area (in a full-covering, air-tight suit, with breathing apparatus), to constantly monitor the possible presence of fibers in the air.

With the present methods, the wet asbestos thus falls onto a plastic-sheeting covered floor, where it is usually picked up by a wet-vacuum device (located either inside or outside the work area), captured in sealable plastic bags, and collected for transport to an approved disposal site. Water jet cleaning has been adapted for a variety of new commercial applications over the past 30 years, but rarely has an industry -- such as the asbestos abatement business -- had an already in-place infrastructure which is so compatible with the introduction of water jet technology.

This paper will describe the development of equipment for use by the asbestos abatement industry to rapidly remove the asbestos layers sprayed onto ceiling surfaces that are particularly difficult to fully clean with the existing methods. Using a self-resonating impulsive water jet nozzle, it has been demonstrated that fully cleaned surfaces can be achieved at rates as much as 50 to 100 times faster, with no need for pre-wetting or a final wiping off of asbestos fibers.

1.2 The SERVOJET™ Self-Resonating Impulsive Water Jet Nozzle

The controlled break-up of a water jet into a series of "slugs" (i.e., large drops) of water has long been known to be effective in increasing the rate of cleaning for a given pump pressure and flow rate. A variety of mechanical devices have shown this increased cleaning phenomenon, due primarily to the so-called "water-hammer" impact stress that is developed when the discrete slug strikes the surface to be cleaned. The magnitude of the water hammer pressure is a function of the average water jet velocity and the properties of the target surface. For instance, the exit velocity of a 10,000 psi (69 MPa; 690 bars) water jet is about 1,218 ft/s (370 m/s). The maximum pressure that a steady jet can generate, the "stagnation pressure," is 10,000 psi (69 MPa) on an infinitely rigid target. If the target is steel, then this pressure from a steady jet will be only about 6,900 psi (48 MPa) (based on the dynamic response properties of steel). An impulsive jet, for the same nozzle pressure drop, will create an impact pressure of about 54,600 psi (376 MPa), an amplification of almost eight! In addition, the interaction of the water slugs with the air tends to flatten and spread the slug (see Fig. 1) thus creating a greatly enlarged "foot-print", in comparison to the diameter of the exiting jet of water. This results in an enlarged contact area for cleaning -- hence more area cleaned, per man-hour, for the operator of the water-jet cleaning tool.

The SERVOJET self-resonating nozzle causes the creation of a high frequency series of slugs by means of a passive, resonance method. As shown schematically in Fig. 2, either tuned resonating chambers, tuned "organ-pipe" segments, or combinations thereof (Chahine, et al., May 1983; Chahine, et al., September 1983; Conn and Chahine, 1985) have proven capable of producing high-frequency, small-scale fluctuations in the mean pressure just upstream of the nozzle exit. Typical frequencies can be in the range of 10 to 30 kHz (dependent on nozzle orifice diameter and jet velocity), and pressure amplitudes are typically only about 5 to 10 percent of the mean pressure for effective slug generation. Although much larger fluctuation amplitudes can be produced by this method, it was found that the larger perturbing amplitudes did not produce effective cleaning jets. The SERVOJET nozzle contains no moving parts, and produces minimal internal pressure losses.

Other attributes of pulsed jets, which contribute to their ability to clean more efficiently are the cycling of the pressures applied to the surface, which promotes unloading pressures that help to debond adhering substances, and the enhanced outflow velocity that can more readily pull away the material that is being removed. The increased cleaning capability of pulsed water jets has been demonstrated over a wide range of pressures (1,000 psi to 10,000 psi; 6.9 to 69 MPa) and flow rates (1 to 20 gpm; 3.8 to 76 l/m), for a variety of commercial cleaning applications ranging from removing graffiti sprayed on concrete; cleaning cars, busses, and trucks; to removing rust, paint, and marine growths from steel surfaces. The ability of any water jet to clean rough and complex surfaces is another important attribute that has contributed to the success of the new asbestos removing equipment described in this paper. In comparison to the tedious effort required to scrape, and then brush away every fiber from a typical steel ceiling -- with its numerous pleats, folds, proturberances for fastening pipe hangers, etc. -- the use of a water jet tool is truly a revolutionary improvement, if the system is designed to be compatible with the requirements of the asbestos abatement industry.

As in any industrial use of water jets, a prime consideration is safety. An inherent facet of the high-frequency fluctuating water jet is its short range of effectiveness. Within about 12 in. (30 cm) from the surface, the slugs are still reasonably intact, and can provide a degree of enhanced cleaning. Beyond distances of about 3 ft (about 1 m), however, the slug-air interaction causes slug disintegration, turning a cleaning device into the producer of a fine spray of relatively harmless very small droplets. Therefore, if the operator of the SERVOJET cleaning tool inadvertently misdirects the jet, he is unlikely to harm a fellow worker, if reasonable distances between personnel are maintained.

2.0 DEVELOPMENT OF THE SYSTEM

The equipment now known as the SWAABS (SERVOJET Waterjet Asbestos Abatement System) was developed at an actual on-going asbestos abatement site, a multi-story office building with sprayed-on layers covering the ceilings (see Fig. 3) in thicknesses ranging from about 3/4 to 1.5 in. (19 to 38 mm). The typical cleaning rates at this job site were averaging about 27 sq. ft (2.5 sq. m) per man-day (8-hour shifts), due to the complexity of the metal surface, and the difficulty of reaching into the gaps between the ceiling surface and the criss- crossing steel I-beams. A portable, diesel-powered pump unit was brought to the site, hoses deployed, and an existing water jet gun was affixed with a series of sizes of SERVOJET nozzles. Flow rates were varied from about 1 to 5 gpm (3.8 to 18.9 l/m); pump pressures from 2,000 to 10,000 psi (13.8 to 69 MPa). The abatement company's staff was trained in the safe and effective usage of a water jet tool, and a series of timed trials over measured areas of the ceiling were performed. Both as-sprayed as well as previously partially-scraped surfaces were cleaned. Although some cleaning was seen at the lower pressures, reasonable cleaning rates were not measured until about 4,000 psi (27.6 MPa), and efficient cleaning did not begin until a pump pressure of about 7,000 to 8,000 psi (48.2 to 55.1 MPa) for this particular surface and asbestos/binder mixture. One of the principal criterion for efficient removal of asbestos by a water jet is the ratio of volume of asbestos removed to the volume of water required. The ideal goal is to have virtually all of the water soaked up by the asbestos, thus leaving no excess water to be vacuumed up from the floor. At a pressure of 10,000 psi (69 MPa), with a flow rate of about 2 gpm (7.6 l/m) this goal was essentially achieved: almost no excess water was seen on the plastic-lined floor. After some experience was gained, the contractor's operators were able to average about 250 sq. ft per hour (23.2 sq. m), for this 3/4 to 1.5 in. (19 to 38 mm) thick asbestos; hence an asbestos-to-water volume ratio of about 1.5. Comparable removal rates have subsequently been achieved on much thicker layers of asbestos, up to as much as 5 to 6 in. (127 to 152 mm); in this case the asbestos to water volume was over seven -- and virtually no extra water remained. When a quick bulk removal of asbestos (with hand-held metal scrapers) was followed by jetting to remove all of the remaining material, then rates as high as 800 to 900 sq. ft/man-hour (74 to 84 sq. m/man-hour) were achieved. This rate should, of course, be modified to account for the time required to do the bulk removal -- unfortunately the times for this were not measured as this scraping had been done prior to our water-jetting trials. Based on these developmental efforts, the system described in the next section was designed, built, and delivered to the asbestos abatement contractor.

3.0 DESCRIPTION OF THE SYSTEM

A block diagram of the complete, four gun, electric-motor driven version of the SWAABS is shown in Fig. 4. This system has been named the Model 4E, referring to four SERVOJET water-jet cleaning tools ("guns"), and "E" for the electric motor drive. Other versions of the SWAABS are powered by a diesel engine, and there are one and two gun models. In this paper we will describe those features of the Model 4E which are particularly relevant to some of the unique requirements of the asbestos abatement industry -- an industry that is essentially completely unfamiliar with the use of high pressure water jetting equipment. An important consideration, therefore, in addition to attempting to design equipment which is as simple to operate and maintain, is the training which must accompany such a system. It is essential to teach the users of this equipment how to use it safely and effectively. Although these skills may not actually be that difficult to learn, it should be understood that the typical asbestos remover has, until now, been dealing only with metal scrapers and small brushes!

3.1 The Pump Unit

As shown in Figs. 5 and 6, the 60 hp (44.7 kW) electric motor is belt-coupled to the three-plunger, positive displacement pump. The motor was placed above the pump, to allow the unit to be as narrow as possible. The 34 in. (0.86 m) width was selected to allow the unit to be rolled through the 36 in. (0.91 m) doorways frequently found in U.S.A. buildings. This width will also allow the pump unit to be put into most freight elevators, for effective use in high-rise buildings that were so often fire-proofed with sprayed-on layers of asbestos during the first half of this century. Included on the pump unit is a pressurizable, 40 gal (151 l) water tank to which the feed water hose is connected. Ordinary house pressure is enough to pressurize this tank and provide the desired input pressure to the pump. In this manner it is not necessary to monitor the input water pressure after it is initially established as adequate during set up of the system. If, during operations, a worker sees that his gun is not ejecting water, he must then call for shut off of the pump, and a check must be made to see whether the problem is due to interruption in the input flow water source. Since the pump is oil (and not water) lubricated, it is possible to run the pump briefly in such a situation without harming the equipment.

The user of this system may have, as an option, a device for injecting wetting agents, or other chemicals, into the input flow pipe leading to the pump. This chemical injector works on the venturi-suction principle; in operation, one merely has to place the end of a plastic hose into the chemical container, and adjust the intake valve to achieve the desired flow rate for the chemical. This injection of a wetting agent is often required by law in certain local jurisdictions, although our testing has indicated that, for the objective of suppressing free fibers of asbestos in the air, this injection of a wetting agent is not needed. During the development of the SWAABS, the personal and room monitor filters were routinely checked, by TEM (transmission electron microscope), and no fibers of asbestos were found on these filters. During the removal process by the SERVOJET, either adequate immediate wetting, and/or the misting action described above, are responsible for insuring that any free fibers will fall rapidly to the plastic floor covering, and will stay there until vacuumed up with the bulk material. Also on the pump unit are: the motor starter and control box; a pressure relief valve to automatically release the system pressure in case of inadvertent overpressurization; gauges to indicate the input and output pressures at the pump; and 8 in. (20 cm) industrial caster wheels, to facilitate rolling the unit into position inside the building being abated. The pump unit weighs about 3,000 lbs (1,360 kg), but it can easily be pushed around by one or two people on a level surface. In general, except perhaps for very high buildings, it will probably be possible to wire the pump into the power source, hook up the input water hose, and leave the pump at that one position for the duration of that abatement effort. Because of the low flow rates, and the excess system pressure capacity, long hose runs between the pump unit and the Manifold/Diverter (M/D) unit (see next section) can be tolerated. The total pump output is 8 gpm (30.3 l/m) at 10,000 psi (69 MPa). If 1/2-in. (12.7 mm) hose is run between the pump and M/D units, the pressure drop, per 100 feet (30.5 m) of hose, will only be about 50 psi (0.34 MPa). Thus, the pump output can be carried up many levels in a high rise building before the pressure decreases below the value of about 8,000 psi (55.1 MPa) which we found to be an effective pressure for removing asbestos -- at a favorable ratio of asbestos-to-water.

3.2 Manifold/Diverter (M/D) Unit

The purpose of this part of the system is, first, to distribute the flow of high pressure water from the pump unit to each of the four SERVOJET guns. It's second job is to automatically divert the flow from any one (or more) of the guns, when that operator releases the trigger on his tool. Since these are "dry guns", that is, no water is dumped from the gun when the trigger is released, the flow to that gun must be rerouted when the valve is shut off by releasing the gun trigger. The heart of the M/D unit is, therefore, the nitrogen-gas compensated diverter valve. A small nitrogen bottle is provided with the unit (see this bottle at the right side of Fig. 7); in this photograph, the diverter valve is in the center, and the manifold for the high pressure water flow distribution is at the left.

When the system is being first set up at the work site, the nitrogen gas pressure in the diverter valve is set, to compensate the full flow of 8 gpm (30.3 l/m) at the desired system operating pressure, e.g., 10,000 psi (69 MPa). Once this pressure balance has been set initially, the nitrogen bottle is shut off and is no longer needed. The static gas pressure thereafter automatically compensates for the amount of flow that needs to be diverted, depending on how many of the four guns are being used. The valve is automatically opened the requisite amount, to allow anywhere from zero to the full 8 gpm (30.3 l/m) to pass through, and thus maintain, at all times, the preset system pressure. The M/D unit has been designed to operate inside the area where asbestos removal is taking place; two men can carry it through the air locks and set it up in the center of the abatement area. The four lengths of hose are then deployed, fastened to each gun, and the system is ready to go to work.

3.3 SERVOJET Asbestos Removal Tools

A photograph of one of the four "guns" is shown in Fig. 8; a close-up of the resonating chamber is in Fig. 9 (compare the schematics in Fig. 2). Some of the components of this gun, moving from left-to-right in Fig. 8, are: the shoulder rest, to ease working on surfaces directly overhead; the quick-disconnect for the high pressure hose; the gun "trigger" (water output control valve; a manual shut-off safety valve; the SERVOJET resonating chamber; the 3-ft (0.91-m) long lance; and the end-coupling for the tip nozzle. By varying the size of the orifice of the tip nozzle, any desired percentage of the available full system flow of 8 gpm (30.3 l/m) can be put through any one gun; of course, the total exit areas of all guns in use at any one time cannot exceed the predetermined value, if the peak system pressure of 10,000 psi (69 MPa) is desired. If each gun is to be operated at 2 gpm (7.6 l/m) at 10,000 psi (69 MPa), then each of the four tip nozzles must have an orifice diameter of about 0.031 in. (0.79 mm). The usual hose size between the M/D unit and each gun is 3/8 in. (9.5 mm). With 2 gpm (7.6 l/m) to a gun, the pressure drop, per 100 ft (30.5 m) of this hose is only about 20 psi (0.14 MPa), a negligible amount. Hence, if required, the guns may be located a significant distance from the M/D unit if this becomes necessary on a given job site.

4.0 CONCLUDING REMARKS

This paper has described the adaptation of water jet technology for use in a new and growing industry. Although to date the SWAABS has been used primarily for its original design intent -- namely asbestos removal from large ceiling areas, it may find usage in other aspects of the problem, such as removing asbestos-bearing floor tiles or roof tiles. In its use in removing layers of sprayed-on ceiling asbestos, the SWAABS has already proven itself to be a significant labor and cost saving method. By combining the prewetting, bulk-removal, and final clean-up step into one, and eliminating the tedious, over-the-head scraping and brushing work, water jet technology should play an important role in reducing the huge cost of the abatement of this planet's health hazard due to asbestos.

5.0 REFERENCES

1. Chahine, G.L., Conn, A.F., Johnson, V.E., Jr., and Frederick, G.S.: "Cleaning and Cutting with Self-Resonating Pulsed Water Jets". Proc. 2nd U.S. Water Jet Conf., Rolla, Missouri, May 1983, pp 167-175.

2. Chahine, G.L., Conn, A.F., Johnson, V.E., Jr., and Frederick, G.S.: "Passively- Interrupted Impulsive Water Jets". Proc. 6th Int'l. Conf. on Erosion by Solid and Liquid Impact, Cambridge, England, September 1983, pp 34-1 to 34-9.

3. Conn, A.F. and Chahine, G.L.: "Ship Hull Cleaning with Self-Resonating Pulsed Water Jets". Proc. 3rd U.S. Water Jet Conf., Pittsburg, PA, May 1985, pp 44-62.

6.0 ACKNOWLEDGMENTS

The author wishes to thank the following individuals and organizations for their help and valuable inputs during the development, design, and construction of the equipment described in this paper: At Marcor, Inc., Mr. Ron Acee, Mr. Michael Balanoff, and Mr. Richard Clarke; at Tracor Hydro-Services, Inc., Mr. Billy Watson, Mr. Pat DeBusk, Mr. Kim Terry, and Mr. Tom Thrash; and Tracor Hydronautics, Inc., the author's former employer, for graciously allowing its patented nozzle system, the SERVOJET™, to be included in this new asbestos abatement system.

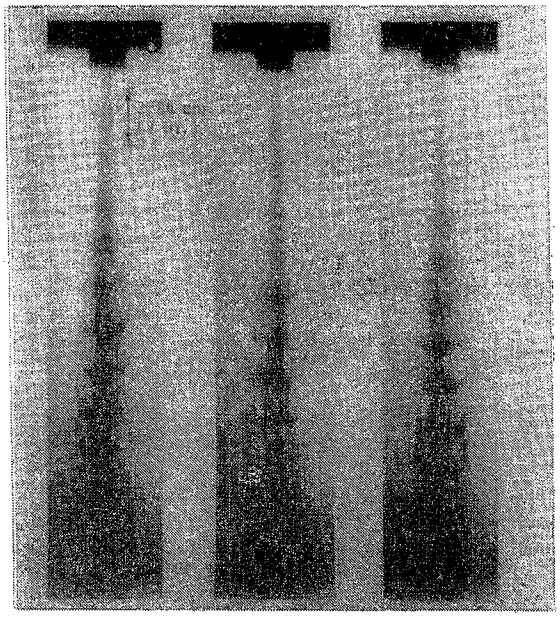

Fig. 1 Slugs formed by resonating jets (frames from high-speed movies)

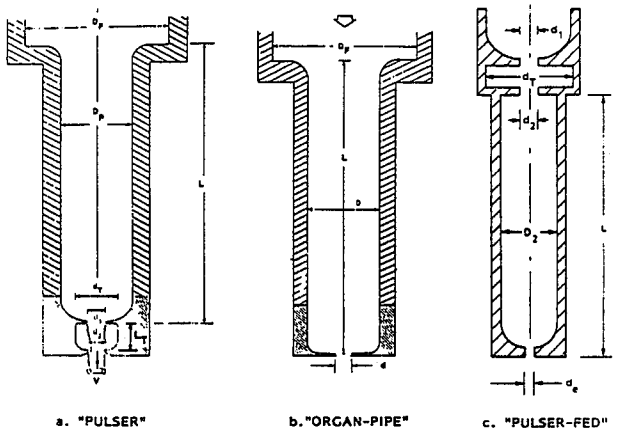

Fig. 2 Self-resonating nozzle system designs

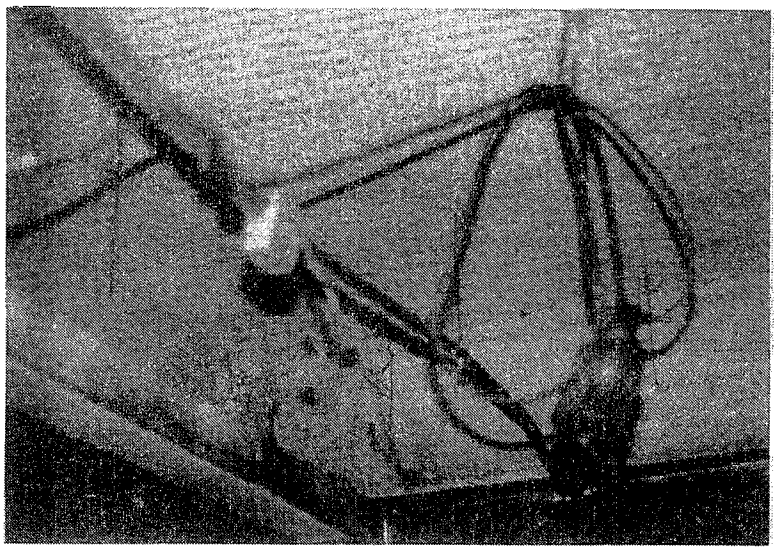

Fig. 3 Asbestos-covered metal ceiling and I-beams

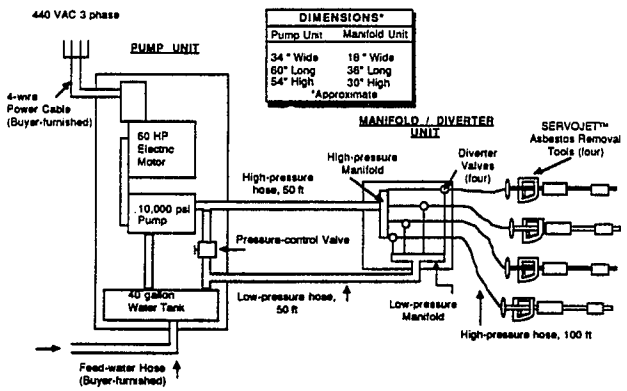

Fig. 4 Block diagram of the Model 4E SWAABS (SERVOJET™ Waterjet Asbestos Abatement System)

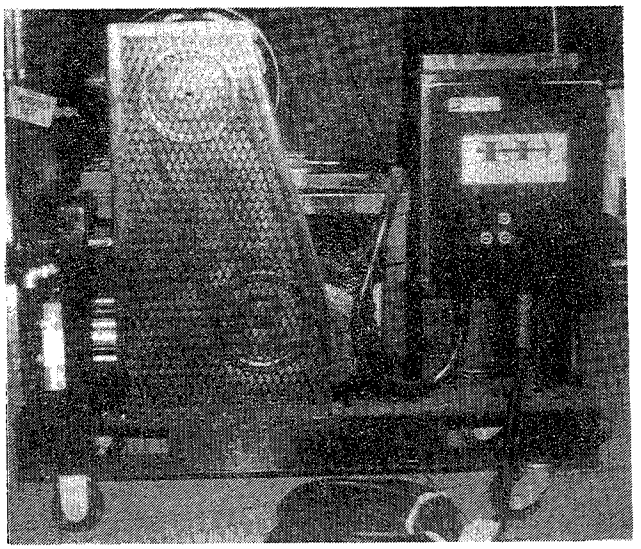

Fig. 5 Pump unit, side view

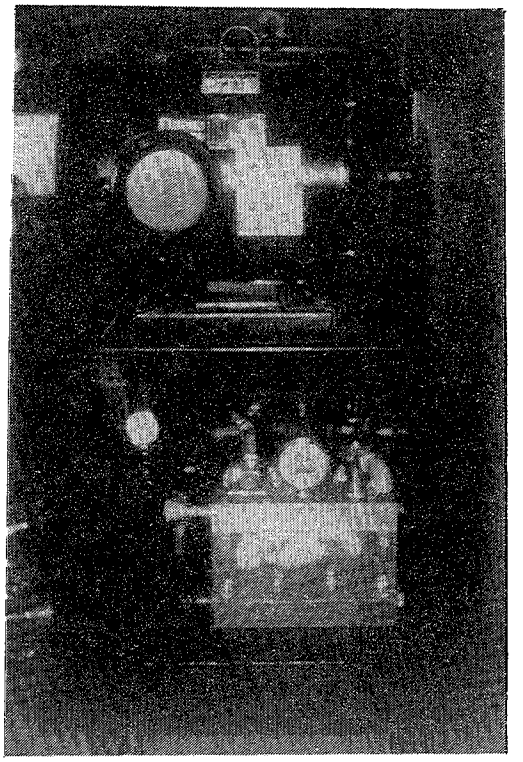

Fig. 6 Pump unit, end view

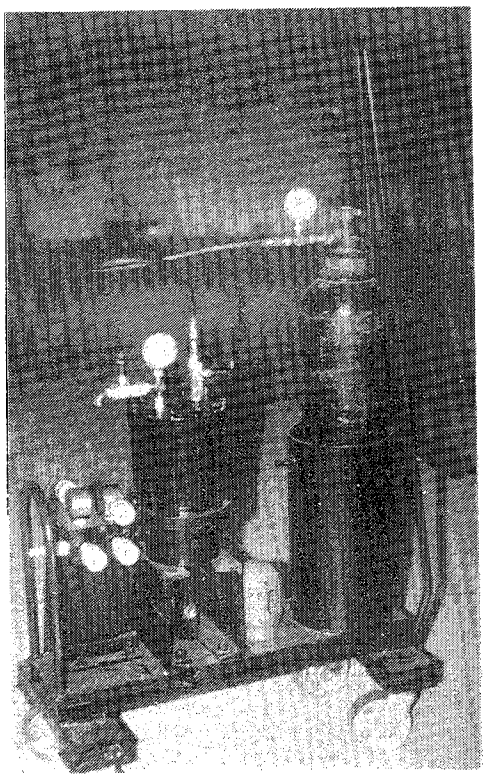

Fig. 7 Manifold/Diverter unit

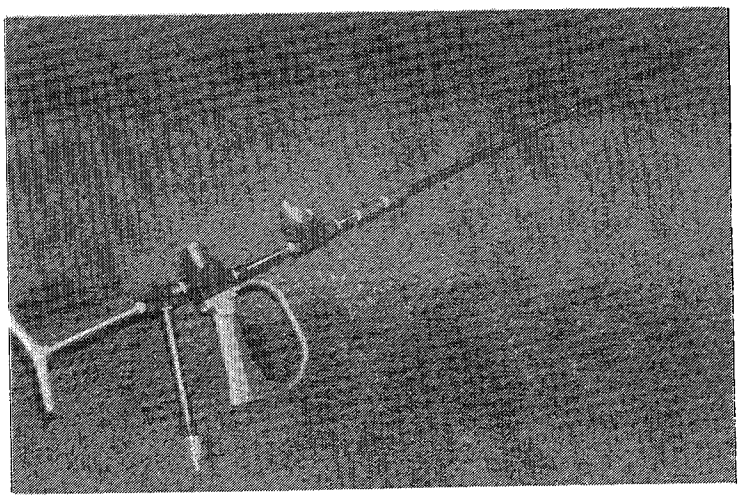

Fig. 8 SERVOJET asbestos removal tool

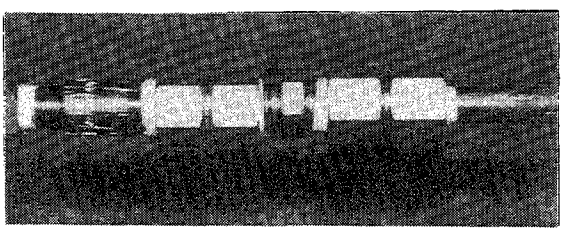

Fig. 9 SERVOJET resonator

5th American Water Jet Conference
August 29 - 31, 1989: Toronto, Canada

Paper / Communication 14

HIGH-PRESSURE WATER JET AS A CUTTING TOOL

A. Klich AND A. Kalukiewicz
Institute of Mining and Dressing Machines and Automation
University of Mining and Metallurgy
30-095 Cracow, Poland

ABSTRACT: In this paper results of the inquiry into a small-diameter water jet produced in a prototype device making it possible to obtain pressures to 200 MPa have been presented. In particular, the range of jet action and the change of its effectiveness with the growing distance from the nozzle outlet have been determined.
The authors have also presented results of the investigation of cutting concrete with water jet. The concrete in question had varying compressive strength at the use of water pressures from 110 to 200 MPa, at the nozzle diameters from 0.8 to 1.2 mm and the nozzle outlet velocity in relation to concrete from 0.76 to 2.85 m/sec.

RÉSUMÉ : Cette communication décrit les résultats de l'étude sur un jet d'eau de petit diamètre produit par un prototype de dispositif permettant d'obtenir des pressions atteignant 200 MPa. On a déterminé en particulier la gamme des actions du jet et son rendement en fonction de la distance à la sortie de la buse.
Les auteurs ont aussi présentés les résultats de l'étude sur la coupe du béton avec des jets d'eau. La résistance à la compression béton en question varie selon la pression de l'eau (110-200 MPa), le diamètre de la buse (0,8-1,2 mm) et la vitesse de sortie de la buse par rapport au béton (0,76-2,85 m/s).

Organized and Sponsored by the National Research Council of Canada and the U.S. Water Jet Technology Association.

1. Introduction.

Already in the years 1950 - 1960 trials were made to use water jets as rock cutting tools. Hydraulic systems to enable cutting, haulage, and horizontal and vertical transport of winning were constructed in Poland and abroad. Those systems produced jets of about 10 mm diameters at the pressure of water of 10 - 30 MPa. However, the above jet parameters determined large discharges of water from the systems. Such masses of water had a harmful effect on the rock surrounding an underground working and brought about radical worsening of climatic conditions under which miners had to work.

Since 1974 [2] investigations have been carried out at the Institute of Mining and Dressing Machines and Automation of the University of Mining and Metallurgy in Cracow, Poland, to use water jets of 1 mm diameter and the outlet pressure of 100 - 200 MPa and more for cutting rock.

A new pressure generator [3] was built and subjected to thorough testing [1] to determine suitable characteristics. This was followed by the examining of the parameter variability of jets forced out to the atmosphere. A series of tests was performed on concrete slabs having various compressive strength. Trials were made to cut and mine hard coal in a real working underground. Basing on those investigations, dependences of the cutting depths, water discharges, unit energy of cutting and mining on the hydraulic parameters of the jet and the way of its positioning and handling in the mine space were determined.

2. Test stand.

Owing to the lack of very high-pressure pumps, an experimental machine was constructed. It produces a quasi continuous jet on the basis of multiplication.

The machine, whose simplified diagram is presented in Fig.1, consist of two units, i.e. a hydraulic supply station I and a monitor II.

The hydraulic supply station includes an asynchronous motor 1 of 90 kW power driving a main pump 2 and the auxiliary one 3. The pump 2 with stepless controlled delivery of 0 - 238 dcm^3/min feeds oil into the monitor. The pressure of oil is controlled by an overflow valve 4 within the range of 5 - 20 MPa.

A gas high-pressure accumulator 6 is incorporated in a feeding conduit 5. Analogously, a gas low-pressure accumulator 8 is incorporated in an oil run-off outflow conduit 7.

The monitor II consists of a rotary part 9 in which three intensifiers 10 are placed in parallel. They form pressure converters with the ratio 1:10 from

20 to 200 MPa.

The intensifiers are supplied with oil from the low-pressure side of the station I. Water is fed through conduits 11 from high-pressure side. Due to high pressure, water as a cutting agent is forced out through a nozzle 12. The possition of the nozzle axis can be changed in relation to the axis of the rotary part 9, and thus during the rotation of the monitor the jet cuts circles with the radii of 0 - 150 mm.

During operation the rotary part 9 of the monitor rotates around the axis parallel to the intensifiers axes and positioned in the axis of their geometric centre. The rotations of part 9 are produced by a hydraulic motor 13 with controlled rotational speed through a chain transmission 14. During one rotation of the monitor part 9, each of the three intensifiers completes one work cycle. A rotary distributor 15 is used to control successive inflow and out flow of oil to each intensifier.

The production of a continuous jet in a prototype system is shown in Fig.2. This figure presents the dependence of rotations maximum water efficiency and oil absorptivity of the monitor on pressure p for various diameters of the nozzle d_o. The above dependences resulted from the investigations were presented in details in the paper read during the 'Hydromechanisation 4' conference in the German Democratic Republic [4].

3. Study of the variability of the water jet dynamic force as the function of the measuring point distance from the nozzle outlet.

The objective of this enquiry was to establish the dependence of the jet dynamic force on presure p, the nozzle diameter d_o, and the distance of a measuring point from the nozzle outlet l_o.

The following parameters were submitted to changes:

- p - pressure (100 - 200 MPa) measured as the pressure feeding oil to the intensifiers multiplied by m = 10,
- q_d - discharges from oil unit having the values of 57, 116, 174 and 236 dcm^3/min,
- d_o - nozzle diameter (0.8; 1.0; 1.2 mm),
- l_o - distance of the jet dynamic force sensor varying from 3 to 700 mm from the nozzle outlet,
- n - monitor rotations matching the delivery q_d (see Fig.2) adjusted in such way as to obtain full piston strokes of the hydraulic intensifiers.

To measure pressures in the oil unit, strain gauges (Fig.3) were used. The gauges had linear characteristics for the whole measuring range. Similarly, to measure the jet dynamic forces a sensor was employed. It could be moved along the jet axis (Fig. 4).

The carrier frequency of the recording apparatus equalled 5 kHz ± 1% . An oscilloscope made by Tetranix, furnished with a memory system, was used.
The dependences of the jet dynamic force P_d on the distance l_o of the sensor from the nozzle outlet are presented in Figs. 5, 6, 7 for the respective nozzle diameters d_o.
Fig. 8 presents the results obtained with the P_d/P_{d3} ratio introduced on the Y-axis and the l_o/d_o ratio on the X-axis.
The dependence obtained is described by the following equation:

$$\frac{P_d}{P_{d3}} = 92.7 \cdot e^{-2,89^{-3} \cdot \frac{l_o}{d_o}}$$

The results obtained during the invastigations were processed on Wang 2200 microcomputer. Thanks to the software it was possible to compute the coefficents for the functions described analytically. Elements of statistical regression were also determined.

4. Laboratory tests of rock cutting with high-pressure water jets.

The aim of these investigations was to determine the influence of the principal parameters of a water jet and its kinematics on the effect of cutting rock of various strength.
Owing to financial, time and organizational reasons, the investigations were limited to concrete samples.
During the tests the following parameters were changed:

- pressure p - 110, 150, 200 MPa;
- nozzle diameter d_o - 0.8, 1.0, 1.2 mm;
- traverse speed - v_w.

The following parameters were stable:

- radius of the nozzle rotation r = 150 mm;
- stand - off distance l_o = 20 mm;
- velocity of the monitor travel from top to bottom v_m = 1.2 m/min.

For each of the three pressures rock samples were cut at three different velocities using three different nozzle diameters.
The tests were carried out for six rock samples of various strength.
The investigation comprised of $3d_D \cdot 3p \cdot 3v_m \cdot 6\sigma_o$ = 162 experiments.
To evaluate the effects of jet cutting the following were taken into consideration:

g - depth of incisions cut;
l_s - length of incisions cut;
F_s - surface of incisions cut;
q - cutting surface rate ;

q_w - water consumption per unit ;

E_{je} - energy consumption per cutting.

Concrete slabs with the dimensions of 450 x 450 x 120 mm were made of the composition of sand and cement using various combinations of components to obtain rock samples of varying strength. During testing the slabs were fixed to a stand additionally prepared (Fig.9).

Each mixture submitted to setting to dense plastic consistence was used to make six slabs and six cylindrical samples of ø 80 mm and height h = 80 mm. Cylindrical samples were used to determine the compressive strength of each mixture after it had set.

The mean value calculated from the four results was accepted as the compressive strength.

The results are shown in Table 1.

Table 1.

	Number of rock sample					
	1	2	3	4	5	6
σ	2.3	3.3	8.3	10.5	15.9	32.0

Jet cutting was tested in the following way: the stand with a sample fixed was placed in front of a nozzle. The required working parameters of the device were adjusted. After setting in motion the monitor, it was lowered on the manipulator extension arm in such a way that the nozzle moving with the motion cosisting of a rotary motion on the radius r = 150 mm and that of transportation v = 0.05 m/sec. caused the formation of incisions on the slab surface (as seen in the photographs in Figs. 10 and 11).

On account of the small transportation velocity v_m in relation to the velocity of the nozzle in the rotary motion, the nozzle velocity towards the rock sample was calculated from the following equation:

$$v_w = \frac{\pi}{30} rn \ m/s \ .$$

A piece of thin wire (0.7 mm) and a slide caliper were used to measure the incisions obtained. From each series of the incisions obtained for the assumed parameters, five incisions were chosen at random and their length and depth were measured at five points. The surface of the incisions was calculated from the formula:

$$F_c = g \cdot l_s \quad cm^2 \ .$$

The cutting surface rate was given by the formula:

$$Q_F = \frac{F_c}{t_w} \quad cm^2/sec$$

and the water consumption per unit by

$$q_w = \frac{v_w}{F_c} \quad cm^3/cm^2$$

where: v_w - displacement volume of the high-pressure part of the intensifier

$$v_w = \frac{\pi}{4} s \cdot d_w^2$$

$s = 6.3$ cm - piston stroke

$d_w = 2.5$ cm - piston diameter.

The rate of energy of cutting was formulated as

$$E_{jc} = \frac{E_j}{F_c} \quad MJ/m^2$$

where: E_j - energy consumed to force out the water volume v_w at the pressure p.

Using the results obtained, diagrams $g(\sigma_c)$ for p = 110, 150, 200 MPa (Fig.12) were prepared. In those diagrams the values d_o and v_w were neglected. Thus, each of the points results from the statistical averaging of the values obtained for different nozzles and at the velocity v_w. Acting in a similar way dependences $g(\sigma_c)$ for d_{01}, d_{02}, d_{03}, (Fig.13), and $g(\sigma_c)$ for v_{w1}, v_{w2}, v_{w3}, (Fig.14) were obtained. Analogously, dependences $E_{jc}(\sigma_c)$, presented by the diagrams in Figs. 15, 16, 17, were obtained.

The curves in Figs. 12, 13, 14 are described by the equations in the form:

$$g = a_2 e^{b_2 \delta_c}$$

Table 2.

Coefficients a_2, b_2 for g(p), σ_c (Fig.12).

p(MPa)	a_2	b_2	error (standard)
110	39.3	-7.88^{-2}	0.32
150	49.8	-6.95^{-2}	0.19
200	52.6	-5.65^{-2}	0.28

Table 3.

Coefficients a_2, b_2 for $g(d_o)$, σ_c (Fig.13).

d_o mm	a_2	b_2	error (standard)
0.8	29.3	-7.3^{-2}	0.32
1.0	45.77	-6.2^{-2}	0.31
1.2	65.12	6.51^{-2}	0.12

Table 4.

Coefficients a_2, b_2 for $g(v_w)$, σ_c (Fig.14).

v_w m/s	a_2	b_2	error (standard)
0.76	63.2	-7.13^{-2}	0.30
1.68	43.2	-6.26^{-2}	0.24
2.85	34.0	-6.06^{-2}	0.23

The dependences of the rate of energy of cutting concrete sample E_{jc} kJ/dcm^2 on their compresive strength σ_c MPa are presented by the straight lines in Figs. 15, 16, 17.

Generally these dependences were described by the equation

$$E_{jc} = a_3 + b_3 \sigma_c .$$

Coeficients for individual cases are presented in Tables 5 - 7.

Table 5

Coefficients a_3, b_3 for E_{jc} (p), σ_c (Fig.15).

p MPa	a_3	b_3	error (standard)
110	-4.06	3.22	7.11
150	1.99	2.63	3.40
200	10.87	2.19	6.70

Table 6

Coefficients a_3, b_3 for E_{jc} (d_o), σ_c (Fig.16).

d_o mm	a_3	b_3	error (standard)
0.8	-1.07	3.54	5.70
1.0	6.25	2.03	6.15
1.2	3.54	2.47	3.87

Table 7

Coefficients a_3, b_3 for E_{jc} (v_w), σ_c (Fig.17).

v_w (m/s)	a_3	b_3	error (standard)
0.76	1.71	4.81	6.30
1.68	3.84	2.12	5.06
2.85	3.39	1.71	3.59

5. Conclusions.

1. The device made at the Institute of Mining and Dressing Machines and Automation of the University of Mining and Metallurgy, Cracow, Poland produces water jets of the diameters d_o = 0.8; 1.0 and 1.2 mm at the outlet pressures to 200 MPa, and makes it possible to handle them in the mine space.
2. A small-diameter, high-pressure water jet after leaving the nozzle is coherent enough to be used for cutting (mining) rock, e.g. hard coal.
3. The patented [5] and used in practice method of cutting rock with water jet presents unquestionable advantages, ensuring, in particular, the obtaining of high relative jet velocities along the rock.
4. Water jets let out to the atmosphere at high presure undergo dispersal. The jet dynamic force initially decreases more intensively, later on its drop is milder. At the distance of about 800 nozzle diameters the jet is almost completely dispersed.
5. It was found that the depth of cutting concrete considerably depends on its compressive strength. The higher the concrete strength the smaller the cutting depth.
6. From among the independent parameters, the greatest influence on the cutting effects is exerted by the velocity of jet displacement along the concrete surface. The effect of the changes of the nozzle displacement velocity is greater for the higher compressive strength of concrete.
7. To increase the depth of cutting it is advisable to enlarge the jet diameter d_o, the more so as the enlargement d_o does not intensify the the rate of cutting energy, and in the case of less compact rock it even brings about the decrease of E_{jc}.
8. The increase of pressure p is advantageous with regard to E_{jc} for high-strength rock. With smaller-strength rock, the intensifying of pressure results in the growth of the rate of cutting energy.
9. During model testing no crushing of rock between incisions was observed. It could be caused by the small length of incisions, by the lack of loading the samples with external forces, and by the structural properties of the samples (lack of planes of weakend cohesion). Since the rock cut did not crush, it was not possible to determine the dependence of mining through cutting on the variability of the parameters of cutting.

At a later date, the testing device was installed in a mine working underground where it was used for mining coal. This experiment proved the applicability and high efficiency of a water jet as a cutting tool. Low

unitary energy of mining was obtained, and large coal grades were found in the output. No strong scattering of coal and no excess water in the working were observed.

6. References.

1. Kalukiewicz A. - Study of Mining Coal with Water Jet (doctoral dissertation) (in Polish) Kraków, 1984.

2. Kawecki Z., Puchała J., and others - Study of the Technique of Mining Rock with High-pressure Pulsating Jet (A report for Mining Mechanization Centre KOMAG Gliwice 1974.)

3. Kawecki Z., Puchała J., and others - The Method of Mining Rock with Continuous Water Jet and the Device to Meet This Purpouse (Polish Patent No 98322/30 1981)

4. Klich. A., Kalukiewicz A. - Versuchsergebnisse an einer Hochdruckwasserstrahlanlage für Stei- und Kohlegewinnung "Hydromechanisation 4", Karl-Marx-Stadt, DDR 1985.

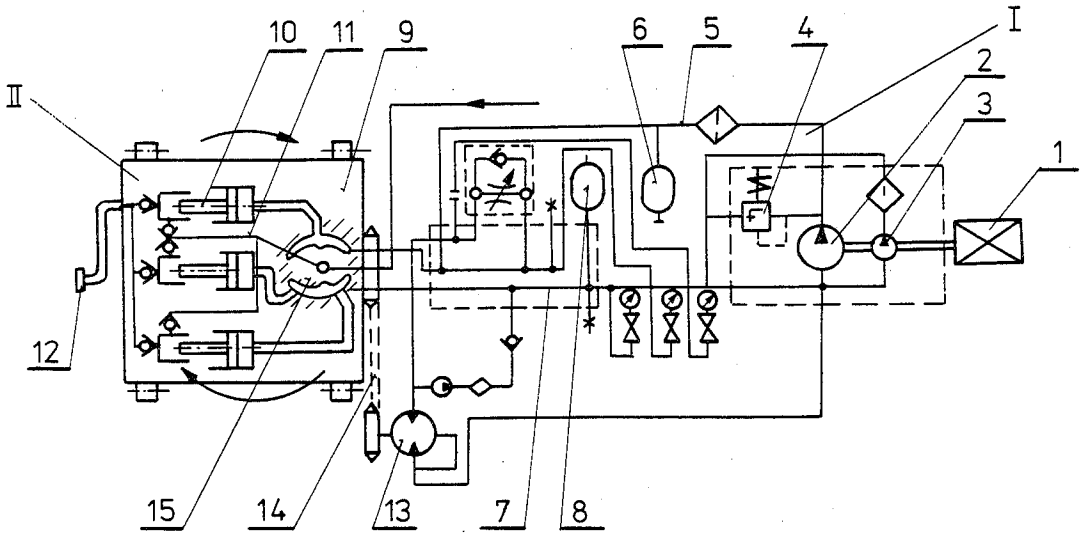

Fig. 1. The simpified diagram of the hydraulic system of the testing device.

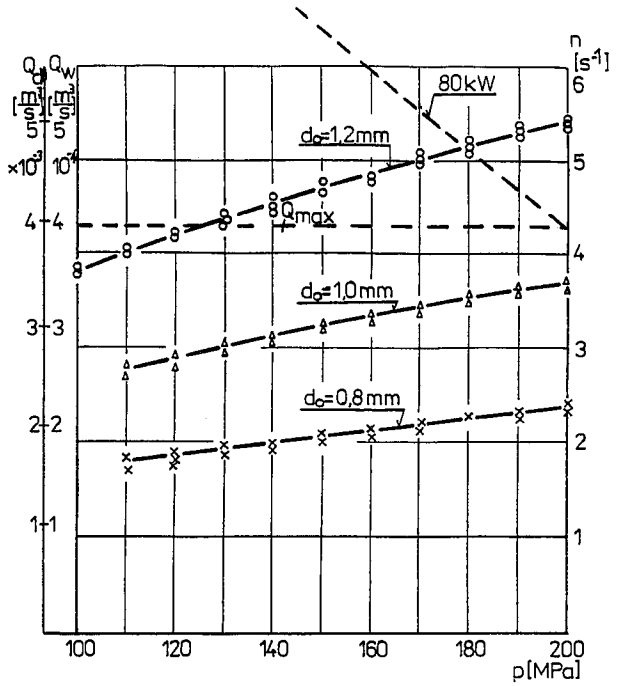

Fig. 2. The dependences of rotations, maximum water delivery and oil absorbing capacity of the monitor on pressure p for various nozzle diameters d .

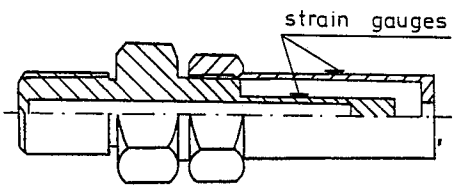

Fig. 3. Pressure sensor.

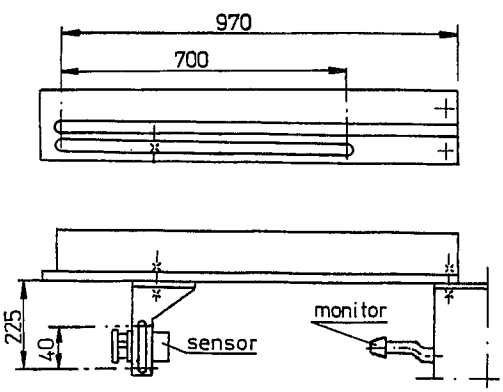

Fig. 4. Sensor of the dynamic force jet.

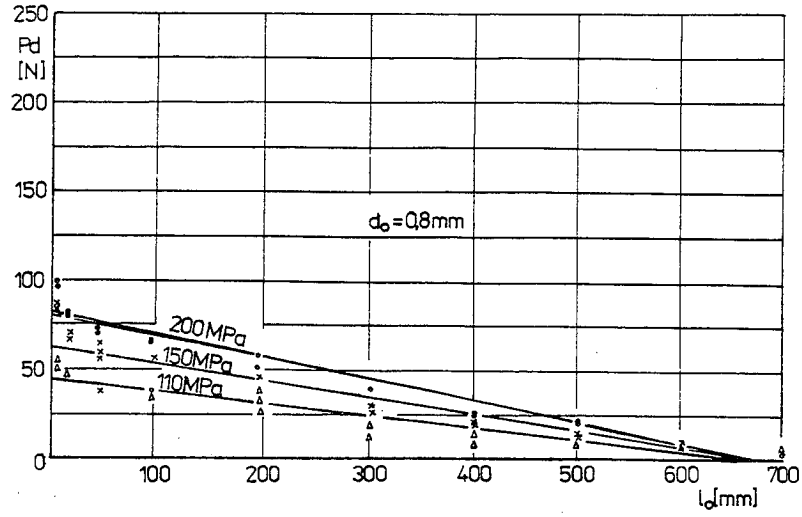

Fig. 5. The dependence of the jet dynamic force on the distance of the measuring point from the nozzle outlet (for d_0= 0.8 mm).

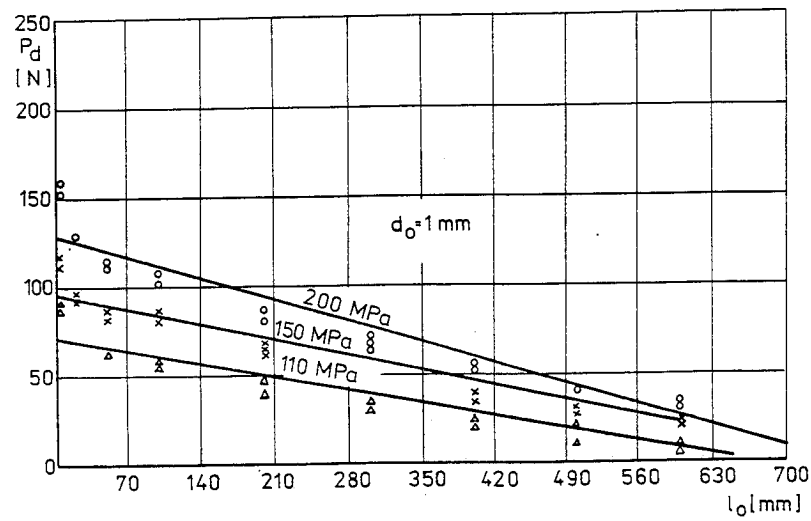

Fig. 6. The dependence of the jet dynamic force on the distance of the measuring point from the nozzle outlet (for d = 1.0 mm).

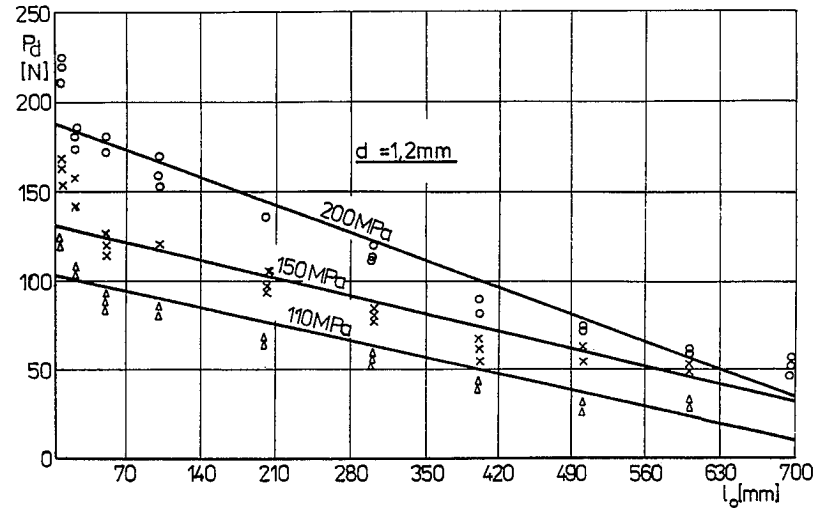

Fig. 7. The dependence of the jet dynamic force on the distance of the measuring point from the nozzle outlet (for d_0 = 1.2 mm).

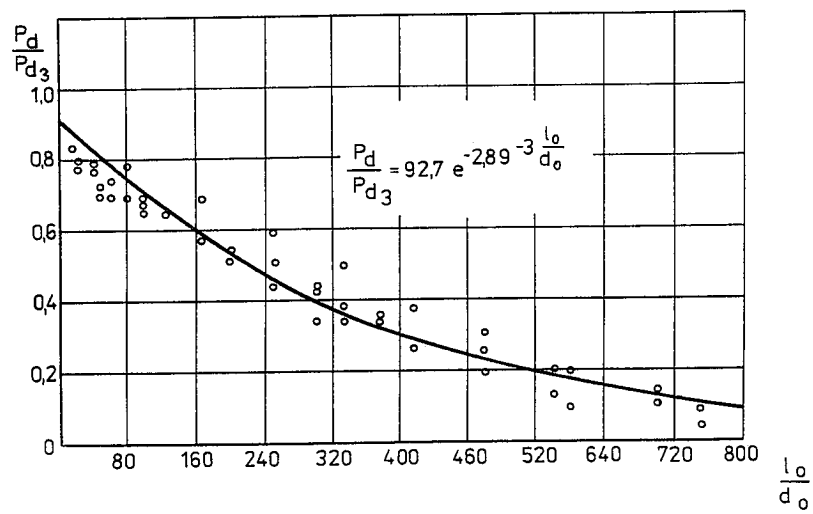

Fig. 8. The dependence of the reduction coefficient of the jet dynamic force P/P^3 on distance calculated by the nozzle diameters l /d .

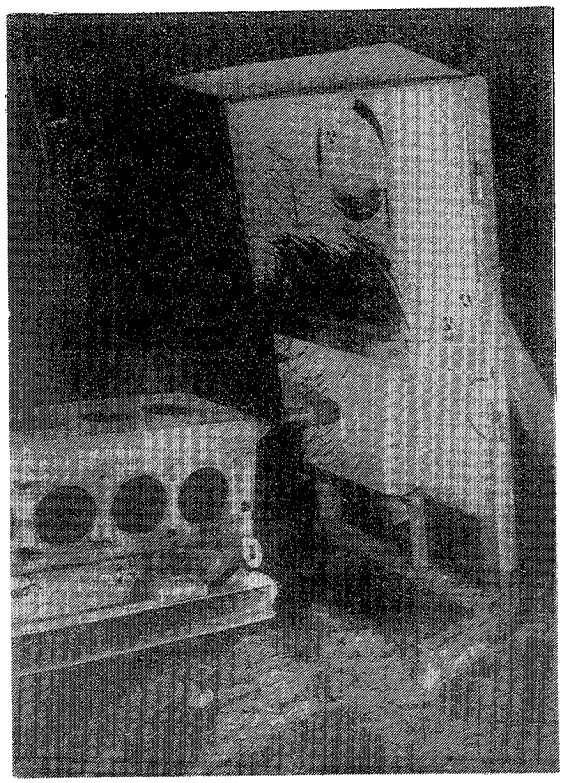

Fig. 9. The stand with a sample fixed.

Fig. 10. Incisions made in concrete during testing.

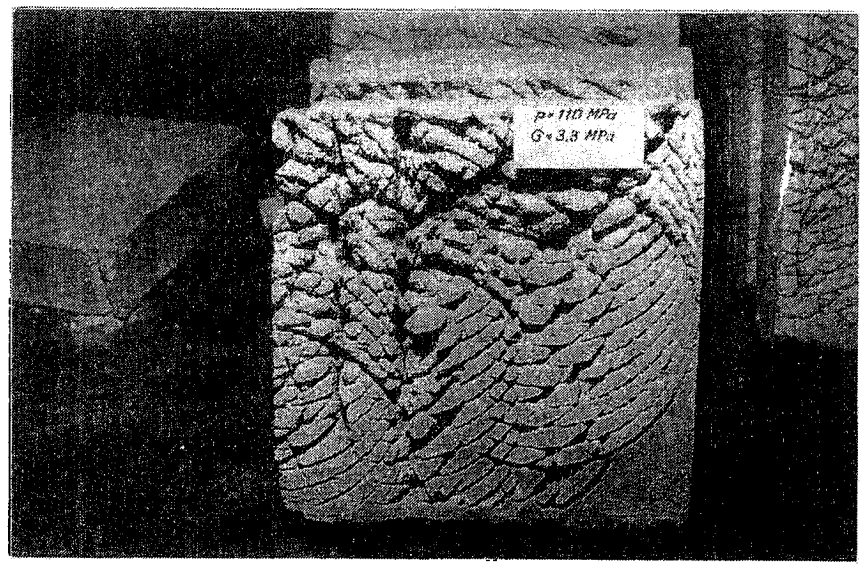

Fig. 11. Incisions made in concrete during testing.

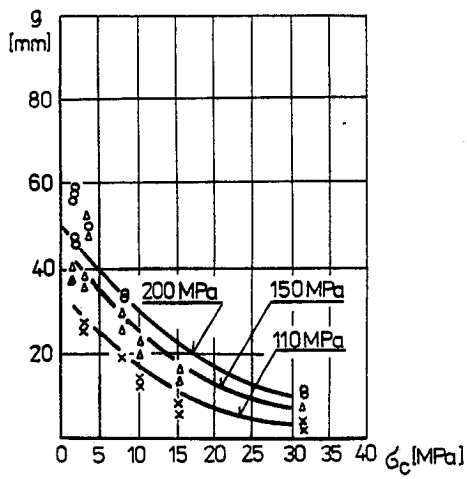

Fig. 12. The dependence of the depth of cutting concrete on its compressive strength σ_o for p = 110, 150, 200 MPa.

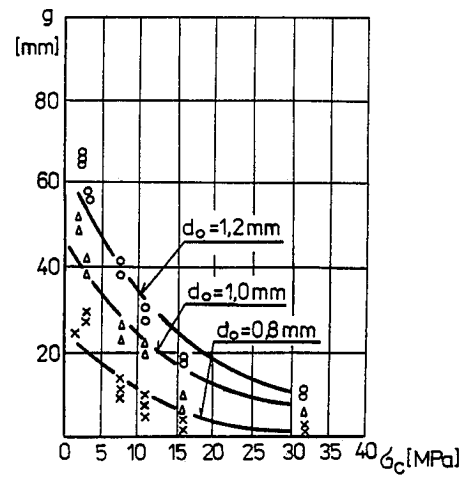

Fig. 13. The dependence of the depth of cutting concrete on its compressive strength σ_o for d_o = 0.8, 1.0, 1.2 mm.

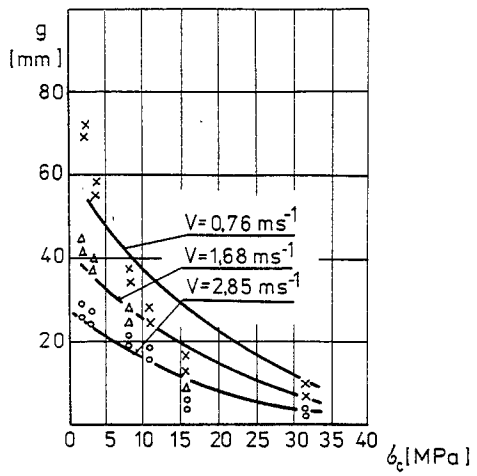

Fig. 14. The dependence of the depth of cutting concrete on its compressive strength σ_o for v_w = 0.76, 1.68, 2.85 m/s.

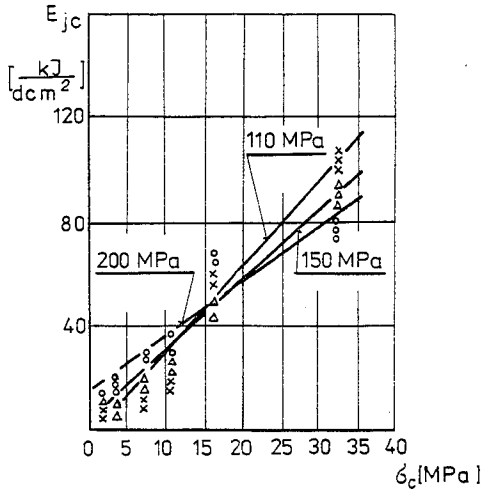

Fig. 15. The dependence of the unitary energy of cutting concrete E_{jc} on its compressive strength σ_c for p = 110, 150, 200 MPa.

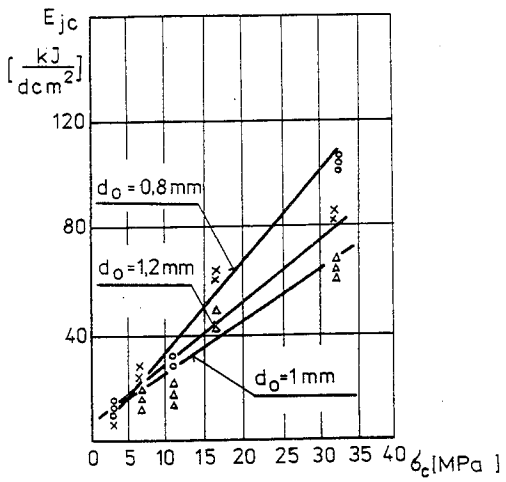

Fig. 16. The dependence of the unitary energy of cutting concrete E_{jc} on its compressive strength σ_c for d = 0.8, 1.0, 1.2 mm.

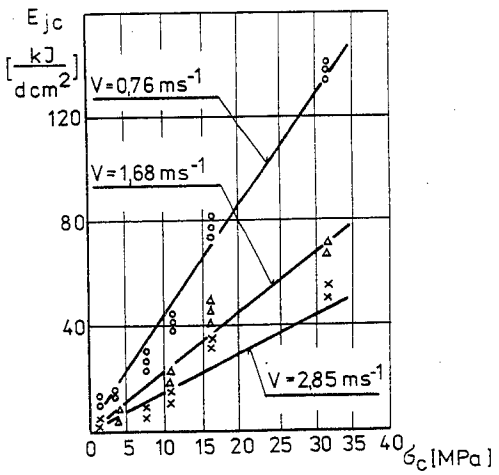

Fig. 17. The dependence of the unitary energy of cutting concrete E_{jc} on its compressive strength σ_c for v = 0.76, 1.68, 2.85 m/s.

5th American Water Jet Conference
August 29 - 31, 1989: Toronto, Canada

Paper / Communication 15

HIGH PRESSURE HYDROMILLING OF CONCRETE SURFACES

R.F. Schmid
Flow International Corporation
Kent (Seattle), Washington 98032, USA

ABSTRACT: Concrete bridges and structures are failing at an alarming rate due to concrete corrosion. It has been shown that high pressure waterjets are a cost-effective and sometimes preferred repair method for concrete scarification.
In this Paper the application of high pressure waterjets for the scarification of concrete will be discussed. The following topics will be introduced: An overview of how concrete is cut, cost advantages of using high pressure waterjets over percussive tools, and increased concrete bond strength for an overlaid surface. Also covered will be a presentation of both test data and field data for how production levels are affected for various operating pressures from 15,000 PSI (1,034 Bars) to 55,000 PSI (3,793 Bars).

RÉSUMÉ : Les ponts et les ouvrages de béton s'effondrent à un rythme alarmant à cause de la corrosion de ce matériau. Il a été démontré que les jets d'eau à haute pression constituent une méthode de réparation économique et parfois de prédilection pour la scarification du béton.
La présente communication porte sur l'application des jets d'eau à haute pression à la scarification du béton. Les sujets suivants seront abordés : aperçu de la manière dont le béton est coupé, avantages économiques des jets d'eau à haute pression sur les outils à percussion et adhérence accrue du béton de revêtement. Des données d'essai et des données de terrain seront aussi présentées sur la variation des niveaux de production en fonction de la pression d'application de 15 000 lb^2 (1 034 bars) à 55 000 lb^2 (3 793 bars).

Organized and Sponsored by the National Research Council of Canada and the U.S. Water Jet Technology Association.

1.0 INTRODUCTION

It is estimated there are 250,000 bridges considered substandard and in immediate need of repair in the United States of America alone. They are considered substandard because the structural integrity of the bridge is degraded by corroded or deteriorated concrete. Some 100,000 bridges are either closed or have posted weight limits. Nationwide funding (1989) for bridge "4R" work (resurfacing, rehabilitation, restoration, and reconditioning) amounts to approximately 4.4 billion dollars. Concrete corrosion occurs mainly as a result of freeze thaw cycling and placement of chloride based de-icers.

Freeze thaw cycling tends to introduce microcracks into the concrete structure. This increases permeability of the concrete and allows roadwater and/or chloride de-icing agents to penetrate to the steel reinforcing bar lattice. When these elements attack and corrode the steel bar, the corrosion introduces very high expansive forces into the parent concrete material which further cracks the concrete and debonds it from the rebar lattice. In general, concrete will debond or delaminate in layers parallel to the lay of the rebar lattice.

Typically, concrete structures are repaired by removing concrete down below the rebar level that is affected by 3/4 inch (1.90 cm) to 1 inch (2.54 cm). The steel reinforced bar is then inspected and either replace or cleaned of all rust. After that a new concrete layer is poured. Concrete is removed today by three different methods: Mechanical grinders, which can only grind to the reinforcing bar level, hand-held percussing tools, and mechanized high pressure waterjet scarification systems.

2.0 SYSTEM COMPONENTS

2.1 Pump

The high pressure water pump is diesel-driven and mounted on a truck or trailer so it can be mobilized on site easily. Concrete cutting requires pumping units in excess of 300 BHP (304 HP Metric).

There are two ranges of pumps used in the field today. They are medium high pressure pumps and ultra-high pressure pumps. Medium high pressure pumps operate in the range of 13,000 PSI (896 Bars) to 20,000 PSI (1,379 Bars). These units are usually very high horsepower units in excess of 500 HP (507 HP Metric) and operate with high flow rates of up to 70 GPM (265 LPM). Ultrahigh pressure pumps operate in the range of 25,000 PSI (1,701 Bars) to 35,000 PSI (2,381 Bars) and operate at horsepowers as low as 300 HP (304 HP Metric) and water flow rates as low as 13 GPM (49 LPM).

2.2 Cutting Robot or Tractor

The high pressure cutting head is carried on a mobile rubber-tired vehicle that drives down the road. The cutting head is reciprocated on a linear traverse mechanism back and forth perpendicular to the direction of travel of the tractor. This rate of traverse is adjustable to allow different cutting depths. The cutting head is composed of a nozzle. The nozzle contains one to three waterjets that are available in different geometries. As the cutting head reciprocates, the motion of the nozzle in conjunction with the geometry defined by the nozzle, cuts a kerf into the concrete. The geometric nozzle allows the waterjet to "reach" under the rebar to prevent leaving a shadow of uncut concrete under the reinforcing bar. After a trench is cut to a desired depth, the tractor increments forward a programmed distance and another trench is cut (see Figure 1). The proper overlap and blending of these trenches leads to a very uniform bottom surface. Concrete is normally removed in multiple pass traverse strokes (see Figure 2).

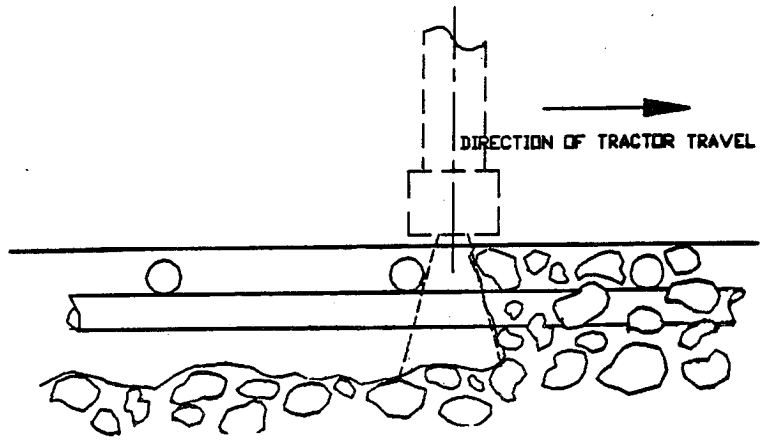

Figure 1 **Cutting of Trench by Tractor**

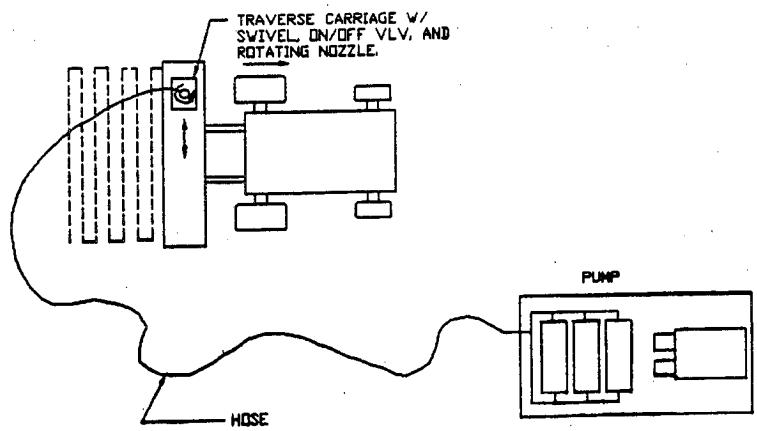

Figure 2 **Coordination of Traverse Mechanism to Pump**

2.3 High Pressure Hose

The pump is coupled to the cutting vehicle by means of a high pressure hose. The use of flexible high pressure hose increases the mobility of the cutting vehicle. The hose is shielded with an auxiliary burst/abrasion shield that protects the operators in the event of a hose bust. For very long delivery distances or paralleling of more than one high pressure pump, multiple hoses can be used.

3.0 ECONOMICS HYDROMILLING™ VERSUS JACKHAMMERING

3.1 Productivity

Virtually all States limit jackhammer sizes to 30 pounds (14 kilogram). Some States specify 15 pound (7 kilogram) chipping hammers. These limitations are imposed to minimize additional damage to a structure while removing deteriorated concrete with a percussive impact tool.

Typical jackhammer productivity is 1 to 1.5 cubic feet (0.03 to 0.04 cubic meter) of concrete removal per hour. Typical HydroMilling™ productivity is 20-30 cubic feet (0.5-0.8 cubic meter) per hour. Hence, Hydromilling™ productivity equates to approximately 20 jackhammers.

3.2 Economics

Equipment, maintenance and fuel for a 30 pound (14 kilogram) jackhammer amounts to approximately 5 US Dollar per hour. Labor costs dominate the contractor's costs for jackhammering as shown in Table I. Fixed and variable costs and contractor's gross margin requirements associated with HydroMilling™ amount to approximately 12 US Dollar per cubic foot (0.028 cubic meters) of concrete removed. Consequently, HydroMilling™ can effectively compete with jackhammering whenever local pay (exclusive fringe benefits and overhead) exceeds 12 US Dollar per hour. Economics particularly favor HydroMilling™ for large jobs involving the removal of 5,000 cubic feet (141 cubic meter) or more of concrete and tight completion schedules in order to minimize traffic disruptions. Therefore, the rehabilitation of interstate and major arterial bridge decks in urban areas are prime targets for high productivity HydroMilling™.

Table 1 Review of Contractor's Costs using the Jackhammering Method

Wages (USD/Hour) (excluding Fringe and Overhead)	Cost of Jackhammering USD/Cubic Foot(Cubic Meter)
10	17 (600)
15	23 (812)
20	29 (706)
25	35 (1,235)
30	41 (1,447)

4.0 BOND STRENGTH OF AN OVERLAID SURFACE FOR A HYDROMILLED SURFACE VERSUS A JACKHAMMERED SURFACE

4.1 Introduction

It has been proven that a hydromilled surface gives better surface interface bonding than a jackhammered surface. In an independent test conducted by Construction Technology Laboratories (C.T.L.) for Flow International, it was shown that shear strengths were 2.3 times higher and pull-off strengths were 3.1 times higher for a hydromilled surface versus a jackhammered one.

4.2. Testing Procedure and Results

The objective of the test was to evaluate the effects of hydromilled and jackhammer scarification methods on microcracking in the upper surface of a scarified base concrete lab, and to evaluate the bond strengths of both by conducting direct single shear and bond pull-off strengths of overlays applied to the base concrete lab. The test was conducted as follows:

1. A concrete slab was cast, using Washington State D.O.T. class AX concrete.

2. In one area, the top 2-3 inches (5-8 centimers) of concrete were scarified, using 34,000 PSI (2,344 Bar) HydroMilling™ Equipment.

3. In another area of the slab, the top 2-3 inches (5-8 centimeters) of concrete were removed, using 30 lbs. (13.6 kg) pneumatic jackhammers.

4. Latex modified concrete was placed on the scarified surfaces in accordance with Washington State D.O.T. standards.

5. The bond strength of the overlayed latex modified concrete to the base slab was tested, using direct shear and pull-off tests.

6. Thin polished sections of the upper regions of the scarified surface were examined petrographically to determine presence and/or absence of microcracks.

The results of the bond strength tests are shown in Figure 3.

		SHEAR STRENGTH TESTS:		PULL-OFF TESTS:	
Test Section	Core No.	Shear Strength PSI/Bar	Failure Plan	Bond Strength PSI/Bar	Failure Plan
34,000 PSI	1	355/24.5	Base Concrete	291/20.1	Base Concrete
ditto	2	**	----------	248/17.1	Base Concrete
ditto	3	222/15.3	Interface	118/ 8.1	Interface
ditto	4	312/21.5	Base Concrete at Rebar	275/18.9	Base Concrete
Jackhammer	13	**	----------	6/ .4	Base Concrete
ditto	14	188/12.9	Interface	95/ 6.5	Interface
ditto	15	117/ 8.1	Interface	122/ 8.4	Interface
ditto	16	92/ 6.3	Undetermined	--------	----------

** Peterographic

Figure 3 **Bond Strength Tests**

4.3 Peterographic Analysis

Peterographic examinations were done using ASTM C 856-83 "Standard Practice for Peterographic Examination of Hardened Concrete". The findings of Construction Technology Laboratories is as follows: No cracks or microcracks were found in the upper regions of the base concrete in the 34,000 PSI (2,313 Bar) scarified concrete. However, microcracks wre present in the base material in the jackhammer prepared surface. The cracks occurred within 3 mm of the bonded overlay, and are sub-parallel to the overlay/substrate bond line.

5.0 PRODUCTION TEST DATA

5.1. Production rate for a given pressure as a function increasing horsepower

Tests were conducted in February 1987 by Flow International on the I-5 Dearborn Street Interchange Bridge in Seattle, Washington. This concrete was 20 year old Washington State ax mix with a compressive strength of 6,500 PSI (442 Bar). Tests were conducted, using standard Flow HydroMilling™ equipment. This equipment was operated at 25,000 PSI (1,701 Bar) with a flow rate from 15 GPM (57 LPM) to 44 GPM (167 LPM). All operating parameters were kept constant i.e.: traverse velocity, nozzle standoff, nozzle rotary speed, angle of nozzle, and forward drive increment. The only variable introduced was changing of the nozzle diameter to increase flow rate hence: increased horsepower. Figure 4 shows the Graph of the results.

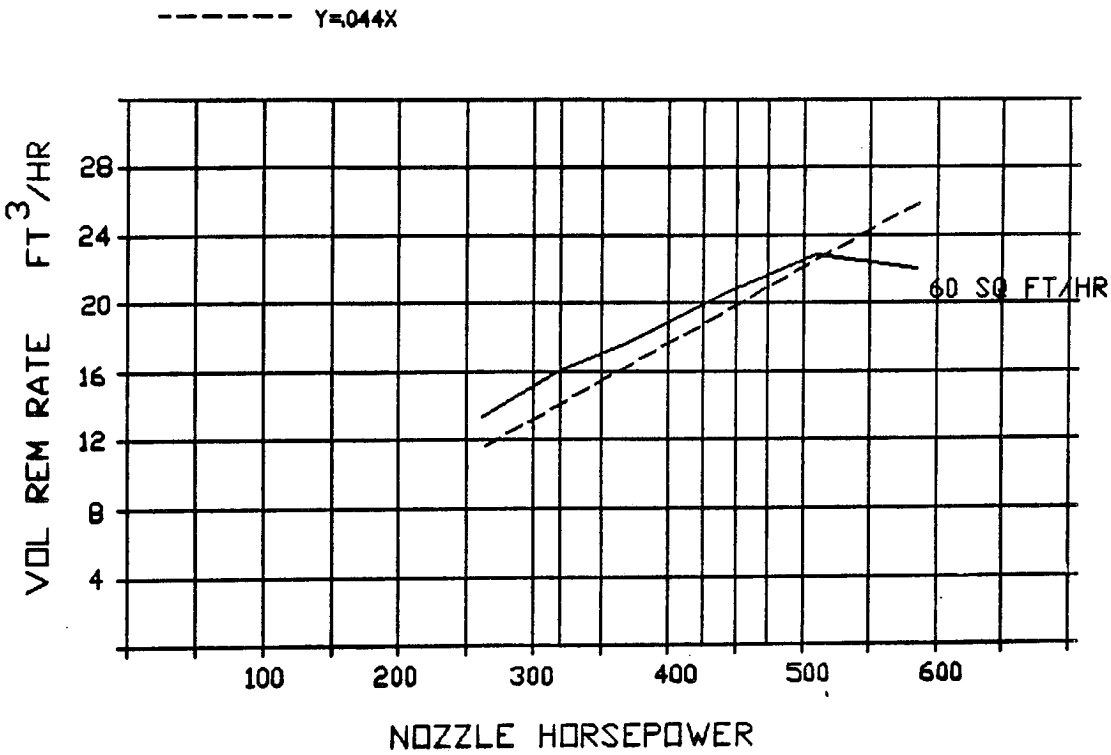

Figure 4 **Production Rate vs. Horsepower For A Given Set Of Operating Parameters (Non-Optimum)**

5.2 Production rate for increasing pressure at a given horsepower

These tests were conducted on the same bridge deck as in section 5 with the same equipment. This time the objective was to cut 3-3.5 inches (8-9 centimeter) deep at optimum operating parameters for different pressures. At each operating pressure, skilled technicians wre allowed to adjust the equipment until peak productivity was achieved. This was to accommodate for the fact that at different pressures maximum productivity is obtained by different operating parameters, and this test was designed to evaluate bulk production rate as a function of operating pressure. Figure 5 shows a graph of the results.

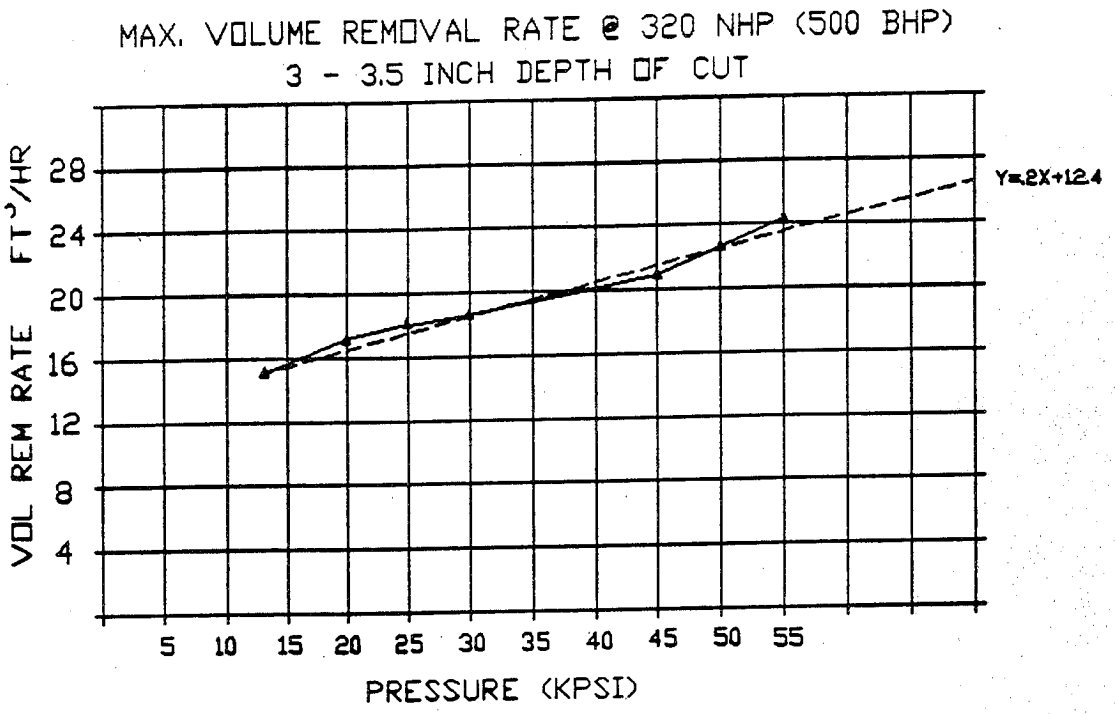

Figure 5 Volume Removal Rate Versus Pressure
At 320 N.H.P. At Optimized Conditions

5th American Water Jet Conference
August 29 - 31, 1989: Toronto, Canada

Paper / Communication 16

STATISTICAL CHARACTERIZATION OF SURFACE FINISH PRODUCED BY A HIGH PRESSURE ABRASIVE WATERJET

C.D. Burnham* AND T.J. Kim,
Waterjet Laboratory
Department of Mechanical Engineering
University of Rhode Island
Kingston, RI 02881, USA

ABSTRACT: An experimental study was conducted to ascertain the surface finish associated with high pressure abrasive waterjet process by a statistical approach. Three different types of materials; sintered alumina, stainless steel, and graphite composites, were used to generate a data base for the analysis. The results of study revealed that the surface roughness can be predicted by the statistical manipulation of certain process parameters. It was also found that the surface roughness can be predicted by the workpiece reactive force.

RÉSUMÉ : Une étude expérimentale a été menée pour vérifier statistiquement la finition de surfaces obtenue avec des jets d'eau abrasifs à haute pression. Trois différents types de matériaux (alumine frittée, acier inoxydable et composés au graphite) ont été utilisés pour produire une base de données d'analyse. Les résultats de l'étude ont révélé que la rugosité des surfaces peut être prévue par le traitement statistique de certains paramètres de processus. On a aussi constaté que la rugosité des surfaces peut être prévue par la force de réaction des éprouvettes.

*Present Address: Flow International Inc., Kent, Washington, USA

Organized and Sponsored by the National Research Council of Canada and the U.S. Water Jet Technology Association.

1. INTRODUCTION

The surface finish produced by conventional machining methods is generally uniform. Therefore, the surface finish of the machined surface can simply be characterized by measuring the surface roughness of any portion of the machined surface. However, with abrasive waterjet (AWJ) cutting, the surface finish varies as a function of the cutting depth of a workpiece. The most pronounced characteristics of the AWJ machined surface is the development of striation marks which transpire below an area of relatively smooth surface finish. The striation marks or transione lines appear when the high pressure stream of water and abrasive loses a significant amount of energy.

The inconsistency in roughness distribution is a unique characteristic of an AWJ cut. The surface quality degenerates as the jet stream approaches the bottom of the cut. Studies by Hashish [1,2] revealed two stages of material removal modes associated with abrasive waterjet process. The mechanism of jet cutting process generally depends on the process parameters but it greatly depends on the workpiece geometry; namely the thickness. In the first stage of cutting, the abrasive particles strike the surface at a shallow angle producing a relatively smooth surface. The material removal phenomenon associated with this process of cutting is called the cutting wear mechanism. The secondary region, displaying unsteady cutting with striation marks as shown in Figure 1, is called the deformation cutting zone. This is the secondary penetration process, which is primarily responsible for the striation marks at the bottom of the kerf. The material removal is controlled by erasive wear by particles impacting at large angles of attack.

Surface finish and tolerance of the AWJ machined components are two major process parameters which are critical for precision machining applications. To quantify the surface finish associated with AWJ cutting, a force sensor system was developed by the Waterjet Laboratory of the University of Rhode Island [3]. The system was used to characterize and to control the surface finish produced by the AWJ cutting. The force sensor technique developed for abrasive waterjet cutting applications provides a near-real-time output of a measured watejet process variable. It was successfully used for monitoring and controlling the cutting efficiency of a workpiece with variable thickness [4,5].

The purpose of this study is to characterize the surface finish generated by an AWJ process using statistical analysis. The data base obtained from cutting experiments were used to examine the roughness pattern and to establish a correlation in terms of the process variables. A series of emperical equations for roughness value are derived and tested for a limited range of AWJ process variables.

2. EXPERIMENTAL SETUP AND PROCEDURE

The high pressure system used for this study consists of an 11X-6 series dual intensifier pump connected to a PASER nozzle assembly; both manufactured by Flow International Inc. The PASER assembly is manipulated by a GMF A-200 robot with a KAREL controller. It has an AC servo drive system and a repeatability of ± 0.0508 mm. The robot can be programmed by teaching points or by geometrically defining the motions off-line:

A surface profilometer (Model ADR-22) manufactured by Federal Products was used to measure the average roughness (R) of the AWJ cuts. The amplifier of the profilometer has a sensitivity and cutoff set at 0.300 and 0.03 inches (7.62 and 0.726 mm). The probe has a 0.0004 inch (0.01 mm) radius diamond stylus. It is also equipped with a built-in skid which follows the contour of the surface being measured. The motor-drive moves the probe over the specimen surface with a specific stroke length, 0.3 inch (7.62 mm) in this case. As the probe is profiling the contour of the surface, the digital readout gradually approaches the actual Ra surface roughness on the specimen. It takes approximately 10 to 20 seconds for the digital readout to asymptotically reach the approximate value of an AWJ cut.

2.1 Materials Selection and Properties

The materials chosen for this study meet the test criteria. The materials are able to withstand surface roughness measurements without damage to the surface. If the stylus indents the surface, as is the case with some aluminum, then the results are not accurate. The materials are also relatively consistent in composition so that any variability in a cut surface can be attributed to the cutting process. The workpiece materials are able to be machined with the AWJ process at reasonable cutting rates in order to avoid inaccuracy of the manipulator motion speed. The workpieces used are of different compositions to cover a wide spectrum of material types. The workpiece materials are aluminum oxide ceramic (AD 85), graphite composite, and 304 stainless steel. The graphite epoxy composite material has a fiber volume percent of approximately 63, and Poisson's ratio of 0.38. Since the graphite fibers oriented in one direction, the modulus of elasticity and tensile strength properties are different from directions of 0 to 90 degrees. For this reason, a separate value is given for 0° and 90° in each of these attribute catagories. The mechanical properties of the workpiece materials are listed in Table 1.

2.2 Test Procedure

To perform the statistical analyses of the surface roughness produced by abrasive waterjet machining, a data base was created by cutting the materials. The significance of roughness variation with respect to position on the workpiece was specifically investigated. A data base was created by machining the three materials, each with numerous cutting speeds, and recording the roughness measurements for each cut. This data base was then statistically analyzed.

Statistical analyses were conducted, beginning with roughness average (R) measurements of the machined surfaces. The profilometer measured the roughness in a grid like fashion. This grid pattern is shown in Figure 2. The numbers shown on the face are average roughness readings obtained from the ceramic sample; cutting speed equal to 0.4-0.5 inches per minute. The roughness variation across and down the cut face was investigated. By using four levels in the vertical direction, the curve fit may be as high as third order. Similarly, three levels used in the horizontal direction allow for a fit of up to second order. Orthogonal polynomial regression method was used to determine the significant variation in roughness value due to horizontal or vertical change in grid location at 95% confidence level. Finally, the multiple regression was used to generate an emperical equation by a curve-fit method.

To minimize the inter-parametric influence on the statistical characterization of the surface finish, all waterjet process parameters are held constant except the nozzle traverse rate, workpiece materials, and workpiece thickness. For the purpose of generating the database for this study, the workpiece materials with constant thickness were used. The values of the AWJ parameters used for cutting tests are:

A. Hydrodynamic Parameter	
1. Water Pressure	35000 psi [241 MPa]
2. Orifice Size	0.018 inch [0.46 mm]
3. Nozzle diameter	0.062 inch [1.57 mm]
4. Nozzle length	2 inch [50.8 mm]
B. Abrasive Parameters	
5. Abrasive material type	garnet
6. Particle size	80 mesh
7. Mass flow rate	1.0 lb/min [7.56 kg/s]
8. Grain shape	angular (random)
C. Mixing Parameters	
9. Mixing method	suction
10. Abrasive condition (wet,dry)	dry
11. Mixing chamber size	.4 cu inch [6.5E-5 m^3]
12. Abrasive hose diameter (ID)	0.25 inch [6.35 mm]
13. Abrasive hose length	72 inch [1.83 m]

D. Cutting Parameters

14. Nozzle traverse rate	variable
15. Nozzle/workpiece standoff	0.05 inch [1.27 mm]
16. Number of passes	1
17. Impingement angle	90 degrees
18. Workpiece material	variable
19. Workpiece thickness	variable

3. SURFACE FINISH CHARACTERIZATION

The data base for measured average roughness for AD85 ceramic, stainless steel, and graphite composite are used to generate the regression equation with a relatively high confidence level. The results show that no statistically justifable variation in roughness (R) is present in the lateral direction for all workpieces tested. The results also indicate that for the given range of cuttting speeds for each material, the variation in surface roughness with depth varies as:

$$\begin{aligned} R &= 181 - 111.6D + 33.9D^2 \quad \text{(Ceramic for S=.75 ipm)} \\ R &= 106 + 12.6D \quad \text{(Steel for S=2 ipm)} \\ R &= 142.8 + 16D \quad \text{(Graphite for S=5 ipm)} \end{aligned} \tag{1}$$

where:

R = surface roughness (μ-inch)
D = depth of surface (inch)
S = cutting speed (ipm)

Figure 3 exhibits the measurement scatter associated with R sampling for a ceramic workpiece cut at .75 ipm. The scatter increases as the depth increases. The similar results were obtained for two other workpiece materials cut at four different cutting speeds. Figure 4 illustrates the curve shifting as the cutting speed increases. The method of predicting R in terms of the depth of cut D requires a separate curve for each cutting speed.

A linear regression model for the ceramic workpiece gives the correlation coefficient (Cr) of .84. But the second order regression model for AD 85 expressed by equation (1) increases the correlation coefficient to .9486 yielding a 90% prediction.

3.1 Multiple Regression Model

The single regression model developed for the depth variable is extended to include both depth and cutting speed. To accomplish this three computer programs (MUTIPOL, MULTYINTER, and MULTIALL) [6] for multiple regression procedures were developed. The first program (MULTIPOL) develops a first order equation. The average roughness measurements for each specific depth and cutting speed are entered. The second program, (MULTYINTER), includes the interaction between depth and speed, and the third program (MULTIALL) combines both the interaction effect and the squared terms for speed and depth. Each program yields the characteristic equations, correlation coefficients and the estimate of the standard error. If the MULTIPOL program yields a low correlation coefficient, the second program is employed which includes additional terms. The MULTYINTER program gives a better fit than MULTIPOL since it incorporates the interaction terms. Similarly, the MULTIALL program can be used if the degree of fit is still not acceptable. For example, the AD 85 ceramic yielded only .8274 correlation coefficient for S and D regression model by MULTIPOL program. This model includes the first order terms only. A better correlation can be found by expanding the equation including an interaction effect. The correlation coefficient increases to 0.9351311. That is 87.45% of the data is represented by the equation. Next, the squared terms of both the depth and the speed can be included to further increase the value of Cr. By incorporating the interaction and the square terms into the multiple regression model, one can obtain the correlation coefficient of 0.97 which implicates 94.60% of the data representation by the equation expressed as:

$$R = 131 - 121.4D - 51.15 + 2241.6D^2 - 1.5S^2 + 1397.9DS \quad (2)$$

Figure 5 shows the roughness distribution expressed in terms of the depth on workpiece for S = 0.75 ipm. The multiple second order regression model for AD 85 expressed by equation (2) gives very close correlation with the data.

Similarly, the multiple regression model was applied for steel and graphite composite materials [6]. The stainless steel model developed by including the interaction effect yields a satisfactory correlation coefficient of .97. The graphite composite also only requires the interaction effect yielding a correlation coefficient of 0.9838. The corresponding linear multiple regression models with D & S interaction effects for steel and graphite composites are expressed as:

$$R = 123.3 - 88.7D - 7.95 + 108.8\ DS \quad \text{(steel)}$$
$$R = 128.7 - 18.7D + 3.7S + 18.4DS \quad \text{(graphite)} \quad (3)$$

3.2 Accuracy of Multiple Regression Model

To ascertain the accuracy of multiple regression models developed in the previous experiments, a group of materials with similar composition is cut with the AWJ and the surface roughness was measured. Since the ceramic workpiece produced the higher order characteristic equation, it was chosen as the test material for this experiment. A 0.25 inch thick material with a range of speed from 0.5 to 1.2 ipm (0.21 to 0.51 mm/s) was tested for the same values of the processing parameters used in the previous experiments. The result of this experiment revealed that 85.7% of data are represented by the derived multiple higher order regression model.

This portion of the study has revealed three valuable informations concerning the surface finish characterization. (1) A curve fit equation can be generated which predicts the surface roughness in terms of the depth and cutting speed. (2) The surface roughness measured at the bottom of the workpiece always gives the highest value. (3) No significant variation in roughness is present in the horizontal direction (laterally across the cut face). The last two characteristics listed above can be used to define a measurement method of surface roughness for an AWJ cut surface. One point reading taken at the bottom of the cut at any eight lateral positions will yield a value corresponding to the roughest portion of the cut face. This "worst case" scenario is often adequate for industrial applications.

4. SURFACE ROUGHNESS AND FORCE CONTROL

Having defined the surface roughness applicable to AWJ cutting process, the next step is to control the roughness. The surface control is achieved by use of the material removal kinetics, namely the cutting force.

4.1 Abrasive Waterjet Dynamometer

A beam force transducer developed for measurement of cutting force was used as a dynamometer for this investigation [3]. The output of the four active arm Wheatstone Bridge circuit mounted on a beam is expressed in terms of the applied force P as:

$$\frac{\Delta V}{V} = \frac{G_f ca}{2IE} (P) \quad (4)$$

where G_f is the gage factor for four identical strain gages used. The constants a and c are beam geometry, E is the modulus of elasticity, and I is the cross section moment of inertia of the beam. Several different force sensing beam designs were initially attempted. The beam which is used in this study is versatile, accurate, easy to operate, and tends to minimize the drift. The drift is largely caused by the expansion or contraction of the beam due to temperature change. The output from the beam transducer was measured using an analog recording devices. A BAM bridge amplifier was wired to the four strain gages. The analog signal from the BAM was then sent to a process computer through a 200 gain op-amplifier, filtered to remove frequencies above 15 HZ, and fed into an A/D board in an IBM PC. A computer program written in interpretive basic sampled the force data at a frequency of 50 HZ.

4.2 Surface Roughness Versus Cutting Force

The cutting force detected by the AWJ dynamometer is known to represent the measure of the cutting efficiency. Since the AWJ cutting efficiency can generally be controlled by adjusting the waterjet process variables, the cutting force can be used as a kinetic parameter to control the efficiency of cut, i.e. the surface roughness:

$$R = J_p \; F \; (f_w) \qquad (5)$$

where J_p is a modified waterjet process parameter and f_w is the level of force output. In a previous study the inverse of equation (5) was used in optimization of the AWJ process by a force feedback control [5]. However, there are several unanswered questions regarding the role of individual AWJ parameter in f_w and R relation, especially the role of material properties and microstructure. This study clearly reveals the material dependency on the surface roughness and force relation.

An experiment was conducted to ascertain the role of material parameter on the establishment of R and f_w relations. All three materials (AD 85, stainless steel, and graphite composites) were used to generate the force-roughness relation as shown in Figure 6. The cutting test was conducted using the workpieces with the same thickness (.385 inch) at a wide range of cutting speeds to attain the force level between 0.5 and 2.1 lbs (2.2 to 3.94N). This eliminates a coupling effect of the geometric parameter (thickness) on the R and f_w relation. It is, however, interesting to note that the linear regression model derived from this experiment indicates a separate trend between brittle material (ceramics) and ductile and psudo-ductile materials (steel and graphite composite). The regression model for all three materials are:

$$\begin{aligned} R &= -111.5 + 232.4\, f_w && \text{(Ceramic, Cr =.96)} \\ R &= 69.1 + 232.4\, f_w && \text{(Steel, Cr = .95)} \\ R &= 109.9 + 91.8\, f_w && \text{(Graphite, Cr =.99)} \end{aligned} \qquad (6)$$

where the slope of steel and graphite composites are the same and Cr is the correlation coefficient.

In order to investigate the influence of the microstructure of a family of materials, the similar cutting test was conducted using a family of sintered Al_2O_3 ceramics. The three grades of alumina ceramics (Ad 85, AD 94, and AD 99.5) were tested. The mechanical properties of all three grades of alumina are listed in Table 1. Each of the materials was cut at a range of speeds to generate the reactive forces ranging between 0.5 and 2.1 lbs. Figure 7 shows the roughness distribution plotted in terms of the cutting force for all three sinter alumina ceramics (the same thickness) at a varying cutting speed. The second order regression model for this experiment is derived as:

$$R = 151.5 - 173\, f_w + 112.4\, f_w^2 \qquad (7)$$

with a relatively high correlation coefficient, Cr = 0.93. The result indicates that the kinetic parameter (f_w) can actually be used to establish an exact functional relation for a group of the same material family with different microstructure, at least for alumina. Although this result is not conclusive enough to extend the same functional relation to other groups of material family, it clearly reveals a possible correlation between the AWJ generated surface morphology and the mechanical properties of the workpiece materials.

REFERENCES

1. Hashish, M., "Steel Cutting with Abrasive Waterjet", Proceedings of the Sixth International Symposium in Jet Cutting Technology, BHRA Fluid Engineering, April 1982, pp. 465-487.

2. Hashish, M., "A Modeling Study of Metal Cutting with Abrasive-Waterjets," ASME Journal of Engineering Materials and Technology, January 1984, pp. 88-100.

3. Kim, T.J. and Field, G., "Workpiece Reaction Analysis Applied to Abrasive Waterjet Processes," Waterjet Lab Report No. 85-2, Department of Mechanical Engineering and Applied Mechanics, University of Rhode Island, Kingston,RI August 1985.

4. Hunt, D.C., Burnham, C.D. and Kim T.J., "Surface Finish Characterization in Machining Advanced Ceramics by Abrasive Waterjet," Presented at the 4th U.S. Waterjet Conference, Published in Conference Proceedings, August 1987.

5. Hunt, C.D., Kim, T.J., and Reuber, M., "Surface Finish Optimization for Abrasive Waterjet Cutting," Presented at the 9th International Symposium on Jet Cutting Technology, Sendai, Japan, October, 1988. Published in the BHRA Conference Proceedings.

6. Burnham, C.D., "Surface Finish Characterization and Control for an Abrasive Waterjet" M.S. Thesis, University of Rhode Island, Kingston, RI, May 1989.

TABLE 1 Mechanical Properties of Workpieces

Materials	Specific Gravity	Modulus of Elasticity (GPA)	Tensile Strength (MPA)	Compressive Strengthy (MPA)	Hardness
316 STL STEEL	8.03	207	552		20 HRB
AL_2O_3 (AD 85)	3.42	227	124	1654	75 HR45N
AL_2O_3 (AD 94)	3.62	287	186	2067	78 HR45N
AL_2O_3 (AD99.5)	3.84	358	262	2067	81 HR45N
GRAPHITE COMP.	1.61	414	11		

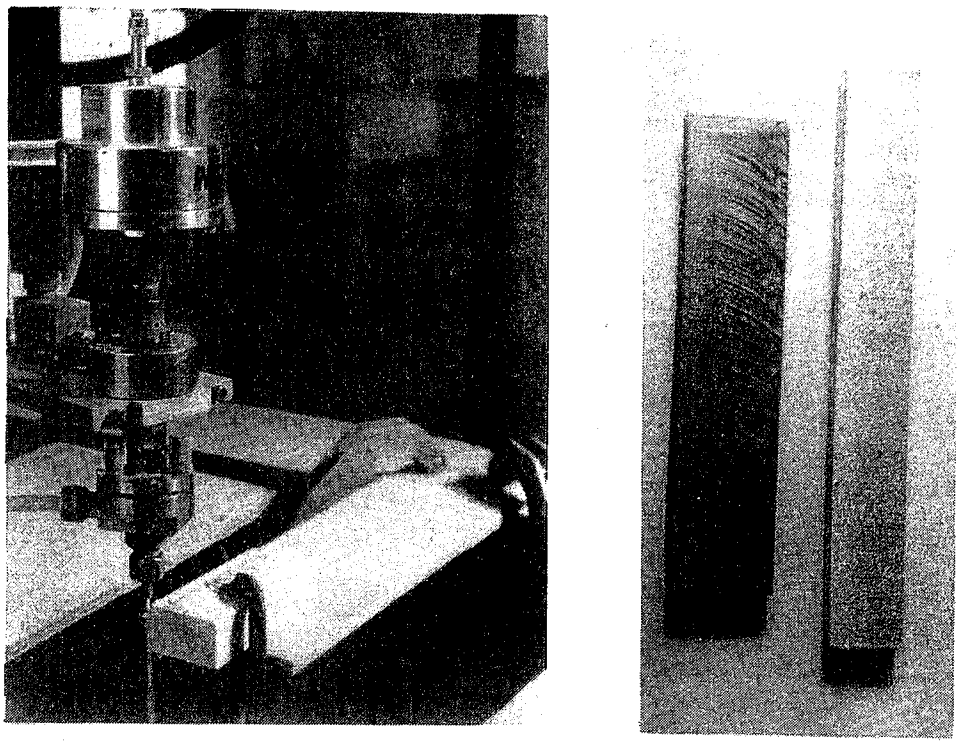

FIG. 1 AWJ CUTTING SETUP AND STRIATED SURFACE

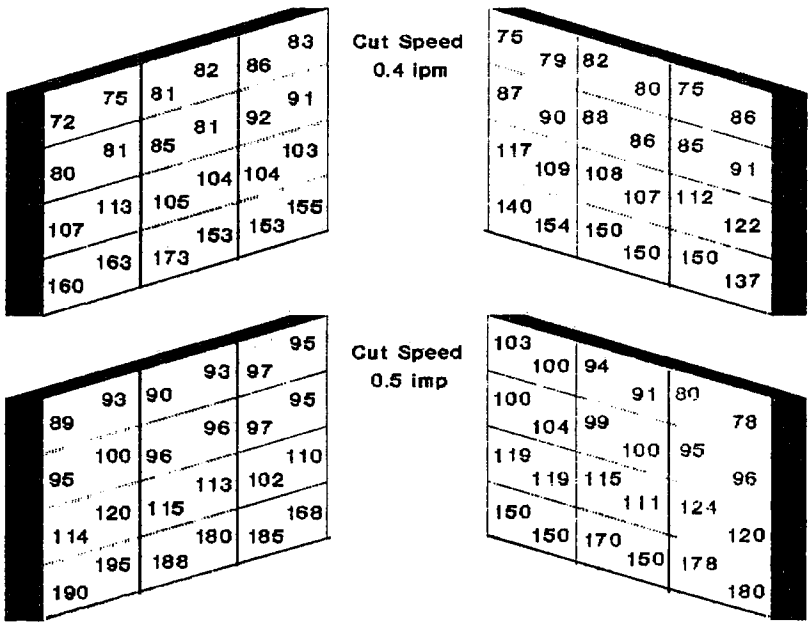

FIG. 2 GRID PATTERN FOR SURFACE ROUGHNESS MEASUREMENT

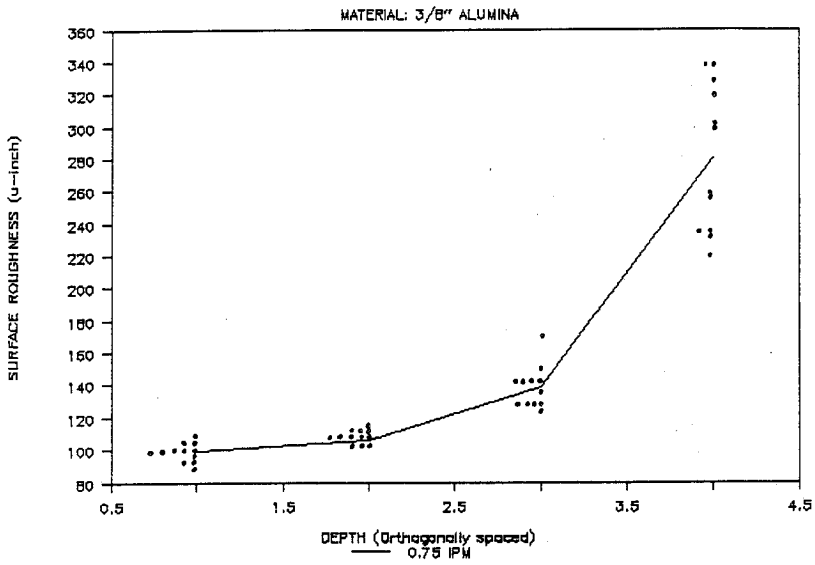

FIG. 3 ROUGHNESS VERSUS DEPTH (AD 85)

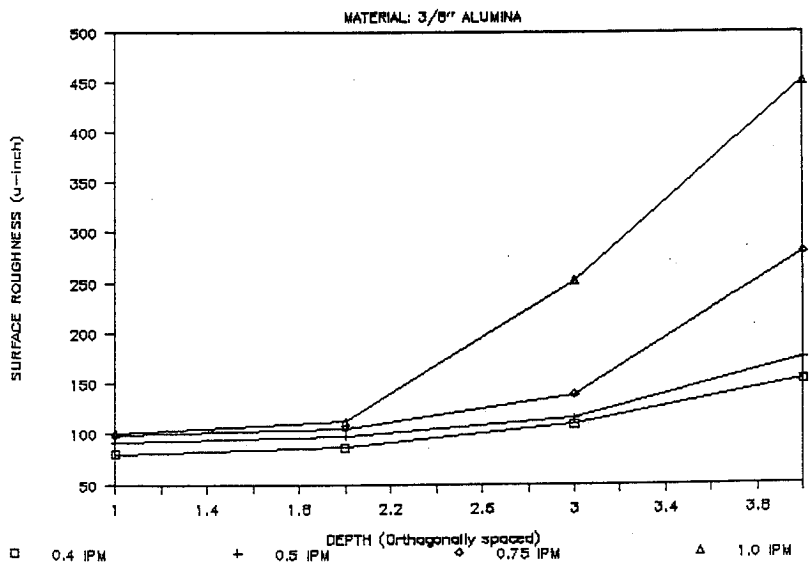

FIG. 4 ROUGHNESS VERSUS DEPTH AT FOUR DIFFERENT SPEEDS (AD 85)

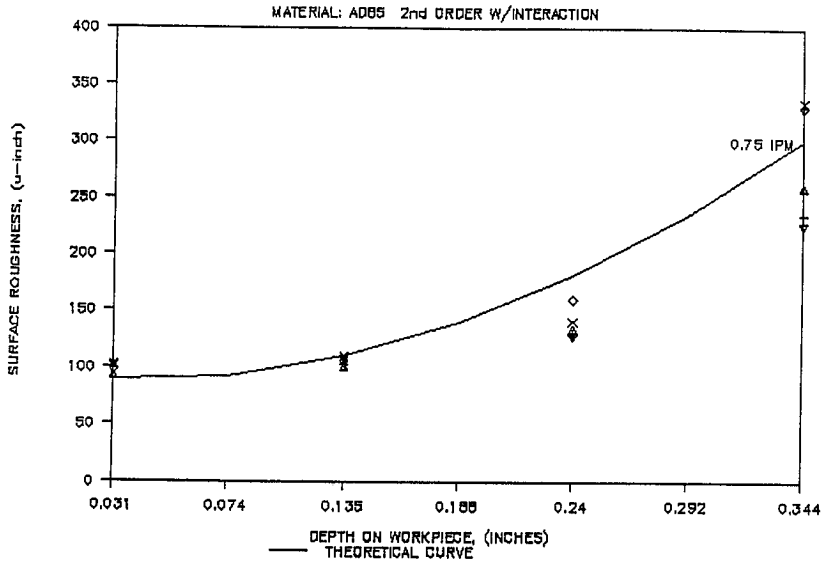

FIG. 5 VERIFICATION OF MULTIPLE REGRESSION MODEL (AD 85)

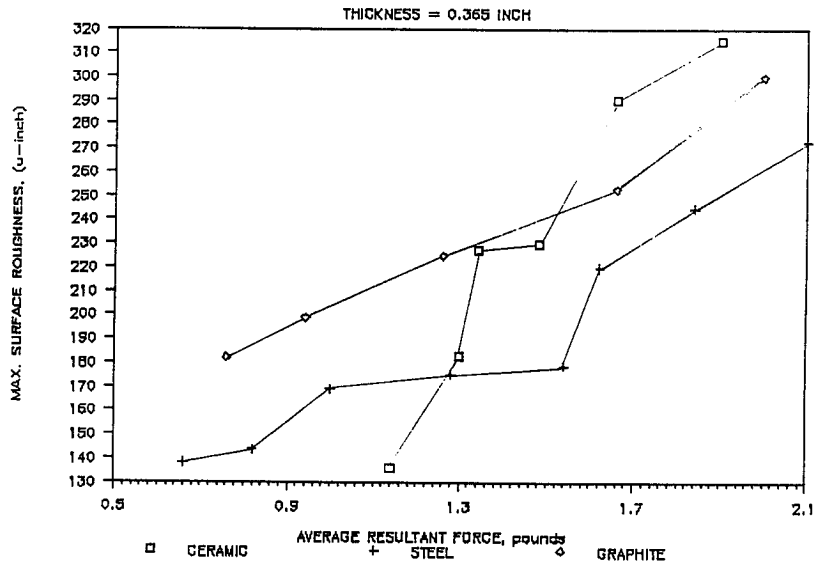

FIG. 6 FORCE VERSUS RESULTANT FORCE

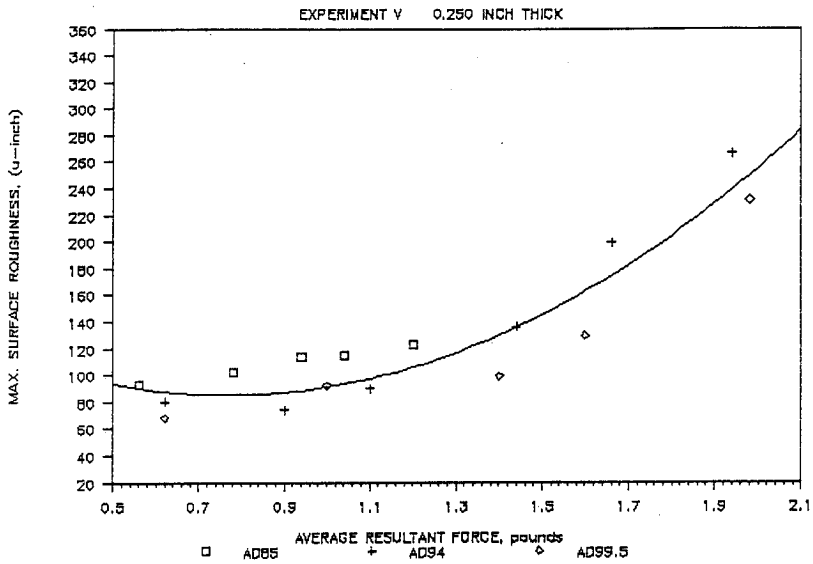

FIG. 7 SURFACE ROUGHNESS VERSUS RESULTANT FORCE (AD 85, AD 94, AD 99.5)

5th American Water Jet Conference
August 29 - 31, 1989: Toronto, Canada

Paper / Communication 17

AN ANALYSIS OF THE MIXING AND CUTTING PERFORMANCE OF ABRASIVE WATER JETS

E. Nadeau, D.J. Burns, G.D. Stubley
University of Waterloo
Department of Mechanical Engineering
Waterloo, Ontario, Canada

ABSTRACT: The study of abrasive waterjet cutting is complex due to the number of parameters that have to be accounted for: water pressure at the orifice, orifice diameter, mixing tube diameter, abrasive flow rate, abrasive material characteristics including size, traverse rate and number of cutting passes, standoff distance and target material properties.
A numerical mixing model has been developed to provide a better understanding of the evolution of the jet prior to cutting. Shallow kerfing experiments have been used to investigate the relationship between cutting performance and abrasive impact velocity and density.
The proposed paper presents the numerical mixing model, results of the aforementioned experiments and reanalyses some of the data previously published by others.

RÉSUMÉ : L'étude de la coupe par jet d'eau est complexe à cause des nombreux paramètres dont il faut tenir compte : pression de l'eau à l'orifice, diamètre de l'orifice, diamètre du tube de mélange, débit d'abrasif, caractéristiques du matériau abrasif dont la taille, la vitesse de traversée et le nombre de passes de coupe, la distance de garde et les propriétés du matériau cible.
Un modèle de mélange numérique a été mis au point pour mieux comprendre l'évolution du jet avant la coupe. Des expériences sur des traits peu profonds ont permis d'étudier la relation entre le rendement en coupe et la vitesse d'impact et la densité de l'abrasif.
La présente communication décrit le modèle de mélange numérique, les résultats des expériences susmentionnées et refait l'analyse de certaines données publiées antérieurement par d'autres auteurs.

Organized and Sponsored by the National Research Council of Canada and the U.S. Water Jet Technology Association.

5th American Water Jet Conference
August 29 - 31, 1989: Toronto, Canada

Paper / Communication 18

THE DYNAMICS OF MULTI-PHASE FLOW IN COLLIMATED JETS

A.L. Miller, R.W. Kugel AND G.A. Savanick
U.S. Department of the Interior, Bureau of Mines
Minneapolis, Minnesota 55417-3099, USA

ABSTRACT: The dynamics and thermal characteristics of a small-diameter, high-speed waterjet expanding into a larger diameter open-ended pipe were studied by the Bureau of Mines. The void created as the jet expands into the larger pipe are filled by vaporization or by entrainment of backflowing air from the pipe exit. The resulting mixture exits the larger pipe as a well dispersed multi-phase fluid. Observation of the vaporization/dispersion phenomena through glass pipes indicated three distinct flow regions: I) jet breakup, II) collimation, and III) backflow. Mass-flow distribution measurements in region II suggest a system of well-dispersed droplets. Pressure and temperature measurements in the first two regions are consistent with vaporization equilibrium values and show little variation. A computer simulation of evaporation rate was used to verify that vaporization equilibrium is reached in a fraction of the residence time of the fluid in the pipe. Surface conductivity measurements indicate the absence of a water film on the inner pipe walls up to region III, where a significant increase in surface conductivity occurs. The boundary between regions II and III is marked by a considerable discontinuity in pressure and temperature. These observations will be used to develop a model to determine flow losses and momentum transfer in the multi-phase flow.

RÉSUMÉ : La dynamique et les caractéristiques thermiques d'un petit jet d'eau à haute vitesse qui se détend dans un tuyau ouvert plus gros ont été étudiées par le Bureau of Mines. Le vide qui s'établit quand le jet grossit dans le tuyau plus grand est rempli par vaporisation ou par entraînement de l'air de retour aspiré par le tuyau. Le mélange résultant sort du tuyau sous la forme d'un fluide multiphasés dispersé. L'observation des phénomènes de vaporisation et de dispersion dans des tuyau de verre a révélé l'existence de trois régions d'écoulement distinctes: I) décomposition du jet, II) collimation et III) écoulement de retour. Des mesures de la distribution des écoulements de masse dans la région II révèlent la présence d'un système de gouttelettes bien dispersées. Les mesures de pression et de température dans les deux premières régions concordent avec les valeurs d'équilibre de vaporisation et fluctuent peu. Une simulation sur ordinateur de la vitesse d'évaporation a permis de vérifier que l'équilibre de vaporisation est atteint dans une fraction du temps de séjour du fluide dans le tuyau. Les mesures de conductivité en surface indiquent qu'il n'y a pas de pellicule d'eau sur les parois intérieures du tuyau jusque dans la région III où la conductivité superficielle augmente sensiblement. La limite entre les régions II et III est marquée par une discontinuité importante de pression et de température. Ces observations serviront à mettre au point un modèle de calcul des pertes d'écoulement et de transfert de quantité de mouvement dans l'écoulement multiphasé.

Organized and Sponsored by the National Research Council of Canada and the U.S. Water Jet Technology Association.

1.0 INTRODUCTION

The Bureau of Mines has patented and licensed for manufacture a new type of hard-rock drill which uses a "collimated" abrasive jet, i.e., a jet which retains cutting power for distances of over 3 m by confining (collimating) the abrasive jet in a pipe. Collimated jets undoubtedly have further applications in mining, but such applications await an improved understanding of the physics involved.

The cutting apparatus consists of a small-diameter (2 mm) coherent water jet entering a 15.9-mm-diameter "collimating" pipe, into which abrasive material is inducted via a port immediately downstream of the jet nozzle (fig. 1). Using only 69 MPa (10,000 psi) water pressure, this configuration has been used to cut hard rock (quartzite with 73,000-psi compressive strength) at distances of over 3 m from the jet nozzle. This is postulated to be a result of efficient momentum transfer between the jet and the abrasive particles, and low flow losses due to the containment of the jet within the pipe. The aim of present research is to characterize the flow of the three-phase abrasive slurry inside the collimating pipe. This paper presents results of a study of the dynamic and thermodynamic behavior of the water jet as it disintegrates into the pipe. Extensive flow visualization studies, using glass collimating pipes, have identified three regions as shown in figure 2. Region I, the breakup region, is where the jet is disintegrating and expanding to fill the collimating pipe. Expansion of the 2-mm jet into the much larger pipe yields the very high void fraction of 0.984. In region II, the dispersed fluid is a "collimated" mixture flowing in the pipe. Region III is the region in which air is backflowing from the pipe exit. In order to understand the vaporization behavior of the water as it flows through these regions, experiments were designed to accurately measure temperature and pressure profiles in the collimating pipe. These profiles were measured in various collimating pipe configurations, and were limited to the flow of water and its own vapor, i.e., without air or abrasive entrainment. In order to verify the degree to which the jet disperses in the pipe, the radial distribution of mass-flow was measured in region II of the flow using a small-diameter probe to collect samples of the collimated fluid at equally spaced intervals across the pipe diameter. Experimental data indicate that the jet disperses significantly throughout the pipe diameter and that conditions of vaporization equilibrium prevail.

2.0 EXPERIMENTAL

2.1 Flow Visualization

A 2-mm nozzle was directed into a 15.9-mm-I.D. glass pipe without air entrainment. The pump pressure to the nozzle was increased gradually from 0 to 10,000 psi and the resulting flow dynamics observed. Liquid dye was injected at various points in the collimating pipe to help identify flow patterns. A He-Ne laser was used to investigate the light transmitting properties of the various flow patterns which occurred in the pipe.

A dual contact conductance probe was incorporated in the pipe wall in order to determine if a liquid film existed at the wall. Two 3-mm aluminum contacts were mounted flush with the wall and spaced approximately 2 mm apart. The current between them was measured with a conductance meter.

2.2 Pressure Measurements

The local static pressure in the glass collimating pipes was measured at ports consisting of 5-mm-I.D. glass nipples attached perpendicularly to the 1.2-m collimating pipes at 10-cm intervals. Vacuum pressure transducers were attached to the glass nipples with vacuum tubing and mounted on a rack parallel to the collimating pipe as shown in figure 3. Shut-off valves were incorporated to prevent damage to the sensitive transducers during pump starting and warmup. The transducers have a range from 0 to 1 atmosphere absolute, and were calibrated before each run using a mercury manometer. Their output was routed via an analog digital conversion board to the interactive software which stored the data in a spreadsheet.

2.3 Temperature Measurements

Temperature data were obtained by insertion of 1.57-mm stainless steel sheathed thermocouples into glass nipples mounted perpendicularly on the outside of the collimating pipe (fig. 3). The thermocouples were the bare-ended type and were centered in the nipple by a cylindrical rubber spacer so as to minimize the influence of heat transfer from the pipe walls. The thermo-couple ends were placed as close to the flow stream as possible. The high velocity of the collimated fluid prevented placement of the thermocouples in the moving stream. The feedwater temperature was monitored at the nozzle entrance for all experiments. This provided

an initial reference temperature for thermodynamic processes in the system. Typical feedwater temperatures ranged from 16 to 20° C.

2.4 Mass-Flow Distribution

The mass flow rate was sampled at various points in the collimated flow of region II. Figure 4 is a schematic of the experimental apparatus. The collection probe was a 1.08-mm-I.D. stainless-steel hypodermic needle, which had been honed to produce a sharp leading edge at the entrance point. The needle was long enough that it allowed placement of the entrance point upstream of the exit disturbances, i.e., into region II. The needle was supported by a streamlined cone of stainless steel which was attached to a piece of 6.3-mm steel tubing. The fluid entering the probe was channeled through the cone and tubing to a collection container. The entire probe assembly was traversed in equal increments across the diameter of the collimating pipe. The mass-flow rate at each point was determined from the mass of fluid collected in a given time interval at that point.

3.0 RESULTS

Flow pattern development was easily observed in a glass collimating pipe. At pump pressures below 4.7 MPa (680 psi), the pipe was full of low-velocity liquid into which the jet diffused its momentum. At approximately 4.7 MPa, the jet momentum was great enough to expel this liquid plug from the collimating pipe, and a new flow pattern resumed. This new flow was characterized by extreme turbulence and it was found by injection of dye at the pipe exit that air was flowing backward along the pipe walls to fill the voids created by the expanding jet. At a pump pressure of 7.25 MPa (1,050 psi), the jet momentum increased to a point where the backflowing air could no longer reach the nozzle. The ensuing flow pattern is that pictured in figure 2. The area of regions I and II becomes evacuated, as no air can rush in to fill the voids created by the expanding jet. As pump pressure is raised, the boundary between regions II and III extends further and further toward the pipe exit. It is within 3 cm of the exit at nozzle pressures of 55.2 MPa (8,000 psi) or greater.

At the normal system operating pressure of 69 MPa (10,000 psi), the conditions of region II prevail in nearly the entire pipe length. This region is, therefore, of particular interest. Pressure measurements in this region indicate a nearly constant pressure of approximately 18 torr (fig. 5), with a sudden discontinuity at the boundary between regions II and III, where the pressure jumps to that of the ambient atmosphere (760 torr). Analysis of the experimental data indicates a slightly positive pressure gradient of .007 - .038 torr/cm in region II and a much larger positive gradient of 15-200 torr/cm in region III.

Temperature measurements in region II indicate a nearly constant temperature within 0.5° C of the feedwater temperature. At the boundary between regions II and III, an abrupt temperature rise is measured, and temperatures in region III were found to be 10 to 13° C warmer than the feedwater (fig. 6). The warmer temperatures may be due to stagnation effects of backflowing air and possible adiabatic compression of the low-pressure vapor with subsequent rapid condensation. The temperatures and pressures measured in region II coincide with vapor pressure equilibrium values calculated for water.

Results of mass-flow distribution measurements appear in figure 7. The graph presents results of two test setups, which were identical except for a slight difference in longitudinal alignment of the jet with the pipe axis. The data show that the mass flow is well distributed across the pipe diameter, although somewhat sensitive to jet-pipe alignment. The horizontal line on the graph represents the theoretical average mass-flow rate expected through the probe at the operating conditions of this experiment, using the ideal assumptions of a) homogeneous fluid continuum, b) constant velocity across the duct, c) 100-pct collection probe efficiency.

Assuming constant mass flow in the system and ignoring inherent corrections required to account for pipe geometry and asymmetrical flow structure, the area under all curves in figure would be equal. Comparing the areas under the two data curves with that under the ideal curve yields overall collection efficiencies of 97 and 113 pct. This suggests that the combined errors due to pipe geometry, asymmetric flow structure, and probe inefficiency are only 3 to 13 pct. This is to say that to a first order approximation, the measurements indicate that the mass is well distributed throughout the pipe cross section.

4.0 DISCUSSION

Experimental results indicate that the coherent jet breaks up and disperses throughout the collimating pipe. The mechanics of this breakup process are not readily discernable, nor has a method been devised for droplet size measurement in this system. Size and distribution of droplets, although difficult to determine, are important in understanding flow dynamics in the

collimating pipe. To this end, jet break-up theory was used to investigate likely breakup scenarios and the expected drop sizes they would produce.

4.1 Mechanical Breakup

The tendency for a jet to disperse into droplets begins with the natural instabilities prevalent in even the most coherent jets. The theory of capillary instability, sometimes called Raleigh breakup, predicts breakup distances that are many times the jet diameter, (Wingquist, S. C., 1986), but fails to address the topic of shear at the jet surface. It is well known that high-velocity jets produce aerodynamic shear at the surface, which results in rapid shedding or peeling of droplets from the surface. The maximum expected size of such droplets has been determined (Weber M. G., 1919). Weber showed that the mechanical breakup of droplets is due to aerodynamic forces overcoming the surface tension forces which hold the droplets together. The ratio of aerodynamic forces to surface tension forces which exist in a given flow field is called the Weber number and is written as:

$$W_e = (U_d - U_g)^2 \rho D/\sigma \qquad \text{Equation (1)}$$

Equation (1) is used to define the critical Weber number, where "D" is the maximum stable droplet size, $(U_d - U_g)$ the velocity difference between droplets and the vapor phase, (ρ) the density of the vapor and (σ) the surface tension of the droplets. This has been determined experimentally for various vapor-droplet environments. Critical Weber numbers typically range between 6 and 14, but have been reported as low as 1.9 for high quality steam-water nozzle flow (Alger, T. W., 1978). In addition, it is noted (Deich, M. E., 1972) that accurate droplet size predictions in a two-phase nozzle could be achieved using a critical Weber number less than 1. This suggests that the breakup process in high-speed turbulent two-phase dispersions may be accounted for by choosing a critical Weber number near unity.

The maximum stable droplet size in the collimated jet is estimated using equation (1) in the region where the jet expands into the collimating pipe. The jet is assumed to break up into droplets due to the aerodynamic forces generated between the jet and the surrounding low pressure vapor. The vapor is assumed to be stagnant in the region surrounding the expanding jet. The jet velocity is assumed to be 360 m/s. The droplet surface tension is assumed to be that of plane surfaces. A value of unity is assumed for critical Weber number as suggested.

Incorporating these assumptions and rewriting equation (1) gives:

$$D = (\sigma)/\rho(U_d - U_g)^2 = 34.5\ \mu m \qquad \text{Equation (2)}$$

This represents a maximum stable droplet size expected due to aerodynamic breakup. Actual drop sizes in the flow would be expected to be in this range or smaller.

4.2 Thermodynamic Breakup

In addition to mechanical breakup there are thermodynamic effects producing atomization in the collimated jet. As the liquid jet exits the nozzle, it encounters a low-pressure environment in the collimating pipe. This low pressure is transmitted through the jet at the speed of sound in water (approximately 1,400 m/s) and within approximately 0.71 μs, practically instantaneously, the pressure is felt at the jet core. When this pressure is below the saturation pressure value corresponding to the local liquid temperature, i.e., when the liquid is superheated with respect to its surroundings, instantaneous pressure-boiling or flashing will begin at nucleation sites in the liquid. The subsequent expansion of numerous vapor bubbles in the jet causes the jet core to disintegrate rapidly as seen in figure 8 which is sketched based on photos found in Fedoseev (Fedoseev, V. A., 1958).

Another thermodynamically motivated breakup mechanism is that referred to as the boiling breakup model (Crowe, C. T. and W. J. Comfort, 1978). The boiling is driven by a temperature gradient between the center of a droplet and the surrounding vapor. If the droplet surface is cooled approximately instantaneously by evaporation, the temperature at the droplet core will lag behind, due to a lower heat transfer rate in the liquid, resulting in internal boiling and subsequent disintegration of the droplet. In the boiling breakup model, droplet disintegration will begin when the saturation pressure corresponding to the droplet core temperature is equal to the ambient pressure plus the pressure due to surface tension of the droplet. This is written as:

$$P_{(T\ core)} = P_{(T\ vapor)} + 4(\sigma)/D \qquad \text{Equation (3)}$$

$$\text{or } D = 4\ (\sigma)/P_{(T\ core)} - P_{(T\ vapor)} \qquad \text{Equation (4)}$$

where: $P_{(T\ core)}$ is the vapor pressure corresponding to the temperature at the core, $P_{(T\ vapor)}$ is the vapor pressure corresponding to the temperature at the surface of the droplet, σ is the surface tension of the droplet, and "D" is the diameter of the droplet. A detailed model based on this approach (Crowe, C. T., 1978) predicts droplet sizes of a few microns. The droplet size expected using this model is dependent on the slope of the vapor pressure versus temperature curve for the temperature range applicable to the experiment. At the temperature range of the collimated jet, this slope is rather shallow, which results in larger droplet sizes than those predicted by Crowe and Comfort. It is, therefore, expected that this type of boiling breakup phenomenon aids only in disintegration of larger droplets, while finer atomization is due to dynamic forces.

4.3 Evaporation Model

A computer model[1] was developed to calculate temperatures, pressures, and evaporation rates in the collimated waterjet. The model assumed water droplets of various uniform sizes were placed in a void space initially at zero pressure and allowed to evaporate so that the water vapor pressure built up to its saturation (equilibrium) value. Evaporation and condensation rates were calculated using kinetic molecular theory, experimental condensation coefficients (Delaney, L. J., R. W. Houston, and L. C. Eagleton, 1964), and the assumption that the rate of evaporation is equal to the rate of condensation which would prevail if the vapor pressure were equal to its saturation value.

Using this model and a void fraction of 0.984 (corresponding to a jet diameter of 2.0 mm and a collimating pipe diameter of 15.9 mm) and starting with water droplets of diameters between 1 and 50 μm at 15° C, relative evaporation rates were calculated as a function of time. The results of these calculations are shown in figure 9. These results clearly indicate that vaporization equilibrium is established rapidly for well-dispersed droplets at these starting conditions. Since, for the reasons presented above, the average droplet diameter in the collimated jet is likely less than 50 μm, vaporization equilibrium should be well established in much less than 200 μs (or well within 6 cm of pipe length for an average flow velocity of 300 m/s). These calculations are consistent with the observation that measured temperatures and pressures in the collimating pipe correspond to equilibrium values.

5.0 SUMMARY

Characterization of the multi-phase flow in the collimating pipe does not lend itself to theoretical treatment by standard methods of fluid mechanics. The high void fraction and the measured mass distribution indicate that the fluid would behave as a gas, yet based on known mass-flow rate, the average density is over 1,000 times that of gaseous water vapor. Standard analyses using momentum and energy conservation principles are complicated by characteristics of the system such as the presence of a positive pressure gradient and the density variation caused by phase change. A model which characterizes the collimated flow must address the unique physics of the system. Experimental results and theoretical analysis have shown that when the pump pressure is above a particular value (7.25 MPa for the collimating pipe tested), the following are true:

1. The jet prevents air from backflowing, and voids in the pipe must be filled by vaporization.
2. The pressure and temperature in region II, which includes most of the pipe, are at values that reflect vaporization equilibrium.
3. The mass of the collimated fluid is found to be well dispersed in the pipe.
4. No continuous film is detected at the wall.
5. The time required for vaporization equilibrium to be established is very fast compared to the residence time of the fluid in the pipe.

These deductions lead to the following preliminary flow characterization. Initially, the coherent jet is influenced externally by aerodynamic forces and internally by thermodynamic disequilibrium, both of which instigate jet instability and droplet formation. Mass-flow distribution experiments indicate that the system of droplets thus formed is well dispersed in the pipe. Pressure and temperature measurements indicate that evaporation fills the voids between droplets and establishes an equilibrium pressure in the pipe. Any variation in this

[1]The Fortran program used a finite element analysis with a time increment of 0.01 microseconds and was run on a Masscomp super-micro computer.

pressure leads to extremely rapid phase change, thereby, maintaining vaporization equilibrium even at high-flow velocities. In a pressure discontinuity near the pipe exit, the pressure rises quickly to that of the ambient atmosphere.

In order to quantify flow characteristics, further research should include development of a model which incorporates the above observations.

It will be important to address the interactions between flow dynamics and phase transition using energy conservation principles. A model which includes this energy balance and allows for an adverse pressure gradient and discontinuity near the exit will lead to determination of overall flow losses and ultimately to estimates of wall shear effects and momentum degradation in the collimating pipe. Such a model will lead to optimization of the collimated abrasive jet drill and possibly to development of other mining tools based on the collimated jet principle.

6.0 REFERENCES

1. Crowe, C. T., and W. J. Comfort: "Atomization Mechanisms in Single-Component, Two-Phase, Nozzle Flows." International Conference on the Liquid Atomization and Spray Systems, Tokyo, 1978, pp. 45-50.

2. Alger, T. W.: "Droplet Phase Characteristics in Liquid-Dominated Steam-Water Nozzle Flow." Technical Report UCRL-52534, Lawrence Livermore Laboratory, Aug. 1978, 233 pp.

3. Deich, M. E., G. V. Tsklauri, V. K. Shanin, and V. S. Danilin: "Investigation of Flows of Wet Steam in Nozzles." High Temperature, Vol. 10, No. 1, Jan-Feb 1972, 102-107 pp.

4. Fedoseev, V. A.: "Colloid Journal (Kolloidnyi Zhurnal)." Vol. 20, No. 4, 1958, pp. 463-466.

6. Winquist, S. C., Corradini, M.L.: "Modeling the Atomization of a Liquid Jet and Application of the Model to Large Diameter, Molten Corium Jets." M.S. Thesis, University of Wisconsin-Madison, Mech. Eng. Dept., Madison, WI, 1986, 122 pp.

7. Delaney, L. J., R. W. Houston, and L. C. Eagleton: "The Rate of Vaporization of Water and Ice." Chemical Engineering Science, No. 19, 1964, pp. 105-114.

8. Savanick, G. A., and W. G. Krawza: "An Abrasive Water Jet Rock Drill." In: Proceedings of Fourth U.S. Water Jet Technology Conference, Univ. of California, Berkeley, CA, Aug. 26-28, 1987, pp. 129-132.

9. Wallis, G. B.: "One-Dimensional Two-Phase Flow." McGraw-Hill, Inc., 1969, 408 pp.

10. Weber, M. G.: "Jahrbuch der Schiffbautechnischen Gesellschaft." Berlin 1919, pp. 355-477.

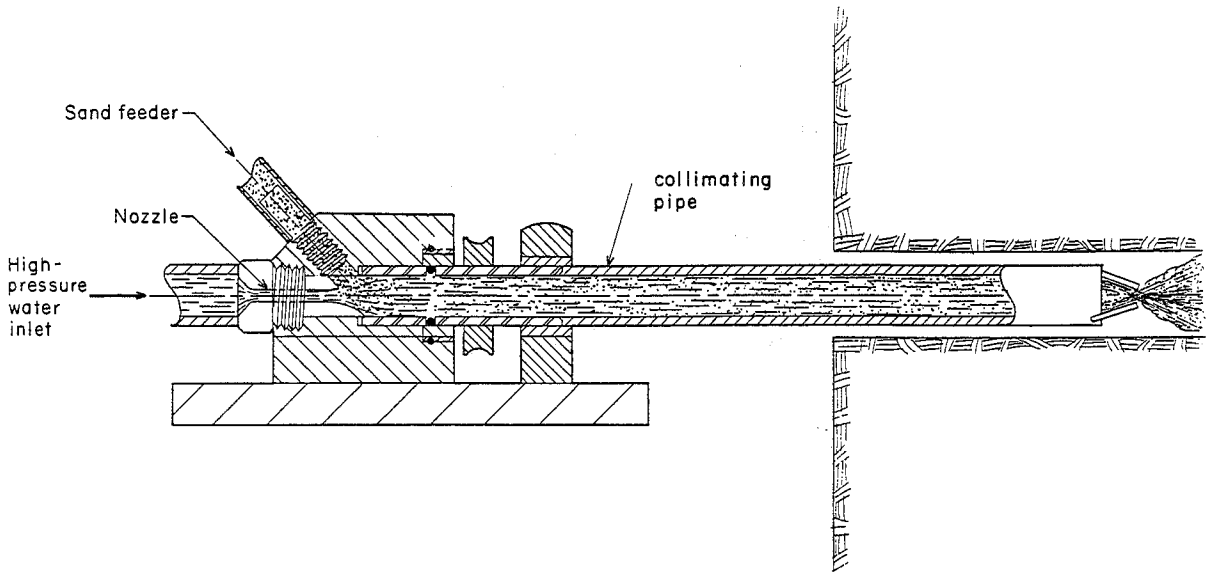

FIG. 1 SCHEMATIC OF PROTOTYPE COLLIMATED ABRASIVE JET

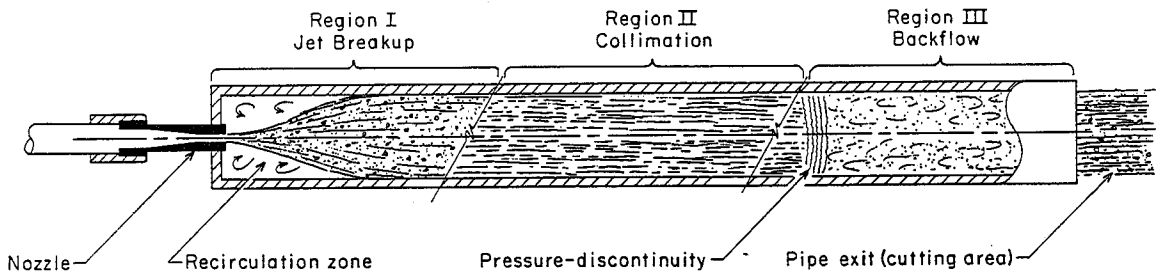

FIG. 2 DIAGRAM OF THREE REGIONS IN COLLIMATED FLOW

FIG. 3 PHOTOGRAPH OF INSTRUMENTATION INSTALLATIONS FOR PRESSURE (LEFT) AND TEMPERATURE MEASUREMENT

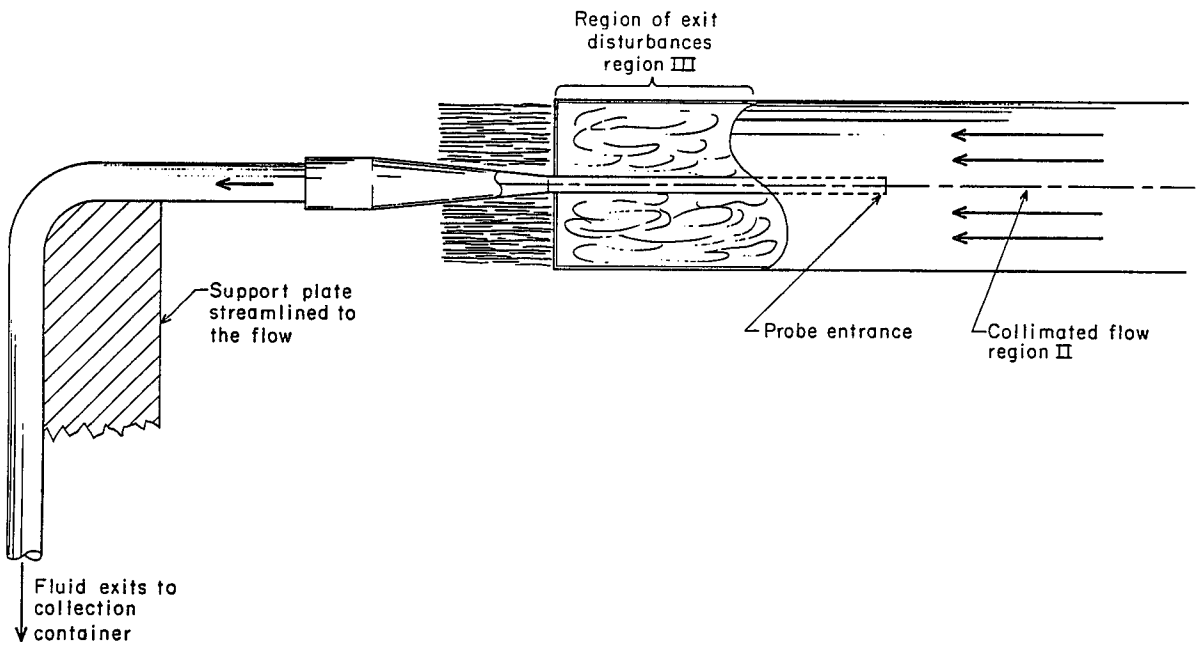

FIG. 4 SCHEMATIC OF MASS COLLECTION PROBE

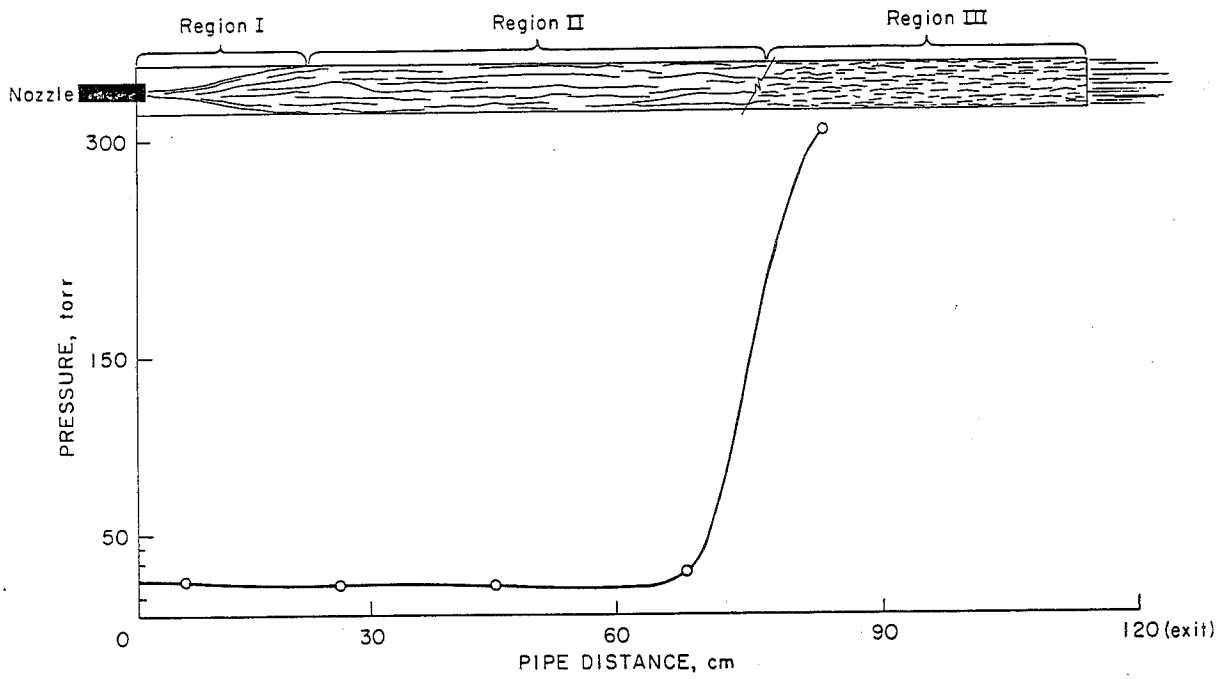

FIG. 5 AXIAL PRESSURE PROFILE IN COLLIMATING PIPE

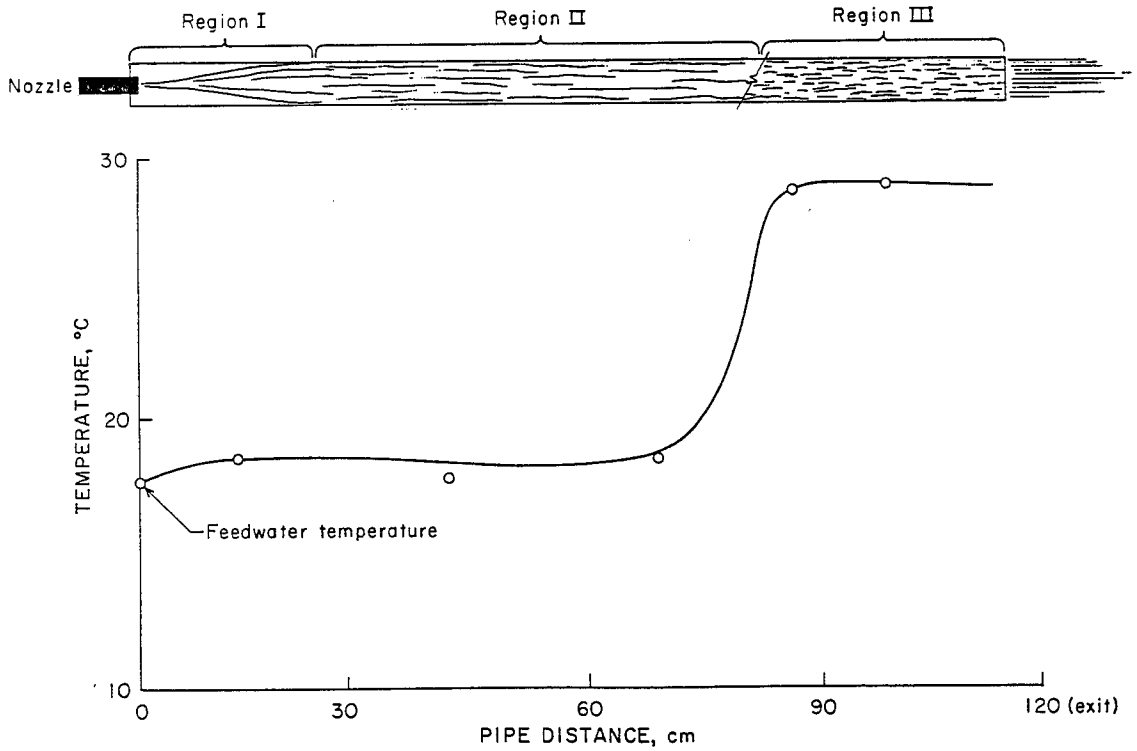

FIG 6 AXIAL TEMPERATURE PROFILE IN COLLIMATING PIPE

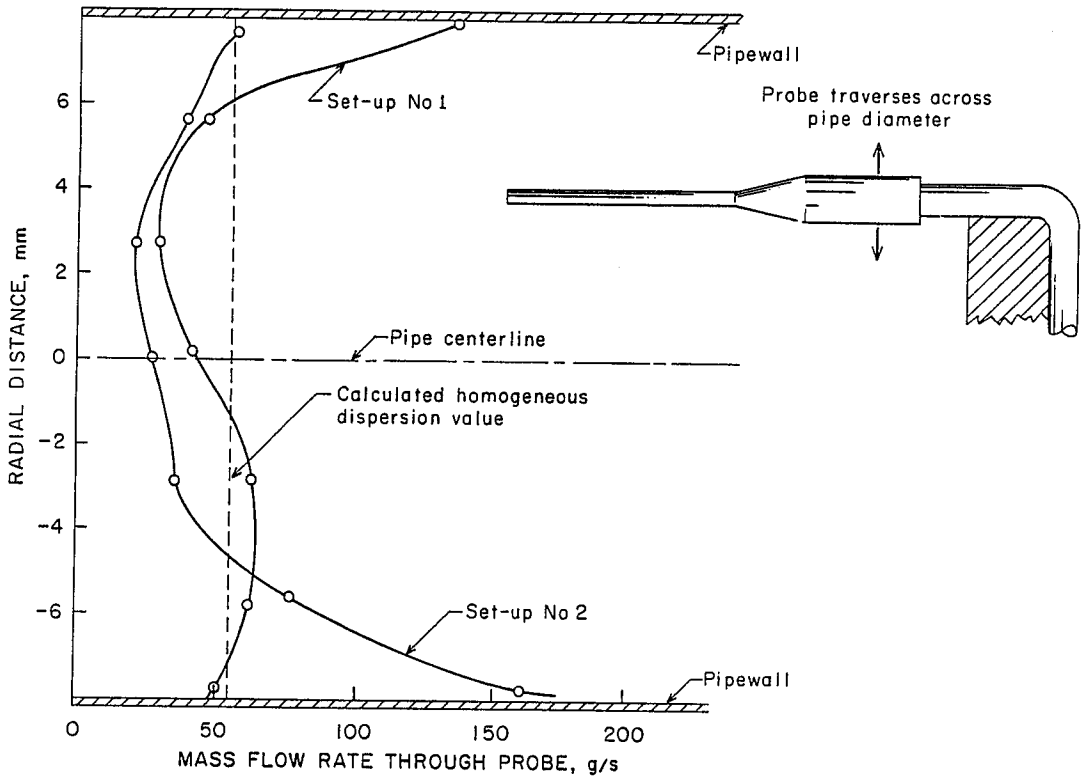

FIG. 7 RADIAL DISTRIBUTION OF MASS IN COLLIMATING PIPE

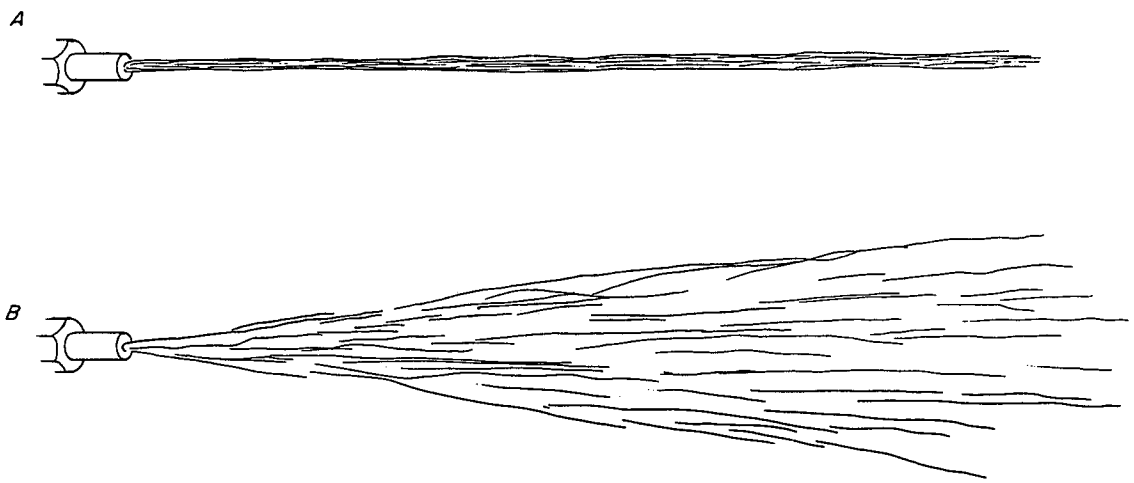

FIG. 8 JET BREAKUP DUE TO SUPERHEAT
A) NONSUPERHEATED JET; B) SUPERHEATED JET

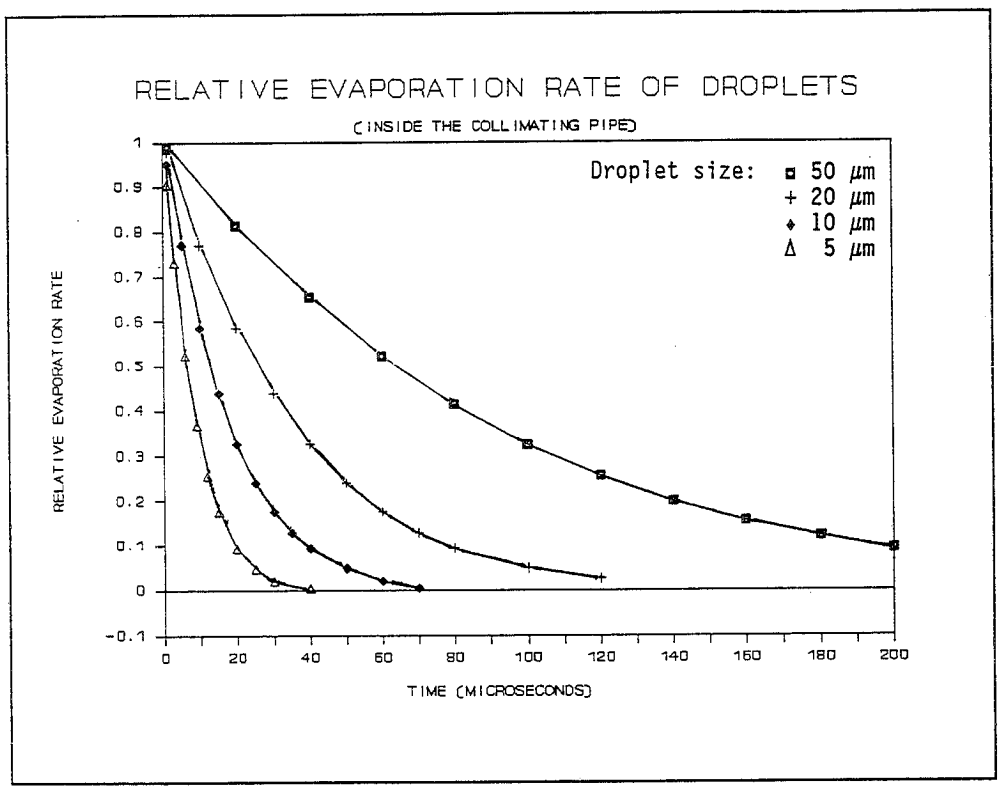

FIG. 9 TIME REQUIRED FOR VAPORIZATION EQUILIBRIUM

5th American Water Jet Conference
August 29 - 31, 1989: Toronto, Canada

Paper / Communication 19

ABRASIVE JET MACHINING OF CERAMIC PRODUCTS

B. Freist, H. Haferkamp, A. Laurinat AND H. Louis
Institute of Materials Science
University of Hannover
Hannover, FRG

ABSTRACT: This paper reports about modified application of abrasive water jets for three-dimensional machining of ceramics. The concept for a complete manufacturing method is introduced. Basic idea of this concept is to break up the workpiece geometry into several single steps of machining by abrasive kerfing. For this aim kerf geometry has to be described by mathematical functions and influences of process parameters and material parameters on the accuracy of matching as well as on the surface properties have to be investigated. Results concerning the first steps of this concept are shown in the paper.

RÉSUMÉ : Cette communication traite d'une variante de l'application des jets d'eau abrasifs à l'usinage tridimensionnel des céramiques. Le principe d'une méthode complète de fabrication est présenté. Ce principe consiste à ramener la géométrie de l'éprouvette à plusieurs étapes d'usinage simples en réalisant des traits à l'aide d'un abrasif. A cette fin, la géométrie des traits doit être décrite par des fonctions mathématiques, et les effets des paramètres de processus et des paramètres des matériaux sur la précision de la correspondance ainsi que sur les propriétés de surface doivent être examinés. Les résultats des premières étapes sont présentés dans la communication.

Organized and Sponsored by the National Research Council of Canada and the U.S. Water Jet Technology Association.

1. Introduction

Today the abrasive water jet technique is normally used for cutting applications in the case of machining steel, concrete and reinforced plastics. In addition a field of useful and efficient application is the machining of materials when it is problematic to do this by other methods. Regarding this fact the field of materials of interest was extended also to ceramics. Although the production of ceramic products is mainly done by near net shaping methods an industrial demand for machining methods for ceramics is rising up. Reasons for the necessity to machine ceramics are:

- Complex shaped workpieces with partial thin walls or webs that cannot be manufactured by common methods like hot isostatical pressing to generate a homogenous structure and high strength. In this case the production of a block with the desired properties and the subsequent machining is a sufficient way.
- Workpiece geometry itself is to complex to be produced by casting or forging e.g.
- Shrinkage during cooling of hot pressed workpieces is too high. That requires a machining procedure to reach accuracy and surface quality.

Amongst common techniques like grinding and sawing with diamond tools, ultrasonic treatments, spark erosion or laser treatment /1-4/ also the abrasive water jet can be used in this case /5-6/. This paper contents informations about the first work carried out in the frame of the development of a manufacturing method for three-dimensional machining of ceramics. Three-dimensional machining in this context includes cutting, turning and milling and for the manufacturing of special workpiece geometries a combination of these treatments. In case of milling the aim of this project is to devide the desired workpiece geometry into several single machining steps based on the results of single and multiple pass kerfing tests.

2. Concept for the development of a manufacturing method

The concept for this new manufacturing method mainly consists of the analysis of the desired workpiece geometry and the mathematical breakup into several single steps of machining that can be produced by abrasive water jets. Each of these single steps should produce a smooth kerf. Machining sharp edged kerfs is expected to be insufficent because in this case the interaction between neighbouring kerfs during machining will lead to jet deflection which may cause secondary kerfing at the opposite flank. The desired shape of the workpiece should be worked out of a massive material running this sequence of single passes. For this aim the analysis of the kerf geometry generated under various conditions and its mathematical description is of great importance and the basis of the manufacturing method. The whole working package for the generation of his manufacturing method is devided into three parts as follows:

A. Basic studies based on single pass kerfing tests

Suitable description functions for kerf geometry have to be determined as well as the influence of process parameters on the accuracy of the selected description functions. Another point is the determination of error levels for description of surface geometry which is important looking to part B. Border zone properties (e.g. roughness) have to be determined to make a forecast for quality of machined parts. Preliminary studies have also to face the interaction between single pass kerfs in case of machining deep kerfs or wide grooves respectively.

B. Modelling of the machining process

This part concerns about the prediction of workpiece geometry based on single pass data in case of multiple pass and parallel kerfing as well as multiple-directional kerfing. Beside this also the prediction of workpiece roughness and waviness is of interest. For this aim suitable modells have to be set up and verified.

C. Generation of a machine and self-adaptive control system

Based on data for material and abrasive treatment parameters, special geometry parameters and surface properties as a function of abrasive treatment resulting from part A and B a machine control system has to be generated. To improve the performance of the manufacturing method a self-adaptive control system has to be set up. This concerns the registration of the actual size and shape of the workpiece during machining while the next machining step runs to minimize the error level concerning the desired shape. This point includes the development of sensor systems as well as special software.

This paper reports on the results concerning the beginning of this working package.

2. Test facilities

In principle any abrasive cutting system can be used to carry out single and multiple-pass kerfing tests. Therefor it is planed to do these tests as well with a premixed abrasive jet as with a conventional injector system. With the last mentioned system the first test were carried out. A cutting head with 0.25 mm diameter of water jet nozzle, 1.2 mm diameter and 50 mm length of focussing nozzle was used /7/. Pressure was generated by an intensifier up to 4000 bars at a flow rate up to 4 l/min. Specimen were made of dry pressed and sintered alumina with a purity of 99.7% and a density of 97% of theoretical density. Abrasive media used was garnet sand (diameter: 0.25 - 0.60 mm). The geometry of the kerfs and the topography of the ground of the kerfs was determined by a pick-up system with a flat datum. Because of the expected depth of the kerfs a special stylus beam was build. With this equipment kerfs of a depth up to 2 mm were measurable.
Measurements were done unfiltered to get the geometry of the kerfs and filtered in case of the determination of the surface roughness.
All tests were carried out in air to get a continuous transition between the uneffected surface of the specimen and the kerf. Certainly kerfing can be done also under water, however, in this case sharper bounded kerfs are produced /8/. This fact complicates the description of the kerfs by simple functions. Impingement angle was always 90 deg. as was found to be optimal for maximal volume removel rate in case of erosion of alumina /9/.

3. Single pass kerfing tests

Tests were carried out in a range of parameters as:

pressure:	1000 to 3000	bars
abrasive feed rate:	1 to 10	g/s
traverse rate:	50 to 200	mm/min
working distance:	20 to 100	mm

To minimize the number of specimen a standard condition was used as follows:

pressure:	1000 bars
abrasive flow rate:	4 g/s
traverse rate:	100 mm/min
working distance:	80 mm

To get an idea about the influence of process parameters for example on kerf geometry or surface roughness based on this standard only one parameter was changed.

The geometry of the kerfs generated by the abrasive jet cutting technique is mainly influenced by parameters of the process like pressure, working distance or the geometry of the focussing nozzle. Fig. 1 gives an example for the range of different kerf-geometries when changing the working dis-

tance. A small working distance leads to sharp edged kerfs with smooth surface of the flanks. Increasing working distance leads to decreasing depth and increasing width of kerf while the surface becomes more and more rough and irregular. Increasing working distance causes first an increasing of volume removal rate. If a certain working distance is exceeded the volume removal rate decreases again. Using standard conditions this optimal working distance was in the range of 60 to 80 mm.
Different kerfing conditions lead to different rates of volume removal. Fig. 2 shows the influence of some parameters on the volume removal rate which is increased when increasing the parameters 'pressure', 'abrasive feed rate' and 'traverse rate'.
Increasing the pressure while other parameters are unchanged causes increasing water jet velocity and accordingly a increasing abrasive particle velocity. This leads to a higher impact energy of each particle and as one result to an increasing rate of particle volume to material removal volume.
Increasing abrasive feed rate leads to an increasing number of impacts and due to this fact to an increasing volume removal rate as an integral effect. Dramatically increasing the abrasive feed rate will lead to an increasing plugging of the kerf with abrasive particles so that it is expected that an optimal volume removal rate will occure at a certain value of abrasive feed rate.
Increasing traverse rate also increases volume removal rate because the interaction between abrasive particles during machining that means the number and violence of collisions is decreased. This will cause an increase of the ratio of abrasive particle volume to material removal volume. It is expected that in case of further increasing of the traverse rate a steady state level of volume removal rate will be reached.

In contrast to the application of the abrasive technique in case of cutting - normally very small and deep kerfs are created -in case of the manufacturing method we want to build up the kerfs have to be more flat. That means that the ratio of width of kerf to depth of kerf is changed to higher values. Due to this fact the kerf geometry is quite sensitive to irregularities of the structure of the abrasive jet. These irregularities will cause variations between the expected and the machined kerf geometry. This point is of great importance because errors during single-pass kerfing will be added up in case of multiple-pass kerfing when machining complicated geometries. As a consequence one has to ensure that the abrasive head is well adjusted. In particular the water jet has to flow in the center of the focussing nozzle. Deviations from this requirement will lead to non symmetrical kerfs as shown in fig. 3. In this case the focussing nozzle was not adjusted exactely but so that the pure water jet touched the edge of the inner diameter of the focussing nozzle at its outlet. This can be seen as the poorest condition of adjusting.

Another fact has to be regarded in this context, that means the wear of the focussing nozzle during operation. In opposite to cutting applications where the wear of the focus leads to a slightly increase of width of the slot and to a decrease of depth of slot as well as cutting efficiency in case of kerfing the influence of the wear of the focus on the geometry of the kerf is distinct. Fig. 4 gives an idea of this phenomena.
For the description of the kerfs by regression it has to be ensured that the more or less accidentally choosen profile is representative for the geometry of the kerf. Under normal conditions the place where the profile for regression is taken from is indifferent (see fig. 5) although there is a scattering which depends on materials properties and on mechanism of material removal as well as on process parameters. In this context "normal conditions" means that the surface topography of the kerf is quite smooth. The eight single profiles of fig. 5 were taken from one specimen with a misalignment of 1 mm. It can be seen that all profiles show a good confirmity.

4. Mathematically description of the kerf geometry

Describing the kerf geometry generated under various conditions is one important column in the frame of the envisaged working station. The kerf geometry is characterized through a local minimum (deepest point of the kerf), two inflection points and two local maximums. Types of functions that are applicable in principle for that geometry are for example polynomial of grade 4 at least, sine

or cosine respectively or a bell-shape distribution. From our point of view cosine-functions are qualified for this approach very well because they have some immanent advantages compared to other types of functions as there are for example:

- matching is easy to realize by variation of the wavelength and of the amplitude
- superposition of single-kerf can be done using addition theoremes

Exemplary fig. 6 shows the good confirmity between measured profile and a cosine-function like:

$$y(x) = c * (\cos x - 1)$$

Parameter c was determined by the method of least squares using a commercial software package for matrix-calculations. This very simple function seems to be sufficient for the description of the geometry of the kerfs generated by abrasive water jets. Variable x runs from 0 to 2π. A multiple-parametric cosine-function like:

$$y(x) = c * \Sigma (\cos x - 1)$$

was expected to give a better matching compared to an one-parametric one. Fig. 7 indicates that in this case the grade of matching decreases when 2 to 4-parametric cosine-functions are used mainly because the depth of the kerf is not represented by the functions in a sufficient way. This is of great importance because the depth of the machined kerf is not permitted to exceed the depth of the mathematically predicted depth using a cosine function.
In case of an one parametric cosine function parameter c represents the half value of the depth of kerf. So for the prediction of kerf geometry a function like

$$y(x) = 0.5\, d_k\, (\cos x - 1)$$

should be used. Variable x - as mentioned running from 0 to 2π - represents the width of kerf. Therefore the width of kerf has to be equated 2π. Table 1 shows the results for depth and width of kerf depending on the combination of parameters.

The quality of description of the kerfs depends on a lot of process and material parameters. First results show that the quality of description increases with increasing the ratio of width to depth of the kerf and with decreasing surface roughness. Fig. 8 shows the best and the worst results found during the tests. The root-mean-square deviation was 1.9 % and 10 % respectively.
Because ceramics are very brittle materials surface properties for example roughness as a result of the machining process has a great influence on workpiece strength. Therefore it is of interest how surface roughness is influenced by the main process parameters as e.g. pressure, abrasive feed rate and traverse rate. Fig. 9 indicates that surface roughness increases when increasing pressure while the abrasive feed rate seems to has no significant influence on surface roughness. Variations in traverse rate lead to a lower value of surface roughness when increasing the traverse rate. Each value represents the average of four measurements taken from the ground of the kerfs with a scattering of $\pm$ 15% maximal.
Chronological development of roughness is given in fig. 10 in case of multiple pass kerfing. As can be seen roughness is increasing during the first passes before reaching a steady level because damage of material by solid impact is a time dependent phenomena.
These presented results only shall give an idea of the dependence of process parameters on surface roughness and should not be seen as absolute values. Comparing the values of roughness that are generated under similar conditions one can see that there is a range of scattering up to 20% although all tests were carried out very carefully and specimen were produced under similar conditions. This scattering indicates that there is a influence of deviations of materials properties on surface roughness.
Some additional tests were carried out to lower the roughness of machined surfaces by a subsequent treatment using high speed water jets without abrasives. This way was choosen not to change workpiece geometry essentially. First a kerf was machined using standard conditions. The subsequent

treatment was done with 1000 bar, 200 mm/min and 80 mm working distance. The results show that there is no significant improvement when running one or two passes under these conditions. Even the increasing of the pressure up to 3000 bar leads to no significant change of roughness. So an improvement only can be expected using an optimized sequence of operations and perhaps a smoother abrasive for finishing.
Finally fig. 11 shows some SEM-photographs taken from the unaffected surface as well as from the flank and the bottom of the kerf created under standard conditions. The unaffected surface (fig. 11a) shows some micro flaws as intercristalline cracks and pores. Fig. 11b was taken from the transition between unaffected surface and kerf showing some first pits. Fig. 11c was taken from the flank of the kerf while fig. 11d was taken from the bottom of the kerf. Both fig 11c and 11d are showing no significant differences indicating that surface topography is mainly influenced by material properties and of course by process parameters and not by the different intensity of the jet at its periphery. Fig. 11e was taken from a specimen from the bottom of the kerf that was treated by 3000 bars while other parametres were standard conditions. Compared to fig. 11d the surface shows some more severe cavtities which cause the increase of center line average shown in fig. 9.

5. Conclusions and Outlook

A new concept for manufacturing ceramics was introduced based on the idea to devide the desired workpiece geometry into several single steps of machining that can be done by abrasive water jets. Basis for this approach is the description of kerf geometry produced by abrasive water jets by mathematical functions. It was found that simple cosine functions are suitable to describe kerf geometry in a sufficient way.
Following the concept now it is necessary to demonstrate the possibility to predict the workpiece geometry as a result of single steps of machining by mathematical methods.
Due to the sensibility of strength of ceramic products on surface roughness further work has to find also a solution for improvements regarding this fact. In case there is no possibility to lower surface roughness nevertheless a combination of near net machining by abrasive water jets and surface finishing by ultra sonic treatment e.g. could improve performance of machining of ceramics at all. Especially the volume removal rate will be increased and so the total machining time can be lowered.

6. References

/1/ Haas, R.:
"Ultraschall-Erosion - Verfahren zur dreidimensionalen Bearbeitung keramischer Werkstoffe"
Sprechsaal, Vol. 121, No. 12, 1988, p. 1166-1172

/2/ Chryssolouris, G. and J. Bredt:
"Machining of ceramics using a laser lathe"
Interceram, No. 2, 1988, p. 43-45

/3/ Spur, G. et al.:
"Überblick über trennende Fertigungsverfahren zur Hartbearbeitung von Keramiken"
Sprechsaal, Vol. 120, No. 6, 1987, p. 516-520 and Sprechsaal, Vol. 120, No. 11, 1987, p. 1021-1025

/4/ Moreland, M.A. and D.O. Moore:
"Versatile performance of ultrasonical machining"
Ceramic Bulletin, Vol. 67, No. 6, 1988, p. 1045-1047

/5/ Hashish, M.:
"Milling with abrasive-waterjets: a preliminary investigation"
Proc. 4th U.S. Water Jet Conference, The american society of mechanical engineers, New York, 1987, p. 1-10

/6/ Hashish, M.:
"Turning, Milling and drilling with abrasive-waterjets"
Proc. 9th Int. Symp. on Jet Cutting Technology, BHRA, Cranfield, 1988, p. 113-131

/7/ Haferkamp, H.; Louis, H. and G. Meier:
"Cutting of contaminated material by abrasive water jets under the protection of a water shield"
Proc. 9th Int. Symp. on Jet Cutting Technology, BHRA, Cranfield, 1988, p. 271-287

/8/ Blickwedel, H.; Decker, B.; Haferkamp, H. and H. Louis:
"Submerged cutting with abrasive water jets"
Proc. 8th Int. Symp. on Jet Cutting Technology, BHRA, Cranfield, 1986, p. 265-275

/9/ Mehrotra, P.K. and H. Conrad:
"Multiparticle erosion of pyrex glass"
in: "Erosion: Prevention and useful applications"
STP 664, 1977, p. 77-100, ASTM, Philadelphia

Parameter	Width of kerf in mm	Depth of kerf in mm
1000 bars	11.44	0.422
2000 bars	11.36	0.960
3000 bars	11.31	1.804
1 g/s	11.20	0.134
2 g/s	10.98	0.230
4 g/s	11.44	0.422
6 g/s	11.52	0.440
8 g/s	12.29	0.500
10 g/s	13.44	0.538
50 mm/min	11.05	0.844
100 mm/min	11.44	0.422
200 mm/min	11.18	0.268
20 mm	4.00	0.922
40 mm	6.88	0.600
60 mm	9.92	0.582
80 mm	11.44	0.422
100 mm	15.04	0.314

Parameters other than listed are:
pressure: 1000 bars
abrasive feed rate: 4 g/s
traverse rate: 100 mm/min
working distance: 80 mm

Table 1: Influence of process parameters on depth and width of kerf

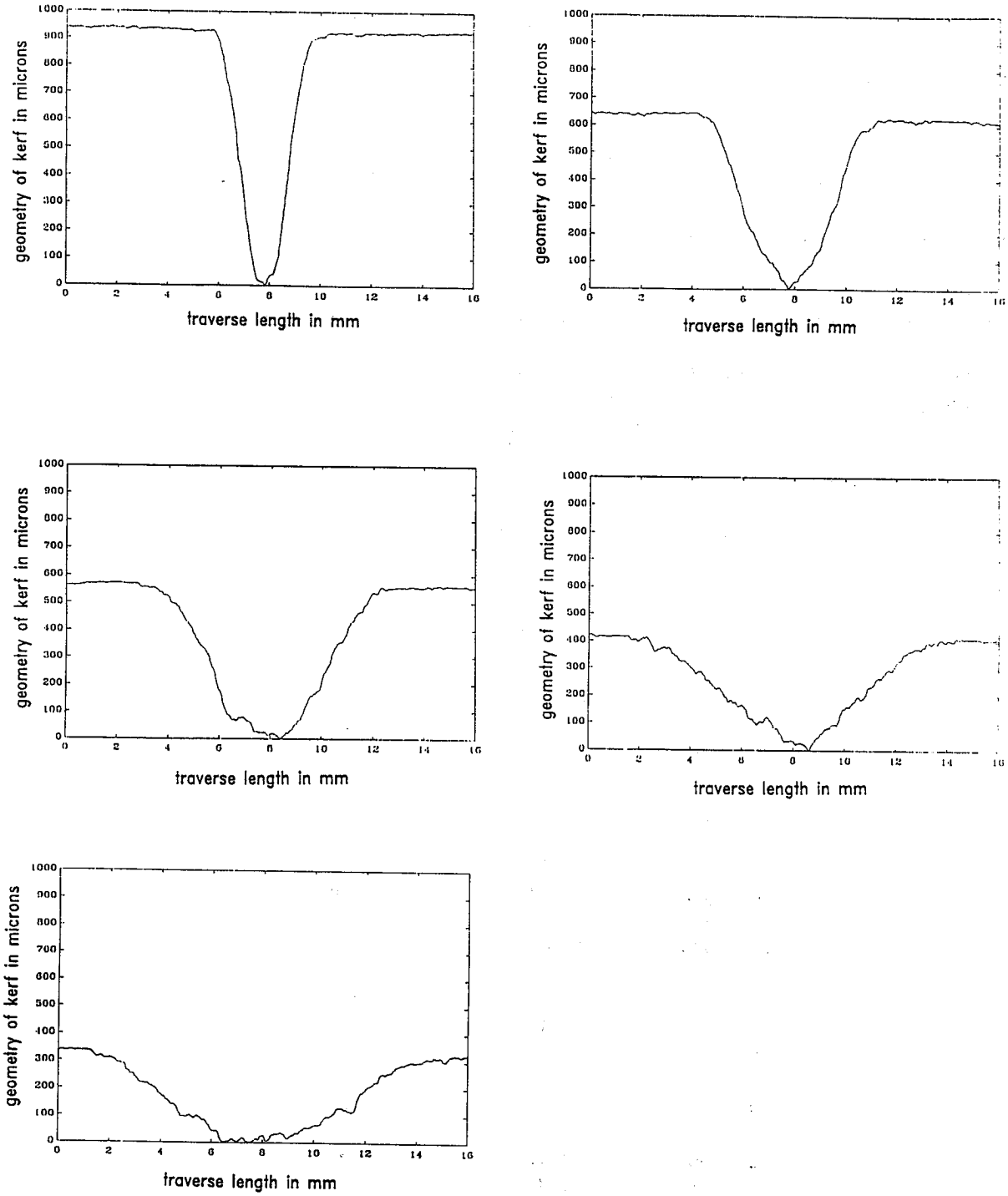

Fig. 1: Influence of working distance on kerf geometry
working distance from top: 20, 40, 60, 80, 100 mm
parameters: standard condition

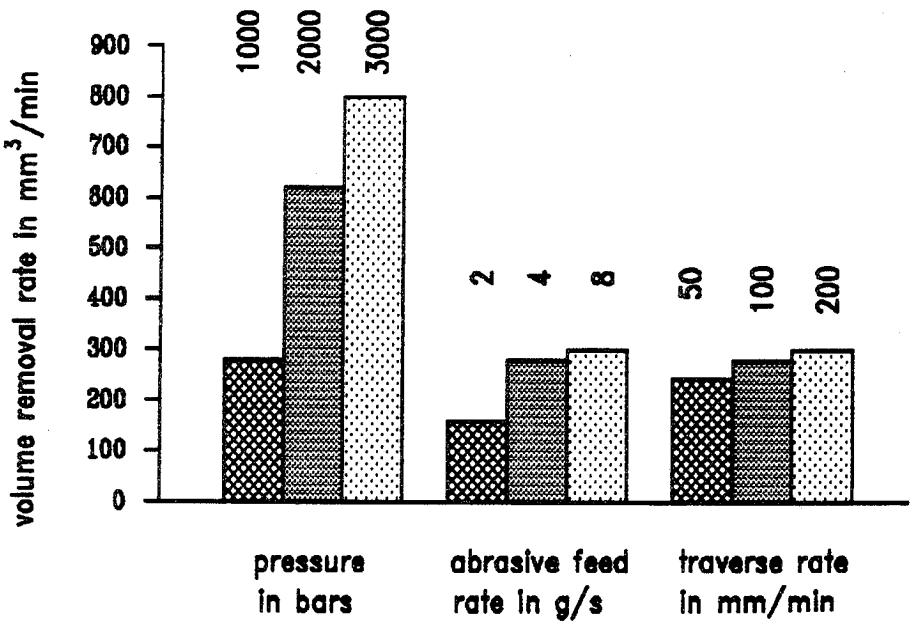

Fig. 2: Influence of pressure, abrasive feed rate and traverse rate on volume removal rate
parameters other than listed: standard condition

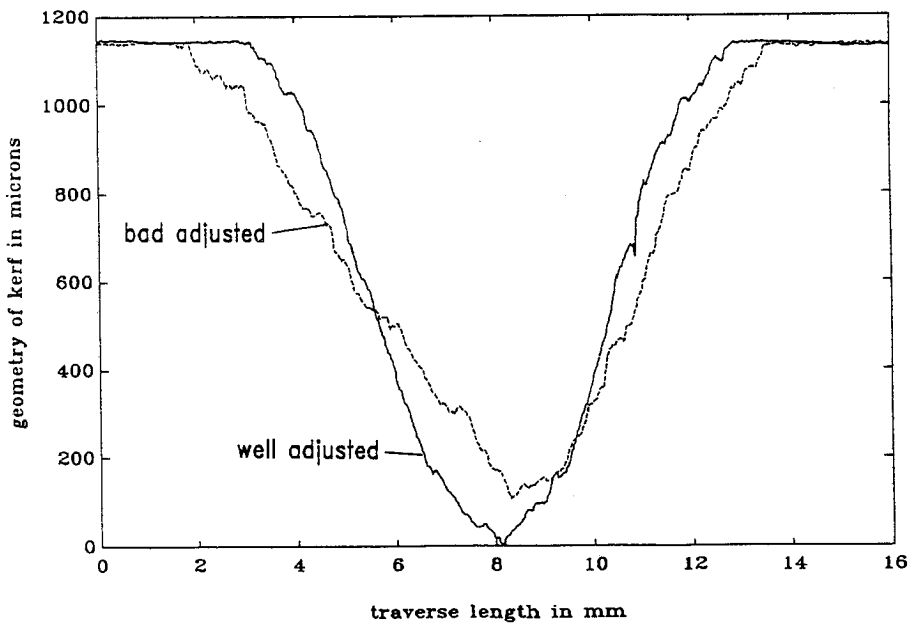

Fig. 3: Effect of adjusting of the focussing nozzle on kerf geometry
parameters: standard condition

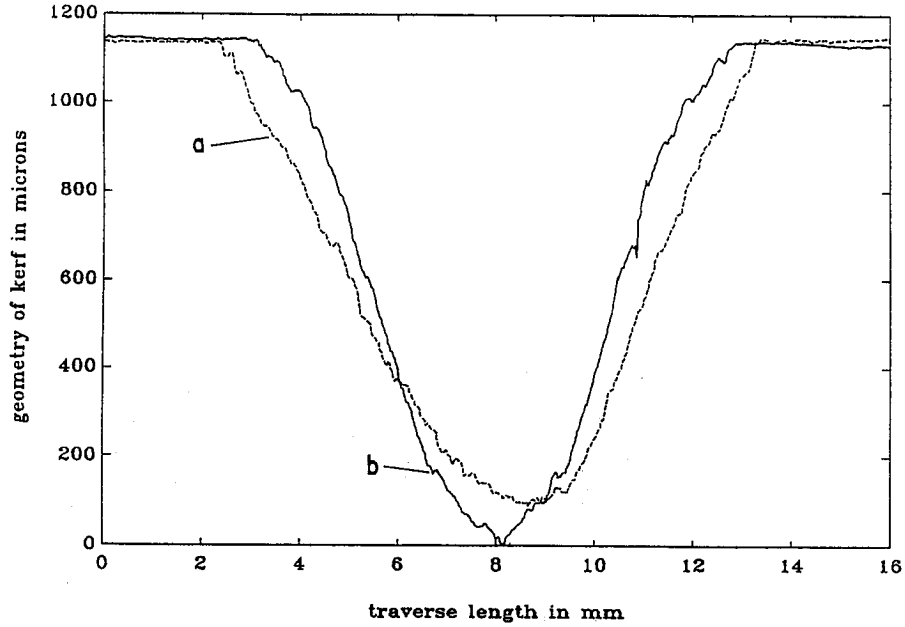

Fig. 4: Influence of focussing nozzle wear on kerf geometry
a: focussing nozzle used about 3 h
b: new focussing nozzle
parameters: standard condition

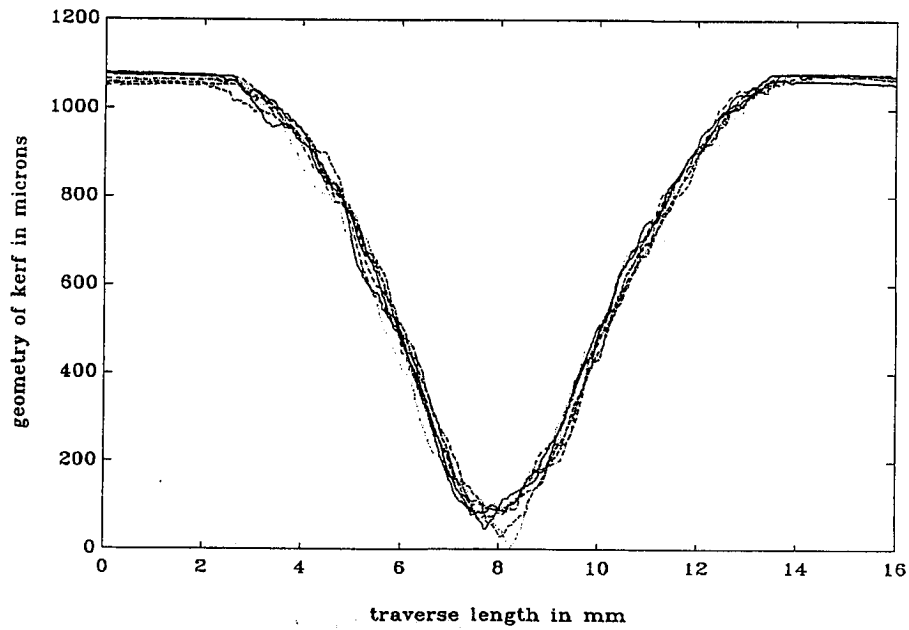

Fig. 5: Scattering of 8 profiles taken from one specimen with a misalignment of 1 mm
parameters: standard condition

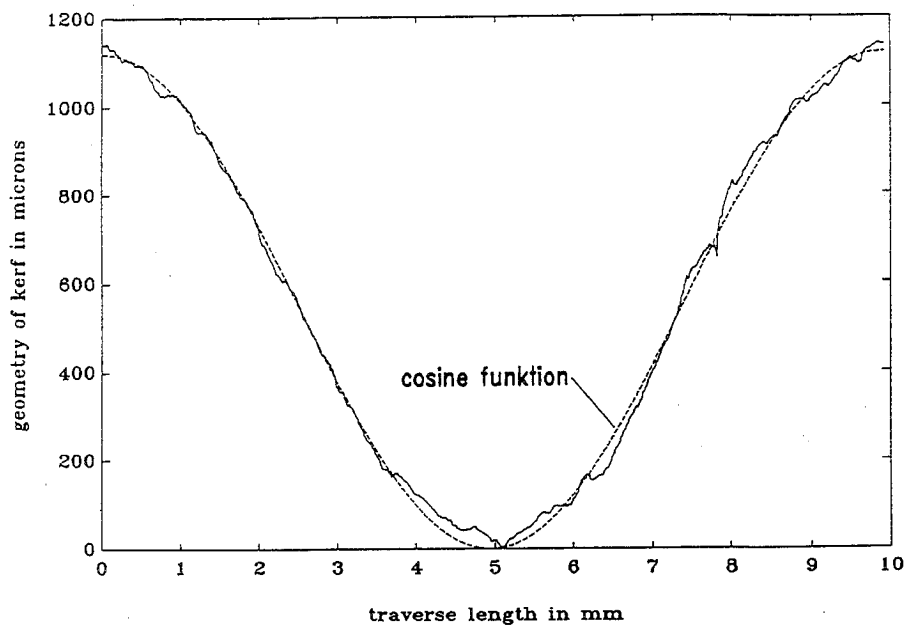

Fig. 6: Matching of profile by cosine function
parameters: standard condition

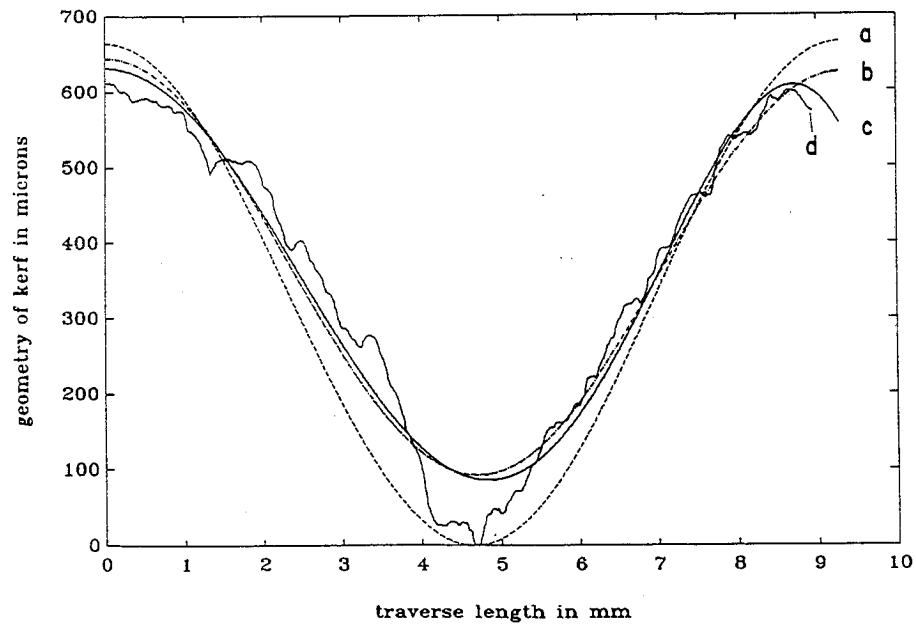

Fig. 7: Comparison between 1-, 2-, 3- and 4-parametric cosine function for matching a profile
a: 1-parametric, b: 2- and 3-parametric, c: 4-parametric
d: measured profile
parameters: pressure: 3000 bar, abrasive: glass pearls,
parameters other than listed: standard condition

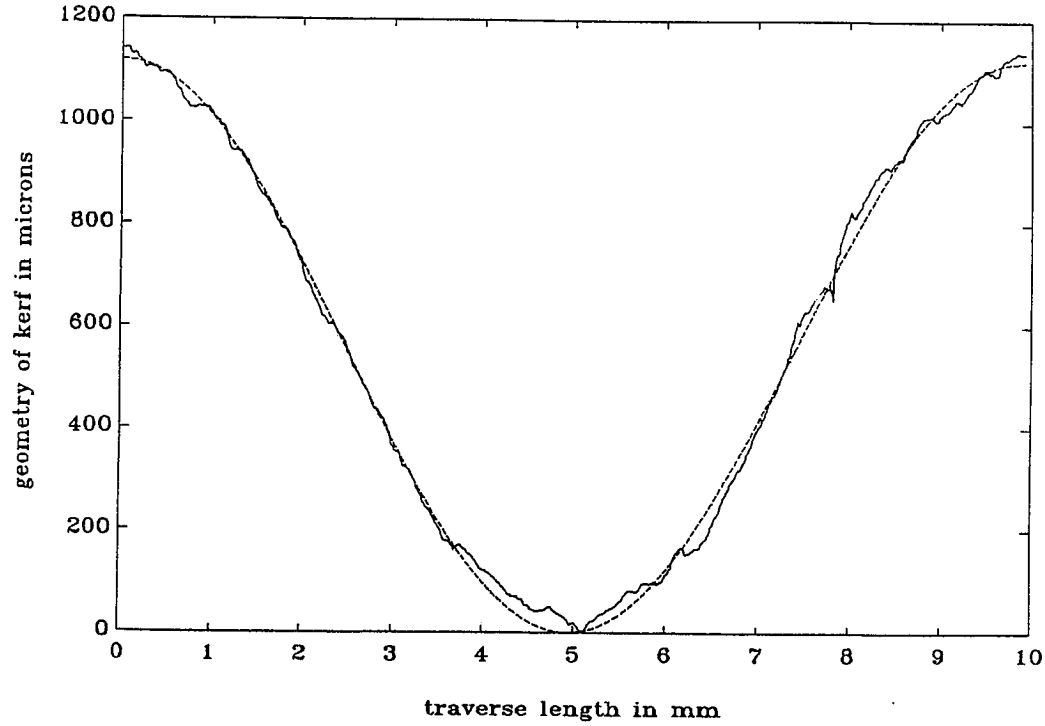

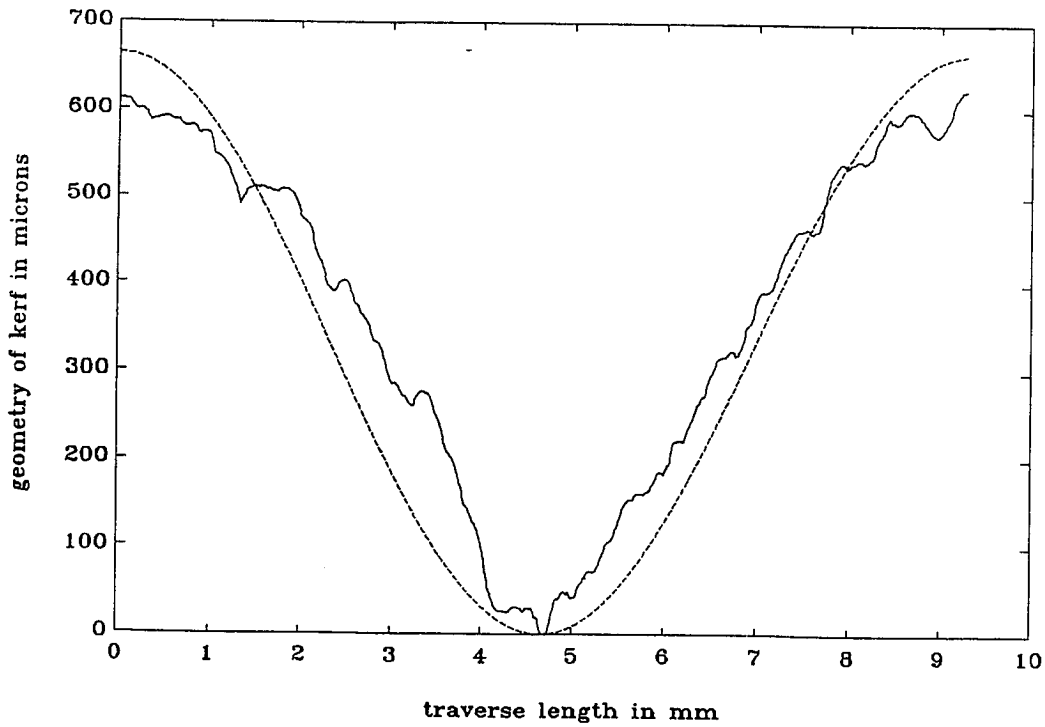

Fig. 8: Influence of surface smoothness on grade of matching
mean-square-deviation: top: 2% bottom: 10%
parameters: top: standard condition
bottom: see fig. 7

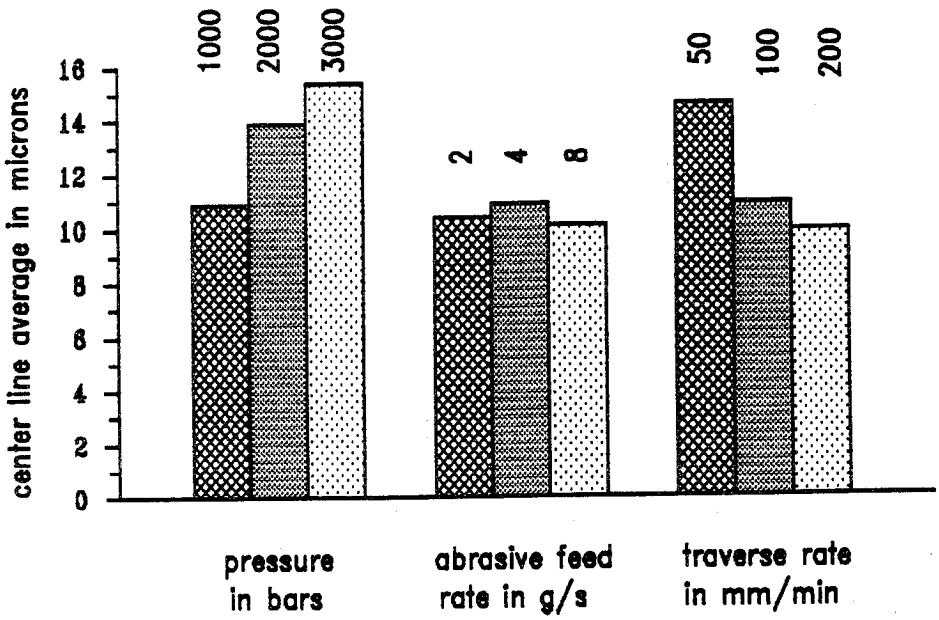

Fig. 9: Influence of pressure, abrasive feed rate and traverse rate on surface roughness
parameters other than listed: standard conditions

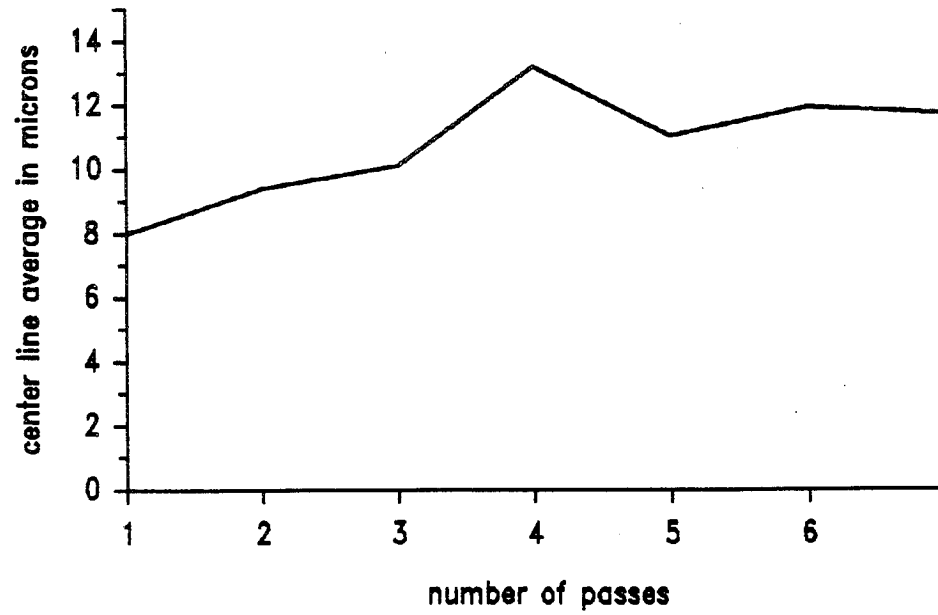

Fig. 10: Influence of number of passes on surface roughness
traverse rate: 200 mm/min
other parameters: standard conditions

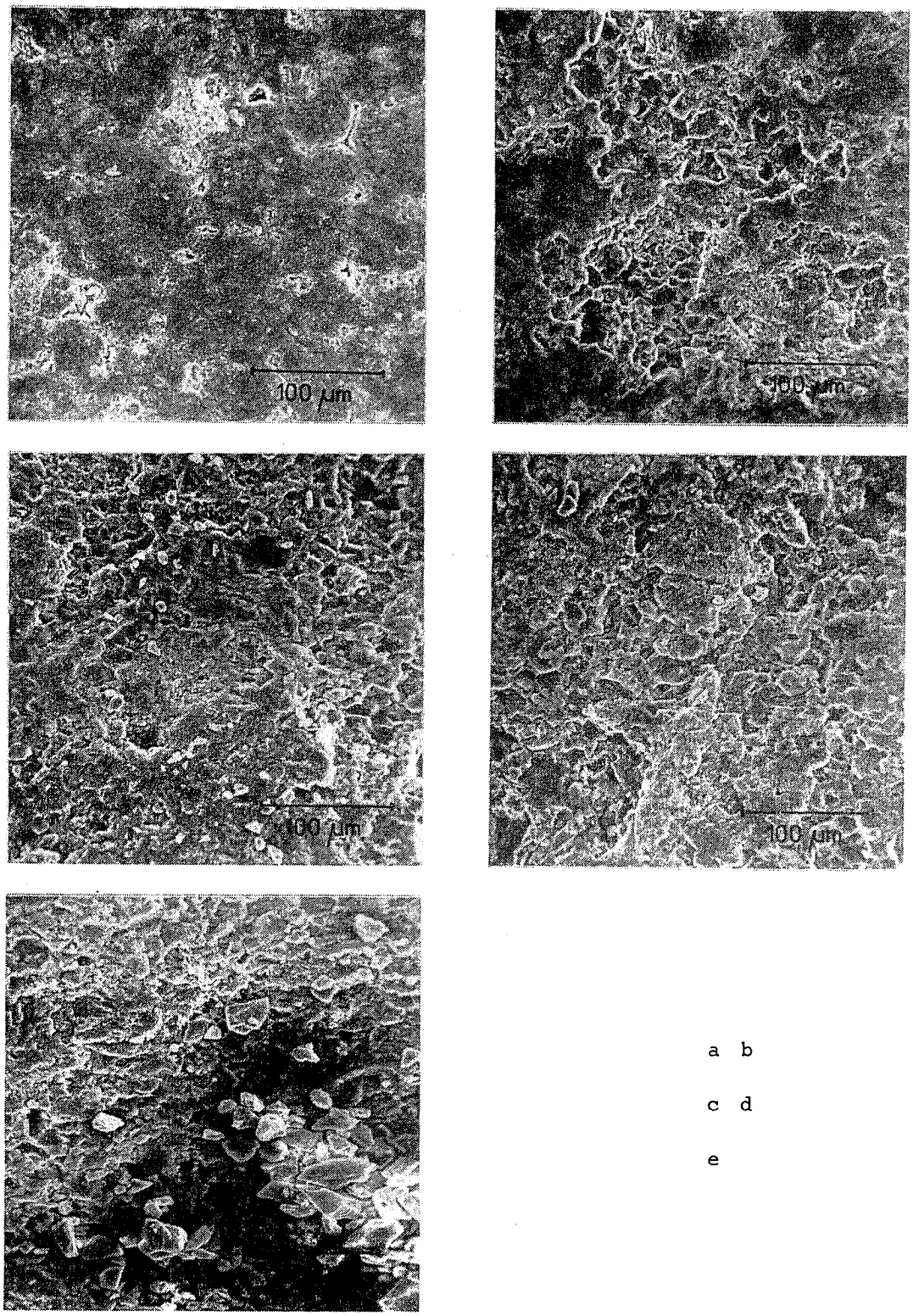

Fig. 11: SEM-photographs of kerfed alumina
a: unaffected surface b: transition between unaffected surface and kerf
c: flank d,e: bottom
parameters: a-d: standard condition; e: pressure: 3000 bars, other standard

5th American Water Jet Conference
August 29 - 31, 1989: Toronto, Canada

Paper / Communication 20

FACTORS INFLUENCING THE ABRASIVE MIXING PROCESS

T.J. Labus
University of Wisconsin-Parkside, USA

K.F. Neusen, D.G. Albert AND T.J. Gores
University of Wisconsin-Milwaukee, USA

ABSTRACT: A basic investigation of the factors which influence the abrasive jet mixing process was conducted, aimed at reducing abrasive consumption and increasing nozzle life. Particle size analysis for "as-received", once through the nozzle, and after passing through the target material were accomplished for a controlled grit size. Grit size distributions were obtained using sieve analysis and water and air collectors. Two different mixing chamber geometries were evaluated, as well as pressure, abrasive feed rate, cutting speed, and target material properties effects on particle size distribution. An analysis of the particle size distribution shows that the main particle breakdown is from 180 directly to 63 microns for a nominal 80 grit garnet. This selective breakdown occurs in both the mixing nozzle and cutting process.

RÉSUMÉ : Une étude fondamentale des facteurs qui influe sur le mélange des jets abrasifs a été menée dans le but de réduire la consommation d'abrasifs et d'augmenter la durée des bues. Une analyse granulométrique d'abrasifs avant utilisation, après passage dans la buse et après pénétration dans la cible a été réalisée pour en contrôler la taille. Des distributions des diamètres des particules abrasives ont été établies par analyse au tamis et utilisation de collecteurs à eau et à air. Deux géométries de chambre de mélange ont été évaluées, ainsi que les effets de la pression, du débit d'alimentation en abrasif, de la vitesse de coupe et des propriétés de la cible sur la distribution des tailles des particules. L'analyse granulométrique révèle que la principale tranche granulométrique va de 180 directement à 63 microns pour des particules de grenat de 80 microns de diamètre nominal. Cette séparation sélective se produit dans la buse de mélange et le processus de coupe.

Organized and Sponsored by the National Research Council of Canada and the U.S. Water Jet Technology Association.

1.0 INTRODUCTION

The introduction of abrasive water jets has broadened the potential base of fluid jet technology applications. Hard metals, ceramics, and thick composites are only a few of the materials which can be machined using abrasive fluid jets. But, with this expanded applications base, comes some challenging problems.

Typical operating/maintenance costs for "water-only" jets range from $0.90/hr to $2.74/hr, while "abrasive" jet costs range from $9.98 to $29.92/hr; approximately a factor of ten (10) increase(1). This increase in costs can be attributed to two factors:

1. the type and amount of abrasive utilized
2. life of the abrasive nozzle or mixing tube

Hence, minimizing the amount of abrasive consumed and extending the life of the mixing tube will have a substantial impact on the economic viability of abrasive jets versus conventional methods. Work by Hashish, et al(2) has shown that the amount and size of abrasive used significantly affects the wear in mixing tubes, (as measured by the change in diameter). Lower abrasive flow rates, and smaller particle sizes reduced nozzle wear. While these conditions produce favorable economics they are not conducive to increasing jet performance in terms of depth of cut produced(3,4). Hence, there must be tradeoffs between performance and mixing tube life/abrasive consumption related to the abrasive jet formation process.

Understanding the mixing process which creates the abrasive jet is a key step to developing intelligent cost/performance tradeoffs. This process is a complex, 3-phase, 3-substance flow which at present, eludes theoretical considerations. To address the mixing process the abrasive jet must be characterized in terms of abrasive particle size, velocity, and density distribution within the jet. This is predicated on the assumption that in hard materials the abrasive particles cause the primary cutting action, and the water jet is used as the accelerating mechanism.

The primary focus of this paper is the effects of various process parameters on the particle size distribution in an abrasive jet. The influence of pressure, abrasive flow rate, cutting rate, mixing chamber design and material properties on cutting performance are investigated. To accurately establish the effects of these parameters the jet condition must be described as it issues from the mixing tube, and after it exits the target material.

2. EXPERIMENTAL CONSIDERATIONS

The breakdown of particles in the abrasive jet cutting process occurs in two stages:

1. particle/particle, particle/water jet and particle/wall collisions in the mixing chamber/tube assembly.
2. particle/particle, and particle/target collisions on the target cutting surface.

Therefore, to establish particle size distribution in the abrasive material samples of the abrasive were taken before entering the abrasive mixing chamber, after exiting the mixing tube, and after cutting through the test specimen. In this way the effects of mixing chamber/tube design changes could be separated from target material and operating condition effects.

Garnet abrasive was used in all the tests with a nominal 80 grit size. The size distribution of this type of abrasive is given in table 1 below (based on mass).

Table 1
Size Distribution of Nominal 80 Grit Garnet

Particle Size Range (μm)	Percent of Sample
Greater than 250	5.9
180 < s < 250	71.7
150 < s < 180	19.1
125 < s < 150	2.6
106 < s < 125	0.5
75 < s < 106	0.1

The main mass fraction of this nominal 80 grit (i.e. the size range of 180 < s < 250 μm) was used in all tests to provide a more controlled initial size range for the abrasive.

Fig. 1 shows the high pressure intensifier pumping system and pneumatic abrasive feed unit. This is a standard commercially available unit, and it formed the basis for all subsequent testing. The first series of tests were run with the abrasive jet issuing into a catcher without impinging on a target, as shown in fig. 1a. From this test the distribution of particles delivered to the target surface could be established, as a function of operating conditions and nozzle geometry. As part of the initial investigation two catchers were employed, 1.) a water catcher, and 2.) an air catcher. The air catcher was similar to that employed by Galecki and Mazurkiewicz (5), both in size and length, while the water catcher was also tubular but only 10.2 cm. in diameter and 122 cm. long. Fig. 2 shows a comparison of particle size distributions for both types of catchers operating under identical conditions of nozzle size, pressure, and abrasive flow rate. For each catcher the amount of abrasive placed into the hopper and the amount recovered from the catcher were recorded to insure accurate results. Typical losses on a mass basis were in the range of 1 to 2% of the initial input mass. As shown the difference between the two catchers occurs outside the range of 75 to 150 micrometers. As will be shown later, this range of particle sizes is not afffected as they pass through the nozzle. Hence, either of the catchers could be used, but the air type was chosen because of the ease of operation and handling. Note, that both catchers indicate that only 20 to 22% of the particles in the initial range of 180 to 250 micrometers survive the passage through the abrasive nozzle assembly. This agrees with the data of Galecki and Mazurkiewicz (5) for comparable nozzle sizes and operating pressures. Hence, a substantial increase in the number of particles in the initial range of 180-250 micrometers may be possible if the significant operating conditions, and nozzle design parameters can be identified. As will be shown in later sections of this paper, it is this range of particles which produces the majority of the cutting action for this nominal size abrasive.

With the experimental method established, the effects of various operating conditions and nozzle design parameters can now be evaluated.

3.0 OPERATING CONDITIONS AND NOZZLE DESIGN VARIATIONS STUDY

The next series of tests were conducted to establish the effects of pressure, abrasive feed rate, and mixing tube length on the particle size distribution of the jet as it issues from the mixing tube. A 0.35mm primary water jet nozzle, and a 1.2mm mixing tube nozzle diameter were employed for all tests. Fig's. 3 through 6 show the effect of pressure on particle size distribution for various mass flow rates(the % sample size on the vertical axis is based on mass). Note the similarity of the distributions for each abrasive mass flow rate, and the relatively weak effect of pressure on particle size distribution, in the range of typical operating pressures as shown in fig. 7. The bulk of the particle breakdown occurs in the pressure range of 0 to 205 MPa. Increasing the pressure beyond this level decreases the percent of particles in the initial size range of 180 to 250 micrometers and increases the fines, with the change from 205 MPa to 274 MPa being greater than the change from 274 MPa to 342 MPa. Also, the more lightly loaded jets (i.e lower abrasive mass flow rates), show a greater sensitivity to pressure changes than the heavier loaded jets, as shown in fig. 8. The decrease in the larger particles generally shows up in a increase in the fines (i.e. particles sizes less than 63 micrometers), rather than a equal distribution across the full range of particle sizes, as shown in fig's. 3 through 6. Thus, in the range of 63 through 125 micrometers particle size distributions remain relatively constant over the range of pressures investigated.

Fig. 9 shows the effect of mixing tube length on the particle size distribution for variations longer and shorter than the standard length of 51 mm. As shown, the changes in the distributions are not significant, Hence, longer mixing tubes which would provide greater accessibility to the working surface do not impose any penalties in terms of altering the particle size distribution.

Fig. 9 also suggests that the particle breakdown that occurs during the mixing process is concentrated within the mixing chamber area. Fig. 10 shows the geometry of the standard mixing chamber employed during the initial phase of the tests. The tapered inlet on the mixing tube, fig. 10a, is considered to be part of the mixing chamber. Fig. 11 shows an alternate mixing chamber

design where the taper on the mixing tube is replaced with a flat surface, but the mixing tube diameter is kept the same as it was with the tapered inlet design. This design was subjected to the same type of test as the standard unit to determine the particle size distribution as it exits from the mixing tube. Fig. 12 shows a comparison of the two designs under identical operating conditions. The modified nozzle produces lower amounts of particles in the range of 180 micrometers, but does not produce as many fine particles (i.e. less than 63 micrometers) than the standard design. The impact of this and other design/operating changes can be gauged only by evaluating the net effect on the work piece, which is the subject of the next section.

4.0 TARGET AND OPERATING CONDITION EFFECTS

In the previous section the jet exiting from the abrasive mixing tube was characterized in terms of particle size distribution. A major question regarding the observed distributions is whether or not they are the proper type for effective cutting, based on the target material and operating conditions. A series of tests were performed using the test system shown in fig. 13. As shown, a pneumatic cylinder with speed controls is used to pass a flat steel specimen under the abrasive nozzle. This traversing mechanism is fixed to the outside cap on the catcher assembly, and is timed so that the abrasive jet is "ON" for the same amount of time before it engages the target. This time is kept to a small percentage of the total test time. The cut length on the specimen is fixed at 2.86 cm, and the abrasive weight in the hopper is recorded before and after each test to establish the amount consumed. Each test is also timed so that cutting rate and abrasive flow rate can be established.

Fig. 14 shows the effect of cutting rate on particle size distribution after the jet has passed through a 1018 cold rolled steel target 6.4mm thick, with a hardness of 84 to 97 Rockwell B. Over the range of 63 to 125 micrometers the distributions remain relatively constant as the cutting speed is increase from 6.35 cm/min to 25.4 cm/min. The primary effect of increased cutting speed on particle size distribution is to decrease the amount of particles in the 150 to 180 micrometers range and increase the fine particles, less than 63 micrometers. This data and the results from the previous section clearly shown why recirculation of the abrasive will not produce the same level of cutting as unused abrasive, since the mixing/cutting process is selective in nature, and the breakdown that occurs in the process is from large particles to fines.

Fig. 15 shows the effect of target thickness on the particle size distribution for cold rolled steel. The same trend is again evident in the shift from 180 to less than 63 micrometers in particle size. This trend is attributed to the increase in target/particle collisions due to increased thickness, just as faster cutting rates also increase target/particle collisions and cause the same shift as was shown in fig. 14.

Fig. 16 shows the effect of target hardness on the particle size distribution for steel specimens. A fixed thickness of 6.04 cm was used and the target materials were a 1018 cold rolled steel (Rockwell hardness of 95 Rb, nominal), and a high strength steel, quenched and tempered, (Rockwell hardness of 26 Rc, nominal) of the following composition:

Carbon.....	.22-.27 %
Manganese....	1.4 %
Phosphorus...	.02 %
Sulphur.....	.015 %
Aluminum.....	.015 %

Again, the same trend in terms of shift from 180 to less than 63 micrometers in particle size is exhibited for both test specimens. The harder material also shows an increase in the particles less than 75 micrometers as compared to the softer steel.

One measure of cut quality is the surface roughness of the cut surface produced by the abrasive jet. Fig. 17 shows the particle size distribution for various abrasive flow rates when cutting 1018 cold rolled steel with a hardness of Rockwell 88 Rb, at a constant pressure and cutting rate. Fig. 18 shows the resulting surface finishes (measured in micrometers), which correspond to the particle size distributions of fig. 17. Measurements of surface roughness were taken at the top, middle and bottom of the cut. As shown, the surface roughness increases from top to bottom, and decreases with increasing abrasive mass flow rate. These trends have been observed by other researchers in metals and non-metalics.

5.0 CONCLUSIONS

From the results of the investigation the following conclusions are relevant.

First, the amount of abrasive of the initial mass fraction which survives the transit through the mixing nozzle is in the range of 20-25%.

Second, the particles in the main mass fraction affect the cutting action of an abrasive jet. The remaining particles of the main mass fraction exiting the mixing tube are reduced, via collision with the work surface, to fine particles in the range of sizes less than 63 micrometers. Particles in the size range of 75 to 150 micrometers do not seem to be affected during transit through the nozzle, or during the cutting operation.

Third, changes in mixing tube length do not affect the particle size distribution, but changes in mixing chamber geometry do affect the particle size distribution.

Fourth, thicker materials cause a greater decrease in the main mass fraction of the abrasive, and an increase in the fines. This suggests that recycling is more viable for thin sections than for thick sections, since more of the main abrasive mass fraction remains intact.

Fifth, over the typical operating pressure range of 205 MPa to 342 MPa the jet pressure has a specific effect on altering particle size distributions, in that the main mass fraction is reduced to fine particle sizes less than 63 micrometers. The main mass fraction change is more substantially affected by pressure changes in the range of 0 to 205 MPa.

REFERENCES

1. "Manufacturing Technology Review of Abrasive Waterjet Cutting", US Army Industrial Engineering Activity, Project No. 2211-002, Rock Island, Illinois, Pg. 23, Feb., 1989.
2. Hashish, M., Kirby, M.J. and Craigen, S.J., "Abrasive Waterjet Cutting Data for Thine Sheet Metal and Wear of Mixing Tubes", Flow Industries Tech. Rept. No. 404, April, 1987.
3. Hashish, M., "Application of Abrasive-Waterjets to Metal Cutting", Proc. of Nontraditional Machining Conference, Pg. 9, American Society for Metals, Cincinnati, Ohio, Dec., 1985.
4. Hashish, M. "Milling with Abrasive Waterjets: A Preliminary Investigation", Proc. of Fourth U.S. Water Jet Conference", Pg. 2, ASME Publication No. I00245, Univ. of California, Berkeley, Aug., 1987.
5. Galecki, G. and Mazurkiewicz, M., "Hydroabrasive Cutting Head Energy Transfer Efficiency", Proc. of Fourth US. Waterjet Conference, Pg. 109-111, ASME Publication No. I00245, Univ. of California, Berkeley, Aug., 1987.

NOMENCLATURE

Dw = Water jet nozzle diameter (mm)
Da = Abrasive nozzle diameter (mm)
Ma = Abrasive flow rate (Kg/min)
t = Target specimen thickness (mm)
p = Jet Pressure (MPa)
v = Cutting Velocity (cm/min)
s = Particle size (microns)
Rb = Rockwell Hardness (B Scale)
Rc = Rockwell Hardness (C Scale)
L = Mixing Tube length (mm)

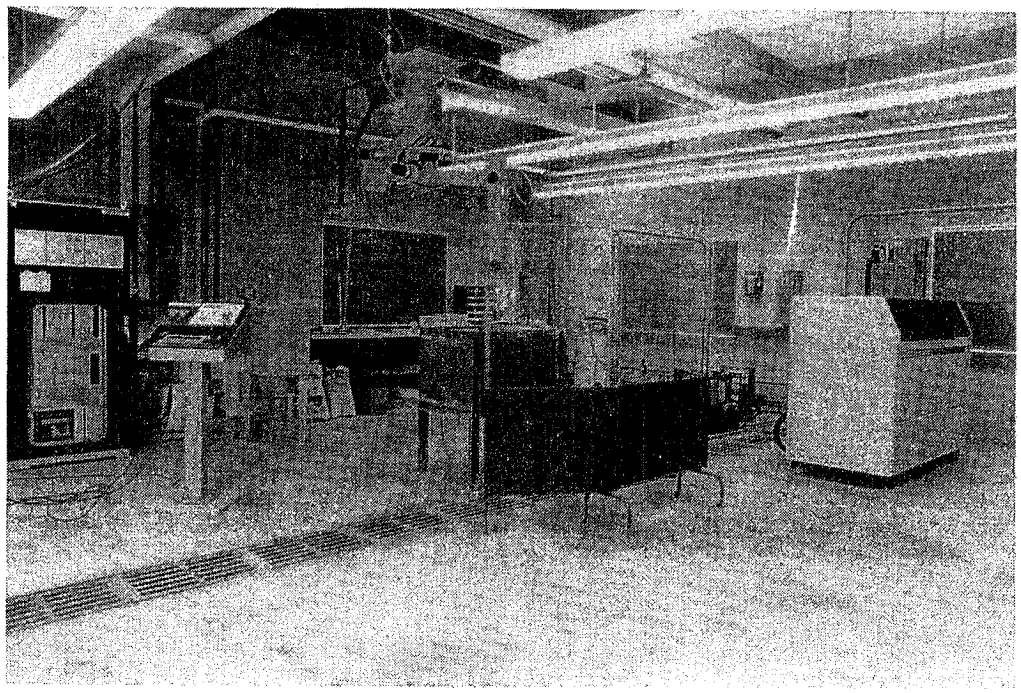

Fig. 1 High Pressure Pumping System and Pneumatic Abrasive Feed Unit

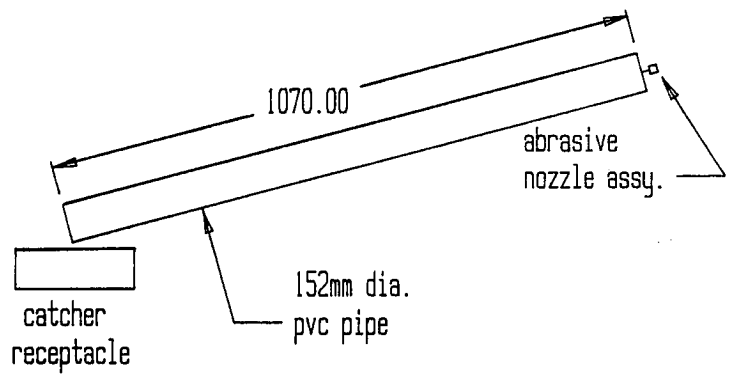

Fig. 1a Air Catcher Test System

Fig. 2 Comparison of Water Vs. Air Type of Catchers

p=274 MPa, Du/Da=.33/1.2 mm, Ma=.45 Kg/min

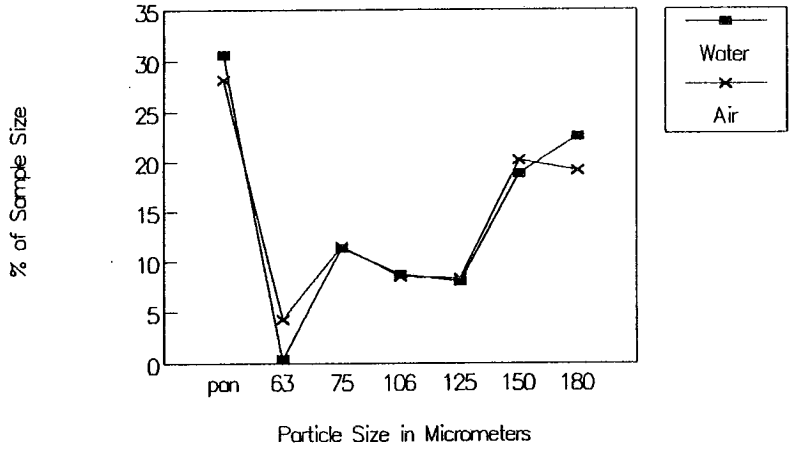

Fig. 3 Effect of Jet Pressure on Particle Size Distribution

Du/Da=.33/1.2 mm, Ma=.227 Kg/min

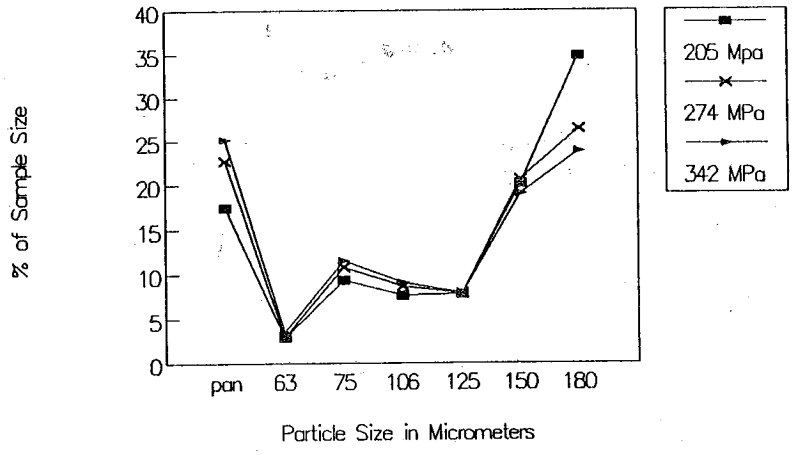

Fig. 4 Effect of Jet Pressure on Particle Size Distribution

Du/Da=.33/1.2 mm, Ma=.45 Kg/min

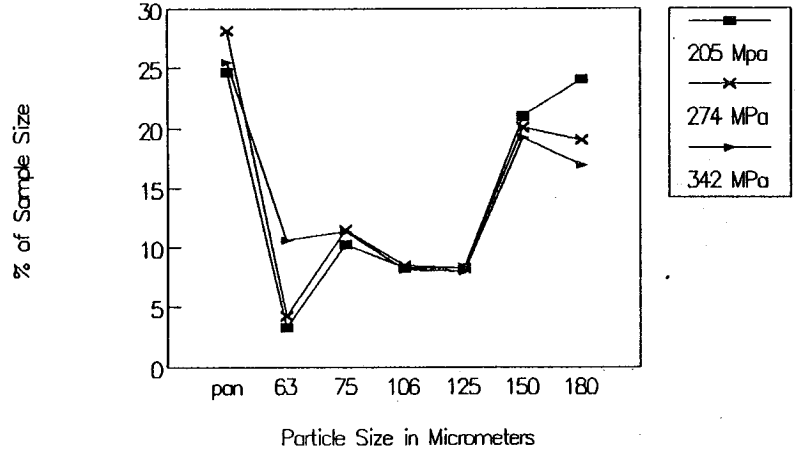

Fig. 5 Effect of Jet Pressure on Particle Size Distribution

Du/Da=.33/1.2 mm, Ma=.681 Kg/min

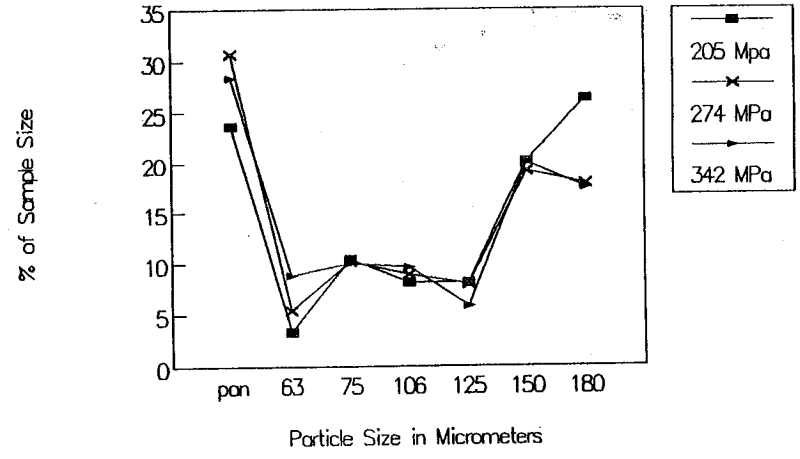

Fig. 6 Effect of Jet Pressure on Particle Size Distribution

Du/Da=.33/1.2 mm, Ma=.908 Kg/min

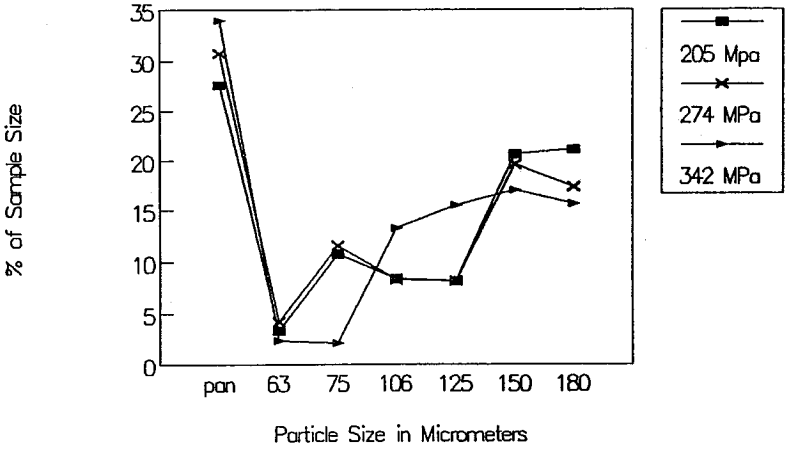

Fig. 7 Effect of Jet Pressure on Particle Size Survival

Du/Da=.33/1.2 mm, Ma=.227 Kg/min, Initial Particle Range 180<s<250

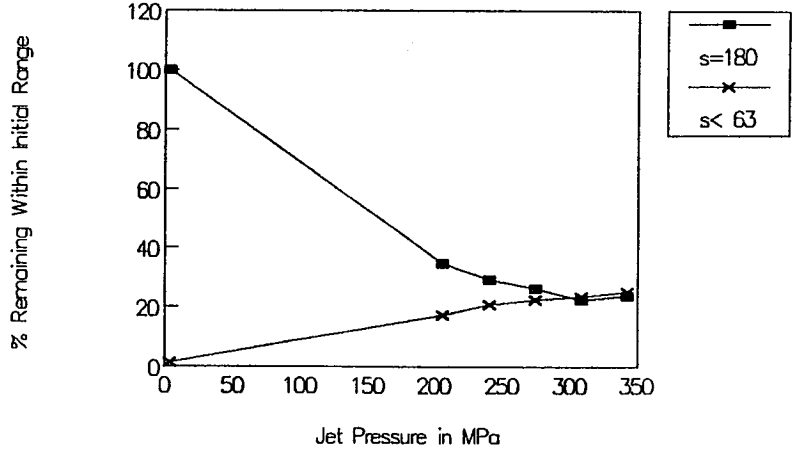

Fig. 8 Effect of Abrasive Flow Rate on Particle Survival

Du/Da=.33/1.2 mm, Initial Particle Size 180<s<250

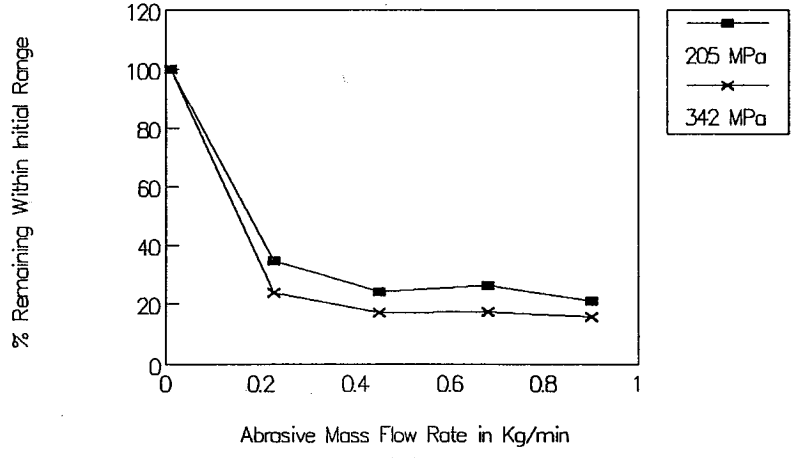

Fig. 9 Effect of Mixing Tube Length on Particle Size Distribution

Du/Da=.33/1.2 mm, Ma=.45 Kg/min, p=274 MPa

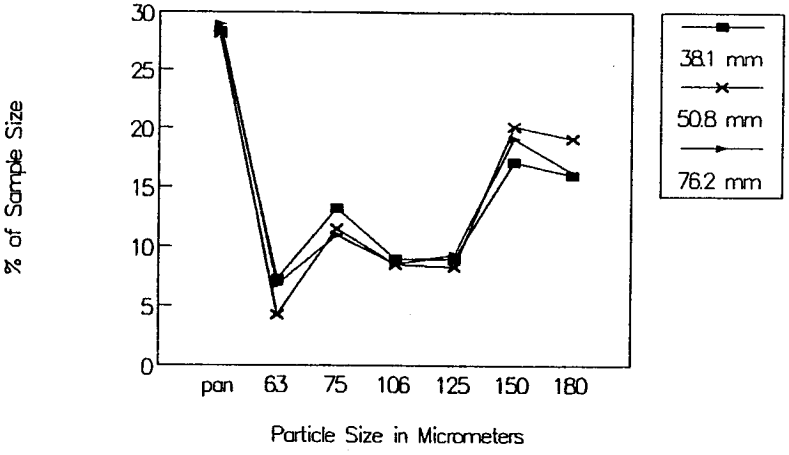

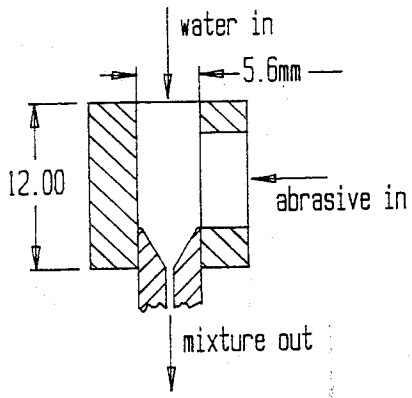

Fig. 10 Standard Mixing Chamber Geometry

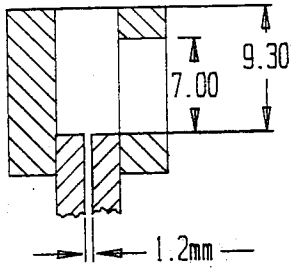

Fig. 11 Modified Mixing Chamber Geometry

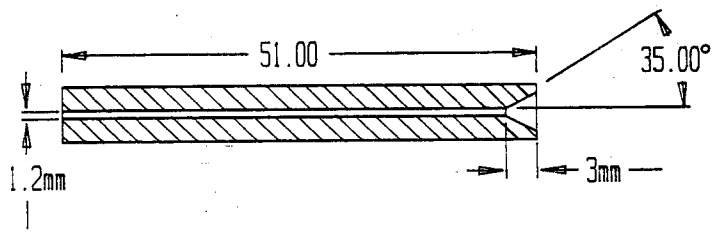

Fig. 10a Mixing Tube Geometry

Fig. 12 Effect of Mixing Chamber Geometry on Particle Size Distribution

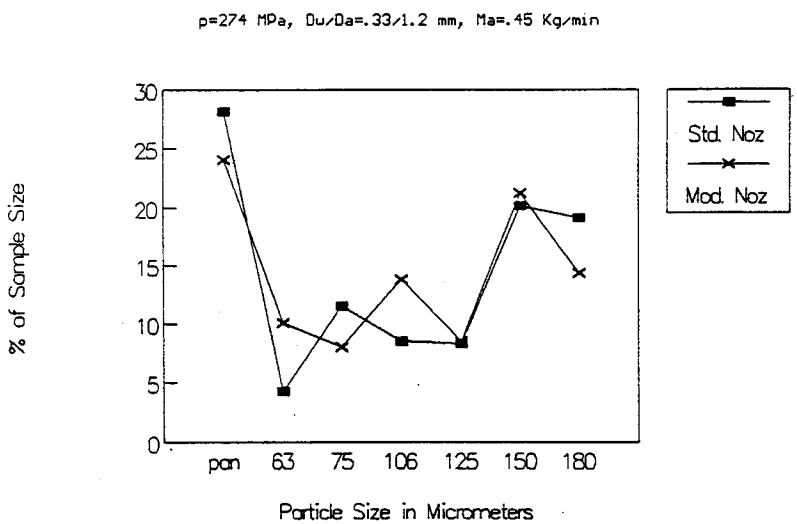

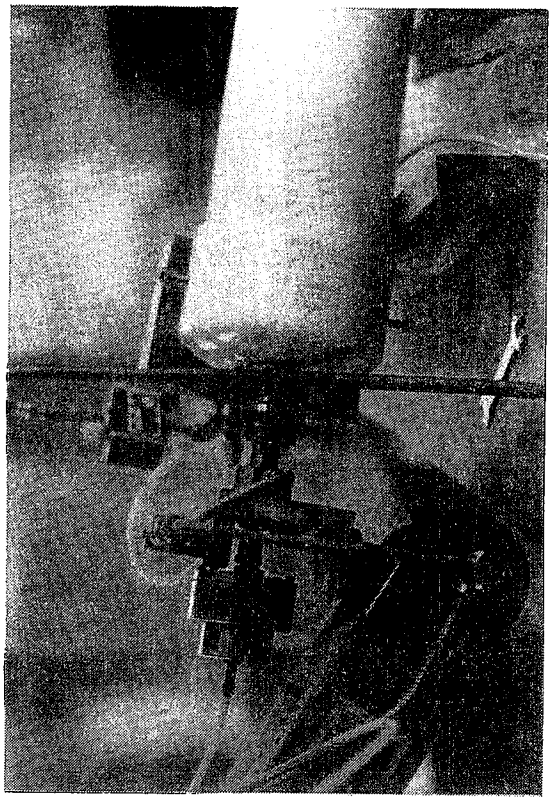

a.) Nozzle Mounted to Cap & Attached to Air Catcher

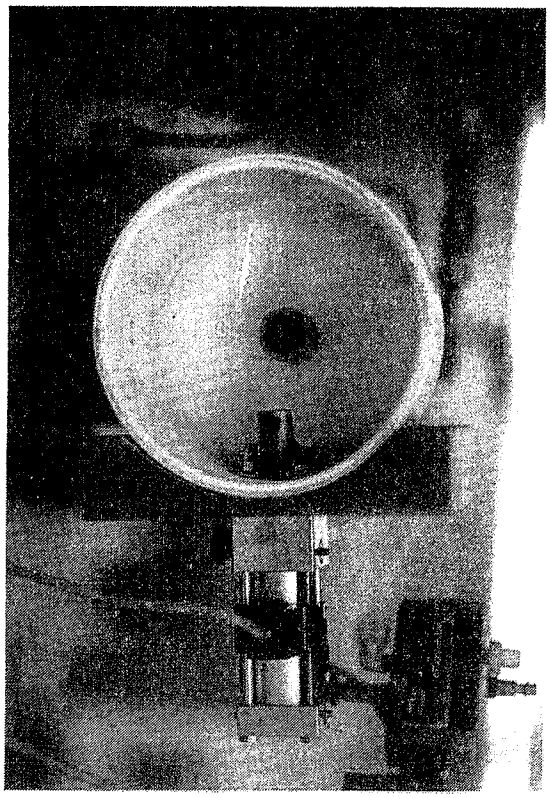

b.) Pneumatic Cylinder Assembly Used to Feed Cutting Specimens

Fig. 13 Cutting Test System Configuration

Fig. 14 Effect of Cutting Speed (cm/min) on Particle Size Distribution

Du/Da=.33/1.2 mm, Ma=.45 Kg/min, p=274 MPa

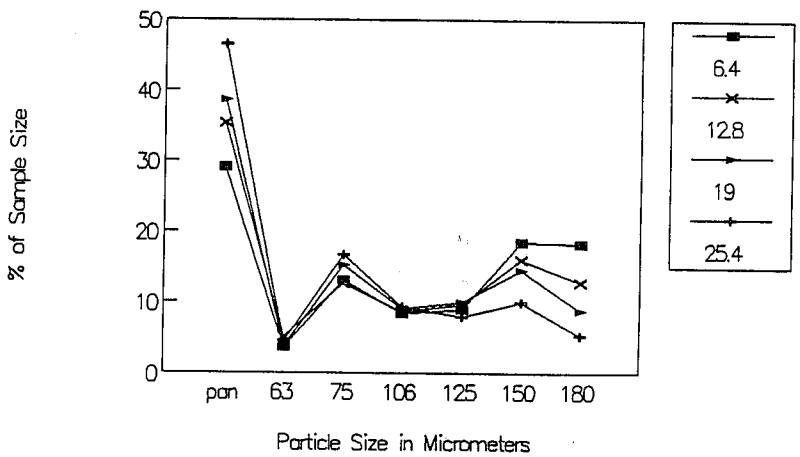

Fig. 15 Effect of Specimen Thickness of Particle Size Distribution

p=274 MPa, v=12.06 cm/min, Du/Da=.33/1.2 mm, Ma=.45 Kg/min

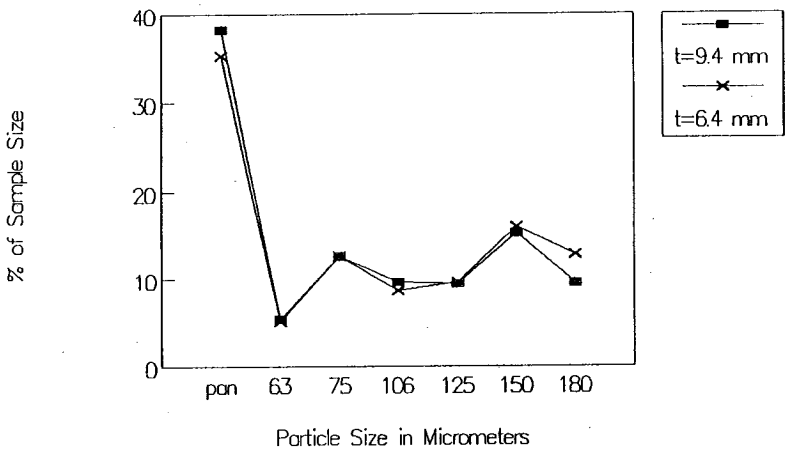

Fig. 16 Effect of Hardness on Particle Size Distribution

Du/Da=.33/1.2 mm, Ma=.45 Kg/min, p=274 MPa, V=12.4 cm/min, T=6.4 mm

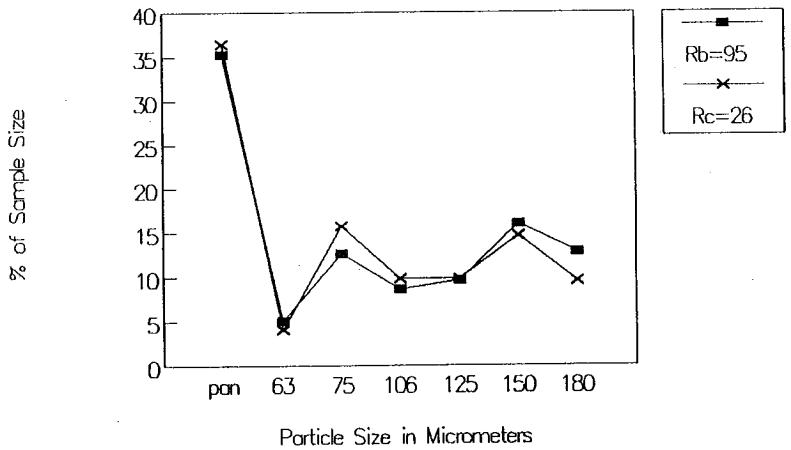

Fig. 17 Effect of Abrasive Flow Rate (Kg/min) on Particle Size Distribution

Du/Da=.33/1.2 mm, p=274 MPa, V=12.4 cm/min, T=9.5 mm, Rb=88

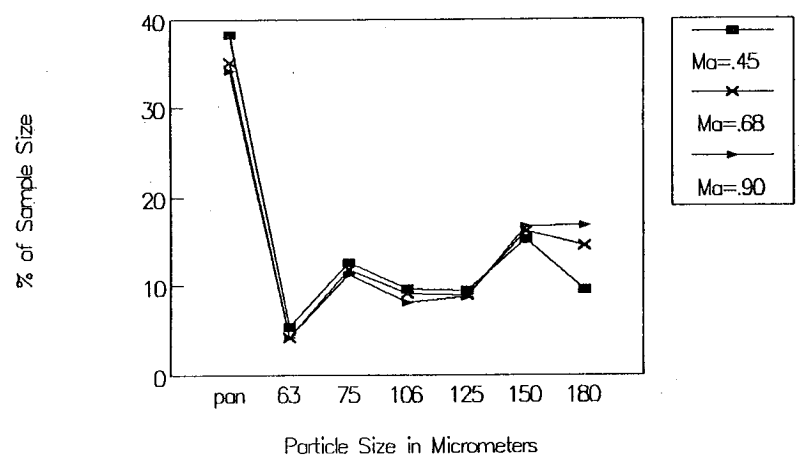

Fig. 18 Effect of Abrasive Flow Rate (Kg/min) on Surface Finish

Du/Da=.33/1.2 mm, p=274 MPa, V=12.4 cm/min, T=9.5 mm, Rb=88

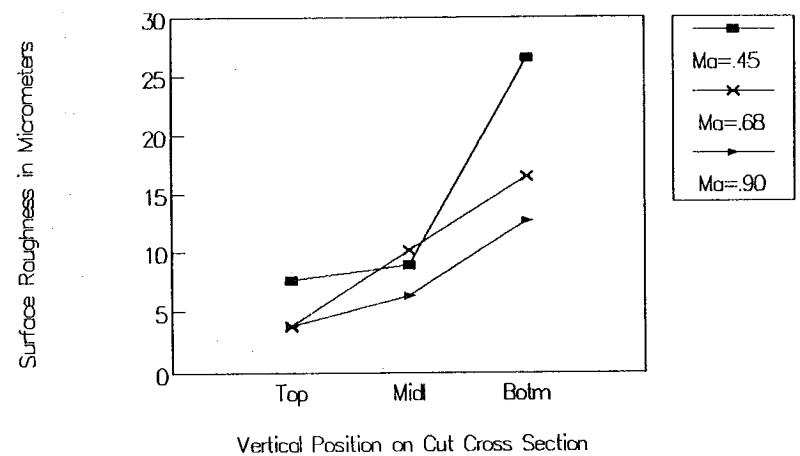

5th American Water Jet Conference
August 29 - 31, 1989: Toronto, Canada

Paper / Communication 21

INVESTIGATION OF ANATOMY OF AN ABRASIVE WATERJET

E.S. Geskin, W.L. Chen, S.S. Chen, F. Hu, M.E. H. Khan AND S. Kim
New Jersey Institute of Technology
Newark, NJ, USA
AND
P. Singh AND R. Ferguson
Ingersoll-Rand Company

ABSTRACT: The study was concerned with the distribution of abrasive particles within an abrasive water jet. Three independent experimental techniques were utilized in this study. High frequency filming (10,000 frames per second) was used to visualize particle motion. A copper vapor laser was employed as the source of the light to make the motion of the particles visible. Another experimental technique involved the investigation of erosion of a polished surface of a stainless steel plate subjected to the impingement of the moving jet. The topography of the eroded surface was examined by SEM and optical microscope. Particle distribution was also studied by collecting the central portion of the jet using different diameters of diamond washers. The results of the experiments have shown that particles in the jet are distributed randomly and emitted in intermittent clusters.

RÉSUMÉ : L'étude a porté sur la distribution des particules abrasives dans un jet d'eau abrasif. Trois techniques expérimentales indépendantes ont été utilisées à cette fin. Le mouvement des particules a été visualisé par photographie ultra-rapide (10 000 images à la seconde). Un laser à vapeur de cuivre a été utilisé comme source de lumière pour rendre visible le mouvement des particules. Une autre technique expérimentale a porté sur l'étude de la surface polie d'une plaque d'acier inoxydable exposée au jet en mouvement. Le relief de la surface érodée a été examiné au microscope électronique à balayage et au microscope optique. La distribution des particules a aussi été étudiée en collectant la partie centrale du jet au moyen de rondelles en diamant de différents diamètres. Les résultats des expériences ont montré que les particules dans le jet sont distribuées au hasard et émises en nuages intermittents.

Organized and Sponsored by the National Research Council of Canada and the U.S. Water Jet Technology Association.

I. INTRODUCTION

The cutting capability of the abrasive waterjet (AWJ) is determined by forces developed through the interaction between individual particles and a work piece. The success of cutting depends on the velocity field of the particles entrained by the water flow. The generation of the particles water flow involves suction of the particles into a mixing chamber, entrainment of these particles into a high velocity water flow, and their subsequent redistribution in the carbide tube and in the free jet, caused by turbulent diffusion. The distribution of particles in a jet stream, exiting the nozzle, is a criterion of nozzle effectiveness. Because of the experimental difficulties and the lack of data describing the abrasive jet, the availability of information about particles distribution is limited. M. Hashish et. al. suggests that particles are concentrated at the central part of the jet [1]. Our recent work determines that the loose particles, the particles outside the mainstream, have a substantial effect on the results of cutting [2]. Information about some features of the particles distribution in the jet is given in [3,4]. It is necessary, however, to obtain a more comprehensive description of this principal feature of the jet flow. The acquisition of such information is the objective of this study.

II. EXPERIMENTAL

The work involved measuring the properties of a high velocity jet containing a large number of abrasive particles. Since the direct measurement of the particles trajectory was not feasible, three independent experimental techniques were used to study the desired distribution.

The first technique involved an attempt to obtain a visual image of the water-particles mixture. The procedure was based on high frequency (10,000 frames/sec) filming of the jet with copper vapor as the source of light. Each individual frame was examined by an analytical projector. Use of a laser light made the jet at least partially transparent and enabled us to identify the individual particles and the change in the shape of the jet under different conditions of the formation.

The second procedure involved an examination of the erosion of a polished surface by an impinging jet. The erosion pattern was characterized by multiple dimplets resulting from particles impact. It was assumed that the distribution of the dimples was a meausure of the distribution of the active particles having sufficient energy to deform a target material. The jet-surface interaction was carried out at such speeds that dimples, formed by individual particles, could be identified.

We can also indirectly derive the particle distribution across the jet by examining the kerf profile of a material being cut. First we can set up a mathematical model. We assume that the depth of the jet penetration for any site of the impingement zone is proportional to the duration of the jet-workpiece interaction. This assumption is correct if the particles are uniformly distributed across the jet and if the mean mass of material removal per particle is constant. Let us consider an arbitary point C at kerf cross-section (Fig. 1). The distance between this point and the axis of the kerf is equal to the abscisa x of the point C. The duration of the jet impingement on the site of C is 2AC/v, where AC represents the part of the jet which was brought into contact with site C, and v is the speed of jet motion in the cutting direction. Then we can assume that the depth of jet penetration at point C, denoted by z, is

$$z = k*AC \qquad [1]$$

where k is the constant for the given cutting conditions, accounting for material removal per particle and speed v, AC is the length of the abrasive waterjet passing over the point C. From Fig. 1 it follows

$$AC = r*\sin\Theta \qquad [2]$$

where

$$\sin\Theta = \sqrt{\frac{r^2 - x^2}{x}} \qquad [3]$$

After a simple manipulation Equations [1] and [3] yield :

$$\frac{x^2}{r^2} + \frac{y^2}{k^2 r^2} = 1 \qquad [4]$$

Equation [4] shows that the profile of the kerf is an ellipse, having axes equal to the depth and width of the kerf when particles are evenly distributed within the jet cross-section.

In order to validate the constructed equation a number of kerf were developed on a polished surface of a steel plate. Pictures of the obtained kerf cross-sections were made and used to determine the coordinates of the profiles. Then the coordinates were determined by the use of equation (4) where the parameter, kr, was taken equal to the depth of the kerf. Comparison of observed and computed values of the kerf coordinates was used to evaluate the validity of the assumption about the particles distribution.

The third experimental technique involved the assessment of the amount of the particles passing through a selected sub-region of the jet cross-section. The ratio between this amount and the total amount of the abrasive, exiting the nozzle in the course of particles accumulation, enabled us to estimate the relative mass flow rate of the particles through a selected area of the jet cross-section. The values of this ratio for several sub-regions determined particle distribution within a jet.

This experiment involved the jet impingement on a plane surface holding a circular washer with a hole (or orifice) containing an orifice of a given cross section area (Fig. 2a, b) and subsequent evaluation of the weight of the particles accumulated beneath the washer. By changing the diameter of the orifice, we evaluated the mass flow rate of the particles at different regions in the jet. The accuracy of the coaxial alignment of the jet and the orifice determined the accuracy of this experiment.

The preliminary tests showed that only a diamond washer can be used in these experiments, although the diamond eroded somewhat during the interaction with the abrasive jet. Coaxiality of the orifice and the jet was attained by proper positioning of the nozzle. To achieve this, the system was run at low presuure and the water jet part of the washer was carfefully observed. Proper alignment was said to have been achieved when this jet was visually observed to have maximum intensity. This procedure assured the parallelism of the nozzle and orifice axis. Further improvement in the system alignment was attained by identifying the center of the area on the washer surface eroded by the jet impingement through microscope. The deviation of this center from the axis of the washer was determined and used to fix the nozzle's position. The erosion of both the diamond and carbide made it necessary to measure diameters of the carbide and diamond orifices before and after each experiment. The duration of mixture collected was equal to 10 seconds. It has been shown that by measuring the forces exerted by the jet on a workpiece that the duration of the transient processes in a jet does not exceed 1 second [5]. Thus, during the 10 second impingement, the steady state condition of the jet was obtained. At the same time, the erosion of the diamond and the carbide, during water jet cutting, did not adversely affect the experimental conditions.

The mixtures collected, with and without the diamond washer, were stored in two operate beakers and their volumes and weights are recorded. Each mixture was held in a beaker, until the particles settled down. The excess clear water was drained and the particles were dried by heating the mixture to a temperature of more than 100^{o} C and weighed again. Such a procedure enabled us to determine the volume and mass fraction of the mixture and the fraction of the abrasive that passed through the washer.

The above experiments were carried out for diamond orifices having a initial internal diameters of 0.005, 0.010, and 0.015 in. The experiments were carried out at different combinations of sapphire and carbide diameters as well as at the different flow rates of abrasive. Barton Garnet 80 mesh and 220 mesh were used in this study.

III. RESULTS AND DISCUSSION

1. High speed filming.

The high speed camera was used to investigate 20 different conditions of jet formation. Both clean waterjet and abrasive jets with particles of different sizes were examined. The film showed that the flow constituted with a jet surrounded by an array of droplets and particles. The jet was subjected to violent oscillations, both transversal and longitudinal. These oscillations grew into large disturbances along the jet, and eventuallly destroyed the continuity of the jet. In some cases individual particles distributed randomly within the jet body were observed (Fig. 3). No region of preferable particle concentration was found.

2. Investigation of the topography of the erosion zone.

The shape of the polished surface subjected to erosion by a moving AWJ is shown in Figs. 4-6. The presented micrographs demonstrate random dimple concentration and constant mean density. The image of the erosion zone, Fig. 7 was constructed by the use of a database, representing the surface (Matrix, 1988). The presented micrographs show that in the longitudinal direction the density of dimples changed periodically due to the mode of the particles distribution within a jet. Clusters of particles formed in the jet create clusters of dimples in the impingement zone. No zone of dimple concentration in the transversal cross-section was observed.

3. Examination of the kerf geometry.

The measured shapes of the kerf and the shapes determined by the equation (4) are given in Fig. 8. The difference between the theoretical and the experimental data demonstrates that for the given conditions of the kerf formation the assumption made about uniform density of the active particles distribution is valid for the central part of the jet [7]. This assumption is less accurate for the jet periphery.

4. Investigation of particles distribution by flow separation.

The results obtained by measuring the strength of the flow, separated by the diamond washer, were used to construct Figs. 9-10 which demonstrate the distribution of the mixture and particles across the jet [8]. The strength of the flow of the mixture through the washer is characterized by the weight of mixture collected beneath the washer. Correspondingly, the strength of the separated flow of abrasive is characterized by the weight percentage of particles passing through the orifice. Figs 9 and 10 show a relationship between the fractions of the abrasive and the mixture collected beneath the washer. The effect of the orifice diameter on the strength of mixture and abrasive flow is depicted in Figs 11-14. The graphs presented in Figs 9-14 show a strong correlation between the strength of the flow of abrasive and mixture. This correlation shows that the time average of particles density for different points of the jet cross-section is uniform.

In Figs 9-14 the following notations are used for flow indentification:
#80 and #220 indicate the particles size in mesh, 10-30 and 7-30 denote the diameters of the sapphire nozzle and carbide tube in milliinches, #5, #7 and #10 show the flow-rate of the abrasive. For abrasive #80 these flow-rates are 0.240 lb/min, 0.66 lb/min, and 0.95 lb/min; and for particles #220 the flow-rates are 0.140 lb/min, 0.43 lb/min, and 0.70 lb/min, respectively.

5. Effect on Cutting

The observation above indicates that the jet mainstream is a pulsating, flow with mean uniform distribution of particle clusters. The uniformity of the flow imposes the limitations on the width of the kerf and the maximal depth of cutting. The reduction of the diameter of the jet can be achieved by the reduction of the diameter of the carbide mixer. This objective can also be accomplished by improving the mixing conditions in the tube.

Clustering of the particles and pulsation of the jet do have an impact on the maximum cutting speed, kerf width, and the finish of the cut surface. Improvements in these areas can be made by improving the jet's stability.

IV. CONCLUSIONS

1. Time average of the particles's density within the jet main stream is uniform. This result is not altered by reasonable variations in the flow rate, particle type or size and sapphire or carbide nozzle diameters.

2. Individual particles form clusters along the longitudinal direction. These clusters enhance non-uniformities in the material cutting rate.

3. The abrasive water jet becomes quickly unstable and the instabilities are strong enough to be observed in the form of severe oscillations and cluster formation.

4. A new experimenatal technique, devised to measure particle distribution across the jet, successfully provided a direct measurement of such distribution.

V. ACKNOWLEDGEMENT

This work was supported by NSF Grant # DMC 8810659 and a grant from Ingersoll Rand Co.

VI. REFERENCES.

1. Hashish, M.A., et al.: "Method and Apparatus for forming a High Velocity Liquid Abrasive Jet." USA Patent 4,648,215 of March 10, 1987.

2. Geskin, E.S. ,Chen, W.L. and Lee, W. T.: "Glass Shaping by the Use of Abrasive Water Jet." Glass Digest, November 1988, pp. 60-64.

3. Swanson, R.K., et al.: "Study of Particles Velocity in Water Driven Abrasive Water Jet." Proceedings of the fourth US Water Jet Conference, ASME, 1987, pp. 103-109.

4. Galecki, G. and Mazurkiewicz, M.: "Hydroabrasive Cutting Head-Energy Transfer Efficiency." ibid., pp. 109-111.

5. Li, H.Y.: "Investigation of Forces Developed in the Course of the Water Jet-Work Piece Interaction, MS Thesis, NJIT, Newark, 1988.

6. Matrix Vidiometrix Inc, Econoscope, Manual, 1988.

7. Chen, S.S.: "Investigation of the Dynamics of Surface Generation in Waterjet Cutting." Master Thesis, NJIT, May 1989 (to be submitted).

8. Kim, S. : "Investigation of Particles Distribution across Abrasive Waterjet" Master Thesis, NJIT, May 1989 (to be submitted).

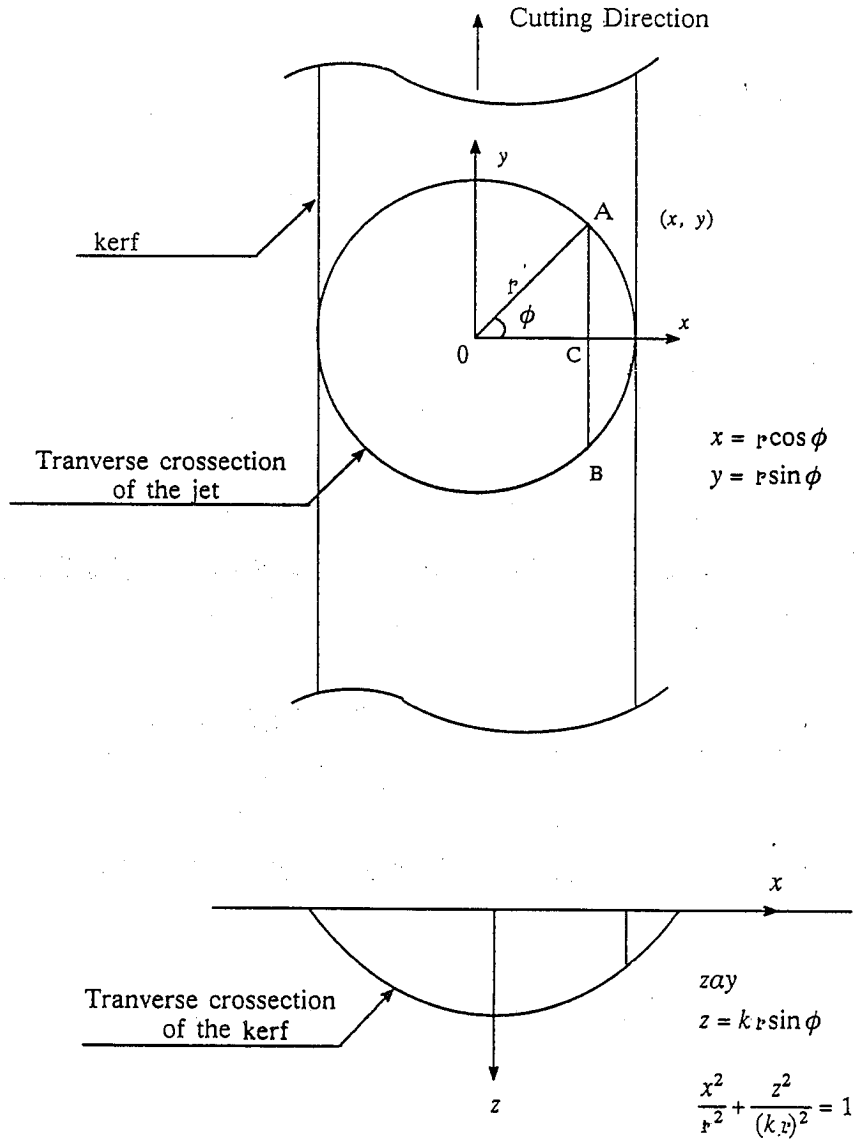

FIG. 1 SCHEMATIC OF THE KERF GENERATION

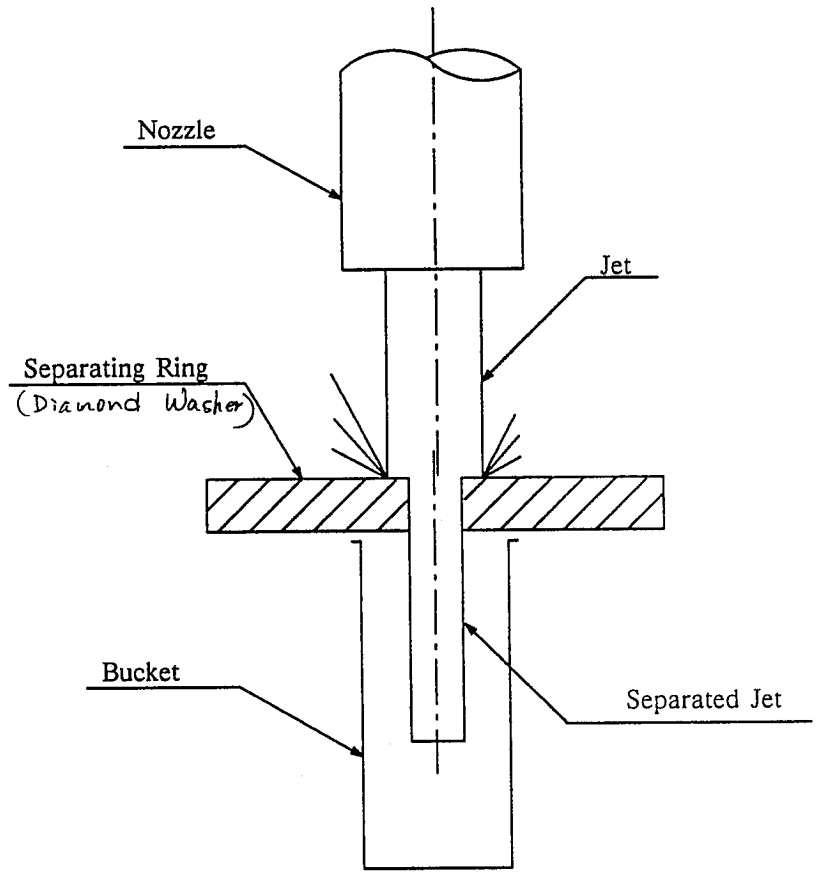

FIG. 2a SCHEMATIC OF FLOW SEPARATION AND COLLECTION

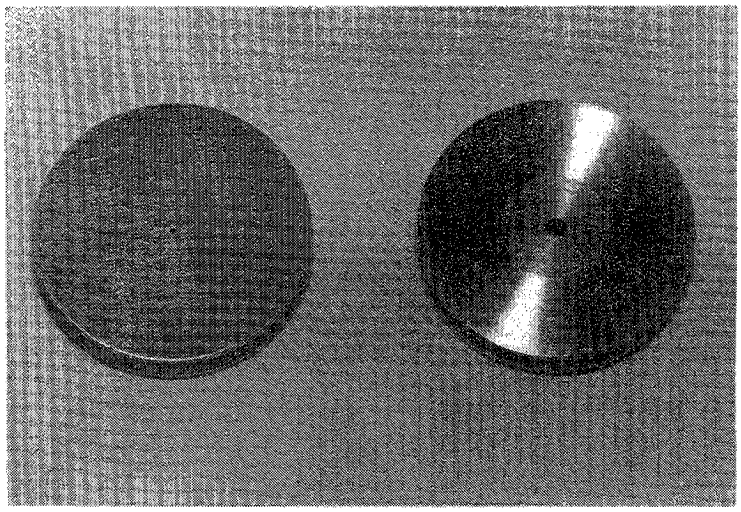

FIG. 2b DIAMOND WASHER AND WASHER HOLDER

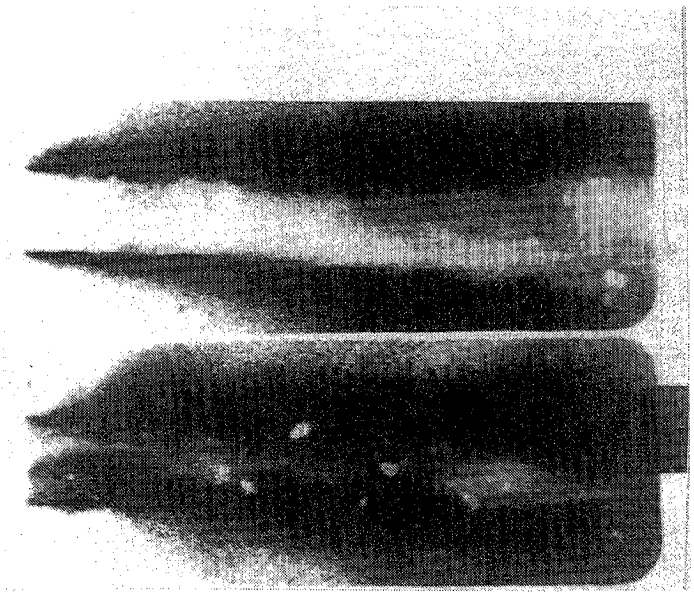

FIG. 3 Frames of the jet film showing behavior of the jet at the exit of the nozzle. Time interval between frames= 0.0001 secs. Size of particle= 50 mesh, particle flow= #10(540 g/min), diameter of sapphire nozzle= 0.010 in., diameter of carbide tube= 0.093 in. White spots on the jet body represent particles. Notice random distribution of particles within the flow.

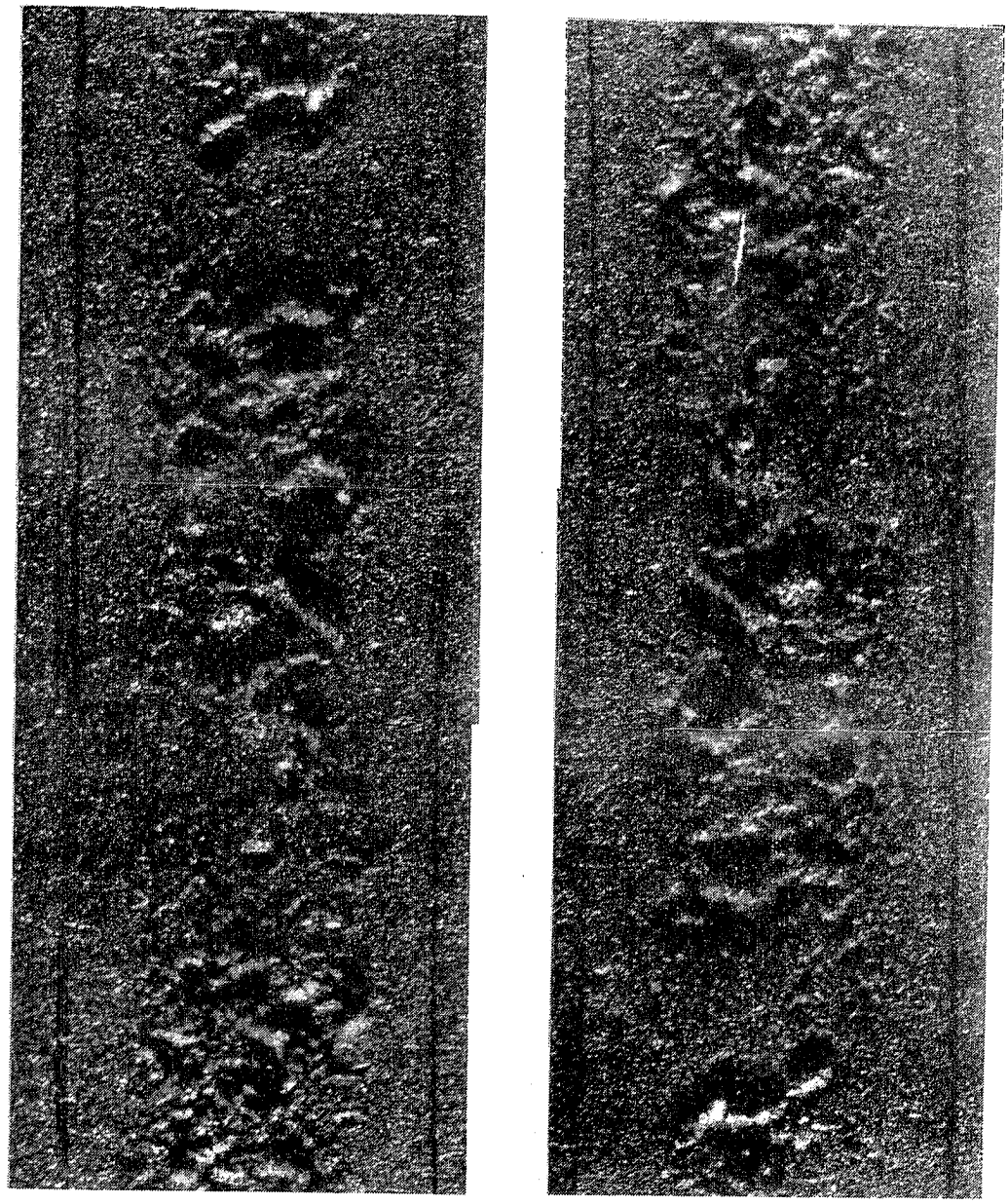

Fig. 4 Micrograph of the surface of a stainless steel plate subjected to AWJ impingement, X65. Particle size= 50 mesh, particle flow rate= #3(94.6 g/min), diameter of sapphire nozzle= 0.010 in., diameter of carbide tube= 0.030 in., speed of the nozzle motion= 2400 in/min. Notice the periodical distribution of dimples and constant mean density of particles in the transverse cross-section.

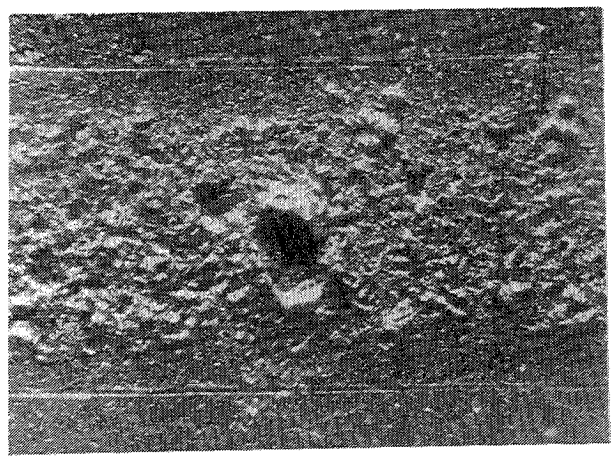

Fig. 5 Micrograph of the surface of a stainless steel plate subjected to AWJ impingement, X65. Particle size= 220 mesh, particle flow rate= #3(48.9 g/min), diameter of sapphire nozzle= 0.010 in., diameter of carbide tube= 0.030 in., speed of the nozzle motion= 2400 in/min. Notice that the mean density of dimples and deep crates generated by impinging clusters of particles is uniform.

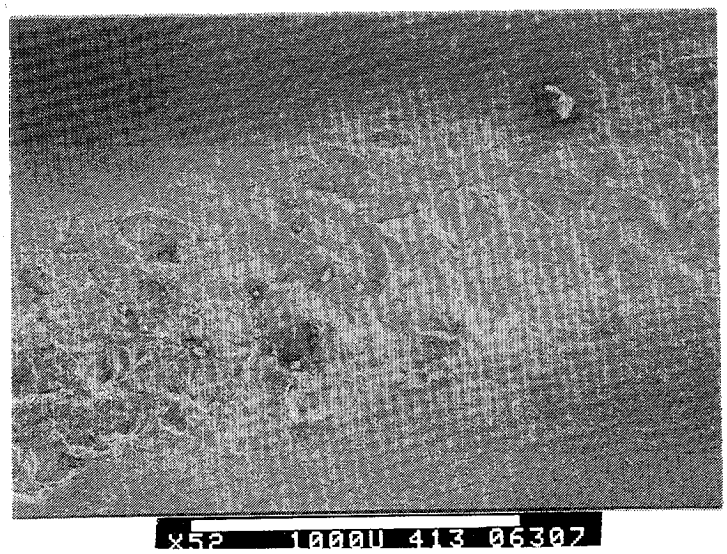

Fig. 6 SEM micrograph of the surface of a stainless steel plate subjected to AWJ impingement, X52. Particle size= 50 mesh, particle flow rate= #3(94.6 g/min), diameter of sapphire nozzle= 0.007 in., diameter of carbide tube= 0.010 in., speed of the nozzle motion= 2400 in/min. Notice the clustering of dimples in the longitudinal direction and random distribution of clusters.

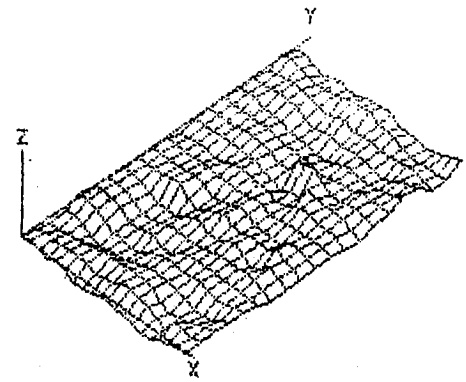

X-Y-Z Plot

Viewing Angle
Theta = 315
Phi = 45

Sample Size
X Axis .03
Y Axis .05
Inspect Lens
10X
Data Points
400

Amplification: 1

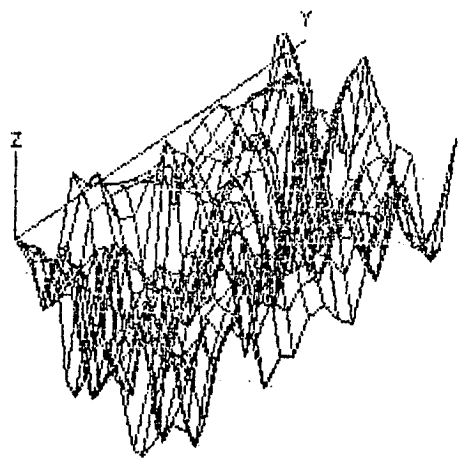

X-Y-Z Plot

Viewing Angle
Theta = 315
Phi = 45

Sample Size
X Axis .03
Y Axis .05
Inspect Lens
10X
Data Points
400

Amplification: 10

Fig. 7 Topograph of the surface of a stainless steel plate subjected to AWJ impingement. Particle size= 50 mesh, particle flow rate= #3(94.6 g/min). The image obtained by Econoscope system shows even distribution of craters across the erosion zone.

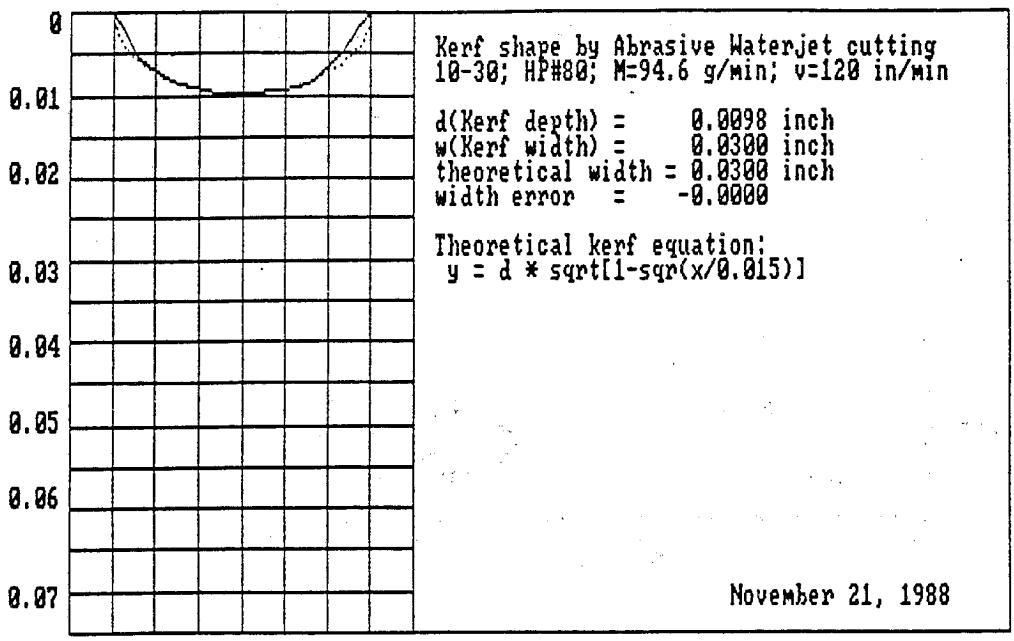

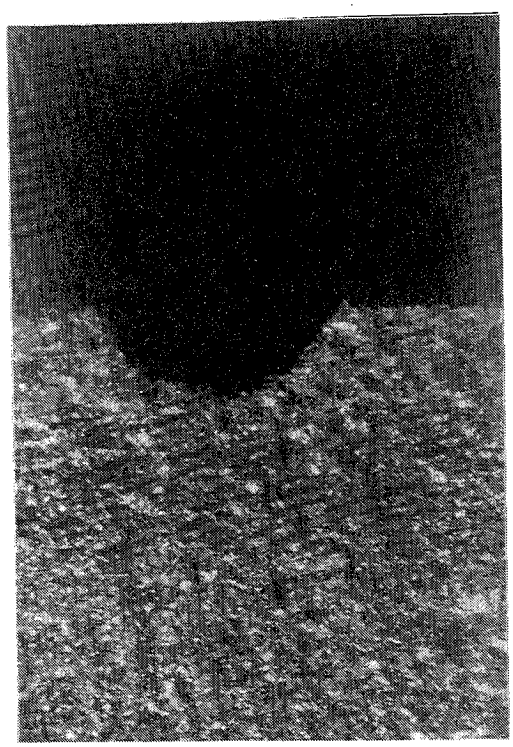

Fig. 8 Comparison between theoretical (dotted line) and experimental shapes of the kerf. Notice a good similarity between predicted and experimentally obtained lines in the center of the kerf but this prediction deviates somewhat at the kerf periphery.

Fig. 9 CORRELATION BETWEEN PERCENT ABRASIVE WITH PERCENT MIXTURE FLOW. Sapphire D= 0.010 in., Carbide D= 0.030 in.

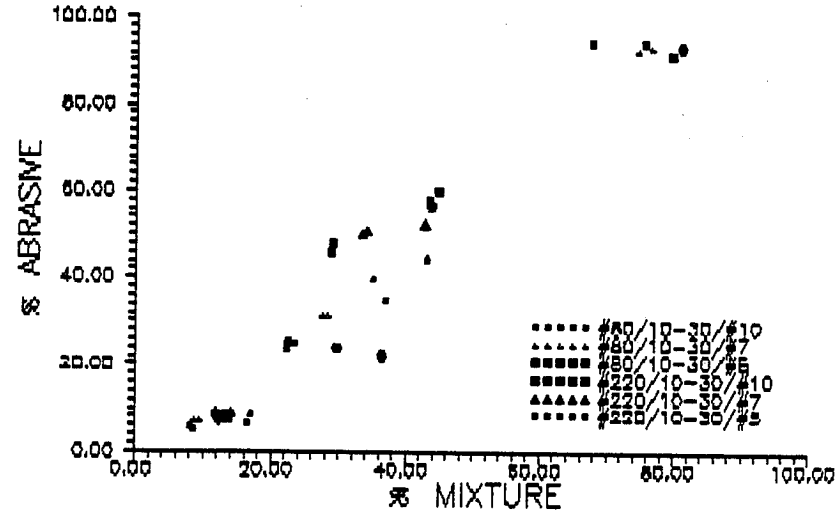

Fig. 10 CORRELATION BETWEEN PERCENT ABRASIVE WITH PERCENT MIXTURE FLOW. Sapphire D= 0.007 in.,Carbide D= 0.030 in.

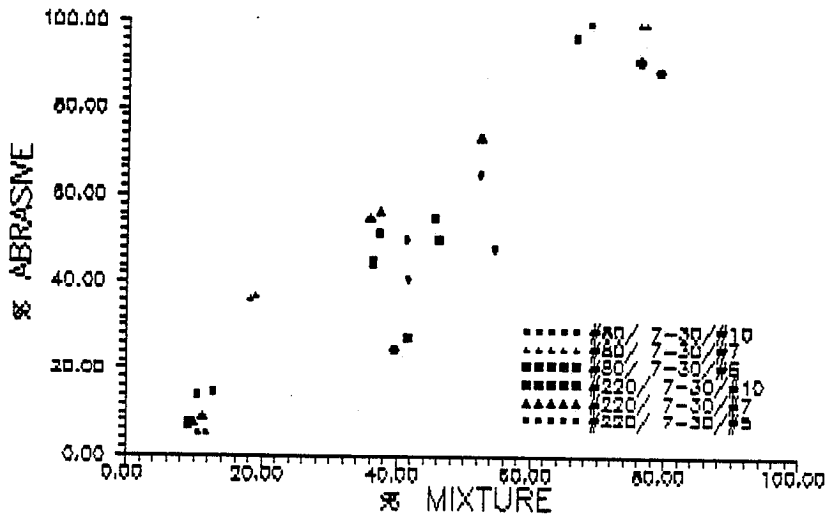

Fig. 11 CORRELATION BETWEEN PERCENT AREA CHANGE WITH PERCENT ABRASIVE FLOW. Sapphire D= 0.010 in.,Carbide D= 0.030 in.

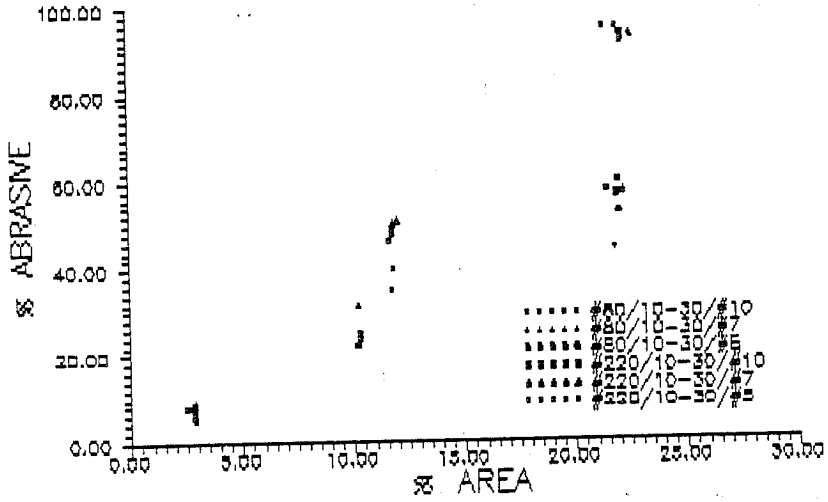

Fig. 12 CORRELATION BETWEEN PERCENT AREA CHANGE WITH PERCENT ABRASIVE FLOW. Sapphire D= 0.007 in.,Carbide D= 0.030 in.

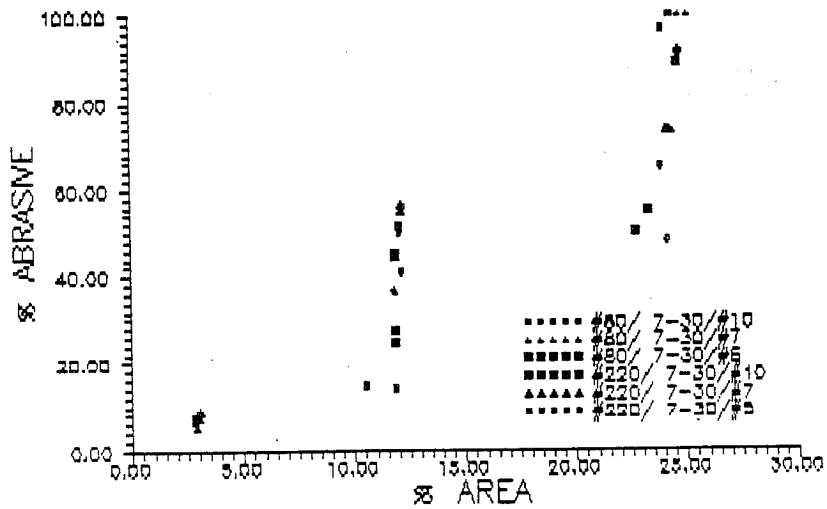

Fig. 13 CORRELATION BETWEEN PERCENT AREA CHANGE WITH PERCENT MIXTURE FLOW. Sapphire D= 0.010 in., Carbide D= 0.030 in.

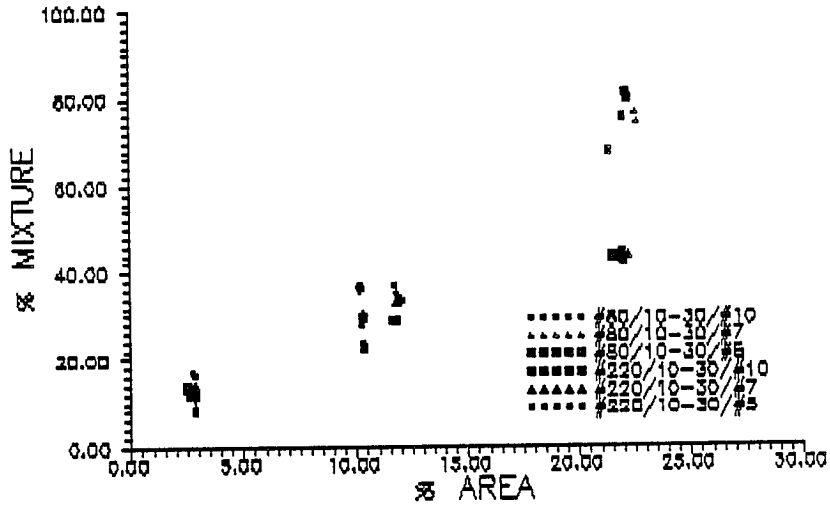

Fig. 14 CORRELATION BETWEEN PERCENT AREA CHANGE WITH PERCENT MIXTURE FLOW. Sapphire D= 0.007 in., Carbide D= 0.030 in.

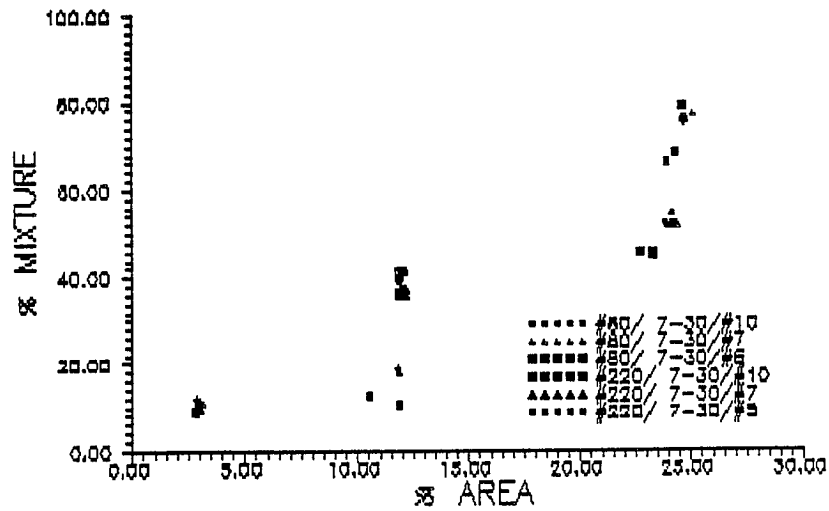

5th American Water Jet Conference
August 29 - 31, 1989: Toronto, Canada

Paper / Communication 22

"WATERJET CUTTING IN A PRODUCTION ENVIRONMENT"

THREE CASE HISTORIES:

AUTOMOTIVE BUMPERS
CARPETING
PRINTED CIRCUIT BOARDS

D.E. Snider
Water Jet Specialties Inc.
Burlington, Ontario L7M 1A6, Canada

ABSTRACT: Waterjet cutting methods cover a vast spectrum of applications in a variety of industries. This short synopsis depicts three automotive related applications previously involved with conventional cutting tools and manual operation.
Progressive industrial involvement with automated machinery employ the waterjet process into some unique production workcells.
No longer a curiosity, 24 hour production lines have verified the process and hardware reliability, as well as convincing ourselves this tool is no longer "non-conventional".

RÉSUMÉ : Les méthodes de coupe par jets d'eau couvrent une vaste gamme d'applications dans une variété d'industries. Ce résumé décrit trois applications dans l'industrie de l'automobile qui nécessitaient auparavant des outils de coupe classiques et des opérations manuelles.
L'introduction progressive dans l'industrie de machines automatisées comporte l'utilisation de jets d'eau dans certaines étapes de production particulières. Ce n'est plus une nouveauté! Des lignes de production fonctionnant 24 h sur 24 ont vérifié la fiabilité des méthodes et du matériel, et nous ont convaincu que cet outil n'est plus "expérimental".

Organized and Sponsored by the National Research Council of Canada and the U.S. Water Jet Technology Association.

1.0 INTRODUCTION

1.1 BACKGROUND

New materials, higher production quotas, and intricate profiling manipulation are only a few overwhelming challenges posing considerable problems to traditional methods of cutting. Streamlining manufacturing processes and technology is a key to economic global competitiveness and selecting the right technology depends on reviewing the benefits.

Concentrating and sustaining the 40 or 60 horsepower resulting in a needle-like jet stream takes some thought into fixture design and wearability of all components. The ability to cut omnidirectionally without shock, vibration, or thermal deformation with little vertical or lateral forces enhances the process economics. Flexibility, reduced costs for tooling, fixturing, re-finishing and material savings are added benefits. Environmentally, the compressive shear of the jet eliminates airborne dust for a cleaner work area. The following case histories have taken advantage of all or a combination of the above benefits.

2.0 ABRASIVEJET AND WATERJET CUTTING WORK TOGETHER TO INCREASE PRODUCTIVITY

2.1 THE PROBLEM

A leading Canadian manufacturer supplies carpets for automobile interiors. With yearly design changes and improved, tougher carpet materials, they needed an economical and efficient way to produce the premolded carpeting pieces.

Automobile carpeting is like regular carpeting except for a layer of epoxy on the bottom. A blank of the carpet is placed on a three-dimensional, contoured aluminum-epoxy resin mold that has precut openings for seat supports, seat belt boltdowns, and so on. Each mold has an integral set of cooling-water pipes underneath.

A heated press conforms the carpet to the mold until the epoxy melts. Then the cooling-water circulated in the pipes lowers the temperature until the epoxy hardens to hold the carpet into the required contours after the press is removed. Workers trimmed the excess carpet away from the outside edges and inside openings by hand using carpet knives - a tedious, slow, and eventually painful process for the employees.

The new carpet materials proved almost impossible to cope with by hand. In addition to the heat and fumes, the three-dimensional contours and tough material caused so much wrist fatigue that production was unacceptably slow. The company cared about their workers' comfort and safety, and they were particularly worried by the high employee turnover rate and the many wrist-injury claims that resulted from this hard work.

2.2 THE SOLUTION

The workcell developed with this user consists of retooling an existing robot (see Figure 1) with a high pressure waterjet nozzle. The integration is powered by a 40 H.P. electronically shifted intensifier pump and high pressure robot swivels are carefully installed at the key robot axis centerlines. This allows the nozzle flexibility to contour a three dimensional plane throughout the full robot work envelope maximizing its payback. The cutting pressure is 3500 bars using a 0.23 mil. (.009") sapphire at 1200 mm per second.

Designing in safety is an ultimate priority. This workcell, as well as many others, incorporates optical and tactile sensors that can instantly abort movement and pressure.

The waterjet follows the same cutting path slats previously used by the manual knife slitters. The mold itself required only a catcher pan for the water and Kerf material.

Additional cost savings for new mold slotting was an unexpected benefit for this user. The preformed carpet mold base arrives on-site as a 3-D "blank". The waterjet nozzle is fitted with an abrasive mixing chamber and the robot tool center point is reprogrammed. This operation consists of a multi-pass procedure whereas the mold can vary in thickness from 15mm to 100mm of Aluminum-Epoxy. Careful monitoring of the abrasive flow rates ensure the interior cooling system is not damaged.

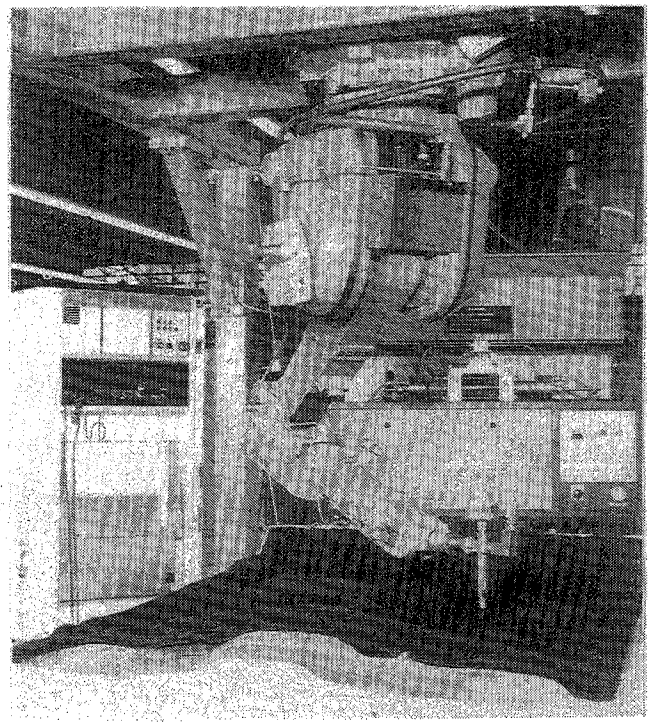

FIGURE 1

3.0 WATERJET CUTTING SAVES RETOOLING COSTS OF NON-STANDARD PARTS.

3.1 THE PROBLEM

A leading manufacturer of extruded, high-impact plastic automobile bumpers had to supply a non-standard bumper to meet the automobile maker's demand for a limited edition sports car model. The front bumper needed precise modification by adding four 3/4" holes and two controlled-radius scallop cuts to clear headlamp housings. In addition, two 18" linear cuts were needed to remove two 3" ledges, leaving behind a perfectly smooth face on the inside corners.

With only a few thousand units required, the company couldn't justify the high cost of retooling their extrusion process to produce this special part. They considered modifying an existing bumper design by hand. However, the intricate contouring of the tough bumper material would have increased labour costs and manual inaccuracies, which made this alternative equally unattractive.

The company needed a fast and economical way to modify a standard extruded bumper to meet their customer's demand for this special, limited edition design.

3.2 THE SOLUTION

The waterjet cutting tool cuts in any direction - even tight inside corners - and uses the full capability of robotic manipulation that is often limited by the geometry of a mechanical tool.

The workcell involved a 25 H.P. intensifier pump at 3700 bar, and plumbing an articulated arm robot (see Figure 2) with the high pressure nozzle and designed a special 0.20 (.008") coned orifice. This patented design retained the waterjet's coherence, so it could cut the required contour up to three inches away from the nozzle position. The system included optical position sensing, and vacuum and operator safety interlocks. (see Figure 3) The controls were easy to operate, and the low thrust of the waterjet cutting tool eliminated the need for elaborate part-support structures.

The waterjet's speed was impressive and its omnidirectional cutting ability even made it possible to remove the two 18" ledges from the inside corners flush to the vertical face without leaving a ridge. No additional hand finishing was needed.

The company found the waterjet cutting tool enabled them to program precise, intricate changes to a standard product without retooling.

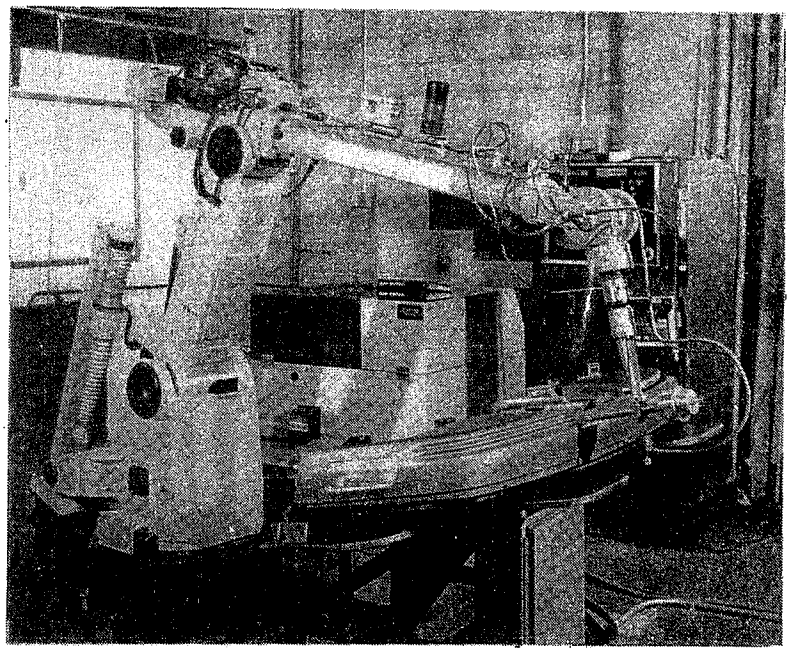

FIGURE 2

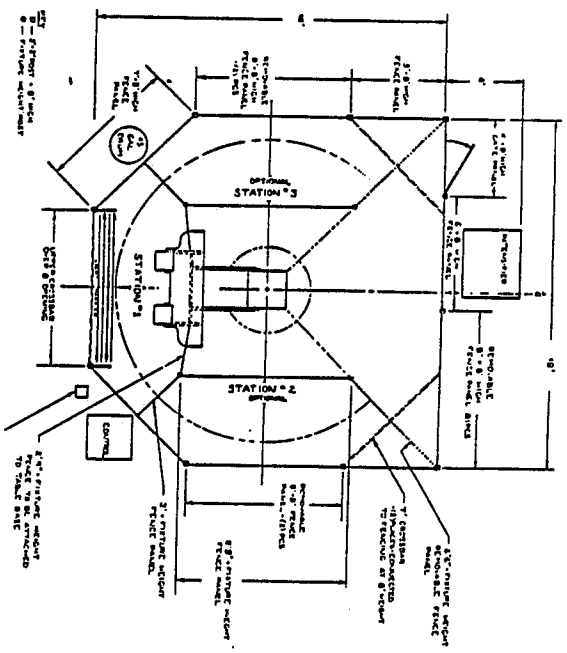

FIGURE 3

4.0 WATERJET CUTTING SAVES MONEY AND DOUBLES PRODUCTIVITY

4.1 THE PROBLEM

A major automotive electronics manufacturer in Toronto produces electronic components and printed wiring boards (PWBs). After assembling surface-mounted components and circuitry on 29-, 21- and 16-boards, they used a routing drill to cut peripheral slots defining the individual circuit boards. This process left small tabs that had to be sheared by hand or with drop shears to divide the master panels into individual circuit boards.

Tab removal by this stop and go method was too slow for the company's high production rates. Manual shearing caused operator fatigue problems, and they lost time and money replacing worn out shearing blades at a high cost.

Worse, the component connections on these PWBs are extremely sensitive to a variety of hazards in the production process. Shocks, bending, vibration, heat and dust all contributed to unacceptably high reject rates. Dulling shears and too frequent handling caused microscopic cracks or delamination, which also resulted in numerous rejects.

The company needed a fast, clean and way to cut the panels into separate boards without tool wear delamination, operator fatigue, or excessive handling of the intricate circuit boards.

4.2 THE SOLUTION

The waterjet cutting tool cut the 3/32" thick panels at speeds of up to 120 inches per minute with pinpoint accuracy.

The rotary table work cell was integrated with an X-Y system and Allen Bradley Model 8400 machine tool control. A single operator loaded and unloaded the boards at the external station of a four-station rotary index table. The operator selected one of several stored cutting path programs depending upon the configuration of the joined circuit boards.

At the operator's signal, the piece was rotated first into an idle station, then into a cutting station where dual waterjet nozzles moved along continuous paths automatically programmed to separate the boards. The final quadrant of the rotary index table housed an electrostatic drying curtain.

Because the operator's hands never had to enter the cutting area while the system was on, the board separator was much safer to use than drop shears.

The 60 H.P electronic intensifier pump at 2900 boars and the hair-this diameter of the jets (typically 0.23 mil or .009") exerted little vertical or lateral pressure on the boards and created minimal kerf. The sapphire life over 330 hours is attributed to a reverse osmosis system. The nozzle never came into contact with the boards and the small amount of kerf was carried away by the waterjet and vacuum/filtration system. (See Figure 4)

This vibration-free, low-force system cut quickly without heat or delamination to the boards and the savings in routing tool replacements costs, **the system paid for itself in just five months!** The doubled production rate was a bonus.

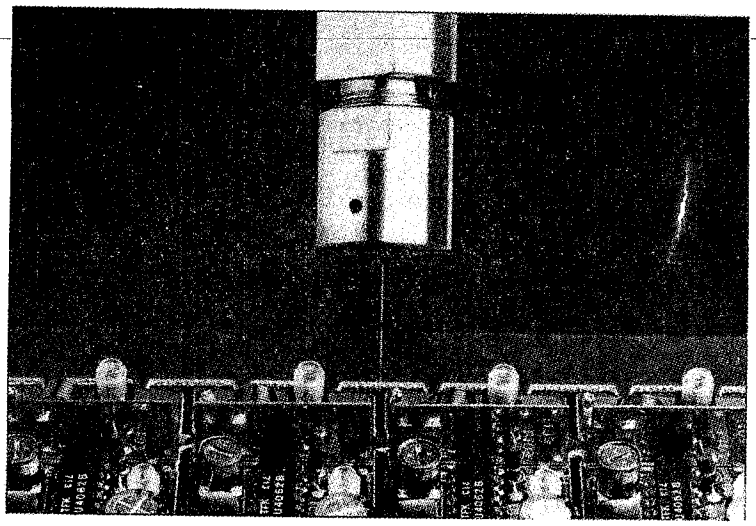

FIGURE 4

5.0 CONCLUSION

Waterjet cutting has a definitely unique niche as an industrial production tool. Feasibility of the process is initially established through parametric cutting of the part and material. Optimization of the process depends upon the hardware demands created by proper orifice sizing, pressure requirements, mechanical fatigue (RE: High speed applications and/or pressures.), etc. The human factor is above all and will remain to be, the most important factor of a successful production system. All key personnel must have a thorough understanding of the theory and mechanics of the system. Respect of the process from a safety point of view, as well as, a production uptime stance depends upon proper training instructions and understanding simple machine dynamics.

5th American Water Jet Conference
August 29 - 31, 1989: Toronto, Canada

Paper / Communication 23

JOB SHOPPING WITH WATERJET/ABRASIVE WATERJET

F.A. Patell, D.A. Scott AND K. Saari
Advanced Systems
Atomic Energy of Canada Ltd.
Mississauga, Ontario L5K 1B2, Canada

ABSTRACT: Upon starting up operations, Advanced Systems of Atomic Energy of Canada Ltd. acquired a waterjet machine with the abrasive waterjet option and an XY gantry robot for demonstration purposes. Considerable interest in the facility and its capability became apparent in the form of many requests for custom and in some cases production cutting. Late in 1988 the decision was made to promote the facility in the job shopping role and in November the doors opened for business. This paper traces briefly the evolution of AECL-Advanced Systems as it found itself in the job shopping role but of more interest, some of the lessons learned since inception.

RÉSUMÉ : Dès sa mise en exploitation, Advanced Systems de l'Energie atomique du Canada Limitée a fait l'acquisition d'une machine à jets d'eau admettant des abrasifs et d'un portique XY robotisé de démonstration. L'installation et sa capacité ont suscité un grand intérêt comme en font foi les nombreuses demandes de travaux de coupe spéciaux et parfois en série. Vers la fin de 1988, il a été décidé de promouvoir la recherche de commandes pour l'installation et, en novembre, l'installation était prête à recevoir les commandes. Cette communication retrace brièvement l'évolution d'Advanced Systems dans son rôle de recherche de commandes, mais surtout rappelle certaines leçons qui ont été tirées depuis la création du service.

Organized and Sponsored by the National Research Council of Canada and the U.S. Water Jet Technology Association.

1.0 INTRODUCTION

Waterjet/Abrasive waterjet job shopping is a material cutting or shaping service generally for small production quantities or special applications. The unique characteristics of the waterjet process lend themselves to applications demanding complex contours and shapes, materials otherwise difficult to cut, and wherever surface finish, thermal effects and work hardening are critical factors. Some of these characteristics are noted below:

- The waterjet is omnidirectional, enabling fully automated three–dimensional cutting and almost unlimited creative potential.

- Due to a relatively narrow jetstream, the kerf width is relatively small, resulting in higher yields.

- Waterjet is a beam cutting technology versus mass removal methods such as drilling or machining. This results in significantly greater cutting and energy efficiencies.

- The process imparts minimal force in any direction. This virtually eliminates work hardening of the cut edge, while permitting the cutting path to come very close to the work piece edge without tearing it. This also eliminates ragged or crushed edges on softer materials such as non wovens, and greatly simplifies material handling.

- Extremely low heat generation makes it ideal for cutting thermally sensitive materials. Metals don't require post heat treating, and plastic edges are not melted.

- The waterjet carries away kerf, eliminating airborne dust.

- As a fully programmable beam technology, waterjet minimizes tooling and set up requirements making it ideal for a J.I.T. environment.

- Waterjet produces a high quality cut edge, reducing the need for finishing or grinding operations.

- Waterjet integrates several processes (e.g. drilling, cutting, bevelling, machining), thereby reducing the number of workstations in most manufacturing situations, resulting in improved efficiency and product quality.

- Waterjet and Abrasive waterjet are applicable to almost every type of material in existence, making them the most versatile of all cutting technologies.

2.0 BACKGROUND

AECL Advanced Systems (referred to elsewhere as Advanced Systems) was formed at the start of 1986 to provide engineering skills for industrial automation and turnkey integrated solutions. This was part of a corporate diversification strategy. It was decided to acquire Waterjet facilities and technology shortly after the inception of Advanced Systems, as a key part of an overall market entry programme.

Waterjet was chosen for various reasons as noted herein.

(i) As a technically well developed but commercially emerging technology, it blended well with existing resources and business objectives.

(ii) Being an omnidirectional beam cutting technology, it was readily adaptable to computer and robotic integration, making it a ideal example of an automated work cell, attractive to modern flexible manufacturing concepts.

(iii) While the process technology was well proven, its application to specific needs was evolutionary, lending itself to Advanced Systems' focus on solution engineering.

(iv) The technology required a high level of technical competency to be successfully utilized and integrated with complimentary systems. This was perceived as a good fit with Advanced Systems resources.

(v) Acquiring the equipment would enable the development of new applications as well as provide a customer demonstration facility.

Once the system was purchased and installed, work commenced for various potential clients and applications. Interest grew in the unique abilities of the waterjet process, and increasing requests for custom cutting of difficult materials were received. This resulted in a greater depth of knowledge and experience with waterjet and abrasive waterjet applications. The concept of strategic materials for waterjet and abrasive waterjet evolved out of this experience. Simply stated, this identified certain materials and applications which were the most technically and commercially feasible candidates for this process; e.g., glass, ceramics, Stellite, or other high value added applications. At the same time, it seemed that job shopping could provide a more immediate return on our capital investment than the commercially evolving market for turnkey systems. This complemented our systems strategy, and resulted in the evaluation of various job shop models. Some of them were as follows:

(i) A stand alone, general purpose job shop.

(ii) A client already involved in a target industry for job shopping, who could operate a general purpose job shop when not using it for their product.

(iii) A strategic material or related industry job shop; e.g., a glass cutting job shop which could also handle stone or marble, etc.

In consideration of the above Advanced Systems elected to undertake the stand alone, general purpose job shop at its own facilities. This would make further use of the existing technical and capital equipment resources, while keeping Advanced Systems on the cutting edge of this technology.

3.0 SYSTEM DESCRIPTION

The design and selection of the system was based on the following parameters.

(1) **Versatility:**

The System was to be versatile in terms of cutting ability and materials handling. This led to the selection of an x–y gantry robot, to move the jet across the work piece with speed, accuracy and repeatability. The waterjet

intensifier, (i.e. the water pressure generator), was also sized with this in mind. It was decided to add the abrasive waterjet option so as to include a much wider range of materials to be cut, and hence a broader spectrum of potential systems applications.

(2) **Marketability:**

The system was to be representative of the type most commonly needed in industry. This affected the robot design earlier mentioned, performance requirements such as speed, accuracy, repeatability, and work envelope. This also affected cost and price considerations.

(3) **Quality:**

It was decided to purchase high quality components such that the system's performance would not be compromised and so that the inherent process advantages could be fully realized.

The equipment selected for integration into the waterjet cutting facility consisted of the following, as illustrated in Table 1. The entire facility as currently in use is shown in Figure 1.

4.0 TYPICAL JOBS COMPLETED

Laminated Plate Glass:

This job involved various cut outs and shapes from 5 FT. x 9 FT. (1.5m x 2.7m) sheets of 1" (25 mm) laminate. The purpose of these sheets of glass was to serve as the structural and display walls of interactive kiosks for a major international business development. Figure II shows a photograph of one of these panels after abrasive waterjet cutting. Figure III shows a close up of a curved cut edge shape.

The single greatest challenge in abrasive waterjet cutting of glass sheets is the materials handling aspect. Improper handling results in cracking and breakage during the cutting operation. However, when properly handled, there is no cause for concern, and the resulting cut produces a smooth edge requiring minimal surface finishing.

Flat Rolled Stellite:

Several orders have been completed involving rectangular, wedge, ring and disc shaped cuts out of 1/4" to 1/2"(6mm to 13mm) thick Stellite sheet. This costly material is especially well suited to abrasive waterjet cutting. Conventional cutting of Stellite involves abrasive sawing and grinding, processes which are slow and generate considerable waste; (at $200 to $300 per pound, this is a critical factor). Abrasive waterjet leaves a smooth cut edge, virtually eliminating the need for grinding after cutting. It also removes far less material during the cut. The net effect is significant time and materials savings for the customer. Nesting of parts is easily accomplished with the system's computer capabilities.

Granite and Marble:

Abrasive waterjet is certainly the process of choice for cutting and shaping granite and marble. The ability to cut complex shapes in brittle materials without mechanical shock damage is highlighted in these applications. Jobs undertaken include black granite logos inlaid in white marble.

Polished Brass: (Figure IV)

Several jobs have involved cutting out company or product logos for display signs. These are generally complex shapes, and require the CIMEX hardware and software to generate the necessary controller code for the ESAB robotic gantry.

Miscellaneous Materials:

Rubbers, plastics, ceramics composites, metals and alloys, magnetic materials and food products, are some of the other materials cut with Advanced Systems' waterjet or abrasive waterjet. However, since the inception of the job shop, the real demand has been for abrasive waterjet cutting. Most waterjet applications, (as opposed to abrasive waterjet), tend to be dedicated, high volume production units, (as in diaper cutting or fiber insulation slitting). Thus, the main focus in job shopping will probably continue to be abrasive waterjet cutting.

5.0 LESSONS LEARNED

Several items need to be addressed when setting up a waterjet system. The first and most obvious is that sufficient space must be provided for getting the items to be cut onto the work table. However, if possible provision should be made for handling items larger than the work table by the use of table extensions.

Secondly, the environmental factors of noise and overspray and splashing need to be addressed in the overall system design.

Noise is controlled by limiting the path of the waterjet through air, by proper design and placement of a catcher tank.

Overspray and splashing can be accommodated by means of vacuum suction piping at the source, as well as proper ventilation, and wash down with a spray hose fixture.

Other observations on the operation of a job shop include the following.

- Regular preventive maintenance of the major mechanical components is of great importance, preventing costly downtime and ensuring the system's longevity. The manufacturer's instructions are quite adequate in this regard.

- Set up time can easily be underestimated, even though the overall process is low on this requirement as compared to others. Programming the shape to be cut and doing test cuts prior to the job are most commonly underestimated. This can be due to inadequate definition of the requirements or unfamiliarity with the software's programming requirements.

- Cost considerations must cover capital equipment, fixed overheads, and variable overheads including operating costs. Operating costs must account for power usage, water supply, effluent disposal, abrasive, and normal wear parts such as nozzles and orifices.

TABLE 1

SYSTEM DESCRIPTION

Functional Items Description	*Make and Model*
55000 psig (379 MPa) Ultra High Pressure Intensifier Pump	Flow Systems Model 11X
Abrasive Jet Delivery System	Flow Systems Model 425 Paser™
Computer Numerical Control for ESAB Robotic Gantry	ESAB Auto–Path GX
X–Y (2 Axis) Robotic Gantry	ESAB Silver Bullet
Computer Integrated Manufacturing System (to automatically generate the tool path for down loading directly into the CNC robotic controller). (Acquired later).	CIMEX Line Tracer

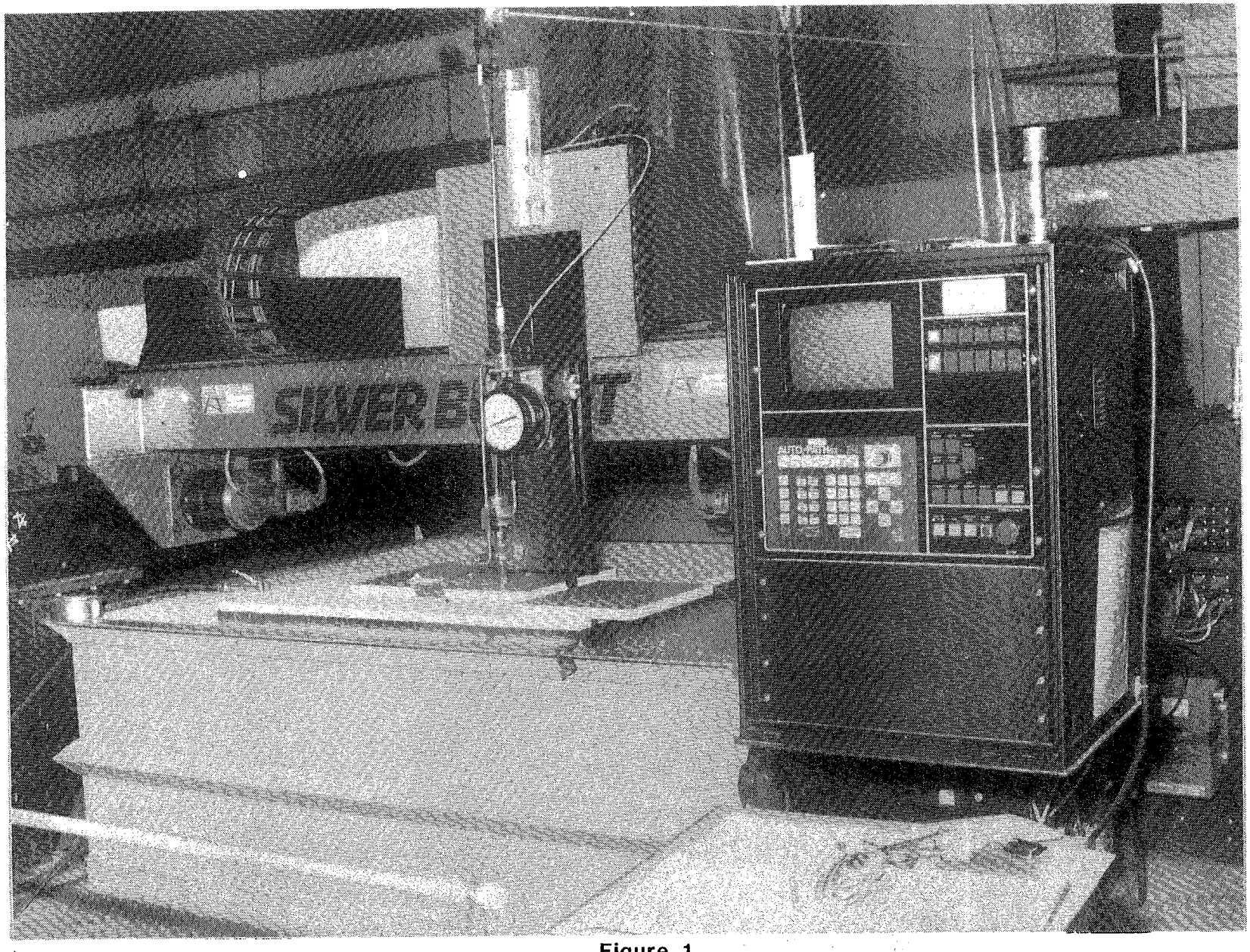

Figure 1

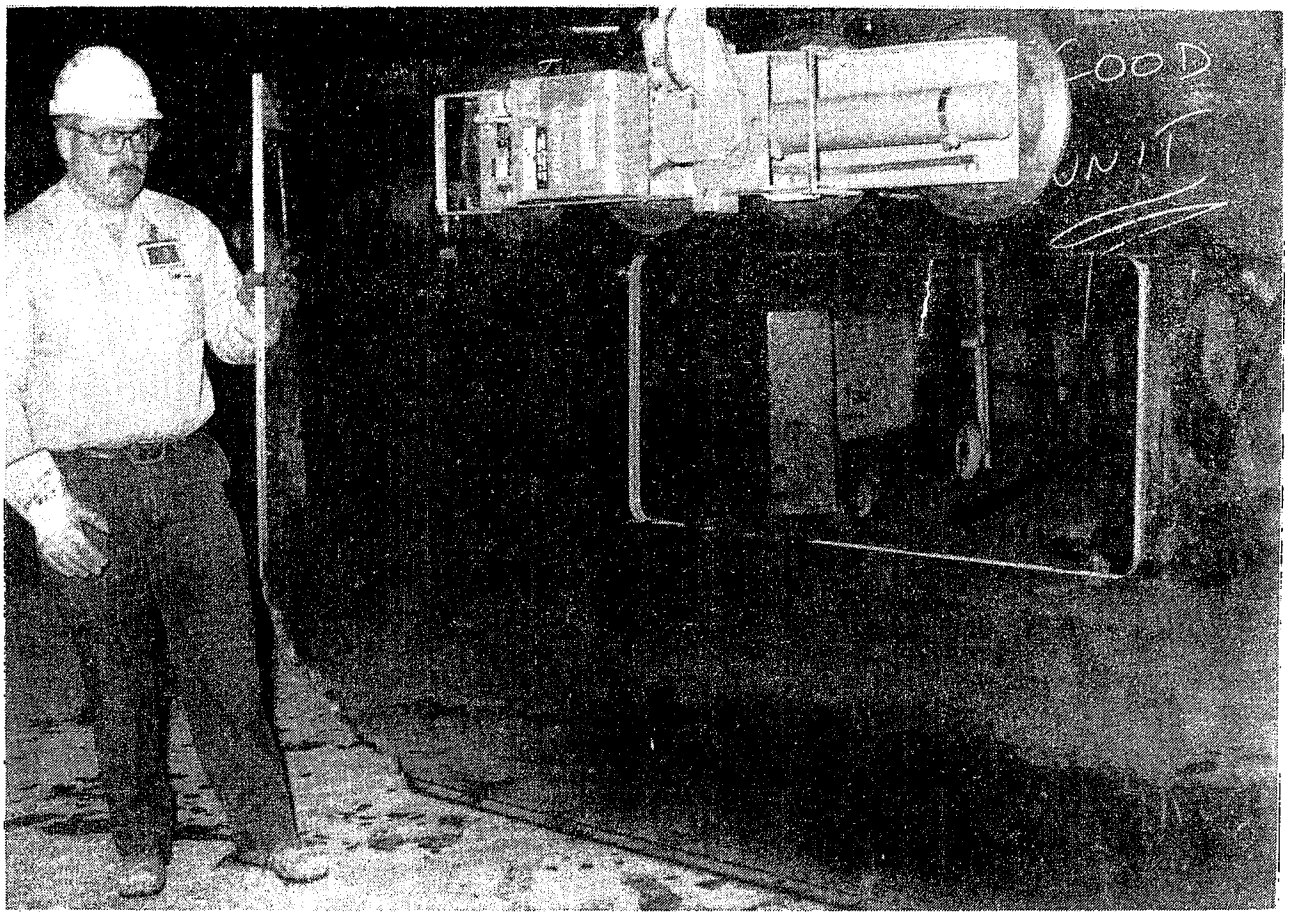

Figure 2

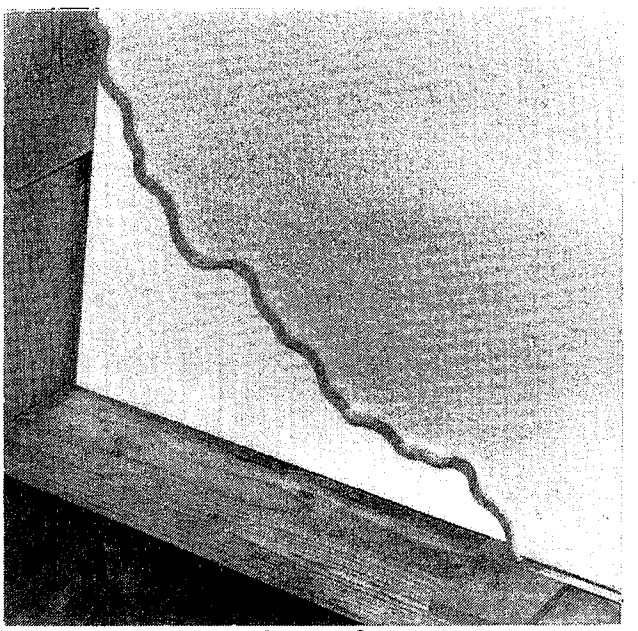

Figure 3

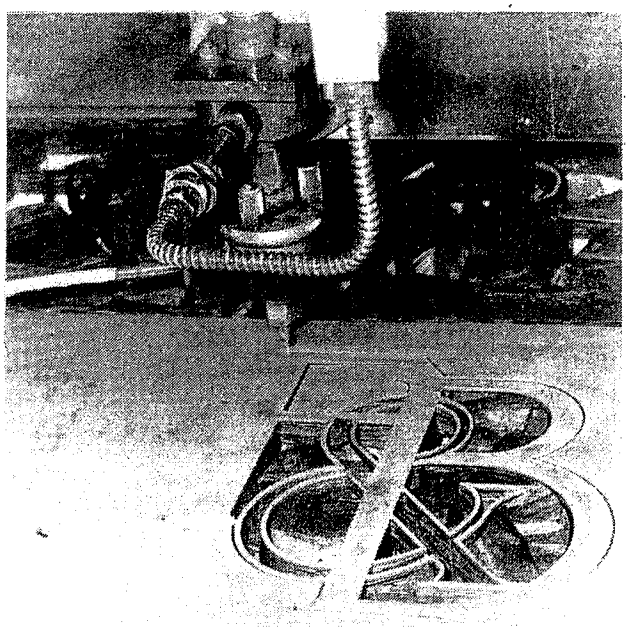

Figure 4

5th American Water Jet Conference
August 29 - 31, 1989: Toronto, Canada

Paper / Communication 24

PRECISION CUTTING WITH A LOW PRESSURE, COHERENT ABRASIVE SUSPENSION JET

R.H. Hollinger, W.D. Perry AND R.K. Swanson
Instrumentation and Space Research Division
Southwest Research Institute
San Antonio, TX 78284, USA

ABSTRACT: Conventional water/abrasive jet cutting relies upon entrainment of abrasive particles in a water jet. The abrasive and high velocity water are combined in a mixing chamber and subsequently refocused through a focusing tube or "director nozzle". Significant velocity and energy losses occur in this process, the flow is turbulent and the jet is divergent. Since the focusing tube has a much larger diameter than the primary orifice, kerf widths are relatively large. By mixing the abrasive with properly treated water prior to pumping, the mixture can be pumped directly through a small orifice resulting in higher individual particle velocity and greatly improved efficiency. The high-viscosity suspending medium (treated water) yields a coherent jet at the reduced pressures required and little divergence occurs before impingement on the target. Under such circumstances, narrow kerfs are produced with greatly reduced cutting pressures and total flow rates, compared to conventional water/abrasive jet performance.
In this paper, examples are shown in which an abrasive suspension of this kind, pumped through a 0.25 mm (0.01 in.) diameter diamond orifice, produces a cut through 6 mm (0.25 in.) steel plate with a kerf width of about 0.8 mm (0.03 in.), with a total pressure of 7500 psi. Similar cuts have been made in brass, aluminum, glass and composite materials at pressures between 3000 and 7500 psi.
In other experiments using the abrasive suspension-jet technique with smaller orifices, cuts with kerf widths of only .075 to 0.10 mm (0.003 to 0.004 in.) through quartz wafers only 0.15 mm (0.006 in.) thick have been produced. In these experiments, the working pressure was limited to only 5000 psi.
Current work involves an investigation of the rheological and flow properties of these suspensions, and the effect of orifice configuration as a function of pressure, on jet coherence and overall cutting performance.
The coherent, abrasive suspension-jet cutting technique shows great promisé for precision cutting of small parts to relatively close tolerances, and for cutting materials which are difficult to cut by other methods. Equipment promises to be relatively small, lightweight and inexpensive.

RÉSUMÉ : La coupe classique par jet eau-abrasif est basée sur l'entraînement de particules abrasives dans un jet d'eau. L'abrasif et l'eau à haute vitesse se combinent dans une chambre de mélange pour ensuite s'aligner dans un tube de mise au point ou une "buse directrice". Des pertes importantes de vitesse et d'énergie se produisent dans ce processus, l'écoulement est turbulent et le jet est divergent. Comme le tube de mise au point a un diamètre beaucoup plus grand que celui de l'orifice, les traits obtenus sont relativement larges. En ajoutant l'abrasif dans une eau convenablement traitée avant le pompage, le mélange peut être pompé directement dans un petit orifice, ce qui augmente la vitesse des particules et améliore grandement le rendement. Le milieu de suspension très visqueux (eau traitée) produit un jet cohérent aux basses pressions requises, jet qui diverge avant d'atteindre la cible. On obtient ainsi des traits étroits avec des pressions de coupe et des débits totaux beaucoup moindres que ceux des jets eau-abrasif classiques.
Cette communication renferme des exemples dans lesquels une suspension abrasive de ce genre, pompée au travers d'un orifice de 0,25 mm de diamètre, permet de découper une plaque d'acier de 6 mm avec une largeur de trait de 0,8 mm environ, à une totale de 7500 lb/po^2. Des coupes semblables ont été réalisées dans du laiton, de l'aluminium, du verre et des matériaux composites à des pressions comprises entre 3000 et 7500 lb/po^2.
Dans d'autres expériences, la technique des jets de suspension abrasive au travers d'orifices plus petits a produit des coupes avec des traits de seulement 0,075 à 0,10 mm de large dans des disques de quartz de seulement 0,15 mm d'épaisseur, à des pressions limitées à seulement 5000 lb/po^2.
Les travaux en cours portent sur une étude des propriétés rhéologiques et d'écoulement de ces suspensions, et de l'effet de la géométrie de l'orifice en fonction de la pression sur la cohérence du jet et son rendement global en coupe.
La technique de coupe au jet cohérent de suspension abrasive semble très prometteuse pour la coupe de précision de petites pièces avec des tolérances assez faibles et la coupe de matériaux difficiles à couper par d'autres méthodes. Le matériel s'annonce relativement peu encombrant, léger et peu coûteux.

Organized and Sponsored by the National Research Council of Canada and the U.S. Water Jet Technology Association.

1.0 INTRODUCTION

1.1 Background

In the field of high pressure water jet cutting, efforts have been made to reduce the divergence of the water jet through orifice, or nozzle, design and the use of water soluble polymer additives. Nozzle design has concentrated on the shaping of the orifice entrance to reduce turbulent entrance effects, and the water soluble polymers enhance the flow of fluid at a given pressure. In some cases, polymeric additives do seem to improve jet coherence in that more fluid is contained in the core of the jet and less in the surrounding cone. The jet, however, remains turbulent.

The water/abrasive jet, used in the cutting of metals, composites, rock, and masonry, utilizes a conventional, turbulent flow, free jet of water which is introduced into a mixing chamber. Abrasive particles are aspirated into the mixing chamber, entrained in the jet, and the whole is re-formed into a larger diameter, turbulent flow, free jet by means of a focusing tube. Mixing inefficiencies lead to abrasive particle velocities less than that of the jet core, (1) and the increased diameter of the focusing tube reduces the exit velocity of the re-formed jet. The velocity of the re-formed jet may be increased by increasing the orifice flow into the mixing chamber. This is effective until the flow is sufficient to flood the chamber and stop the abrasive particle feed.

Recently, Southwest Research Institute has devised a method of pumping a water/abrasive mixture directly through an orifice to form a free jet in which the abrasive particles are accelerated, together with the water, to the jet velocity dictated by the orifice diameter, the driving pressure, and the orifice coefficient. In order to prevent the abrasive from settling in the flow lines and reservoir, different polymeric additives were used to increase the viscosity of the water. The free jets formed by these solutions were not divergent at pressures where ordinary free jets are divergent, but were coherent and showed no outer cone. Cuts made with these abrasive suspension jets show narrower cut widths than with conventional water/abrasive jets and use lower pressures.

1.2 Suspension Preparation

Three methods for suspending abrasive particles were studied: (1) the use of a gel; (2) the use of a microemulsion; and (3) the use of a high viscosity water solution of a polymer.

The gel based suspension proved unsatisfactory since preparation of the suspension required up to six hours, and the abrasive particles tended to concentrate along the "threads" of the gel structure as the gel began to set. The high local concentration of particulates would cause orifice clogging.

The microemulsion, or high internal phase emulsion, would have required more investigation than time permitted, and, while still a viable alternative, further work was set aside in favor of high viscosity solutions.

The use of a high viscosity solution as the suspending medium is based on the Stokes' law settling velocity of spherical particles. If the solution viscosity is high enough, the settling velocity will be so low that a practical suspension is achieved. Methyl cellulose solution and a solution of a commercially available thickening agent[1] were used to form suspensions of garnet sand in two size ranges, 53 - 75 micrometers diameter and 75 - 106 micrometers diameter. The apparent viscosities of the two solutions are shown in Table 1. In both cases, the solutions are shear thinning when measured in the low shear region by rotational viscometer. By Stokes' law, if a settling velocity of five millimeters per hour is used for a garnet particle of 106 micrometers diameter, a solution apparent viscosity of 12700 centipoises is required. The two weight percent methyl cellulose solution easily exceeds this value within the measured range, while the commercial thickener, at a weight concentration of 1.5 percent, approaches the required value at low shear rates. The high viscosities thus keep the particles suspended when the solution is at rest or only lightly sheared, but the shear thinning effect makes the suspension easily pumpable.

---

[1]Super Water™, Berkeley Chemical

TABLE 1. VISCOSITY OF POLYMER SOLUTIONS

Spindle Speed (RPM)	Apparent Viscosity (Centipoises) 2% Methyl Cellulose[1]	1.5% Commercial[2]
20		1,730
20	14,700	2,768
10	21,250	5,450
4	28,200	9,300

[1]Brookfield No. 4 spindle
[2]Brookfield No. 2 spindle

1.3 Apparatus

In order to pump the abrasive suspension, the apparatus shown schematically in Figure 1 was used. The use of a floating piston cylinder allows steady flow of the suspension at the pressure dictated by the high pressure intensifier setting. Multiple cylinders can be used in order to have continuous flow.

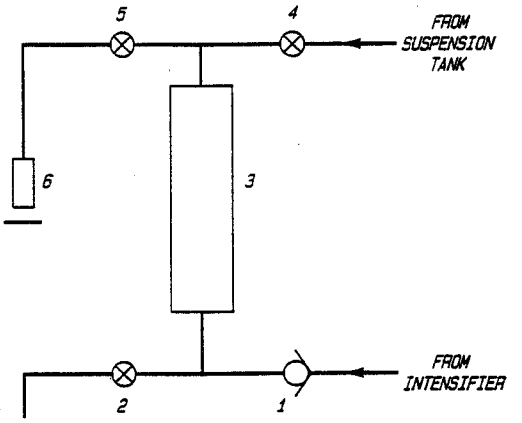

1. INLET CHECK VALVE
2. DEPRESSURIZING VALVE
3. FLOATING PISTON CYLINDER
4. SUSPENSION CHARGING VALVE
5. SUSPENSION OUTPUT VALVE
6. ORIFICE AND ORIFICE HOLDER

Figure 1. Abrasive Suspension Jet Schematic Diagram

The orifices used for the coherent abrasive suspension jet are single crystal, diamond wire drawing dies with housings modified to create high pressure edge seals. Standard sapphire orifices show excessive wear in from three to four minutes when used with the suspension at jet velocities of 254 meters per second (833 feet per second).

2.0 EXPERIMENTAL

2.1 Abrasive Suspension

The abrasive suspension used in cutting various substrates of 0.635 centimeters (0.25 inches) thickness was composed of 1.5 weight percent commercial thickener, and garnet abrasive in the 75 - 106 micrometer diameter range at a weight concentration of 105.7 grams per liter (0.88 pounds per gallon) of thickened water. For an orifice having a diameter of 254 micrometers (0.01 inches), higher abrasive concentrations or larger particle sizes, led to orifice clogging.

2.2 Cutting with the Coherent Abrasive Suspension Jet

The results of cutting tests using five different substrates are summarized in Table 2. The suspension jet was capable of cutting through all substrates, except steel, at 51.67 MPa (7500 psi) at a traverse speed of 10.2 centimeters per minute (4.0 inches per minute). Penetration of steel required a 50 percent reduction in traverse speed.

TABLE 2. CUTTING VARIOUS SUBSTRATES WITH COHERENT ABRASIVE SUSPENSION JETS

Substrate	Pressure, MPa (PSI)	Cut Depth, % Thickness[1]	Kerf Width, CM (IN)
Aluminum	51.7 (7,500)	100	< 0.079 (< 0.031)
Aluminum	69.0 (10,000)	100	0.079 (0.031)
Aluminum	103.4 (15,000)	100	0.16 (0.062)
Mild Steel	51.7 (7,500)	50	< 0.079 (< 0.031)
Mild Steel	69.0 (10,000)	66	0.079 (0.031)
Mild Steel	86.2 (12,500)	50	0.16 (0.062)
Mild Steel	103.4 (15,000)	40	0.16 (0.062)
Mild Steel	(51.7) (7,500)[2]	100	< 0.079 (<0.031)
Plate Glass	51.7 (7,500)	100	0.079 (0.031)
	103.4 (15,000)	100	0.32 (0.125)
Yellow Brass	51.7 (7,500)	100	< 0.079 (< 0.031)
Lead	51.7 (7,500)	100	0.079 (0.031)

[1]Substrate thickness was 0.635 centimeters (0.25 inches).
[2]Traverse speed was 5.1 centimeters per minute (2.0 inches per minute).

At the lowest pressures, kerf widths are 0.079 centimeters (0.031 inches) or slightly less. Above 69 MPa (10,000 psi), kerf widths grow larger indicating a loss of jet coherence. The loss of coherence is best illustrated in the data for steel, where not only do kerfs grow wider, but penetration decreases. At 103.4 MPa (15,000 psi) penetration is actually less than at 51.7 MPa (7,500 psi).

A comparison of the conventional water abrasive jet (WAJ) and the abrasive suspension jet (ASJ), based on cuts in steel, is shown in Table 3. The cuts are made through 98-100 percent of a 0.635 centimeter (0.25 inch) thickness of steel using a 0.0254 centimeter (0.01 inch) orifice for both jets. The conventional jet used a 0.11 centimeter (0.045 inch) diameter focusing tube. The suspension jet uses less power and abrasive per unit length of cut but has a slightly higher water use per unit length of cut. This is chiefly a result of a higher orifice coefficient resulting from the polymeric additive (WAJ, c_o = 0.67 ASJ, c_o = .79), and the slower traverse speed.

TABLE 3. COMPARISON OF WATER ABRASIVE JET AND ABRASIVE SUSPENSION JET CUTTING

	Conventional Jet (WAJ)	Suspension Jet (ASJ)
Pressure	206.9 MPa (30,000 psi)	51.7 MPa (7,500 psi)
Traverse Speed	10.2 cm/min (4 in/min)	5.1 cm/min (2 in/min)
Power	65.7 kcal/min	9.4 kcal/min
Power/cm	6.4 kcal/min/cm	1.8 kcal/min/cm
Abrasive Consumption	271 grams/min	81.6 grams/min
Abrasive Consumption/cm	26 grams/cm	16 grams/cm
Abrasive Used	60/80 grit garnet	75 - 106 micrometer garnet
Abrasive Concentration or Flow	271 grams/min	102.9 grams/L
Water Use/cm	0.129 L/cm	0.152 L/cm
Kerf Width	0.16 cm	< 0.079 cm

Figures 2 and 3 show cuts in aluminum and steel at a traverse speed of 10.2 centimeters per minute (4 inches per minute) using a conventional jet (WAJ) at 206.9 MPa (30,000 psi) and the suspension jet (ASJ) at 51.7 MPa (7,500 psi).

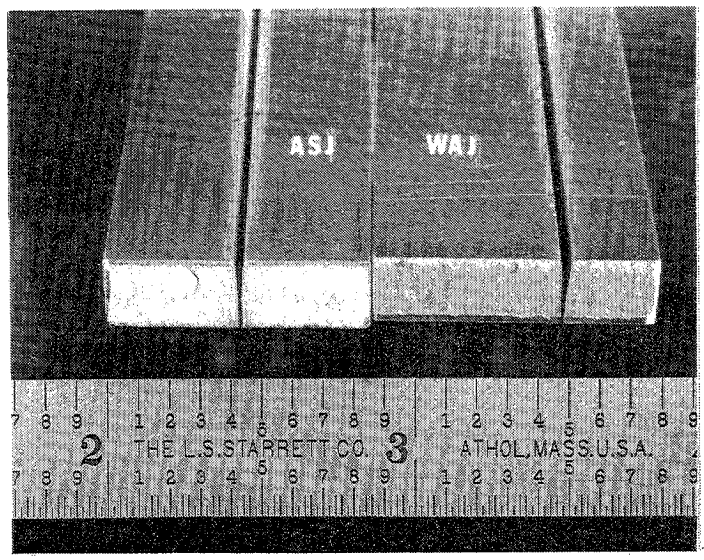

Figure 2. Cuts in Aluminum

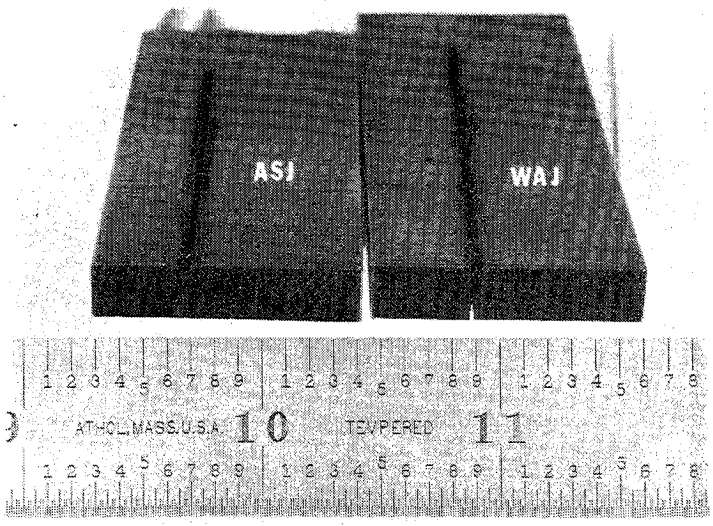

Figure 3. Cuts in Steel Plate

3.0 MICROJET CUTTING

3.1 Background

The coherent abrasive suspension jet opens an area for precision cutting that is, at best, difficult with the conventional jet. The use of a fine size abrasive suspension and a small diameter diamond orifice produces extremely narrow kerfs. The kerf for a conventional abrasive jet is limited by the diameter of the focusing tube and the ability to feed fine size abrasive powders.

3.2 Experimental

In order to make precision cuts through 0.015 centimeter (0.006 inch) thick gold coated quartz wafers, a suspension of 10 micrometer alumina abrasive was prepared.. A 1.5 weight percent proprietary thickener with water formed the suspending medium, and the alumina concentration was 26.4 grams per liter (0.22 pounds per gallon). With a 0.0076 centimeter (0.003 inch) diameter orifice, a traverse speed of 1.27 centimeters per minute (0.5 inches per minute), and a pressure of 34.5 MPa (5,000 psi), cuts with kerf widths of 0.008 - 0.010 centimeters (0.003 - 0.004 inches) were obtained. Figure 4 shows two parallel cuts in gold coated quartz spaced only 0.03 centimeters (0.011 inches) apart. Closer cuts can be made depending on the precision of the positioning mechanism. Figure 5 is a scanning-electron micrograph of one of the cuts and illustrates the extremely narrow cut width. Other precision cuts have been made in 0.094 centimeter (0.037 inch) thick glass (Figure 6) and in 0.32 centimeter (0.125 inch) thick glass (Figure 7).

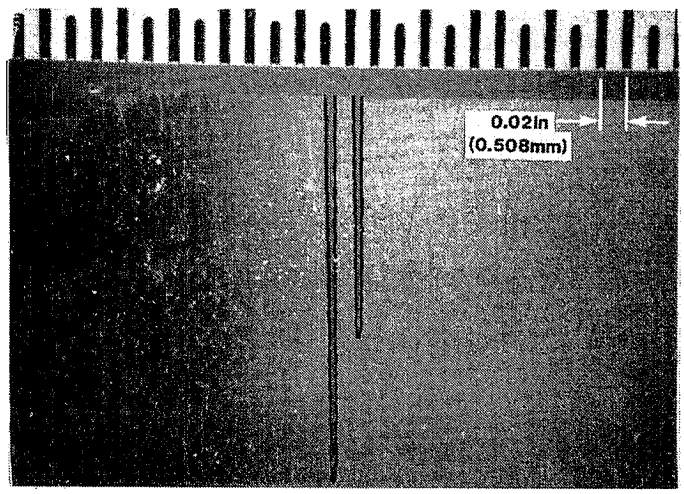

Figure 4. Parallel Microcuts

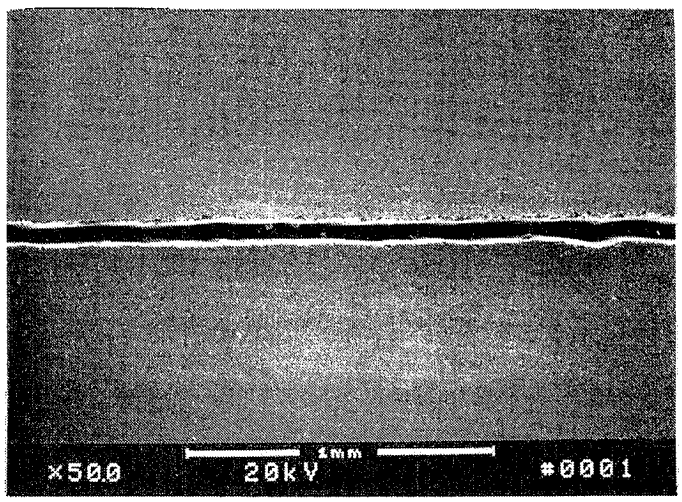

Figure 5. Electron Micrograph of Microcut

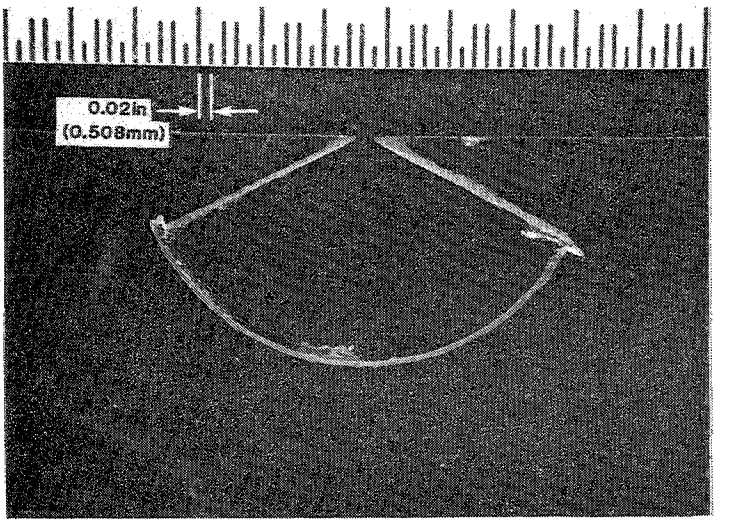

Figure 6. Cut Section in Glass

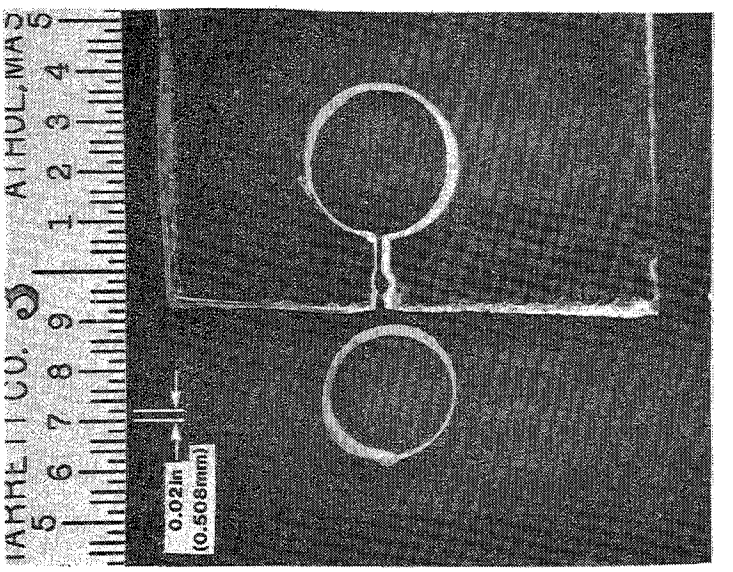

Figure 7. Small Circular Cut in Glass

4.0 CURRENT WORK

Current work involves studying microjet cutting using different fine size abrasives. Other work involves studies of the effects of the rheological properties of the suspending medium and of orifice configurations on the coherence of the jet at pressures above 69 MPa (10,000 psi).

5.0 CONCLUSIONS

The main conclusions to be drawn from this work are:

1. The coherent abrasive suspension jet offers a path to producing narrow kerf precision cuts in small parts.

2. The low pressures and low flows do not require heavy, high volume apparatus. This is especially true of the microjet.

3. Because of lower pressure operation, apparatus and operating costs can be reduced.

6.0 REFERENCES

1. Swanson, R.K., Kilman, M., Cerwin, S., Tarver, W., and Wellman, R., "Study of Particle Velocities in Water Driven Abrasive Jet Cutting, "Proceedings of Fourth United States Water Jet Conference, Berkeley, California, June 1987.

5th American Water Jet Conference
August 29 - 31, 1989: Toronto, Canada

Paper / Communication 25

ALUMINUM GRINDING WITH HIGH PRESSURE WATER JET ASSISTANCE

J. Borkowski
Koszalin Technical University
Koszalin, Poland

M. Mazurkiewicz
University of Missouri-Rolla
Rolla, Missouri, USA

ABSTRACT: Conventional grinding of soft and ductile materials is seriously hindered because of loading of the working surface of the grinding wheel and an accompanying loss of its grinding ability. The conditions of grinding operations improve considerably with the application of a water jet of the pressure of approximately 2 MPa for cleaning the grinding wheel. This report deals with the problems connected with grinding of aluminum alloys. The dependences and relations between the cutting parameters, cutting speed, depth of cut, grinding wheel parameters, and workpiece material, and water jet parameters, type of nozzle, flow ratio, pressure, used liquid, on the one hand and workpiece surface quality and the life of the grinding wheel on the other hand and presented in this report. It was concluded that the application of proper grinding wheel cleaning conditions can increase by several times the time of its life which at estimated costs attractively present the economical aspects of application of such a way of cleaning the working surface of the grinding wheel.

RÉSUMÉ : Le meulage classique des matériaux mous et ductiles est sérieusement compromis lorsque la surface de meulage se charge du matériau à meuler, ce qui diminue sa capacité à meuler. Les conditions de meulage s'améliorent considérablement par l'application d'un jet d'eau à une pression d'environ 2 MPa pour nettoyer la meule. Ce rapport traite des problèmes liés au meulage des alliages d'aluminium. Les liens de dépendance et les relations qui existent entre les paramètres de coupe, la vitesse de coupe, la profondeur de coupe, les paramètres de la meule et du matériau de l'éprouvette, et les paramètres du jet d'eau, le type de buse, le rapport des débits, la pression, le liquide utilisé, d'une part, et la qualité de la surface de l'éprouvette et la durée de la meule, d'autre part, sont présentés dans ce rapport. On conclut qu'un nettoyage adéquat de la meule peut allonger de plusieurs fois sa durée de vie. Une telle méthode de nettoyage de la surface de travail d'une meule constitue selon une estimation des coûts une solution économique intéressante.

Organized and Sponsored by the National Research Council of Canada and the U.S. Water Jet Technology Association.

1. Introduction

Grinding is one of the most popular machining methods as it ensures shaping of machine elements with high precision. However, the application of conventional grinding technique for machining soft and ductile materials is not effective. The reason for that is very quick loading of the grinding wheel's working surface with the chips which are pressed into the pores existing between the grains. This leads to grinding wheel cutting ability restriction, intensive friction, and heat buildup in the cutting zone as well as to deterioration of the workpiece surface quality. This results in necessity of frequent dressing of the grinding wheel, which is both expensive and time consuming.

In order to avoid this state it is useful to clean the working surface of the grinding wheel during the process of grinding. One of the ways which considerably improve the conditions of grinding soft and ductile materials is the application of a high pressure water jet directed at the grinding wheel's working surface. Proper directing of such additional water jet (Fig. 1) ensures the removal of the chips pressed into the grinding wheel's working surface thus allowing for maintaining high cutting ability and considerable lengthening of the time of the tool's life (Ref. 1, 2). Thanks to this the general output and efficiency of the grinding process also increase as there is clear reduction in the number of grinding wheel dressing operations.

The application of intensive water jet also presents itself as one of the more efficient ways of carrying away of heat arising in the cutting zone (Ref. 3, 4). This reduces to minimum heat interaction with the workpiece surface. Thus this technique of grinding hard workable materials prevents the occurrence of heat impairments in the material's structure (Ref. 4). Furthermore, in such conditions a decrease of vibration level and grinding force was observed which contributes to stabilization of dimensional deviations of the workpiece (Ref. 4, 5).

This study deals with problems of aluminum alloys grinding with high pressure water jet assistance. It presents the relations occurring between such cutting parameters as cutting speed and depth of cut at grinding with grinding wheels of various parameters and parameters of the water jet, especially types of water nozzles or liquid used, pressure of its working jet, and the quality of machined surface and efficiency of grinding process.

2. Research Methodology

Lubricoolant systems used nowadays in modern grinding machines in general ensure the supply of proper amount of liquid to the wheel/workpiece interface. The flow of this liquid usually provides good lubrication and cooling conditions in this zone but in general do not remove metal chips pressed between the grains of the working surface of the tool. In order to clean the grinding wheel off the chips it is necessary to install a special system which would ensure a supply of high pressure spray jet onto the grinding machine's working surface.

The system of delivering a high pressure water jet was built utilizing a typical grinding machine's suds sump, ensuring a closed circuit of the liquid in the grinding machine's water system. However, separate water pump and filter system and additional pressure vessel, acting as hydraulic accumulator were used. To generate lower range pressures (to 2 MPa) membrane pump was used and in systems requiring higher liquid pressures gear pump was used. The latter solution required a more precise filtering of the grinding liquid which was performed with the use of a band filter.

The most important, from the point of view of cleaning efficiency, part of the pressure system is the spray nozzle. Various types of nozzles were mounted on the safety cover of the machine (Fig. 2) so that they might change their position in respect to the working surface of the wheel. After careful thought it was decided to use single spray nozzles produced by Spraying Systems Co. of the following types:

1. Narrow Angle Injector Fulljet nozzle type 1/8 GG-SS 30.04 (fullcone spray),
2. Wide Angle Fulljet nozzle type 1/8 GG-SS 3. (fullcone spray),
3. Square Spray Fulljet nozzle type 1/8 G-SS 3.6SQ (fullcone spray),
4. Whirl Jet nozzle type 1/8 B-SS 3-5W (hollowcone spray),
5. Wash Jet nozzle type 1/4 MEG 40.07 (flat spray),
6. Solid Stream nozzle type 1/8 H-USS 0006 (straight jet).

In the studies of the grinding process there were used grinding wheels on ceramic binder of aloxite grains of various granularity and hardness. They were straight type grinding wheels of the following parameters:

T1 350x32x127 99A46H6V
T1 350x32x127 99A46K6V

T1 350x32x127 99A46N6V
T1 350x32x127 99A60K6V

The wheels were used for grinding cubicoid aluminum samples sized 150x20mm. Samples for straight type grinding were made of two types of aluminum alloys in the form of rolled sheets. Material PA1 (according to Polish Standard PN-59/H-88026), containing an additive of 1.0 ÷ 1.6% Mn was characterized by tensile strength of R_m=130 MPa and hardness of 30 BHN. The other material PA27 (according the Polish Standard PN-59/H-88026), containing the following additives: (4.8 ÷ 5.5) % Mg and (0.3 ÷ 0.6) % Mn, was characterized by tensile strength of R_m=315 MPa and hardness of 70 BHN. Additionally in technological trials there were used roll samples sized 40 x 200 made of aluminum alloy PA7 (according to Polish Standard PN-59/H-88026) having the following alloy additives:
(3.8 ÷ 4.9) % Cu, (1.2 ÷ 1.8) % Mg and (0.3 ÷ 0.9) % Mn. This material had the following mechanical parameters: tensile strength R_m=520 MPa, hardness of 70 BHN.

The grinding process was carried out with the grinding wheel's tangential velocity of approximately 31 m/s with the displacement of the workpiece with speed changing within the range of v_w = 0.1 ÷ 0.3 m/s. The depth of cut was changed within the range of g = 0.01 ÷ 0.03 mm.

As the grinding liquid 2...10% water solution of oil emulsion was used. This liquid was delivered to the spray nozzle under the working pressure of from 0.7 to 2.1 MPa. It was expected that within this range of pressures the liquid jet would gain the speed ensuring effective cleaning of the grinding wheel's working surface off the loading caused by workpiece chips.

3. The Results and Their Evaluation

From the point of view of efficiency of cleaning of the grinding wheel's working surface the nozzle is the most important element of the cleaning system. The type of nozzle used is decisive for the surface cleaning quality and its extensiveness. In order to provide complete spray coverage of the grinding wheel with narrow jets, it is necessary to use a set of spray nozzles. For practical reasons it is not advised to use Solid Stream type nozzles (No. 6), which provide only slender spray with narrow jet. For these reasons it is advised to use only such nozzles whose spray angle at working pressure is at least 30 degrees. This condition is fulfilled by the other nozzles used (Number from 1 to 5).

The grinding wheel's working surface cleaning efficiency with the application of these nozzles is illustrated, as example, by histograms on Figure 3. As the diagrams show the application of additional cleaning with a water jet multiplies the time of the grinding wheel's life, whose working surface in general remains in a better condition than after a shorter time of conventional grinding. The best effects are provided with the use of nozzle No. 3 (with square section of the jet) and nozzle No. 5 type 1/4 MEG -40.07 providing as flat spray nozzle (No. 5) and a considerable width of cleaning at relatively small discharge of water only such nozzles were used in further research. The nozzles were mounted on the inner side of the safety cover of the machine at the distance of 50 mm from its working surface.

For all cases of grinding flat samples the angle of mounting of the nozzle was set at β =180 degrees and of grinding roll samples this angle was considerably smaller (β 90 degrees). Throughout the experiments it was observed that the angle of mounting of the nozzle against the grinding wheel's working surface should not exceed the value of 90 degrees. An increase of the angle over this value is not desirable as the grinding wheel's working surface cleaning efficiency deteriorates which causes a decrease of its life and deterioration of the machined surface roughness.

The use of cleaning of the grinding wheel with a water jet lessens the influence of the grinding wheel's parameters on aluminum alloys grinding efficiency. For example, within the range of the parameters examined here no considerable influence of the grinding wheel's hardness was noticed. Very important, however, are the pressure of the cleaning water jet and the parameters of the grinding operation. The easiest basis for examining this influence is to examine the example of roughness generated at grinding flat surfaces.

The diagrams on Figure 4 illustrate the shaping of surface roughness in the function of the number of passes of the grinding wheel. As the figure indicates, in the beginning phase of grinding the roughness of the workpiece increases with an increase of the number of the grinding wheel's passes which corresponds to an increase of capacity of the ground off material. The worst effects occur in conventional grinding conditions, i.e. without the assistance of water jet cleaning the working surface of the grinding wheel. Thanks to the use of additional water jet cleaning the working surface of the wheel the machined surface is less rough and, furthermore, after 20-30 passes of the wheel the roughness practically stabilizes at

the level depending from the pressure of the liquid. With an increase of the pressure of the liquid the roughness of the machined surface decreases. However, an increase of both the speed of the workpiece and the depth of cut causes deterioration of the workpiece surface roughness. It can be seen, for example, from a comparison of the values of diagrams shown on Figure 4 mentioned above with corresponding dependances shown on Figure 5. The character of these changes is clearly illustrated by the diagrams shown on Figure 6 from which it appears that an increase of the depth of cut in every case contributes to an increase of the roughness of the machined surface.

It is fully understandable as the total of the chips increasing with the growth of the depth of cut is pressed more easily into the pores in the grinding wheel becoming a basis for faster sticking of further chips, which in consequence leads to the loading of the working surface of the grinding wheel. If this condition exceeds a certain critical limit of loading of the grinding wheel there follows a considerable deterioration of the machined surface quality as the chips attached to the working surface of wheel hinder the course of the grinding process entailing the seizing of the machined surface. It is illustrated on a photo of such seized surface of machined material shown on Figure 7. In the case when high pressure cleaning is used, the chip (Figure 8) are washed out of the working surface of the wheel and removed along with other products of the grinding process. In such conditions the grinding wheel has almost unchangeably sharp working surface, which allows for best grinding of aluminum alloys with a greater surface finish (Figure 9).

4. Economical Aspects

The use of additional water system for cleaning the working surface of the grinding wheel should be preceded by an estimation of costs of such enterprise. On the basis of the results of the above research important economic profits can be expected thanks to an increase of the life of the grinding wheel.

Estimated cost for the dressing of grinding wheels used for, as an example, grinding the surface of casts looks as follows. Depending from the conditions and type of the workpiece it is necessary to dress the grinding wheel every 10-15 minutes of the machine's work, and each operation takes 1-2 minutes. Taking into account only average values it is easy to estimate that for this kind of grinding operations approximately 12% of machine time is spent on dressing the wheel. At approximately 25 dollars per hour for skilled labor on a yearly basis. The labor cost equates to approximately 6,000 dollars. To this should be added further costs connected with premature wear of the wheel, shutdown of machines necessary for dressing, balancing or changing the grinding wheel, etc., which considerably rise the sum estimated above.

Basing on the above it can be stated that the costs connected with a system designed for high pressure cleaning of the grinding wheels will pay back already in the first year of work of such equipped grinding machine.

5. Summary

On the basis of the experiments carried out it can be stated that the use of a water jet for permanent cleaning of the working surface of the grinding wheel used for grinding soft and ductile materials, especially aluminum alloys, is very useful. This prohibits the loading of the working surface of the grinding wheel with chips of the machined material and multiplies the time of the life of the grinding wheel and reduces and frequency of dressing operations. No differences were noticed in the efficiency of cleaning of the grinding wheel during grinding of either flat surfaces or rolls. The stated dependances and tendencies are in both cases of grinding the same.

The biggest influence on efficiency of cleaning of the grinding wheel exerts the type of nozzle used and the pressure of water jet. It is advised to use nozzles providing water jet of square or flat intersection. The system used for cleaning the grinding wheel should ensure the pressure of 2 MPa.

On the basis of the experiments carried out no considerable influence of grinding wheel's parameters, especially its hardness, on effects of grinding and the length of the life of the tool was stated. The time of the life of the grinding wheel decreases with an increase of the depth of cut and the speed of ground material. Alternative criteria decisive for the moment of dressing the wheel may be: the occurrence of traces of loading of the working surface of the wheel or an increase of surface roughness of the workpiece.

Taking into account the above conclusions and the fact that the estimated cost of introduction of such a method of cleaning grinding wheels are profitable, this method of grinding should be recommended for general use in machining soft and ductile materials.

6. References

1. Borkowski J.: Podstawy teoretyczne, narzedzia i technologia obrobki scierniwem zwiazanym. Skrypt WSInz. Koszalin, Poland 1984.

2. Kubik K., Bienia F.: Opracowanie metody aktywnego oczyszczania sciernicy do intensyfikacji procesu obrobki w szlifowaniu walkow. Raport No 275 ITBM Politechniki Wroclawskiej.

3. Chudobin L.W.: Primienienie podwiznych sopel dla ochlazdienia pri slifovanii. Stanki i Instrument, 1968, No3.

4. Eda H., Kiski K.: Improvement of grinding process for difficult -togrina materials by acting the jet infusion of grinding fluids. Proc. Int. Conf. Prod. Eng. Tokyo, 1974, pp.665-670.

5. Chudobin L.W., Poljanskow I.W.: Powysenie tocnosti geometriceskoj formy izedlej pri gidroocistkie slifowalnych krugow. Wiestnik Masinostrojenia, 1969, No.3.

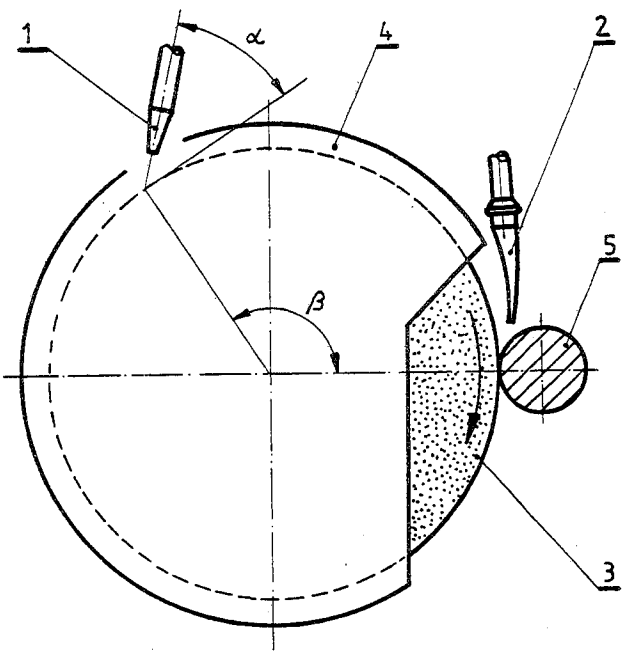

Figure 1. Diagram of mounting high pressure nozzle used for cleaning of the working surface of the grinding wheel: 1-high pressure nozzle, 2-standard nozzle, 3-grinding wheel, 4-safety cover of the grinding wheel, 5-workpiece, α-the angle of setting of the nozzle, β-the angle of mounting of the nozzle.

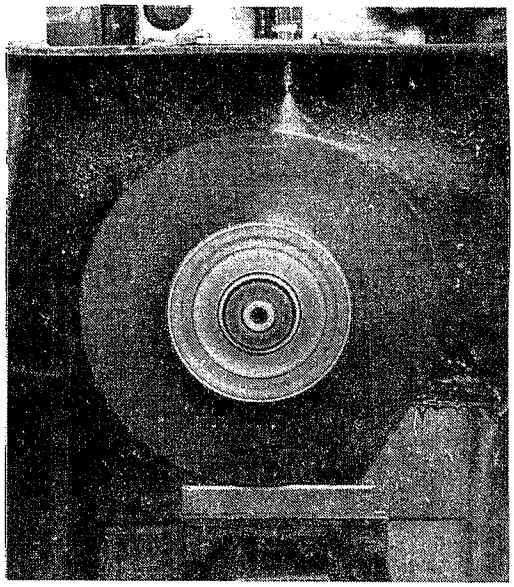

Figure 2. Cleaning of the grinding wheel with a water jet directed from the nozzle mounted on the safety cover of the grinding wheel.

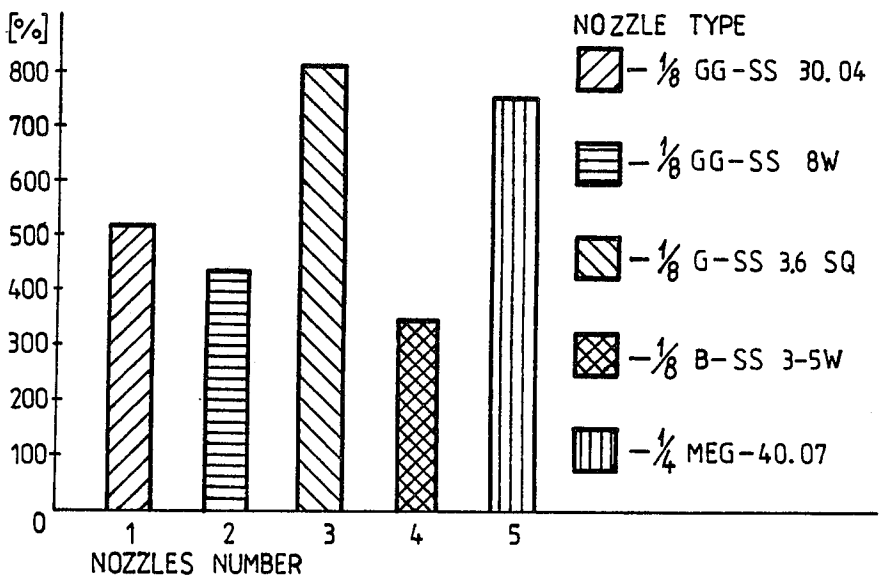

Figure 3. An increase of the life of grinding wheels T1 350x35x127 99A46K6V cleaned with a water jet at pressure of 2.1 MPa delivered through various spray nozzles set at the angle α=90 degrees compared with the life of grinding wheels used for conventional grinding of PA7.

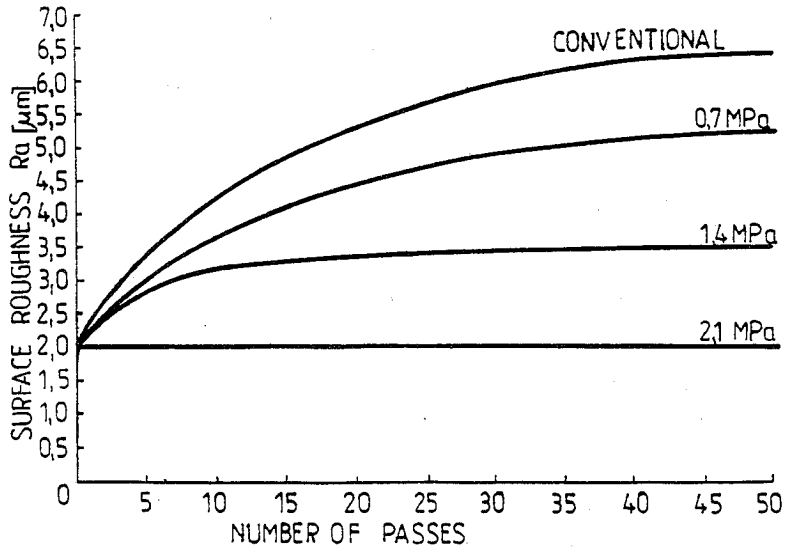

Figure 4. Surface roughness vs. number of passes at 0.0125mm cut/pass for grinding of PA 27 aluminum.

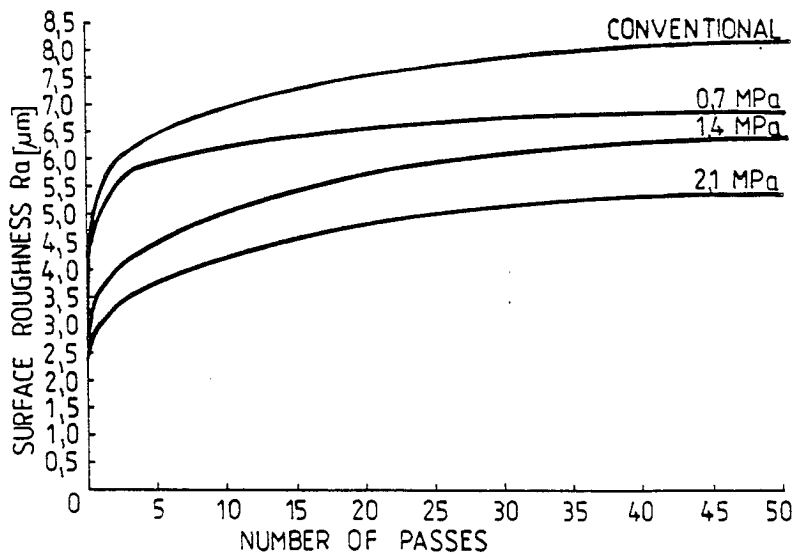

Figure 5. Surface roughness vs. number of passes at 0.025mm cut/pass for grinding of PA27 aluminum.

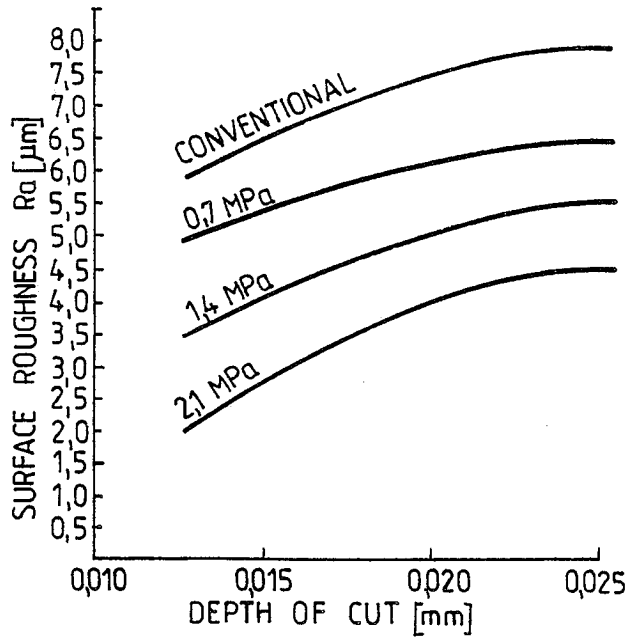

Figure 6. Surface roughness vs. depth of cut after 30 passes for grinding of PA27 aluminum.

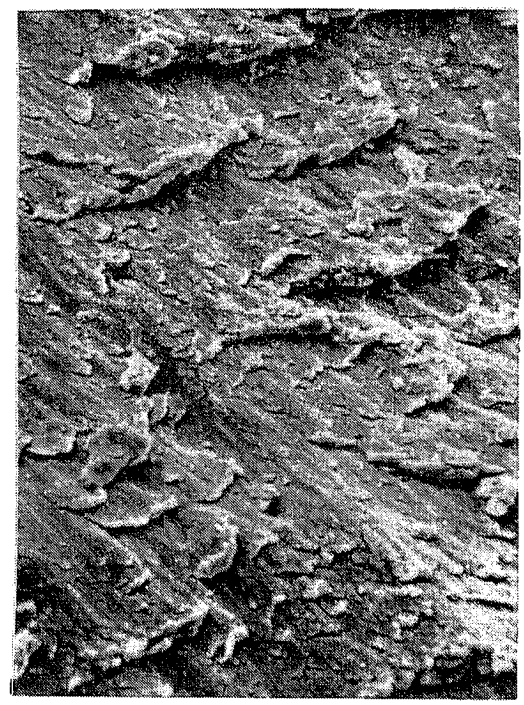

Figure 7. Traces of seizing on the workpiece surface of PA1 alloy machined with a grinding wheel with loaded working surface (x100).

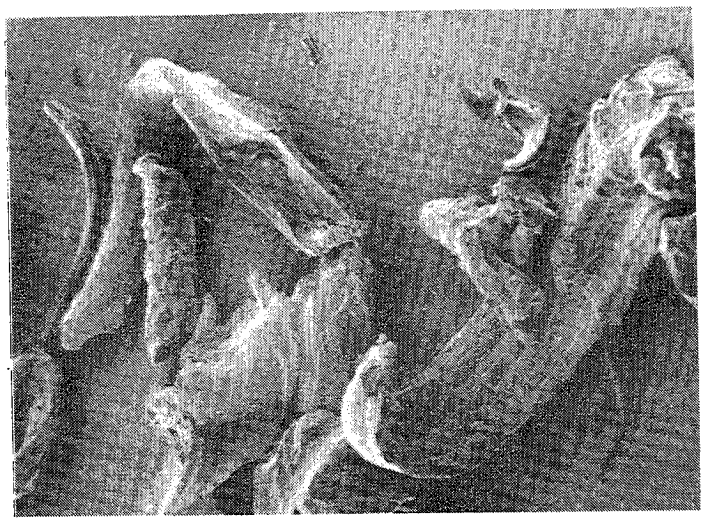

Figure 8. Typical shapes of chips arising during grinding of PA1 alloy with a grinding wheel T1 350x35x127 99A46K6V with water jet assistance at pressure of 2.1 MPa (x100).

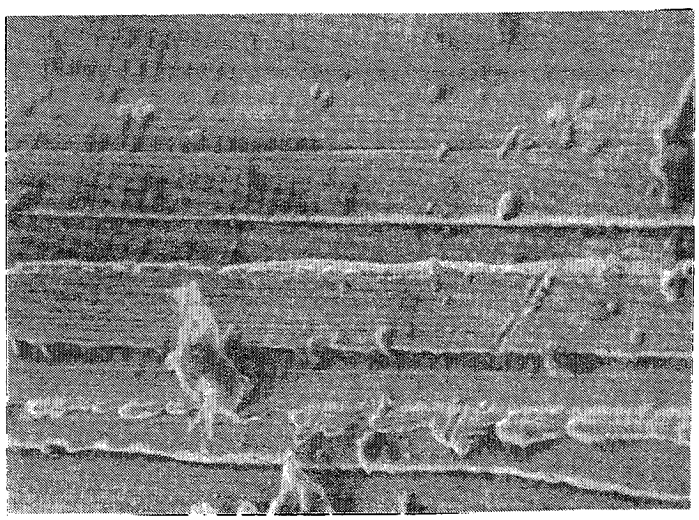

Figure 9. Typical stereometry of the surface (PA27 alloy) machined with high pressure water jet assistance (x100).

5th American Water Jet Conference
August 29 - 31, 1989: Toronto, Canada

Paper / Communication 26

INDUSTRIAL NEEDS SURVEY – WATERJET CUTTING

J.G. Klavuhn AND C.B. Baker
University of Pittsburgh at Johnstown
Johnstown, PA 15904, USA

ABSTRACT: A survey has been conducted to assess the metalworking industries' needs in waterjet cutting technology. The survey addresses five major areas of waterjet cutting technology. These include research and development, standards, systems, new products, and training and service. The survey was mailed to approximately 1400 individuals of which approximately 200 responded. The results have been analyzed for the entire group and various sub-groups. These include waterjet users, suppliers, and neither users nor suppliers. There are specific questions in the various categories on which all respondents agree and weigh approximately equal. The Waterjet Technology Association may have an interest in addressing specific questions concerning the survey and survey responses.

RÉSUMÉ : Un sondage a été réalisé pour évaluer les besoins de l'industrie de la métallurgie en matière de technologie de la coupe par jet d'eau. Il porte sur cinq grands secteurs de la technologie de la coupe par jet d'eau : recherche et développement, normes, systèmes, nouveaux produits, formation et service. Un questionnaire a été distribué à environ 1 400 particuliers, et 200 y ont répondu. Les résultats ont été analysés pour le groupe au complet et divers sous-groupes: utilisateurs de jets d'eau, fournisseurs, autres. Il y a des questions spécifiques dans les diverses catégories sur lesquelles tous les répondants s'entendent et auxquelles ils accordent à peu près la même importance. L'Association de la technologie des jets d'eau pourrait avoir intérêt à se pencher sur des questions particulières concernant le sondage et les réponses au sondage.

Organized and Sponsored by the National Research Council of Canada and the U.S. Water Jet Technology Association.

INTRODUCTION

High pressure waterjet cutting (WJC) is a new technology for the metalworking industry. It is providing a viable alternative for material cutting processes particularly where conventional techniques have failed. Since WJC is new to the metalworking industry, its full potential will require some time to evolve. A survey has been conducted to assist the WJC and the metalworking communities in developing the potential of this technology. This survey prioritizes the industrial needs in high pressure WJC based on the opinions of individuals with an interest in this technology.

The survey form was developed after a general study of the WJC industry. The form was distributed to approximately 1400 persons with various interests in WJC. The overall response was about 14%. Since a copy of the final report was used as an inducement to respond to the survey, it is believed that the respondents share a real interest in WJC technology.

The survey contained questions in six major categories: (1) organizational questions, (2) research and development, (3) standards, (4) systems, (5) new products, and (6) training and service. Responses were analyzed for four different respondents groups: (1) all respondents, (2) WJC users, (3) WJ equipment suppliers, and (4) neither WJC users nor WJ equipment suppliers.

SURVEY DATA

Organizational Questions

The results for the organizational questions are provided in Figure 1. The vertical axis scale is the fractional value calculated from the data for each particular group of respondents. The letters along the horizontal axis correspond to the questions as labeled beneath the figure. The numerical values adjacent to each question are those calculated for each respondent grouping and plotted in Figure 1.

From this figure it is interesting to note that:

1. 80% of all respondents are involved with defense contracting.
2. 40% of all respondents are WJC users.
3. 59% of all respondents and 64% of the respondents that are neither users or suppliers are considering a WJC system.
4. 91% of all respondents are seeking more information about WJC.

WJC Technology Questions

This part of the survey addresses five specific areas of WJC technology. These are 1) research and development, 2) standards, 3) systems, 4) new products, and 5) training and service. Respondents were requested to answer the questions on the priority scale provided. The scale range is from 0 to 5 (0 designates the lowest priority and 5 designates the highest priority). A descriptive needs ranking based on the priority scale is as follows:

Needs Ranking	Priority Mean Value
High priority	4.0 or greater
Important	3.5 to 4.0
Attention is required	3.0 to 3.5
Low priority	less than 3.0

Graphical and numerical results for questions in this category are given in Figures 2 through 6. The numerical values on the vertical axis represent the mean values for the priority. The roman-arabic numerals along the horizontal axis correspond to the survey subject areas and question numbers respectively.

Research and Development

For this group of items the response of WJC users and suppliers is considered a good indicator for the future direction of developments in WJC technology. These trends can be observed in Figure 2 which contains both the graphical and tabulated results of the items in the research and development category. A summary of the responses is as follows:

	Item	Users	Suppliers
1.	Basic research on cutting principles	Important	Important
2.	High pressure nozzle design	Important	High Priority
3.	Intensifer pump design	Low priority	Important
4.	Abrasive injection systems	Important	High priority
5.	Jet catcher development	Important	Attention is required

Item 3 is the only area in which there is a significant disagreement in the responses of the WJC suppliers and users.

Standards

The results for the responses in this group of questions are given in Figure 3. The response of all the combined groups appear to be fairly indicative of the priority ratings for the items in the standards list. The ordered priority ratings are:

	Item	All Respondents
4.	Performance standards	High priority
2.	Safety standards	Important
3.	Environmental standards	Attention is required
5.	Standardized system specs.	Attention is required
1.	Hardware standards	Low priority

Systems

None of the items in this group were given a high priority rating. Both Items 1 (system integration) and 6 (robotics or NC controller systems) are rated as being important on the priority scale. Note that these items are closely related. The respondents in the users group consider item 2 to be important. The users probably have a better feel for the problems involved with abrasive handling systems than other respondent groups. Therefore, their opinion would dictate the priority of this item. The graphical and numerical results are given in Figure 4. The priority order for the system category is as follows:

	ITEM	PRIORITY
1.	Systems Integration	Important
6.	Robotic or NC controller system	Important
2.	Abrasive handling systems	Important
3.	Tool design	Attention is required

5.	Disposal systems	Attention is required
4.	Water conditioning systems	Low priority

New Products

This category of items is a "mixed bag." It is difficult to decide how to treat the opinions of those respondents that are neither users nor suppliers of WJC equipment. The survey was not designed to establish the respondents level of knowledge about the survey material. Consequently, the response of only the users and suppliers of WJC equipment will be used to set the priority for these items. The graphical and numerical results are given in Figure 5. A summary of the users and suppliers priorities is:

	Item	Users	Suppliers
1.	High pressure quick disconnects for	Attention is required	Important
2.	High pressure swivel joints with longer service life	Attention is required	Important
3.	Automatic nozzle alignment system for abrasive jet nozzles	Important	High priority
4.	Jet catchers that operate in all positions	Important	Attention is required
5.	Transport system for abrasives	Attention is required	Attention is required

It is interesting that the suppliers give Item 1 a higher priority rating than the users. The difference in the priority rating for Item 4 is understandable since suppliers are not generally as concerned with multi-position cutting as users are.

Training and Service

There is very little spread in the responses to the items in this category. There is an interesting little anomaly in the responses to Items 1 (operator training) and 4 (short courses for potential users). The suppliers rank Item 1 at a value of 3.57 and Item 4 at a value of 3.05. Whereas, the respondents in the neither category rate these items at 3.15 and 3.58 respectively. Suppliers want operator training to teach users proper equipment operation and maintenance, and respondents in the neither category want short courses to better understand WJC technology. Both of these items should be rated as important. The graphical and numerical results are given in Figure 6. A summary of the ordered priorities is as follows:

	ITEM	PRIORITY	RESP. GR.
5.	Handbook with cutting data for various materials	High priority	All
4.	Short courses for potential users	Important	Neither
1.	Operator training	Important	Suppliers
6.	Water jet cutting test and demonstration	Important	All
3.	Manufacturing engineering training	Important	All
2.	Maintenance training	Attention is required	All

CONCLUSIONS

The results of this survey show a high priority need to establish:

- A data base on water jet cutting that contains the necessary technical data (i.e. nozzle size, pump pressures, abrasive type, nozzle speed, etc.) for cutting various types of metals using high pressure water jets; this information must be made available to the entire WJC community.

In addition, the results indicate there is an important need:

- To establish a WJC demonstration center that can be used for cutting tests, short courses for potential users, and operator training;

- To establish organized efforts in hardware development which should include automatic nozzle alignment, abrasive injection and handling systems, jet catchers, system integration, and basic research on cutting principles.

RECOMMENDATIONS

It is recommended that:

1. A directed effort be made to centralize the collection of WJC data

2. An on-line computerized database be established which would be available to the WJC community

3. A WJC facility be designated to generate the data needed to complete the database, provide demonstrations, and assist in the improvement and development of WJC hardware

4. A seminar of interested people in the WJC community be convened to define the format of the water jet cutting database and the parameters to be included in the database

ACKNOWLEDGMENT

Work on this survey was funded by the U.S. Navy's MANTECH program through the National Center for Excellence in Metalworking Technology (NCEMT) which is part of Metalworking Technology, Inc. (MTI). A copy of the survey report may be obtained by writing to Metalworking Technology, Inc., 1450 Scalp Avenue, Johnstown, PA 15904.

Organizational Questions

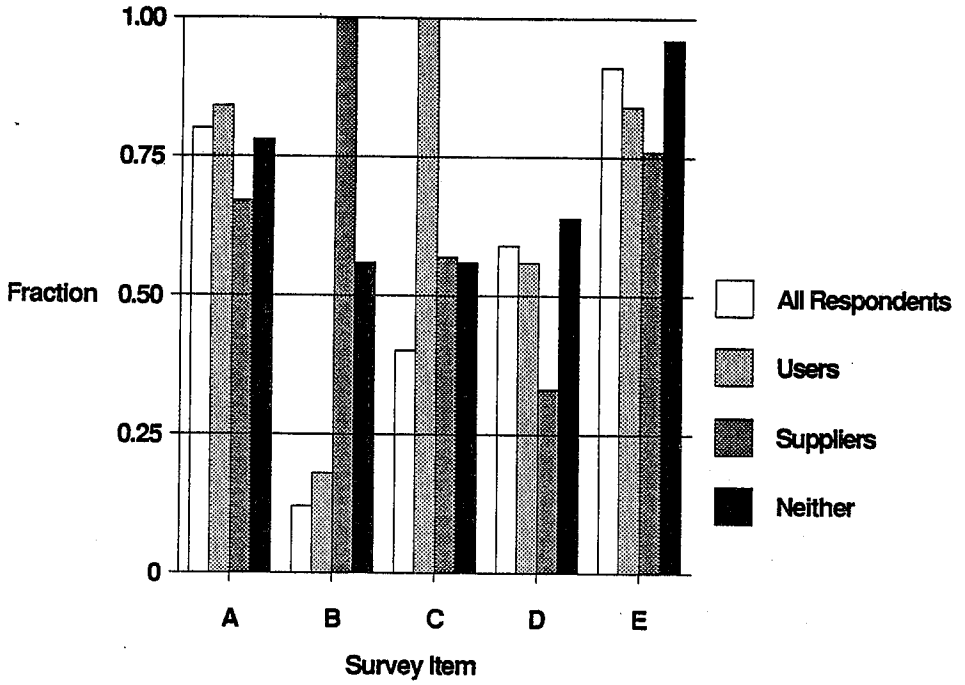

Survey Item	Respondent Group No.			
	1	2	3	4
Is your organization	All	Users	Supp.	Neither
A. Involved with defense contracting?	0.80	0.84	0.67	0.78
B. A supplier of water jet or abrasive jet cutting systems or components?	0.12	0.18	1.00	0.56
C. Using water jet or abrasive jet cutting?	0.40	1.00	0.57	0.56
D. Considering a water jet cutting system?	0.59	0.56	0.33	0.64
E. Seeking more information about water jet cutting?	0.91	0.84	0.76	0.96

Figure 1

Research and Development Needs

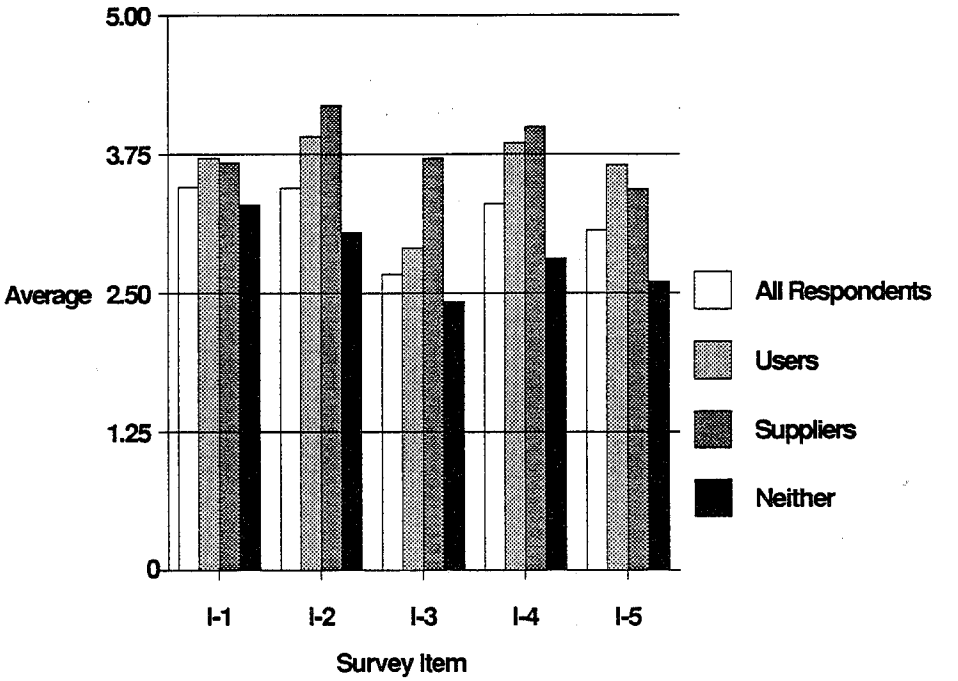

Survey Item	Respondent Group No. 1 All	2 Users	3 Supp.	4 Neither
I. Research and Development				
1. Basic Research on Cutting Principles	3.45	3.71	3.67	3.29
2. High Pressure Nozzle Design	3.44	3.91	4.19	3.04
3. Intensifier Pump Improvement	2.67	2.90	3.71	2.42
4. Abrasive Injection Systems	3.30	3.85	4.00	2.81
5. Jet Catching Development	3.06	3.65	3.43	2.60

Figure 2

Standards

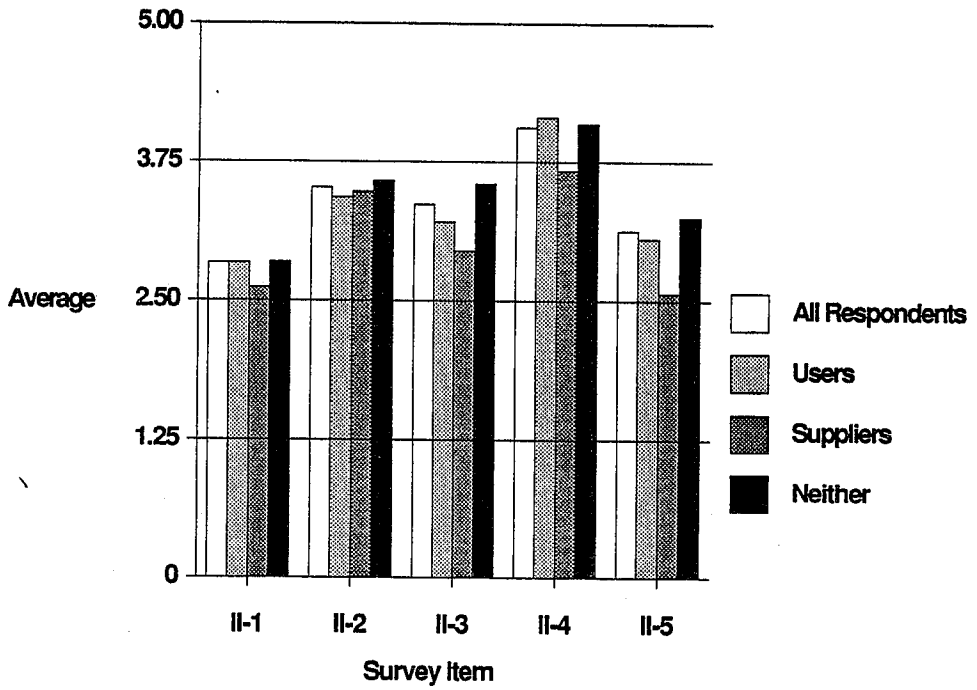

Survey Item	Respondent Group No. 1 All	2 Users	3 Supp.	4 Neither
II. Standards				
1. Hardware Standards	2.84	2.84	2.62	2.85
2. Safety Standards	3.52	3.43	3.48	3.58
3. Environmental Standards (e.g. Noise, Moisture, etc.)	3.37	3.21	2.95	3.55
4. Performance Standards (Cutting Speeds, Tolerances, Finish, etc.)	4.06	4.15	3.67	4.09
5. Standardized System Specs.	3.13	3.06	2.57	3.25

Figure 3

Systems Needs

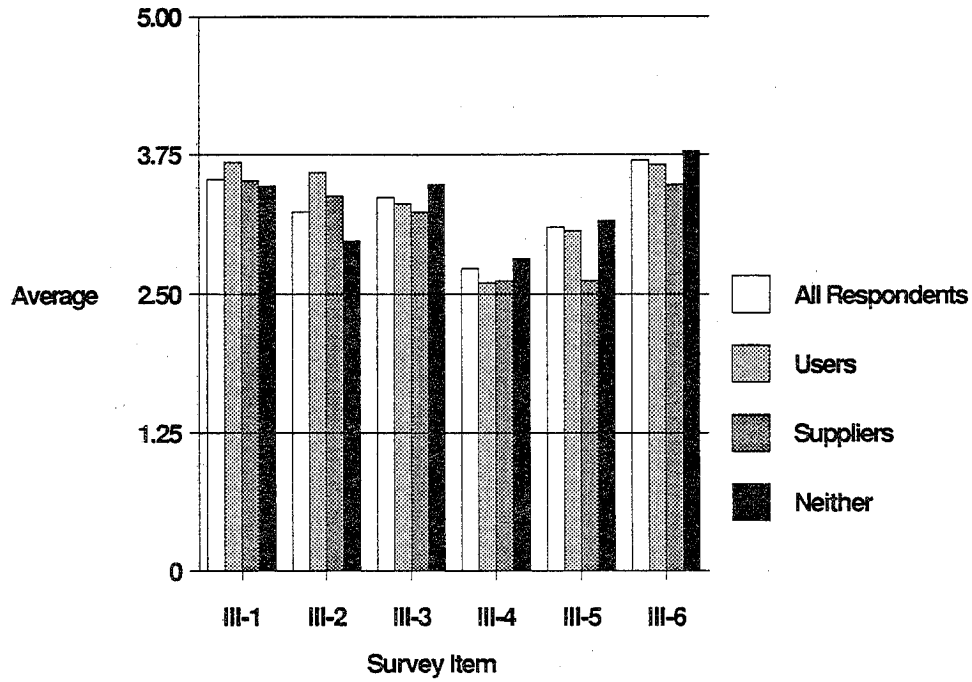

Survey Item	Respondent Group No. 1 All	2 Users	3 Supp.	4 Neither
III. Systems				
1. System Integration	3.53	3.68	3.52	3.47
2. Abrasive Handling Systems	3.24	3.59	3.38	2.98
3. Tooling Design	3.37	3.31	3.24	3.48
4. Water Conditioning Systems	2.73	2.60	2.62	2.82
5. Disposal Systems	3.10	3.07	2.62	3.16
6. Robotic or NC Controller Systems	3.70	3.66	3.48	3.78

Figure 4

New Products

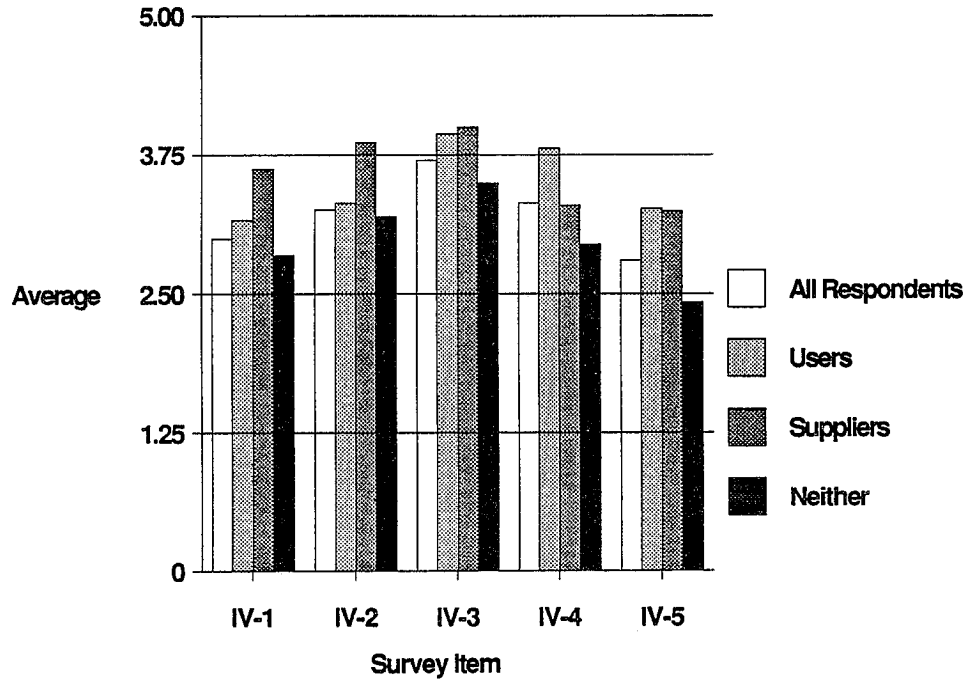

Survey Item	Respondent Group No. 1 All	2 Users	3 Supp.	4 Neither
IV. New Products				
1. High Pressure Quick Disconnects for Robot Tool Change	2.99	3.16	3.62	2.84
2. High Pressure Swivel Joints with Longer Service Life	3.25	3.31	3.86	3.19
3. Automatic Nozzle Alignment System for Abrasive Jet Nozzles	3.70	3.94	4.00	3.49
4. Jet Catchers that Operate in all Positions	3.31	3.81	3.29	2.94
	2.80	3.26	3.24	2.42

Figure 5

Training and Service

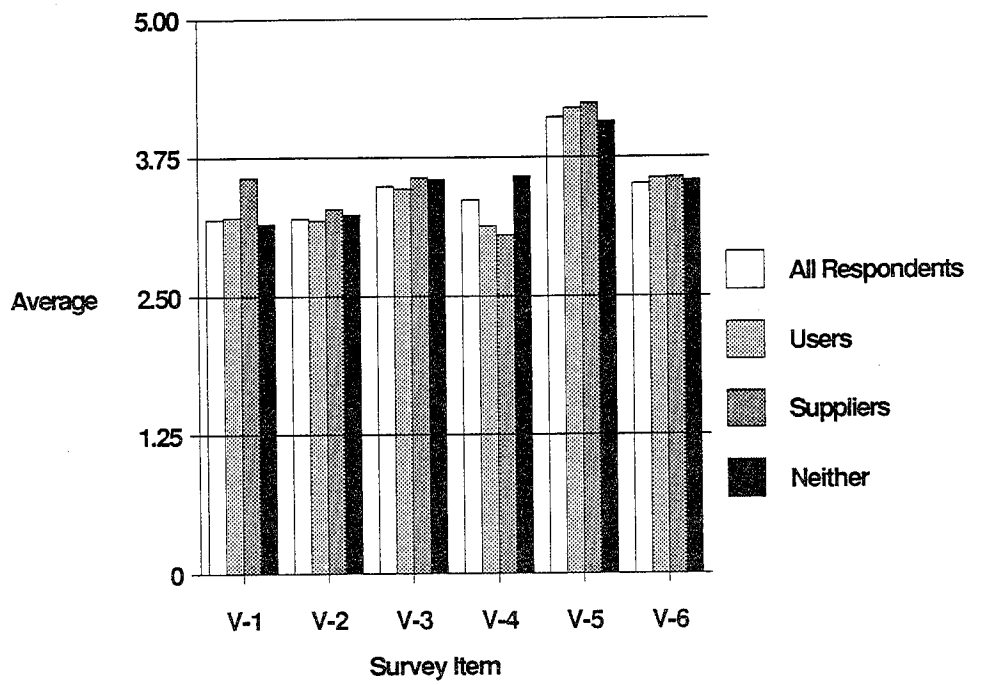

Survey Item	Respondent Group No. 1 All	2 Users	3 Supp.	4 Neither
V. Training and Service				
1. Operator Training	3.19	3.21	3.57	3.15
2. Maintenance Training	3.20	3.18	3.29	3.24
3. Manufacturing Engineering Training	3.49	3.47	3.57	3.55
4. Short Courses for Potential Users	3.37	3.13	3.05	3.58
5. Handbook with Cutting Data for Various Materials	4.11	4.19	4.24	4.07
6. Water Jet Cutting Test and Demonstration Center	3.51	3.56	3.57	3.54

Figure 6

5th American Water Jet Conference
August 29 - 31, 1989: Toronto, Canada

Paper / Communication 27

A HYDRAULIC JET MINING TECHNIQUE FOR RECOVERING BITUMEN FROM ALBERTA OIL SANDS

B. Singh, K. Redford AND V.R. Puttagunta
School of Engineering, Lakehead University
Thunder Bay, Ontario P7B 5E1, Canada

ABSTRACT: This paper describes the results of an experimental investigation of using hydraulic jet cutting to recover bitumen from frozen oil sands. The effect of various parameters including nozzle type, flow rate, sweep speed, and oil sand grade on the slurrying efficiency were studied. A single jet of hot alkaline solution was impinged on a 30 cm x 30 cm x 12 cm block of frozen oil sand. The objective was to crumble the oil sand into a slurry with a minimum of working solution. It was found that optimum amount of bitumen was slurried when a 0.1 weight percent sodium hydroxide solution at 98°C was impinged with a flat jet nozzle at a flow rate of 1.4 kg/minute. Also, air samples in the vicinity of the experimental set up were analyzed for alkali content to evaluate the environmental effects caused by the process and it was found that insignificant amounts of sodium hydroxide escaped into the atmosphere.

RÉSUMÉ : Cette communication décrit les résultats d'une recherche expérimentale sur l'utilisation de jets d'eau pour récupérer du bitume dans des sables bitumineux gelés. L'effet de divers paramètres comme le type de buse, le débit, la vitesse de balayage et la qualité des sables sur le rendement de conversion en boue a été étudié. Un seul jet de solution alcaline chaude a été projeté sur un bloc de 30 cm sur 30 cm sur 12 cm de sable bitumineux gelé. L'objectif était de convertir les sables bitumineux en boue avec un minimum de solution de travail. On a trouvé que la quantité optimale de bitume est mise en suspension lorsqu'on projette une solution titrant 0,1 % d'hydroxyde de sodium en poids à 98°C avec une buse à jet étalé à raison de 1,4 kg/min. En outre, on a dosé la teneur en alcalis d'échantillons d'air ambiant pour évaluer les effets sur l'environnement d'un tel procédé, et on a constaté que des quantités importantes d'hydroxyde de sodium s'échappent dans l'atmosphère.

Organized and Sponsored by the National Research Council of Canada and the U.S. Water Jet Technology Association.

1.0 INTRODUCTION

The oil sands deposits in Alberta contain reserves of crude bitumen estimated to be more than 180 billion cubic meters (Camp, F.W., 1976). Existing methods to recover bitumen from these deposits may be generally divided into those which depend on surface mining, combined with some further processing, and those which operate on oil sands in situ. The surface mining techniques are applicable to shallow deposits (less than 40 meters of overburden), and in situ methods are suitable for deposits deeper than 200 meters. The surface mining based techniques result in recovery of over 90% of the bitumen in the mined oil sands, but require very large capital investments, and thus restrict the size of producing plants to be over 10,000 cubic meters of bitumen per day. A large part of the capital investment as well as operating costs is due to the use of heavy machinery (e.g. bucket wheels) and the associated power plant requirements for strip mining operations. In the two plants (Syncrude Canada Ltd., and Suncor Ltd.) currently producing bitumen by surface mining techniques, the mining and solids transport operations account for 30% of the capital investment, and the utilities account for another 19%, of which a large portion is used to supply power to the mining operations (Bowman, C.W., 1983). The in situ methods require smaller capital investments and permit plants producing as little as 200 cubic meters of bitumen per day to be economically feasible, and unlike surface mining, in-situ methods provide possibilities for gradual build-up of capacity as cash flows develop. However, in situ methods result in recovery of less than 30% of the available bitumen (for example, one of the most successful in-situ method based project, the Imperial Oil Cold Lake Heavy Oil Project, recovers only about 21% of the bitumen available). Further, the lack of communication between wells due to low effective permeability of the deposit is a major problem in in situ recovery techniques. Current fracturing techniques to link injection and production wells in intermediate and deep oil sands reservoirs are not universally successful (Plewes, H.D., et al., 1985). Finally, there is no suitable method available at present to recover bitumen from the zones of intermediate depths (40 to 200 meters). The amount of bitumen available in these zones is as much as 25% of the total resource (Camp, F.W., 1976). Thus there is need for the development of a bitumen recovery method which: (1) reduces requirements for capital investments and makes smaller projects feasible for shallow deposits; (2) allows gradual build-up of capacity as cash flows develop; (3) permits high recovery of the resource; (4) can be used to develop and maintain controlled fractures; and (5) allows production of bitumen from the zones of intermediate depths. It is to meet these requirements that the use of high pressure hydraulic jets to cut oil sands is of some interest.

The hydraulic jet cutting of oil sands has been investigated by several researchers (Gates, E.M., and R.R. Gilpin, 1981; Gates, E.M., et al., 1984; Law, D.J., et al., 1987; Wagner, C.G., and E.L. Hodges, 1985; McRoberts, E.C., et al., 1988), but although the mechanical effects of jet have been documented, none of these has examined the addition of an enhancing agent (such as an alkali) to assist in the separation of bitumen from the sand particles. The formulation of this study was based on the conjecture that the mechanical action of the jets of hot alkaline solution would serve to crumble the oil sand and emulsify the bitumen which has been softened by the thermal and chemical action of the working solution in the impinging jets. Only the emulsions will be transported away from the mined zone and most of the solids would be left on-site. The jets can be operated below the overburden and thus the method can be used for deeper deposits as well.

The objective of the present work is to study experimentally the slurrying of rich and medium grade oil sands by a jet of hot alkaline solution under controlled but realistic conditions. A controlled experiment is required to get a meaningful comparison between oil sands of diffrent grades. Although only a limited amount of data is presented here, the experimental apparatus and method used is simple enough that it could serve as a screening device for a wide variety of oil sands. The equipment allows an evaluation of the combined effect of the thermal, mechanical and chemical energies of the jet on the slurrying process.

2.0 EXPERIMENTAL APPARATUS AND PROCEDURES

2.1 Description of Apparatus

The basic laboratory arrangement is presented schematically in Figure 1. A high pressure metal cylinder was used as the storage tank for the working solution. The tank was immersed in a hot water bath kept at the desired temperature. High pressure nitrogen from a compressed gas cylinder was used to deliver the working solution to the oil sand block. Nozzle sizes ranging in capacity from 0.3 to 4.0 kg/min. at 1.7 MPa were used to achieve different flow rates.

A robotic device was designed and constructed to hold the impinging jet at a predecided distance from the face of the oil sand block. The device is essentially a three axis cartesian robot with fully programmable automatic controls for the individual axes. The robot has a work envelope of 30 cm x 30 cm x 12 cm, and it

can be programmed to achieve desired sweep speeds and sweep patterns.

The oil sand used in the laboratory originated from the Suncor (previously G.C.O.S) site of the Athabasca deposit at Fort McMurray. A test sample block was prepared by manually compacting the sand into a 30 cm x 30 cm x 12 cm mold to a specific gravity of 2.1. The blocks were then kept in a freezer at -21 ^{0}C for at least 48 hours. Upon removal from the freezer, the block of oil sand was mounted in the apparatus and the jet cutting test carried out. Appropriate catch basins were installed to keep account of the oil sand removed from the block during the test and the amount of bitumen separated from the oil sand.

2.2 Experimental Procedure

To begin each test run, the mass of the catch basins, full cylinders and oil sand block were recorded. The oil sand block was placed in the test stand above the sludge tray and enclosed within plastic protective curtains. The appropriate jet nozzle was installed, and the robotic device was programmed for the desired sweep pattern and sweep speed. The storage tank containing the working solution was then placed in the hot water bath several hours before the run. The nitrogen cylinder valve was then opened and the system was pressurized. When the temperature of the working solution reached and stabilized at the desired level, the toggle valve to release the working solution to the impinging jet was opened, and the experiment commenced. The flow rate of the working solution was controlled by regulating the pressure imparted on the solution contained in the tank. The time from start to finish of each run was recorded. Appropriate samples from the sand block, the sand in the catch basin and the bitumen slurry were collected and were analyzed for tbe bitumen content.

To assess the environmental impact of the proposed method in a cold climate such as in northern Alberta, outdoor tests were also conducted during the cold winter months in Thunder Bay. The test procedure for the outdoor runs was kept same as those for the indoor runs except that only hand held jet was used in outdoor tests. The Gilian 113 air sampling system was used to sample large volumes of fog generated in outdoor tests. The air samples were analyzed for alkali content to assess the air pollution caused by the proposed method.

3.0 PRESENTATION OF RESULTS

Experiments were designed to study the cutting and removal of the oil sand, and the separation of bitumen from sand particles for various jet parameters. Two performance criteria were selected to evaluate the relative importance of parameters. These criteria were: (1) slurrying efficiency, and (2) percent residual oil in the slurried sand. The parameters were: (1) nozzle type, (2) flow rate, (3) sweep speed, and (4) oil sand grade. Others parameters of importance to be evaluated in future tests are the effect of jet temperature and jet pressure. The tests reported in this paper were carried out at 98 ^{0}C and 1.7 MPa gauge. The jet distance from the sand face was kept at 2.5 cm for all the tests.

3.1 Slurrying Efficiency

The term slurrying efficiency was coined as a measure of the performance of jet cutting and defined as the mass of oil sand removed per unit mass of the working solution used.

3.1.1 Nozzle Type

Two types of nozzles were tested. These were: (1) flat jet, and (2) conical jet nozzles. Figure 2 presents the plot of slurrying efficiency for the two nozzles at various flow rates. A high grade oil sand (15% bitumen content by weight) was used for these tests. It is evident from figure 2 that the flat jet nozzle is more efficient than the conical jet nozzle in removing oil sand from the block. Since the amount of chemical energy available was same for both nozzles, it may be concluded that the loss of mechanical and thermal energies was greater in the conical nozzle. The formation of a solid cone in the conical nozzle causes the loss of mechanical (pressure) energy, and also the enlarged surface area of the cone results in relatively greater evaporation and hence the loss of thermal energy. It is also seen from figure 2 that at higher flow rates there was not much difference between slurrying efficiencies achieved by the two nozzles. This may be explained by the fact that as the flow rate increases, there is not much of additional loss of thermal and mechanical energies for the conical nozzle, while at high flow rates the flat jet nozzles results in poor performance due to excessive splatter of the working solution.

3.1.2 Solution Flow Rate

Figures 2 and 3 present the effect of flow rate on slurrying efficiency. It is evident that there is an optimum flow rate for each situation. This may be explained by considering the mechanisms involved in the slurrying of the oil sand. The thermal energy of the jet helps to soften the oil sand by reducing bitumen viscosity. As it is seen from Figure 4, the viscosity of cold bitumen is usually so high that at temperatures below -20 ^{0}C, the oil sand is as hard to cut as steel. However, as temperature rises, the viscosity decreases and sand becomes very easy to cut. Further, the chemical energy of the jet help in disengaging the bitumen from sand graines. Finally, the mechanical energy of the jet helps to remove the softened oil sand from the block. At low flow rates, there is very little penetration of the impinging jet and hence very little heat transfer resulting in the block remaining cold and inhibiting the slurrying process. However, at very high flow rates, there is insufficient time for the heat transfer process and the thermal energy of the jet is not utilized effectively. At optimum flow rates, there is efficient utilization of the mechanical and thermal energies of the jet.

3.1.3 Oil Sand Grade

Two different grades of the oil sand were used for the experiments reported here. The bitumen content of the high grade oil sand and medium grade oil sand was 15% and 10% respectively. As is shown by Figure 3, more high grade oil sand is slurried per given flow rate of working solution as compared to the medium grade oil sand. It is also seen from Figure 3 that the peak slurrying efficiency for medium grade oil sand occurs at a higher mass flow rate (2.0 kg/minute) than that for the high grade oil sand (1.4 kg/minute). This may suggest that for the medium grade sand the mechanical cutting action is relatively more important, while for the high grade oil sand the thermal and chemical action are more important. Binding action of the high grade oil sand is due mainly to the presence of the bitumen. Thermal and chemical energies affect bitumen by reducing viscosity and increasing jet penetration. On the other hand, medium and low grade oil sands are bound together by clays and shales, along with bitumen, and greater mechanical energy is perhaps required to slurry oil sands with these impurities.

3.1.4 Sweep Speed

To evaluate the effect of sweep speed on slurrying efficiency, the sweep speed was varied from 1.5 cm/second to 7.5 cm/second. Figure 5 presents the plot showing the influence of sweep speed on slurrying efficiency. Although there is considerable scatter in the plotted data, it appears that there is slightly higher slurrying efficiency at higher sweep speeds. For a single jet, the sweep speed does not seem to be an important parameter, but its influence may be more important in field situation where an array of jets is to be employed.

3.2 Residual Oil in Slurried Sand

In most jet cutting applications, the only objective is to remove the material. However, for successful application in recovering bitumen from the oil sands, in addition to cutting action, the separation of bitumen from the slurried oil sand is essential. Ideally, the process should be designed as to remove all bitumen from the oil sand so that only bitumen-water emulsion needs to be transported for further processing and the sand remains on site. For this purpose, appropriate samples were taken from the slurried oil sand and were analysed for oil content. Also, to improve the overall process, it was decided to give an additional wash to the slurried oil sand to maximize bitumen separation for some of the experiments. Figure 6 indicates that residual oil in the slurried sand increases at higher solution flow rates. As mentioned previously, the optimum slurrying efficiency of medium grade oil sand was found to occur at a flow rate of 2 kg/minute, and it was found that at this condition the residual oil content was about four percent. Thus, almost 60% of the bitumen was separated from the oil sand. On washing the slurried sand once with an equal volume of hot 0.1% NaOH solution, the oil content was reduced to less than 0.5%. Thus, with one wash, more than 95% of the bitumen was removed from the oil sand. The efficiency of this wash does not appear to depend on the amount of oil removed during initial slurrying.

During the experiments, it was noticed that lower sweep speed removed a greater percentage of oil from the slurried sand. Figure 7 presents the effect of sweep speed on the residual oil content in the slurried sand and the trend is toward higher residual oil content in the slurried sand at higher sweep speeds.

3.3 Environmental Impact of Using Caustic Solution

Seven tests were conducted outdoors in atmospheric temperatures ranging from -15 to -25 ^{0}C. Air samples were collected within 30 cm of the impinging jet. On analysis, it was found that the concentration of NaOH in the samples was less than 0.013 ppm in all cases and on the average it was only 0.004 ppm. There was considerable amount of fog generated, and the smell generated was that of hot bitumen. It was found that the caustic entrainment into the atmosphere was negligible, and even that was restricted to a very small area around the jet. In an actual field situation, a plastic portable bubble can be used to cover the affected area, thus minimizing air pollution as well as heat losses in the process.

4.0 DISCUSSION OF RESULTS

It is useful to interpret the results obtained in this study from the point of view of applicability to field situations. As such, the best slurrying efficiency achieved in these tests (0.65 kg of oil sand slurried/kg of working solution) does not compare favorably with the Clark's hot water process used in the existing surface mining based plants. The ratio of hot water required in the Clark's process is approximately 1 kg/kg of oil sand processed. However, a closer look at the experimental set up indicates that the proposed method will work better in a field situation. In the laboratory, there were considerable losses of heat from the boundaries of the oil sand block. In an actual field situation, the heat lost to the surrounding oil sand will in effect be utilized in raising its temperature and thus facilitating the cutting process. Further, in the field situation, especially for the zones of intermediate depths, the oil sand temperature will be high enough to require considerably less working solution for jet cutting. A mathematical model of the process and the appropriate scaling criteria are being developed at present to assist in further evaluation of the process.

5.0 CONCLUSIONS

The experimental results indicate that in addition to mechanical energy (which is the most important parameter in commonly used jet cutting applications), thermal and chemical energies are of importance in jet cutting of oil sands. It appears that high grade oil sand would benefit more from thermal and chemical energy, while lower and medium grade oil sands would respond better to mechanical energy. It may also be concluded that an optimum level exists for the influence of flow rate on the slurrying efficiency. Use of a flat jet nozzle was found better as compared to a conical nozzle.

6.0 ACKNOWLEDGEMENTS

This work has been supported by the Federal Department of Energy, Mines and Resources and by the Natural Sciences and Engineering Research Council. The assistance provided by Mr. Jim Kuper in conducting the experiments is greatly appreciated.

7.0 REFERENCES

1. Bowman, C.W., **Oil Sands Technology and Economics,** Short Course Notes, Alberta Research Council, 1983.

2. Camp, F.W., **The Tar Sands of Alberta, Canada,** Cameron Engineers Inc., Denever, Colorado, 1976.

3. Gates, E.M., and R.R. Gilpin, "Jet Piercing of Oil Sands," **Transactions of the ASME, Journal of Energy Resources Technology,** Vol. 103, pp. 330-335, December 1981.

4. Gates, E.M., R.W. Toogood, and B.W. Simms, "A Model for Drilling by High Pressure Water Jet," paper D5, 7th International Symposium on Jet Cutting Technology, Ottawa, Canada, June 26-28, 1984.

5. Gilpin, R.R., E.M. Gates, and W.T.R. Chau, "Jet Cutting of Oil Sands," 5th International Symposium on Jet Cutting Technology, Hanover, 1980.

6. Law, D.H., J.H. Masliyah, and K. Nandakumar, "Ablation of Frozen Oil Sands Under the Influence of Turbulent Axisymmetric Jets," **AOSTRA Journal of Research,** Vol. 3, pp. 177-181, 1987.

7. McRoberts, E.C., D.S. Cavers, "Geotechnical Considerations in Borehole Hydraulic Mining of Oil Sands OSLO New Technology," 4th UNITAR/UNDP Conference on Heavy Oil and Tar Sands, Edmonton, August 7-12, 1988.

8. Plewes, H.D., J.D. Scott, and T.R. Hsu, "Dynamic Fracturing of Oil Sands," presented at the Heavy Oil and Oil Sands Technical Symposium, University of Calgary, February 20, 1985.

9. Wagner, C.G., anf E.L. Hodges, "Downhole Hydraulic Mining System," Third International Conference on Heavy Crude and Tar Sands, Long Beach, California, 1985.

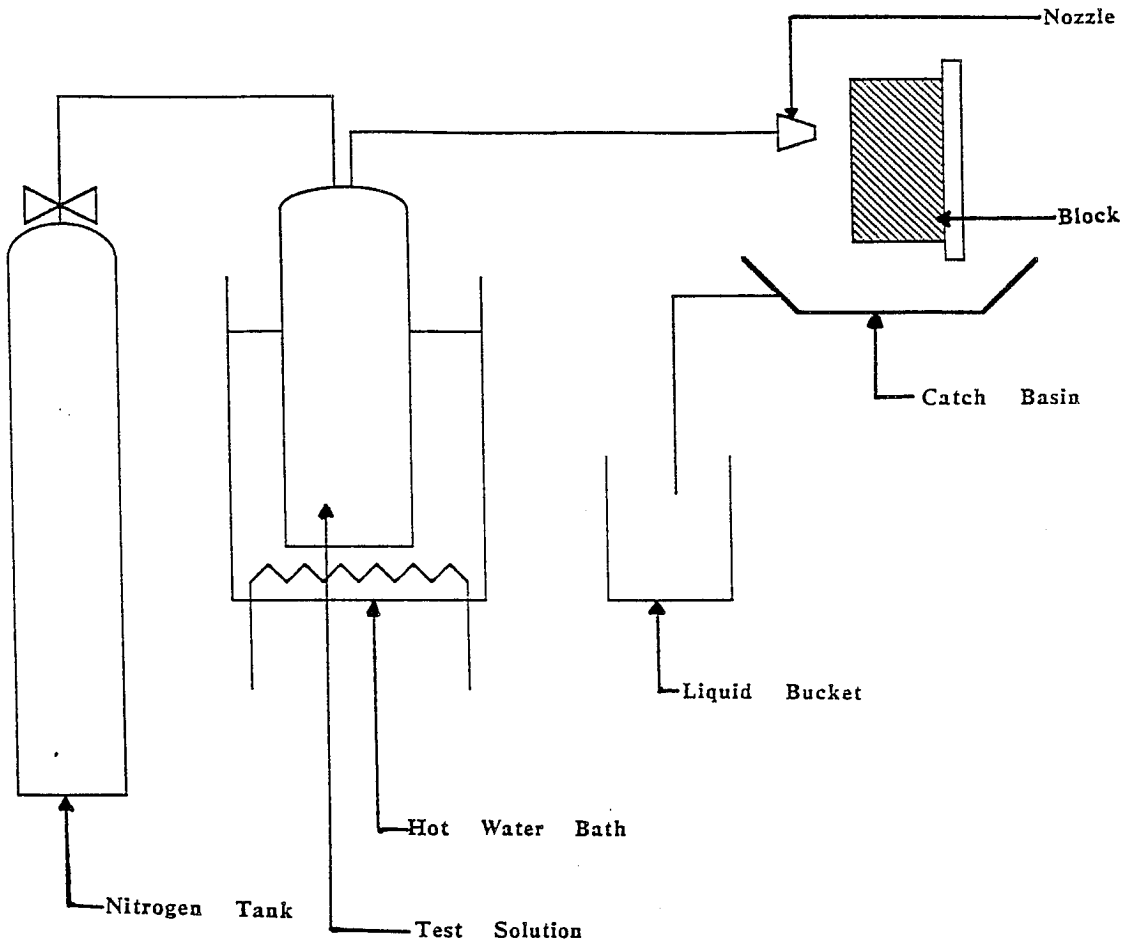

FIG. 1 SCHEMATIC OF THE APPARATUS

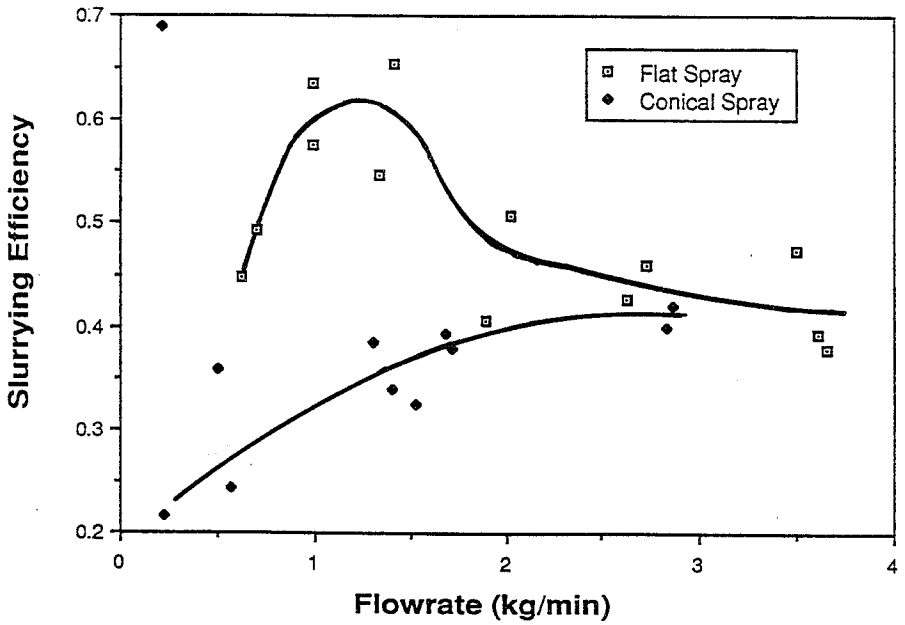

Fig. 2 Plot of Slurrying Efficiency vs. Flowrate of High Grade Ore for Different Nozzle Types

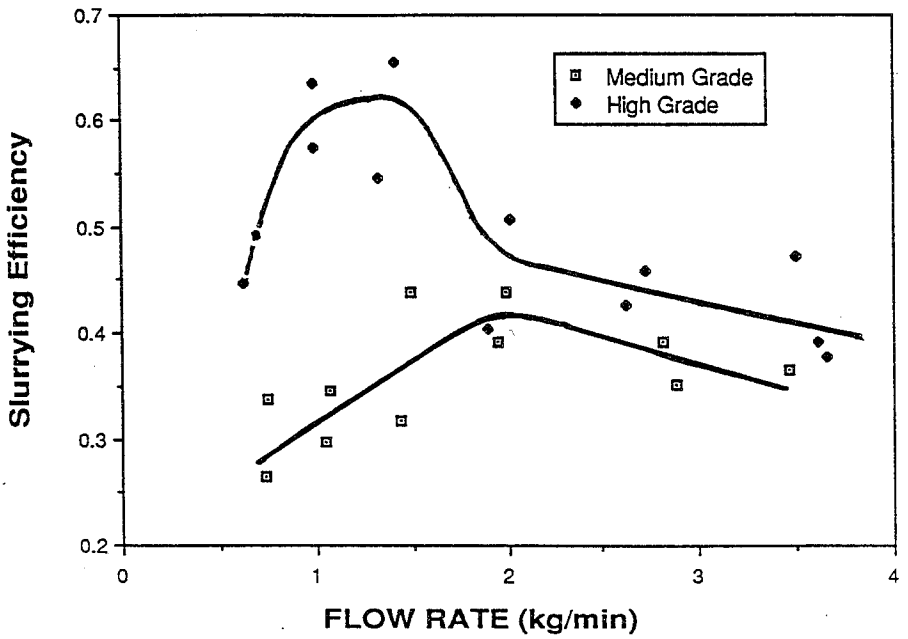

Fig.3 Plot of Slurrying Efficiency vs. Flowrate For High Grade and Medium Grade Ore

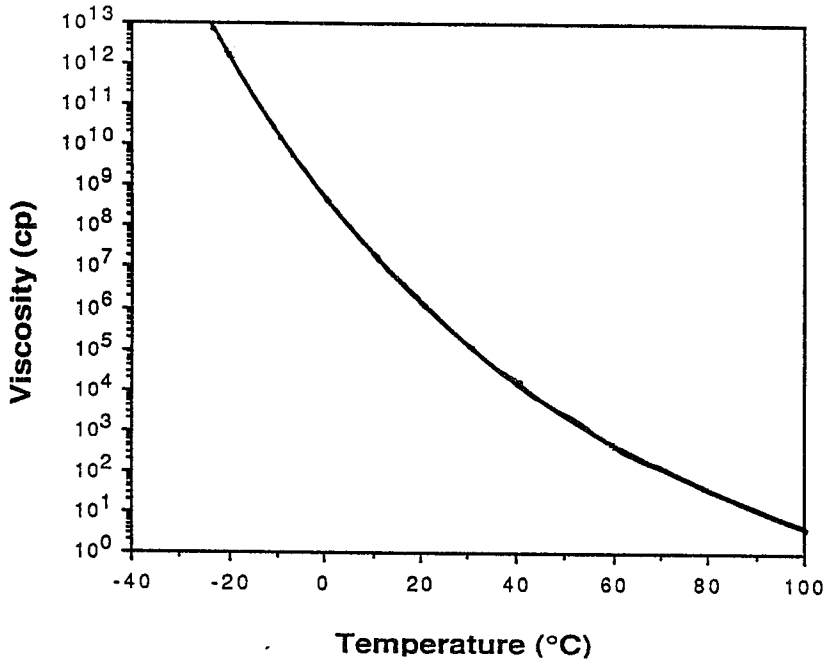

Fig. 4 Bitumen Viscosity vs. Temperature

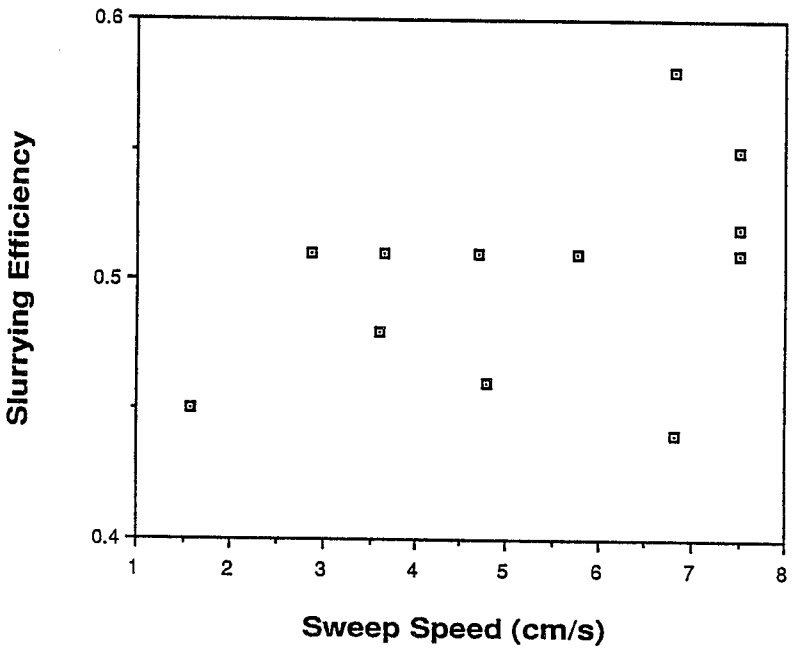

Fig. 5 Sweep Speed vs. Slurrying Efficiency

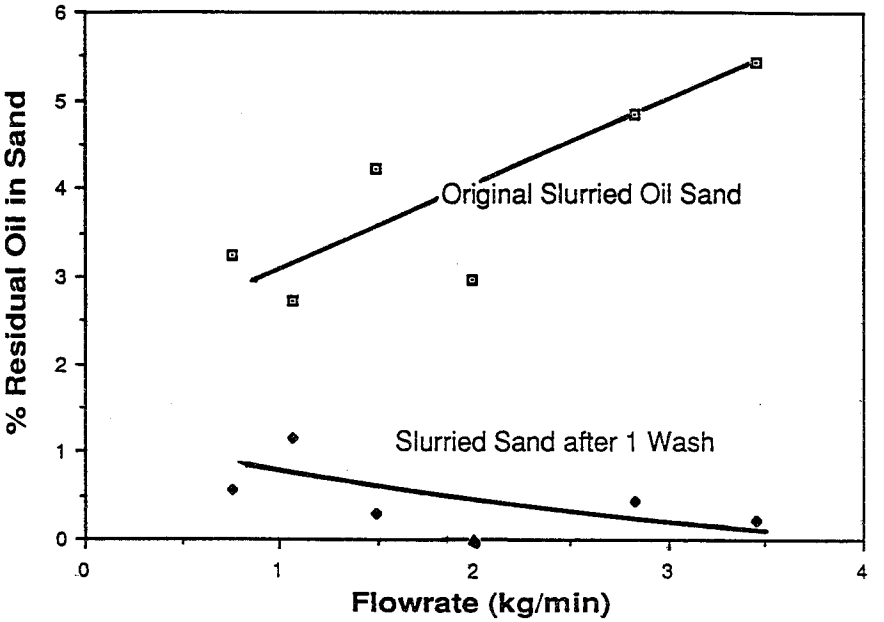

FIG. 6

% Residual Oil in Sand from Medium Grade Ore Before and After Washing

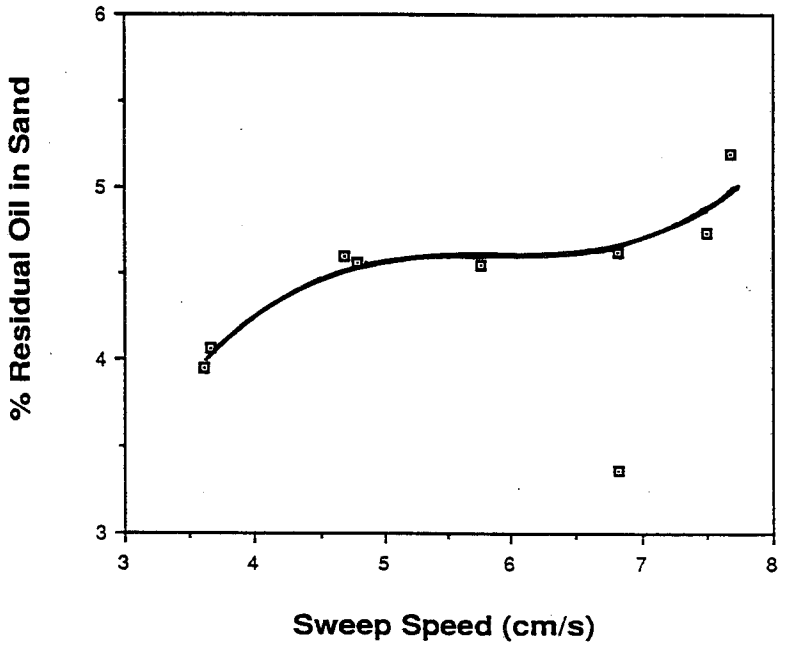

Fig. 7 %Residual Oil in Sand vs. Sweep Speed

5th American Water Jet Conference
August 29 - 31, 1989: Toronto, Canada

Paper / Communication 28

EFFECTIVENESS OF COAL COMMINUTION BY HIGH PRESSURE WATERJET

G. Galecki AND M. Mazurkiewicz
High Pressure Waterjet Laboratory
Rock Mechanics Facility
University of Missouri-Rolla
Rolla, Missouri 65401, USA

ABSTRACT: The results of the work conducted on the coal response for high pressure waterjets attack are presented. The paper covers different types of waterjets such as: solid jets, cavitating jets, and rotating jets and also the results of coal disintegration effectiveness. The concepts of the models of comminuting machines are presented. The coal disintegration in relationship to these models and the process efficiency based on energy consumption are discussed.

RÉSUMÉ : Les résultats des travaux effectués sur le comportement du charbon sous l'effet de jets d'eau à haute pression sont présentés. La communication traite de différents types de jets d'eau tels que : les jets solides, les jets avec cavitation et les jets rotatifs, ainsi que des résultats sur l'efficacité à désintégrer le charbon. Les principes des modèles de machines de fragmentation sont présentés. La désintégration du charbon en rapport avec ces modèles et le rendement du procédé en termes de consommation d'énergie sont analysés.

Organized and Sponsored by the National Research Council of Canada and the U.S. Water Jet Technology Association.

1.0 INTRODUCTION

From the basic mechanistic point of view, in order for a particle to be fractured, a stress must be induced which exceeds the fracture strength of the material. The mode of fracture and the path that it follows depends on the material, the shape and structure of the particle, and on the way and rate at which the load is applied. The way in which the load is applied will control the stresses that induce fracture extension within the particle. The force used to induce this growth can be one of simple compression, which causes the particle to fracture in tension, either at a slow or fast rate. Alternatively the applied load may be in shear, such as is exerted when two particles rub against each other, or the load may be applied as a direct tensile force on the particle. There are many terms which have been used to describe the mechanisms of single particle fracture, such as abrasion, cleavage, and shattering. A new term must now be added - one which describes crack and microcrack hydro-fracture during waterjet attack.

For optimum comminution, a shattering fracture is most beneficial; this occurs when the energy applied to the particle is well in excess of that required for fracture. Under these conditions, very rapid crack growth is induced and will cause crack bifurcation; thus, the multiplicity of areas in the particle that are simultaneously over stressed will combine to generate a comparatively large number of particles with a wide spectrum of sizes. Shattering usually occurs under conditions of rapid loading (e.g., a high velocity impact) with maximum size reduction occurring around the impact points. According to existing theory, the finest product sizes are generated in the zone around the impact point, when insufficient energy is applied to cause total fracture of the particle. The localized nature of the applied stress and the high energy required for this ultra-fine grinding make this process relatively inefficient.

Size reduction involves rupturing the chemical bonds within the material in order to generate new surfaces. Thus, the chemical processes associated with fracture will significantly affect the energy required to induce this fracture. This influence extends beyond the bonds themselves to include the surrounding environment. For example, the presence of water at the crack of water at the crack tip will lower the forces required to expand the crack and improve efficiency, especially where the water contains inorganic ions and organic surfactants [1,2]. One explanation for this effect is that the additives penetrate into microcracks ahead of the major crack front and thus take part in the highly reactive events that occur during fracture. Because the capillary flow of these fluids into the material ahead of the main front runs at the velocity of crack propagation it provides a means of transmitting energy more easily within the crack area. Because the material surrounding the reaction zone is less affected, there is a degree of confinement of the energy to the crack tip zone.

With the advances in the high pressure waterjet technology, one of the potential applications of this science is in the area of material disintegration. Coal was chosen as the subject of interest because of the ongoing search for an alternative source of energy and also coal is very brittle and has a structure that is filled with micro-cracks.

The theoretical model for comminution of coal by high pressure waterjets was based on Griffith's theory [3,4].

2.0 EXPERIMENTAL EQUIPMENT, PROCEDURE AND DISCUSSION OF RESULTS

As mentioned, three types of jets were tested, i.e., solid, cavitating and rotating jets. In all tests the comminuted particles below 75 microns (200 mesh) was separated by a wet sieve analysis [5] and the specific energy levels calculated. The calculated specific energy consumption was the energy of the water stream alone and does not include the energy consumed by the system as a whole. In this chapter each series of experimental equipment, experimental procedure and the results achieved will be discussed separately for each kind of jet.

2.1 Solid Waterjets

The first series of tests was concerning the use of solid waterjets for coal comminution. The initial task was to find dependence of the initial test conditions on comminution effectiveness [6].

All tests were conducted on selected coal particles 20 mesh (840 microns). The pressure range was from 69 MPa to 276 MPa and the waterjet diameter was 0.35 mm. Figure 1 shows a schematic view of the equipment set up for each test condition. Disintegration product was collected and a wet sieve analysis was used to separate the coal particles.

Energy consumption was calculated for comminuting the coal sized below 75 microns only. There was no practical way to divide the energy consumed in the comminution process between the various size fractions of the coal obtained. Thus, in considering all the input energy as being used to generate coal particles in the size range below 75 microns, one is over estimating the actual energy required for this process.

In Table 1, Figure 2 and 3 respectively are given the results of sieve analysis and energy consumption for different test conditions. The lowest level of the energy consumption was observed for test no. 12, where relatively low percentage of the coal particles in size below 75 microns was created. The pressure used for test number 12 was 69 MPa. This is an important remark from a practical point of view, because lower pressures are easier to generate and does not require expensive equipment.

As conclusions from this part of the tests, it can be stated that:
-energy consumption for tested systems is pretty high, range 400-1400 kWh/ton. One of the possible reasons is that particles had a chance of getting in touch with the jet only one time during entering the nozzle.
-coal under high pressure waterjet impact shows breakage typical for brittle materials. Scanning microscope picture study of comminuted coal, Figure 4 does not show any plastic deformation or abrasion between the coal particles.

2.2 Cavitating Waterjets

The second series of experiments were for cavitating jets. The cavitation number which defines the inception and subsequent growth and collapse of cavitation bubbles is given by the equation:

$$\sigma = \frac{P_o - P_v}{\rho U_o^2/2}$$

where P_o and U_o are the ambient values of pressure intensity and velocity, and P_v and ρ are the vapor pressure and the density of the liquid, respectively. For maximum cavitation in the chamber, the outlet pressure should be approximately 1% of the inlet pressure. To control these conditions, a specially designed cavitation chamber was used, Figure 5 [7].

Two types of nozzles were used. The first series utilized the Lichtarowicz's type nozzle. For this series the coal was loaded into the cavitation cell and acted by the high pressure waterjet.

Using the cavitation nozzle, tests were conducted for jet action time of 5.0 seconds at an inlet pressure of 34.5 MPa for a mass of 200 grams. The results showed that an almost linear relationship existed between the initial coal size and the energy consumption. The lowest energy consumption was for the smallest coal particle size of 30 mesh. As the coal size was increased the energy consumption increased. These results can be explained by the fact that for the same coal mass but smaller grain size, the total surface area of coal which comes into contact with the cavitation bubbles is greater. Cavitation is a micro-phenomenon and the area of contact is very important. For this reason, the erosion process observed during the cavitation phenomenon is proportional to the coal grain size.

For the same initial coal size of 30 mesh, as the time of jet action was increased to 10.0 seconds, a drastic increase in the energy consumption occurred (13,502 kWh/ton for the 10 second tests as compared to 839 kWh/ton for the 5.0 second test). These results indicate the importance of the slurry concentration. To further emphasize these results, tests were conducted for constant pressures but for different amounts of initial coal of 200, 400 and 600 grams. The results show that as the initial coal mass was increased the energy consumption decreased.

In the second series a solid waterjet nozzle was used; combined with a mixing chamber, slurry nozzle and the cavitation cell, Figure 6. The coal entering the mixing chamber was attacked by the high pressure waterjet and exists through the slurry nozzle into the cavitation chamber. Inside the cavitation chamber erosion of the coal particles takes place due to the cavitation phenomenon and high turbulence in the chamber.

The tests were conducted for a nozzle diameter combination of d=1.04mm and D=3.04mm for pressures of 24MPa and 38MPa. The initial coal particle size was 30 mesh. The tests were conducted for different back pressures, as shown in Figure 7.

The lowest energy level achieved for a final product size of minus 75 microns was 407 kWh/ton for an inlet pressure of p=24MPa. Also, the results show that no significant changes in the energy level was observed at higher pressures. Slight changes in the back pressure caused no significant change in the energy consumption.

From this series of experiments it could be concluded that:
-the coal should not be surrounded by water
-a higher slurry concentration would produce better results
-as the initial particle size was decreased the energy consumption decreased.

2.3 Rotating Waterjets

A specially designed and machined test rig was used in conducting these experiments [8]. The primary system component was the rotating spindle. Three nozzles were attached to the nozzle head. The rotating spindle was supplied with high pressure water through the rotary coupling. The maximum speed of rotation for this rotary coupling was limited to 600 rpm. The system was driven by an electric motor. A schematic view of the assembly can be seen in Figure 8. The coal was filled into both a perforated and imperforated container. The container placed on a mechanical lifter made it possible to give vertical movement to the container.

The initial coal particle size was 13.3mm <S< 18.8mm. The tests were conducted for a pressure of 38 MPa using three nozzles each of diameter 0.81mm.

The initial tests were carried out with the nozzles oriented at 3, 8 and 20 degree angles. The first task was to investigate the importance of increasing the volume of water to the comminution process. Tests were carried out for jet action times of 15, 30 and 75 seconds

using an imperforated container. It was seen that as the time of jet action increased the energy consumption increased. To explain this, consider the waterjet action on the coal and the time over which it acts. Increasing the jet action time increases the volume of water utilized. The coal particles tend to become suspended in the excess water. They are in effect, surrounded by a coating of water whose protective ability increases with the volume of water utilized. The waterjets lose energy in penetrating this protective coating in order to come in contact with the coal particles. This energy is not used to create new surfaces during direct collision with coal particles and hence is wasted.

For the same series of tests a perforated coal container was used and waterjet action times of 75 seconds and 150 seconds investigated, with vertical up and down axial movement (8 cycles/minute) of the coal container. A test with a jet action time of 75 seconds was conducted without container movement. The results show, Figure 9, that the energy consumption with coal container movement to be almost half those of the case with rotation only. These results clearly indicate the importance of the kinematic movement of the high pressure waterjets, which gives a better opportunity for the coal particles to come in direct contact with the water jets.

In the next series the orientation of the nozzles were changed. The nozzles were now oriented perpendicular to the spindle axis. The effect of vertical movement of the coal container was investigated for both 3 and 12 full cycles of motion for 2 minute tests. For the purpose of comparison the coal container was also kept stationary. The energy requirements appear almost 20% less for the case when rotating jets were moved up and down 12 times per minute, as compared to other kinematic conditions of the jets for the tests carried out, Figure 10.

As conclusions from this portion of experiments, the importance of the slurry concentration was brought out again. The coal particles should not be surrounded by water. Also the kinematics and dynamics of the interaction between the high pressure waterjets and the material to be comminuted plays a very important role in the effectiveness of the comminution process.

3.0 GENERAL CONCLUSIONS

Based on the experimental results presented in this paper the following conclusions can be formulated:

The energy consumption taken into consideration as a criterion of the effectiveness of the comminution process shows a very strong dependence on:

-jet diameter and pressure
-initial coal particle size
-solid concentration in slurry
-kinematics of the interaction between the high pressure waterjets and coal.

The minimum specific energy input of 400 kWh/ton achieved for presented coal comminution machines represents an improvement in the comminution technology. Typical energy consumption levels associated with fluid energy mills are in the range of 700-800 kWh/ton [9].

It has to be mentioned, that further research and the knowledge gained, gave us a chance to build coal comminution machine based on high pressure waterjet in which the energy consumption level was reduced down to slightly over 12 kWh/ton [10]. This machine undergoes patent pending process.

4.0 ACKNOWLEDGEMENT

Support for this project was provided by the Department of Energy, Pittsburgh Energy Technology Center under contract no. DOE-DE-AC22-86PC-91271. The authors are grateful for this support.

5.0 REFERENCES

1. P. Somasundaran, I.J. Lin, "Effect of the Nature of Environment on Comminution Process", Ind. Eng. Chem. Process. Des. Dev., Vol. 11, pp. 321-331 (1972).

2. P.A. Rehbinder, "On the Effect of Surface Energy Changes on Cohesion, Hardness and Other Properties of Crystals", Proc. 6th Phys. Congr., State Press, Moscos (1928).

3. Griffith, A.A., "The Phenomena of Rupture and Flow in Solids", Phil. Trans. Roy. Soc. of London, A 221 (1921), pp 163-197.

4. Griffith, A.A., "The Theory of Rupture", Proc. 1st Int. Congress Appl. Mech., (1924), pp 55-63.

5. Mazurkiewicz, M. Galecki, G., Technical Progress Report No. 7 on Contract DOE-DE-AC22-86PC-91271, submitted to Department of Energy, Pittsburgh, Pennsylvania, April 1987.

6. Galecki, G., Mazurkiewicz, M., "Coal Comminution by High Pressure Waterjet". 8th International Symposium on Coal Slurry Fuels Preparation and Utilization, Orlando, Florida, May 1986. pp. 852-861.

7. Galecki, G., Mazurkiewicz, M., Summers, D.A., "Cavitation Cell" Invention Disclosure 88-UMR-042.

8. Mazurkiewicz, M., Galecki, G., Technical Programs Report No. 10 on Contract DOE-DE-AC22-86PC-91271, submitted to Department of Energy, Pittsburgh, Pennsylvania, July, 1987.

9. Report of the Committee on Comminution and Energy Consumption "Comminution and Energy Consumption", Publication NMAB-364, National Academy Press, Washington, D.C., 1981, pp. 13-39.

10. Mazurkiewicz, M., Galecki, G., Technical Progress Report No. 21 on Contract DOE-DE-AC22-86PC-91271, submitted to Department of Energy, Pittsburgh, Pennsylvania, June 1988

TABLE 1. TEST PARAMETERS AND SIEVE ANALYSIS BY WEIGHT.

Test #	Test arrangement scheme	Pressure MPa	Sieve analysis %			Remarks
			100 mesh	200 mesh	-200 mesh	
1	C	276	25	17	58	
2	H	276	50	17	33	
3	A_2	276	10	39	51	
4	D	276	25	52	23	
5	E	276	24	20	56	outlet slurry is very hot (70 C)
6	G	276	5	65	30	
7	F	276	24	69	7	outlet slurry is very hot (70 C)
8	A_1	138	34	17	49	
9	A_1	276	22	61	17	
10	B	276	19	66	15	
11	A_2	138	23	27	50	two passes through the disintegrator
12	A_2	69	50	22	28	jamming

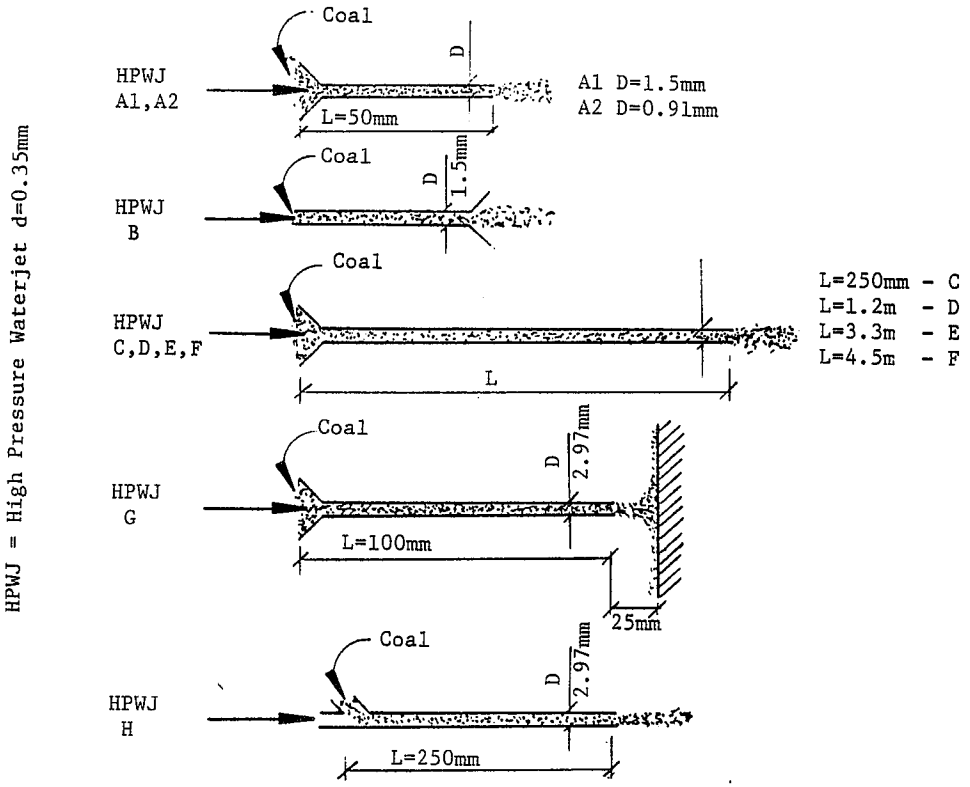

FIGURE 1. TEST ARRANGEMENT SCHEMES FOR SYNCHRONOUS WATER AND COAL STREAM.

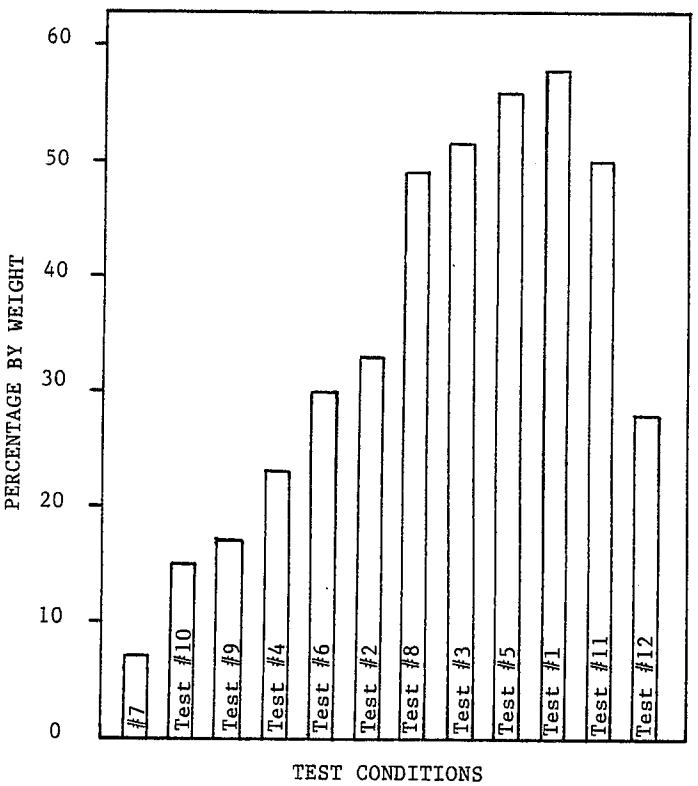

FIGURE 2. PARTICLE SIZE OUTPUT BELOW #200 MESH;
ONE STAGE PROCESS: TEST 1 TO 10 AND 12;
TWO STAGE PROCESS: TEST NO. 11.

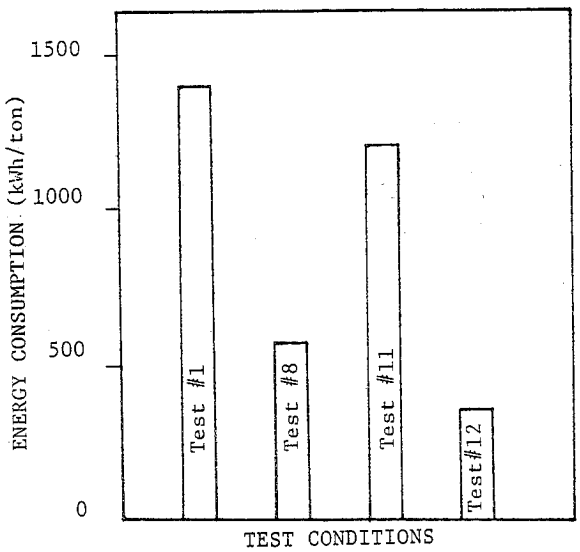

FIGURE 3. ENERGY CONSUMPTION FOR DIFFERENT TEST ARRANGEMENTS.

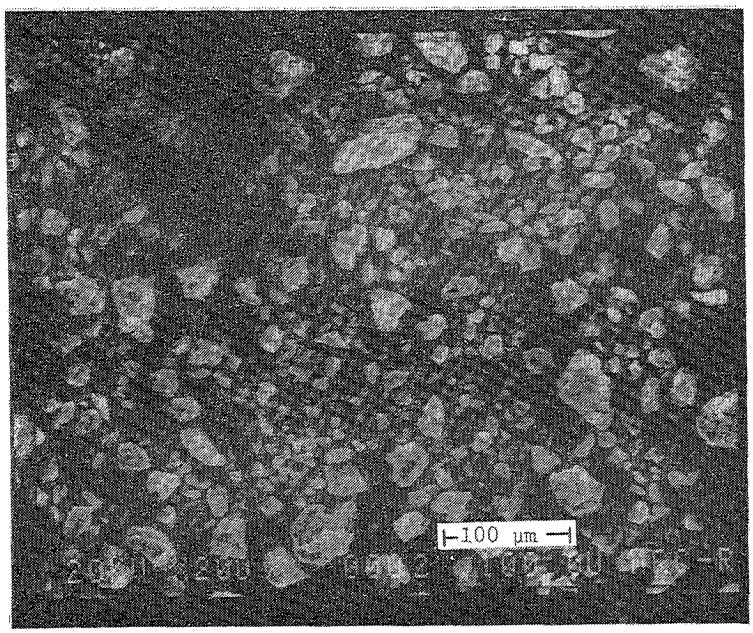

FIGURE 4. COAL PARTICLES OBTAINED AFTER WATERJET ACTION (SEM, X200 MAGNIFICATION)

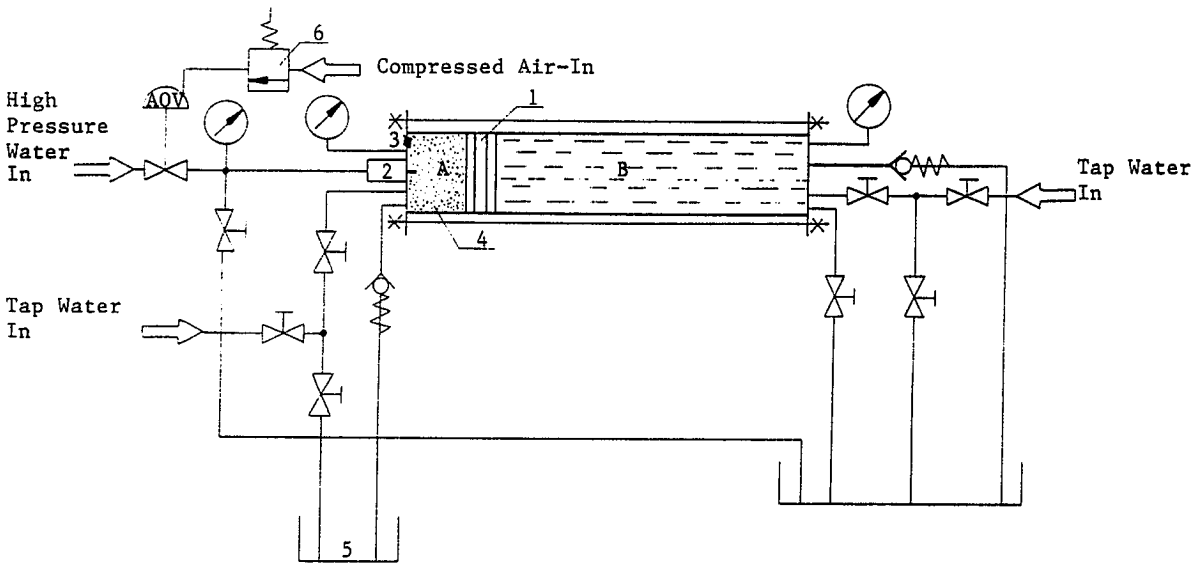

FIGURE 5. SCHEMATIC DIAGRAM OF CAVITATION CELL.
A - COMPARTMENT A OF THE CELL
B - COMPARTMENT B OF THE CELL
1 - PISTON
2 - HIGH PRESSURE WATER JET NOZZLE
3 - LOADING WINDOW
4 - COAL TO BE DISINTEGRATED
5 - DISINTEGRATED PRODUCT CONTAINER
6 - TWO-WAY VALVE FOR REMOTE CONTROL OF DIAPHRAGM AIR

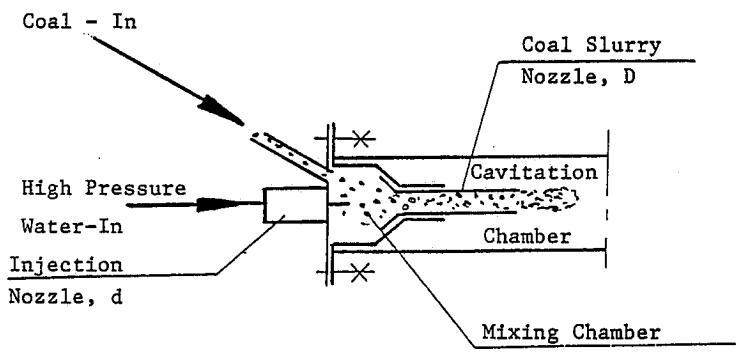

FIGURE 6. SCHEMATIC DRAWING OF APPARATUS FOR SOLID WATERJET TESTS WITH MIXING CHAMBER.

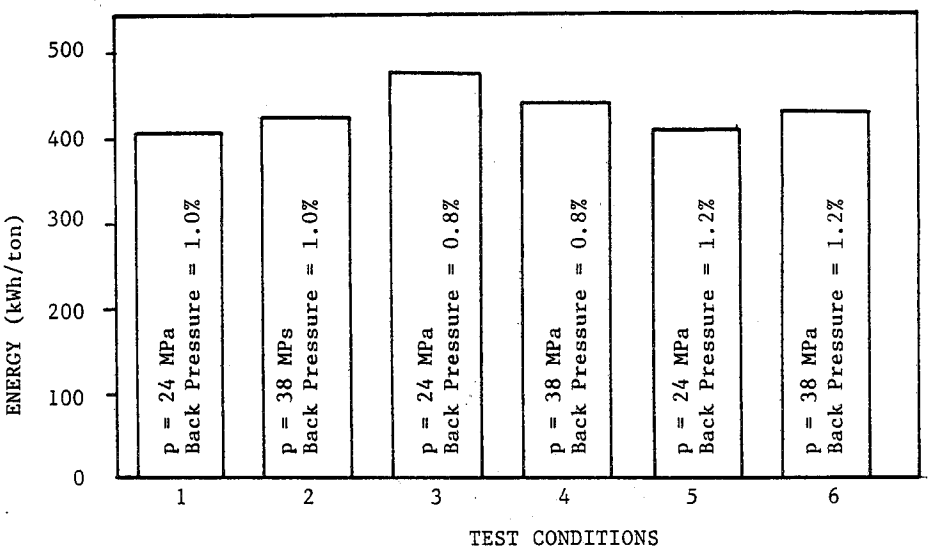

FIGURE 7. GRAPH OF ENERGY VERSUS DIFFERENT COMBINATIONS OF INLET AND BACK PRESSURES FOR CAVITATION TESTS.

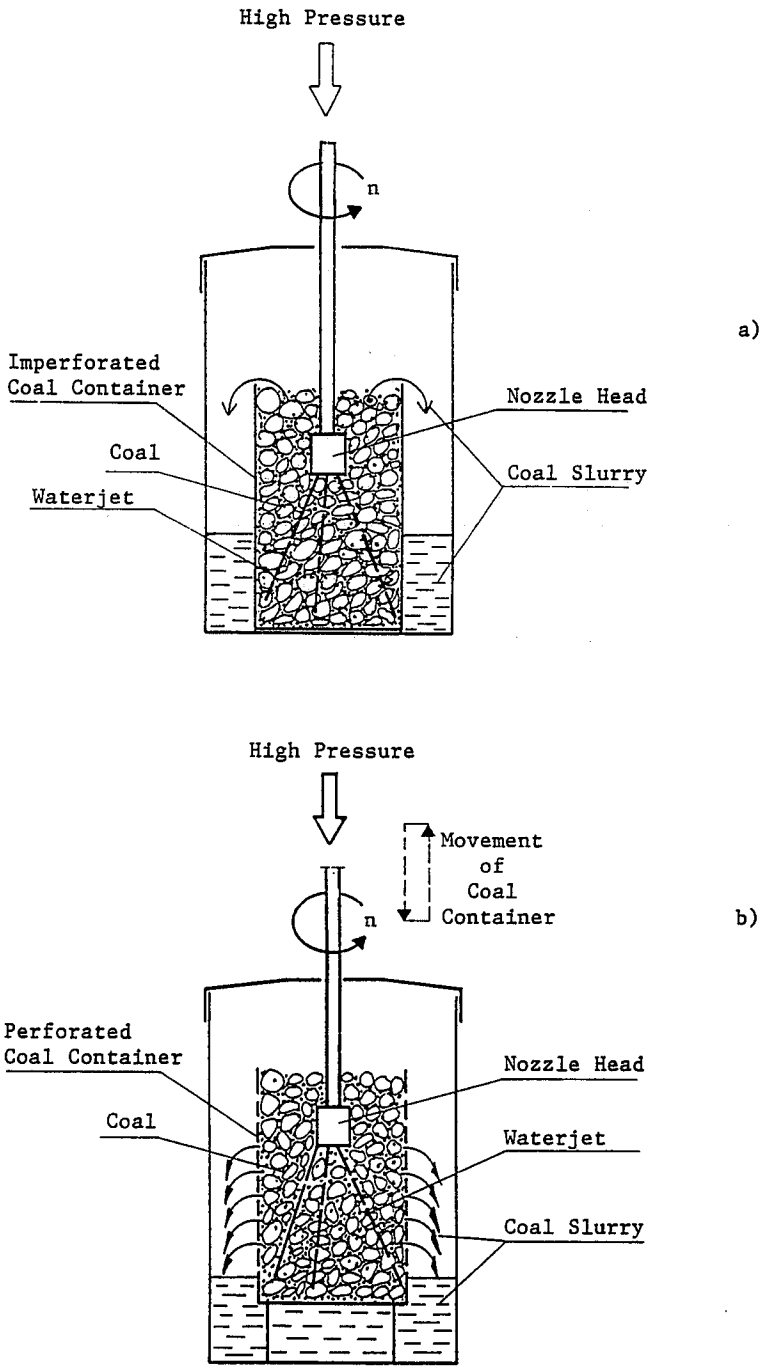

FIGURE 8. SCHEMATIC DRAWING OF ROTATING WATERJET EXPERIMENTAL EQUIPMENT.

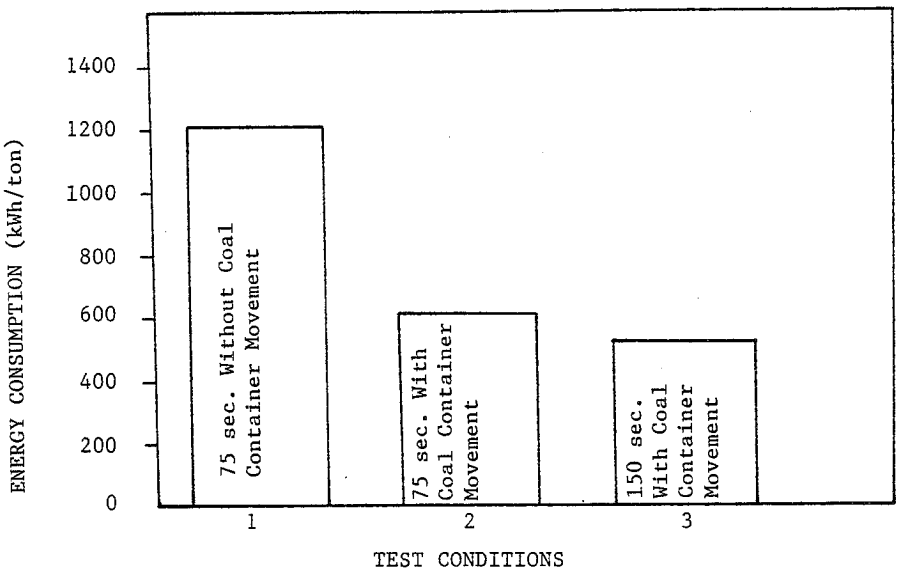

FIGURE 9. GRAPH OF ENERGY VERSUS DIFFERENT TEST CONDITIONS FOR NOZZLES ANGLED AT 3, 8 AND 20 DEGREE ANGLES.

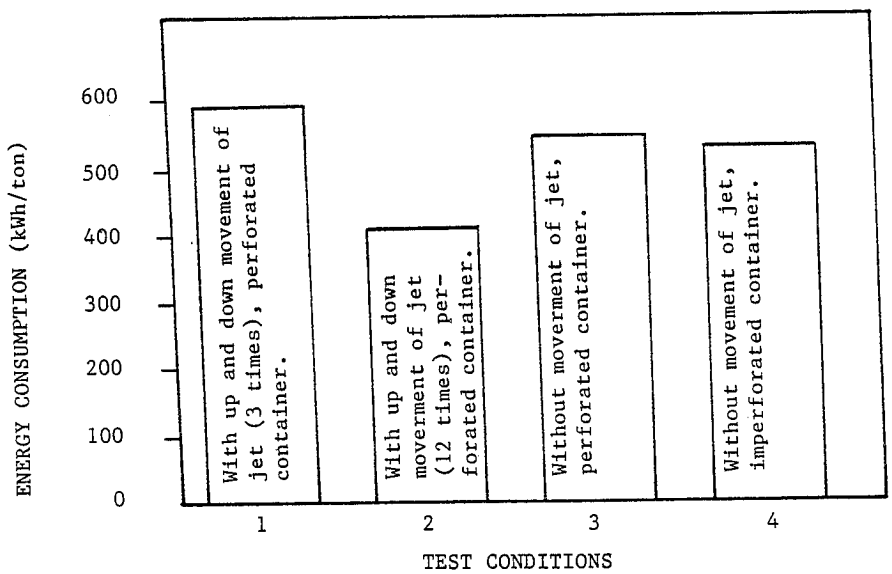

FIGURE 10. GRAPH OF ENERGY VERSUS DIFFERENT TEST CONDITIONS FOR NOZZLES ANGLED PERPENDICULAR TO THE AXIS OF ROTATION.

5th American Water Jet Conference
August 29 - 31, 1989: Toronto, Canada

Paper / Communication 29

THE EFFECT OF PRESSURE AND FLOW RATE ON CUTTING SOIL UTILIZING WATER JET FOR WIDER APPLICATION

H. Yoshida
Kajima Institute of Construction Technology
2-19-1 Tobitakyu, Chofu City, Tokyo 182, Japan

M. Shibazaki, H. Kubo, S. Jimbo, AND M. Sakakibara
Chemical Grouting Co., Ltd.
Minato-ku, Tokyo 107, Japan

ABSTRACT: This paper reports the results of tests which were performed to obtain more accurate knowledge of the relationship between cutting time and cutting characteristics, for the purpose of improving the cutting efficiency and reducing the cost of the Jet Grouting Method. In the tests a water jet with a higher energy (pressure x flow rate) than conventional units was used on model soil. The results of the tests reveal that cutting efficiency is improved by increasing the energy of the water jet. They also prove that increasing flow rate contributes more to improving cutting efficiency than increasing pressure, leading to advantages in terms of economic efficiency.

RÉSUMÉ : Cette communication fait état des résultats d'essais qui ont été mené pour acquérir des connaissances plus précises sur la relation qui existe entre le temps de coupe et les caractéristiques de coupe, en vue d'améliorer le rendement en coupe et de réduire le coût de la Méthode de cimentation par jet. Dans les essais, un jet d'eau plus puissant (pression x débit) que les jets classiques a été utilisé sur du sol modèle. Les résultats des essais révèlent que le rendement en coupe augmente en fonction de l'énergie du jet d'eau. Ils démontrent également qu'un débit accru contribue davantage à l'amélioration du rendement qu'une pression accrue, ce qui présente des avantages en termes de rentabilité.

Organized and Sponsored by the National Research Council of Canada and the U.S. Water Jet Technology Association.

1. INTRODUCTION

The Jet Grouting Method, which is now being used worldwide, was developed by the authors about twenty years ago as one method of soil modification. The results of numerous applications mostly based upon the conventional specifications (pressure of 400 kgf/cm^2 and flow rate of 600 l/min) clarify the characteristics of cutting soil utilizing a water jet. Recently however, improvements providing longer diameters and lower costs have been required. For this purpose, new specifications, which have never been tried, are necessary to replace the conventional ones. This report describes the effect of pressure and flow rate on cutting soil utilizing a water jet, based on the results of tests conducted on model soil with higher pressures and higher flow rates than the standard. Economic efficiency is also addressed.

2. TEST PROCEDURES AND DEVICES

When loose sandy soil is cut by water jet, the factors affecting cutting efficiency include the pressure, the flow rate, the speed of rotation and withdrawal of a nozzle, the pass number and the properties of the soil. Of these five factors, the two basic factors, i.e. the pressure and the flow rate, were tested.

(1) Parameters of Tests

Since the high-pressure pump used in the tests can produce 470 kgf/cm^2 at the maximum, we adopted two other values of 370 kgf/cm^2 and 270 kgf/cm^2 accordingly.

Since the high-pressure pump used in the tests can produce 300 l/min at the maximum, we adopted two other values of 150 l/min and 75 l/min accordingly.

The nine combinations of the respective levels of the pressure and the flow rate are shown in Table 1. The tests were conducted twice for each case.

(2) Test Method and Equipment

As shown in Fig. 1, a test tank 2.2 m in width, 6.0 m in length and 1.83 m in height was filled with sand, with a grain size distribution as is shown in Table 2, and the soil was compacted by watering. The soil properties after compaction are shown in Table 3.

For the tests, a high-pressure pump HDP380 manufactured by Hammelmann was used. Photo 1 shows the test jetting.

In the tests, the cutting velocity of the water jet (cutting time until reaching a particular point) was measured to evaluate the cutting characteristics of the jet.

To detect the passing of the water jet, vibration sensors were fixed on steel nets, which were installed in the model soil at eight points: the first was 1.0 m away from the nozzle with the others spaced at 0.5 m intervals up to a total distance of 4.5 m. The time when the water jet passed a point on a steel net was detected according to the impact vibration caused by the water jet. The measurement procedure is shown by a flow chart in Fig. 2. Photo 2 shows how vibration sensors were placed. Photo 3 introduces the method of recording the data detected by the vibration sensors.

3. TEST RESULTS

The data obtained by the vibration sensors are shown in Fig. 3. The relationship between the distance from the nozzles to each measuring point and the time until the water jet passed the point is shown in Fig. 4.

4. EVALUATION

(1) Discussion of Test Results

When the distance from the nozzle to each measuring point and the time until the water jet passed the point are taken as characteristic values, it was judged that the distance (L), pressure (P) and flow rate (Q) are each independently, related to T.

Then correlative equation for these parameters are given below.

$$T = 63{,}700 \times L^{2.21} \times P^{-1.72} \times Q^{-1.88} \quad \ldots (1)$$

where,

T: Time until passing (sec)
L: Distance between the nozzle and measuring point (cm)
P: Discharge pressure of water jet (kgf/cm^2)
Q: Discharge flow rate of water jet (cm^3/sec)

If the cutting velocity (V: V=l/T) at a particular point is taken as a characteristic value, Eq. (1) can be transformed to the following equation.

$$V = 7.10 \times 10^{-6} \times L^{-1.21} \times P^{1.72} \times Q^{1.89} \quad \ldots (2)$$

The results of calculations using Eq. (1) are shown in Fig. 4 with dotted lines.

(2) Comparison of Effects of Pressure and Flow Rate on Cutting Distance

Eq. (1) was used to calculate distances for different combinations of pressure and flow rate for a representative jetting period of 0.1 second, and Fig. 5 shows the results accordingly. The dotted lines show the constant hydraulic energy (P x Q).

Furthermore, the figure obviously indicates that, for a given level of hydraulic energy, higher flow rates produce larger cutting distances than higher pressures. For example, a jet stream with a pressure of 600 kgf/cm^2, a flow rate of 2000 cm^3/sec, and a jetting period of 0.1 second reaches 225 cm, while another stream with a pressure of 200 kgf/cm^2, a flow rate of 6000 cm^3/sec, and a jetting period of 0.1 second produces a cutting distance up to 250 cm, a gain of approximately 10 percent.

Since the absolute value of the exponent for Q exceeds that for P in Eq. (1), it can be said that the effect of Q on the cutting is more influential than that of P.

Although an increase of hydraulic energy causes an exponential increase of jetting distance, the latter does not increase as much as the former.

(3) Economic Effect

According to Fig. 5, doubling hydraulic energy results in an increase of some 1.8 times of the cutting distance. Since the Jet Grouting Method, however, cuts soil in a horizontal disc shape, the cut area corresponds to the square of the cut radius.

This means that doubling hydraulic energy consequently produces an increase of 3.2 times of the cut area, and this increased energy can contribute greatly to cutting efficiency.

As was mentioned previously, an increase of flow rate is more effective in improving the cutting efficiency than an increase of pressure, hydraulic energy being the same. However, as there is only a slight difference in the exponential values, you may not think the effects of increasing pressure differ much from those of increased flow rate.

From a practical point of view, however, higher pressure requires a super high-pressure pump and also the improvement of the pressure holding capacities of hoses and pipes resulting in cost increases due to changes in materials, thickness, etc.

On the other hand, higher flow rate requires the expansion of plunger diameter of the pump, for example, resulting in a relatively simple and low cost change.

Taking into account applications to actual execution, therefore, it is believed that an increased flow rate rather than increased pressure is more efficient for the overall improvement of the method.

5. CONCLUDING REMARKS

The cutting tests were performed on model soil which consisted of sand in a test tank. However, it is supposed that some quantitative problems remain if the test results are to be applied directly to natural soil strata. Therefore, it is planned that verification tests will be conducted on actual ground soil in the near future.

In the present tests, out of all the factors relevant to cutting distance, the speed of rotation and withdrawal, the cutting frequency and the properties of the soil were excluded from consideration. Future tests will be definitely focused on the relationships between cutting distance and these factors accordingly..

Reference

Teruo Yasuhiro, Hiroshi Yoshida, and Kenji Nishi, Simplified Construction Technology--Underground Engineering Method Using Water Jet, in Japanese

Table 1 Classes regarding between Pressure and Flow Rate

		Discharge Pressure (kgf/cm²)		
		470	370	270
Discharge Flow Rate (ℓ/min)	300	○	○	○
	150	○	○	○
	75	○	○	○

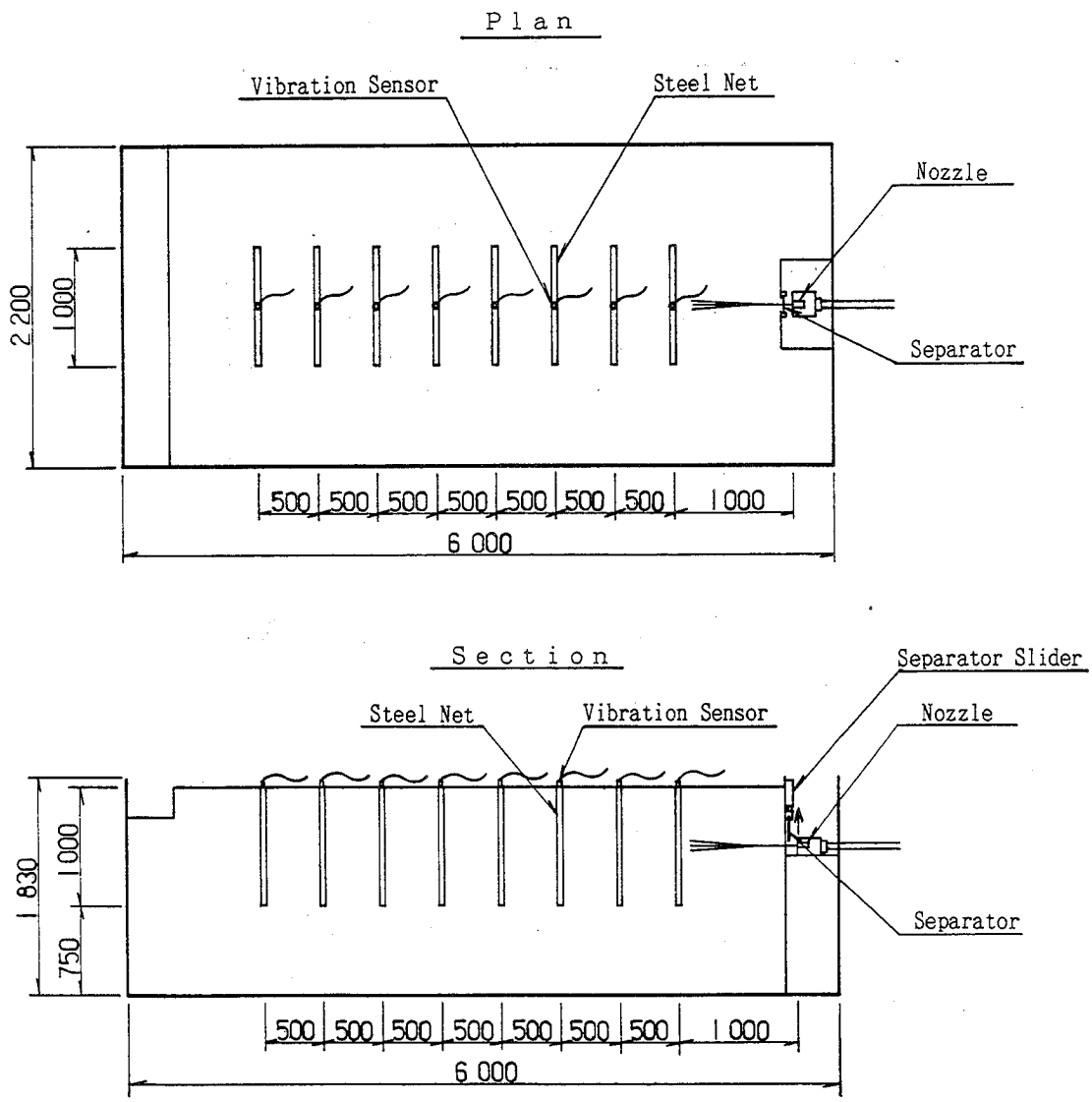

Fig.1 The Size of the Test Tank filled with Test Soil and Placement of Vibration Sensors

Table 2 Grain Size Distribution of Filled Sand

Gravel	(more than 2000μm)	%	6
Sand	(74～2000μm)	%	90
Silt	(5～74μm)	%	4
Clay	(less than 5μm)	%	
Maximum Grain Size		mm	19.1
Coefficient of Uniformity		U	2.4
Coefficient of Curvature		Uc'	1.0
Specific Gravity of Soil Particle		Gs	2.3

Table 3 Soil Properties after Compaction by Watering

Natural Moisture Content		%	22.6
Compaction Characteristic	Optimum Moisture Content	%	24.0
	Maximum Dry Density	t/m³	1.5
N - Value (Average) (SPT)			2～3

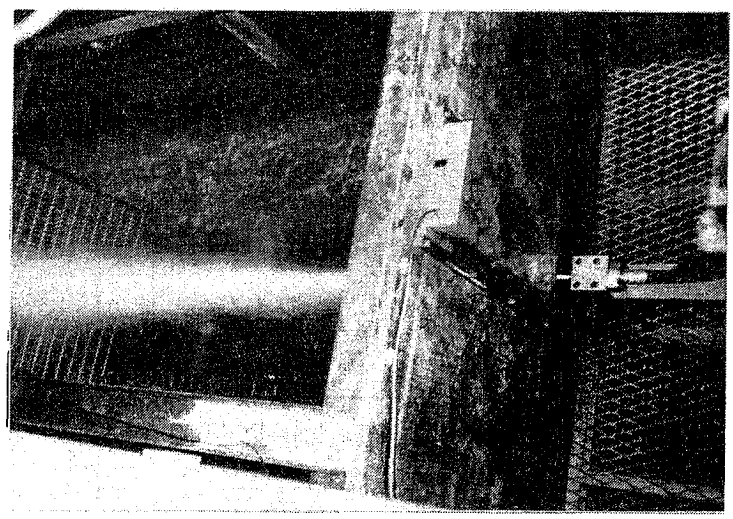

Photo 1 The Test Jetting

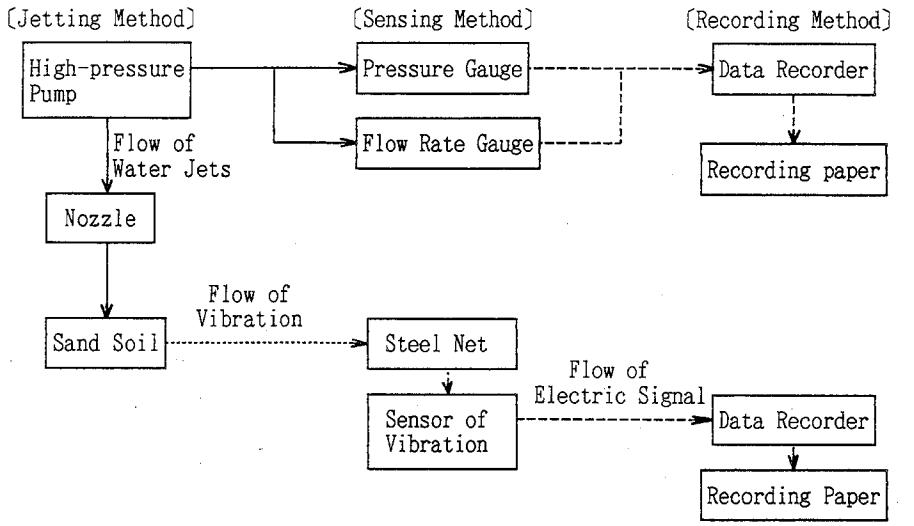

Fig.2 Flow Chart of Jetting, Sensing and Recording

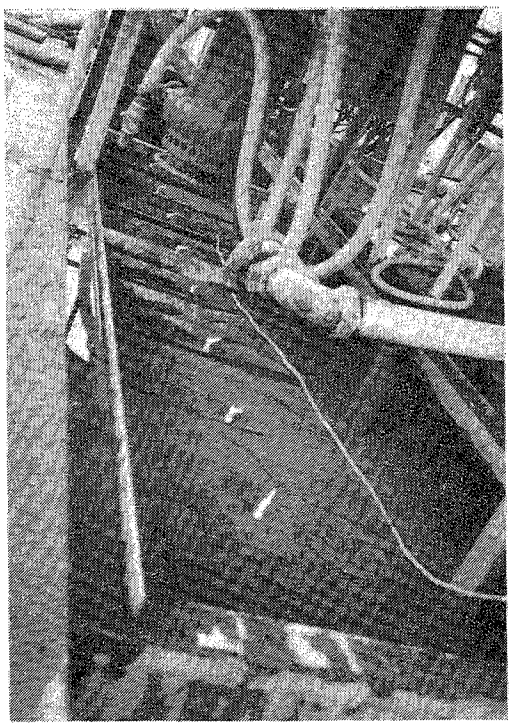

Photo 2 A Situation of Vibration Sensors

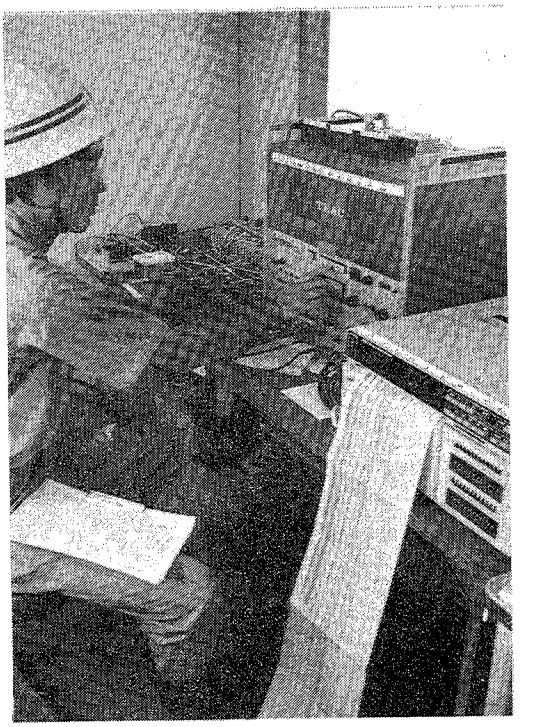

Photo 3 Output of the Data obtained by the Vibration Sensors

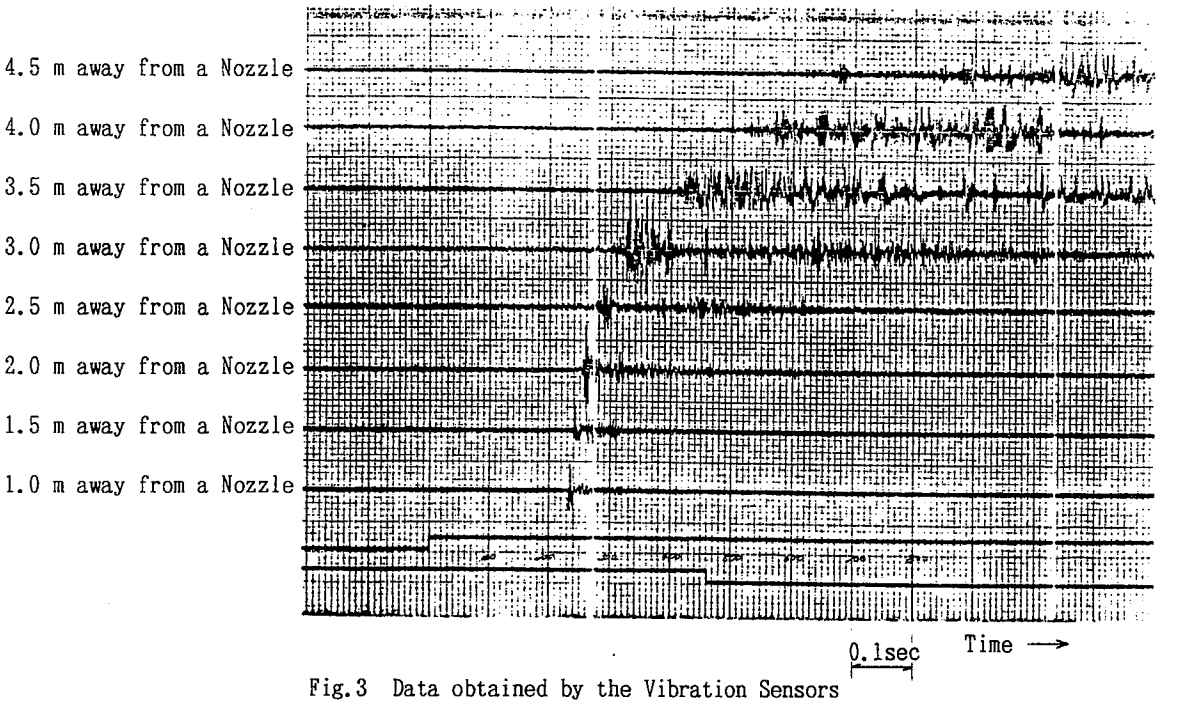

Fig.3 Data obtained by the Vibration Sensors

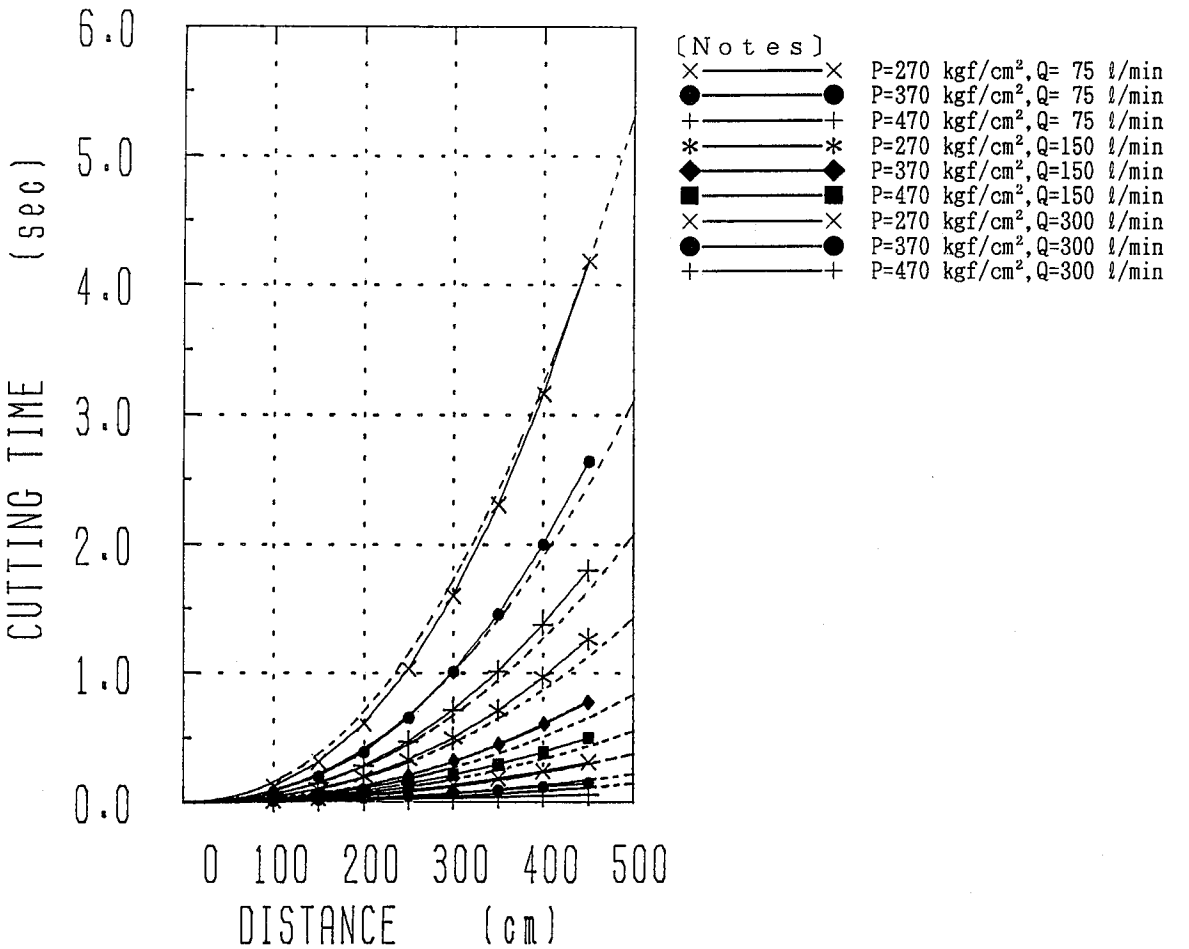

Fig.4 The Relationship between the Distance of each Measuring Point and the Time until the Water Jet passed the Point

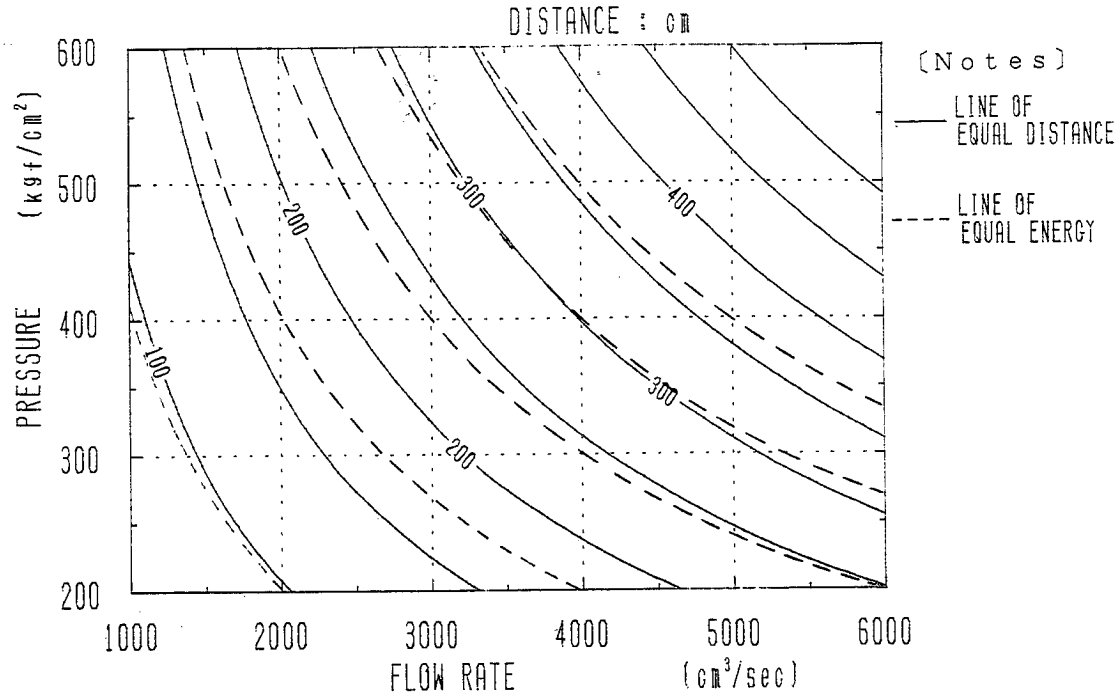

Fig.5 The Distances reached for different Combinations of Pressure and Flow Rate, and the Constant Hydraulic Energy

5th American Water Jet Conference
August 29 - 31, 1989: Toronto, Canada

Paper / Communication 30

MAJOR ADVANTAGES OF ENTRY DRIVAGE WITH SWING-OSCILLATING JET IN HIGH METHANE CONCENTRATION COAL SEAM

D. Cheng, Z. Zou AND C. Guo
China University of Mining and Technology

X. Zhang
Kailuan Coal Mine Administration

G. Li, Z. Wang, Y. Jia AND Z. Xiao
Xintai Coal Mine Administration
China

ABSTRACT: Swing-oscillating jet has been used for entry drivage in the high methane concentration coal seam in two mines, Xiandewang Coal Mine in Hebei and Matian Coal Mine in Hunan. It speeds up drivage and raises economic benefits greatly, also shows its specific advantages in improving the face of the environment, making the coal face safe and the tunnel good quality.
A portable swing-oscillating jet excavator tunnels coal at a speed of 229.2m per month in Xiandewang Coal Mine. The drivage cost decreases by more than 1/3.
Major advantages:
(a) Gas releases uniformly, and accidents are prevented.
(b) Coal dust is greatly restrained, the average dust content is below 10mg/m^3.
(c) There is no possibility of gas or coal dust explosion as no spark is induced.
(d) Air around the face is very fresh and noise is very low, which is good for the workers' health.
(e) Since no damage to surrounding coal body, the tunnel is shaped quite well. The amount of maintenance work is greatly reduced.
The new drivage technology is now becoming more popular at Xiandewang and other Coal Mines.

RÉSUMÉ : Des jets oscillants ont été utilisés pour creuser des galeries dans des couches de charbon riches en méthane dans deux mines, celle de Xiandewang dans le Hebei et celle de Matian dans le Hunan. La technique accélère le creusement et améliore grandement la rentabilité; elle comporte aussi des avantages particuliers pour l'environnement du front de taille : conditions d'exploitation sécuritaires et tunnel de grande qualité.
Un excavateur à jet oscillant portatif creuse le charbon au rythme de 229,2 m par mois dans la mine de Xiandewang. Le coût de creusement est réduit de plus du tiers.
Principaux avantages :
(a) Le gaz s'échappe uniformément et les accidents sont empêchés.
(b) La poussière de charbon est grandement limitée, la teneur moyenne étant inférieure à 10 mg/m^3.
(c) Les coups de grisou ou de poussières sont impossibles car il n'y a pas d'étincelles.
(d) L'air près du front de taille est très frais et le bruit est très faible, ce qui est bon pour la santé des travailleurs.
(e) Comme le charbon encaissant n'est pas endommagé, la paroi du tunnel est très régulière, ce qui diminue les travaux d'entretien de beaucoup.
La nouvelle technologie d'excavation est maintenant répandue à Xiandewang et dans d'autres mines de charbon.

Organized and Sponsored by the National Research Council of Canada and the U.S. Water Jet Technology Association.

1.0 INTRODUCTION

Some achievements have been yielded in basic, industrious and experimental research on coal cutting with swing-oscillating jet in China(1)(2). It has been proved by experiments both at home and in site that jet energy can be fully used and efficiency of brittle material cutting can be raised noticeablly by using working way of perpendicular swing-oscillating. Therefore, swing-oscillating jet can be considered as a new working way of jet with great prospects.

Drivage in high methane concentration coal seam is often accompanied with dangers of gas content exceeding safe limit, gas outbursting or exploding, so that it has been a difficult and important project in excavation which needs to be solved as soon as possible.

Research on using the swing-oscillating jet for drivage in high methane concentration coal seam has been conducted at Matian Coal Mine in Hunan and then at Xiandewang Coal Mine in Hebei.

2.0 TECHNICAL REQUIREMENTS BY DRIVAGE IN HIGH METHANE CONCENTRATION COAL SEAM

Generally, coal in high methane concentration coal seam is softer, accidents would often take place if improper drivage technique is used, for example

(a) When gas content exceeds safe limit due to too much gas released, drivage has to be interrupted for removing gas until its content below the limit, it used to be often the case taking place at Xiandewang Coal Mine.

(b) Gas and coal outburst resultsfrom too much gas gushes suddently. It used to happen many times at Matian Coal Mine. Sometimes hundreds of tons of gas burst.

(c) When gas content exceeds the limit in drivage face, gas explosion will often happen if there exists any spark.

According to the practice at Matian and Xiandewang Coal Mine, coal cutting process must possess the following three major requirements for drivage in high methane concentration coal seam in order to ensure safety and continuity:

(a) Coal must be split seam after seam so as to release gas uniformly. Only by doing so, can production be safe and continuous.

(b) No violent vibration to the surrounding coal body must be caused to avoid appearing of gas outburst.

(c) No spark must be induced to prevent gas from exploding during drivage.

3.0 CHARACTERISTICS OF DRIVAGE WITH SWING-OSCILLATING JET

Because of the specific properties of jet and coal seam, coal winning process

with swing-oscillating jet has the following characteristics:

(a) Drivage with swing-oscillating jet is based on jet cutting, coal will not be broken or won unless it is cut by jet.

(b) Amount of coal won by swing-oscillating jet contains direct breaking part and indirect breaking part.

(c) In some loose coal seams with developed bedding and joint, coal collapsing is usually induced after cutting.

To keep safe and continuous drivage in high methane concentration coal seam, we must make full use of jet energy and characteristics of swing-oscillating jet for coal cutting. At the same time, proper technique for coal cutting and drivage process must be employed.

4.0 PROCESS AND MAJOR TECHNICAL PARAMETERS FOR DRIVAGE WITH SWING-OSCILLATING JET IN HIGH METHANE CONCENTRATION COAL SEAM

Process of drivage with high pressure waterjet includes: (a) jet cutting procedures, that is, feeding ways and travelling track of coal cutter; (b) coal cutting, loading, transporting and supporting, etc..

Process of coal cutting with jet is shown in Fig.1. The first step of drivage is always to cut deep bottom slots, which aims at increasing free faces of coal body instead of at coal cutting. The deeper the bottom slots, the larger the coal cutting capacity. To deepen the slots, travelling speed of the swing rod of coal cutter must be lowered, usually less than 100-150mm/s. Two to three or more times of cutting is required if necessary. The swing rod then moves up gradually along a zigzag course, and the nozzle moves a certain height (about 350-450mm) every time. The small coal columns between breaking zones formed by horizontal cutting will collapse by both their own weights and the vertical component of jet. The horizontal speed of swing rod is increasing with the lance moving up. The whole drivage face will have been finished when the lance moves from bottom to top.

Having been formed initially, the face must be cut 1-2 times along its two vertical sides to make itself regular. After the tunnel has been formed, holes for setting support must be cut by way of extending the rear swing rod and contracting the front swing rod. Process of jet drivage is shown in Fig.2.

No one is allowed to stand in front of the cutter when it is working. At this time, workers except the driver are preparing support materials. And the cutter must not operate during loading coal and supporting. The driver maintains machine at the same time to make full use of working time.

It must be pointed out that cutting bottom slots is a very important link in the drivage process, but this does not mean that the depth of bottom slots is proportional to cutting time. Depth of the bottom slot will increase slowly when

cutting damp coal. Sometimes, depth of 1-1.5m can be reached in a few seconds when the cutting angle is such that the mixture of coal and water can flow out naturally.

In practice, the experience been got is that perfect coal cutting effect can be obtained by the following procedures: cutting from bottom to top, cutting along a zigzag track, increasing horizontal swing speed from low to high and cutting repeatedly after having deep bottom slots.

Technical parameters of swing-oscillating jet used in drivage at Matian and Xiandewang Coal Mine are as follows:

working pressure 300-500 bar
nozzle diameter 1.9-2.4 mm
horizontal speed of swing rod 100-300 mm/s
amplitude of lance(at nozzle exit) 100 mm
frequency of lance about 14 Hz
standoff 0-150 mm

5.0 MAJOR ADVANTAGES OF DRIVAGE WITH HIGH PRESSURE SWING-OSCILLATING JET IN HIGH METHANE CONCENTRATION COAL SEAM

Practice at Matian and Xiandewang Coal Mine has born out that except a faster drivage speed and higher economic benefits, drivage with swing-oscillating jet in high methane concentration coal seam shows its unique advantages, such as improving safe condition at working face and ensuring tunnel quality.

5.1 Reducing Procedures, Shortening Time For Each Operating Cycle And Raising Drivage Speed

As shown in table 1, procedures of drivage with swing-oscillating jet can be reduced by 8 compared with conventional blasting. Time for each operating cycle is shortened from 83 to 57 minutes(average 26 minutes), so that drivage speed is raised.

According to data obtained at Xiandewang Coal Mine in 1988, average drivage length per month was 217m, the highest was 229.2m. Each work team needed only 9 workers(used to need 11). Drivage cost was reduced by more than one third and noticeable economic benefits were obtained.

5.2 Unique Advantages of Drivage in High Methane Concentration Coal Seam With High Pressure Waterjet

(a) A good coal cutting technique, shallow spliting and repeated cutting, has been found for drivage with swing-oscillating jet at Matian and Xiandewang Coal Mine. Coal body will be split seam after seam without vibration. So that gas can release uniformly and is easy to be controlled. Accidents such as gas exceeding the safe limit and outburst are prevented.

(b) When swing-oscillating jet with pressure of 300-500 bar is used for drivage in high methane concentration coal seam, coal dust content can be lowered obviously, the average content is usually lower than 10mg/m^3. It can be seen from table 2 that the coal dust content of drivage with swing-oscillating jet is 20 times lower than that with blasting.

(c) High pressure waterjet is the power and tool for jet drivage, and no spark will be produced. Therefore, it prevents gas and coal dust from exploding which is often caused by spark when drivage with machine or blasting. It strongly guaranties the safety for production.

(d) Having observed and analysed jet drivage, many experts in hygiene believed that waterjet can increase the number of anion(air vitamin) in air during drivage, which is very good for workers' health. During coal cutting, noise created by high pressure waterjet is far lower than that by blasting or machine. This is also very useful for workers' health and for alleviating workers' fatigue.

(e) No vibration or damage to surrounding coal body and roof is induced by using the technique of shallow spliting and repeated cutting and cutting deep bottom slots. Shapes of tunnels are good.

After drivage with jet and blasting, the moving speed of roof has been measured at Xiandewang Coal Mine. As shown in Fig.3: after drivage with jet, the largest moving speed of roof is about 7mm/day; while after blasting, it is about 37mm/day, and there is effect on the roof for 8-10days. Moving speed of roof when drivage with blasting is about 5-10 times of that when drivage with jet.

Tunnel quality becomes better and maintenance easier due to the slow moving speed of roof caused by jet drivage.

6.0 CONCLUDING REMARKS AND ACKNOWLEDGEMENT

For drivage in high methane concentration coal seam, swing-oscillating jet has many unique advantages over other ways of drivage. Nowadays, the new drivage technique has been popularizing at Xiandewang and other Coal Mines.

The authors wishes to express their thanks for taking part in the project to Prof. Zou Changsheng, Mr. Liu Linsheng, Mr. Wu Banji (CUMT) and Engineer Lu Fuming, Fu Xuejun, Zhao Songnian Xia Xumin (Wuxi Mining Machinery Plant) and Engineer Guo Lisheng (Xintai Coal Mine Administration).

7.0 REFERENCES

1. Cheng Dazhong, Zou Changsheng, etc., "Development of Novel Operating Method of High Pressure Waterjet for Coal Mine Entry Drivage." Proceedings of Mining Machinery and Electro-technology Section, International Symposium of Mining Technology and Science, Sept., 1985, Xuzhou, PRC.

2. Cheng Dazhong, Zou Changsheng, etc., "Preliminary Practice in the Use of a Swing-Oscillating Waterjet in Coal Mine Drivage." Proceedings of the 2nd US Waterjet Symposium, 1983

3. Zou Changsheng, Cheng Dazhong, etc., "Investigation on Anatomy of Continuous Waterjet for Updating Jet Performance." Proceedings of the 3rd US Water Jet Conference, 1985

4. Cheng Dazhong, "The Basic Knowledge About a Novel Technology High Speed Water Jet." (Teaching Material) May, 1986

5. Cheng Dazhong, Zou Changsheng, etc., "Preliminary Development of High Pressure Waterjet 'Less Cutting' Drivage Studying." Proceedings of the International Waterjet Symposium, Sept. 9-11, 1987, Beijing, China

Table 1. Comparision for Procedures and Cycle Time

Blasting			Jet Drivage		
No.	Procedure	Time(min)	No.	Procedure	Time(min)
1	Preparing	3	1	Preparing	5
2	Boring	20	2	Coal cutting	10
3	Filling	4			
4	Workers withdrawing	3			
5	Gas measuring	2			
6	Setting fuse	3			
7	Blasting	1			
8	Smoke removing	10			
9	Gas measuring	3			
10	Workers returning	4	3	Cutting holes	15
11	Coal loading	13	4	Coal loading	10
12	Supporting	20	5	Supporting	15
13	Transporting	12	6	Transporting	12
Total Time		83	Total Time		57

Table 2. Coal Dust and Gas Content

Measuring Process	Coal Dust Content (mg/m^3)			Maximum Gas Density Against/Return(%)	
	Blasting	Jet	Jet Lower Than Blasting	Blasting	Jet
Boring	136	/	/	/	/
Blasting	274	/	/	1.7/2.4	/
Coal Cutting	/	21-27	-247 - -253	/	1.2/1.8
Coal Loading	216	9	-207	/	/
Supporting	93	4	-89	/	/

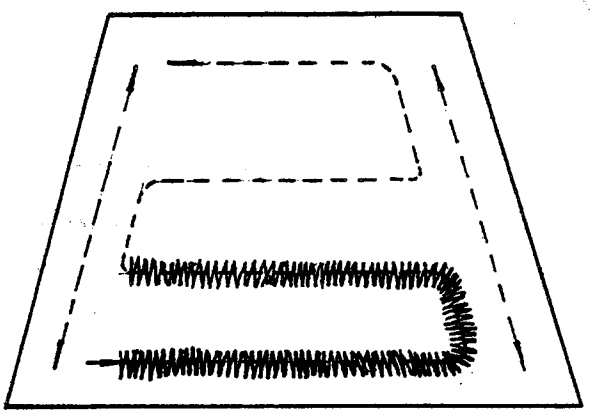

Fig.1 Process of Coal Cutting With Waterjet

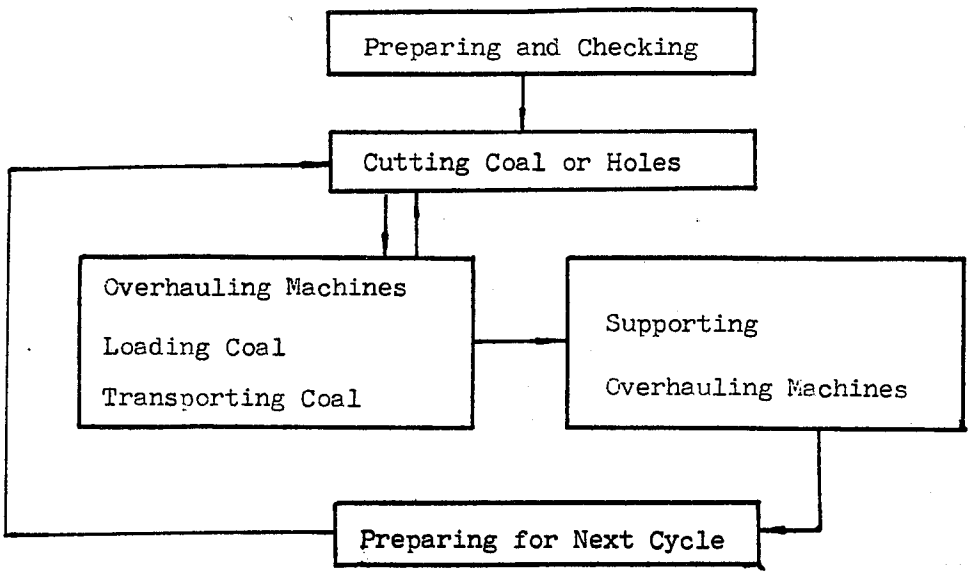

Fig.2 Flow Chart of Jet Drivage Process

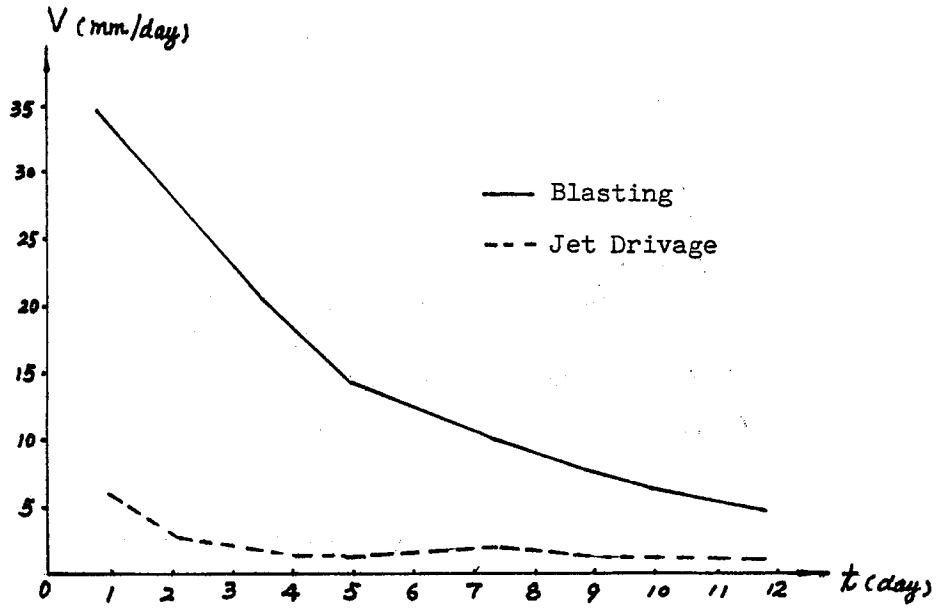

Fig.3 Comparision Between Effects of Blasting and Jet Drivage on the Moving Speed of Roof

5th American Water Jet Conference
August 29 - 31, 1989: Toronto, Canada

Paper / Communication 31

HYDRAULIC BOREHOLE COAL MINING IN DIAGONAL HOLES

R. Kownacki, S. Lasko AND J. Bednarczyk
Research and Design Center of Opencast Mining "Poltegor"
53-332 Wroclaw, Poland

ABSTRACT: We present the results obtained during the design, field-test, and production phases of the Hydraulic Borehole Mining of Coal. The HBM of coal in this example has been associated with process of gas freeing and relaxation of coal stratum.
The holes have been drilled through rock and coal in horizontal and diagonal directions. The HBM device was lowered into the borehole. Generation pressure of cutting jets was 8 up to 11MPa at first and 24 up to 28MPa at experimental series. We compared the results of both series. We obtained triple quantity of coal mining. We generalized results of field-test.

RÉSUMÉ : Nous présentons les résultats obtenus au cours des phases de conception, d'essai sur le terrain et de production du programme d'abattage hydraulique en trou de sonde (AHTS) du charbon. L'AHTS du charbon dans cet exemple a été associé au processus de libération des gaz et de relaxation de la couche de charbon.
Les trous ont été forés dans la roche et le charbon dans des directions horizontales et obliques. Le dispositif d'AHTS a été descendu dans le trou de sonde. La pression des jets d'eau a été de 8 à 11 MPa au début et de 24 à 28 MPa dans la série expérimentale. Nous avons comparé les résultats des deux séries. Nous avons obtenu trois fois plus de charbon abattu. Nous avons généralisé les résultats de l'essai sur le terrain.

Organized and Sponsored by the National Research Council of Canada and the U.S. Water Jet Technology Association.

1.INTRODUCTION

This Hydraulic Borehole Coal Mining /HBM/in diagonal and horizontal holes has been realized in this experiment.The Hydraulic Borehole Mining of Coal has been associated process with gas freeing and relaxation of coal stratum. This experiment concerned the tunnel drilling at -350 m level,in one of the coal mine in Silesia.

The active method leading to the elimination of gas danger /methane/,has been realized by borehole washing or water jet cutting of coal.Technical realization of this method is drilling four series of holes in face of front tunnel to the coal deposite,after leaving rock wall about 2 meters of thickness.To these boreholes has been introduced HBM device.

At the beginning,the generation pressure of water jets has been 8 up to 11 MPa Thus it was hydrowashing process mainly.

The method of gas freeing and relaxation process of coal deposit is effective when the mass of excavated coal is not smaller than 4% of coal stratum.

The old method by hydrowashing was not effective,and absorbing much time. Because of this situation, we have proposed the new method.Then it was used higher generation pressure of water jets and special Nozzle Mining Device.The water pump has had pressure 24 to up 28 MPa, and nozzles with special geometry of holes.

The efficiency of gas freeing and relaxation of coal stratum was triple improved in the relation to the old hydraulic method.

2.HYDRAULIC BOREHOLE MINING DEVICE

The Hydraulic Borehole Mining of Coal system is shown in Fig.1.The water supply hose and filter have been water instalation of coal mine.The miner`s truck was used as the water tank.The water is flowing from tank to high pressure plunger pump by the suction hose.

The pump unit technical data:
type: PT 30/300,
pressure: 32 MPa,
capacity: 0,5 x 10^{-3} cubic meters per second,
el. power:18 kW.

Two the pumps unit PT 30/300 worked in paralleling system.From the pumps the water is directed by the flexible hose to the high pressure swivel.And from swivel the water has flowed by the hole of the hollow rod into the Nozzle Mining Device.The Nozzle Mining Device has had 3 nozzles as shown in Fig.2 and Fig.3.

The high pressure water jets have been cutting coal and have produced coal slurry.The coal slurry was flowing into the space between the pipe and the hollow rod to the swivel.Then the slurry returns by the hose to the reservoir with the stockyard.

The water pressure in the chamber has been generating the flow slurry outside. The rotating of the Nozzle Mining Device has been realised by electromotion or with the hand.The water pressure and pump`s capacity, have been regulated by the feed-back valve.The Nozzle Mining Device has had 3 nozzles diameter 1,5 mm/see Fig.2 and Fig.3./.We have usually used two side nozzles.

The water from the stockyard has returned to the water tank for pumps,but only partly.

3.HBM of COAL-FIELD TEST

In one of coal mine on Silesia coal field, tunnel has been drilled between two shafts.We have used HBM of coal technology with underwater jets cutting system.This Hyraulic Borehole Coal Mining has been associated process with gas freeing and relaxation of coal deposit.

At first, 12 holes drilled from 3m to up 48m length, that is shown in Fig.4. The drilled machine type WDP-1,has bored the holes diameters 76mm up 112mm. Wehave been drilled four series of holes.

In the first series, the diagonal holes Nr.1,2,3, have been drilled with angle -30 degree/-II/6 rd/ and the length from 3m up to 8m.

In the second series the diagonal holes Nr.4,5,10, have been drilled with angle -10 degree /-II/18 rd/,the length from 5m to up 8,5m.
In the third series the diagonal holes Nr.6,7,and 11,have been drilled with angle direction -2degree /-II/90 rd/,length from 11m to up 26m.
In the four series the diagonal holes Nr.8,9,and 12, have been drilled with angle +4 degree / II/45 rd/,and the length from 25m to up 32m.
All the holes have had steel pipes and closed system, in front of the tunnel face.Before using the Hydraulic Borehole Mining of Coal, the coal deposit has been drilled in the same holes.
After drilling 8 holes, it hase come up to hydraulic borehole in the first series of the holes.These holes give a lot of gases and coal slurry with slate flowing.
During HBM, in the holes of the third series, coal stratum between the hole Nr.2 and the hole Nr.8 was broken and then between the hole Nr.11.
While Hydraulic Borehole Coal Mining in hole Nr.6, the slurry was also going out through the hole Nr.12.
The remaining holes didn`t show gasodynamic process and hydroworking was without disturbing.
The period of HBM of Coal for gas freeing and deposites relaxation amounted to 16 working days.So, the time of tunneling was shorted about 2,5 times.
It was obtained medium about 83 kg of coal per hour with the HBM method, thus the increasing of the hydromining was triple.
The above results were very satisfactory, so that is why the Coal Mine uses the HBM device to usual mining phase. That means, tunnel drilling was HBM used at the 500m distance.

4.CONCLUSIONS

1. The Hydraulic Borehole Coal Mining with h.p. water cutting jets in comparison with the Hydrowashing, is more effective for gas freeing and the coal stratum relaxation.This HBM method requires the pump with nominal pressure about 30 MPa, and using special nozzles which are tested for Jet Cutting Technology.

2. The HBMof Coal with the underwater high pressure water cutting jets, can be used as an independent technology for the coal excavation, under the condition localization of convenient coal deposites-in the diagonal, horizontal and perpendicular holes.

3. The application of this technology is technically possible for other minerales besides coal, under the condition that geological structure of overburden and stratum are advantageous.Especially it is recomended for small deposit, where trdicional technology is difficult or economocally not acceptable.

5.REFERENCES

1.J.B.Cheung: " Hydraulic Borehole Mining of Coal".Proc.3rd International Symposium on Jet Cutting Technology.Paper D3.by BHRA, Chicago,U.S.A. /11th-13th May 1976/.

2.Patent USA Nr. 4,615,564.

3. Patent West Germ., Nr.2728853, Nr.2924547.

4.Raport by R.Kownacki,-CPBR 1.4/42-6/ "Poltegor" Wrocław,Poland,/1988/,not published.

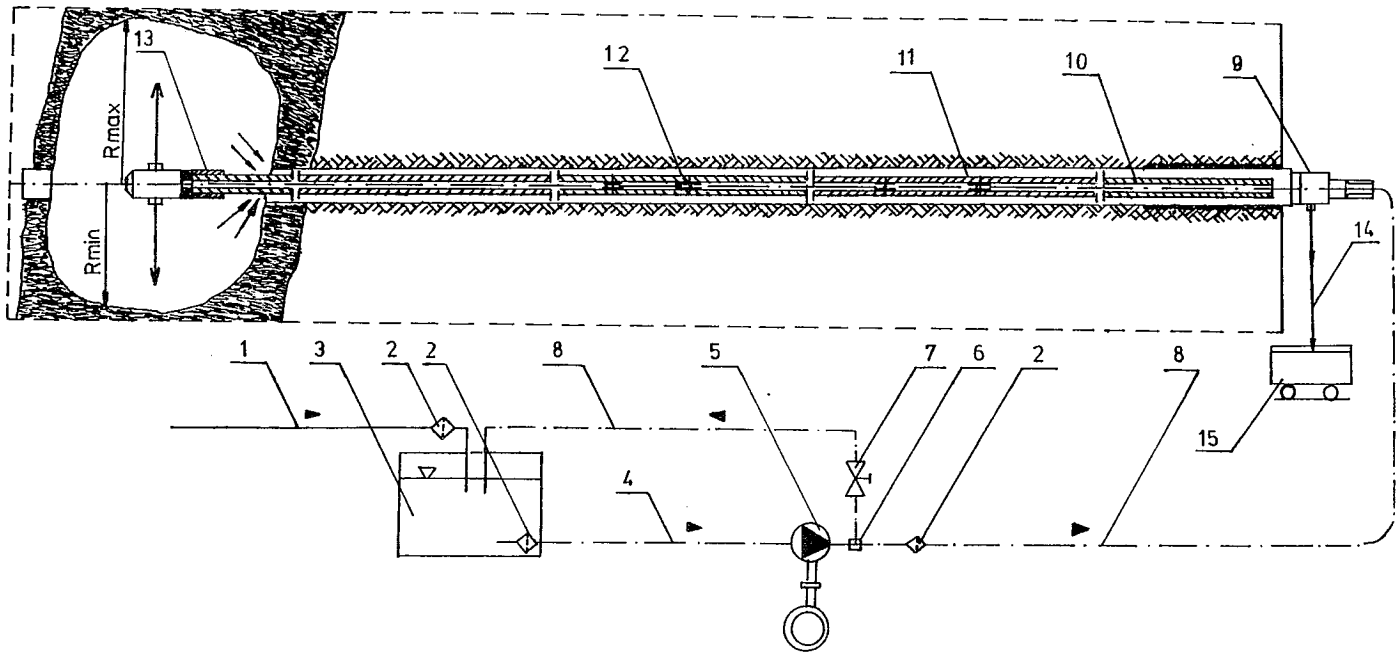

FIG1.HYDRAULIC BOREHOLE MINING OF COAL

1 WATER SUPPLY CONDUIT	6 TEE	11 CONNECTING PIECE
2 FILTER	7 YALVE	12 PRESSURE PACKING
3 WATER TANK	8 H.P.HOSE	13 MINING DEVICE
4 SUCTION CONDUIT	9 SWIVEL	14 RETURN SLURRY HOSE
5 H.P. PUMPS UNIT	10 HOLLOW ROD	15 SLURRY RESERVDIR

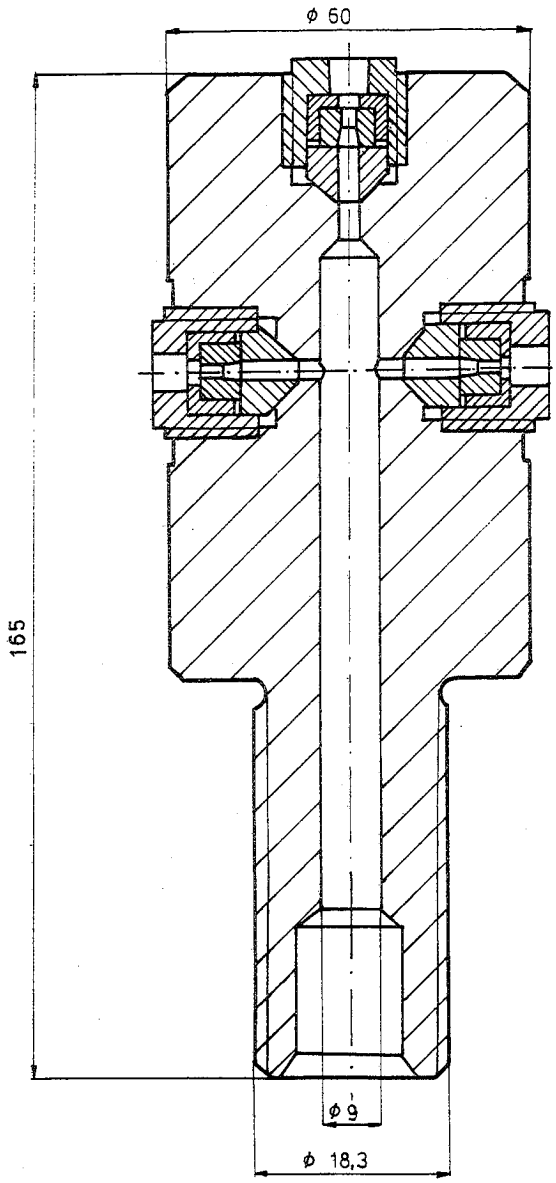

FIG.2 NOZZLE MINING DEVICE DESIGN.

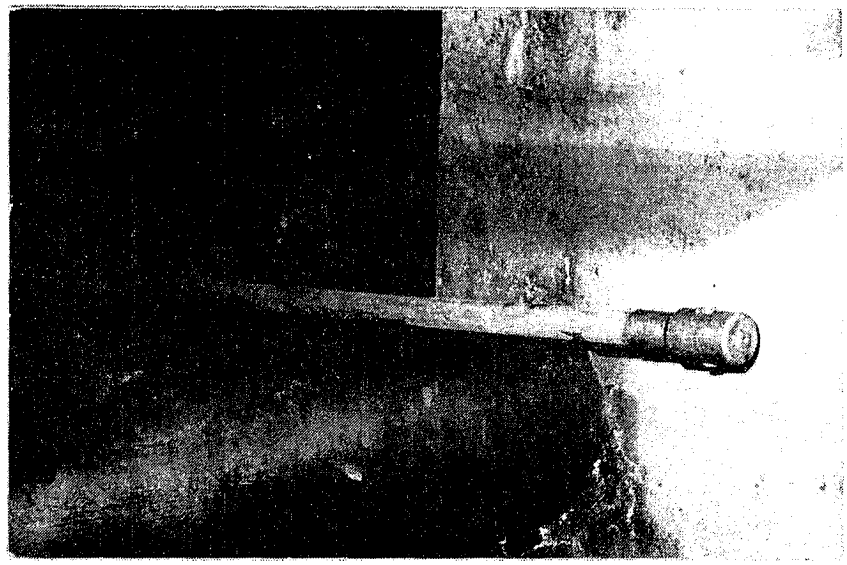

FIG.3 THE VIEW OF HBM DEVICE

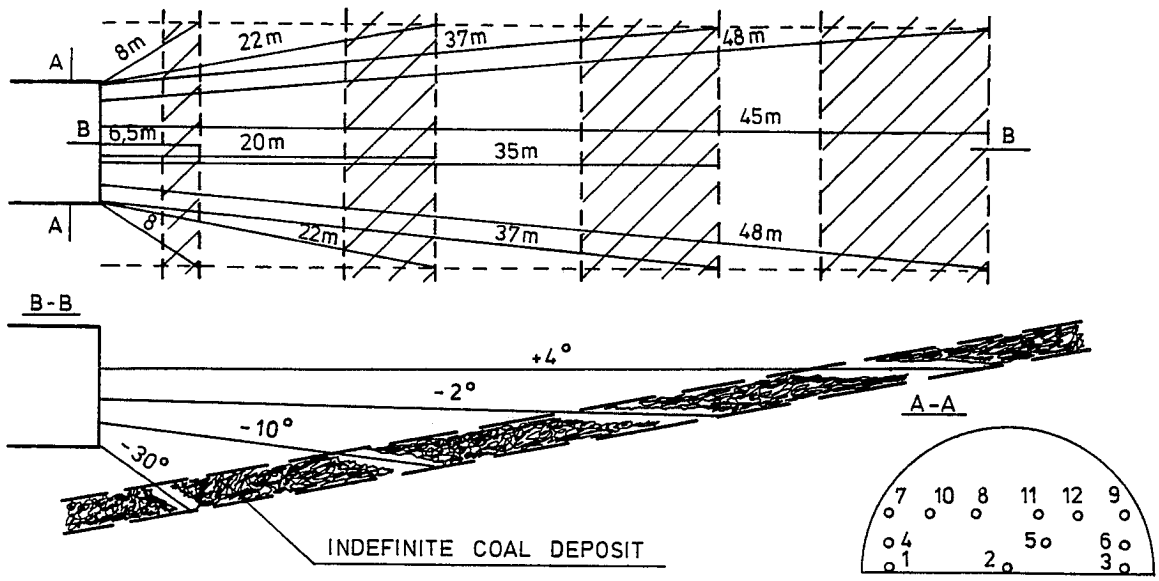

Fig.4. BOREHOLE WASHING FOR TUNNEL LEVEL - 350 m

5th American Water Jet Conference
August 29 - 31, 1989: Toronto, Canada

Paper / Communication 32

THE POTENTIAL OF AN ULTRAHIGH-PRESSURE ABRASIVE-WATERJET ROCK DRILL

M. Hashish
Flow Research, Inc.
Kent, Washington 98032, USA

ABSTRACT: A research study was conducted to determine the feasibility of developing a novel rock drill that employs abrasive-waterjets (AWJs). These jets are formed by mixing high-velocity (up to 700 m/s) waterjets with an abrasive material such as garnet or silica sand. Two concepts are discussed here. In the first concept, a nonrotary drill stem is combined with multiple waterjets, which are used to form a single AWJ. These jets may or may not rotate inside a stationary stem to enhance mixing with abrasives and to provide more uniform energy distribution. The second concept employs two AWJs mounted in a rotary drill stem. The rotation of the jets results in the cutting of concentric circular grooves. The material between these grooves must then be removed using an optimized drill design. Initially, a linear cutting test matrix was generated to determine the parameters for the drill head design. Drill heads were designed based on the above concepts and then tested on granite and sandstone samples. For hard rocks, the rotary drill concept showed the most promising results. The other two concepts were promising for soft rocks. Optimization studies of each concept are needed to define specific usage ranges. Projected drilling costs, based on this study, showed that AWJ drilling is competitive with conventional methods.

RÉSUMÉ : Une recherche a été menée pour déterminer s'il est possible de mettre au point une nouvelle foreuse à jets d'eau abrasifs (JEA). Ces jets sont formés en mélangeant des jets d'eau à grande vitesse (jusqu'à 700 m/s) et un matériel abrasif comme du grenat ou du sable de silice. Deux principes sont abordés. Le premier combine un train de tige et plusieurs jets d'eau en un seul JEA. Ces jets peuvent tourner ou ne pas tourner à l'intérieur d'un train de tige fixe de façon à améliorer le mélange avec les abrasifs ou à produire une distribution d'énergie plus uniforme. Le deuxième principe consiste à monter deux JEA dans un train de tige rotatif. La rotation des jets permet de réaliser des coupes concentriques circulaires. La matière entre les traits concentriques doit ensuite être enlevée selon un plan de forage optimisé. Au début, on a établi une matrice d'essai pour coupe linéaire pour déterminer les paramètres du trépan. Des trépans ont été conçus selon les principes susmentionnés, puis essayés sur des échantillons de granite et de grès. Dans la roche dure, la foreuse rotative a produit les meilleurs résultats. Les deux autres foreuses semblent plus prometteuses dans la roche tendre. Des études d'optimisation de chaque principe s'imposent pour définir des champs d'utilisation particuliers. Les coûts de forage prévus selon cette étude montrent que le forage aux JEA se compare aux méthodes classiques.

Organized and Sponsored by the National Research Council of Canada and the U.S. Water Jet Technology Association.

1. INTRODUCTION

The drilling of holes in rock is a key task in the production of many essential raw materials and in excavation work. Several billions of linear meters are drilled annually to meet mining, construction, and military requirements in the free world.

Current drilling technology relies on cutters using hard metal or diamond projections (drill bits) that are thrust against a rock mass while being rotated and/or impacted. This breaks loose rock fragments via the mechanisms of abrasion, crushing, and tensile/shear fracturing. The fact that most rock is relatively hard and abrasive causes several unavoidable problems for conventional drilling machines:

- o Abrasion and fatigue of the cutting surfaces cause expensive drill bits to wear rapidly.
- o Large and expensive drilling machines are needed to provide the high thrust levels and complex mechanical devices required to exert thrust/rotation/impact forces adequate to achieve economic penetration rates.
- o Maintenance costs are high because mechanical assemblies with precision moving parts must operate in a hostile environment (i.e., dust, moisture, and poor visibility) without proper maintenance.

Although minor improvements are constantly being made in drill bits and machines, there have been no industry-wide advances in drilling technology since the introduction of tungsten-carbide drill bit wear inserts during the early 1950's. The development of hydraulically powered percussive drills, diamond-laminate rotary drill bits, and high-pressure waterjet drills during the 1970's has advanced limited sectors of drilling technology. However, over 97% of all rock drilling is currently done with conventional rotary or percussive drills that have the inherent problems listed above.

The research presented in this paper was conducted to study the feasibility of a novel drill concept that has the potential to reduce drilling costs substantially. This concept uses abrasive-waterjets (AWJs) as cutting tools.

Some advantages of the AWJ drill, in addition to lower drilling costs, include:

- o Fast and consistent drilling speeds in very hard rocks
- o Lighter, smaller, and more maneuverable drilling machines
- o Versatility, (i.e., able to cut and slot rock as well as drill holes)
- o Simplified operation and maintenance, minimizing training requirements
- o Very low thrust
- o Curved drilling (drilling around corners)
- o No sparking and environmentally safe

In this paper, some general background information regarding drilling and AWJ technology is presented first, followed by a discussion of the basic AWJ drill concepts examined in this research. The experimental investigation and results are then discussed in detail. A preliminary cost analysis is also presented. Finally, the conclusions of this study are summarized.

2. BACKGROUND

Conventional Rock Drills

Rock drilling requirements in the free world currently average over 1.5 billion linear meters annually, not including the petroleum industry. Of this total, about 75% is for the placement of explosives for rock excavation in the mining and construction industries. An additional 20% is used for the purpose of installing ground support, mainly roofbolts, in underground coal and metal mines and in construction tunneling projects.

Rock drilling can also be categorized according to hole diameters, which generally range from 25 to 400 mm. About 60% of the total (one billion meters) consists of holes less than 50 mm in diameter. These holes are used primarily for underground excavation, ground support, and construction. Holes less than 50 mm in diameter are normally drilled either with rotary or percussive drills. Soft to medium-hard rocks that are not too abrasive can be drilled with rotary drills. Rotary diamond coring drills are used for deep drilling and sampling, but constitute only a small portion of the total drilling market. The largest application of rotary drilling is the drilling of roofbolt holes in coal mines. Hard abrasive rocks require percussive drills that rapidly impact the drill bit as it is rotated. Blasthole drilling in underground metal mines and construction projects is done almost exclusively with percussive drills.

Waterjet Drilling

The development of high-pressure waterjet rock drills has been in progress since the early 1970's (Refs. 1-6). Waterjet drills using multiple rotating cutting jets (see Figure 1) substantially weaken the rock in front of a drill bit. The cutting assist provided by the waterjets reduces the required drill thrust and torque to 5 to 10% of that required for conventional rotary drag-bit drills. Since the bit does comparatively little work, drill bit life increases to 10 or 20 times that of rotary drills.

Waterjet drills can rapidly drill holes with smaller diameters than conventional drills are capable of drilling. As a result, they are ideal for drilling resin-grouted roofbolt holes, due to speed and resin savings (Ref. 7). Waterjet

drilling has demonstrated bolting productivity 50% higher than conventional drilling, with up to thirty 1.5-meter-long resin-grouted bolts per hour drilled and installed in the hard roof. An average savings of 40% in resin volume was also achieved, enabling a substantial cost savings per bolt. The main disadvantage of waterjet drills is their inability to drill very hard rocks.

Abrasive-Waterjet Cutting

Abrasive-waterjets (AWJs) are formed by either mixing abrasives with high-velocity waterjets (Ref. 8) or by pressurizing a premixed slurry and forcing it through a nozzle (Ref. 9). The impact of the high-velocity particles results in material removal rates an order of magnitude higher than those for plain waterjets (Refs. 10 and 11). A very wide range of materials can be cut effectively and economically with AWJs.

An investigation was conducted to develop a new rock drill based on the AWJ concept (Ref. 12). The developed concept is shown in Figure 2. The mixed water and abrasives are directed toward a deflector at the end of a collimator tube. Some of the drilling results obtained with this drill are given below:

Charcoal granite: 0.10 m/min
Oneotu dolomite: 0.15 m/min
Salem limestone: 0.76 m/min
Sioux quartzite: 0.10 m/min

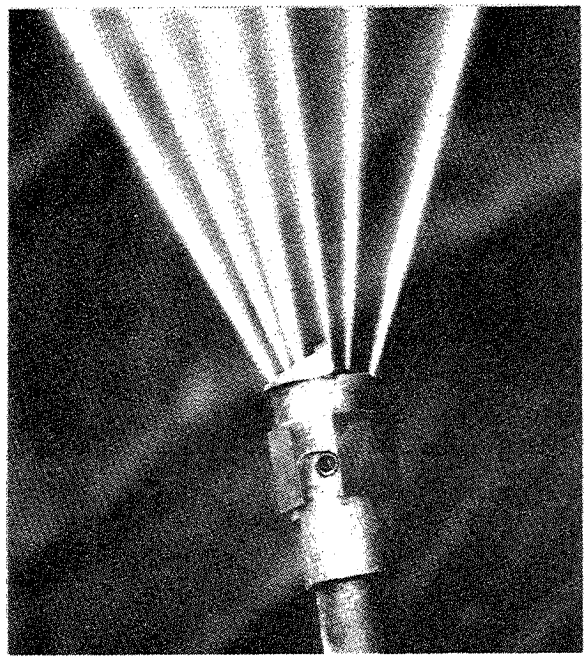

FIG. 1. Waterjet Drill Used in Roofbolting

The above rates are considered low. The objective of this investigation is to develop a drill that can drill the same rocks at least ten times faster than the above rates.

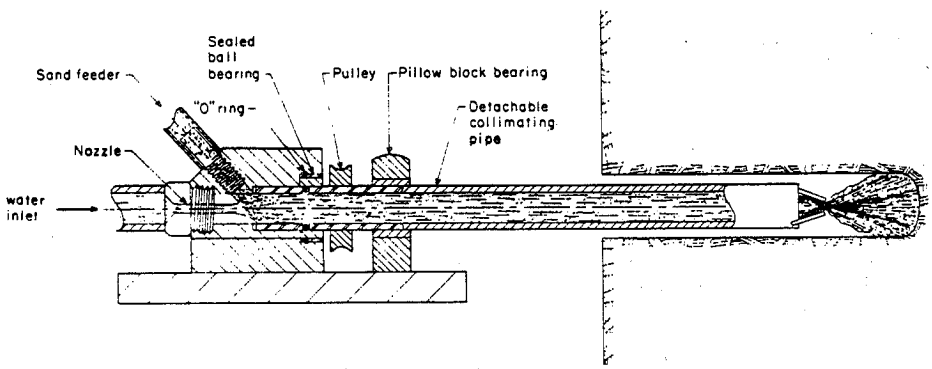

FIG. 2. AWJ Rock Drill with Collimating Tube and Deflectors. Water pressure ≃ 10,000 psi (Ref. 12).

3. ABRASIVE-WATERJET DRILL CONCEPTS

AWJ drills work by delivering sufficient impact energy of abrasives and water to the area to be drilled. This may be accomplished by a single jet comparable in size to the hole to be drilled or by a smaller jet or set of jets that moves to cover the area. In the first case, the available energy will be spread and, consequently, the energy density will be low, while in the second, the energy will be more focused and higher energy density will be obtained.

Figure 3 illustrates several different concepts for an AWJ drill. The space between the drill stem and the high-pressure water supply tube(s) is used to feed the abrasives to the waterjet(s). Figure 3a employs a single waterjet that mixes with abrasives in a mixing tube inside the drill stem. This jet enlarges as the distance increases downstream. The length of the spread zone before the jet impacts the target is controlled by the drill stem. A fan-type jet may also be used, as shown in Figure 3b. Figures 3c, 3d, 3e, and 3f show examples of stationary drill stem concepts. The waterjet tubes in these figures may or may not rotate. Figure 3g shows a concept in which the rotation of jets would be essential. Figures 3h and 3i show a rotary drill stem concept where AWJs are formed at the drill head. When the drill rotates, circular cuts are made. Material between these cuts may be removed as the drill advances and/or with the backflow. A slight mechanical assist of a blade at the tip of the drill head may be required in some situations. For hard rocks, it may be necessary to use multiple jets providing complete coverage of the drilling area. Varying the standoff distance to allow control of jet spreading for full coverage of the rock face may also be essential in the rotary drill concept.

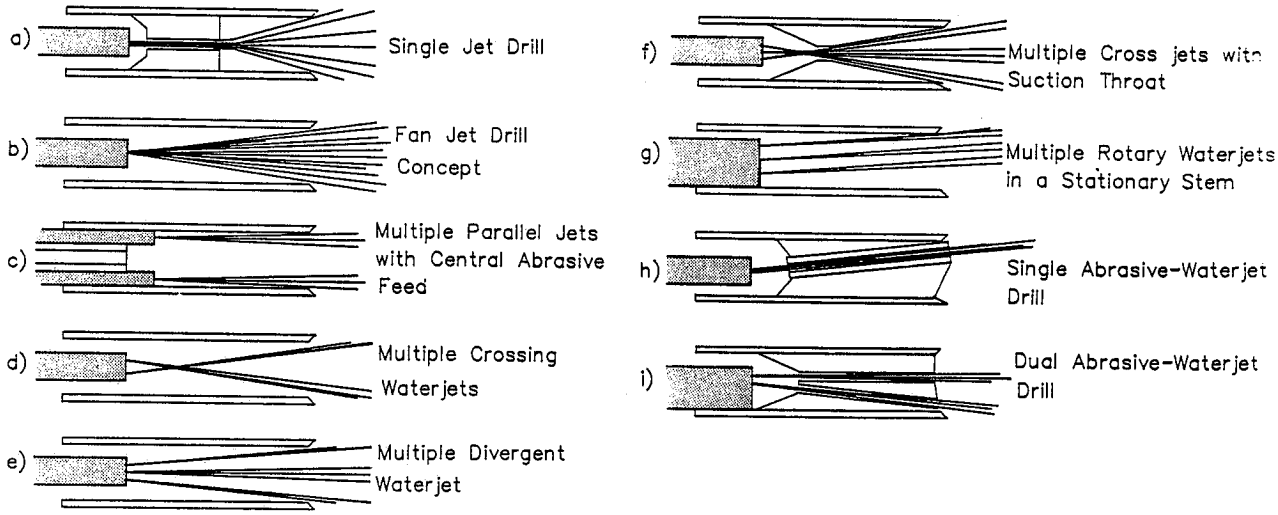

FIG. 3. Concepts for an AWJ Drill

The proper type of drill to be used depends largely on the rock type. For example, soft rocks may be drilled with a single stationary jet that has relatively low energy density. This concept may not be adequate for hard rocks, however, where high energy density is required.

4. EXPERIMENTAL INVESTIGATION

The experimental investigation conducted in this study consisted of the following efforts:

- o Parametric linear cutting tests
- o Tests with different drill heads

4.1 Parametric Linear Cutting Tests

Parametric linear cutting tests were conducted to generate data on the cutting of granite. These tests were designed to simulate the conditions and design restrictions pertinent to a drill design, such as:

- o Parameters of traverse mechanism
- o Design variables and size limitations
- o Practical considerations

The cutting tests were conducted under the following ranges of conditions:

Pressure (p)	- 241 and 345 MPa	Abrasive type	- garnet sand
Nozzle diameter (d_n)	- 0.330 to 0.914 mm	Abrasive size	- 60 and 36 mesh
Mixing tube diameter (d_m)	- 1.981 to 4.801 mm	Traverse speed (u)	- 20 to 200 mm/s
Mixing tube length (l_m)	- 76.2 mm	Standoff distance (sod)	- 2.5 to 40 mm
Abrasive feed rate (m)	- 7.5 to 45 g/s		

A discussion of the results obtained in the parametric linear cutting tests is given below.

Figure 4 shows the effect of traverse speed on the depth of cut for different waterjet sizes at 241 MPa. Figure 5 shows similar trends at 345 MPa. It can be seen that the traverse rate has a strong effect on the depth of cut produced. For example, the top curve in Figure 4 shows that tripling the traverse speed from 20 to 60 mm/s will result in a reduction in the depth of cut from about 38 to 15 mm.

The effect of waterjet size is also shown in Figures 4 and 5. To illustrate this effect, let us assume that a depth of cut of 10 mm is required. Using a 0.381-mm orifice and a pressure of 241 MPa, this depth will be produced at about 32 mm/s (Figure 4). The same depth can be obtained with a waterjet size of 0.635 mm at 90 mm/s, which is approximately 2.8 times faster than in the previous case. The power increase is about 2.7 times. This should not lead to the conclusion, however, that the relationship between depth of cut and hydraulic power is linear. This relationship is affected by other conditions. Mixing parameters, such as the mixing tube diameter and length, have the most influence of these conditions. The parameters should be selected to match the waterjet size, which is a subject of a future detailed study.

The effect of traverse speed on the volume removal rate is illustrated in Figure 6. It is clear that higher traverse speeds (and consequently higher rotational speeds in a rotary drill) will be preferred. It is expected that an optimum traverse speed exists for maximum volume removal rates, as has been observed in metal cutting. Figure 7 shows the effect of traverse speed on the specific energy parameter. The specific energy is defined as the energy required to remove a unit volume. We observe that the specific energy is a strong function of traverse speed and that smaller diameter jets are more efficient than larger jets.

The traverse speed can be replaced with the rotational speed when the drill diameter is known. For a 25.4-mm-diameter drill, Figure 8 shows the effect of rotational speed on the rate of penetration in granite at a pressure of 241 MPa. A useful parameter to express the efficiency of drilling is termed here the Penetration Index, which is defined as the rate of penetration per unit power. Penetration Index data are shown in Figure 9.

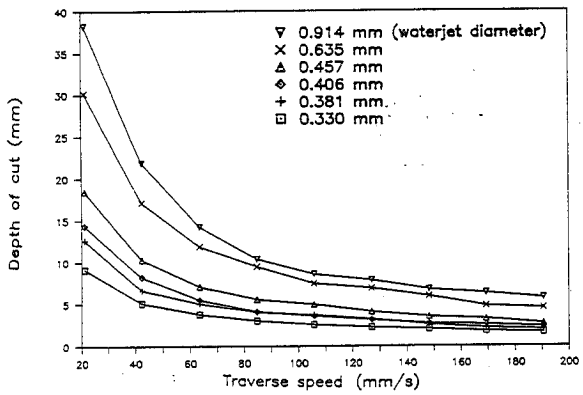

FIG. 4. Effect of Traverse Rate on Depth of Cut in Granite at 241-MPa Pressure for Different Jet Sizes (m = 7.56 g/s; sod = 25 mm)

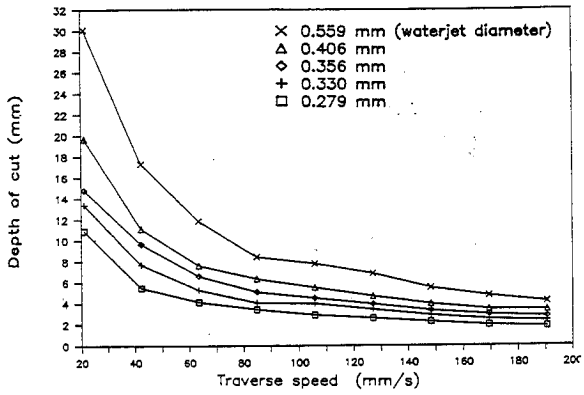

FIG. 5. Effect of Traverse Rate on Depth of Cut in Granite at 345-MPa Pressure for Different Jet Sizes (Garnet; 60 mesh)

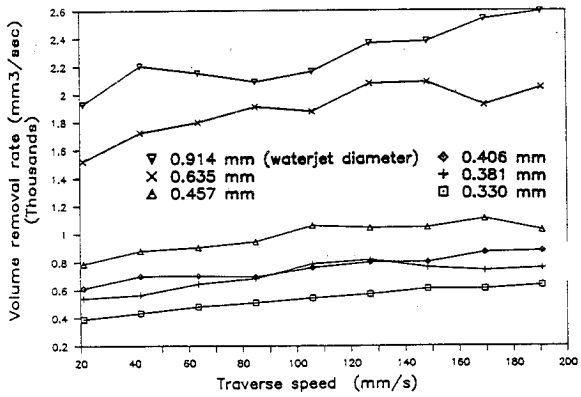

FIG. 6. Effect of Traverse Rate on Volume Removal Rate in Granite at 241-MPa Pressure (m = 7.56 g/s; sod = 25 mm)

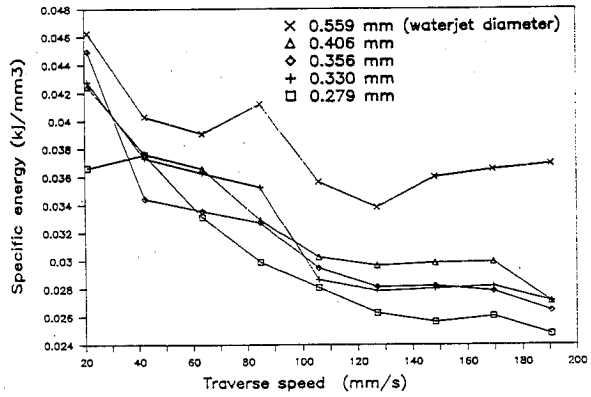

FIG. 7. Specific Energy Values for Granite Cutting at 345-MPa Pressure (Garnet, 60 mesh; sod = 25 mm)

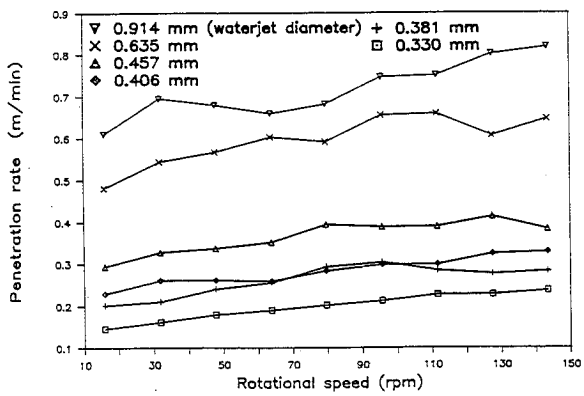

FIG. 8. Effect of Rotational Speed on Rate of Penetration of 25.4-mm-Diameter Hole in Granite at 241-MPa Pressure (m = 7.56 g/s)

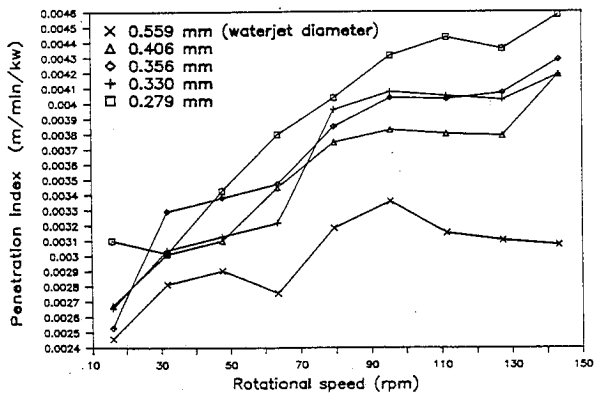

FIG. 9. Penetration Index at 345-MPa Pressure (Garnet, 60 mesh)

At a given pressure, power levels were varied by varying the waterjet size. In this study, two pressure levels and ten waterjet sizes were used. The specific energy data obtained at the different power levels are shown in Figure 10. It can be deduced that the use of higher power will not necessarily lead to higher volume removal rates. It is also shown that low-power jets are more efficient than high-power jets.

The effect of abrasive flow rate is combined with the specific energy term to yield a number termed here the Performance Index, which is the volume removed per unit energy per unit mass of abrasive flow rate. This index is plotted against hydraulic power in Figure 11. It is clearly illustrated that lower power levels are more efficient in material removal. This suggests that multiple smaller jets would be more efficient than a large single jet, which is an important consideration in drill design.

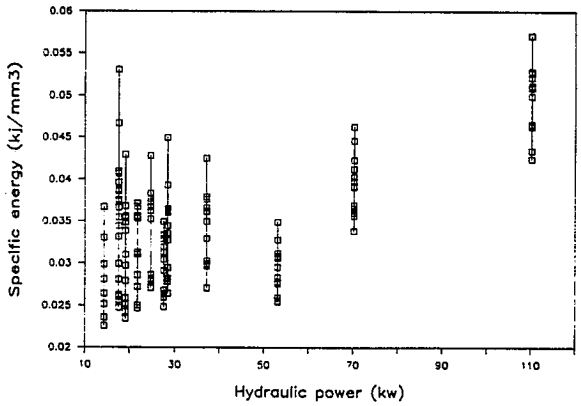

FIG. 10. Specific Energy Versus Hydraulic Power

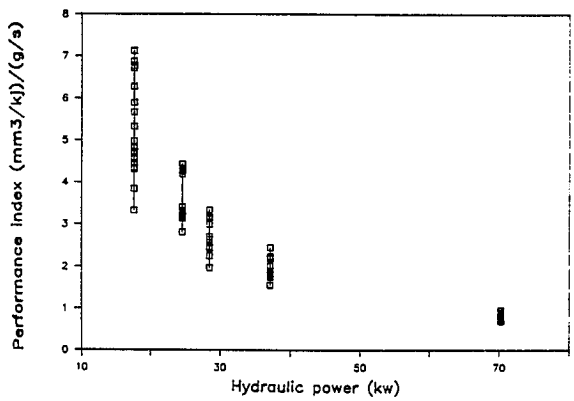

FIG. 11. Performance Index Versus Hydraulic Power at 345-MPa Pressure

4.2 Experimental Investigation with Different Drill Heads

Nonrotary Drill Stem Test Results

Nonrotary AWJ drills employ a stationary stem within which the mixing of abrasives and waterjet(s) takes place. These waterjets may have different distributions and arrangements, and they may also rotate inside the stationary drill stem. Figure 3 shows several related concepts, including:

- o Stationary drill stem with a single stationary waterjet (Figs. 3a, 3b)
- o Stationary drill stem with multiple stationary waterjets (Figs. 3c-f)
- o Stationary drill stem with multiple rotating waterjets (Fig. 3g)

The results of the experimental investigation using multiple waterjets are discussed below.

Figure 12 shows four waterjets emerging from a 10-mm tube. The mixing of these jets with abrasive particles occurs in a common mixing tube. The mixing can be enhanced by one of the following methods:

- o Rotating or oscillating the waterjet supply tube
- o Directing the abrasives toward the crossing zone of cross-divergent jets (Fig. 3f)
- o Increasing the number of waterjets
- o Employing multiple feed ports for uniform entry of abrasives at the mixing area

All of the above methods have been tested in drilling granite and sandstone. Drill heads were built to demonstrate the pattern of hole generation rather than deep drilling.

The experimental investigation consisted of a series of tests on drill heads with several different geometries. For all geometries, the abrasive flow rate and standoff distance were the main variables of investigation at different rotation or oscillation speeds. Other parameters were held fixed as follows:

p = 241 MPa
Abrasive material = garnet
Abrasive size = 60 mesh
Mixing tube internal diameter = 22 mm
t = 10 seconds

Table 1 shows the results obtained with a triple-waterjet drill stem. The three waterjets were divergent at 1°. A convergent-divergent nozzle section was used to direct the abrasives to the minimum cross-sectional area of jets intersecting a normal plane. Observe in Table 1 that rotation significantly increases the volume removal. Also, an optimum rotational speed exists for maximum volume removal. This is observed in the decline in volume removal rates when the rotational speed is increased from 70 to 1000 rpm. The pattern of holes produced is generally convergent and conical in shape with a central uncut core.

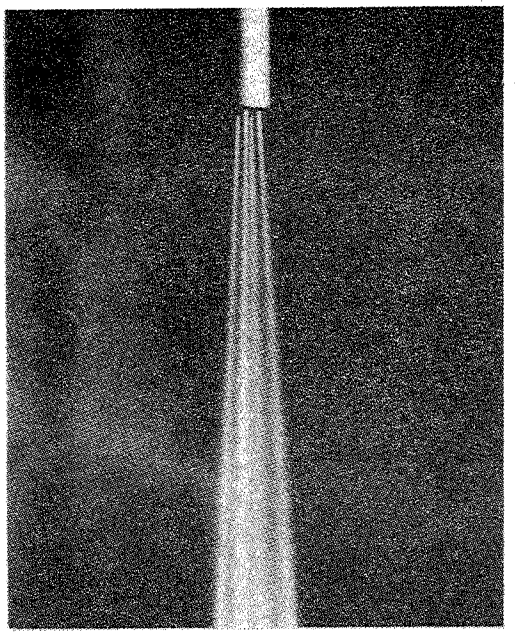

FIG. 12. High-Pressure Tube with Multiple Waterjet Orifices

TABLE 1. Drilling Performance with Triple-Waterjet Drill Head

Target rock : Granite

Test No.	jet arrangement	m g/s	sod mm	rpm	vol. mm3	power kW	spe kJ/mm3	rop m/min
2	3 jets,.559 mm	30	38	0	3500	84.9	0.243	0.055
1	1 deg. divergent	30	38	20	7000	84.9	0.121	0.111
3	angle	41	38	0	5000	84.9	0.170	0.079
4		41	38	20	9000	84.9	0.094	0.142
5		41	25	0	4000	84.9	0.212	0.063
6		41	25	20	9000	84.9	0.094	0.142
7		41	25	1000	7000	84.9	0.121	0.111
8		41	50	0	6000	84.9	0.141	0.095
9		41	50	20	9000	84.9	0.094	0.142
10		41	50	1000	8000	84.9	0.106	0.126
11		41	75	0	7000	84.9	0.121	0.111
12		41	75	20	8200	84.9	0.104	0.129
13		41	75	1000	8000	84.9	0.106	0.126

Other test conditions:
pressure : 241 MPa
drill diameter : 22.2 mm
abrasives : garnet
exposure time : 10 sec
abrasive size : mesh 60

Conical holes are not desirable because they limit the advance per rotation and the subsequent material removal process. The impact of particles on inclined surfaces is not as efficient in removing material as impacts at normal angles. This is particularly true for brittle materials such as rocks. The central core, however, may be removed with additional jets or by allowing different angles of divergence to cover the maximum possible area.

To overcome the problem of conical holes, the jet divergence angle needs to be increased. This will reduce the mixing length so that the jets do not impinge on the tube wall. This may have the adverse effects of reduced particle velocity as well as improper mixing. Consequently, an optimum angle and corresponding mixing length need to be determined for improved drilling.

The rate of penetration data shown in Table 1 are the calculated values from the measured volume removal rate and the cross-sectional area of the drill. Table 2 shows results obtained with a four-jet drill head. Notice that the behavior is similar to the previous case in terms of rotational speed and standoff distance, which also exhibits optimal values. Although the hydraulic power used with the four-jet drill is less than that for the three-jet drill, improved specific energy values are observed. This is due to the improved coverage of the jets over the drilling area. Table 3 shows that when two of the jets are directed inward (1° instead of 3°), a slight decline in performance may result. However, the central core is reduced in size, as expected. There is a relative increase in the volume removal rates in sandstone as compared to the harder granite. Holes produced in sandstone showed an initial straight wall followed by a tapered pattern. Also, with the "softer" sandstone, high rotational speeds seem to be beneficial.

TABLE 2. Drilling Performance with Four-Waterjet Drill Head

Target rock : Granite

Test No.	jet arrangement	m g/s	sod mm	rpm	vol. mm3	power kW	spe kJ/mm3	rop m/min
14	4 jets, .457 mm	41	25	0	2000	75.7	0.424	0.032
15	3 deg. divergent	41	25	20	6000	75.7	0.141	0.095
16	angle	41	25	1000	5000	75.7	0.170	0.079
17		41	50	0	3000	75.7	0.283	0.047
18		41	50	20	9000	75.7	0.094	0.142
19		41	50	1000	6500	75.7	0.131	0.103
20		51	50	0	2500	75.7	0.303	0.039
21		69	50	0	3500	75.7	0.216	0.055
24		51	50	20	7000	75.7	0.108	0.111
25		69	50	20	10000	75.7	0.076	0.158
22		51	50	1000	6500	75.7	0.116	0.103
23		69	50	1000	9000	75.7	0.084	0.142

Other test conditions:
pressure : 241 MPa
drill diameter : 22.2 mm
abrasives : garnet
exposure time : 10 sec
abrasive size : mesh 60

TABLE 3. Drilling Performance with Dual-Angle Four-Waterjet Drill Head

Target rock : Granite

Test No.	jet arrangement	m g/s	sod mm	rpm	vol. mm3	power kW	spe kJ/mm3	rop m/min
26	4 jets, .457 mm	41	50	0	4000	75.7	0.189	0.063
27	two at 2 deg.	41	50	20	7000	75.7	0.108	0.111
28	two at 3 deg.	41	50	1000	7000	75.7	0.108	0.111

Target rock : Wilkeson Sandstone

29		41	50	0	6000	75.7	0.126	0.095
30		41	50	20	23000	75.7	0.033	0.363
31		41	50	1000	26000	75.7	0.029	0.411

Other test conditions:
pressure : 241 MPa
drill diameter : 22.2 mm
abrasives : garnet
exposure time : 10 sec
abrasive size : mesh 60

Table 4 shows drilling performance results using five jets, one being an axial jet directed so as to remove the central core. The holes produced confirm that the central core does not form. The specific energy and rate of penetration are comparable to the previous cases. This confirms that improved energy distribution is an important criterion. Note that the jet sizes are specified such that the power levels are nearly equal for the different cases.

Table 5 shows results obtained when oscillation, rather than rotation, was used. The potential advantage of oscillation is improved removal of cut solids. This is due to the momentary dwell of the jets at the end of each oscillation stroke to produce a deeper cut, which allows cores to be easily removed. A rotating oscillation may be required for uniform advance. This was not attempted in this study.

Figure 13 shows patterns obtained with the stationary drill head concept on a granite rock sample.

TABLE 4. Drilling Performance with Five-Waterjet Drill Head

Target Rock : Wilkeson Sandstone

Test No.	jet arrangement	m g/s	sod mm	rpm	vol. mm3	power kW	spe kJ/mm3	rop m/min
32	5 jets, .406 mm	41	25	0	9000	74.6	0.083	0.142
34	four at 2 deg.	41	25	50	26000	74.6	0.029	0.411
33	one central	41	50	0	16000	74.6	0.047	0.253

Target Rock : Granite

35	same as test 32	41	25	0	3000	74.6	0.249	0.047
36		41	25	50	8000	74.6	0.093	0.126
37		41	50	0	5000	74.6	0.149	0.079
38		41	50	50	9000	74.6	0.083	0.142
39	5 jets, four .457	41	50	0	5500	81.5	0.148	0.087
40	mm at 2 deg. and a .254 mm central	41	50	50	9500	81.5	0.086	0.150

Other test conditions:
pressure : 241 MPa exposure time : 10 sec
drill diameter : 22.2 mm abrasive size : mesh 60
abrasives : garnet

TABLE 5. Drilling Performance with Oscillating Waterjet Drill Head

Target rock : Granite

Test No.	jet arrangement	m g/s	sod mm	rpm	angle deg.	vol. mm3	power kW	spe kJ/mm3	rop m/min
41	5 jets, four .457	41	50	60	45	5000	81.5	0.163	0.079
42	mm at 2 deg. and a .254 mm central	41	50	6	60	8000	81.5	0.102	0.126

Target Rock : Wilkeson Sandstone

43		41	25	6	60	20000	81.5	0.041	0.316
44	same as test 35	41	25	6	60	31000	74.6	0.024	0.490
45		41	25	60	60	28000	74.6	0.027	0.442
46	5 jets, four .381	41	25	60	60	25000	71.5	0.029	0.395
47	mm at 2 deg, and	41	25	6	60	25000	71.5	0.029	0.395
48	a .457 mm central	51	25	6	70	25000	71.5	0.029	0.395
49		69	25	6	70	29000	71.5	0.025	0.458

Other test conditions:
pressure : 241 MPa exposure time : 10 sec
drill diameter : 22.2 mm abrasive size : mesh 60
abrasives : garnet

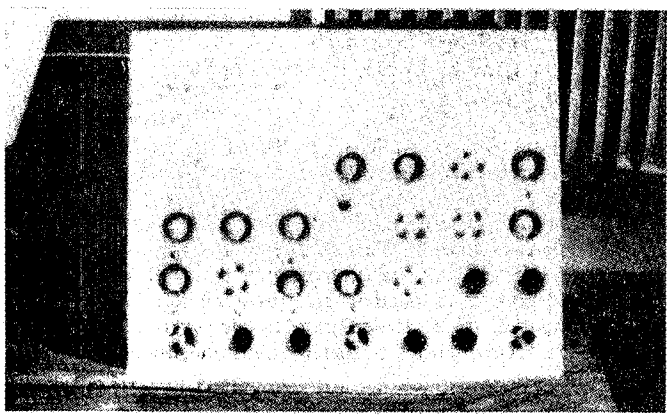

FIG. 13. Sample Rock Showing Patterns of Holes Produced with Stationary Drill Head

Rotary Drill Head Design and Testing

The design of this drill incorporates a high-pressure water tube mounted inside a drill stem. Two waterjets are formed at one end of the water tube. Each waterjet enters a mixing tube that is oriented at a specific angle. Abrasives flow in the space between the outer stem and the high-pressure water tube. Each jet entrains a portion of the abrasives at the mixing tube entry. The abrasives enter the angular space through an abrasive swivel, through which the high-pressure water tube passes. This high-pressure tube is attached to a high-pressure swivel, which allows tube rotation. Figure 14 shows a front view of the drill head, illustrating the location of the mixing tubes. Figure 15 shows the drilling assembly. The drill head also incorporates a carbide blade to protect the front of the drill head from wear, as the drill head may strike the rock face.

Table 6 shows the parameters and results of the drilling tests. Granite was used in the parametric study. Other types of rock were tested to qualitatively determine if there are any other important features of the drilled holes. The power level was held constant at 64.7 kW for all tests. The duration of drilling was kept at 10 seconds for all tests to recognize the patterns of the holes produced and the energy distribution. For longer durations of drilling, these patterns will form deeper in the hole, which makes them difficult to inspect. The hole geometry yields information on the effectiveness of each jet and on the effect of different parameters.

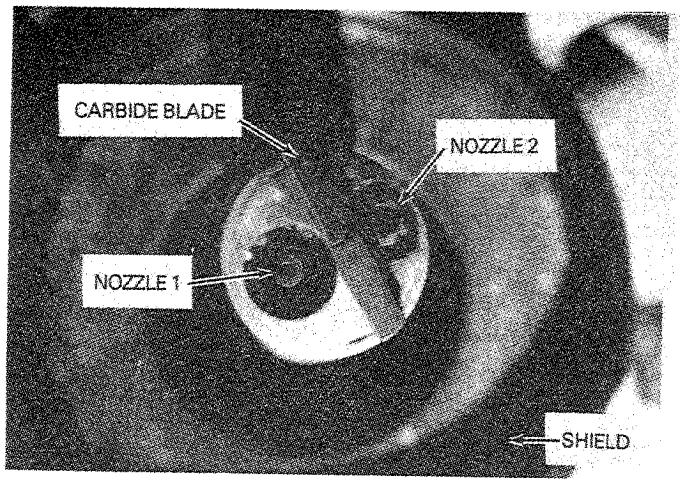

FIG. 14. Front View of AWJ Drill Head

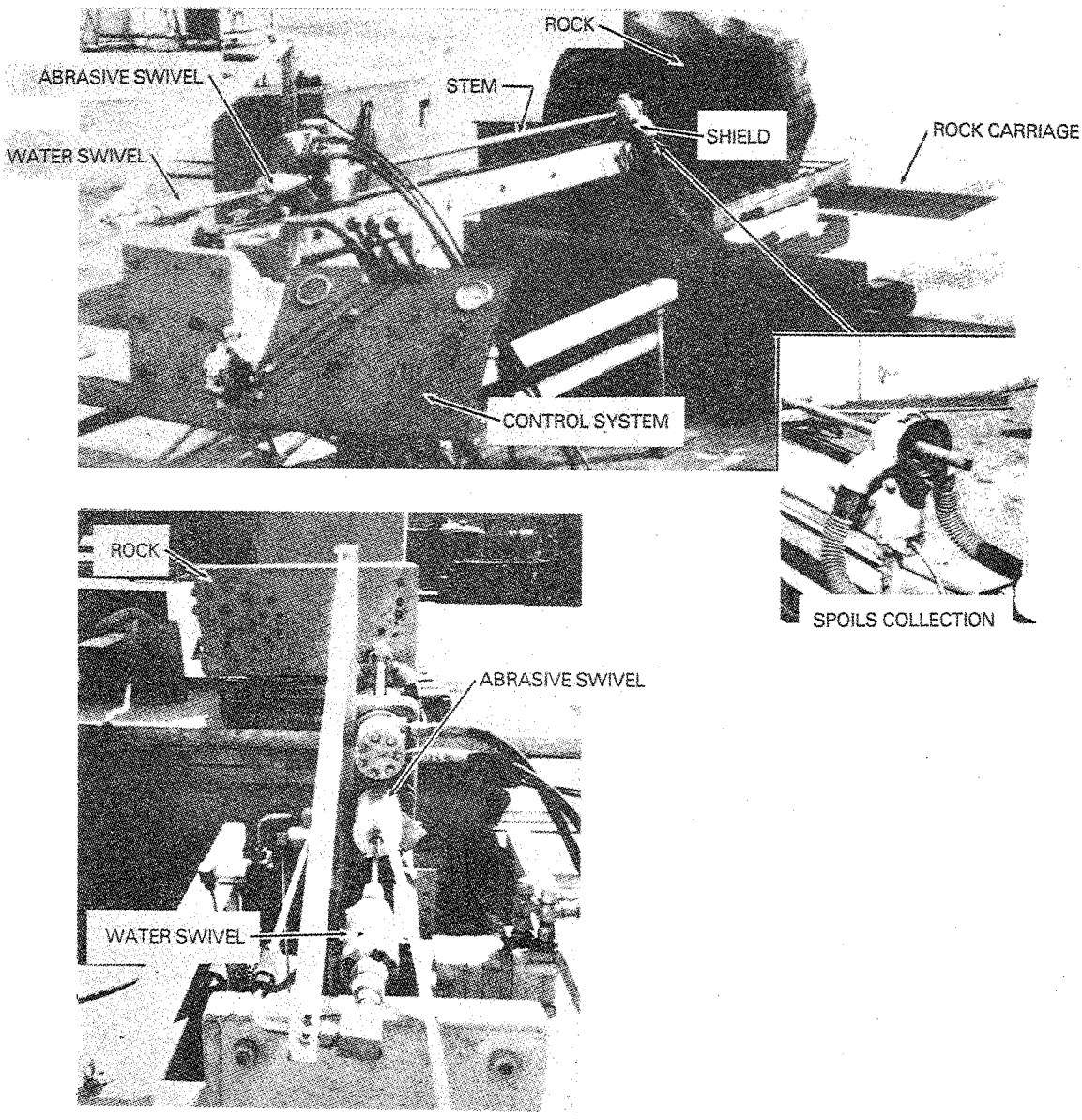

FIG. 15. Test Setup for Rotary AWJ Drill

TABLE 6. Test Results of Drilling in Granite with Rotary AWJ Drill

Test No	m g/s	size mesh	rpm	p MPa	dm1 mm	dm2 mm	power kW	vol. mm3	spe kJ/mm3	dh mm	rop m/min
1	28	60	325	241	1.78	3.18	64.7	14000	0.046	28	0.166
2	42	60	325	241	1.78	3.18	64.7	18000	0.036	28	0.213
3	59	60	325	241	1.78	3.18	64.7	20000	0.032	29	0.237
4	29	40	325	241	1.78	3.18	64.7	17000	0.038	29	0.201
5	43	40	325	241	1.78	3.18	64.7	22000	0.029	27	0.261
6	59	40	325	241	1.78	3.18	64.7	28000	0.023	27	0.332
7	31	36	325	241	1.78	3.18	64.7	22000	0.029	29	0.261
8	47	36	325	241	1.78	3.18	64.7	31500	0.021	29	0.373
9	60	36	325	241	1.78	3.18	64.7	36000	0.018	30	0.426
10	31	36	325	172	1.78	3.18	39.2	16000	0.024	30	0.190
11	47	36	325	172	1.78	3.18	39.2	18000	0.022	27	0.213
12	60	36	325	172	1.78	3.18	39.2	26000	0.015	27	0.308
13	31	36	325	310	1.78	3.18	94.6	38000	0.025	27	0.450
14	47	36	325	310	1.78	3.18	94.6	43000	0.022	27	0.509
15	60	36	325	310	1.78	3.18	94.6	52000	0.018	27	0.616
16	31	36	600	241	1.78	3.18	64.7	19000	0.034	31	0.225
17	47	36	600	241	1.78	3.18	64.7	31000	0.021	30	0.367
18	60	36	600	241	1.78	3.18	64.7	34000	0.019	27.5	0.403
19	31	36	180	241	1.78	3.18	64.7	18000	0.036	26.5	0.213
20	47	36	180	241	1.78	3.18	64.7	30000	0.022	27	0.355
21	60	36	180	241	1.78	3.18	64.7	32000	0.020	29	0.379
22	31	36	325	241	1.78	2.34	64.7	26000	0.025	27	0.308
23	47	36	325	241	1.78	2.34	64.7	21000	0.031	27	0.249
24	60	36	325	241	1.78	2.34	64.7	31000	0.021	27	0.367
25	31	36	325	241	1.78	3.80	64.7	22000	0.029	29	0.261
26	47	36	325	241	1.78	3.80	64.7	28000	0.023	28	0.332
27	60	36	325	241	1.78	3.80	64.7	27000	0.024	29	0.320

inner waterjet orifice diameter : 0.457 mm
outer waterjet orifice diameter : 0.711 mm
drill outside diameter : 25.4 mm
abrasives material : garnet
exposure time : 10 sec
mixing tube(s) length : 76 mm

The effect of abrasive flow rate is shown in Table 6 in conjunction with the effects of rotational speed, pressure, abrasive size, and mixing diameter. The effects of abrasive flow rate and particle size are represented by the first nine tests. The coarser abrasives (36 mesh) were found to be the most effective. The rate of penetration in Table 6 is calculated by dividing the measured volume removal rate by the cross-sectional area of the drill stem. This is not representative of the geometry of the hole, which in many tests was irregular. Jet size and number optimization is required to control the shape of the produced hole. At optimized conditions, it is expected that volume removal rates or specific energy values will improve only slightly.

The effect of pressure is also shown in Table 6. Observe that the specific energy does not vary significantly with changing pressure. The penetration rate, however, increases when the pressure increases. Table 6 also shows an optimum rotational speed of about 325 rpm. The effect of mixing tube diameter, as given in Table 6, indicates similar performance for the range of mixing tube diameters used.

Figure 16 shows a granite sample with drilled hole patterns. The time of drilling was 10 seconds. Many of the holes shown contain an uncut portion, which is either a solid or a hollow core. This indicates that more jet coverage is needed. A three-jet rotary drill will be more efficient if an extra jet is directed so as to remove the uncut core. Figure 16 shows that the uncut cores, especially the hollow ones, are thin and do not represent significant material removal problems.

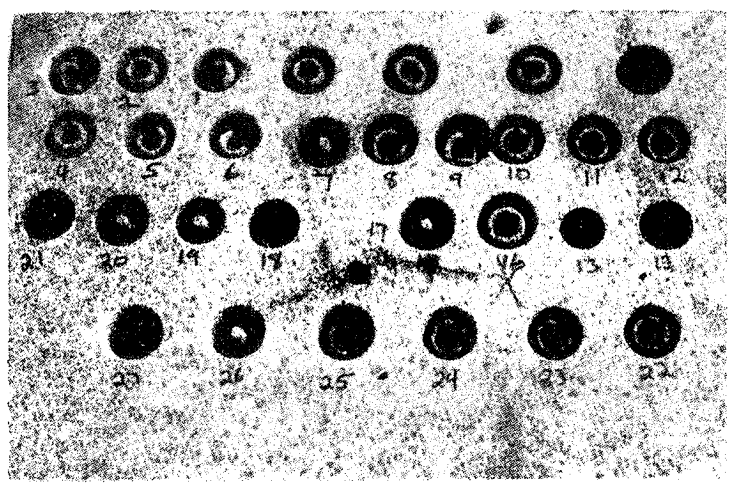

FIG. 16. Holes Produced in Granite with Dual AWJ Drill

5. COST ANALYSIS

A comprehensive economic model of cutting with AWJs is beyond the scope of this paper. However, a simplified analysis is given here to recognize the contribution of each cost element to the overall cost of operation. The elements that contribute to the cost of this technique are:

- o Equipment depreciation
- o Abrasives consumption
- o Nozzle wear and replacement
- o Power utilization
- o Maintenance costs

It is assumed that an AWJ system utilizing 75 kW will have an initial cost of $100,000. We will assume that the system will be paid off after (y) years with no residual value. Payments will be made in equal monthly installments at a yearly interest rate of R%. The equipment will be used a total of T hours. Assuming a linear relationship between system power (bhp) and initial fixed cost (FC), we obtain FC = kW * 1333. The total hours of use per month (t) are given as t = T/(y * 12). The hourly cost (C_1) of equipment is C_1 = MI/t, where MI is the monthly installment. The cost of abrasives depends on the abrasive flow rate m (g/s) and on the type of abrasives. Typical costs (C) of abrasives are as follows:

Garnet: 0.22 $/kg
Silica sand: 0.11 $/kg
Steel grit: 1.10 $/kg

The hourly cost (C_2) of using abrasives without recycling is $C_2 = (m * 3.6x10^6) * C$.

The replacement of AWJ mixing tubes depends on the limits of acceptable performance. If no more than a 10% reduction in depth of cut is allowed, then a typical nozzle lifetime is about 4 hours at a consumption rate of 33 g/s of garnet abrasives. Assuming a linear relationship between abrasive flow rate and nozzle lifetime, then the useful lifetime (t_l) in hours based on the abrasive flow rate m is t_l = m [(4 hr)/(33 g/s)].

The typical cost of a mixing tube is about 2.6 $/cm, based on limited quantities. For a tube with a mixing length l_m, the hourly cost (C_3) will be $C_3 = 2.6\ l_m$ m. Recent observations indicate that increasing the mixing tube length increases its lifetime; however, this relationship has not been verified. For a conservative estimate, the above formula can be used.

The maintenance cost of a 22-kW single-intensifier unit is about $1.75/hr. For a 55-kW dual-intensifier unit, this cost is $3/hr. Using these two figures, and assuming a linear relationship between the maintenance cost and motor power, the following equation can be derived for the maintenance cost (C_4) in $/hr as $C_4 = 0.03$ kW + 0.9 .

The total hourly cost can be determined from the costs specified above as follows: $C_1 + C_2 + C_3 + C_4$.

Figure 17 shows a plot of the cost of drilling one meter in granite versus the power used for drilling. The data include a wide range of parameters. Comparing the range of costs shown to the cost of drilling with rotary and percussive drills, it can be concluded that AWJ drilling is competitive with these conventional methods. Figure 17 demonstrates that optimization of drilling parameters is important and that further optimization will further reduce drilling costs.

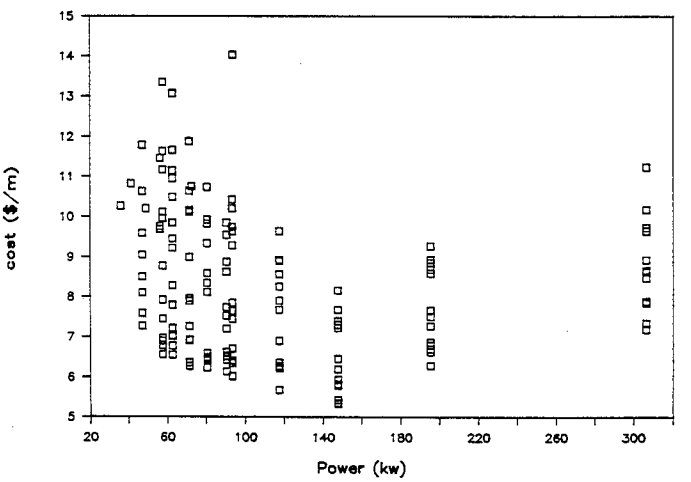

FIG. 17. Projected Cost Range of Granite Drilling (25.4-mm-diameter Hole) with an AWJ Drill

6. CONCLUSIONS

- Linear cutting tests show that AWJ drills have great potential for drilling hard rocks at high penetration rates.
- Drilling with nonrotary drill stems with either stationary or rotary waterjet(s) requires high power levels and high abrasive flow rates to obtain fast penetration rates.
- Uniformity of abrasive kinetic energy distribution is an important criterion for a nonrotary stem AWJ drill.
- Optimization of the mixing process is an important task for the development of a nonrotary stem AWJ drill.
- The use of multiple small waterjets rather than a single waterjet using the same amount of power is more efficient in material removal. However, mixing length and jet distribution require optimization.
- The rotary dual (or multiple) AWJ drill concept is the most promising concept because high-efficiency jets can be used at optimum mixing conditions.
- In rotary dual (or multiple) AWJ drills, jet position is an important parameter for optimization.
- High penetration rates can be achieved in hard rocks with rotary dual AWJ drills.
- The projected cost of drilling with AWJ drills is approximately $5/m. This is competitive with conventional drilling methods. Further optimization of the AWJ drill could result in substantial annual savings in drilling costs.

ACKNOWLEDGEMENT

The author acknowledges the support of the NSF under the SBIR program.

REFERENCES

1. Nagano et al., "The Development of a Waterjet Drilling Machine," *Proc. of the 2nd Int. Symp. on Jet Cutting Technology*, BHRA, 1974.
2. Hoshino, et al., "The Development and the Experiment of the Waterjet Drill for Tunnel Construction," *Proc. of the 3rd Int. Symp. on Jet Cutting Technology*, 1976.
3. Summers, D. A. and Bushnell, D. J., "Preliminary Experimentation of the Design of the Waterjet Drilling Device," *Proc. of the 3rd Int. Symp. on Jet Cutting Technology*, 1976.
4. Veenhuizen, S. D. and Cheung, J. B., "Waterjet Drilling of Small-Diameter Holes," *Proc. of the 4th Int. Symp. on Jet Cutting Technology*, BHRA, 1978.
5. Wang, F. D. and Wolgumott, J. E., "Development of Waterjet-Assisted Drag Bit for Drilling Coal Mine Roof Bolt Holes," *Mining Technology for Energy Resources: Advances for the 80's*, ASME, 1978.
6. Vijay, M. M. and Brierley, M. I. E. D., "Drilling of Rocks with Rotating High-Pressure Waterjets: An Assessment of Nozzles," *Proc. of the 5th Int. Symp. on Jet Cutting Technology*, BHRA, 1980.
7. Veenhuizen, S. D. and O'Hanlon, T. A., "Development of a System for High-Speed Drilling of Small-Diameter Roofbolt Holes," Flow Industries Report No. FTD-117, 1978.
8. Hashish, M., et al., "Method and Apparatus for Forming High-Velocity Liquid Abrasive Jet," U.S. Patent Number 4,648,215.
9. Fairhurst, R. M., et al., "Diajet - A New Abrasive-Waterjet Cutting Technique," *Proc. of the 8th Int. Symp. on Jet Cutting Technology*, BHRA, Durham, England, Sept. 1986, pp. 395-402.
10. Hashish, M., "The Application of Abrasive-Waterjets to Concrete Cutting," *Proc. of the 6th Int. Symp. on Jet Cutting Technology*, BHRA, England, April 1982, pp. 447-464.
11. Hashish, M., "Application of Abrasive-Waterjets to Metal Cutting," *Proc. of the Nontraditional Machining Conf.*, ASM, Cincinnati, Ohio, December 1985, pp. 1-11.
12. Savanik, G. A. and Krawza, W. G., "An Abrasive-Waterjet Rock Drill," *Proc. of the 4th U.S. Waterjet Conf.*, Berkeley, Calif., August, 1987, pp. 129-132.

5th American Water Jet Conference
August 29 - 31, 1989: Toronto, Canada

Paper / Communication 33

EVALUATION OF ABRASIVE-ENTRAINED WATER JETS FOR SLOTTING HARD ROCKS

M.M. Vijay
Gas Dynamics Laboratory
National Research Council of Canada
Ottawa, Ontario K1A 0R6, Canada

ABSTRACT: Extensive previous work conducted on drilling and slotting of hard rocks in the laboratory has indicated, beyond doubt, that simple plain water jets are not economically attractive for processing of hard rock materials which are generally found in the mines or quarries. While a number of alternative techniques are in progress in the laboratory for dealing with rocks, in this paper test results pertaining to slotting with abrasive-entrained water jets are presented. Tests were conducted on Barre Granite, using it as a standard for comparison, dolomite and blocks of mining samples containing both ore-bearing and waste materials. Nozzle pressures and traverse speeds were in the range of 69 to 140 MPa and 0.38 to 1.67 cm/s respectively, whereas the standoff distance was generally close to 2.5 cm. Abrasive (Iron slag) feed rate was varied from 0.227 to 1.8 kg/min. It is shown that (1) not all types of rocks can be cut with abrasive-entrained water jets, (2) abrasive mixing process and the amount of abrasives have considerable influence on performance, and nozzle life which is directly related to reliability and acceptability, and (3) deep slotting still remains a problem.

RÉSUMÉ : Des recherches approfondies effectuées en laboratoire sur le forage et le rainurage dans la roche dure ont révélé, au-delà de tout doute, que l'utilisation de simples jets d'eau ordinaire n'est pas rentable pour le traitement de la roche dure qu'on trouve en général dans les mines ou les carrières. Même si plusieurs techniques de remplacement sont mises au point en laboratoire pour traiter la roche, la présente communication décrit les résultats d'essais de rainurage au moyen de jets d'eau avec abrasifs. Les essais ont été menés sur du granit de Barre, l'étalon de comparaison, sur de la dolomite et sur des blocs d'échantillons de mine contenant des matériaux tant minéralifères que stériles. Les pressions et les vitesses de traversée de la buse ont varié de 69 à 140 MPa et de 0,38 à 1,67 cm/s respectivement, tandis que la distance de garde a été en général voisine de 2,5 cm. Le débit d'alimentation d'abrasif (scorie de fer) a varié entre 0,227 et 1,8 kg/min. Il ressort que (1) tous les types de roche ne peuvent être taillés par des jets d'eau avec abrasifs, (2) le processus de mélange de l'abrasif et la quantité d'abrasif ont un effet considérable sur le rendement et la durée de la buse qui est une mesure directe de fiabilité et d'acceptabilité, et (3) la réalisation de rainures profondes demeure un problème.

Organized and Sponsored by the National Research Council of Canada and the U.S. Water Jet Technology Association.

1.0 NOMENCLATURE

A_s Surface area of the slot = L X h, cm^2
d Diameter of water nozzle, mm
D Inside diameter of ceramic tubing or slurry nozzle, mm
E_a Specific kerfing energy = H_p/hV_{tr}, J/cm^2

E_a^* Specific kerfing energy based on total depth of slot, J/cm^2

E_a^{**} Minimum specific energy for a particular slot, J/cm^2
E_r Specific energy per unit depth of penetration, particularly used in drilling = H_p/R, J/cm
h Depth of cut, total or per pass, cm
H_p Hydraulic power input, kW
L Length (in the direction of cutting) of slot, cm
L_c Length of ceramic tubing, cm (Fig. 1B)
L_n Length of high pressure tubing upstream of the nozzle, cm (Fig. 1B)
m_a Rate of flow of abrasives, kg/min
m_w Rate of flow of high pressure water, kg/min (constant at 67.9)
N Rotational speed of the device, RPM
P Water jet nozzle pressure, MPa
R Rate of penetration, cm/min
V_{tr} Traverse speed of the device, cm/s
W Width of slot, mm

2.0 INTRODUCTION

Recently, based on the extensive work conducted in the laboratory on drilling and slotting of hard rocks with high pressure plain water jets, the author asserted that plain water jets alone are not economically attractive for processing of hard rock materials (Ref. 1). He also stated that the only way that the water jets could be used, particularly for mining applications, is to combine them with the mechanical cutters, be it water-jet-assist or mechanical assist, and further, that improvements could probably be achieved by incorporating into these hybrid systems the newly developing techniques, viz., abrasive-entrained, cavitating or pulsed jets. Work is in progress in the laboratory to study the effectiveness of all of these techniques for processing of hard rocks. Results reported in this paper, limited due to the continuing nature of the investigation, pertain to slotting with abrasive-entrained water jets. The work was undertaken because it was felt that the results available in the literature (Refs. 2 to 8) were not sufficient to fully evaluate the potential and the problems associated with the abrasive-entrained water jets.

Initially, in order to assess the feasibility of cutting rocks with abrasive-entrained water jets, some preliminary tests were conducted on dolomite using the conventional nozzle designs shown in Fig. 1A (Ref. 9). Realizing the limitations of such nozzle designs for deep penetrations into the rocks, the nozzle design was altered to that shown in Fig. 1B. Attempts were made to drill samples of Barre Granite (this rock specimen, as discussed later, is always used as a standard against which the performance of water jets on all other rock materials can be compared) at 200 RPM (Ref. 1). The rotational speed was deliberately kept low in order to obtain smooth entraining of abrasives (garnet) in the rotating water jets. At a pressure of 117 MPa (hydraulic power = 124 kW), and an abrasive feed rate of 6.4 kg/min, the rate of penetration (R) was 20.2 cm/min, yielding a specific energy (E_r) of 3.70×10^5. Considerable wear in the nozzle was noticed (Fig. 2). It should be emphasized that for applications such as mining, in addition to improvements in performance, the life of the operating systems is of utmost importance. It was felt that the wear was due to high abrasive feed rate, and therefore the abrasive rate was decreased to 4 kg/min, while increasing the pressure to 138 MPa (hydraulic power = 158 kW), keeping the RPM still constant at 200. The result was, in short, very disappointing. As the orifices wore out, within a span of a few seconds, in the process of drilling, the jet quality degraded considerably, resulting in a penetration rate of only 11.80 cm/min ($E_r = 8.0 \times 10^5$). With pure water jets at 138 MPa and the same hydraulic power & RPM the rate of penetration was 137.6 cm/min ($E_r = 7.0 \times 10^4$). Although steps are in progress to improve the method of producing rotating twin abrasive-entrained water jet systems, results reported in this paper on slotting were conducted with a single orifice nozzle, still rotating the device, to obtain a well mixed slurry.

3.0 EQUIPMENT, MATERIALS AND METHOD

As stated above, the test results presented herein were obtained with the abrasive-water nozzle device shown in Fig. 1B. The device consists of 17 different components to investigate the effect of various parameters, e.g., the length (L_c) of slurry accelerating

ceramic tubing. The whole unit was designed to operate from 0 to 1000 RPM, if required. Abrasives, mixed with water, to avoid clogging, can be fed to the hopper by gravity, which then travel down the annular space between the high pressure water tubing and the outer housing tubing. Abrasives are then entrained by the high speed water jet in the gap (the mixing chamber) between the nozzle and the slurry accelerating ceramic tubing. At the tip of the ceramic tubing one can attach any type of exit nozzles to produce rotating or stationary, multiple or single, slurry jets. The length (L_n) of the high pressure tubing upstream of the water nozzle can be changed to study the effect of the length of the mixing chamber (gap) on the nature of the slurry jet. The whole unit was designed to operate at a maximum pressure (P) of 138 MPa (20000 psi), water flow rate of 68 litres/min (m_w = 67.9 kg/min) and an abrasive flow rate (m_a) of 9.1 kg/min (20 lb_m/min). As the flow rate was kept constant at 68 litres/min, the water nozzle diameters (d) were 1.97, 1.78, 1.659 mm respectively for the operating pressures of 69, (H_p = 78 kW) 103.5 (117kW), and 138 MPa (156kW).

In order to facilitate deep drilling or slotting (using angled jet or jets), compromise had to be made to keep the overall outer diameter of the abrasive housing tubing as small as possible, and yet obtain sufficient annular gap width to allow smooth flow of abrasives to the mixing chamber. This required a gap width of a minimum of 3.2 mm, and since the outer diameter of the high pressure tubing, upstream of the nozzle was 9.525 mm, the outer diameter chosen for the abrasive housing tubing was 22.225 mm. The design and dimensions of the ceramic accelerating tubing was even more critical. In principle, the length to completely accelerate the particles to the speed of the jet would be infinite (Refs. 10 & 11). Several of these tubings were fabricated, hoping to find the optimum design by experimentation. The one selected in the present investigation had an internal diameter of 3.175 mm, a length of 13.97cm and a converging angle of 20° at the inlet (Fig. 1B). The single orifice ceramic nozzle, fabricated from aluminium oxide, had the same inner diameter (D/d varied from 1.61 to 1.91). The abrasive used in the experimental work was chilled iron grit and shot, G-40 (particle diameters ranged from 0.3 to 1.0 mm). Smooth flow of the abrasives through the annular gap was achieved by mixing them with water and rotating the device at about 100 RPM.

Most of the tests were conducted on blocks of barre granite (average size = 80x55x40cm). Barre granite was selected for the study because, apart from its commercial uses, it is fairly homogeneous and has well defined properties, albeit somewhat varying. When assessing the performance of any new technique, it is quite important, particularly in rock work, to minimize the dubious effects of variations in material properties on the performance. The blocks were confined within a matrix of reinforced concrete to eliminate the edge effects and also to impose in situ stress conditions. The micro-structural properties and the composition of the rock material were obtained by taking the optical and electron micrographs of several thin sections taken from several samples (Figs. 3A & B). The rock material is a muscovite biotite granite of medium grain size and consists mostly of feldspars (64%), and quartz (21%). Other minerals are biotite (7%), muscovite (7%), chlorite (0.4%) with some accessory minerals such as apatite (0.5%). As shown in Fig. 3B, open cracks were common around the grain boundaries, and some through the grains themselves. In cutting with plain water jets, flow of water through these cracks enhances the cutting ability of jets (Ref. 12). A discussion of how the same cracks or microfractures influence the abrasive bearing jets is beyond the scope of this paper. Rock properties measured in the laboratory had the following values:

Compressive strength (146 MN/m^2), tensile strength (8.0 MN/m^2), grain size (0.976 $\pm$ 0.614 mm), porosity (1.4%), and permeability at 1 atm (0.16mD).

Continuing the work on ore-bearing and non-ore-bearing samples (Ref. 12), a number of tests were conducted on some of these samples with the abrasive-entrained jets. Only photographs, depicting qualitative observations are reported in this paper (Fig. 4).

The experimental method was quite straight forward. Once the operating variables (m_a, P, and V_{tr}) were set at the desired values, the rock sample was traversed under the slurry nozzle. The standoff distance was generally constant at 2.54 cm (varied somewhat due to the uneven top surface facing the jet). After each pass, the nature of the slot and any other peculiarities, such as, for instance, the wear of the slurry nozzle, were noted, and the width and depth of the slot were measured. This procedure was repeated until a desired depth of cut was achieved or the rock was completely sliced. During the experimentation, for a given pressure (69,103.5, & 138 MPa), abrasive feed rate and traverse speed were varied as follows:

$$m_a = 0,\ 0.454,\ 1.05,\ \text{and } 1.814 \text{ kg/min; and } V_{tr} = 0.38 \text{ to } 1.67 \text{ cm/s}.$$

Nozzle device performance was assessed based on (i) total depth or depth of cut per pass, (ii) specific kerfing energy (E_a = energy spent per unit surface area of the slot = H_p/hV_{tr}),

and (iii) wear of the components, particularly the ceramic accelerating tubing and the slurry nozzle which is quite important from the standpoint of reliability in the industrial continuous mode of operation.

4.0 PRESENTATION OF RESULTS

Qualitative results are illustrated in Fig. 4 (A to G). These are included to point out some of the prominent differences between slotting with the plain and the abrasive-entrained water jets. Raw data acquired in the investigation are plotted in Fig. 5 which shows the cumulative depth of cut after a certain number of passes and also for one set of operating conditions, the depth of cut in each successive pass. The calculated values of specific kerfing energy (E_a) for each successive pass are plotted in Fig. 6. Specific energy values based on the total depth of cut for a particular slot are plotted in Fig. 7 as a function of the traverse speed. Finally, the minimum values of specific energy achieved for a particular slot are plotted in Fig. 8. All of the results plotted in these figures pertain only to BARRE GRANITE. It should be stated that the data points are connected by lines only for the sake of clarity, and for the same reason, only sample results are included in the plots. Errors in the measurement of raw data are estimated to be in the neighbourhood of 15 percent. The scatter in the data, indicated particularly in Fig. 7 (open circles) are probably due to the variations in the structural properties of the rock material of the same block or from one block to another.

5.0 DISCUSSION

One of the variables which is not included in the presentation of the results is the width of the slot. In slotting with abrasive-entrained water jets, although the width was fairly uniform for a particular slot, it generally varied from slot to slot depending on the pressure, traverse speed and the concentration of abrasives in the jet, i.e., m_a/m_w (Figs. 4C,F & G). In cutting tests with plain water jets, as the rock often spalled, at least in the first couple of passes, the slots were not well defined, rendering measurement of slot width difficult (Figs. 4B & D). There are some anomalies in the slot widths which are difficult to explain. For instance, consider slot #15 and #16 in Fig. 4C. These slots were obtained at the same pressure (103.5 MPa) and concentration of abrasives (m_a/m_w = 0.015), but at different traverse speeds. For #15, V_{tr} was 1.0 cm/s, and for #16, it was 0.66 cm/s. The mean (the mean taken from top to the bottom) width of slot #15 was 19 mm and that of #16 was 7 mm. One would expect the slot width to decrease as the traverse speed increased, other conditions remaining constant, contrary to what was observed in these tests. Fig. 4 also clearly demonstrates that not all rocks can be cut with abrasive-entrained water jets, at least not at the same operating conditions (compare Fig. 4E with F & G).

Fig. 5 brings out several important points, although scatter in the data, as pointed out earlier (Fig. 7), makes it quite difficult to arrive at firm conclusions. It is quite clear that the addition of abrasives to the water jet increases the depths of cut, but not as dramatically as claimed by some investigators (for example, Refs. 4 & 5). The trend of data indicates, at the same operating conditions of pressure and traverse speed, the depth of cut increases as the concentration of abrasives in the jet is increased. However, as pointed out earlier, increasing the amount of abrasives without changing the dimensions of the components has an adverse effect on their life span. Another interesting observation is that abrasive-entrained jets appear to have better cutting ability in the second and upto fourth passes compared to plain water jets. This is probably due to the accelerating, confining, and focusing effects created by walls of the slot generated during the previous pass. However, these contributions seem to diminish after about the 5th pass. The maximum depth of cut achieved was 22 cm after 12 passes.

Values of the specific kerfing energy, which is a measure of the efficiency of the technique, calculated for each pass of cutting, vary considerably from one pass to the next, Fig. 6. The positive slopes of the curves, disregarding the scatter, indicate that the process is becoming more and more inefficient from one pass to the next. In other words, the depth of cut is getting smaller and smaller in each successive pass. The hydraulic power which is constant for a given pressure, is being simply wasted due to the friction of the walls of the slot. The minimum point observed at the 9th pass at 138 MPa could be spurious or real due to the focusing effect alluded to above. The plain water jet appears to loose power much faster than the abrasive water jet.

Often in practice, one is generally interested in a certain finite depth of cut, regardless of the number of passes required to achieve it. In Fig. 7, values of specific energy, based on the total depth of cut, are plotted as a function of the traverse speed. The results for both types of jets follow the same, well proven trend (Ref. 1) namely, that the magnitude of specific energy decreases as the traverse speed is increased upto a certain limit. Although no data were obtained at traverse speeds beyond 1.67 cm/s, the slopes of the lines

appear to indicate that this value of the traverse speed is probably close to the optimum. Magnitudes of specific energy obtained with abrasive water jets appear to be slightly better than those achieved with plain water jets.

In Fig. 8 magnitudes of minimum values of specific energy pertaining to a particular slot are plotted against the nozzle pressure (very limited). As the power input per pass is constant, and the depth of cut may increase or decrease in each successive pass (depends whether the focusing effect contributes in enhancing the cutting ability), it is possible to achieve minimum values of specific energy in a slot. Further slotting without changing the operating conditions will result in diminishing returns, as the efficiency of cutting is reduced. Although the data are scattered somewhat, it appears that improvements in cutting performance can be obtained at pressures close to 138 MPa (20000 psi).

It was stated earlier that the results obtained with abrasive-entrained water jets in this investigation were not as dramatic as reported by other investigators. A great number of variables influence the cutting process with abrasive jets, including the type and concentration of abrasives. The concentration of abrasives in this work is quite low compared to those used by others (Refs. 5 to 8). In order to fully assess the potential of abrasive jets for mining and quarrying applications, the effect of all of these variables on the performance, including the life of the components, needs to be investigated. In the present study, although the slurry nozzle survived more than 3 hours of operation, there were problems with the ceramic accelerating tubing, as the abrasives penetrated through walls of the tubing. New tubing had to be placed twice during the period of investigation. In the laboratory setting, this is probably adequate. However, in continuous commercial operations, the components have to function satisfactorily for more than three hours. Furthermore, with a single straight orifice the depth of cut that can be achieved is probably limited to no more than 30 cms. With the rotating angled plain water jets, slots as deep as 3.4 m have been achieved in the field trials in a quarry (Ref. 13). The advantage of abrasive-entrained water jets appear to be during the initial passes where they seem to penetrate deeper into the rock than the plain water jets. Therefore, if an abrasive jet device can handle slurry nozzle with two or more angled jets (Fig. 2), then the system would be attractive for deep hole drilling or slotting. Work to address some of these problems is in progress in the laboratory. Since abrasive-entrained water jets are finding their way in many industrial applications, (Refs. 14 to 24), it is only appropriate to consider the potential of the technique for mining and quarrying of rock materials.

6.0 CONCLUSIONS

From the experimental results presented in this paper, it is possible to draw the following conclusions:

1. Abrasive-entrained water jets do have the potential for processing of some types of rock materials, at the operating conditions employed in the investigation. Whether other types of hard rocks, e.g., non-ore-bearing rock, can be processed at higher pressures, abrasive flow rates, etc., remains to be investigated.
2. A life of the order of 3 hours for the abrasive handling components is certainly an improvement, but it is not adequate for continuous commercial operations, be it mining, quarrying or any other applications.
3. The design requires refinements to achieve deep drilling and slotting in hard rocks.
4. Further work is required to understand why some types of rock material e.g., granite,can be readily cut with abrasive-entrained jets while on some others, e.g., non-ore-rock material, they hardly make a scratch.

7.0 ACKNOWLEDGMENTS

The author gratefully acknowledges Mr. N. Paquette, Technical Officer, Gas Dynamics Laboratory, and Mr. McMullin, who assisted him in acquiring the experimental data in the laboratory. The author is thankful to Mr. W. Yan, Daqing Petroleum Institute, Anda City, Heilong Jiang Province, China, for developing and designing the rotating abrasive-entraining nozzle device, and to Dr. P.E. Grattan-Bellew, Institute for Research in Construction, NRC, for the petrographic analyis of rock samples. It is a pleasure to acknowledge Dr. R.G. Williamson, Head, Gas Dynamics Laboratory, for the interest shown in the project. Thanks are also due to Mrs. H. McDonald for typing the manuscript of this paper.

9.0 REFERENCES

1. Vijay,M.M., and Yan,W.: Water Jet Cutting for Processing of Hard Rock Material. Paper K4. Proc. 9th International Symposium on Jet Cutting Technology. BHRA. England. 1988. pp.545-560 (Also in International Journal of Surface Mining. V.3. No.2. 1989).
2. Maurer,W.C.: Advanced Drilling Techniques. Chapter 5. Petroleum Publishing Co.

Tulsa, OK 74101, U.S.A. 1980. pp.19-27.
3. Saunders,D.: A Safe Method of Cutting Steel and Rock in Hazardous Atmospheres. Paper K5. Proc. 6th International Symposium on Jet Cutting Technology. BHRA. England. 1982. pp.503.518.
4. Hashish.M., Loscutoff,W.V., and Reich,P.: Cutting with Abrasive Water Jets. Proc. 2nd U.S. Water Jet Conference. Rolla, Missouri, U.S.A. May 1983. pp.391-406.
5 Yie, G.G.: Cutting Hard Rock with Abrasive-Entrained Water Jet at Moderate Pressures. Ibid. pp.407-422.
6. Savanick,G.A.,Krawza,W.G., and Swanson,D.E.: An Abrasive Water Jet Device for Cutting Deep Kerfs in Hard Rocks. Proc. 3rd U.S. Water Jet Conference. Pittsburgh, U.S.A. May 1985. pp.101-122.
7. Marlowe,A.C.,Worsley,S.L., and Price,C.J.: The Use of Abrasive-entrained High Pressure Water Jets as a Tool for the Non-explosive Winning of Gold Bearing Quartzites. Paper 11. Proc. 8th International Symposium on Jet Cutting Technology. BHRA. England. 1986. pp.113-123.
8. Savanick,G.A., and Krawaza,W.G.: An Abrasive Water Jet Rock Drill. Proc. 4th U.S. Water Jet Conference. Berkeley, California, U.S.A. August 1987. pp.129-132.
9. Vijay,M.M., and Grattan-Bellew,P.E.: An Examination of the Application of High Pressure Water Jets for Cutting Rocks. Proc. International Water Jet Symposium. Beijing, China. September 1987.
10. Bohnet,M.: Design of Gas-Solids Injectors. In : Handbook of Fluids in Motion. Edited by : Cheremisinoff,N.P., and Gupta, Ann Arbor Science, The Butterworth Group. Chapter 30. pp. 785-805.
11. Wallis,G.B.: One-Dimensional Two-Phase Flow. Chapter 8. McGraw-Hill Book Company. 1969. pp. 175-242.
12. Vijay,M.M., and Grattan-Bellew,P.E.: An Assessment of Rotating High Pressure water Jets for Drilling and Slotting of Hard Ore-Bearing Rocks. Proc. 3rd U.S. Water Jet Conference. Pittsburgh, U.S.A. May 1985. pp.231-247.
13. Hawrylewicz,B.M., Vijay,M.M., Remisz,J, and Paquette,N.: Design and Testing of Rock Slotter for Mining and Quarrying Applications. Paper G4. Proc. 9th International Symposium on Jet Cutting Technology. BHRA. England. 1988. pp.377-386.
14. Liu,B.L, and Cui,M.S.: Experiment of the Premixed Abrasive Jet to cut Metal Plate. Paper B4. Proc. 9th International Symposium on Jet Cutting Technology. BHRA. England. 1988. pp.85-98.
15. Hunt,D.C.,Reuber,M., and Kim,T.J.: Surface Finish Optimization for Abrasive Waterjet Cutting. Ibid. Paper C1. pp.99-112.
16. Hashish,M.: Turning,Milling and Drilling with Abrasive-Waterjets (AWJ). Ibid. Paper C2. pp.113-132.
17. Bortolussi,A.,Summers,D.A., and Yazici,S.: The Use of Water Jets in Cutting Granite. Ibid. Paper E3. pp.239-254.
18. Haferkamp,H.,Louis,H., and Meier,G.: Cutting of Contaminated Material by Abrasive Water Jets Under the Protection of Water Shield. Ibid. Paper F1. pp.271-288.
19. Seiki,Y.,Nakamura,H.,Narazaki,T., and Yokota,Y.: Application of Water Jet to Dismantlement of Reactor Biological Shield. Ibid. Paper F2. pp.289-296.
20. Yamada,B.,Yahiro,T., and Ishibashi,J.: On the Development and Application of a Method of Remodelling and Utilizing an Abrasive Jet System. Ibid. Paper E1. pp.203-216.
21. Hessling,M.: Recent Examinations Relating to the Effects of the Abrasive Material, Operational Parameters and Rock Properties on the Depths of Cut Obtainable with Abrasive High Pressure Water Jets When Cutting Rock. Ibid. Paper G3. pp.357-376.
22. Fairhurst,R.M., and Roff,M.F.: A Field Application of the Diajet Abrasive Water Jet Cutting Technique. Ibid. Paper H1. pp.387-398.
23. Kokaji,C.,Sakashita,F.,Oura,S., and Sato,M.: Effects of Abrasives on Concrete Cutting. Ibid. Paper L2. pp.571-580.
24. Sugiyama,H., and Tabata,A.: Abrasive Water Jet Method for Effective Cutting of Reinforced Concrete Members (on Vibration Properties when Cutting). Ibid. Paper L3. pp.581-590.

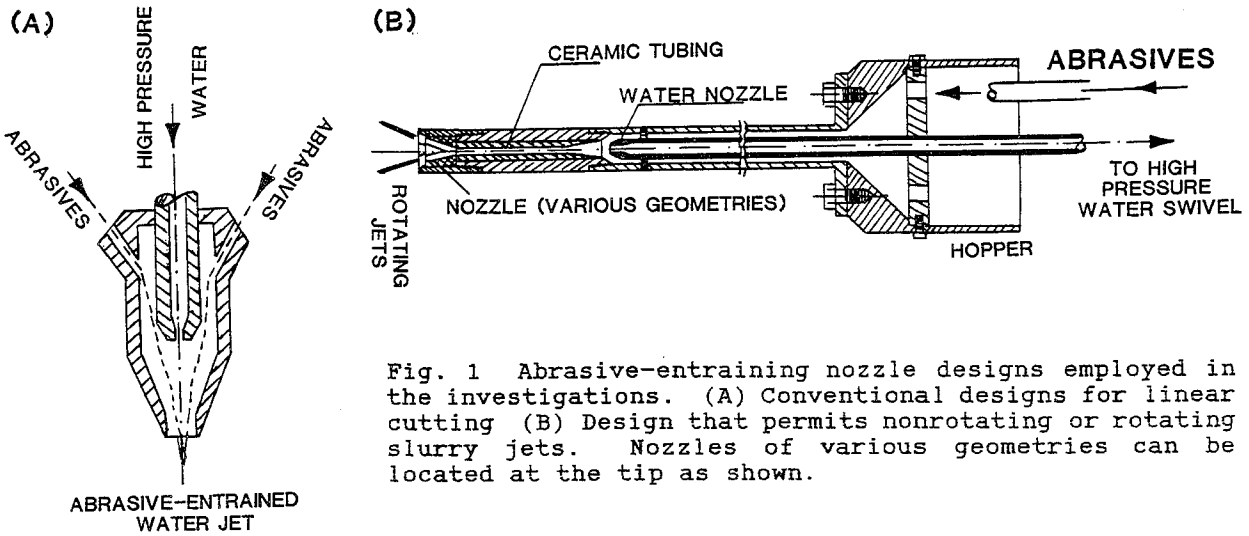

Fig. 1 Abrasive-entraining nozzle designs employed in the investigations. (A) Conventional designs for linear cutting (B) Design that permits nonrotating or rotating slurry jets. Nozzles of various geometries can be located at the tip as shown.

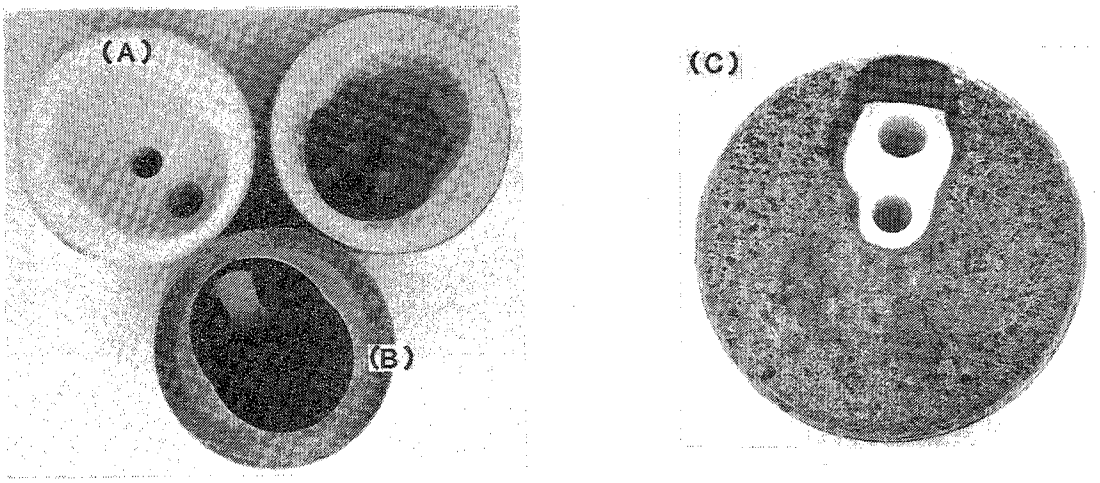

Fig. 2 Twin-orifice nozzles for generating rotating abrasive-entrained water jets for deep drilling and slotting of rocks, employed in the earlier investigations. (A) Nozzles fabricated from hard ceramic, aluminum oxide (B) Nozzle fabricated from hardened 17-4 PH stainless steel, and (C) Erosion of the nozzle holder due to the reverse flow of the slurry in the hole.

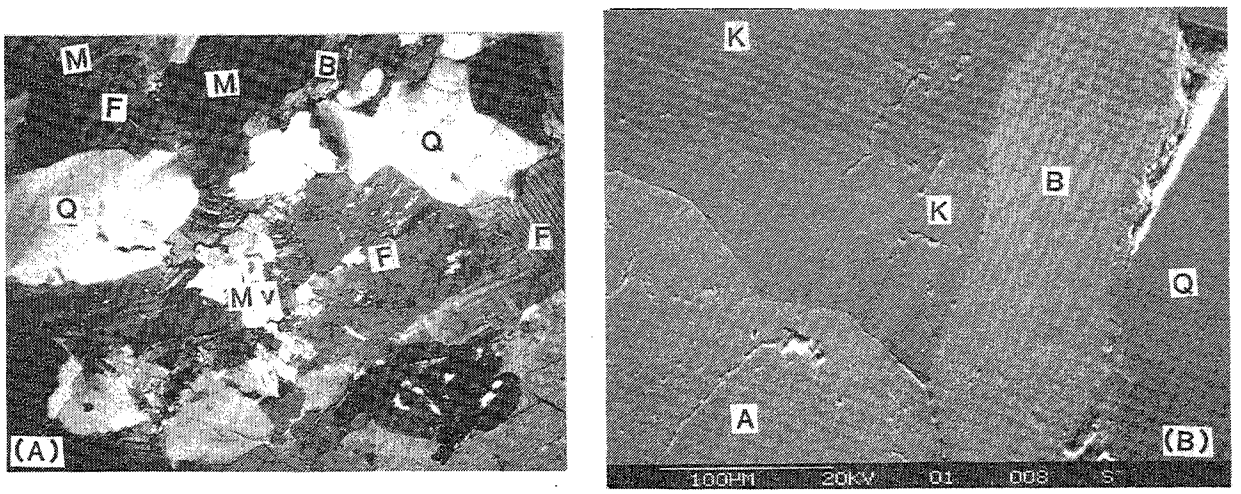

Fig. 3 Optical (A) and scanning electron micrographs (B) of barre granite, showing the grain size distribution and the composition. Note the micro-fractures along the grain boundaries and across the grains. A : Apatite B : Biotite F : Feldspar K : Potassium Feldspar M : Microcline feldspar Mv : Muscovite Q : Quartz

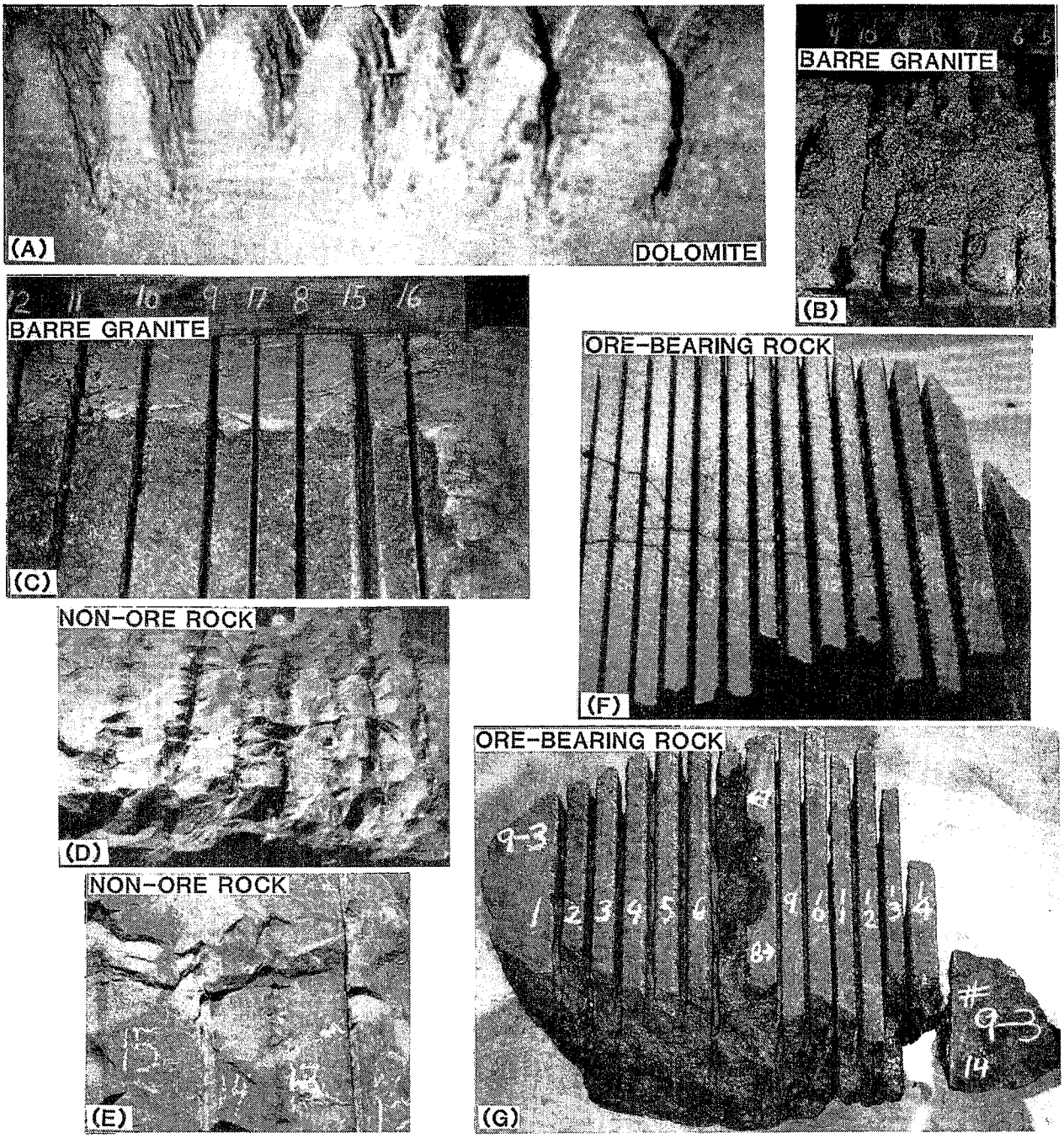

Fig. 4 Slotting different types of rocks with plain and abrasive-entrained water jets. (A) Dolomite slotted with the nozzle (d = 1.6 mm) type shown in Fig. 1A, at P = 69 MPa, V_{tr} = 1.67 cm/s. (B) Barre granite slotted with plain water jets. (C) Barre granite slotted with abrasive-entrained water jets. (D) & (E) Non-ore bearing rock (waste material) slotted with plain and abrasive jets. (F) & (G) Rich ore-bearing rock slotted with abrasive-entrained jets at pressures upto 138 MPa. Note: Generally during the first couple of passes plain water jets tend to spal the rock material (B & D). Abrasive water jets, on the other hand, almost always yield clean cuts with smooth surfaces of the slots. Also, the reinforcing bars are cut through after a few passes and concrete can be cut readily with the abrasive-entrained water jets, at pressures as low as 69 MPa (10000 psi).

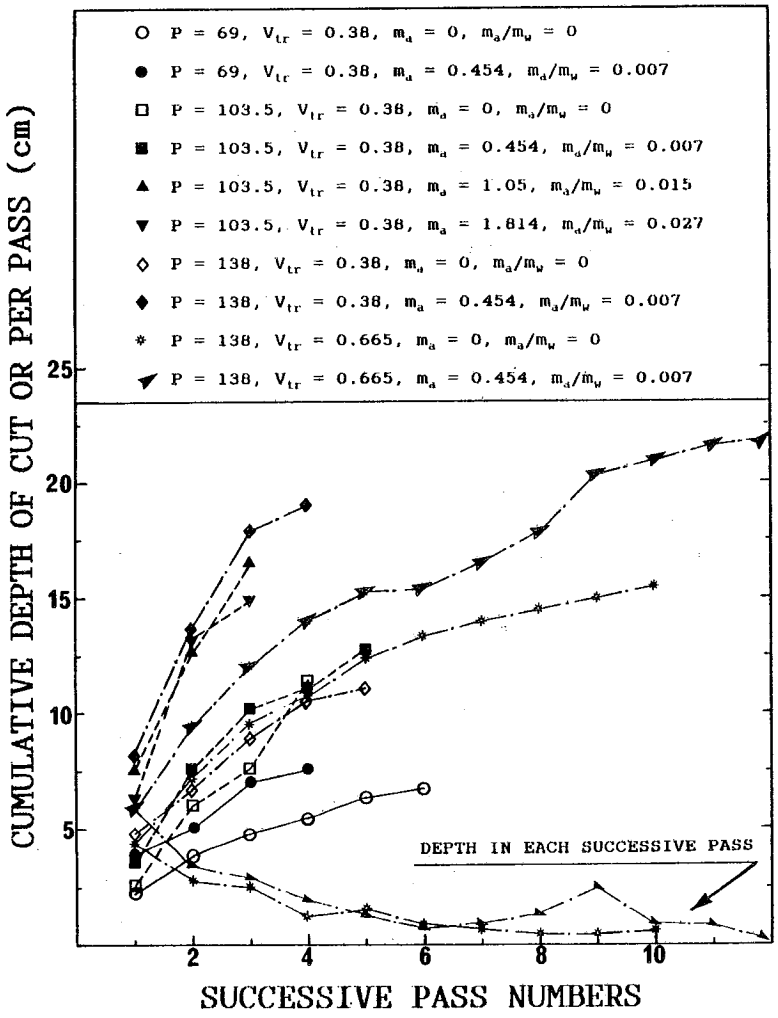

Fig. 5 Plot of cumulative depth of cut against the pass numbers, with pressure, feed rate of abrasives and the traverse speed as parameters.

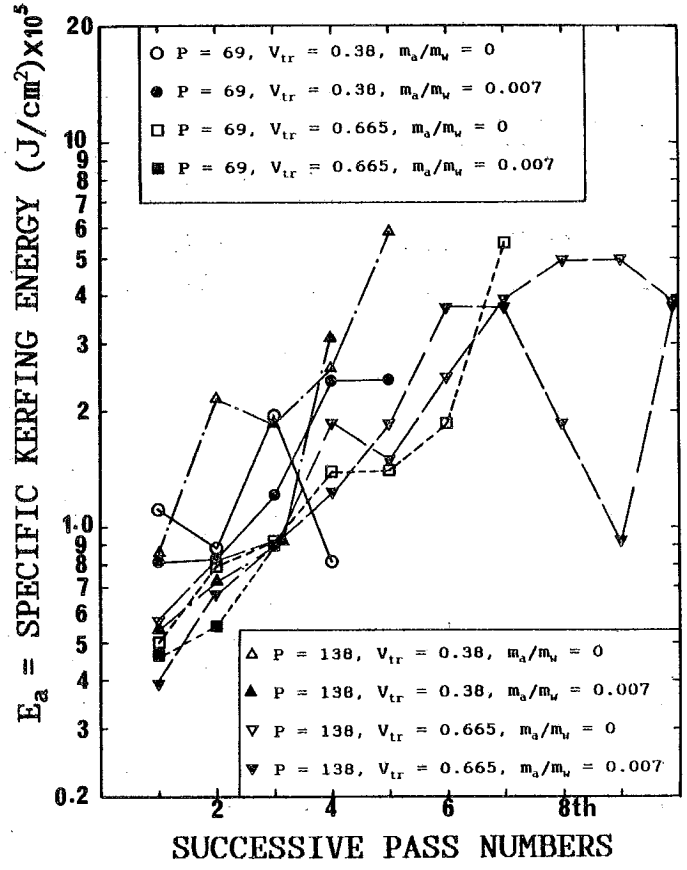

Fig. 6 Plot of specific kerfing energy (E_a) against the pass numbers, with pressure, feed rate of abrasives and the traverse speed as parameters.

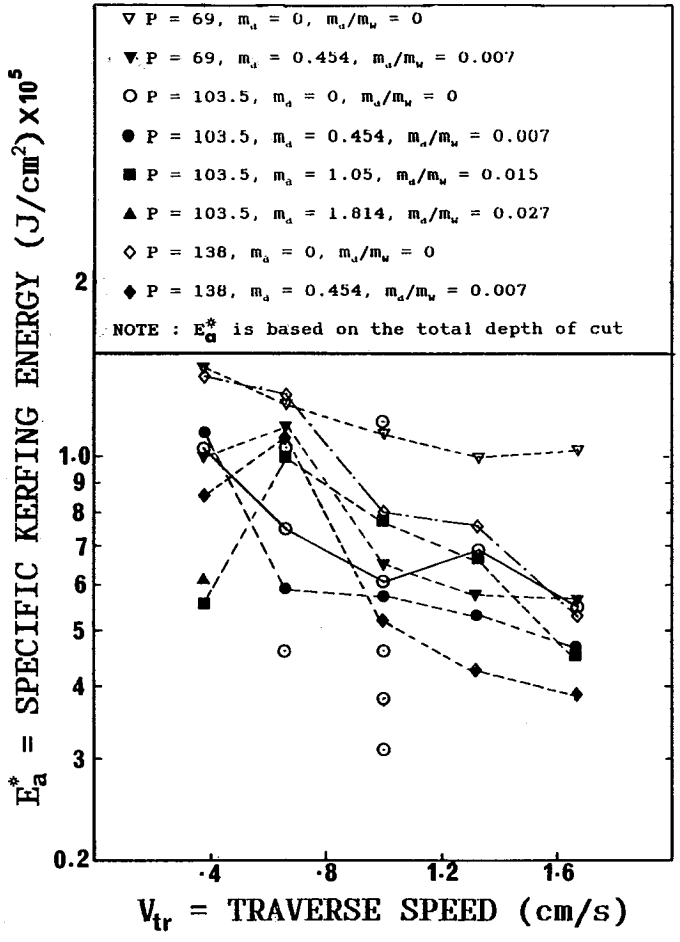

Fig. 7 Plot of specific kerfing energy based on the total depth of the slot (E_a^*) against the traverse speed, with pressure and the feed rate of abrasives as parameters.

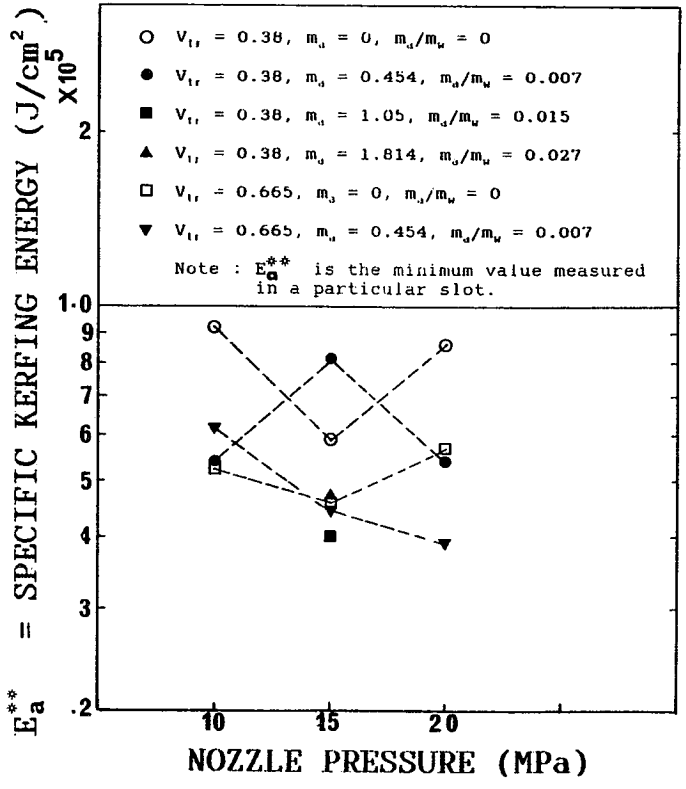

Fig. 8 Plot of minimum specific kerfing energy (E_a^{**}) against nozzle pressure, with the traverse speed and the feed rate of abrasives as parameters.

5th American Water Jet Conference
August 29 - 31, 1989: Toronto, Canada

Paper / Communication 34

THE INVESTIGATION OF DIAJET (DIRECT INJECTION OF ABRASIVE JET) CUTTING OF GRANITE

S. Yazici AND D.A. Summers
High Pressure Water Jet Laboratory
University of Missouri-Rolla
Rolla, MO 65401, USA

ABSTRACT: The drilling and cutting of rock by a DIAjet system can be an alternative to conventional rock removal methods. In order to assess the practicality of this method, an experimental study has been conducted examining the effect which different cutting parameters have on the process. A total of 128 single pass cuts were made on a sample of Georgia granite. Two different nozzle types were used in the program, and seven different abrasives were evaluated. The depth, width and volume of the resulting slot were measured. Based on these values the specific energy and erosion efficiency of the abrasive was calculated as an indicator of cutting efficiency. The following conclusions could be drawn from the results obtained: Depth of cut increases with an increase in jet pressure, abrasive flow rate, particle size and hardness. Depth of cut decreases with an increase in traverse velocity. The relationships found appeared to be similar to those found with conventional abrasive jet entrainment. Pressure and abrasive hardness were found to be the most influential parameters on the resulting depth of cut. A possible optimum depth of cut occurred when the abrasive feed rate reached a value of 100 g/sec. The rate at which the kerf area was generated appeared to reach a maximum when the traverse velocity lay between 35 and 60 cm/min. Nozzle wear was found to increase as nozzle diameter reduced and as particle size increased. Order of magnitude values for the specific energy of DIAjet cutting in granite was 20,000 to 30,000 MJ/m^3 and erosion efficiency was 0.005 cm^3 of granite/g of abrasive.

RÉSUMÉ : Le système de forage et de coupe dans la roche DIAjet peut remplacer les méthodes classiques d'enlèvement de la roche. Pour évaluer si la méthode est applicable, on a mené une étude expérimentale sur l'effet de divers paramètres de coupe sur le procédé. En tout, 128 coupes en une seule passe ont été réalisées dans un échantillon de granite de Georgie. Deux types de buses ont été utilisés dans le programme, et sept abrasifs ont été évalués. La profondeur, la largeur et le volume du trait résultant ont été mesurés. Ces valeurs ont permis de calculer l'énergie spécifique et la capacité d'érosion de l'abrasif comme indices du rendement en coupe. Les conclusions suivantes pourraient être tirées des résultats obtenus : la profondeur de coupe augmente avec la pression du jet, le débit d'abrasif, la taille et la dureté des particules. Elle diminue avec la vitesse de coupe. Les relations établies semblent se rapprocher de celles établies pour une coupe au jet abrasif classique. La pression et la dureté de l'abrasif se sont avérées les paramètres déterminants en ce qui a trait à la profondeur de la coupe. La profondeur de coupe a semblé optimale lorsque le taux d'alimentation en abrasif a atteint 100 g/s. La vitesse à laquelle la surface du trait s'est développée a semblé atteindre un maximum lorsque la vitesse de coupe était comprise entre 35 et 60 cm/min. L'usure de la buse a augmenté lorsque son diamètre a été réduit, et la taille des particules, augmentée. L'ordre de grandeur de l'énergie spécifique de DIAjet dans le granite est de 20 000 à 30 000 MJ/m^3, et sa capacité d'érosion, de 0,005 cm^3 de granite/g d'abrasif.

Organized and Sponsored by the National Research Council of Canada and the U.S. Water Jet Technology Association.

1.0 INTRODUCTION

The use of high pressure water jets as a tool for cutting and drilling rock has been the subject of many investigations. Results have shown that the technique can be successful in relatively soft or granular rock (7, 8). In harder rock it is necessary either to use the jet to assist mechanical cutting, or to add abrasive to the jet. Conventional waterjet abrasive systems are impractical in mines, because the very high pressure equipment required has stringent water quality demands, and environmental cleanliness standards which cannot be found in most mines. Use of the lower pressure DIAjet system suggests a possible alternative approach, which may overcome these difficulties with simpler equipment (6,10).

Before starting a field project, one should find the parameters which control the DIAjet performance. The parameters studied in this investigation included jet pressure, abrasive flow rate, nozzle diameter, traverse speed and abrasive properties. In order to correlate the results with previous studies of plain waterjet cutting and conventional abrasive jet systems, the DIAjet study was carried out on Georgia granite.

2.0 EQUIPMENT AND MATERIALS USED

2.1 Jet Cutting Equipment

A commercially available DIAjet unit (Jetnife 5000) was purchased by the UMR High Pressure Waterjet Laboratory (HPWL) in 1988. The main system components are a storage hopper, a pressure vessel and a small slurry pump. Abrasives are automatically mixed with water in the hopper and fed into the pressure vessel. When cutting is required a selector valve is used to feed the abrasives into the hose which carries pressurized water from the pump to the cutting nozzle. A more detailed description of the unit is given elsewhere (1, 9).

Two nozzle types were used in this study; 2.18 cm long carbide inserts used in conventional waterjet cutting, and the longer nozzles supplied with the DIAjet equipment. The first design has a 12° tapered entrance and a very short straight section, nozzle diameters of 1.98, 2.39 and 2.77 mm were tested in the program. The DIAjet nozzle has a 60° tapered section, followed by a 4.45 cm long straight passage with a 2.80 mm diameter. High pressure water was supplied by a 113 kW (150 Hp) Aqua-Dyne pump capable of providing flows of up to 96 L/min (25 gpm) at a pressure of up to 69 MPa (10,000 psi). The abrasive injection equipment was connected into the 15.2 m (50 ft) long, 1.27 cm (0.5 in.) ID high pressure hose which carried water from the pump to the nozzle.

2.2 Abrasives

Seven abrasives were used, differing in size, hardness and density (Table 1). Average size was calculated from the size distribution data, particle density was measured at the HPWL and a hardness value was obtained from the literature (3).

Table 1. Properties of Abrasives

Abrasive	Average Size, micron	Density, g/cm^3	Bulk Density, g/cm^3	Mohs Hardness
Garnet # 60	296	3.89	2.04	7.5
Garnet # 40	586	3.91	2.27	7.5
Garnet # 36	867	3.84	2.23	7.5
Garnet RUF	1250	3.65	2.16	7.5
Quartz Sand	401	2.60	1.65	7.0
Boiler Slag	336	2.65	1.40	--
Aluminum Oxide	341	3.87	2.23	9.0

2.3. Granite Target Material

Granite samples were obtained from the remaining blocks left from the construction of the UMR Stonehenge. Georgia granite is reported to have a compressive strength of 179 MPa, (26000 psi) and a density of 2.69 g/cm^3 (168 lb/ft^3). The tests were carried out on blocks measuring 58 by 58 by 180 cm.

3.0 EXPERIMENTAL PROCEDURE

3.1 Cutting Experiments

The tests were carried out in two parts. The shorter nozzles were used to provide information on the effects of jet pressure, nozzle diameter, abrasive flow rate and traverse speed. The DIAjet nozzle was used to study the effects of pressure, abrasive flow rate and type, and traverse speed (Table 2).

Cutting experiments began by bringing the supply pump to pressure, and then opening the supply circuit which injected abrasive into the flow. For the first 10 seconds the jet was exhausted into the air until it reached full abrasive flow, the nozzle was then traversed over the granite block, starting from an edge, until it had cut a slot 5.0 to 7.5 cm long. The nozzle assembly was moved to a fresh surface, and the steps above repeated for the next test. It should be noted that, while rock anisotropy has a considerable on jet cutting ability with plain waterjets, it has been found to have little effect in abrasive waterjet cutting (5).

Table 2. Parameters Investigated in DIAjet Cutting

Parameters	Number of Levels
A) Experiments with 2.18 cm long Carbide Inserts	
Abrasive: Garnet # 60	1
Rock Type: Georgia Granite	1
Stand off Distance: approximately 1.27 cm	1
Pressure: 20.7, 27.6, 34.5 MPa	3
Abrasive Flow Rate: 46, 105, 149 g/sec	3
Nozzle Diameter: 1.98, 2.39, 2.77 mm	3
Traverse Speed: 15.24 cm/min	1
B) Traverse Speed Experiments	
Traverse Speed: 3.76, 8.08, 23.77, 43.08, 51.56, 91.19 cm/min	6
Pressure 27.6 MPa, nozzle diameter 2.39 mm, abrasive flow rate 105 g/sec,	
Other parameters as in Series A.	
C) Initial Experiments with DIAjet Nozzle	
Abrasive Type: Garnet # 60, #40, #36, RUF, Boiler Slag, Quartz Sand, Aluminum Oxide	7
Rock Type: Georgia Granite	1
Stand off Distance: approximately 1.27 cm	1
Pressure: 20.7, 27.6, 34.5 MPa	3
Abrasive Flow Rate: Varied with abrasive type (20 to 120 g/sec)	3
Nozzle Diameter: 2.80 mm (DIAjet Nozzle)	
Traverse Speed: 17.22 cm/min	1
D) Traverse Speed Experiments with DIAjet Nozzle	
Traverse Speed: 3.76, 8.08, 23.77, 43.08, 51.56, 91.19 cm/min	6
Pressure 27.6 MPa, abrasive flow rate varies with abrasive type (20 to 120 g/sec)	
Other Parameters as in Series C.	

Traverse speed was controlled through an electronic control box. Pressure values were taken from a gauge on the injector instrument panel. Abrasive flow rate was adjusted using a gauge on the front panel of the injector and converted to a value in grams/sec using calibration charts developed at the HPWL for the different abrasives.

After each cut, the depth, volume and width of the slot, were measured to assess performance. It was necessary to measure the volume of the slot and the depth since the slot was not rectangular but narrowed in the middle and become enlarged at the bottom.

Cross sectional area was determined by dividing the volume by the length of the slot. Measurements were taken at 2 to 5 different locations and averaged to give the final result.

3.2 Nozzle Wear

Nozzle wear was measured by weighing the nozzle before and after a specified set of experiments carried out with each abrasive. The variation of wear with pressure and abrasive flow rate, was not determined. A high precision balance with an accuracy of 0.0001 gram was used for this evaluation.

4.0 RESULTS AND ANALYSIS

4.1 Results

The variation of depth of cut, specific energy and erosion efficiency with change in the tests parameters was plotted (Fig. 1 to 12) for results obtained using the shorter carbide inserts and Garnet #60 as the abrasive. Because the results of tests with the other abrasives, and with the DIAjet nozzle show similar variations, they are not included. The width of the cut did not show a significant and consistent variation with change in any of the cutting parameters, but lay in the range of 0.2 cm to 0.4 cm.

Specific energy is a calculated value of the amount of energy consumed to remove unit volume of material. Erosion efficiency is the calculated volume of material removed by unit weight of abrasives consumed. Reducing specific energy and increasing erosion efficiency are both required to improve the cutting process. They are calculated as follows:

$$SE = 2.12 \times 10^6 \frac{P^{1.5}\, d^2}{CS\ S\ \rho^{0.5}} \qquad (1)$$

$$ER = 0.0167 \frac{CS\ S}{AFR} \qquad (2)$$

where:

SE = specific energy, MJ/m^3 ,
ER = erosion efficiency, cm^3/g,
P = pressure at vessel, MPa,
d = nozzle diameter, cm,
CS = cross sectional area, cm^2,
AFR = abrasive flow rate, g/sec,
S = traverse speed, cm/min and
ρ = mass density of water, 102 $kg\text{-}sec^2/m^4$.

Nozzle wear (Tables 3 and 4) was defined as:

$$W = \frac{WN}{WA} \qquad (3)$$

where:
W = wear of the nozzle, g/g,
WN = weight of the material removed from the nozzle, g
WA = weight of the abrasives passing, g.

Except for tests run with aluminum oxide, where wear was faster, a run of 45 minutes with any abrasive increased the DIAjet nozzle diameter enough to drop jet pressure from 34 to 28 to 31 MPa.

Table 3. Wear of 2.18 cm Long Carbide Inserts

Nozzle Diameter, mm	Wear, g/g
1.98	1.048×10^{-6}
2.39	0.868×10^{-6}
2.77	0.357×10^{-6}
Abrasive Material is Garnet # 60	

Table 4. Wear of DIAjet Nozzle

Abrasive Material	Wear, g/g
Garnet # 40	1.273×10^{-6}
Garnet # 36	2.859×10^{-6}
Garnet RUF	7.698×10^{-6}
Quartz Sand	1.040×10^{-6}
Boiler Slag	0.547×10^{-6}
Aluminum Oxide	20.413×10^{-6}

In order to assess the effect of change in traverse speed another parameter was calculated. this is the area of kerf generated in unit time, given by the product of depth of cut and traverse speed. The variation of kerf area generated with traverse speed is given in Figure 13 for all abrasives, but at different abrasive flow rates.

4.2 Regression Analysis

The effect of parameters such as abrasive size, hardness and density was identified by use of regression analysis. The power model used for the evaluation was:

$$CR = e^{C} P_1^{x1} P_2^{x2} \ldots P_n^{xn} \quad (4)$$

where:
CR = a cutting result such as depth of cut,
$P_{1..n}$ = parameters such as pressure and nozzle diameter,
$x_{1..n}$ = exponents and
C = the intercept.

Multiple regression analysis was performed on the DIAjet cutting data, using the statistical package Stat View 512. The results of the analysis are presented in Table 5. In the analysis, the dependent variables examined were depth of cut (cm), cross sectional area (cm^2), specific energy (MJ/m^3), and erosion efficiency (cm^3/g). Although specific energy and erosion efficiency can be calculated from the cross sectional area, a separate analysis was preferred in order to better understand the relationships. For this reason some of the the exponents of cross sectional area are similar to those of specific energy and erosion (Table 5). Since density changes in Equation 2-Table 5 were not significant this parameter was eliminated and a new regression equation presented for prediction purposes.

5.0 DISCUSSION

The discussion will be center on the use of depth of cut as the major criteria of performance, since it is usually the most important parameter for rock slotting. However insights from examining the values found for specific energy and erosion will be addressed.

Table 5. Results of Regression Analysis

1) Garnet # 60 and 2.18 cm Long Carbide Inserts				
T. Speed, cm/min	15.24			
Parameter	Depth of Cut, cm	Cross Sec., cm^2	S. Energy, MJ/m^3	Erosion, cm^3/g
Intercept	-3.2703	-4.8411	9.7711	-6.1974
$e^{Intercept}$	3.7994×10^{-2}	7.8982×10^{-3}	1.7520×10^{4}	2.0346×10^{-3}
Nozzle Diameter, mm	0.3077	0.2490 (Ins.)	1.7494	0.2399 (Ins.)
Pressure, MPa	1.0119	1.0207	0.4795	1.0173
Abrasive F.R., g/sec	0.3182	0.4557	-0.4557	-0.5436
Num. of observations	27	27	27	27
R^2	0.95	0.88	0.90	0.90
F	145	55	67	66
$F_{table} = F_{0.05,3,23} = 3.30$				

2) All Abrasives Except Boiler Slag and DIA Jet Nozzle				
Abrasive Type	Garnet # 40, Garnet # 36, Garnet RUF, Quartz sand, Aluminum Oxide			
Parameter	Depth of Cut, cm	Cross Sec., cm^2	S. Energy, MJ/m^3	Erosion, cm^3/g
Intercept	-7.9340	-10.7900	20.4960	-14.8740
$e^{Intercept}$	3.5835×10^{-4}	2.0605×10^{-5}	7.9671×10^{8}	3.4698×10^{-7}
Pressure, MPa	0.9274	1.0080	0.4920	1.1060
Abrasive F.R., g/sec	0.4537	0.5680	-0.5680	-0.4310
Traverse S., cm/min	-0.6799	-0.5930	-0.4070	0.4070
Particle Size, micron	0.4771	0.5450	-0.5450	0.5420
Density, g/cm^3	0.2116(Ins.)	-0.1220 (Ins.)	0.1220 (Ins.)	-0.1150 (Ins.)
Mons Hardness	1.6496	2.0130	-2.0120	1.9990
Num. of observations	78	78	78	78
R^2	0.91	0.89	0.83	0.90
F	121	94	57	103
$F_{table} = F_{0.05,6,71} = 2.24$				

3) All Abrasives Except Boiler Slag, DIA Jet Nozzle, Density is eliminated.				
Abrasive Type	Garnet # 40, Garnet # 36, Garnet RUF, Quartz sand, Aluminum Oxide			
Parameter	Depth of Cut, cm	Cross Sec., cm^2	S. Energy, MJ/m^3	Erosion Eff. cm^3/g
Intercept	-8.5670	-10.4240	20.1320	-14.5290
$e^{Intercept}$	1.903×10^{-4}	2.971×10^{-5}	5.536×10^{8}	4.899×10^{-7}
Pressure, MPa	0.9110	1.0180	0.4820	1.0250
Abrasive F.R., g/sec	0.4660	0.5610	-0.5610	-0.4380
Traverse S., cm/min	-0.6790	-0.5920	-0.4080	0.4070
Particle Size, micron	0.5140	0.5240	-0.5240	0.5220
Mohs Hardness	1.9810	1.8210	-1.8220	1.8190
Num. of observations	78	78	78	78
R^2	0.91	0.89	0.83	0.90
F	143	113	69	125
$F_{table} = F_{0.05,5,72} = 2.15$				
Ins. means insignificant contribution by the variable with a 95 % probability				

5.1 Pressure

An increase in jet pressure causes an increase in depth of cut (Fig. 1), in specific energy (Fig. 5) and in erosion efficiency (Fig. 9). Thus while more energy is consumed, less abrasive is needed to cut a unit volume of material. The exponent of pressure is approximately 1.0 (Table 5), indicating that in the range from 20 to 34 MPa, the depth of cut linearly increases with pressure. This finding is consistent with results from both waterjet cutting and conventional abrasive jet cutting.

5.2 Abrasive Flow Rate

Increase in abrasive flow rate increases the depth of cut (Fig. 2), decreases specific energy (Fig. 6) and decreases the erosion efficiency (Fig. 10). This means that while less energy is consumed, more abrasives are required to cut a unit volume of material as the abrasive volume is increased. This reflects a lower efficiency of energy transfer from the water to the abrasive, and potentially that less of the abrasive being added to the water is being effectively used in cutting. The exponent of abrasive flow rate stays in a range of 0.3 to 0.5 (Table 5). This indicates that the rate of increase in penetration decreases with increasing abrasive flow. For this equipment the maximum flow rate is limited so that it was not possible, in this series, to identify the point at which increasing abrasive flow starts to choke the system, and cause a decrease in cutting depth. The point at which the rate of increase in penetration slows is, however, apparent for Garnet # 60 after 100 g/sec (Fig. 2).

5.3 Nozzle Diameter

Change in nozzle diameter was only studied with one abrasive, Garnet # 60, and the short nozzles. Increase in nozzle diameter caused an increase in depth of cut (Fig. 3), and in specific energy (Fig.7). However the relation between nozzle diameter and erosion efficiency is not very clear (Fig. 11). In general it may be stated that increasing nozzle diameter improved erosion efficiency. The exponent of nozzle diameter is nearly 0.3 in the depth of cut equation (Table 5). This confirms that larger nozzles do not cause much increase in depth of cut under fixed pressure and abrasive flow rate conditions.

5.4 Traverse Speed

An increase in traverse speed decreases the depth of cut (Fig. 4), lowers specific energy (Fig. 8) and increases erosion efficiency (Fig. 12). Thus at faster speeds, less energy is required and less abrasive used to cut unit volume of material. The exponent of traverse speed is around -0.7 (Table 5). However pure waterjet cutting has a similar exponential value of around -0.3 to -0.4, so that considerable savings can be obtained by running the equipment at higher traverse rates and making multiple passes over the same slot. The lower exponent of the DIAjet indicates that a similar strategy will not be as effective with abrasive injection.

A plot of rate of kerf area generated against traverse speed reaches a maximum value at a relatively slow speed, between 35 and 60 cm/sec (Fig.13), for all the abrasives tested. This suggests that slower, deeper cutting may be more effective with abrasive systems, rather than going to the higher traverse speeds of the pure waterjet approach.

5.5 Abrasive Particle Size, Density and Hardness

Increasing particle size led to an increase in depth of cut, improved erosion efficiency and reduced specific energy (Table 5.3). Thus larger particle sizes are more beneficial in DIAjet cutting, provided they are sized to freely pass through an appropriate orifice size.

From an energy transfer point of view there a number of aspects to this phenomenon. Generally bigger sizes can carry more energy, but the same abrasive flow rate carries a lower number of particles. So a gain in energy can be lost by the less number of particles available in the mix. Additionally bigger particles cannot accelerate as fast as smaller ones because of their higher drag coefficient. However the cutting mode may change with particle size. Secondary erosion may take place, as a result of larger particles fragmenting during initial impact and the resulting finer particles continuing to cut (4).

Change in abrasive density did not show any significant correlation with cutting results with a 95 % probability (Table 5). However, the density range of the abrasives used in this study lay between 2.59 to 3.89 g/cm^3 and the number of different values may have been too narrow to reveal a meaningful relationship.

Increasing hardness of abrasive increased the depth of cut, decreased specific energy and increased erosion (Table 5). There was, again, not enough data to show if there was a maximum to the hardness ratio between abrasive and target, as found by Hashish (2).

5.6 Wear of Nozzles

Smaller nozzles wear out faster than larger ones (Table 3) because in a constant abrasive flow, the area of the nozzle in contact with the same amount of abrasives decreases with larger nozzle diameters. Wear of the nozzle also increased with use of larger abrasives (Table 4, Fig. 14) which might be expected since this is similar, in a way, to depth of cut. As expected aluminum oxide, the hardest abrasive, gave the highest wear to the DIAjet nozzle (Table 4). To compare the cutting ability and wear, depth of cut was normalized to abrasive flow rate and plotted with the wear data (Fig. 14). The damage to the nozzle is proportional to the depth of cut, except in the case of aluminum oxide. This shows that the most abrasive material does not necessarily give the deepest cut, or most effective service.

6.0 CONCLUSIONS

1 - Abrasive cutting with a DIAjet is not very different to conventional abrasive cutting. Depth of cut increases with pressure, abrasive flow rate, particle size and hardness and decreases with traverse speed. Pressure and abrasive hardness are the most effective parameters which control the depth of cut.
2 - The rate of increase in depth of cut slows with increased abrasive flow, with a possible optimum above 100 g/sec for #60 mesh garnet.
3 - The largest abrasive size, roughly half the nozzle diameter, should be used in a DIAjet.
4 - Cutting with multiple passes over the same slot is not as efficient as with pure waterjets.
5 - Generated kerf area is a maximum at a traverse speed between 35 and 60 cm/min.
6 - Nozzle wear increases with smaller nozzle sizes, larger and harder particles.
7 - Specific energy of DIAjet cutting of granite is currently around 20,000 to 30,000 MJ/m^3.
8 - Current erosion efficiency of DIAjet cutting is around 0.005 cm^3/g. Thus to remove one gram of granite, 75 grams of abrasive must be used. Hence DIAjet should be employed to slot around blocks rather as a means of totally removing a mass.

7.0 REFERENCES

1. Fairhurst, R. M., R. A. Heron, D. H. Saunders (1986), "DIAJET - A New Abrasive Water Jet Cutting Technique," Proc. of 8th Internat. Symposium on Water Jet Cutting Technology, Durham, England, Sept. 9-11, 1986, pp. 395-402.

2. Hashish, M. (1989) "Data Trends in Abrasive Waterjet Machining", Proc. Clinic on Automated Waterjet Cutting Processes, Southfield MI, May 9-10, 1989, SME.

3. Hurlbut, C. S. JR. (1971), DANA's Manual of Mineralogy, 18th edition, John Wiley and Sons Inc., 579 pp.

4. Maji, J., G. L. Sheldon (1979) "Mechanisms of Erosion of a Ductile Material by Solid Particles" in Erosion -Prevention and Useful Applications, Vail, CO, ASTM STP 664.

5. Summers, D.A., (1989) "Waterjet Use in Quarrying". (In Italian) Presented at the Convegno Internazionale su: Situazione E Prospecttive Dell'Industria Lapidea, Cagliari, Italy, 3-5 Aprile.

6. Summers, D.A., Yazici S. (1988), "Drilling Holes in Rock with Low Pressure Abrasive," 1st IFAC Workshop on Advances in Automation of Underground Hard Rock Mining, Quebec, Canada, Sept. 12-14, 1988, 14 pp.

7. Summers, D.A., T. F. Lehnoff (1977), "Water Jet Drilling in Sandstone and Granite," Proc. of 18th Symp. on Rock Mechanics, Keystone, Colorado, May 1977, pp. 1B6-1 - 1B6-5.

8. Vijay, M. M., et al. (1985), "An Assessment of Rotating Water Jets for Drilling and Slotting of Hard Ore Bearing Rocks," Proc. of 3rd U.S. Water Jet Conference, Pittsburgh, May 21-23, 1985, pp. 231-247.

9. Yazici, S., Summers, D. A., "Abrasive Jet Drilling -- A New Technology" to be presented at the 30th Annual Rock Mechanics Symp. - West Virginia, in June 1989.

10. Yazici, S., (1989), Abrasive Jet Cutting of Rocks, Ph.D. Thesis, UMR, in preparation.

ACKNOWLEDGEMENTS

This work was carried out with the help of Mr. J. Blaine, Mr. L. J. Tyler, Mr. R. D. Fossey, Mr. S. Gabel, and Ms. J. Moutray, of the technical staff of the HPWL at UMR. Some of the garnet was provided by Barton Mines. This assistance is gratefully acknowledged.

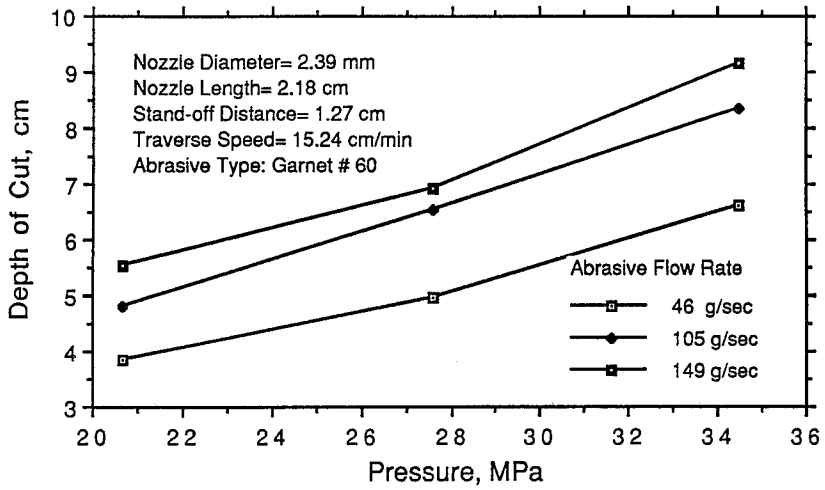

FIGURE 1. THE VARIATION OF DEPTH OF CUT WITH PRESSURE

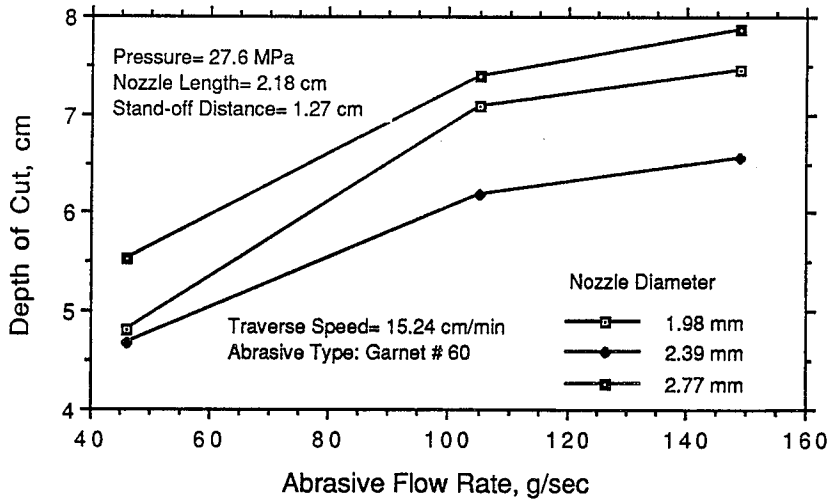

FIGURE 2. THE VARIATION OF DEPTH OF CUT WITH ABRASIVE FLOW RATE

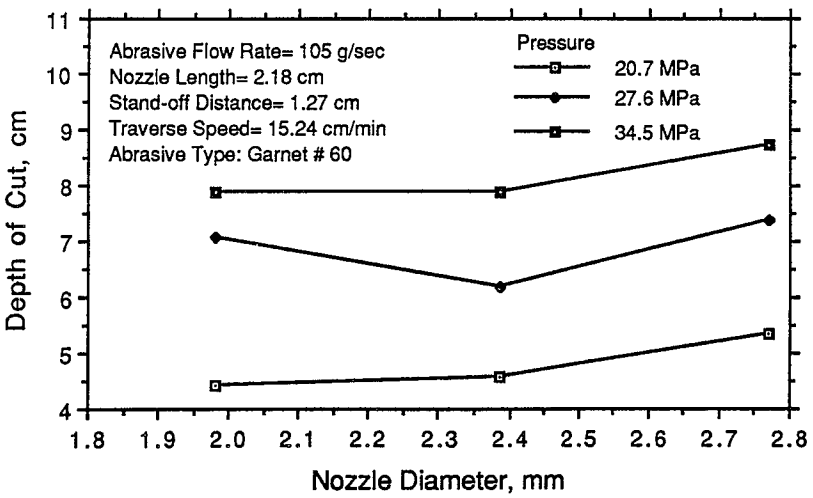

FIGURE 3. THE VARIATION OF DEPTH OF CUT WITH NOZZLE DIAMETER

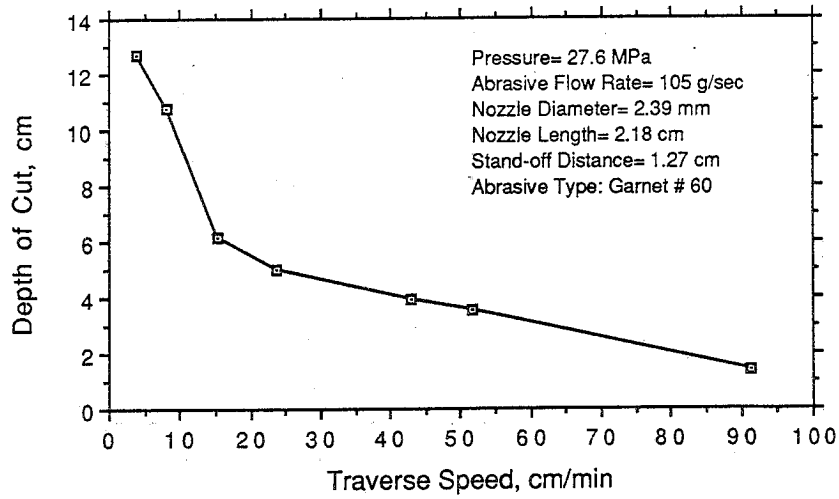

FIGURE 4. THE VARIATION OF DEPTH OF CUT WITH TRAVERSE SPEED

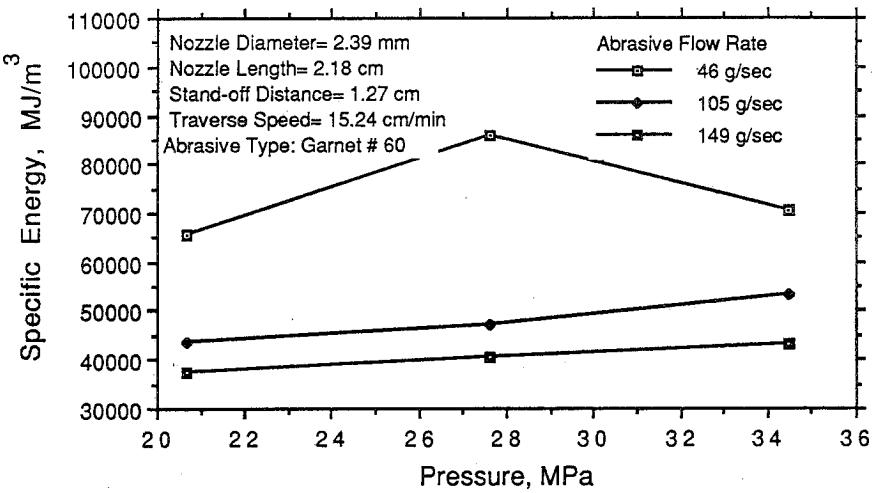

FIGURE 5. THE VARIATION OF SPECIFIC ENERGY WITH PRESSURE

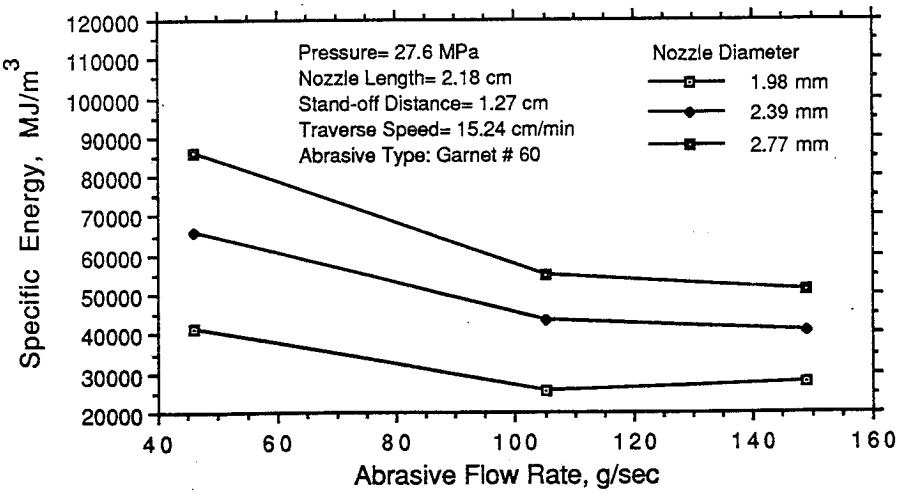

FIGURE 6. THE VARIATION OF SPECIFIC ENERGY WITH ABRASIVE FLOW RATE

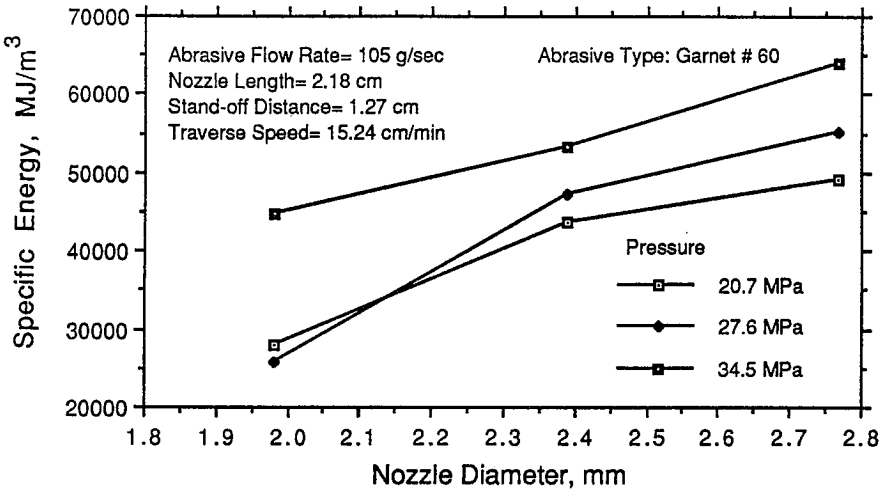

FIGURE 7. THE VARIATION OF SPECIFIC ENERGY WITH NOZZLE DIAMETER

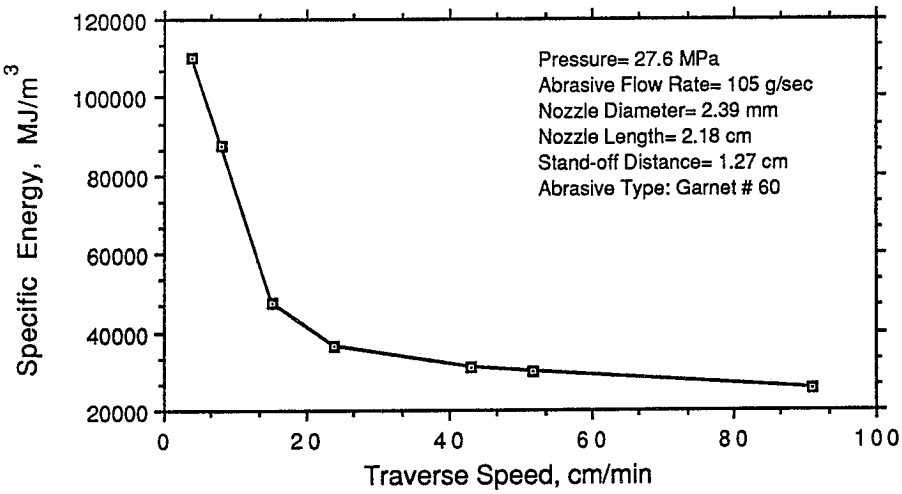

FIGURE 8. THE VARIATION OF SPECIFIC ENERGY WITH TRAVERSE SPEED

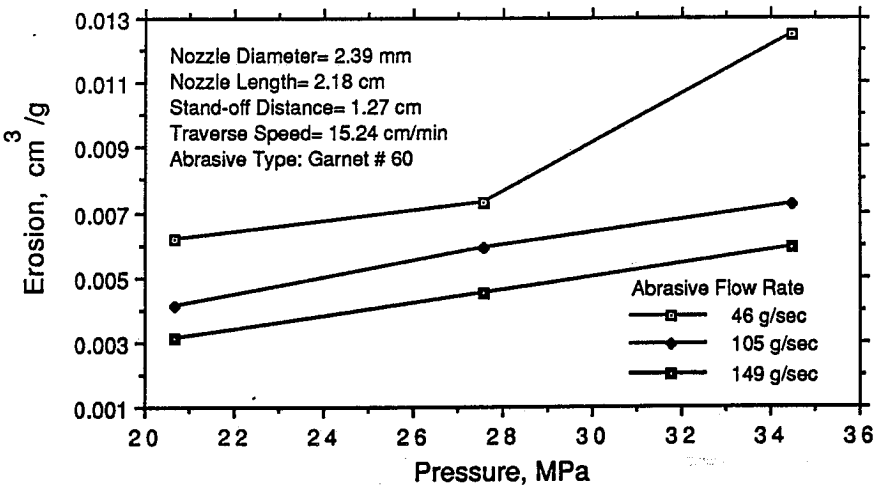

FIGURE 9. THE VARIATION OF EROSION WITH PRESSURE

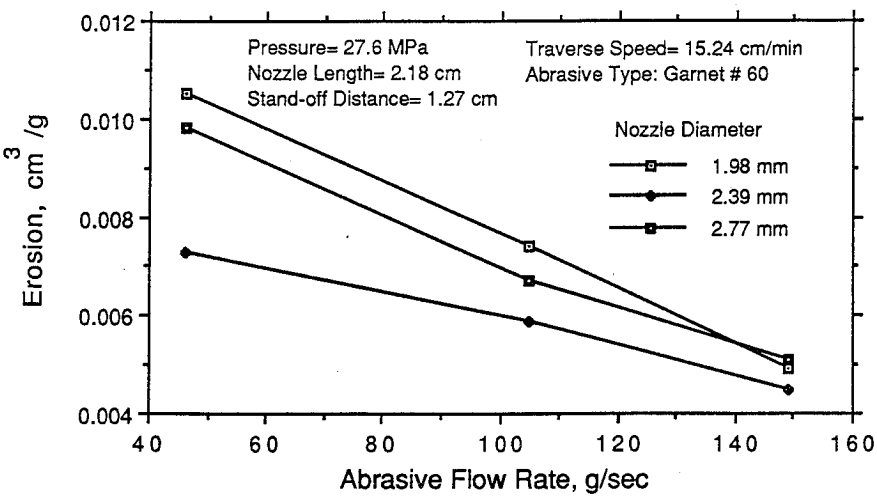

FIGURE 10. THE VARIATION OF EROSION WITH ABRASIVE FLOW RATE

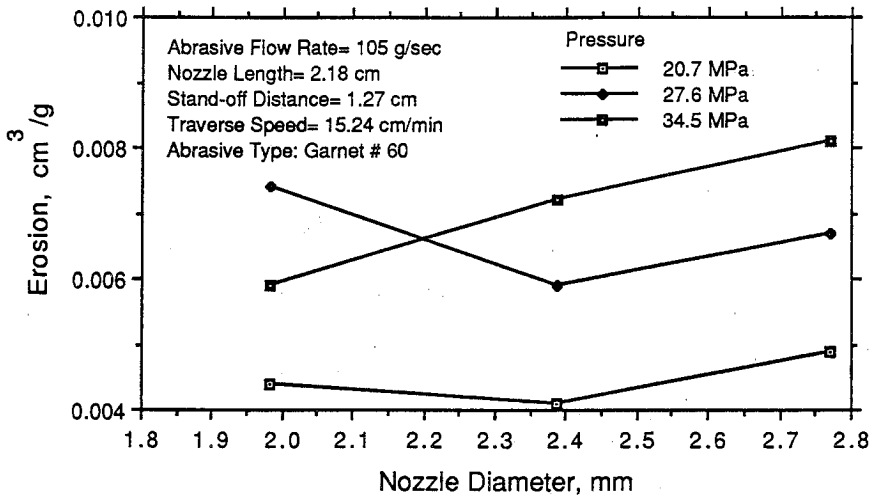

FIGURE 11. THE VARIATION OF EROSION WITH NOZZLE DIAMETER

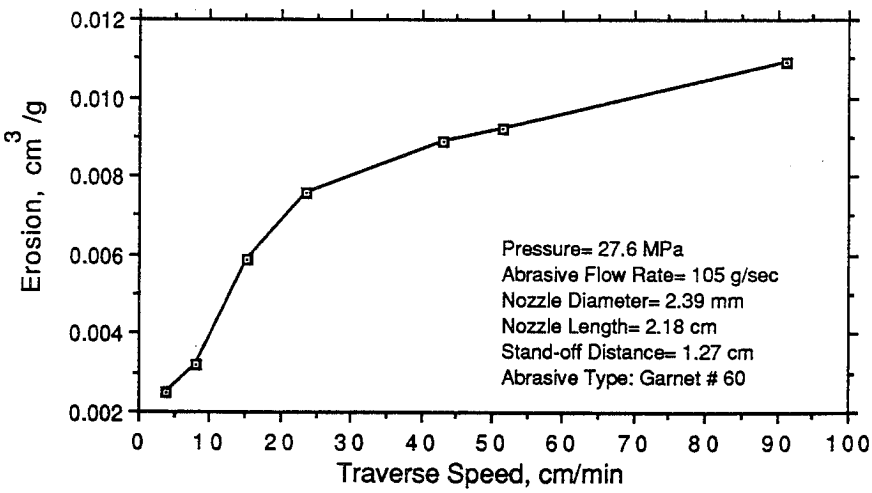

FIGURE 12. THE VARIATION OF EROSION WITH TRAVERSE SPEED

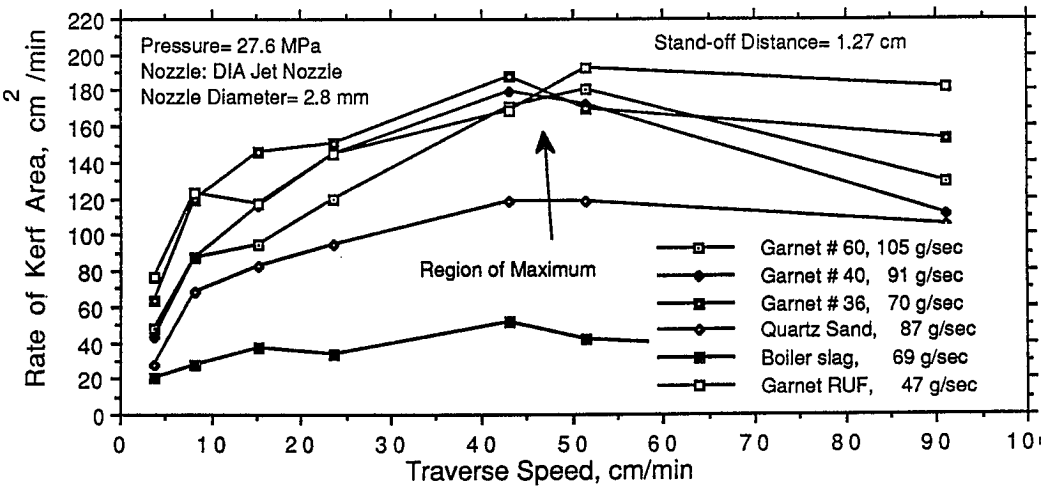

FIGURE 13. THE VARIATION OF RATE OF KERF AREA WITH TRAVERSE SPEED

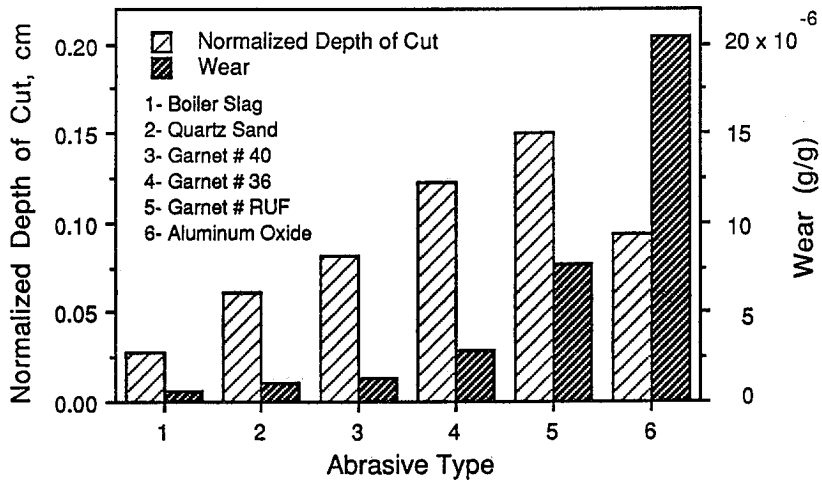

FIGURE 14. THE WEAR OF THE DIAJET NOZZLE

5th American Water Jet Conference
August 29 - 31, 1989: Toronto, Canada

Paper / Communication 35

HYDROMECHANICAL ROCK JETTING - TEST STANDS - RESEARCH PROGRAMME AT THE UNIVERSITY OF MINING AND METALLURGY IN CRACOW

A. Klich AND A. Kalukiewicz
University of Mining and Metallurgy
Cracow, Poland

Z. Student
Mining Mechanization Centre KOMAG
Gliwice, Poland

ABSTRACT: In this paper a new Polish made machine for digging tunnels has been discussed. The machine works on the principle of hydromechanical jetting of hard rock. In this machine disk tools are aided with water jets of high pressure to 200 MPa. The design of the test stands for examining the cutting process with the whole machine has been discussed. The relevant research programme has been included.

RÉSUMÉ : Cette communication porte sur un nouveau tunnelier de fabrication polonaise. La machine repose sur le principe de l'abattage hydromécanique de la roche dure. Dans cette machine, les outils de coupe sont des disques assistés par des jets d'eau à haute pression (jusqu'à 200 MPa). La conception des montages d'essai pour examiner le processus de coupe avec la machine au complet a été analysée. Le programme de recherche pertinent est décrit.

Organized and Sponsored by the National Research Council of Canada and the U.S. Water Jet Technology Association.

Introduction.

In numerous countries of highly advanced mining, research and designing works are carried out to find new solutions of full - face machines for driving tunnels and shafts.
To ensure coal mining in Poland on a satisfactory level, it will be necessary to build new collieries and get coal from deeper extracting levels, in order to reproduce the mining efficiency. Since mining will have to be carried out from more than 45% thin beds and at considerable depths from about 800 to 1000 m, it will be necessary to drive a large number of galleries mainly through stone or stone-coal layers under extremely difficult mining-geological conditions.

Only few world companies are concerned with research into and construction of new types of full-face Tunnel Boring Machines for tunnel workings. The following can be mentioned here. DEMAG and WIRTH in German Federal Republic, ROBINS in the United States, and BOUYGUES in France. In Poland two centres are interested in this question. They are the Institute of Mining and Dressing Machines and Automation at the University of Mining and Metallurgy in Cracow and the CMG KOMAG in Gliwice. A new design of a heading machine, based on new, not used before, mining techniques is presented below. A design of test stands for laboratory and semi-commercial examinations is also given.

1. Work on a new design of the full-face TBM.

A new design of the tunnel machine for driving circular tunnels was prepared at the Institute of Mining and Dressing Machines and Automation. Its technical documentation resembles a similar construction made by the French firm Bouygues. It differs, however, from the French solution mainly in the application of high-pressure water jets to about 250 MPa aiding the operation of discs. Such machine, therefore, can be used in gassy mines, is spark-safe, and can cut rock having the compressive strengt to 180 - 200 MPa.

2. Testing head of the full-face TBM.

To examine the cutting of rock with disc tools placed on four articulated arms, a testing head shown in Fig.1 was constructed. Its parameters are given in Table 1. The head is placed in a testing tunnel shown in Fig2. The tunnel can deflect from - 15° to + 15°. The head is pressed to the tunnel face by

four hydraulic pistons (IX) being, at the same time, moved along special guides. This helps to simulate the working conditions similar to the real ones. The investigations were made on a model rock sample embeded in concrete in a bottom plug screwed to the tunnel face.

Table 1

1	Maximum drilling diameter	4.2 m
2	Maximum dip of working	$\pm 15^{\circ}$
3	Strength of rock R_c	160 MPa
4	Maximum rotations of head	18.6 min^{-1}
5	Maximum pressing force	1200 kN
6	Number of disc tools	4
7	Diameter of disc tool	400 mm
8	Pressure of hydraulic system	16 MPa
9	Power demand	854 kW

The head consists of a guiding-pressing part (I) and of a rotary one (II). The latter is furnished with four articulated arms (III) with disc tools (IV). The disc action is aided by high-pressure water jets (to 256 MPa) forced out from 4 pairs of nozzles (V) fed from four intensifiers (VI) situated in the axis of rotations of the head arms. The swinging motions of the arms are induced by one central hydraulic piston (VII). It sets in motion four cutting arms through a lever-connector system. Four hydraulic motors (VIII) enable the head rotations.

A number of sensors which collect data about the head work are attached to it. On each arm three foil strain gauges in the half-bridge system two acceleration sensors and a pressure pick-up (3) measuring the pressure of oil supplying the intensifier are placed. The data from the above sensors are sent to the switchboard (8) over a measuring cable (9), and from there if needed, they can be sent on. The displacement of the head is measured by a set of displacement sensors (4). The supply pressure of the hydraulic pistons and that of the central piston is measured by pressure pick-ups (6), and the supply pressure of the hydraulic motors by a pressure pick-up (5). A revolution counter indicates the head rotations. The supply of the head (rotary motion, pressing, deflection of the arms) is accomplished. by a

hydraulic unit of 160 kW (pressure to 25 MPa), and the supply of the high-pressure system by a hydraulic unit of 90 kW (pressure of 32 MPa). This enables the work of the head under full power load at the reduced rotational speed of the head (6 to 10 rotations/min) or at the maximum speed but under full load of only two of the four arms, or under partial power load of the all the four arms. By forcing out continuous water jets from eight nozzles, the above power is sufficient to produce jets which have the diameters to 0.3 mm. At larger jet diameters it is necessary to stop the work of some nozzles at full pressure,or to reduce the pressure.

The investigations carried out with the use of the testing head are meant to determine the dependence of the parameters on

- the force pressing the discs to the rock;
- the angular velocity of the arm motion at various rotational speed;
- the kind, compactness and structure of the rock.

The above dependences are compared when the work of the discs is aided with water jets of different pressures and nozzle diameters, the nozzles having various positions.

The answers obtained from the investigation will affect the improvement of the design of the full-face TBM, and the determination of such optimum working parameters as the pressing of the head, torque, the force of arm angular displacement, the pressure of water in the jets. This, in the course of nature, will help to build a supply station which will meet full demand for power for the TBM prototype.

3. Test stand for examining the cutting process with single tools.

A special test stand was designed to examine the efficiency and reliability of the tools for TBM, and to test mining aided by high-pressure water jets. The stand is built in the form of a turning and boring lathe based on a boring rig. The stand consists of (Fig.3) a frame (I) on which a traverse (II) moves vertically along the guides. The traverse is driven by a hydraulic motor through two lead screws (III). A slide (IV) fastened on the traverse is to be moved along it. A disc holder (V) and an intensifier (VI) are attached to the slide. Water of the pressure to 25 MPa is supplied to two nozzles (VIII) through two high-pressure conduits (VII) leading from the intensifier. The nozzles are installed in front of a cutting disc (IX). A rotary table is placed on the frame axis. A container (XI) with a material simulating the rock to be mined is fixed to the table.

When the container with an experimental material and the disc are fixed, the tests may be started. The container is set in a rotary motion at an

assumed speed, and the traverse with the cutting disc is lowered. The disc pressing against the rock is achieved by a hydraulic system, and the disc is moved along the container radius by means of the slide. When the intensifier is switched on mining aided by high-pressure water jets can be examined.

The operation of the stand, i.e. the rotations of the table and the motion of the tool, is accomplished by the hydraulic station of 160 kW furnished with suitable valves electrohydraulically controlled with the possibility to regulate the pressures and flow rate.
The supply of the system intensifying the pressure of water aided mining is accomplished by the station of 90 kW with an infinitely variable adjustment of the pressures and flow rate. It is possible to obtain water jets of 1 mm diameter at the pressure of 256 MPa.

The stand was furnished with sensors to collect the largest possible number of the measurement data. A set of three foil strain gauges 1 attached to the holder is used to measure the forces acting on the disc holder and on the disc itself during its work. Two acceleration sensors 2 are placed on the holder to measure vibrations of the cutting tool. The temperature of disc bearings is measured by the heat sensor 3. The strain gauges 1 were installed in the half-bridge system together with the compensatory strain gauge attached to the stand casing. A pressure pick-up 4 measures the pressure of water aided mining through measuring the pressure of oil supplying the intensifier. Signals from the strain gauges, the pressure and the vibration pick-ups are sent to the switchboard 5 over measuring cables, and from there the parameters measured can be transmitted to the measuring apparatus. Displacement sensors 6,7,8 measure the displacements of the disc round the axis and along the radius of the rock container. The rotations of the container are measured by the proximity detector fixed to the rotary table.

Such a configuration of the sensors helps to measure the dependence of various mining parameters. Comparative investigations can be made at the same disc pressing against the rock without and with the aiding of mining with high-pressure water jets. The productivity of mining at varying pressings of the disc, varying pressures and diameters of the water jet and varying rotational speed of the container can be measured. The results obtained allow one to choose the optimum mining parameters employing disc tools aided by high-pressure water jets. This is indispensable for the continuation of the work on the prototype of the full-face TBM.

4. Analysis - Measurement Centre.

This centre is concerned with the collecting, logging, analysing and

further processing of the measurement data from the test stands,as well as with the optimisation of the working parameters and with the programmed remote control of the devices investigated. Besides, the Centre is engaged in making calculations for the computer aided designing.

The proposed system configuration (Fig.4) consists of two computers working in local network.It is expected that - until the microprocessor data collecting system is introduced - its function will be performed by the computer IBM AT - compatible. Therefore, this computer is equipped with an AD/DA card. This solution enables the sampling of 16 analoque signals with the resolution of 12 bits and the sampling time T = 60 s. An AD/DA card, additionaly introduced, enables the putting in or out of 6 eight-bit signals. This computer is provided with a high-resolution card and a monitor Hercules, a printer a plotter and a scanner.

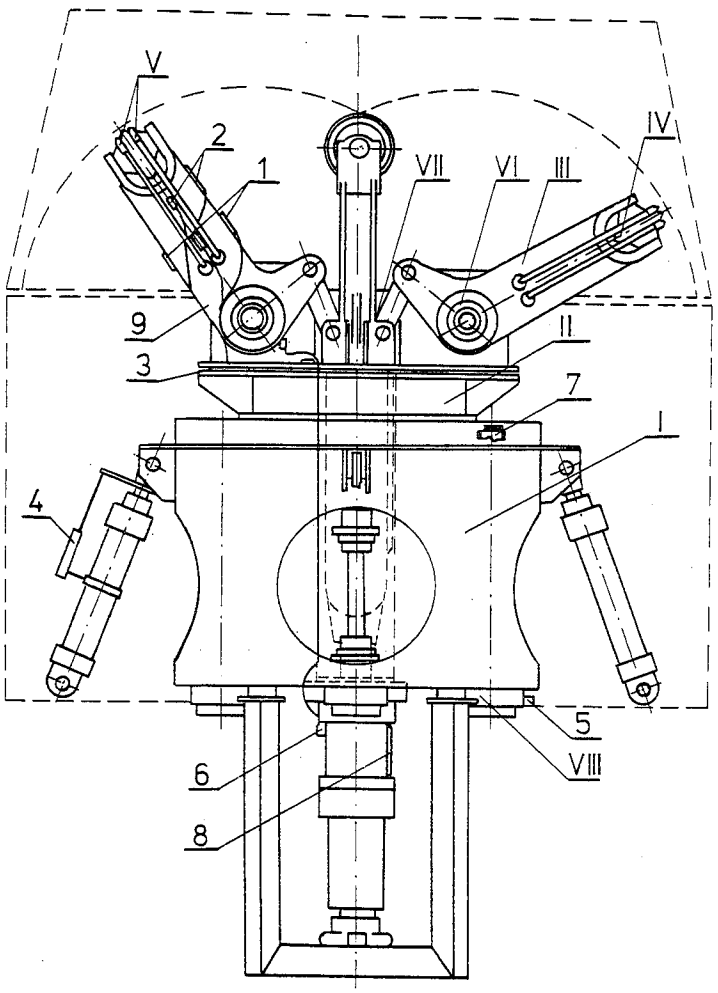

Fig 1. Testing head of TBM.

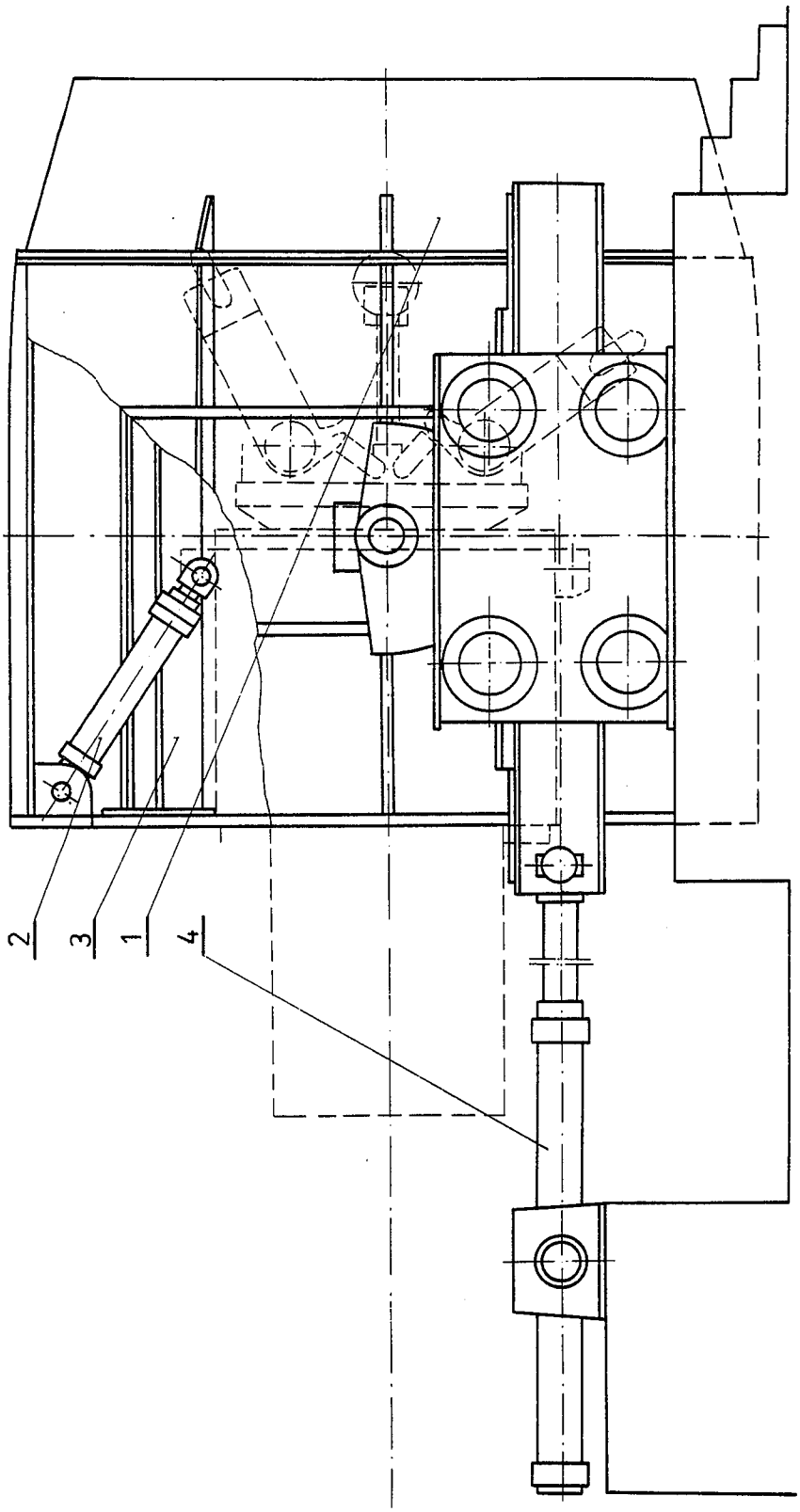

Fig 2. Testing tunnel. 1 - tunnel face with a rock sample fixed, 2 - pressing pistons, 3 - head guides, 4 - pistons deflecting the tunnel.

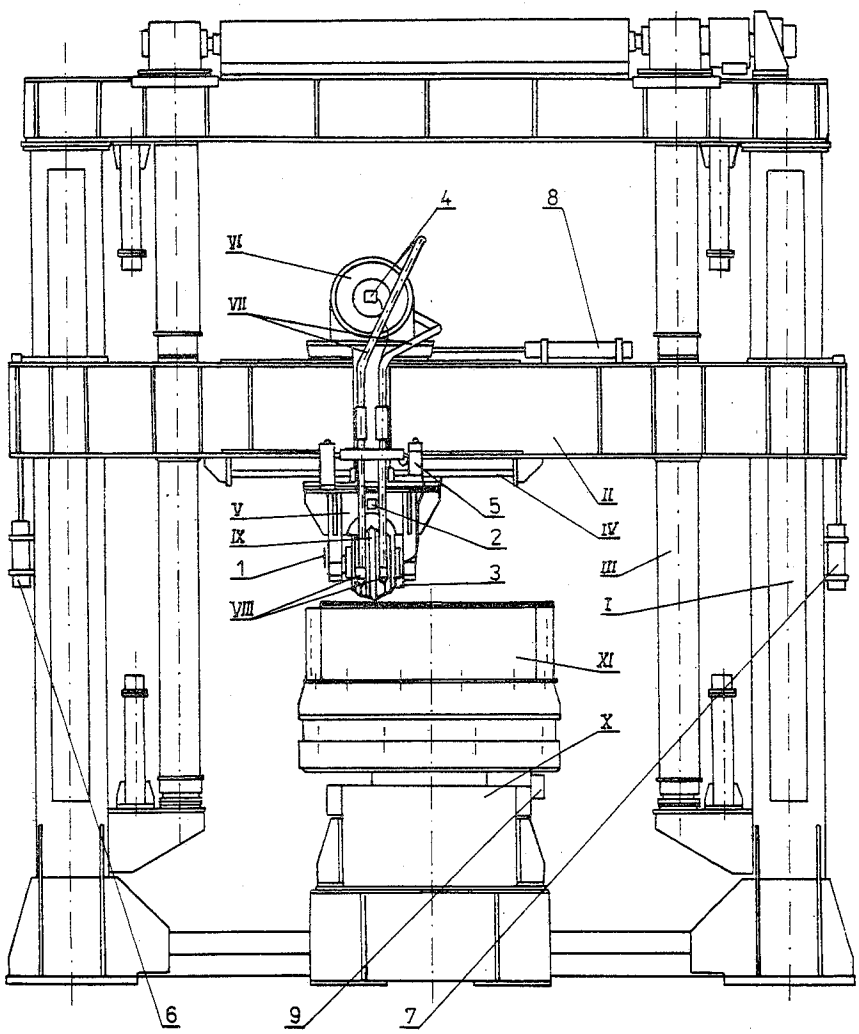

Fig 3. Test stand for single tools.

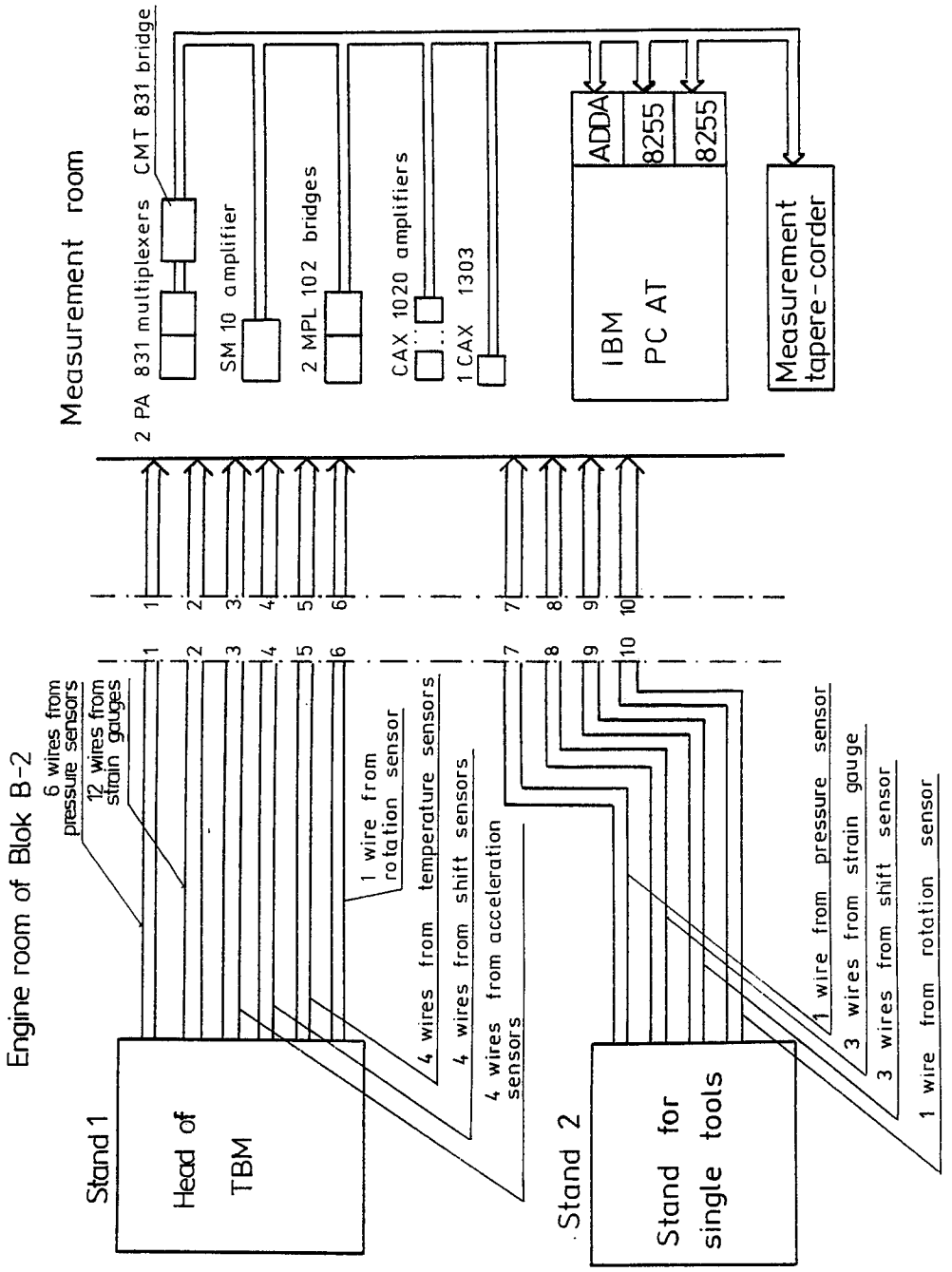

Fig 4. Diagram of the measuring-recording system.

5th American Water Jet Conference
August 29 - 31, 1989: Toronto, Canada

Paper / Communication 36

PREDICTION OF TURBULENT FLOW FIELD FOR DILUTE POLYMER SOLUTION JETS

Q.D. Liao, X.D. Zhao AND T.Y. Long
Shanghai Institute of Mechanical Engineering
Shanghai 200 093, China

ABSTRACT: Basing on turbulent models of pure water jet and some experimental results of polymer solution jet, a $K-\epsilon-Re$ turbulence model to be applied to dilute polymer solution jet is developed, and then solved numerically by using finite difference method. The profiles of mean velocity, turbulent kinetic energy and its dissipation rate, and of Reynolds shear stress are determined. The prediction results are compared with experimental data. The agreements are good with respect to most features of these flows. The numerical results show that, by dissolving a very small amount of polymer additives in water, it can change the properties of distribution of turbulent kinetic energy and its dissipation rate, and reduce the Reynolds stress, enhance coherence, smooth the jet surface, and then markedly improve the jet quality, as compared with pure water jet under identical conditions.

RÉSUMÉ : A partir de modèles turbulents du jet d'eau pure et de quelques résultats expérimentaux sur un jet de solution polymérique, un modèle de turbulence $K-\epsilon-Re$ applicable au jet de solution polymérique diluée est mis au point, puis résolu numériquement par la méthode des différences finies. Les profils de vitesse moyenne, d'énergie cinétique turbulente et de son taux de dissipation, et de la contrainte de cisaillement de Reynolds sont établis. Les prévisions sont comparées aux résultats expérimentaux. L'accord est bon pour la plupart des paramètres d'écoulement. Les résultats numériques montrent que, en dissolvant une très faible quantité de polymère dans l'eau, on peut modifier la répartition de l'énergie cinétique turbulente et son taux de dissipation, et diminuer la contrainte de Reynolds, améliorer la cohérence, lisser la surface du jet, puis améliorer grandement la qualité du jet par rapport à un jet d'eau pure dans des conditions identiques.

Organized and Sponsored by the National Research Council of Canada and the U.S. Water Jet Technology Association.

1.0 INTRODUCTION

The water jets are widely applied to engineering problems, for example, to spray washing, cooling, fire-fighting, mixing, irrigating, drilling, slotting, cutting and destructing, etc. How to improve the jet properties, which is a substantial project, is always a matter of concern to investigators. In recent years, the drag-reduction by additives has been used in water jet. It has been found experimentally that the additives of small amount of long-chain polymer can not only greatly improve the properties of jet, but effectively extend the working period of nozzle as well. Hoyt, J. W. and Taylor, J. J., (1974 a.b) and Liao, Q. D., et al. (1989) verified that, according to their experimental measurements, the spraying rate of jet surface could markedly be suppressed, and the coherence and cutting ability could obviously be enhanced by additives to be dissolved in water. Usui, H. and Sano, Y. (1980) used visualization and photographic analysis to investigate the profiles of mean velocities and velocity fluctuations of polymer solution jet. Their measurements showed that the spreading rate was also reduced, the centerline velocities were larger, and the axial turbulent intensities were higher in the center region and decreased more rapidly in the radial direction, compared to those of solvant jet. Berman, N. S. and Tan, H. (1985) used a Two-Component Laser Doppler Velocimeter to study submerged jets of dilute polymer solutions. The mean velocities, turbulent intensities and Reynolds shear stress were measured, and found that the centerline velocities and axial turbulent intensities were higher, but the radial turbulent intensities and Reynolds stresses were lower, compared to pure water jet. All of them considered the effects of additives in water to suppress or absorb the small scale viscosity eddies, but not to influence or even strengthen, perhaps, the large scale motions.

Although the good many advances in experiments have been made for the polymer solution jets, but the substantial results with respect to theoretical studies and computational analyses have still not been developed. Here, a $K-\varepsilon-$ Re turbulence model which can be applied to analyzing the polymer jets is established. Authord's attempt is of using numerical prediction methods to study quantitatively the influences of polymer additives on the turbulent construction of water jet. The numerical predictions show that, by dissolving very small amount of polymer additives in water, the properties of distribution of turbulent kinetic energy and its dissipation rate can be changed, the Reynolds stresses can be reduced, the jet coherence can be enhanced and the jet surface can be smoothed, and then the jet qualities can markedly be improved, as compared with pure water jet under identical conditions. At last, the calculated results here are compared with the experimental data (Hoyt, T. W. and Taylor, J. J., 1974 a, b; Usui, H. and Sano, Y., 1980; Berman, N. S. and Tan, H., 1985; and Liao, Q. D., 1989; et al.) and are in good agreement.

2.0 GOVERNING EQUATIONS

For pure water jet, Reynolds stress models had respectively been put forward by Launder et al (Launder, B. E., Reece, G. J. and Rodi, W., 1975; Chen, C. J., 1985; Launder, B. E., Morse. A. P., Rodi, W. and Spalding, D. B., 1973), and numerical results with the models had also been obtained. But, up to now, the mechanism of the effects of polymer additives on the turbulent is still a puzzle, so no one has developed the $K-\varepsilon-$ Re model for the polymer solution jets.

According to the experimental data mentioned above, it could be known that the properties of turbulence field had been altered by additives in a certain extent under appropriate conditions. So, it is evident that the Reynolds stress term and the diffusion and production and dissipation terms in model equations must all be modified to account for the effects of additives. It will be noted that problems in free turbulent flow are of a boundary-layer nature, meaning that the region of space in which a solution is being sought does not extend for in a transverse direction, as compared with the main direction of flow, and that the transverse gradients are large. Consequently it is permissible to study such problems with the aid of the boundary-layer equation. Furthermore, the local friction drag in pipe or boundary layer flow are drastically reduced by additives,and in jet flow the dispersion rate is depressed and the centerline velocity is obviously enhanced by additives respectively. Consequently, both the mechanisms above are regarded as similitude by many investigators. And, many experimental data to have been obtained (for example, Berman, N. S. and Tan, H. 1985; Usui, H. and Sano, Y., 1980; et al.) had also testified that the larger the drag-reducing percentage of polymer additives, the better the effects to improve the jet properties with that additives.

A damping factor model for viscoelastic fluids was previously developed (Hassid, S. and Poreh, M., 1975; Mizushina, T. and Usui, H. 1977), using a procedure similar to that of Van Driest with the use of the Maxwell model as a constitutive equation (Van Driest, E. R., 1956). In this paper, basing on turbulence model of pure water jet and some experimental results of polymer solution jet, and referring to the damping factor model, a $K-\varepsilon-$ Re turbulence model to be applied to dilute polymer solution jets is developed. The high Reynolds number, thin shear Layer equations governing the turbulent incompressible polymer solution jet are as follows:

continuity

$$\frac{\partial u}{\partial x} + \frac{\partial v}{\partial y} = 0 \tag{1}$$

momentum

$$u \frac{\partial u}{\partial x} + v \frac{\partial u}{\partial y} = \frac{\partial}{\partial y}(-\overline{u'v'}) \tag{2}$$

turbulent kinetic energy

$$u \frac{\partial K}{\partial x} + v \frac{\partial K}{\partial y} = C_\mu \frac{\partial}{\partial y}\left(f_u \frac{K^2}{\varepsilon} \frac{\partial K}{\partial y}\right) - \overline{u'v'} \frac{\partial u}{\partial y} - f_u \varepsilon \tag{3}$$

turbulent dissipation

$$u \frac{\partial \varepsilon}{\partial x} + v \frac{\partial \varepsilon}{\partial y} = C_\varepsilon \frac{\partial}{\partial y}\left(f_u \frac{K^2}{\varepsilon} \frac{\partial \varepsilon}{\partial y}\right) - C_{\varepsilon 1} \frac{\varepsilon \overline{u'v'}}{K} \frac{\partial u}{\partial y} - C_{\varepsilon 2} f_u \frac{\varepsilon^2}{K} \tag{4}$$

Reynolds stress

$$u \frac{\partial \overline{u'v'}}{\partial x} + v \frac{\partial \overline{u'v'}}{\partial y} = C_s \frac{\partial}{\partial y}\left(\frac{K^2}{\varepsilon} \frac{\partial \overline{u'v'}}{\partial y}\right) - C_\phi \left(\frac{\overline{u'v'}\varepsilon}{K} + C_\mu f_u K \frac{\partial u}{\partial y}\right) \tag{5}$$

where

$$f_u = 1 - \exp\left\{-A_u \, Re_t \left[-\alpha + (\alpha^2+1)^{\frac{1}{2}}\right]^{\frac{1}{2}}\right\} \tag{6}$$

and

$$\alpha = \frac{\rho u_\tau^2 \, [\eta]^2 MC}{NBT \, (1 + [\eta]C)} \tag{7}$$

In expression (7) of α, the friction velocity, u_τ, accounts for the effect of Reynolds number, and the intrinsic viscosity, $[\eta]$, of solution is related to molecular weight, molecular mass distribution, size and elasticity of solution. Consequently, the damping parameter, α, has synthetically expressed the influence of properties and concentration of solution, and of flow Reynolds number on the turbulent flow field of jet. The larger the value of α, the better the damping effect. For the pure water jet, the damping parameter α is put equal to zero.

Boundary conditions for equations (1) - (5) are
symmetry plane, y = 0:

$$v = 0 , \quad \frac{\partial u}{\partial y} = 0 , \quad \frac{\partial K}{\partial y} = 0 , \quad \frac{\partial \varepsilon}{\partial y} = 0 , \quad \overline{u'v'} = 0 \tag{8a}$$

jet edge, y = ∞ :

$$u = 0 , \quad K = 0 , \quad \varepsilon = 0 , \quad \overline{u'v'} = 0 \tag{8b}$$

And then, the model constants complete the specification of the problem, $A_u = 0.012$, $C_\mu = 0.09$, $C_\varepsilon = 0.075$, $C_{\varepsilon 1} = 1.44$, $C_{\varepsilon 2} = 1.92$, $C_s = 0.1$, $C_\phi = 1.5$.

3.0 NUMERICAL SOLUTION AND DISCUSSION

It is advantageous to define a stream function, $\psi(x, y)$,

where,

$$\frac{\partial \psi}{\partial y} = u , \qquad \frac{\partial \psi}{\partial x} = v \tag{9}$$

and equation (1) is then identically satisfied.

Let the dimensionless variables be

$$\xi = \frac{x}{b}, \qquad \eta = \frac{y}{x} \tag{10}$$

and choose the dimensionless stream function, $f(\xi, \eta)$, so that

$$\psi(x,y) = U \times f(\xi,\eta) \tag{11}$$

and then, the velocities, u and v, can easily be expressed as

$$u = U f', \qquad v = U \left(\eta f' - f - \xi \frac{\partial f}{\partial \xi} \right) \tag{12}$$

where the primes, " ' ", indicate derivatives with respect to η .

When the turbulent kinetic energy, k, and its dissipation rate, ε , and Reynolds stress, $\overline{u'v'}$, are also written as dimensionless form

$$\bar{K} = \frac{K}{U^2}, \qquad \bar{\varepsilon} = \frac{b\varepsilon}{U^3}, \qquad \bar{\tau} = \frac{\overline{u'v'}}{U^2} \tag{13}$$

then the dimensionless form for equations (2)-(5) are achieved, viz.

$$\xi f' \frac{\partial f'}{\partial \xi} - f f'' - \xi f'' \frac{\partial f}{\partial \xi} = \frac{\partial}{\partial \xi} (-\bar{\tau}) \tag{14}$$

$$\xi^2 f' \frac{\partial \bar{K}}{\partial \xi} - \xi f \bar{K}' - \xi^2 \frac{\partial f}{\partial \xi} \bar{K}' = C_\mu \frac{\partial}{\partial \eta} \left(f_u \frac{\bar{K}^2}{\bar{\varepsilon}} \frac{\partial \bar{K}}{\partial \eta} \right) - \xi \bar{\tau} f'' - f_u \xi^2 \bar{\varepsilon} \tag{15}$$

$$\xi^2 f' \frac{\partial \bar{\varepsilon}}{\partial \xi} - \xi f \bar{\varepsilon}' - \xi^2 \frac{\partial f}{\partial \xi} \bar{\varepsilon}' = C_\varepsilon \frac{\partial}{\partial \eta} \left(f_u \frac{\bar{K}^2}{\bar{\varepsilon}} \frac{\partial \bar{\varepsilon}}{\partial \eta} \right) - C_{\varepsilon 1} \xi f'' \frac{\bar{\tau} \bar{\varepsilon}}{\bar{K}} - C_{\varepsilon 2} f_u \xi^2 \frac{\bar{\varepsilon}^2}{\bar{K}} \tag{16}$$

$$\xi^2 f' \frac{\partial \bar{\tau}}{\partial \xi} - \xi f \bar{\tau}' - \xi^2 \frac{\partial f}{\partial \xi} \bar{\tau}' = C_s \frac{\partial}{\partial \eta} \left(\frac{\bar{K}^2}{\bar{\varepsilon}} \frac{\partial \bar{\tau}}{\partial \eta} \right) - C_\phi \left(\xi^2 \frac{\bar{\tau} \bar{\varepsilon}}{\bar{K}} + C_\mu f_u \xi \bar{K} f'' \right) \tag{17}$$

The boundary conditions (8) can correspondently be represented by

$$\begin{aligned} \eta = 0 \ : \quad & f = 0, \quad f'' = 0, \quad \bar{K}' = 0, \quad \bar{\varepsilon}' = 0, \quad \bar{\tau} = 0 \\ \eta = \eta_\infty \ : \quad & f' = 0, \quad \bar{K} = 0, \quad \bar{\varepsilon} = 0, \quad \bar{\tau} = 0 \end{aligned} \tag{18}$$

A crucial step in the numerical procedure is to reformulate the problem in terms of a first-order system of partial differential equations. For this purpose we introduce new dependent variables, $u(\xi,\eta)$, $v(\xi,\eta)$, $s(\xi,\eta)$, $t(\xi,\eta)$ and $p(\xi,\eta)$, so that

$$f' = u, \quad u' = V, \quad \bar{K}' = s, \quad \bar{\varepsilon}' = t, \quad \bar{\tau}' = p \tag{19}$$

and then the equations (14)-(17) can be written as:

$$f' = u \tag{20a}$$

$$u' = V \tag{20b}$$

$$\xi u \frac{\partial u}{\partial \xi} - f V - \xi V \frac{\partial f}{\partial \xi} = \frac{\partial}{\partial \eta} (-\bar{\tau}) \tag{20c}$$

$$\bar{K}' = s \tag{21a}$$

$$\xi^2 u \frac{\partial \bar{K}}{\partial \xi} - \xi f s - \xi^2 \frac{\partial f}{\partial \xi} s = C_\mu \frac{\partial}{\partial \eta} \left(f_u \frac{\bar{K}^2}{\bar{\varepsilon}} s \right) - \xi \bar{\tau} V - f_u \xi^2 \bar{\varepsilon} \tag{21b}$$

$$\bar{\varepsilon}' = t \tag{22a}$$

$$\xi^2 u \frac{\partial \bar{\varepsilon}}{\partial \xi} - \xi f t - \xi^2 \frac{\partial f}{\partial \xi} t = C_\varepsilon \frac{\partial}{\partial \eta} \left(f_u \frac{\bar{K}^2}{\bar{\varepsilon}} t \right) - C_{\varepsilon 1} \xi V \frac{\bar{\tau} \bar{\varepsilon}}{\bar{K}} - C_{\varepsilon 2} f_u \xi^2 \frac{\bar{\varepsilon}^2}{\bar{K}} \tag{22b}$$

$$\bar{\tau}' = p \tag{23a}$$

$$\xi^2 u \frac{\partial \bar{\tau}}{\partial \xi} - \xi f p - \xi^2 \frac{\partial f}{\partial \xi} p = C_s \frac{\partial}{\partial \eta} \left(\frac{\bar{K}^2}{\bar{\varepsilon}} p \right) - C_\phi \left(\xi^2 \frac{\bar{\varepsilon} \bar{\tau}}{\bar{K}} + C_\mu f_u \xi \bar{K} V \right) \tag{23b}$$

The boundary conditions (18) are simply

$$\eta = 0 : \quad f = 0 , \quad V = 0 , \quad s = 0 , \quad t = 0 , \quad \bar{\tau} = 0$$
$$\eta = \eta_\infty : \quad u = 0 , \quad \bar{K} = 0 , \quad \bar{\varepsilon} = 0 , \quad \bar{\tau} = 0 \qquad (24)$$

In here, a Keller Box method (Cebeci, T. and Brandshaw, P., (1977) are employed for solving the nonlinear system of partial differential equations given by eqs. (20)-(24).

Let the net points be given by, as is shown in Fig. 1,

$$\xi^0 = 0 , \quad \xi^n = \xi^{n-1} + k_n , \quad n = 1 , 2 , \cdots , NI$$
$$\eta_0 = 0 , \quad \eta_k = \eta_{k-1} + h_k , \quad k = 1 , 2 , \cdots , K \qquad (25)$$

We also employ the notation, for points and quantities midway between net points and for any net function:

$$\xi^{n-\frac{1}{2}} = \tfrac{1}{2}(\xi^n + \xi^{n-1}) , \quad \eta_{k-\frac{1}{2}} = \tfrac{1}{2}(\eta_k + \eta_{k-1})$$
$$g_k^{n-\frac{1}{2}} = \tfrac{1}{2}(g_k^n + g_k^{n-1}) , \quad g_{k-\frac{1}{2}}^n = \tfrac{1}{2}(g_k^n + g_{k-1}^n) \qquad (26)$$

We simply approximate Eqs. (20a), (20b), (21a), (22a) and (23a) using centered difference quotients and average about the midpoint $(\xi^n, \eta_{k-\frac{1}{2}})$ of the segment as in Fig. 1. Eqs. (20c), (21b), (22b) and (23b) are similarly approximated by centering about the midpoint $(\xi^{n-\frac{1}{2}}, \eta_{k-\frac{1}{2}})$ of the rectangle. Thus, the difference equations which are to approximate Eqs. (20)-(23) are now easily formulated. They are

$$f_k^n - f_{k-1}^n - \tfrac{1}{2}h_k(u_k^n + u_{k-1}^n) = 0 \qquad (27a)$$

$$u_k^n - u_{k-1}^n - \tfrac{1}{2}h_k(V_k^n + V_{k-1}^n) = 0 \qquad (27b)$$

$$\alpha_1(Vf)_{k-\frac{1}{2}}^n - \alpha_0[(u^2)_{k-\frac{1}{2}}^n + (V^n f^{n-1})_{k-\frac{1}{2}} - (V^{n-1}f^n)_{k-\frac{1}{2}}] = S_{k-\frac{1}{2}}^{n-1} \qquad (27c)$$

$$\bar{K}_k^n - \bar{K}_{k-1}^n - \tfrac{1}{2}h_k(s_k^n + s_{k-1}^n) = 0 \qquad (28a)$$

$$\frac{C_\mu}{h_k}[(f_u\frac{\bar{K}^2}{\bar{\varepsilon}}s)_k^n - (f_u\frac{\bar{K}^2}{\bar{\varepsilon}}s)_{k-1}^n] + 2\alpha_4(fs)_{k-\frac{1}{2}}^n$$
$$- \alpha_3[(u\bar{K})_{k-\frac{1}{2}}^n + (u^{n-1}\bar{K}^n)_{k-\frac{1}{2}} + (f^{n-1}s^n)_{k-\frac{1}{2}}] = M_{k-\frac{1}{2}}^{n-1} \qquad (28b)$$

$$\bar{\varepsilon}_k^n - \bar{\varepsilon}_{k-1}^n - \tfrac{1}{2}h_k(t_k^n + t_{k-1}^n) = 0 \qquad (29a)$$

$$\frac{C_\varepsilon}{h_k}[(f_u\frac{\bar{K}^2}{\bar{\varepsilon}}t)_k^n - (f_u\frac{\bar{K}^2}{\bar{\varepsilon}}t)_{k-1}^n] - C_{\varepsilon 1}\xi^n(\frac{V\bar{\tau}\bar{\varepsilon}}{\bar{K}})_{k-\frac{1}{2}}^n - C_{\varepsilon 2}(\xi^2)^n(f_u\frac{\bar{\varepsilon}^2}{\bar{K}})_{k-\frac{1}{2}}^n$$
$$+ 2\alpha_4(ft)_{k-\frac{1}{2}}^n - \alpha_3[(u\bar{\varepsilon})_{k-\frac{1}{2}}^n + (u^{n-1}\bar{\varepsilon}^n)_{k-\frac{1}{2}} + (f^{n-1}t^n)_{k-\frac{1}{2}}] = N_{k-\frac{1}{2}}^{n-1} \qquad (29b)$$

$$\bar{\tau}_k^n - \bar{\tau}_{k-1}^n - \tfrac{1}{2}h_k(p_k^n + p_{k-1}^n) = 0 \qquad (30a)$$

$$\frac{C_s}{h_k}[(\frac{\bar{K}^2}{\bar{\varepsilon}}p)_k^n - (\frac{\bar{K}^2}{\bar{\varepsilon}}p)_{k-1}^n] - C_\phi(\xi^2)^n(\frac{\bar{\tau}\bar{\varepsilon}}{\bar{K}})_{k-\frac{1}{2}}^n + 2\alpha_4(fp)_{k-\frac{1}{2}}^n$$
$$- \alpha_3[(u\bar{\tau})_{k-\frac{1}{2}}^n + (u^{n-1}\bar{\tau}^n)_{k-\frac{1}{2}} + (f^{n-1}p^n)_{k-\frac{1}{2}}] = R_{k-\frac{1}{2}}^{n-1} \qquad (30b)$$

where

$$S_{k-\frac{1}{2}}^{n-1} = \frac{1}{h_k}[\bar{\tau}_k^{n-1} - \bar{\tau}_{k-1}^{n-1}] + \frac{1}{h_k}[\bar{\tau}_k^n - \bar{\tau}_{k-1}^n] + \alpha_2(fV)_{k-\frac{1}{2}}^{n-1} - \alpha_0(u^2)_{k-\frac{1}{2}}^{n-1}$$

$$M_{k-\frac{1}{2}}^{n-1} = -\frac{C_\mu}{h_k}[(f_u\frac{\bar{K}^2}{\bar{\varepsilon}}s)_k^{n-1} - (f_u\frac{\bar{K}^2}{\bar{\varepsilon}}s)_{k-1}^{n-1}] + 2\xi^{n-\frac{1}{2}}(\bar{\tau}V)_{k-\frac{1}{2}}^{n-\frac{1}{2}} + 2(\xi^2)^{n-\frac{1}{2}}(f_u\bar{\varepsilon})_{k-\frac{1}{2}}^{n-\frac{1}{2}}$$
$$+ \alpha_5(fs)_{k-\frac{1}{2}}^{n-1} - \alpha_3[(u^n\bar{K}^{n-1})_{k-\frac{1}{2}} + (u\bar{K})_{k-\frac{1}{2}}^{n-1} + (s^{n-1}f^n)_{k-\frac{1}{2}}$$

$$N_{k-\frac{1}{2}}^{n-1} = -\frac{C_\varepsilon}{h_k}[(f_u\frac{\bar{K}^2}{\bar{\varepsilon}}t)_k^{n-1} - (f_u\frac{\bar{K}^2}{\bar{\varepsilon}}t)_{k-1}^{n-1} + C_{\varepsilon 1}(\xi V\frac{\bar{\tau}\bar{\varepsilon}}{\bar{K}})_{k-\frac{1}{2}}^{n-\frac{1}{2}} + C_{\varepsilon 2}(\xi^2)^{n-1}(f_u\frac{\bar{\varepsilon}^2}{\bar{K}})_{k-\frac{1}{2}}^{n-1}$$
$$- \alpha_3[(u\bar{\varepsilon})_{k-\frac{1}{2}}^{n-1} + (u^n\bar{\varepsilon}^{n-1})_{k-\frac{1}{2}} + (t^{n-1}f^n)_{k-\frac{1}{2}}] + \alpha_5(tf)_{k-\frac{1}{2}}^{n-1}$$

$$R^{n-1}_{k-\frac{1}{2}} = -\frac{C_s}{h_k}\left[\left(\frac{\bar{K}^2}{\bar{\varepsilon}}p\right)^{n-1}_{k} - \left(\frac{\bar{K}^2}{\bar{\varepsilon}}p\right)^{n-1}_{k-1}\right] + C_\phi(\xi^2)^{n-1}\left(\frac{\bar{\tau}\bar{\varepsilon}}{\bar{K}}\right)^{n-1}_{k-\frac{1}{2}} + \alpha_5(fp)^{n-1}_{k-\frac{1}{2}}$$

$$- \alpha_3\left[(u^n\bar{\tau}^{n-1})_{k-\frac{1}{2}} + (u\bar{\tau})^{n-1}_{k-\frac{1}{2}} + (p^{n-1}f^n)_{k-\frac{1}{2}}\right] + 2C_\phi C_\mu \xi^{n-\frac{1}{2}}(f_u\bar{K}V)^{n-\frac{1}{2}}_{k-\frac{1}{2}}$$

$$\alpha_0 = \frac{1}{k_n}\xi^{n-\frac{1}{2}}, \quad \alpha_1 = \alpha_0 + 1, \quad \alpha_2 = \alpha_0 - 1$$

$$\alpha_3 = \frac{1}{k_n}(\xi^2)^{n-\frac{1}{2}}, \quad \alpha_4 = \frac{1}{2}(\xi^n * \alpha_3), \quad \alpha_5 = \alpha_3 - \xi^{n-1}$$

The boundary conditions (24) yield, at $\xi = \xi^n$

$$f^n_0 = 0, \quad V^n_0 = 0, \quad s^n_0 = 0, \quad t^n_0 = 0, \quad \bar{\tau}^n_0 = 0$$

$$u^n_k = 0, \quad \bar{K}^n_k = 0, \quad \bar{\varepsilon}^n_k = 0, \quad \bar{\tau}^n_k = 0 \tag{31}$$

When the values, f^{n-1}_k, u^{n-1}_k, V^{n-1}_k, s^{n-1}_k, t^{n-1}_k and p^{n-1}_k, are known for $o \le k \le K$, then Eqs. (27)-(30) are solved by means of Neuton's method, which are solved one by one in succession of the momentum, turbulent kinetic energy, dissipation rate and Reynolds stress equations. The problems are numerically calculated respectively, when the different values of α, o, 15 and 35, are chosen. In order to compare the numerical results with different values of α. the same initial conditions are taken. Because, perhaps the turbulent field of polymer solution jet do not put on a pose of self-similarity, and in order to simplify the calculated process and to obtain the numerical data of spread, dissipation and decay rates in jet flow with different values of α, the centerline velocity, U, and the streamwise coordinate value, b, at starting lateral section are taken as characteristic velocity and representative scale, respectively. The characteristic Reynolds number, iteration convergence criterio$_6$ and equally step length in the ξ coordinate direction are respectively chosen as 40000, 10^{-6} and 0.004. Having variable profiles on 840 lateral sections across the jet along the coordinate, ξ, direction are calculated. There is an interval of forty sections between each two data to be type-written down.

In order to examine the reliability of the model and its numerical results mentioned above, we first calculate the pure water jet and then compare the results with experimental data (Berman, N. S. and Tan, H., 1985). As shown in Fig. 2, we can be sure that, the mean velocity profiles agree satisfactorily and the profiles of Reynolds stress deviate only slightly from the measurements in a small region near the jet edge. The reasons for the derivation may be that the jet flow near the jet edge becomes more random and stochastical, owing to partly mixing with the surrounding fluid at rest and concurrently spread out. So that, both calculation numerically and measurement experimentally are more difficult to obtain their accurate results in this region.

The profiles of f', $\bar{K}$, $\bar{\varepsilon}$ and $\bar{\tau}$ are plotted in Figs. 3-6 for the different values ξ = 1.16, 1.64, 2.28, 2.92 and 3.56. These figures obviously show the deficit state of mean velocities and the decay processes of turbulent fluctuation fields (kinetic energy, dissipation rate and Reynolds stress).

In order to distinguish that the mean velocity profiles and turbulent fluctuation fields behave like self-similarity or not, we can transform the longitudinal coordinate in Figs. 3, 4 and 6 into the similarity coordinate as usual, and thus obtain the Figs. 7, 8, and 9, relatively. It is sure that, as shown in Fig. 7, the mean velocity profile put wholly on pose of self-similarity and the similarity variable is η. But, as shown in Figs. 8 and 9, the kinetic energy profile do not behave like self-similarity and the Reynolds stress profile behave partial and local self-similarity — in the center region it is governed by self-similarity and other region it is not, across jet section. The values of K/U_m^2 and $\overline{u'v'}/U_m$ decrease with the increase of distance far from upstream or toward downstream. These results are also found by some measurements. Write, D. A. (1967), for example, investigated experimentally the mean velocity profiles in axisymmetric jets of dilute polymer solution, and made sure that the velocity profiles appear as a self-similarity as usual. Berman, N. S. and Tan, H. (1985) studied in detail the submerged jets with additives, using Two-Component Laser Doppler Velocimeter, and did not discover that the turbulent intensities have a pose of self-similarity until the distance very far from upstream along streamwise, where the turbulent fluctuations have nearly vanished. Judging from this, the numerical calculated method here, using nonsimilar variables, are reliable and fine, and it is fortunately one of the advantages of K - ε - Re model developed here.

Fig. 10 illustrates the centre-line velocity decay rate with different values of damping parameters, α = 0, 15 and 35. It is worth noted that all of them decay nearly in law of the development of $\xi^{-\frac{1}{2}}$. Basing on this figure, we can also find that the centerline velocity increases with the increase of the value of α, and the difference between one and other in these three curves is larger when the distance far from the initial section becomes farther. The Reynolds stress, $\bar{\tau}$, which are predicted by the present computations at the section, ξ = 2.12, for the different values of α, are given in Table 1. The Reynolds stresses in whole region across jet section reduce continuously with the increase of values of α. By means of the expression (7), the increase of α value means the increase of molecular weight or of intrinsic viscosity or of concentration of solution. Therefore, we can be sure that the larger the drag-reducing percentage of polymer additives, the better the effects to improve the jet properties with the additives. These results are in agreement with experimental data mentioned above.

40. CONCLUDING REMARKS

1. By dissolving very small amount of polymer solution in water, it can markedly enhance the centerline velocity, improve the coherence, strengthen the working ability and raise up the level of quality of water jet. The larger the drag reduction percentage the better the effects to improve the jet property with additives.

2. With the increase in value of α, or, in other words, with the increase of whichever of parameter variables among the molecular mass weight, intrinsic viscosity and concentration of solutions, the profiles of turbulent kinetic energy and its dissipation rate can more effectively be improved, the Reynolds stress can obviously be reduced, and the dispersion rate of jet can evidently be suppressed, under identical initial starting conditions.

3. For polymer solution jets, the mean velocity profiles behave a self-similarity as usual, the Reynolds stress profiles put partially and locally on a pose of self-similarity, but the turbulent kinetic energy profiles do not appear as a self-similarity.

5.0 NOMENCLATURE

B = Boltzmann's constant
b = representative length scale
c = polymer concentration
f = dimensionless stream function
fu = damping function
K = turbulent kinetic energy = $\frac{1}{2}$ ($\overline{u'^2}$ + $\overline{v'^2}$ + $\overline{w'^2}$)
$\bar{K}$ = dimensionless turbulent kinetic energy
M = molecular weight of polymer
N = Avogadro constant
Re = characteristic Reynolds number = $\frac{Ub}{\nu}$
Re_t = turbulent Reynolds number = $K^2/\nu\varepsilon$
T = absolute temperature
U = characteristic velocity
Um = centerline velocity
u = streamwise mean velocity
u_τ = shear velocity
u' = streamwise fluctuation velocity
v = lateral mean velocity
v' = lateral fluctuation velocity
$\overline{u'v'}$ = Reynolds shear stress
w' = span direction fluctuation velocity
x = streamwise coordinate
y = lateral coordinate
$y_{\frac{1}{2}}$ = half width of jet
$\alpha^{\frac{1}{2}}$ = damping parameter
ε = dissipation rate of K
$\bar{\varepsilon}$ = dimensionless dissipation rate
η = dimensionless coordinate
$[\eta]$ = intrinsic viscosity of solution
ν = kinematic viscosity
ξ = dimensionless coordinate
ρ = mass density
$\bar{\tau}$ = dimensionless Reynolds stress
ψ = stream function

6.0 REFERENCES

1. Hoyt, J. W., and Taylor, J. J., "A Photographic Study of Polymer Solution Jets in Air," Proc. Int. Conf. Drag Reduction, 1974a.

2. Hoyt, J. W., Taylor, J. J., and Runge, C. D., "The Structure of Jets of Water and Polymer Solution in Air," J. Fluid Mech., Vol.63, 1974b.

3. Liao, Q. D., Zhong, S. Y., Zhao, X. D., and Zhu, Y., "The Performances of High Pressure Jet of Pure Water and Polymer Solution with Conical Nozzle," J. of Hydrodynamics, Vol. 1, No. 1, 1989. (China Ocean Press - Beijing).

4. Vsui, H., and Sano, Y., "Turbulence Structure of Submerged Jets of Dilute Polymer Solution," J. Chem. Eng. Japan, 13, 401, 1980.

5. Berman, N. S., and Hung Tan, "Two-Component Laser Doppler Velocimeter Studies of Submerged Jets of Dilute Polymer Solution," AIchE J. Vol. 31 No. 2, 1985.

6. Launder, B. E., Reece, G. J., and Rodi, W., "Progress in the Development of a Reynolds-Stress Turbulence Closure," J. Fluid Mech., Vol. 68, 1975.

7. Chen, C. J., "Fluid Mechanics and Heat Transfer," Defence Industry Press - Beijing, 1985, (in Chinese).

8. Launder, B. E., Morse, A. P., Rodi, W., and Spalding, D. B., "The Prediction of Free-Shear Flows - A Comparison of the Performance of Six Turbulence Models," Proc. of the NASA Langley Free Turbulent Shear Flows Conf., Vol. 1, NASA Sp 320, 1973.

9. Hassid, S., and Porch, M., "A Turbulent Energy Model for Flows with Drag Reduction," J. of Fluids Eng. June, 1975.

10. Mizushina, T., and Usui, H., "Reduction of Eddy Diffusion for Momentum and Heat in Viscoelastic Fluid Flow in a Circular Tube," the Physics of Fluid, Vol. 20, No. 10, 1977.

11. Van Driest, E. R., "On Turbulent Flow near a Wall," J. of Aeronautical Science, Vol.23 1956.

12. Cebeci, T., and Bradshaw, P., "Momentum Transfer in Boundary Layers," Hemisphere Publishing Corporation, London, 1977.

13. Vollmers, H., and Rotta, J. O., "Similar Solution of the Mean Velocity, Turbulent Energy and Length Scale Equation," AIAA J., Vol. 15, No. 3, 1977.

14. White, D. A., "Velocity Measurement in Axisymmetric Jets of Dilute Polymer Solution," J. Fluid Mech., Vol. 28, 1967.

Tabble 1. Results for $\bar{\tau}$ using present method

	0	15	35
0.000000	0.000000	0.000000	0.000000
0.024144	0.006882	0.006806	0.006568
0.054312	0.012290	0.012146	0.011692
0.066036	0.013265	0.013107	0.012604
0.078684	0.013679	0.013515	0.012980
0.114444	0.012142	0.011987	0.011440
0.144198	0.009239	0.009085	0.008559
0.174474	0.006243	0.006084	0.005594
0.204054	0.003923	0.003755	0.003299
0.228114	0.002862	0.002638	0.002192

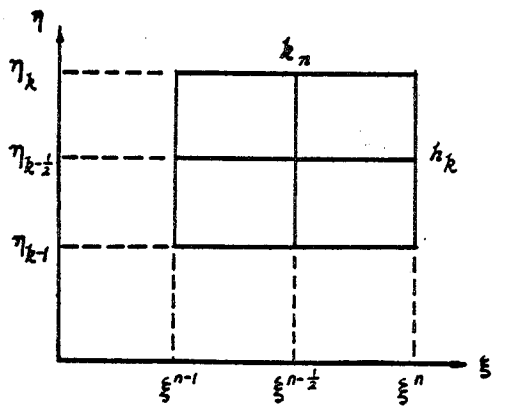

FIG. 1 NET RECTANGLE FOR DIFFERENCE APPROXIMATIONS

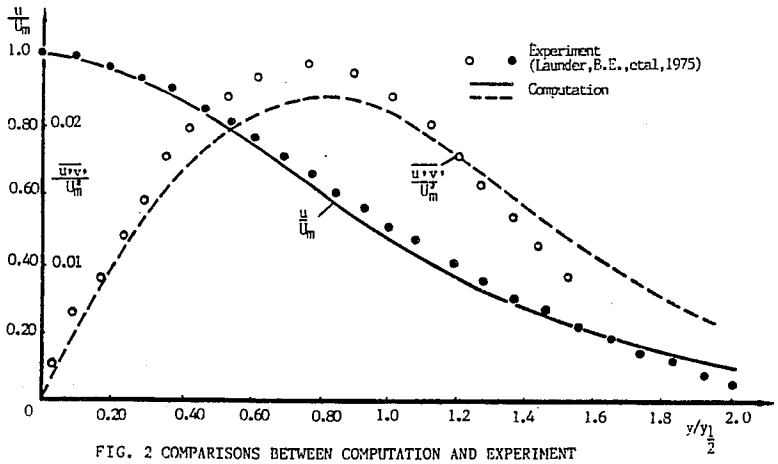

FIG. 2 COMPARISONS BETWEEN COMPUTATION AND EXPERIMENT
FOR THE VALUES OF MEAN VELOCITY AND REYNOLDS STRESS

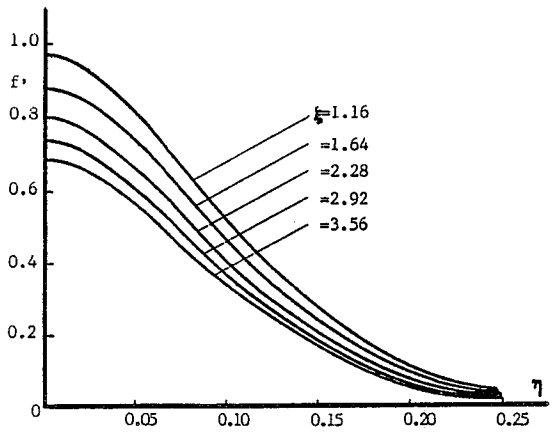

FIG. 3 MEAN VELOCITY PROFILES

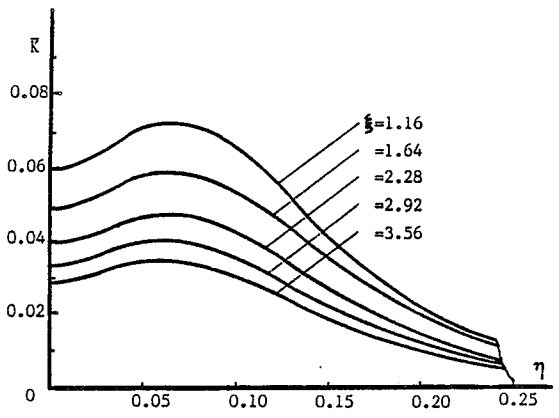

FIG. 4 TURBULENT KINETIC ENERGY PROFILES

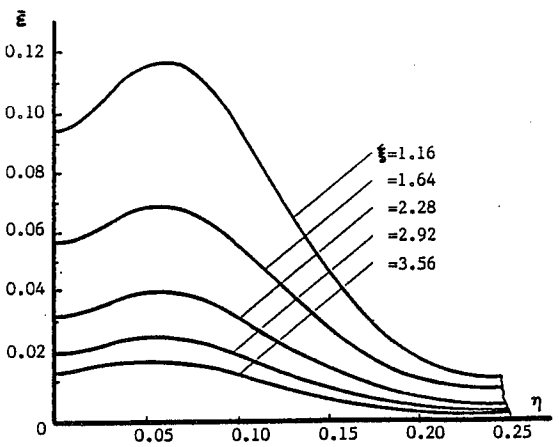

FIG. 5 TURBULENT DISSIPATION PROFILES

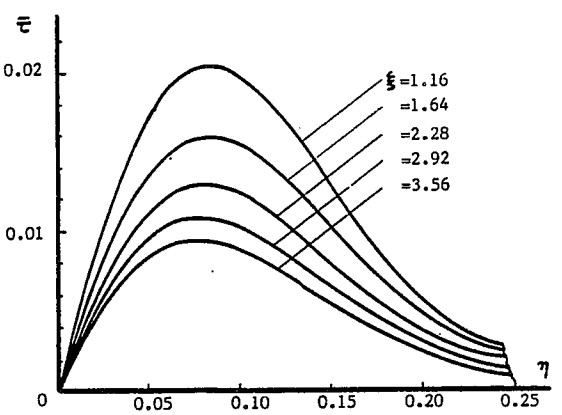

FIG. 6 REYNOLDS SHEAR STRESS PROFILES

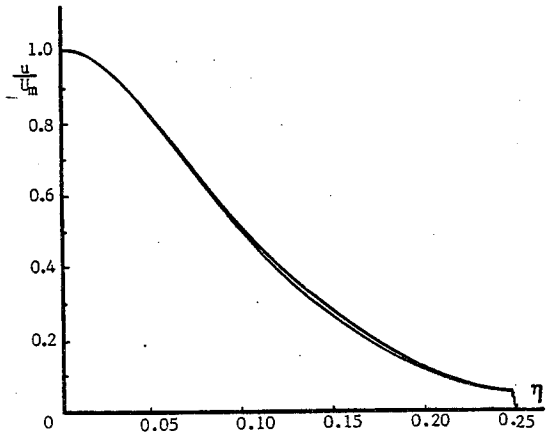

FIG. 7 MEAN VELOCITY PROFILES IN SIMILARITY COORDINATE

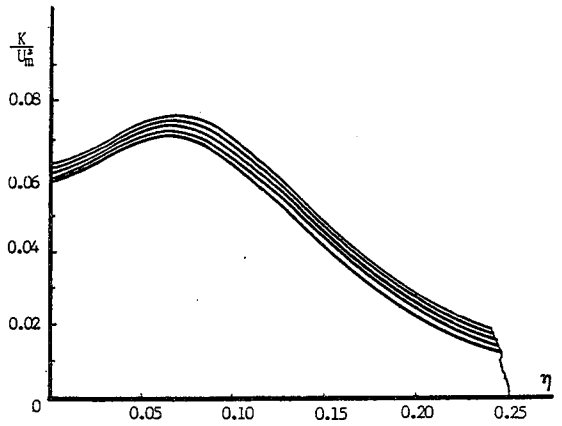

FIG. 8 TURBULENT KINETIC ENERGY PROFILES IN SIMILARITY COORDINATE

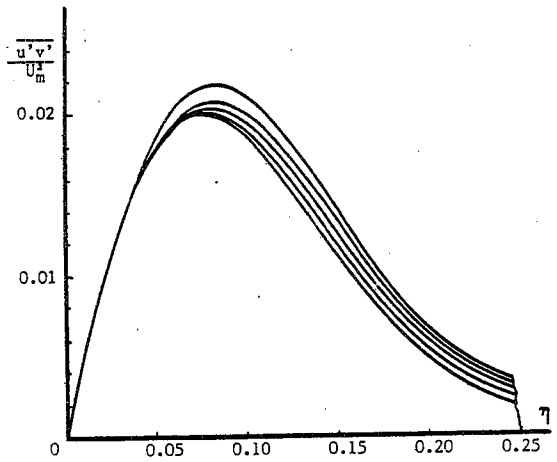

FIG. 9 REYNOLDS STRESS PROFILES IN SIMILARITY COORDINATE

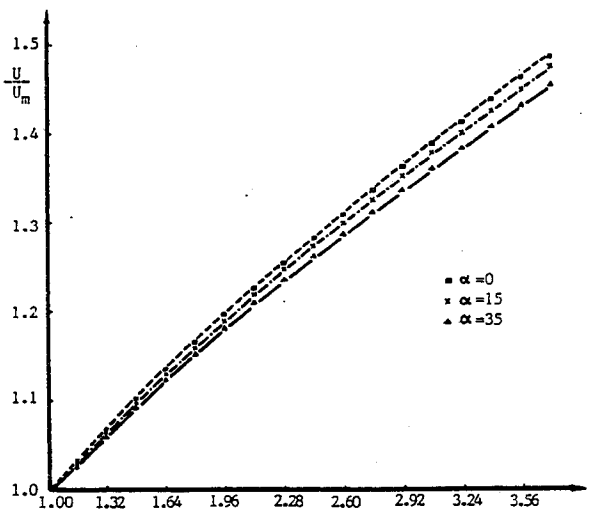

FIG. 10 CENTERLINE VELOCITY DECAY

5th American Water Jet Conference
August 29 - 31, 1989: Toronto, Canada

Paper / Communication 37

MULTIPASS CUTTING OF HIGH VELOCITY WATER JETS UNDER THE CONDITION OF EQUABILITY OF ENERGY

Q.D. Liao, Q. Jin, S.Y. Zhong AND X.D. Zhao
Shanghai Institute of Mechanical Engineering (SIME)
Shanghai 200 093, China

ABSTRACT: It will be discovered from experimental results that the cumulative cutting depths obtained with two or three passes are about 40 per cent or 70 per cent deeper than a single pass respectively under identical cutting energy. It is known as repeated cutting or multipass cutting technology – a very interesting phenomenon. In the presented paper, the effects of repeated cutting in high pressure water jet cutting technology are analysed. Based on continuous water jet cutting equation, the authors have deduced a multipass cutting function. Using the function and prediction equations that we carry out, we can obtain the practical application condition of multipass cutting, and explain the physical essences of it. There is no doubt that it will contribute to exploring the nature of multipass phenomenon and providing theoretical evidence for practical application of multipass cutting technology.

RÉSUMÉ : Des résultats expérimentaux révèlent que la profondeur de coupe cumulée après deux et trois passes est de 40 et 70 % environ plus grande qu'après une seule passe, respectivement, pour la même énergie de coupe dépensée. Cette technologie est appelée la technologie de la coupe répétée ou de la coupe multi-passes, un phénomène très intéressant. Dans la présente communication, les effets de la coupe répétée dans la technologie de la coupe par jet d'eau à haute pression sont analysés. A partir de l'équation de coupe par une jet d'eau continu, les auteurs ont défini une fonction de coupe multi-passes. A partir de cette fonction et des équations de prévision qui sont développées, nous pouvons obtenir la condition d'application pratique de la coupe multi-passes et expliquer ses caractéristiques physiques. Il ne fait pas de doute qu'elle contribuera à l'exploration de la nature du phénomène multi-passes et fournir une preuve théorique de l'applicabilité de la technologie de la coupe multi-passes.

Organized and Sponsored by the National Research Council of Canada and the U.S. Water Jet Technology Association.

1.0 INTRODUCTION

High velocity water jet cutting is a new technology which will widely be applied to engineering problems. It has many advantages:

(1) having strong cutting ability and fast penetration rate;

(2) substituting water for knives and not wearing out cutting tool;

(3) smoothening cutting margin and less materials to be cut off;

(4) lower specific energy and less energy consumption;

(5) lower noise and easy to handle, etc.

Increasing the jet pressure would apparently promote cutting ability. Therefore, new records of high pressure were successively set up in developing higher pressure producer. The jet pressure, for example, produced by two step intensifier which was developed in Japan had reached to 1700 MPa (Cheng, D.Z., 1987). Generally speaking, the present technology level makes it possible to use intensifier equipment which may produce the pressure of 200 MPa - 400 MPa. With the promoting of pressure, however, it will be limited in the aspects of producing equipment and spare parts, and of qualities of materials, and of cost and service life of machine. There is also a safety problem in practically running machine. As a result, how to improve jet properties without very high working pressure so as to reduce the consumption of jet energy has been taken into account since 1970's. For example, the practical application studies of high frequency pulsed jet and cavitating jet, and of abrasive jet and polymer solution jet are all of attempts to get highly economic efficiency under not too high working pressure. Simultaneously, great attentions are paid to the studies of jet flow and cutting mechanism which make it possible to choose optimum cutting parameters so as to get the largest cutting efficiency under the least input. For example, the studies of optimum stand-off distance and optimum feed rate, and of multipass cutting technology are all practical embody of this idea. It is obvious that the better cutting efficiency can be obtained if we can appropriately combine the feed rate and number of passes in the multipass at the same total elapsed-time. A typical experiment (Wang, X.M., 1982) shows that the cumulative depths of cut obtained with two or three passes are about deeper 40 per cent or 70 per cent than a single pass respectively under identical cutting energy. It is known as multipass cutting -- a very interesting phenomenon.

In presented paper, the effects of multipass cutting of high pressure water jet are analysed. Basing on a cutting equations of continuous water jet, the authors have deduced a cutting function of multipass. Using the function and prediction equations that we carry out, the practical application conditions of multipass cutting can be obtained, and the physical essence of this kind of cutting can also be explained. It is no doubt that it will contribute to exploring the nature of multipass phenomenon and providing theoretical evidence for practical application of multipass cutting technology.

2.0 MULTIPASS CUTTING FUNCTION

Based on a control volume analysis to determine the hydrodynamic forces acting on the solid boundaries in the cutting slot, Hashish, M., and Duplessis, M.P., (1978) had derived the generalized cutting equation of high velocity water jet at main region, that is

$$\frac{Z}{d} = \frac{1 - \frac{\sigma_y}{\rho V^2}}{\frac{2C_f}{\sqrt{\pi}}} \left[1 - \exp\left(-\frac{2C_f}{\sqrt{\pi}} \frac{\rho V^2}{\eta u}\right)\right] \tag{1}$$

Let the nondimensional numbers, N_1, N_2 and N_3, be

$$N_1 = \frac{Z}{d}, \qquad N_2 = \frac{1 - \frac{\sigma_y}{\rho V^2}}{\frac{2C_f}{\sqrt{\pi}}}, \qquad N_3 = \frac{2C_f}{\sqrt{\pi}} \frac{\rho V^2}{\eta u} \tag{2}$$

and then, equation (1) can be written as

$$N_1 = N_2(1-e^{-N3}) \tag{3}$$

The comparison between Eq. (3) and experimental results are plotted in Fig. 1. It shows that Eq. (3) is in reasonable consistent with measurement. Consequently, it will be reliable for us to analyse the phenomenon of multipass basing on this equation given here in below.

Under the assumption that the dynamic pressure of jet keeps constant in the inseparable main region, namely $\rho v^2 = 2p \geqslant \sigma y$, the equation (1) can be rewritten as

$$\frac{Z}{d} = \frac{1-\frac{\sigma_y}{2p}}{\frac{2C_f}{\sqrt{\pi}}}\left[1-\exp\left(-\frac{2C_f}{\sqrt{\pi}}\frac{2p}{\eta u}\right)\right] \tag{4}$$

If let

$$R(u) = \frac{1-\exp\left(-\frac{2C_f}{\sqrt{\pi}}\frac{2p}{\eta u}\right)}{\frac{2C_f}{\sqrt{\pi}}\frac{2p}{\eta u}} \tag{5}$$

and then, equation (4) can be written as

$$\frac{Z}{d} = \frac{2p-\sigma_y}{\eta u} R(u) \tag{6}$$

Now, let us analyse the physical meaning of function, R(u). Figs. 2 and 3 illustrated the experimental measurements of multipass at different feed rates and numbers of pass (We, I., and Zhong, Y.T., 1987; Wang, X.M., (1982). As shown in the figures, the cumulative depths of cut increase approximately in same quantity with the increase of number of pass when the stand-off distance are always placed within the inseparable main region of jet. Now, we consider the two cases of multipass for same material, let it be supposed that the numbers of pass are defined as m and n respectively. Supposing the stand-off distance is placed in the inseparable main region of jet, and then from equation (4), the cumulative depths of cut are relatively given out as follows:

$$\frac{Z_m}{d_m} = \frac{1-\frac{(\sigma_y)_m}{2p_m}}{\frac{2C_{fm}}{\sqrt{\pi}}}\left[1-\exp\left(-\frac{2C_{fm}}{\sqrt{\pi}}\frac{2p_m}{\eta_m u_m}\right)\right] \quad m \tag{7}$$

$$\frac{Z_n}{d_n} = \frac{1-\frac{(\sigma_y)_n}{2p_n}}{\frac{2C_{fn}}{\sqrt{\pi}}}\left[1-\exp\left(-\frac{2C_{fn}}{\sqrt{\pi}}\frac{2p_n}{\eta_n u_n}\right)\right] \quad n \tag{8}$$

It has practical significance for us to study the multipass effectiveness under the same condition of equability of energy. So-called multipass at equability of energy means that the total elapsed time and the jet energy (that is jet pressure and nozzle diameter) are kept in same constants respectively when the multipass at different feed rate and in different numbers of pass are employed in cutting of same material. Therefore, we can get it to $d_m=d_n=d$, $p_m=p_n=p$, $C_{fm}=C_{fn}=C_f$, $\eta_m=\eta_n=\eta$, $(\sigma_y)_m=(\sigma_y)_n=\sigma_y$ and $u_m/m=u_n/n$ .Then, according to equations (6), (7) and (8), we obtain

$$\frac{Z_n-Z_m}{Z_m} = \frac{R(u_n)-R(u_m)}{R(u_m)} \tag{9}$$

where

$$R(u_m) = \frac{1-\exp(-\frac{2C_f}{\sqrt{\pi}}\frac{2p}{\eta u_m})}{\frac{2C_f}{\sqrt{\pi}}\frac{2p}{\eta u_m}} \tag{10}$$

$$R(u_n) = \frac{1-\exp(-\frac{2C_f}{\sqrt{\pi}}\frac{2p}{\eta u_n})}{\frac{2C_f}{\sqrt{\pi}}\frac{2p}{\eta u_n}} \tag{11}$$

It is obvious that effectiveness of multipass in which the equability of energy is always kept may be indicated by function R(u). So the function R(u) is defined as multipass function of cut under the condition of equability of energy.

3.0 ANALYSIS AND DISCUSSION

Multipass function R(u) can simply be written as

$$R(u) = \frac{1-e^{-N_3}}{N_3} \tag{12}$$

or

$$R(u) = \frac{u}{c}(1-e^{-c/u}) \tag{13}$$

where

$$N_3 = \frac{2C_f}{\sqrt{\pi}}\frac{2p}{\eta u}, \qquad c = \frac{2C_f}{\sqrt{\pi}}\frac{2p}{\eta}$$

To the same kind of cutting material and same jet pressure, the parameter, c, is a constant. The derivative function of R(u) with respect to u can be obtained when c = constant.

$$\frac{dR(u)}{du} = \frac{1}{c}(1-e^{-c/u} - \frac{c}{u}e^{-c/u}) \tag{14}$$

The curve of function R(u) versus nondimensional number N_3 is plotted in Fig. 4. Clearly, for functions R(u) and dR(u)/du , there are two terminal limit values as is shown in the following:

$$R(u) \to 1, \quad \frac{dR(u)}{du} \to 0, \quad \text{as } N_3 \to 0 \text{ or } u \to \infty$$

$$R(u) \to \infty, \quad \frac{dR(u)}{du} \to \frac{1}{c}, \quad \text{as } N_3 \to \infty \text{ or } u \to 0 \tag{15}$$

The relative error between R(u) and $1/N_3$ can be expresed as:

$$ER_1 = \frac{1/N_3 - R(u)}{1/N_3} = e^{-N_3} \tag{16}$$

Apparently, the limited value of ER_1 when the value of N_3 is approaching to infinity is zero, that is

$$\lim_{N_3 \to \infty} ER_1 = 0$$

Some calculation values of ER_1 are listed in Table 1. We can find that ER_1 is less or equal to 5 per cent when N_3 is greater than or equal to 3.0, and the relative error function, ER_1, decreases progressively with the increase of N_3. Therefore, the function R(u) can be substituted by $1/N_3$ within certain error limits (i.e. $ER_1 \leqslant 5\%$). And then, when $N_3 \geqslant 3.0$, equation (6) can be simplified as

$$\frac{Z}{d} = \frac{2p-\sigma_y}{\eta u} \frac{1}{\frac{2C_f}{\sqrt{\pi}} \frac{2p}{\eta u}} = \frac{\sqrt{\pi}}{2C_f}\left(1-\frac{\sigma_y}{2p}\right) \tag{17}$$

or

$$\frac{2C_f}{\sqrt{\pi}} \frac{Z}{d} = \left(1-\frac{\sigma_y}{2p}\right) \tag{18}$$

Based on general limits of cutting pressure, the jet pressure may be chosen within the range of between $\frac{1}{2}\sigma_y$ and $6\frac{1}{2}\sigma_y$. If so, by means of Eq. (18), the relationship between cutting depth and jet pressure is shown in Fig. 5. Thus, it can be seen that the relation of cutting depth and jet pressure is formulated on non-linear and hyperbolic behaviour when $N_3 \geqslant 3.0$. In this case, the depth of cut has nothing to do with feed rate, and the limited depth, Z, is equal to $\sqrt{\pi}d/2C_f$. The experimental results shown in Fig. 6 (Koji, M., Kirohiko, O., and Cui, M.S., 1987) proved above conclusions. It can be found from Fig. 6 that cutting depth versus jet pressure response characteristic are linear relationship when u is larger, but non-linear when u is smaller. And the curves shape in Fig. 6 are also similar to Fig. 5.

In this time, based on equation (9), the step depths and the cumulative depth of multipass can respectively be expressed as follows:

$$\frac{Z_{n+1}-Z_n}{Z_n} = \frac{R(u_{n+1})-R(u_n)}{R(u_n)} = \frac{1}{n} \tag{19}$$

and

$$\frac{Z_n-Z_1}{Z_1} = \frac{R(u_n)-R(u_1)}{R(u_1)} = n-1 \tag{20}$$

that is $Z_n=Z_1$. This shows that, within certain error limits, $ER_1 \leqslant 5\%$, the multipass at equability of energy mentioned above gets the same effective result as that of at non-equability of energy in which the feed rate of cut keeps constant. The depth of cut increases successively in same quantity with each single pass. That is right away optimum multipass effectiveness.

Now, let's turn to analyse the relative error between R(u) and 1. It can be expressed as

$$ER_2 = \frac{1-R(u)}{1} = \frac{N_3-1+e^{-N_3}}{N_3} \tag{21}$$

Apparently, the limited value of ER_2 is also zero, that is

$$\lim_{N_3 \to 0} ER_2 = \lim_{N_3 \to 0} \frac{N_3-1+e^{-N_3}}{N_3} = 0$$

Some calculation values of ER_2 are listed in Table 2. We can find that $ER_2 \leqslant 5\%$ when $N_3 \leqslant 0.1$, and the relative error function, ER_2, decreases progressively with the decrease of N_3. Therefore, the function R(u) can be replaced by 1 within certain error limits (i.e. $ER_2 \leqslant 5\%$). And then, when $N_3 \leqslant 0.1$, equation (6) can be simplified as

$$\frac{Z}{d} = \frac{2p-\sigma_y}{\eta u} R(u) = \frac{2p-\sigma_y}{\eta u} \tag{22}$$

In this case, the relationship between cutting depth and jet pressure is formulated on linear behaviour, but it is hyperbolic line with feed rate.

From equation (9), we can obtain

$$\frac{Z_n-Z_m}{Z_m} = \frac{R(u_n)-R(u_m)}{R(u_m)} = 0$$

As a consequence, the multipass effectiveness disappeared when $N_3 \leqslant 0.1$ within certain error limits, $ER_2 \leqslant 5\%$.

At last, let's analyse the multipass phenomenon within the range of $0.1 \leqslant N_3 \leqslant 3.0$. Judging by experimental results (Rehbinder, G., 1982), the effective jet pressure for cutting granite (compressive yield strength is about 188 MPa) must exceed 210 MPa, and the optimum pressure limits to be used are about (270 — 320) MPa. So, it means that the optimum pressure is about $p=3\frac{1}{2}\sigma_y$. The figure 7 obtained by measurement for the case of cutting material is limestone (compressive yield strength is about 33 MPa) showed that the specific energy, E, changed with jet pressure. It is found from this figure that there is an optimum jet pressure which makes the specific energy have a minimum value, and the optimum pressure is also about equal to $3\frac{1}{2}\sigma_y$. Similarly, as shown in Fig. 5, the depth of cut increases slowly and the relative consumption of jet power increases quickly with the increase of pressure when the pressure $p \geqslant 3\frac{1}{2}\sigma_y$. Calculated results for some cutting materials are listed in Table 3 as $p = 3\frac{1}{2}\sigma_y$ and $N_3 = 3.0$, 0.1, respectively, which, as a reference, can practically be used to multipass cutting.

From equation (6) and considered $\frac{u_n}{n} \to u_1$, we can easily obtain

$$Z_n - Z_1 = \frac{(2p-\sigma_y)d}{\eta}\,[R(u_n)-R(u_1)]\,\frac{1}{\frac{u_n}{n}} \tag{23}$$

Obviously, under the condition of equability of energy, we have $u_n \geqslant u_1$, so that $(N_3) \leqslant (N_3)_1$ and $R(u_n) \geqslant R(u_1)$. And thus the difference value between cumulative depths of cut, $(Z_n - Z_1)$, increases with the decrease of value . This conclusion was also proved by Fig. 3.

Summarizing above analyses and by facts shown in Eqs. (9)-(15), we can know that multipass effectiveness i.e. the value of $(Z_n - Z_1)/Z_1$ is better when the feed rate is smaller. When $u \leqslant u_{3.0}$ or $n \leqslant u_{3.0}/u_1$, then $N_3 \geqslant 3.0$, so the depth of cut increases at same quantity and the cutting effectiveness is best. But the multipass effectiveness disappears as $u \geqslant u_{0.1}$ or $n \geqslant u_{0.1}/u_1$ and $N_3 \leqslant 0.1$.

4.0 CONCLUSIONS

1. Multipass function of cut under the condition of equability of energy is developed, that is

$$R(u) = \frac{1-\exp\left(-\frac{2C_f}{\sqrt{\pi}}\,\frac{2p}{\eta u}\right)}{\frac{2C_f}{\sqrt{\pi}}\,\frac{2p}{\eta u}}$$

2. The multipass effectiveness is becoming better and better when the feed rate is becoming smaller and smaller or when, in other words, the nondimensional number N_3 is becoming bigger and bigger. The multipass effectiveness is best when $u \leqslant u_{3.0}$ or $N_3 \geqslant 3.0$, and disappears when $u \geqslant u_{0.1}$ or $N_3 \leqslant 0.1$.

5.0 NOMENCLATURE

d = nozzle diameter

p = jet dynamic pressure at nozzle exit

u = feed rate

v = initial jet velocity

Z = depth of cut

C_f = total skin friction coefficient

η = damping coefficient

ρ = density

σ_y = compressive yield strength

6.0 REFERENCES

1. Cheng, D.Z., "The New Technology of Developing High Pressure Water Jet," J. High Preessure Water Jet, No. 1, 1987, (in Chinese).

2. Wang, X.M., "Translation of Cutting Technology Paper," Coal Mechanical Press - Beijing, 1982, (in Chinese).

3. Hashish, M., and Duplessis, M.P., "Theoretical and Experimental Investigation of Continuous Jet Penetration of Solids," Transactions of the ASME, J. Engineering for Industry, Vol. 100, 1978.

4. We, I., and Zhang, Y.T., "Abrasive Water Jet Cutting," J. High Pressure Water Jet, No.2, 1987, (in Chinese).

5. Matsuki, K., and Cui, M.S., "Rock Cutting with High Speed Water Jets both in Air and in Water," proceedings of the international water jet symposium, Beijing, Sept. 1987.

6. Rehbinder, G., "Theory of Cutting Granite with High Pressure Water Jet," J. High Pressure Jet, No. 2, 1982, (in Chinese).

Table 1. Calculation Values of Error Function, ER_1

N_3	2.4	2.6	2.8	3.0	3.2	3.4	3.6	3.8	4.0	4.2	4.4	4.6
ER_1, %	9.07	7.43	6.08	4.98	4.08	3.34	2.73	2.24	1.83	1.50	1.23	1.01

Table 2. Calculation Values of Error Function, ER_2

N_3	0.20	0.15	0.10	0.08	0.06	0.04	0.02
ER_2, %	9.37	7.14	8.48	3.90	2.94	1.97	0.99

Table 3. Calculation Results for Some Materials

Material	σ_y Mpa	C_f	η kg/m²s	p=3½, N_3=0.1		p=3½, N_3=3.0	
				$u_{0.1}$ mm/s	$\frac{Z_{0.1}}{d}$	$u_{3.0}$ mm/s	$\frac{Z_{3.0}}{d}$
Elm	28.1	0.005	3.3×10^9	1.44	11.25	0.05	107.20
Poplar	14.6	0.005	1.73×10^9	1.43	11.23	0.05	106.91
Sugar Maple	31.4	000.5	6.13×10^8	8.67	11.24	0.29	111.88
Limestone	33.0	000.6	8.17×10^7	82	9.37	2.73	93.71
Concrete	25.9	0.01	2.2×10^8	40	5.62	1.33	56.07
Polycarbonate	86.2	0.008	4.7×10^8	50	7.02	1.66	69.98
Coal	6.9	0.008	1.73×10^7	108	7.03	3.60	70.17
White Granite	134.5	0.015	1.37×10^8	498	3.75	16.62	37.42

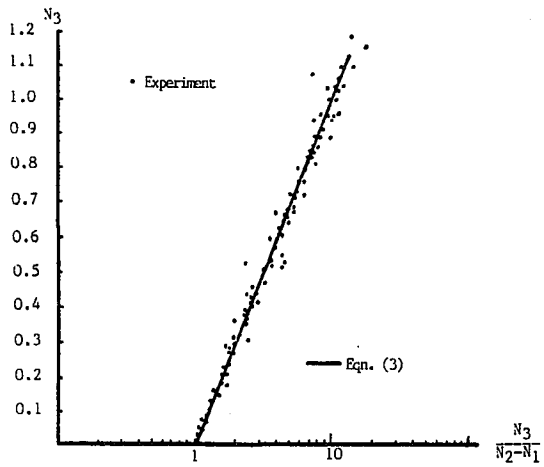

FIG. 1 COMPARISON BETWEEN EXPERIMENTAL RESULTS AND THEORETICAL EQUATION(3)

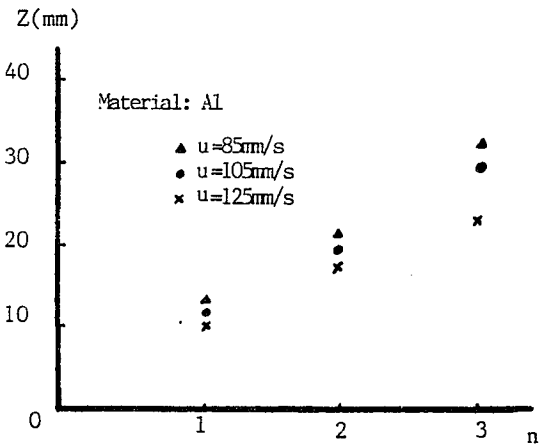

FIG. 2 EXPERIMENTAL RESULTS OF MULTIPASS CUTTING

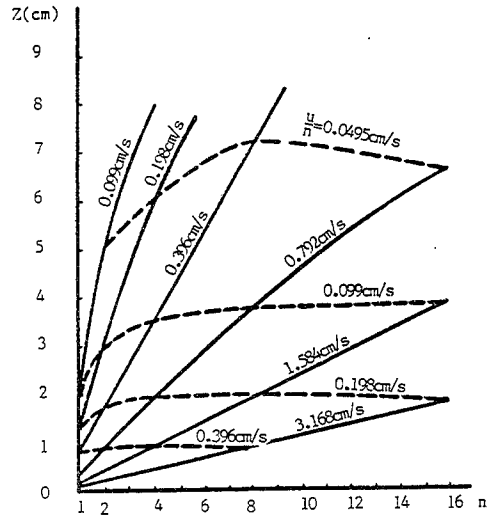

FIG. 3 CURVES OF MULTIPASS CUTTING

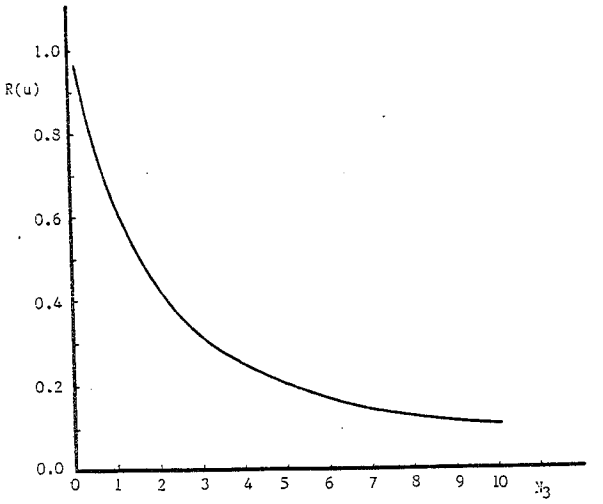

FIG. 4 CURVE OF MULTIPASS FUNCTION

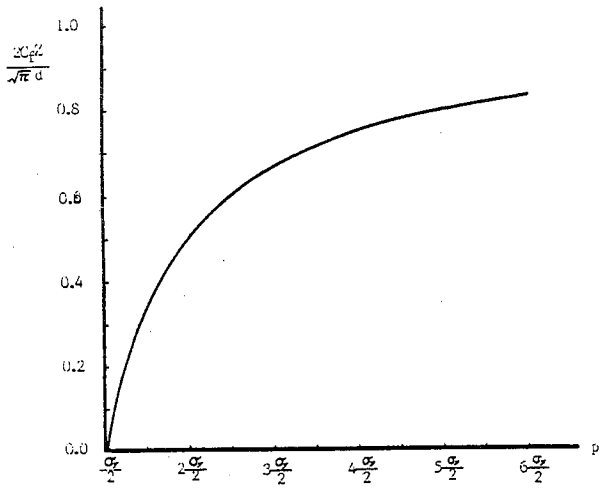

FIG. 5 CUTTING DEPTH VARYING WITH PRESSURE FOR $N_3 \geq 3.0$

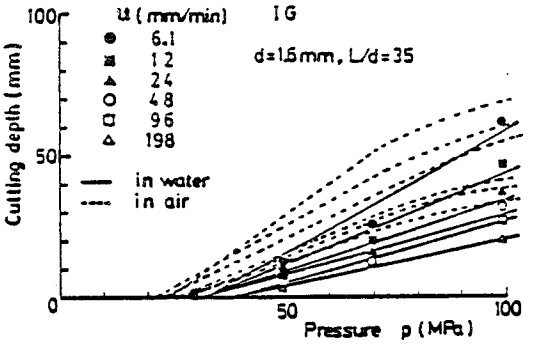

FIG. 6 EFFECT OF PRESSURE AND FEED RATE ON CUTTING DEPTH

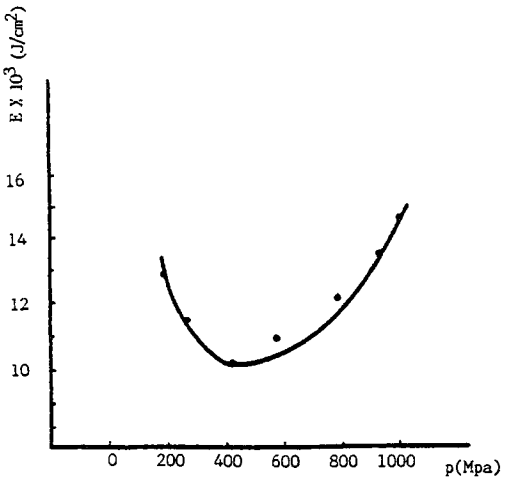

FIG. 7 SPECIFIC ENERGY AS A FUNCTION OF PRESSURE

5th American Water Jet Conference
August 29 - 31, 1989: Toronto, Canada

Paper / Communication 38

RESEARCH ON THERMAL PERFORMANCE OF HIGH PRESSURE ROTARY SEALS

Z. Chen AND J. Yang
Hei Long Jiang Institute of Mining
Jixi City, Hei Long Jiang Province, China

ABSTRACT: This paper deals with the thermal performance of high pressure seals. Two kinds of sealing materials chosen are packing polytetrafluoroethylene(PTFE) and nylon. Temperature distribution along sealing chamber has been measured for the two kinds of sealing materials and changing rules of temperature field in the center of sealing parts have been calculated by the heat - transfer theory. Changing rules of temperature with pressure and heat - durability of sealing materials are analyzed. Theoretical bases are provided for selecting materials. Therefore, when sealing materials are chosen, they must have characteristics of resistance to wear, thermal stability and anti-maturity.

RÉSUMÉ : Cette communication traite de la performance thermique de deux matériaux pour joints sous pression élevée, le polytétrafluoroéthylène (PTFE) et le nylon. La répartition des températures dans la chambre d'isolation a été mesurée pour les deux matériaux, et les régimes variables du champ de température au centre des joints ont été calculés par la théorie des transferts de chaleur. Les régimes variables de température en fonction de la pression et la durabilité thermique des joints sont analysés. Des bases théoriques sont présentées pour le choix des matériaux. Les matériaux choisis doivent donc avoir des propriétés de résistance à l'usure, de stabilité thermique et de non-vieillissement.

Organized and Sponsored by the National Research Council of Canada and the U.S. Water Jet Technology Association.

1.0 INTRODUCTION

High pressure rotary sealing device(swivel) is the important part on water jet tunneling and drilling machine , which plays a role in linking rotary parts with stationary parts . If the seal of swivel ceases to be effective , there will be bad effects on normal operation and working life of machine , such as tunneling machine and driling machine .

With its development , high pressure water jet technology has been applied in coal, petroleum and drilling technology gradually. High pressure rotary seal is one of the critical problems met in this technology. This paper deals with the thermal performance of rotary sealing materials with sealing diameter 30 mm under a certain pressure

Packing PTFE and nylon are used for rotary sealing materials[1, 2, 3]. Most non-metallic materials , such as plastics , nylon and polymers , are characteristic of , softening or melting when heated , hardening after cooled , and this prcess can be repeated . The stability of materials are easily affacted by temperature. Under the action of high pressure and high temperature , plastic flow or deformation will take place on the materials so-called , 'creep'.

Therefore , temperature measurement and theoretical calculation for sealing materials are made so as to analyse the heat-durability of sealing materials .

Thermal stability of sealing materials is not ideal through experiments . For the rotary shaft revolution of 745 rpm. , under the action of the working pressure of 350 bars , after continous operation for 1.5 hours , sealing materials will occur in heat-deformation and working life of sealing materials would be affacted seriously. It is necessary that thermal performance be analized by temperature measurement and theoretical calculation .

2.0 PRINCIPLE AND METHOD OF TEMPERATURE MEASUREMENT

We use thermocouple to measure the temperature of sealing parts . Thermocouple has higher accuracy for temperature measurement . Thermocouple has the ability of remote-transfer of signals and multipoint on-off measurement since it can change temperature signal into electronic signal . Chomel-copper thermocouple is chosen for measurement . It is an inexpensive metallic thermocouple . Thermoelectrical potential rate of the thermocouple is bigger than other usual thermocouples . So it is often used to measure temperature .

In order to measure temperature , first of all , Fourier's law is introduced (see Fig.1) [4] .

$$Q=-\lambda F\frac{\partial t}{\partial x} \qquad (1)$$

Q: Heat quantity of transfer (W)

λ: Coefficient of heat conductivity (W/m · ℃)

$\frac{\partial t}{\partial x}$: Gradient of temperature (℃/m)

F: Surface area (m^2)

Thermal formula of unit lenth is derived from equation(1)(see Fig.2) for single layer cylindrical wall.

$$Q=\frac{2\pi\lambda(t_1-t_2)}{\ln(r_2/r_1)} \qquad (2)$$

As shown above , thermal formula of unit lenth is derived (see Fig.3) for multi-layer cylindrical wall .

$$Q=\frac{2\pi(t_1-t_4)}{\ln(r_2/r_1)/\lambda_1+\ln(r_3/r_2)/\lambda_2+\ln(r_4/r_3)/\lambda_3} \qquad (3)$$

As shown in Fig.1 , holes are drilled on the sealing body . There are six hohes at three different positions on the body. Two holes are not the same in depth on the same circumference. Diameter of hole is 2 mm so that temperature values can be easily calculated.

3.0 EXPERIMENTAL APPARATUSES AND MEASUREMENT PROCEDUCE

Experimental apparatuses include WKZ-122 immersion type multipoint on-off switch , UJ33a portable D.C. potentiometer , thermometer and stopwatch (see Fig.5) .

Relative voltage values produced by thermocouple and room temperature are measured by experimental apparatuses at the same time . then relative voltage values are changed into absolute voltage values . Temperature values have been consulted according to absolute voltages of chomel-copper thermocouple and temperature contrast table . [5, 6]

Our purpose is to measure the temperature of sealing parts . From the structure of seal , it is equal to the heat-transfer of multi-layer cylindrical wall . Thus , the thermal flow rates of every measuring points are calculated by formula (2) at first . Because the thermal flow rates are equal along the radial flow .

$$Q=\frac{2\pi\lambda(t_1-t_2)}{\ln(r_2/r_1)}$$

t_1 , t_2 : Temperature values measured
r_1=22 mm , r_2=32 mm
λ : Coefficient of heat conductivity of the body (49.8W/m · ℃)
The temperature values (T_1, T_2, T_3) of internal diameter of the body are calculated by formula (2) after thermal flow rates have been calculated

4.0 RESULTS OF MEASUREMENT AND ANALYSES

Temperature of sealing parts for two kinds of sealing materials has been measured respectively. Temperature with the pressure , temperature with time and temperature under the condition of equilibrium have been obtained .

The pressure selected are 50 bars , 100 bars , 150 bars , 200 bars , 300 bars and 350 bars . According to the measurement results , temperature values produced by two kinds of sealing materials are equal on the whole in operation. Therefore , nylon material is discussed . Pressure , time , temperature and thertmal flow rate have been measured for the nylon material after equiliberium temperature (see Table 1 , Table 2 , Table 3) .

In order analyze thermal performance of seal , Fig.6 shows the relations between temperature and pressure for measuring points 1 , 2 and 3 . From Fig.6 , the changes of temperature increase with pressure increment .

Fig.7 shows the relations between temperature and time (pressure is constant) for measuring point 2 in the course of equiliberium temperature . The pressure of curves 1 , 2 and 3 are 100 bars , 200 bars and 300 bars respectively . From the changing rules of the curves , temperature of sealing parts reaches maximum with some time and equiliberium temperature after a few minutes . Because decrease of leakage rates has resulted in maximum temperature in operation . Owing to decrease of leakage rates . Heat quantity taken away by leakage is decreased , thus resulting in increase of temperature .

Temperature field distribution along the center of sealing part is calculated by formula (3)

For measuring point 1 :
Coefficient of heat conductivity of nylon
λ_1=0.34W/m · ℃
Coefficient of heat conductivity of water
λ_2=212W/m · ℃
r_1=15 mm , r_2=16 mm , r_3=19 mm
Pressure : P=350 bars
T_1=43.79℃ , Q_m=475.62 W

$$Q_m=\frac{2\pi(T_1in-T_1)}{\ln(r_3/r)/\lambda_1+\ln(r_3/r_2)/\lambda_2}$$

Thus : $T_1in=222.68(2.97-\ln r)$ (4)
($15 < r < 16$)

For measuring point 2 :
Coefficient of heat conductivity of nylon
λ_1=0.34W/m · ℃
Coefficient of heat conductivity of rubber
λ_2=0.29W/m · ℃
r_1=15 mm , r_2=16 mm , r_3=19 mm
Pressure : P=350 bars
T_2=43.84℃ , Q_m=846.55W

$$Q_m=\frac{2\pi(T_2in-T_2)}{\ln(r_3/r)/\lambda_1+\ln(r_3/r_2)/r_2}$$

Thus : $T_2in=396.30(3.08-\ln r)$ (5)
($15 < r < 16$)

For measuring point 3
Coefficient of heat conductivity of nylon
λ_1=0.34W/m·℃
r_1=15 mm , r_2=19 mm
Pressure : P=350 bars
T_r=44.54℃ , Q_n=802.15W

$$Q_n=\frac{2\pi(T_1in-T_r)}{\ln(r_2/r)/\lambda_1}$$

Thus : $T_1in=375.68(3.06-\ln r)$ (6)
$(15 \leq r < 19)$

Temperature distribution along the center of sealing part can be seen in Fig.8 . Curve 1 shows temperature distribution of section 1-1 .Curve 2 shows section 2-2 . Curve 3 shows section 3-3 . Temperature produced by sealing part in the section 2-2 is 147℃ and temperature of the area is maximum when working pressure is 350 bars . From pressure measurement , the area is that pressure drop is biggest and wear is most serious .Therefore , sealing part will produce heat-deformation at high temperature [7] . From the experiment , when rotary sealing device works continuosly for 1.5 hours , the seal has high leakage and performance of the seal is good after stopping for a certain time . That has shown thermal stability of the sealing material is not good , producing heat-deformation , resulting in ineffect .

As shown in Fig.9 , total heat quantity produced by sealing part is shown by equation (7)

$$Q=Q_1+Q_2+Q_3+Q_4 \quad (7)$$

Q_1 : Heat dissipating capacity of radial direction and obtained by measurement

Q_2 , Q_3 : Heat dissipating capacity of axial direction and nelected .

Q_4 is heat quantity taken away by leakage water and very large . But according to modern measurement method it is difficult to measure the heat quantity for the seal of the structure accurately . Because temperature of internal diameter for sealing part comes to maximum of 147℃ , when leakage water goes through sealing part , water will be steamed and gas bubble will be produced . The phenomenon is called 'conduit steaming' The clearance between sealing part and shaft can be called heat pipe .

The flow velocity of liquid affacts the steaming course . When liquid acted under the pressure difference makes gas bubble and liquid flow together, thus , complicated gas-liquid two-phase flow is formed

It is confirmed that actual temperature of internal diameter for sealing part is larger than temperature calculated because many factors are neglected in the course of measurement , and the changes of leakages result in the complexity of temperature changes.

5.0 CONCLUSIONS

1.0 : Through the experiment , the smaller the measuring temperature hole , the more accurate temperature measurement . But the measuring temperature hole is too small and thermocouple wires would not be put into it

2.0 : Temperature changes for sealing material increase with pressure increment gradually .

3.0 : Temperature distribution along axial direction for sealing part tends to be uniform .

4.0 : Decrease of leakage rates has resulted in temperature maximum in operation .

5.0 : Temperature produced by sealing part in the section 2-2 is maximum . From pressure measurement , pressure gradient is biggest , wear is most serious and damage is most quick at section 2-2

6.0 : From the experiment , when rotary sealing device works continuously for 1.5 hours , sealing part will produce heat-deformation . That has shown thermal stability of the sealing .

7.0 : When sealing materials are chosen , they must have characteristics of resistance to wear, good thermal stability , good heat dissipating and anti-maturity , making them have longer working life .

6.0 : ACKNOWLEDGEMENTS

The authors would like to thank Professor Sun Jiajun and Mr.Guo Chuwen for various assistance .

7.0 : REFERENCES

1. : Gong Yunbiao , Shi Anfu《Polymer Sealing Materials》
2. :《Solid Anti-Wear Materials》Published by Mechanical Engineering Industry Press
3. : I.M. Ward < Mechanical Properties of Solid Polymers》Second Edition
4. : Yang Shiming 《Heat Transfer》
5. : Ye Dajun 《Measurement Technology on Thermal Machine》
6. : Wu Yongsheng , Fang Keren 《Thermal Measurement and Gauges》
7. : H.D. Harris , 'An Elastohydrodynamic Analysis of the Sleeve Type High Pressure Seal' ASME Paper 72-Lub-M .

Table 1 Measuring point 1

Pressure (bars)	Time (min)	Temperature(T_1) (℃)	Thermal Flow Rate(Q_{n1}) (W)
50.00	29.09	27.24	25.04
100.00	28.37	27.56	95.11
150.00	35.59	31.15	168.55
200.00	51.38	37.98	240.37
300.00	31.48	39.84	381.51
350.00	42.15	43.19	475.62

Table 2 Measuring point 2

Pressure (bars)	Time (min)	Temperature(T_2) (℃)	Thermal Flow Rate(Q_{n2}) (W)
50.00	28.30	27.59	75.12
100.00	29.30	27.73	168.33
150.00	37.01	31.40	350.42
200.00	52.24	39.98	420.31
300.00	32.43	40.92	730.35
350.00	42.41	43.84	846.55

Table 3 Measuring point 3

Pressure (bars)	Time (min)	Temperature(T_3) (℃)	Thermal Flow Rate(Q_{n3}) (W)
50.00	28.36	27.45	83.47
100.00	29.00	28.13	180.51
150.00	36.25	32.09	320.42
200.00	53.32	39.75	640.53
300.00	32.16	40.78	770.43
350.00	43.04	44.54	802.15

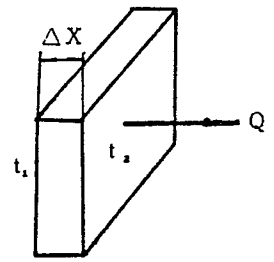

Fig.1 Schema of heat-transfer

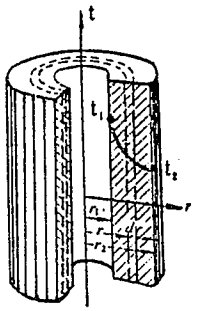

Fig.2 Single layer cylindrical wall

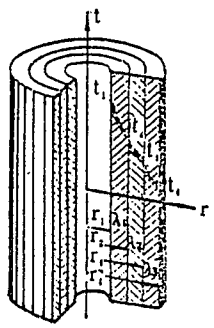

Fig.3 Multi-layer cylindrical wall

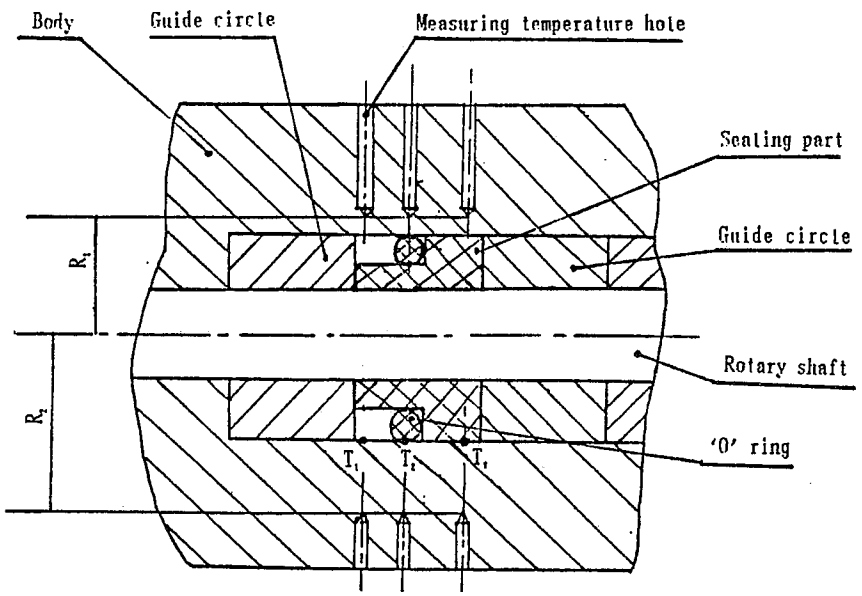

Fig.4 Schema of sealing structure

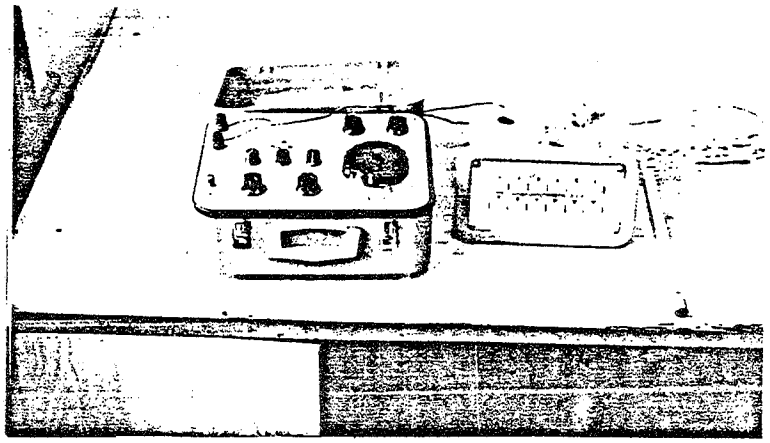

Fig.5 Measuremement apparatuses

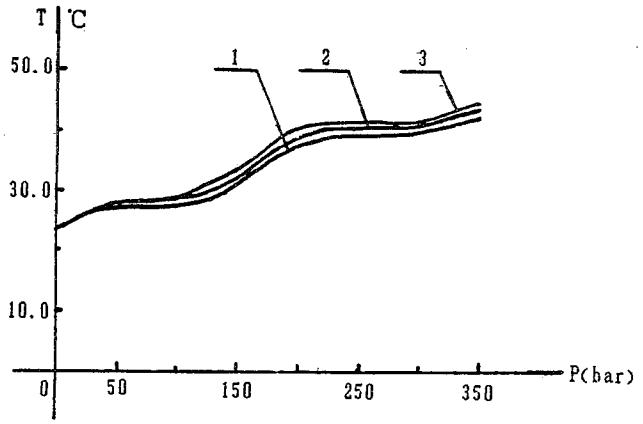

Fig.6 Relations between temperature and pressure for measuring points 1, 2 and 3

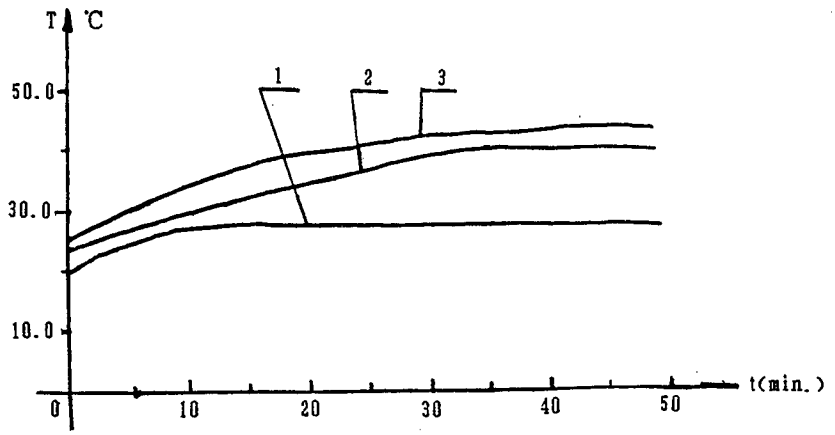

Fig7.Relations between temperature and time(pressure is constant) for measuring point 2 in the course of equiliberium temperature

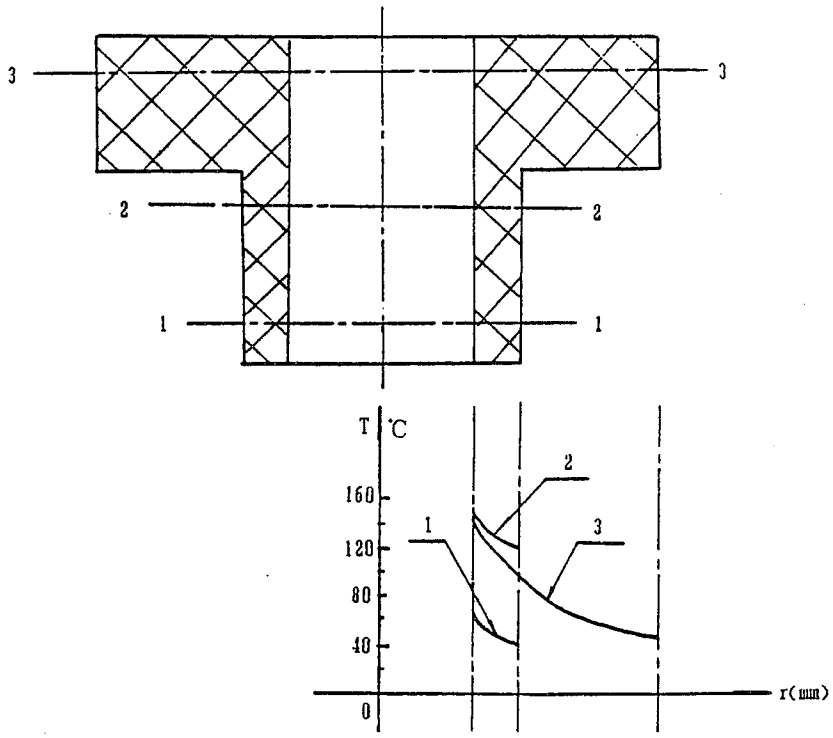

Fig. 8 Temperature distribution along the center of seating part

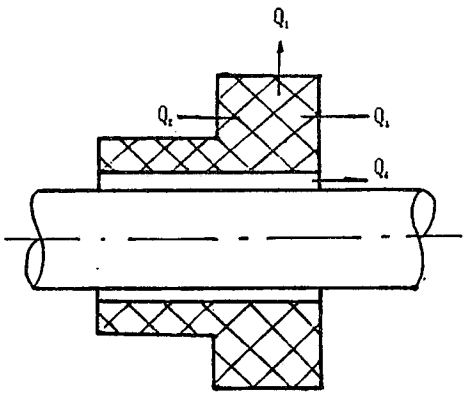

Fig. 9 Schema of analysis on heat quantity

5th American Water Jet Conference
August 29 - 31, 1989: Toronto, Canada

Paper / Communication 39

STUDIES OF HIGH VELOCITY JETS IMPINGING ON A FLAT PLATE

G. Wu, Z. Jing, S. Zhong
Department of Power Engineering
Shanghai Institute of Mechanical Engineering
Shanghai 200093, China

ABSTRACT: A numerical procedure for predicting the contour and the pressure distribution of high velocity jets impinging on a flat plate is presented in this paper. The finite difference method is used to solve the N – S equations combined with a simplified $k - \epsilon$ model for the free jet in order to obtain the impact velocity distribution. The one-dimensional impact equation is then employed in calculating the impact pressure.
To verify the results of theoretical analysis, experiments were conducted on a high velocity water jet cutting device. Both the working pressure at nozzle exit and the jet flowrate are adjustable through a control valve. The nozzle pressure and impact pressure were measured with a Bourdon pressure sensor and a pressure transducer respectively. A number of combinations of the nozzle diameter and the stand-off distance were examined in the experiments. The jet velocity at nozzle exit was up to 300 m/s. The experimental results show that the measured data and the computed results are in a reasonable agreement.

RÉSUMÉ : Cette communication décrit une méthode numérique de prévision de la forme et de la distribution de pression des jets à grande vitesse sur une surface plane. La méthode des différences finies est utilisée pour résoudre les équations N – S pour un modèle $k - \epsilon$ simplifié du jet libre et obtenir la distribution de vitesse d'impact. L'équation d'impact à une dimension est ensuite utilisée pour calculer la pression d'impact.
Pour vérifier les résultats de l'analyse théorique, des expériences ont été menées sur un dispositif de coupe par jet d'eau à grande vitesse. Un robinet de commande permet de régler la pression à la sortie de la buse et le débit du jet. La pression à la buse et la pression d'impact ont été mesurées avec un capteur de pression de Bourdon et un transducteur de pression respectivement. Les expériences ont été répétées avec différentes combinaisons diamètre de la buse-distance de garde. La vitesse du jet à la sortie de la buse a atteint 300 m/s. Les résultats des expériences montrent que les données mesurées et les résultats calculés concordent assez bien.

Organized and Sponsored by the National Research Council of Canada and the U.S. Water Jet Technology Association.

1.0 INTRODUCTION

The fluid dynamics of a free jet impinging on a flat plate surface is basic to the study of jet cutting technology. On examination of the literature, quite a few numerical procedures have been proposed to predict the pressure distribution over a flat plate target. It is considered that when the impact velocity is higher than a certain value, high transient pressure will be generated on the solid surface because of the compressible deformation of the water jet front. Field et al [1] have reported that the initial peak impact pressure is dependent on the shape of the jet front. Impact pressure-time curves at different impact velocities and angles of incidence were experimentally obtained in their studies. Heymann [2] has found that the peak impact pressure resulted from the compressible flow depends on the velocity of compression wave, and in turn on the jet velocity. A numerical procedure which allows solution of the Navier-Stokes equations in conjunction with a two-equation turbulent model was presented by Amano et al [3]. With special treatments to a wall function, the pressure distribution and velocity profile in a free jet were then calculated. Huang et al [4] first studied the unsteady, two-dimensional liquid-solid impact phenomena numerically and reasonably succeeded.

This paper presents a relatively simple numerical procedure for predicting both the contour and pressure distribution of the high velocity jet impinging on a flat plate. The computation includes two steps: by solving the N-S equations combined with a simplified turbulent k-ε model for a free jet, the velocity distribution at different stand-off distances is computed; on the basis of obtained jet velocity profile, the impact pressure can then be calculated through the one-dimensional impact equation. To verify the validity of the present procedure, experiments were performed in the Hydraulics Laboratory of the Shanghai Institute of Mechanical Engineering (SIME). The experimental results show a reasonable agreement with the calculated ones.

2.0 NOMENCLATURE

C_1, C_2, C_μ	=	coefficients in turbulence model
d	=	nozzle exit diameter
k	=	turbulent kinetic energy
p	=	pressure
p_r	=	reservoir pressure
r	=	radial coordinate
x	=	coordinate parallel to nozzle axis
u	=	velocity in x direction
v	=	velocity in r direction
s	=	stand-off distance (nozzle-to-plate distance)
ρ	=	fluid density
μ_T	=	turbulent viscosity
ε	=	turbulence energy dissipation rate
σ_k, σ_ε	=	turbulent Prandtl numbers for diffusion of k and ε respectively
ψ	=	stream function
p'	=	impact pressure
ρ'	=	fluid density at impact pressure
C', C_o	=	impact velocity and sonic velocity respectively

Subscripts

D	=	downstream nodes of the grid network at x along a streamline
D_+, D_-	=	upper and lower nodes of D at x
E	=	outer boundary of the jet
I	=	inner boundary of the jet
U	=	upstream nodes of the grid network at $x-\Delta x$ along a streamline
U_+, U_-	=	upper and lower nodes of U at $x-\Delta x$

3.0 THEORETICAL ANALYSIS

3.1 Governing Equations

Considering the free turbulent jet process, a k-ξ model is used as it appears to be more realistic than the other two-equation models [5]. In order to analyse the jet flow mathematically, the following assumptions are made:

(1) two-dimensional, steady and turbulent flow with homogeneous fluid density;

(2) body forces can be neglected.

The equation of motion under the above assumptions, in a coordinate system where r is the radial coordinate, and x is the axial coordinate, becomes

$$\frac{1}{r}\left[\frac{\partial}{\partial x}(\rho uur)+\frac{\partial}{\partial r}(\rho uvr)\right]=\frac{\partial}{\partial r}\left(r\mu_T\frac{\partial u}{\partial r}\right)-\frac{dp}{dx} \tag{1}$$

The continuity equation is

$$\frac{\partial}{\partial x}(\rho ur)+\frac{\partial}{\partial r}(\rho vr)=0 \tag{2}$$

Turbulent kinetic energy equation:

$$\frac{1}{r}\left[\frac{\partial(k\rho ur)}{\partial x}+\frac{\partial(k\rho vr)}{\partial r}\right]=\frac{1}{r}\frac{\partial}{\partial r}\left(\frac{r\mu_T}{\sigma_k}\frac{\partial k}{\partial r}\right)+\mu_T\left(\frac{\partial u}{\partial r}\right)^2-\rho\varepsilon \tag{3}$$

Turbulent energy dissipation equation:

$$\frac{1}{r}\left[\frac{\partial(\varepsilon r\rho u)}{\partial x}+\frac{\partial(\varepsilon r\rho v)}{\partial r}\right]=\frac{1}{r}\frac{\partial}{\partial r}\left(\frac{r\mu_T}{\sigma_\varepsilon}\frac{\partial\varepsilon}{\partial r}\right)+C_1\frac{\varepsilon}{k}\mu_T\left(\frac{\partial u}{\partial r}\right)^2-C_2\frac{\rho\varepsilon^2}{k} \tag{4}$$

Turbulent viscosity hypothesis:

$$\mu_T=C_\mu\rho\frac{k^2}{\varepsilon} \tag{5}$$

where coefficients C_1, C_2, C_μ, σ_k and σ_ε are empirical constances [6]. Their values taken in this paper are $C_1 = 1.44$; $C_2 = 1.92$; $C_\mu = 0.09$; $\sigma_k = 1.0$ and $\sigma_\varepsilon = 1.0$ respectively.

Then we introduce a stream function ψ which satisfies

$$G_1=\rho u=\frac{1}{r}\frac{\partial\psi}{\partial r} \tag{6}$$

$$G_2 = \rho v = -\frac{1}{r}\frac{\partial \psi}{\partial r} \tag{7}$$

Equations (1) through (5) can be written in the following general expression:

$$\frac{\partial \phi}{\partial x} + (a + br)\frac{\partial \phi}{\partial r} = \frac{\partial}{\partial r}\left(c\frac{\partial \phi}{\partial r}\right) + \frac{\Phi}{G_1} \tag{8}$$

where

$$a = -\frac{1}{\psi_E - \psi_I}\frac{d\psi_I}{dx} \tag{9}$$

$$b = -\frac{1}{\psi_E - \psi_I}\frac{d(\psi_E - \psi_I)}{dx} \tag{10}$$

$$c = \frac{r\mu_T}{\sigma_\phi(\psi_E - \psi_I)} \tag{11}$$

ϕ represents u, v, k, ε, etc. The corresponding Φ are listed in Table 1.

Table 1. Correspoding Φ for given ϕ

ϕ	Φ
u	$-\frac{dp}{dx}$
k	$\mu_T(\frac{\partial u}{\partial r})^2 - \rho\varepsilon$
ε	$C_1\frac{\varepsilon}{k}\mu_T(\frac{\partial u}{\partial r})^2 - C_2\rho\frac{\varepsilon^2}{k}$

3.2 Numerical Procedure

Basic equation (8) will be solved by use of finite difference approximation. For the purpose of the derivation of the finite difference equation, we shall suppose that the flow field has been covered by a grid network, and the nodes of the finite difference grid correspond with the intersections of the grid lines (see Fig.1). Here U and D refer to the upstream and downstream nodes of a portion of the grid at a given x respectively, and symbols + and - indicate the upper and lower neighbouring nodes. To use the step-by-step forward integration, the values ϕ are assured known at the upstream nodes.

Equation (8) may be integrated over the indicated portion of the grid. The left-hand side of it can be written as

$$\left\{\int_{x_U}^{x_D}\int_{r_1}^{r_2}\left[\frac{\partial \phi}{\partial x} + (a + br)\frac{\partial \phi}{\partial r}\right]drdx\right\} / (x_D - x_U)(r_2 - r_1)$$

where the finite difference approximations may be made:

$$\int_{x_U}^{x_D}\int_{r_1}^{r_2}\frac{\partial \phi}{\partial x}\,drdx = \int_{r_1}^{r_2}(\phi_D - \phi_U)dr \approx (\phi_D - \phi_U)(r_2 - r_1)$$

$$\int_{x_U}^{x_D}\int_{r_1}^{r_2} a\frac{\partial\phi}{\partial x}\,dr\,dx \approx \frac{1}{4}a_U(\phi_{D+} + \phi_{U+} - \phi_{D-} - \phi_{U-})(x_D - x_U)$$

$$\int_{x_U}^{x_D}\int_{r_1}^{r_2} br\frac{\partial\phi}{\partial r}\,dr\,dx \approx \frac{1}{4}b_U(\phi_{D+} + \phi_{U+} - \phi_{D-} - \phi_{U-})(r_1 + r_2)$$

Thus, this side of Eq. (8) can be reduced to

$$g_1\phi_{D+} + g_2\phi_D + g_3\phi_{D-} + g_4$$

where the values of g_i (i = 1, 2, 3, 4) can easily be calculated from the known coefficients and values of ϕ and ψ at x_U.

Likewise, the finite difference expression of the right-hand side of Eq. (8) may be given as

$$[(c_{U+} + c_U)(\phi_{D+} - \phi_D)/(r_{D+} - r_D) - (c_U + c_{U-})(\phi_D - \phi_{D-})/(r_D - r_{D-})]/(r_{D+} - r_{D-})$$
$$+ (\mathfrak{T}/G_1)_U + [\frac{\partial}{\partial\phi}(\mathfrak{T}/G_1)]_U(\phi_D - \phi_U)$$

Combining both sides shown above yields the finite difference equation corresponding to Eq.(8), which may be further reduced to

$$\phi_D \approx A\phi_{D+} + B\phi_{D-} + C \tag{12}$$

where A, B and C can also be calculated from the known values. Finally the linear equations (12) are solved by use of the tri-diagonal matrix algorithm (TDMA).

3.3 Boundary Conditions

The boundary conditions for the jet impinging on a flat plate are shown in Fig.2. The boundary E is an external free boundary where the time-average shear stress and velocity may be assumed to be zero, and thus the turbulent kinetic energy k and eddy viscosity ε vanish there. Therefore, the conditions on the boundary E ($r = r_E$) are given as

$$u = 0, \quad k = 0, \quad \varepsilon = 0 \tag{13}$$

The symmetrical axis of the jet I is considered to be the internal boundary where the derivatives of u, k and ε with respect to r are all equal to zero. Thus, the conditions on the boundary I (r = 0) are written as

$$\frac{\partial u}{\partial r} = 0, \quad \frac{\partial k}{\partial r} = 0, \quad \frac{\partial\varepsilon}{\partial r} = 0, \quad v = 0 \tag{14}$$

In addition, the velocity profile at the nozzle exit (x = 0) can be regarded as uniform. Thus, we obtain

$$u \approx \text{constant}, \quad v = 0 \tag{15}$$

In the computation, ψ_I and ψ_E , which are functions of x, should be selected carefully. It is convenient that ψ_I is taken as a constant so that ψ_E equals ψ_I plus flowrate.

3.4 One-dimensional Impact Equation

Considering the fact that the high velocity of the jet impinging on the target and the steep velocity gradient near the outer boundary play a more important role than the pressure gradient, the later term in Eq. (1) may be regarded as negligible. When the impact velocity is not high enough, the jet flow is considered to be incompressible. However, the compressibility of the flow has to be taken into account in the computation when the velocity is increased up to a certain level. So far, it is still difficult to determine at which velocity the shock wave will occur. The following one-dimensional impact equation [7] will be used in the calculation:

$$p' = \rho' C' u \tag{16}$$

where p' is the impact pressure, ρ' is the fluid density at p', and C' is a velocity constant related to the impact velocity.

When the impact velocity is lower than 600 m/s, C' and ρ' can be given as follows

$$C' = 0.5u \; ; \qquad \rho' = \rho_o \tag{17}$$

where ρ_o is the density of water just before impinging on the target. Thus, p' becomes the stagnation pressure along the centerline of the jet.

When the impact velocity is between 600 and 1000 m/s, the value of C' is taken as

$$C' = C_o \tag{18}$$

where C_o is the sonic velocity.

When the impact velocity is higher than 1000 m/s, the following approximate equation is suggested [8]:

$$\frac{C'}{C_o} = 1 + 2\frac{u}{C_o} - 0.1\left(\frac{u}{C_o}\right)^2 \tag{19}$$

In addition, an equation of state [9] should be used in the calculation, which is as follows

$$\frac{p'+m}{m} = \left(\frac{\rho'}{\rho_o}\right)^n \tag{20}$$

where m and n are empirical coefficients depending on the flow temperature. We take m = 300 MPa and n = 7 at 20°C as recommended by Cole [10].

4.0 EXPERIMENTS

A small high velocity jet cutting system was employed for the investigation of the jet impinging on a flat plate target for the case of velocities ranging from 30 to 300 m/s. Fig.3 shows the experimental arrangement schematically. The reservoir pressure, which can be pumped up to desired levels, such as 5, 10, 20 and 30 MPa, was measured with a Bourdon pressure sensor. The jet leaving the nozzle and impinging on the target was quasi-steady in nature. The pressure at nozzle exit and

thus the jet flowrate were adjusted through a control valve. The maximum exit pressure in the experiments was approximately 30 MPa, and the maximum flowrate 1 l/min.

The impact pressure was measured by means of a piezoelectric pressure transducer rigidly attached to the back side of the target (see Fig.3). The transducer, which was arranged in alignment with the nozzle axis, sensed the impact pressure of the jet impinging on the target through a small hole on it. The output from the transducer was displayed and recorded on the secondary instruments.

Because of the small diameter and high kinetic energy of the jet, no velocity measuring device was placed in the jet. Therefore, the nozzle exit velocity determined for the experiments was essentially a calculated velocity on the basis of the measured reservoir pressure. The one-dimensional energy equation taking both the frictional and minor losses produced in the supply pipe and nozzle combination into account was used to calculate the velocity. In these experiments, the fluid used was filtered running water. The target in each experiment was a plexiglass flat plate. A number of combinations were examined through variations of the nozzle exit diameter of 0.3 and 0.5 mm and the stand-off distance in the range of 50 to 180 mm.

5.0 RESULTS AND DISCUSSION

Fig.4 shows the computed velocity profiles at different stand-off distances which were taken as the impact velocity distributions in the calculation of the impact pressure. It can be seen that the velocity profiles computed from the simplified $k-\varepsilon$ model proposed by the authors are quite flat across almost the entire jet cross section, except in the vicinity of the outer boundary where the velocity gradients are steep. Fig.5 illustrates the relations between the impact pressure and the dimensionless stand-off distance s/d, here d is the nozzle exit diameter, at different reservoir pressures. Since the the velocity of the jet in each experiment was lower than 300 m/s, the impact pressure was considered to be the stagnation pressure as mentioned earlier. The calculated results present good agreement with the measured data. It is to be noted that the impact pressure p' is remarkably influenced by the stand-off distance s. The impact pressure decreases rapidly with the increase of the dimensionless stand-off distance s/d. Furthermore, the impact pressure reduces at a higher rate when s/d is greater than 600 than when $s/d < 600$. In the range of $0 < s/d < 600$, an empirical formula for predicting the impact pressure from the reservoir pressure, which was based upon the experimental data, is recommended as follows

$$p' = (0.75 \sim 0.85)\ p_r \tag{21}$$

The relationships between the impact pressure and the nozzle exit velocity are plotted in Fig.6. It can be seen that the nozzle exit velocity has a great influence upon the impact pressure. A comparison of the computed results with the experimental data shows that they are in a good agreement.

Since the limitation of the experimental device, the results calculated from Eqs. (16), (18) and (19) for the impact velocity higher than 600 m/s were compared with the existing experimental data presented by Davies et al [11] and Watson, et al [12]. It is shown that they are in a qualitative agreement. The deviation might indicate that some corrections for the coefficients in these equations ought to be made. More investigations are needed before the more results are given.

6.0 CONCLUSIONS

1. A new numerical procedure for predicting the behaviors of the high velocity jet impinging on a flat plate, which combines the solutions of the full Navier-Stokes equations in conjunction with a simplified $k - \varepsilon$ turbulence model by using the finite difference method with solving the one-dimensional impact equation, is presented in the paper. The results computed by the present procedure show a reasonable agreement with the experimental data.

2. The piezoelectric pressure transducer can be used to indicate the impact pressure with a satisfactory accuracy. It has been found that the impact pressure decreases with the increase of the stand-off distance more quickly when the dimensionless ratio $s/d > 600$ than when $s/d < 600$. An empirical formula for evaluating the impact pressure from the reservoir pressure is also suggested by the authors.

3. It appears that the present numerical method has potential for investigating the turbulent free jet process. Because of the limitation of the experimental set-up, however, more investigations should be made before more results are presented.

The authors wish to express their thanks to the staff at the Hydraulics Laboratory, SIME.

7.0 REFERENCES

1. Field, J.E., et al: "On Erosion by Liquid and Solid Impact." In: Proc. 6th Int. Conf., 1983, p. 9.
2. Heymann, F.J.: "On the Shock Wave Velocity and Impact Pressure in High Speed Liquid Impact." In: Trans. ASME, J. of Bas. Eng., 1968.
3. Amano, R.S., et al: "A Numerical and Experimental Investigation of High-Velocity Jets Impinging on a Flat Plate." In: 6th Int. Symp. on Jet Cutting Tech., 1982, p. 19-99.
4. Huang, Y.C., et al: "Hydrodynamic Phenomena During High Speed Collision Between Liquid Droplet and Rigid Plane." In: Trans. ASME, June 1973, pp. 276-294.
5. Spalding, D.B.: "Concentration Fluctuation in a Round Turbulent Free Jet." In: Chemical Engineering Science, Vol. 26, 1971, pp. 95-107.
6. Singhal, A.K., et al: "Prediction of Two-Dimensional Boundary Layers with the Aid of $k - \varepsilon$ Model of Turbulence." In: Computer Methods in Applied Mechanics and Engineering, Vol. 25, 1981, pp. 365-385.
7. Daniel, I.M.: "Experimental Study of Mechanics of Rock Fracture by Water Jet." Translated into Chinese in the J. of High-Pressure Water Jet, Vol. 1, 1980, pp. 107-121.
8. Huang, Y.C., et al: "A Note on Shock Wave Velocity in High-Speed Liquid-Solid Impact." ORA Report UMICH-03771-11-7, The University of Michigan, 1971.
9. Tait, P.G.: "Report on Some of the Physical Properties of Fresh Water and Sea Water." In: Physical Chemistry, Vol. 2, 1888, pp. 1-17.
10. Cole, R.H.: "Under Water Explosion." Dover, 1965.
11. Davies, J.W., et al: "The Anatomy and Impact Characteristics of Large Scale Water Jets." In: 5th Int. Symp. on Jet Cutting Tech., 1980, pp. 15-32.
12. Watson, A.J., et al: "Impact Pressure Characteristics of a Water Jet." In: 6th Int. Symp. on Jet Cutting Tech., 1982, pp. 93-106.

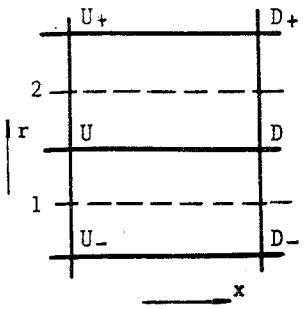

FIG.1 A PORTION OF THE FINITE DIFFERENCE GRID

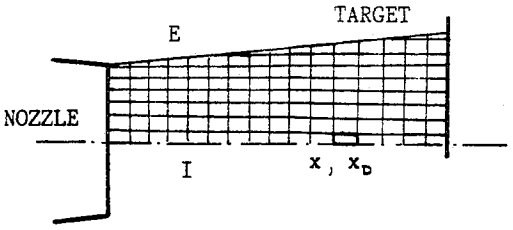

FIG.2 BOUNDARY CONDITIONS

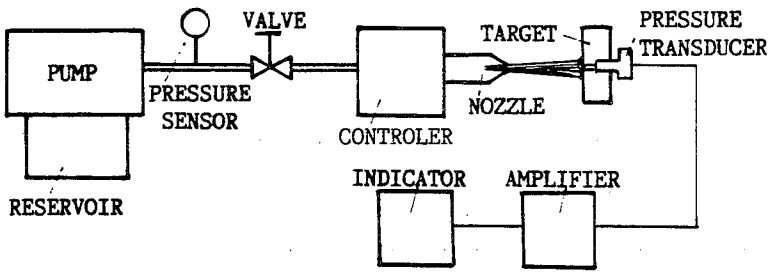

FIG.3 EXPERIMENTAL ARRANGEMENT

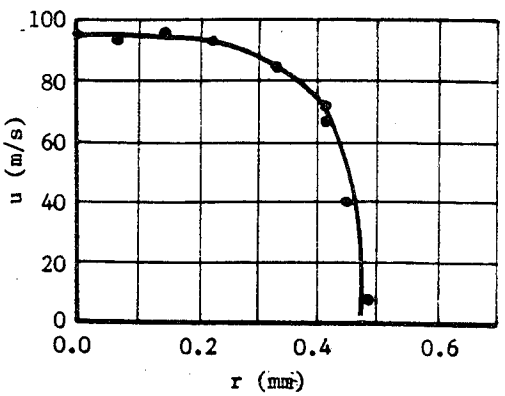

(a) d=0.3mm, s=50mm

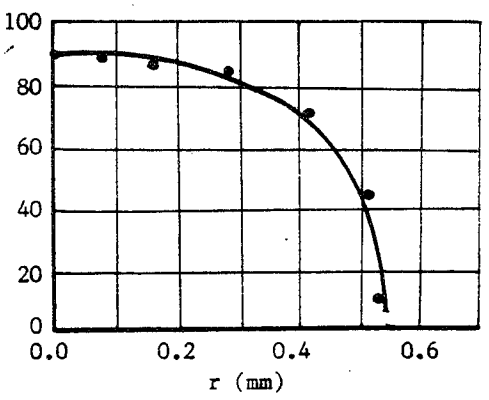

(b) d=0.3mm, s=100mm

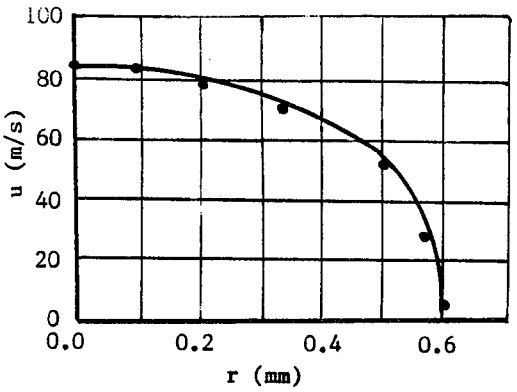

(c) d=0.3mm, s=140mm

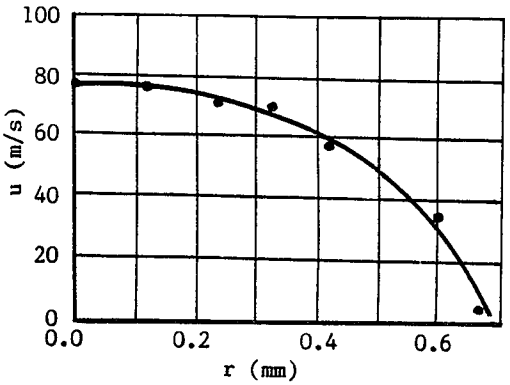

(d) d=0.3mm, s=180mm

FIG.4 COMPUTED VELOCITY PROFILES

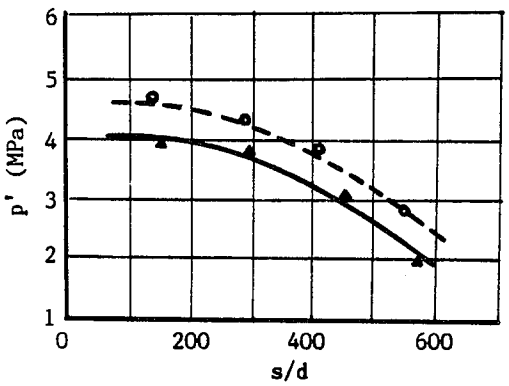

(a) d=0.3mm, p_r=50MPa

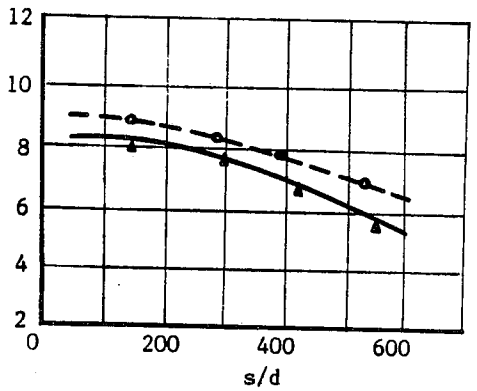

(b) d=0.3mm, p_r=100MPa

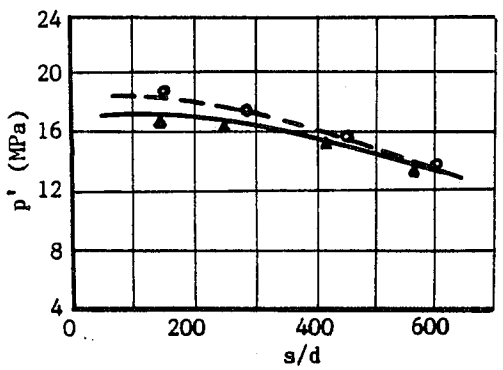

(c) d=0.3mm, p_r=200MPa

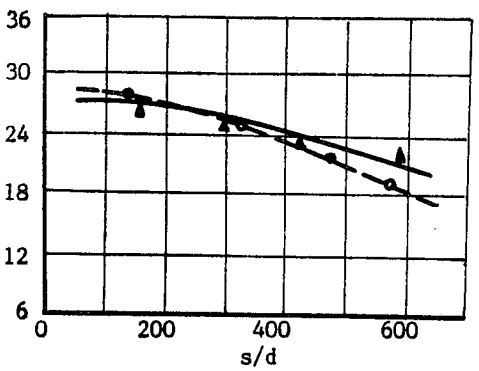

(d) d=0.3mm, p_r=300MPa

o —— computed values, ▲—— measured values

FIG.5 IMPACT PRESSURE VERSUS STAND-OFF DISTANCE CURVES

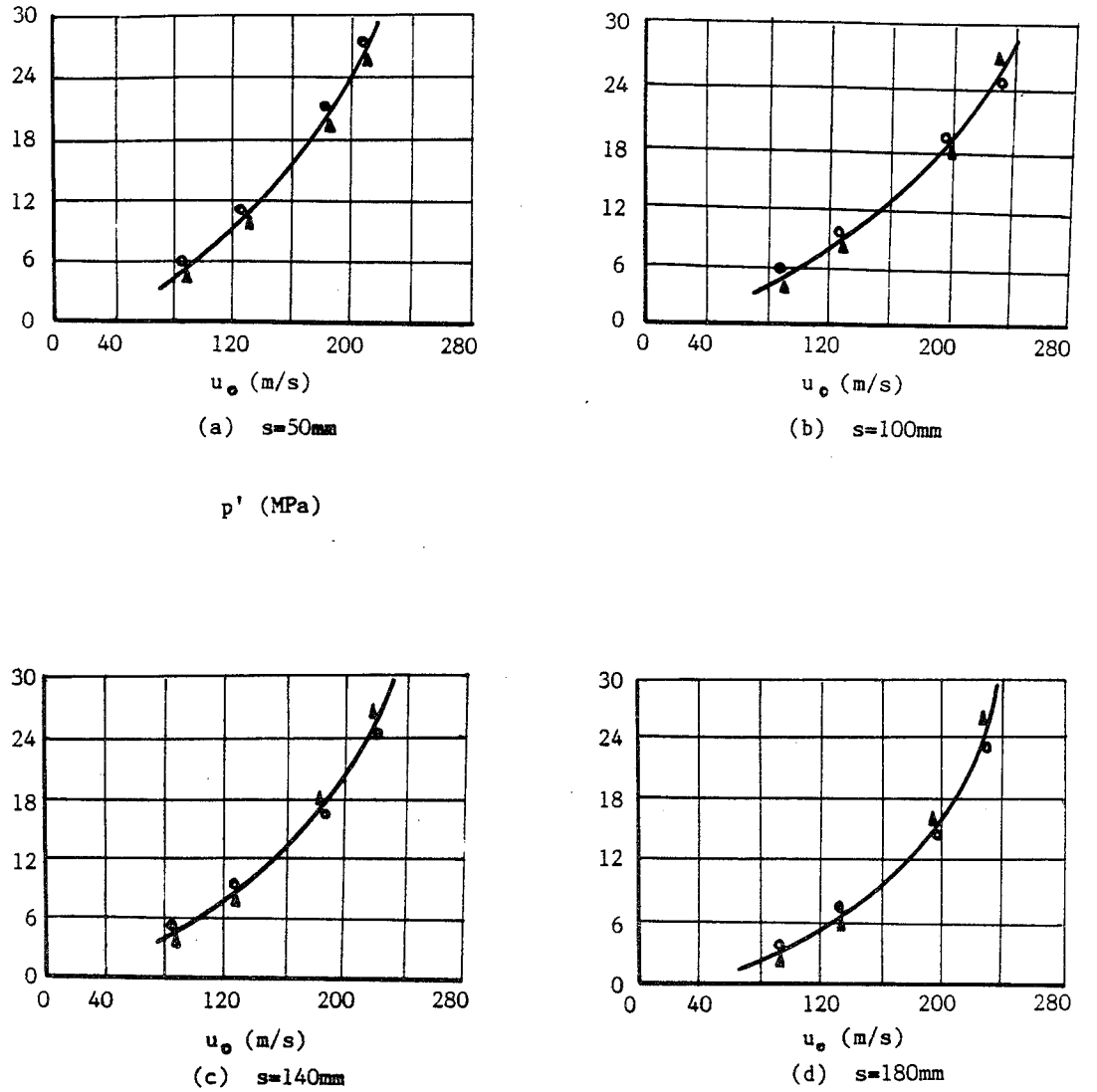

u_e – velocity at nozzle exit, ○ —— computed values, ▲ —— measured values

FIG.6 IMPACT PRESSURE VERSUS NOZZLE EXIT VELOCITY CURVES

5th American Water Jet Conference
August 29 - 31, 1989: Toronto, Canada

Paper / Communication 40

THE WATER-SAND JET CUTTING OF BRICK WALLS

S. Lasko, R. Kownacki, J. Bednarczyk
Research and Design Center of Opencast Mining "Poltegor"
Wroclaw, Poland

ABSTRACT: We present the results obtained at the design, manufacturing and laboratory-test phases of the water-sand jet cutting of a brick wall. Our new idea in the jet cutting technology was to put the nozzle with cutting jet into the previous slot. We obtained the optimal distance between the nozzle and the cutting surface.

RÉSUMÉ : Nous présentons les résultats obtenus lors de la conception, de la fabrication et des essais en laboratoire d'un outil à jet d'eau et de sable pour couper les murs de brique. Nous avons cherché dans cette méthode de coupe par jet de faire repasser la buse dans un trait déjà fait. Nous avons optimiser la distance entre la buse et la surface à couper.

Organized and Sponsored by the National Research Council of Canada and the U.S. Water Jet Technology Association.

1.INTRODUCTION

A lot of buildings has the brick walls.Some of them has become moist and then grow decrepit.

The chemical methods and more effective electro-osmosis drying method is very good, and it can save a lot of original and historical buildings. This method needs making a lot of holes or slots with electrodes.

At present, the boring holes process, needs using the mechanical boring machine.Boring with boring machine is timeconsuming and very troublesome on account of noise, vibration and dustiness.

The cutting of walls by making slots is used rarely because special machine with disk must be used.This process makes troublesome dustiness and we must have diamond disk. The limit of DIA disk takes up limiting of cutting deep slot

All of these difficulties, give occasion to compose a new idea of water-sand jet cutting of brick wall.

The new technology of cutting brick wall needs putting the nozzle with cutting jet into the previous made slot.

We have tested some materials for ejector nozzle.

2.THE NEW METHOD OF WATER-SAND JET CUTTING AND ITS DEVICE

The cutting with the water-sand jet has had pumps for comparatively small generation pressure, that is a very good fact.

At tradicional water jet cutting technology the depth of slot is limited, because water jet energy was consuming by "water pillow" into the slot.Then the ejector's nozzle has situated with constant distance from the wall.The same phenomenon exists at the water-sand jet cutting process.

So, that is very bad phenomenon.

Also, we have proposed a new idea of jet cutting tehnology for cutting of brick walls.At this technology, the nozzle was putting into the slot ,previous made slot.The nozzle with waterjet or water-sand jet, was putting into the slot step by step and then we obtained the effective distance between the nozzle and the cutting surface, in the slot.

The special cutting lance has been designed, and made, for realized of this method.This cutting lance has flat body, and it gives possibility of the motion into the slot.The device for the water-sand jet cutting of the brick wall is shown in Fig.1.This cutting device is composed with two sets:

hp water supply system,

and sand supply system.

The action of the high pressure supply system is fllowing:

The water from low pressure water instalation is flowing to the water reservoir /see pos.1 in Fig.1./ Sucking is realized by h.p. pump /pos.2./, through the valve with filter/pos.3./.And the pumping water is flowing to the cutting lance by hp flexible hose./pos.10./. Then the flow of water jet in the lance was generating the negatve pressure.

The sand supply system has following action:

The dry sand is situated in sand reservoir.From the sand reservoir , sand is sucking to the cutting lance by the flexible hose/ pos.8. in Fig.1./.The sand reservoir was plastic sack with dry sand, and the hoses were the plastic flexible transparet hoses.

The water-sand jet cutting device is shown in Fig.2.In this Fig.2.,the water pump unit technical data is:

max. pressure - 40,0 MPa,
capacity- $0{,}5 \times 10^{-3}$ m^3/s,
el. power- 18,5 kW.

The cutting lance /Fig.3./,was composed with high pressure steel pipe, joined with the water nozzle. At both sides of this pipe, two plastic holes are placed by which dry sand is given to the suck chamber of the ejector.

The suck chamber is a cone hole, which in its narrower part becomes a cylindeical hole.The mixing chamber with a cylinrical hole that is just water-sand jet ejector nozzle.So, there is the clasical ejecter but it hasn't the diffuser.

The ejector body is flat and it gives possibility to put the ejector into the slot.

3.LABORATORY TEST

The laboratory test were carried into effect on three walls built of new bricks.The thickness of walls was 1,5; 2,0; and 2,5 bricks.

The masonry mortar hashad cement Portland 350.

After building the walls, we waited about one month for stabilization of the masonry mortar.And after this time we come up to drilling the holes and cutting the slots.

These are the best results , which we have obtained:

drilling the holes,

thickness of wall	1,5 brick,
granulation of sand	0,6 mm,
DIA of water nozzle	1,5 mm,
DIA of ejector nozzle	3,0 mm,
time of cutting the wall through and through	2-3 min,

the lance doesn't input the hole.

Fig.4.,presents two holes which were cut in this wall, left hole through the brick and the right one trough the mortar.

An interesting fact was the obtaining for the right hole the diameter output about 8 mm at diameetr of the hole input about 15 mm.

cutting of the slot,

thickness of wall	2,0 bricks,
granulation of sand	0,6 mm,
DIA of water nozzle	1,5 mm,
DIA of ejector nozzle	4,0 mmm,
width of the slot irregular,	20 mm /about/,
time of cutting slot width 0,5 m, through and through of wall	15 to 20 min,

Fig.5., presets the phase of cutting the slot on the wall which is two bricks thick.It can see the surface of the wall with output slot.

We tested the water-sand nozzle of ejector which diameters were: 2,0 mm, 3,0 mm; 4,0 mm; and 6,0 mm.

The materials of body nozzle were the following: polyurethan, tephlon, glass, brass, tool steel, and sintered carbides.

The best life of the ejector nozzle was obtained for body nozzle of sintered carbides, about 2 hours.

The test of the life nozzle in its improvement aspect, are continued. And we are working at new construction of the ejector nozzle e.g. assembled nozzles.

4.CONCLUSIONS

1.The cutting of brick walls with water-sand jet can be the competitive technology to the traditional mechanical cutting methods for cutting of brick walls and drilling the holes in those walls.

2.The jet cutting method with cutting lance into the slot gives the possibility of cutting the big rock blocks from body of rock.

3.This cutting technology can eliminate the buster shot as the method of obtaining the big rock blocks.At this technology the conditions of work are much better, and degradation of nature is much smaller.

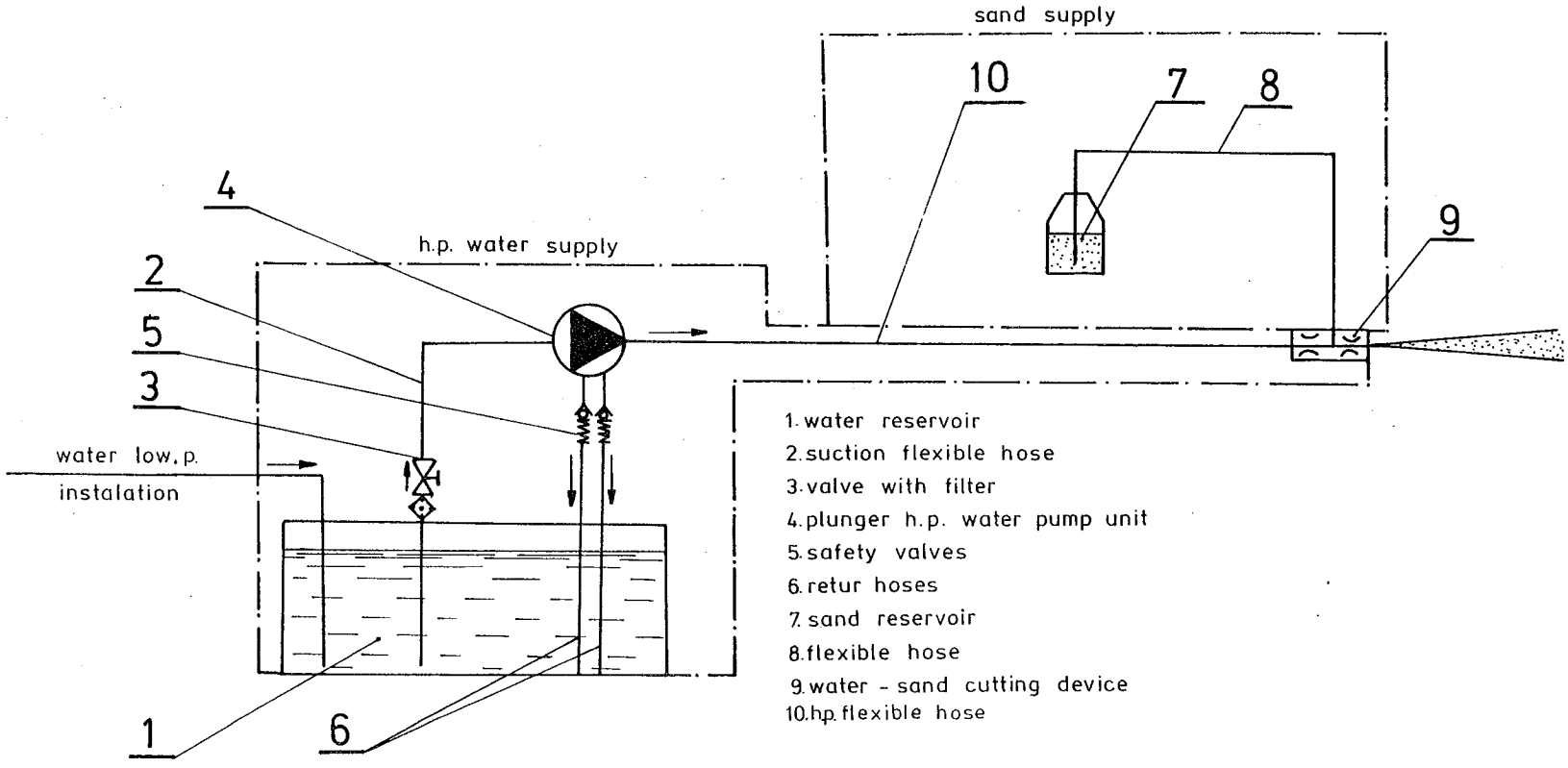

Fig. 1. HYDRAULIC SCHEME OF THE WATER - SAND JET CUTTING FOR THE BRICK WALL.

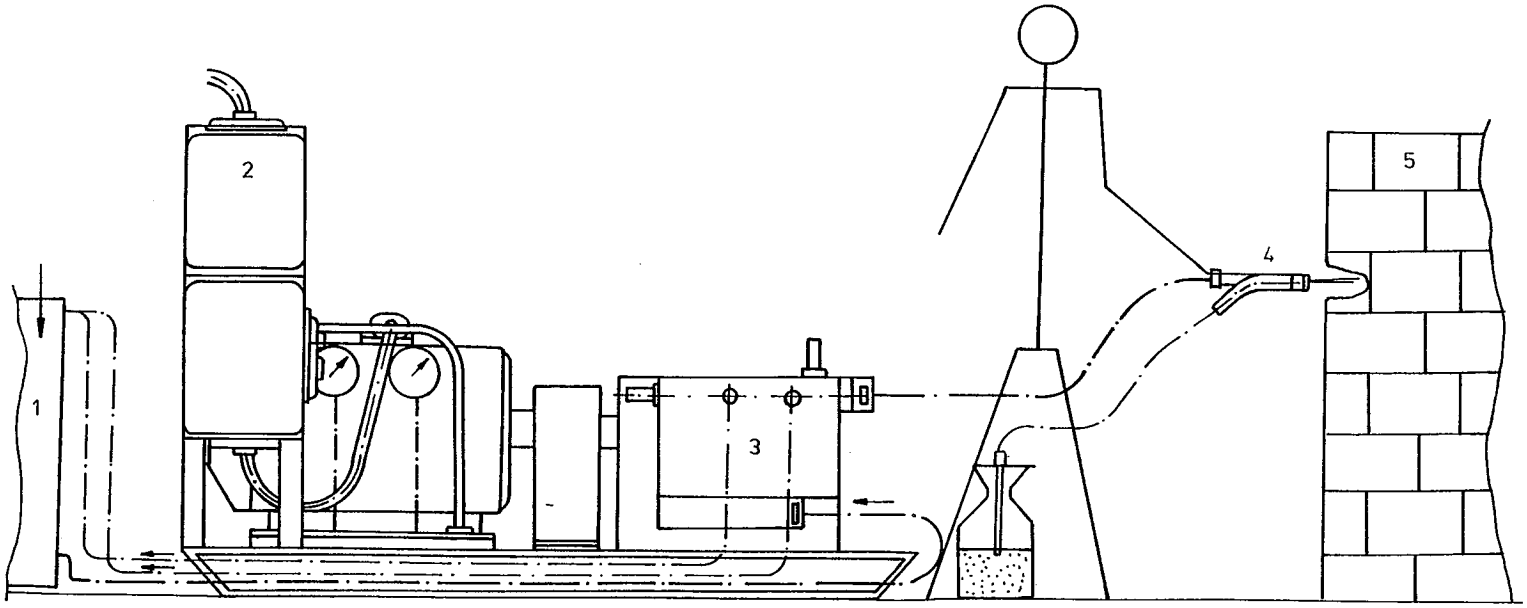

1.water reservoir
2.el. control station
3.plunger h.p. water pump unit
4.water - sand cutting device
5.brick wall

Fig.2. HYDRAULIC WATER - SAND JET CUTTING OF THE BRICK WALL .

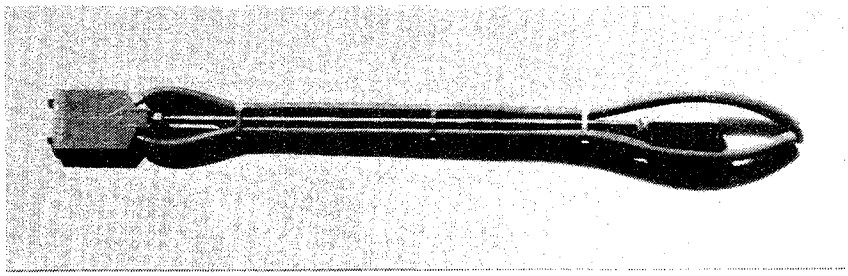

Fig.3. THE WATER SAND CUTTING LANCE

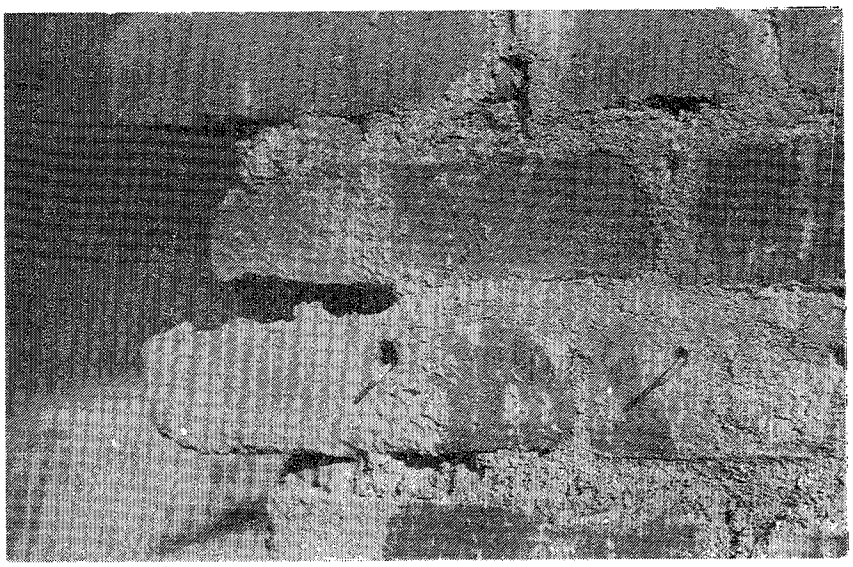

Fig.4. THE HOLES HAVE BORED WATER-SAND JET

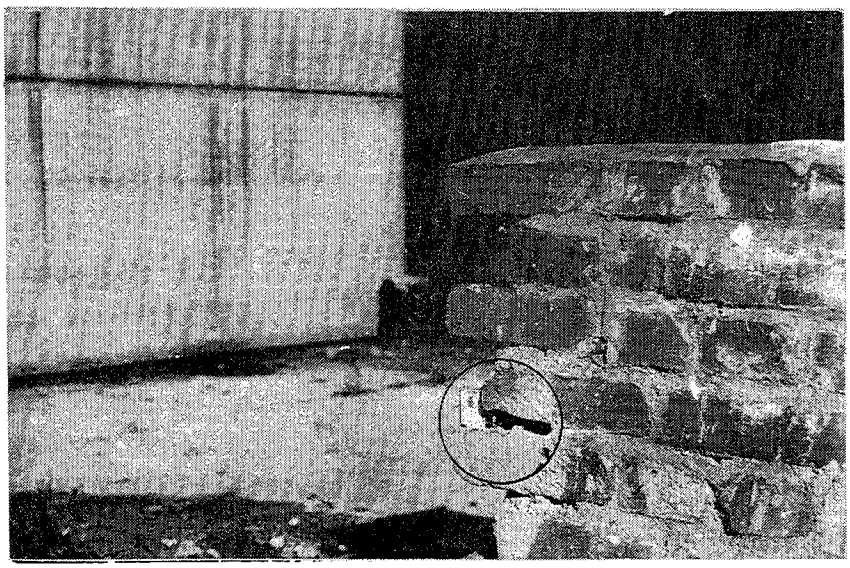

Fig.5. THE SLOT WAS CUTTING BY WATER-SAND JET

5th American Water Jet Conference
August 29 - 31, 1989: Toronto, Canada

Paper / Communication 41

EVALUATING SMALL BORE TUBING FOR DYNAMIC HIGH PRESSURE SYSTEMS

D.M. Fryer
Autoclave Engineers Group
Erie, Pennsylvania, USA

ABSTRACT: The use of small bore (less than 1" [25 mm] ID) tubing for dynamic High Pressure applications is discussed, and various stress analysis concepts are presented.
The stress analysis concepts include basic static stresses, the influence of cyclic service, accommodating mechanical motion stresses and the potential benefits of autofrettage.
The cyclic examination includes both fatigue and fracture analyses. These, and the autofrettage discussion, are in accord with the philosophy of the new High Pressure codes recently issued or currently being developed by the American Society of Mechanical Engineers.
The necessity of good material specification, as well as good Quality Control also is mentioned.

RÉSUMÉ : L'utilisation de canalisation de faible calibre (diam. int. inférieur à 25 mm) pour des applications dynamiques à haute pression est analysée, et diverses notions de l'analyse des contraintes sont présentées.
Les notions de l'analyse des contraintes comprennent les contraintes statiques élémentaires, l'effet d'une utilisation répétée, la prise en compte des contraintes mécaniques de mouvement et les avantages possibles de l'auto-frottement.
L'examen cyclique comprend des analyses de fatigue et de rupture. Ces dernières et l'analyse d'auto-frottement sont en accord avec les nouvelles méthodes à haute pression qui ont été publiées récemment ou qui sont mis au point par l'American Society of Mechanical Engineers.
La nécessité de bien spécifier les matériaux et de bien en contrôler la qualité est aussi mentionnée.

Organized and Sponsored by the National Research Council of Canada and the U.S. Water Jet Technology Association.

1.0 INTRODUCTION

1.1 Small bore tubing is used for many high pressure applications in the Chemical, Petrochemical, Waterjet, Iso-static Pressing and other industries.

1.2 Using the lead of ASME Standard B31.3, Chapter IX, high pressure is defined as greater than ASME B16.5 Class 2500 Flange ratings.

1.3 The primary hazards, of concern regarding both personnel and facilities, are leaks (which can be uncontrolled piercing jets), missiles and whipping tubing.

1.4 Subjects which must be addressed are material quality, static strength and ductility.

1.4.1 Ductility, of course, relates to fatigue and fracture behavior.

2.0 MATERIALS & SIZES

2.1 The materials most commonly used for high pressure tubing are AISI types 304 and 316 stainless steel. To achieve the necessary strength, stainless tubing is manufactured by a process of cold-drawing.

2.1.1 Because of the cold-drawing, such tubing should not be used at excessive temperature or be installed by welding as these will remove the enhanced strength properties.

2.2 Other strength enhanced materials such as precipitation-aged stainless steels, and quenched and tempered alloy steels also may be used.

2.3 Sizes most commonly employed range in inside diameters between 0.062 and 0.688 inches (1.5 to 17.5 mm), and typically have wall ratios from approximately 1.5 to 5.0.

2.3.1 Wall ratio is defined as outside diameter divided by inside diameter. For the balance of this paper, wall ratio will be designated as "Y".

3.0 STATIC ANALYSIS

3.1 There are several static analytical techniques that have been used over the years; all of which are based on some form of safety factor.

3.1.1 It should be recognized; however, if one examines a classical fatigue endurance limit curve, that any so-called design safety factor is valid only for the first cycle.

3.2 The actual Bore and OD Hoop Stresses (Si & So) away from the ends of a length of tubing are shown as (a) and (b) respectively (with P = internal pressure: PSI [MPa]):

(a) $$Si = \frac{P\,(Y^2 + 1}{(Y^2 - 1)} \quad : \text{PSI (MPa)}$$

(b) $$So = \frac{2\,P}{(Y^2 - 1)} \quad : \text{PSI (MPa)}$$

3.2.1 Safety factor is defined as the Ultimate Strength (Sult) of the tubing material divided by Si; and ASME Boiler and Pressure Vessel Code, Section VIII, Division 1 requires the minimum value to be 4.0.

3.3 ASME Code, Section VIII, Division 2 defines a General Primary Membrane Stress (Sm), and calculates this as:

$$(c) \quad Sm = \frac{P\ (Y+1)}{2\ (Y-1)} \quad : \text{PSI (MPa)}$$

Division 2 then requires the minimum safety factor against Ultimate Strength to be 3.0 with this stress.

3.4 An analysis sometimes of interest to high pressure designers, and also required by some legislative jurisdictions around the world, is to calculate the von Mises (or distortion energy) stress (Svm) at the tubing bore:

$$(d) \quad Svm = \frac{\sqrt{3}\ P\ Y^2}{(Y^2 - 1)} \quad : \text{PSI (MPa)}$$

A typical stress limit considered with this concept is the material Yield Strength (Sy) divided by 1.5.

3.5 A more recent approach to rating high pressure tubing has been to estimate the theoretical Burst Pressure (Pb) using the expression:

$$(e) \quad Pb = \frac{2\ Sy\ \ln (Y)}{\sqrt{3}} \left[\ 2 - \frac{Sy}{Sult}\ \right] \quad : \text{PSI (MPa)}$$

Safety factor becomes this value divided by the rated pressure; and typical values have ranged between 2.4 and 4.0.

3.6 The most recent rating method is the requirement introduced in ASME Standard B31.3, Chapter IX, where the full Collapse (or through the wall yield) Pressure (Pc) is calculated by:

$$(f) \quad Pc = \frac{2\ SY\ \ln (Y)}{\sqrt{3}} \quad : \text{PSI (MPa)}$$

The required minimum safety factor between this value and the rated pressure is 2.0.

4.0 DYNAMIC ANALYSIS

4.1 Applications such as water-jet-cutting, cold isostatic pressing and some others expose tubing to very large numbers of high stress cycles. In these cases, fatigue and fracture behavior usually become the controlling design parameters instead of the static analysis.

4.2 The basic technique of evaluating the potential number of service cycles for a section of tubing is the classical Fatigue analysis. This involves calculating what is called the Alternating Stress which then is used in conjunction with endurance limit curves such as the ones in ASME Code Division 2. Attached Figure 1 illustrates a typical curve.

4.2.1 Alternating Stress (Sa) for use with Division 2 type curves is calculated by:

$$(g) \quad Sa = \frac{P\ Y^2}{(Y^2 - 1)} \quad : \text{PSI (MPa)}$$

This stress is one-half the total Stress Intensity (Sint) or range of the stress cycle.

4.2.2 Because of the various factors (2:1 on stress and 20:1 on cycles) built into the Code curves, the resultant number of cycles is considered by some to approximately represent crack initiation rather than ultimate failure.

4.3 A more rigorous approximation of cycles to failure can be made using the procedures of Fracture Mechanics. This involves calculating a theoretical Critical Crack (Ac), assuming an Initial Crack (Ai) size and then calculating the number of cycles for the initial crack to propagate to critical size.

4.3.1 The theoretical critical crack will be a function of the Stress Intensity (Sint: KSI [MPa]) of the stress cycle and the Plane Strain Fracture Toughness (Klc: KSI $\sqrt{\text{inch}}$ [MPa $\sqrt{\text{m}}$]) of the material; and simplified, may be expressed as:

(h) $Ac = (Klc/Sint)^2 / \pi$: inch (m)

4.3.2 The number of cycles from initial crack to critical size may be estimated by integrating across the tubing wall using an expression such as:

(i) $dA/dN = C (\Delta K)^m$: inches/cycle (m/cycle)

where: ΔK = range of stress intensity factor : KSI $\sqrt{\text{inch}}$ (MPa $\sqrt{\text{m}}$); and C and m are factors based on the specific material.

4.4 When assessing the magnitude of maximum stress intensity for the dynamic analysis, it often is necessary to identify pressure spikes caused by pressure source equipment. Such spikes are not always detectable by normal pressure measuring instruments; and as a result, actual behavior may appear not to agree with the analysis.

5.0 QUALITY CONTROL

5.1 As can be seen from the preceding section, manufacturing quality is extremely important since the maximum expected residual defect in the tubing usually is used as the initial crack size.

5.1.1 Basic minimum specifications should include chemistry, ultimate strength, yield strength, elongation, a maximum limit on bore defect size plus some form of continuous non-destructive examination such as eddy-current or ultra-sonics.

5.1.2 In addition, the noble motive, obviously, is to try to specify zero bore defects. Unfortunately the state of the art in tubing manufacturing has yet to reach this level of perfection, so an alternative must be found to obtain optimum cyclic performance.

5.2 Studying the equations in Section 4 above shows that reducing stresses or improving toughness also care candidates for improving cyclic performance. Toughness is inherently high in most materials used for this type of tubing, so this leaves stress as the target; however, remember, required pressure usually is fixed in most processes.

6.0 AN ALTERNATIVE

6.1 Paragraphs 3.2, 3.4 and 3.6 show that there is a substantial stress gradient across the tubing wall and also that it is possible to yield the tubing bore without yielding the OD. It also is well known that if part of the wall is yielded by overpressure, upon release of this pressure the bore will be in a state of residual compressive stress and the outer surface will be in a state of residual tensile stress. This phenomenon is known as AUTOFRETTAGE. Upon subsequent applications of pressure, the actual stress distribution through the wall will be the algebraic sum of the basic imposed stresses and the residual stresses.

6.2 The solid line portions of Figure 2 graphically illustrate the autofrettage mechanism. It shows that not only is the peak stress magnitude reduced, it is moved away from the bore surface where any manufacturing defects normally would be present. By using these reduced stresses in the concepts of Section 4.0, the expected cyclic behavior of the tubing can be shown to be greatly improved.

6.3 By further examining Figure 2, it also can be seen that is the plastic-elastic interface is moved far enough through the wall, the bore can theoretically reach reverse yield; and this would be the limit of any benefit from the autofrettage technique.

6.4 In realty, the full benefit of theoretical reverse yield is not available. A phenomenon known as the Bauschinger effect identifies that once a material has been yielded in tension, the absolute value of its compressive yield strength is reduced.

6.5 The dotted lines on Figure 2 illustrate how the Bauschinger effect can influence the autofrettage residual stress as well as the resultant stress upon re-application of pressure.

6.6 In some situations, autofrettage must be applied with caution; or at least be evaluated in more detail. If bending or torsion stresses are present, these will be highest at the OD. As Figure 2 illustrates, even though the OD stresses from pressure are not as high as elsewhere in the wall, they are higher than normal after autofrettage has been applied. Usually, such combination conditions will manifest themselves most adversely in the vicinity of threads near the ends of the tubing; and special precautions may be required.

6.7 The autofrettage procedure always should be applied to tubing sections longer than required for fabrication so several inches (50 to 60 mm) can be cut off each end afterwards to ensure uniform benefit.

7.0 CONCLUSIONS

7.1 Simple safety factor considerations are not always enough when designing a system involving high pressure tubing, especially when cyclic and other dynamic conditions may be involved.

7.2 The technique of autofrettage is a viable method for reducing effective stresses and thus improving performance when high cyclic service is required.

7.3 A quality program of material property specification, testing and verifying is a must, not just for subjecting tubing to basic high pressure service, but especially if the stress redistribution benefits of autofrettage are to be expected.

7.4 Detailed technical information concerning the concepts presented above may be found via the following list of references.

REFERENCES

1. American Society of Mechanical Engineers, "Boiler and Pressure Vessel Code, Section VIII; 1986 Edition.

2. ASME Standard B31.3, "Chemical Plant and Petroleum Refinery Piping, Chapter IX, High Pressure Piping"; 1987 Edition.

3. Chaaban, A., Leung, K. & Burns, D. J.; "Residual Stresses in Autofrettaged Thick-Walled, High Pressure Vessels"; Volume 110, Proceedings of ASME Pressure Vessels and Piping Conference; 1986.

4. Chen, P. C. T.; "Stress and Deformation Analysis of Autofrettaged High Pressure Vessels"; Volume 110, Proceedings of ASME Pressure Vessels and Piping Conference, 1986.

5. Crossland, B.; "The Collapse or Ballooning Pressure of Thick-Walled Vessels"; Part II, 9th AIRAPT International High Pressure Conference; 1983.

6. Fryer, D. M.; "The Paradox of Safety Factors in High Pressure Equipment"; ASME 2nd National Congress on Pressure Vessels and Piping Technology; 1975.

7. Kendall, D. P.; "The Influence of Bauschinger Effect on Re-Yielding of Autofrettaged Thick-Walled Cylinders"; Volume 125, Proceedings of ASME Pressure Vessels Conference; 1987.

8. Koves, W. J.; "Comparison Pressure Vessel and Piping Fatigue Criteria"; #88-PVP-5, ASME Pressure Vessels and Piping Conference; 1988.

9. Mraz, G. J.; "Development of Criteria for A High Pressure Vessel Design Code"; Volume 98-8, Proceedings of ASME Pressure Vessels and Piping Conference; 1985.

10. Priddy, T. G. & Hughes, W. T.; "Hazards in High Pressure Systems"; Volume 110, Proceedings of ASME Pressure Vessels and Piping Conference; 1986.

11. Sims, J. R.; "Development of Design Criteria For A High Pressure Piping Code"; Volume 110, Proceedings of ASME Pressure Vessels and Piping Conference; 1986.

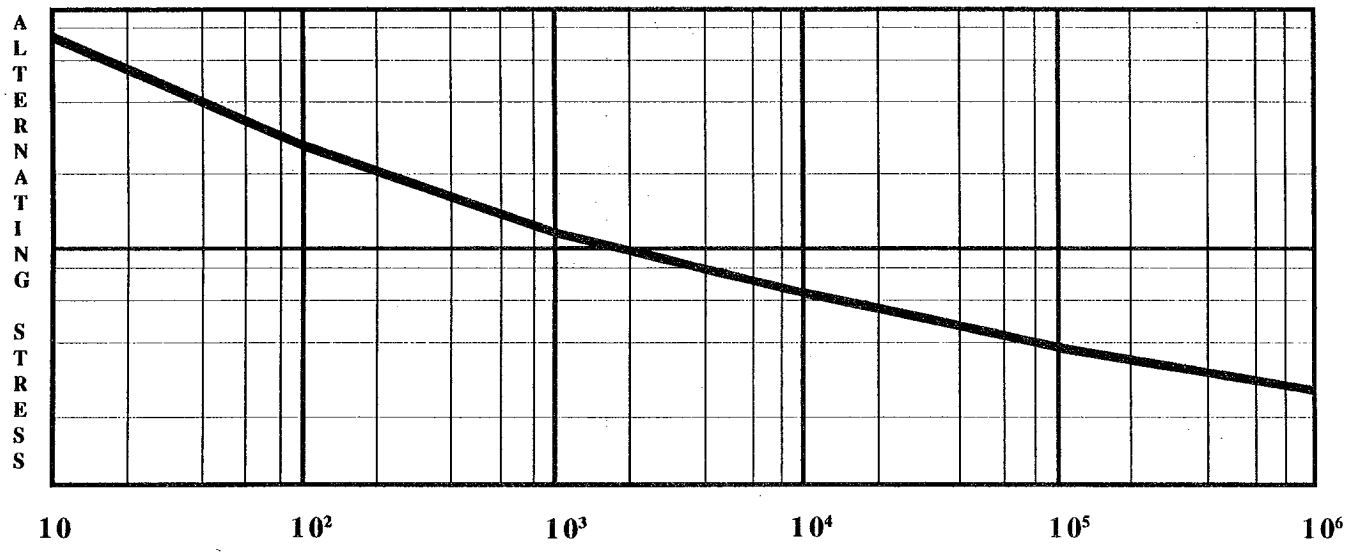

DESIGN FATIGUE CURVE

FIGURE 1

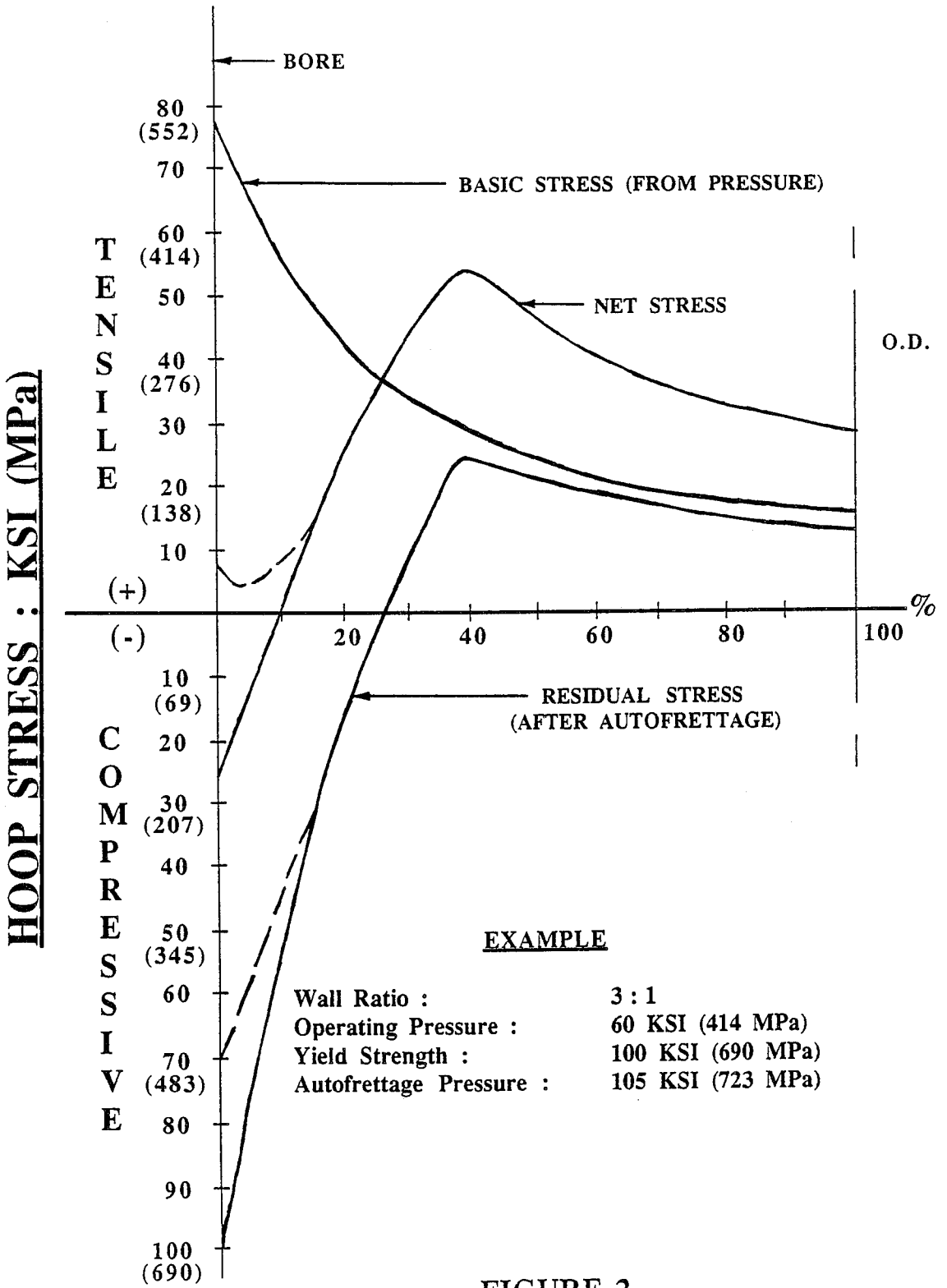

EXAMPLE

Wall Ratio :	3 : 1
Operating Pressure :	60 KSI (414 MPa)
Yield Strength :	100 KSI (690 MPa)
Autofrettage Pressure :	105 KSI (723 MPa)

FIGURE 2

5th American Water Jet Conference
August 29 - 31, 1989: Toronto, Canada

Paper / Communication 42

A CRITICAL EXAMINATION OF THE USE OF WATER JETS FOR MEDICAL APPLICATIONS

M.M. Vijay
Gas Dynamics Laboratory
National Research Council of Canada
Ottawa, Ontario K1A 0R6, Canada

ABSTRACT: In recent years water jets and abrasive-entrained water jets have become increasingly popular for a variety of applications in industry. In the medical and dental fields, although water jets have been used for a number of years for such applications as wound cleansing and oral hygiene, research and development work currently in progress all over the world will no doubt introduce new uses of the technique for other applications. While such wide spread uses and progress are remarkable, the potential dangers accompanying the improper uses of the jets, to human body have also increased enormously. An extensive review of the literature was made in both areas, a brief report of which is given in this paper. The search has revealed (1) the potential of liquid jets for medical applications is indeed bright and (2) the injury caused by the jets should not be treated lightly. Liquid jet injuries should be regarded as *SURGICAL EMERGENCIES and IMMEDIATE MEDICAL ATTENTION SHOULD BE SOUGHT FROM EXPERT PHYSICIANS, NOT THE INEXPERIENCED INTERNS OR RESIDENTS, OFTEN IN ATTENDANCE IN THE EMERGENCY DEPARTMENTS AT THE HOSPITALS. Furthermore,* the operators, and most importantly their SUPERVISORS, should be fully aware of the dangers posed by the jets, should an accident happen.

RÉSUMÉ : Au cours des dernières années, les jets d'eau et les jets d'eau avec abrasifs ont été de plus en plus utilisés dans une variété d'applications industrielles. Dans les domaines de la médecine et de la dentisterie, même si les jets d'eau ont été utilisés pendant de nombreuses années dans des applications telles que le nettoyage des plaies et l'hygiène buccal, les efforts de recherche et développement en cours dans le monde entier déboucheront sans aucun doute sur de nouvelles utilisations de la technique dans d'autres applications. Malgré ces utilisations aussi répandues et les progrès remarquables qui ont été réalisés dans le domaine, les dangers que peuvent présenter pour le corps humain les mauvaises utilisations des jets se sont aussi grandement multipliés. Une étude détaillée de la documentation sur ces deux aspects a été réalisée et est rapportée brièvement dans la présente communication. L'étude a révélé (1) que les applications médicales des jets de liquides sont en fait prometteuses et (2) que les blessures causées par les jets ne doivent pas être traitées à la légère. Les blessures causées par les jets de liquides méritent des INTERVENTIONS CHIRURGICALES D'URGENCE et DES SOINS MÉDICAUX IMMÉDIATS DOIVENT ÊTRE DISPENSÉS PAR DES SPÉCIALISTES ET NON PAR LES INTERNES ET LES RÉSIDENTS INEXPÉRIMENTÉS QUI SONT DE GARDE DANS LES SALLES D'URGENCE DES HÔPITAUX. En outre, les opérateurs, et avant tout leur SUPERVISEURS, doivent être pleinement conscients des dangers que posent les jets en cas d'accident.

Organized and Sponsored by the National Research Council of Canada and the U.S. Water Jet Technology Association.

1.0 INTRODUCTION

A few years ago some tests were conducted in the laboratory to investigate the feasibility of using high pressure water jets for bone surgery (Ref.1). The work started with cutting leg bones taken from dead rabbits at various nozzle diameters and pressures (Fig. 1A). Since the cuts were clean (Fig. 1B) and acceptable to the surgeons involved in the project, the investigation continued on anaesthetized live rabbits (Fig. 2). Although these tests were successful and showed that water jets can be used for amputating bones (Fig. 2C), the rabbits did not survive the ordeal, and passed away after a couple hours. In order to investigate the causes for these unexpected deaths, subsequent tests were conducted with water tainted with a blue dye (Fig. 2B). Furthermore, to evaluate the maneuverability of the jet-lance system, the surgeon conducted some of the tests in this series by holding the nozzle in his hand (Fig. 2B). This procedure was unsatisfactory because the surgeon almost cut his little finger (the skin near the nail was peeled off) during one of the tests. While this information was of great importance, the answer to the question " why did the rabbits die?" will never be known because the principal surgeon in charge left the country and the project was terminated. However, the curiosity to find the answer did not stop. Over the years, the author conducted a search of the literature and found, in addition to the clues on rabbits' death, a wealth of information (Refs. 2 to 122), generally in the medical and dental fields, not only on medical applications of liquid jets but also, the injuries that the jets can cause if one is not careful in employing them. The search also clearly indicated the lack of basic knowledge of the underlying damage mechanisms of the tissues and the limitations of liquid jets for medical applications. With respect to limitations, Fig. 3 shows a typical example. Attempts were made recently in the laboratory, partly based on the test results stated above, to cut into thin sections a specimen of large human bone (equivalent diameter > 5 cm), embedded in a bioplastic material, for histological examination. The depth of cut achieved with a water jet of 0.127 mm at a pressure of 138 MPa was only 6.4 mm after 5 passes. The cut shown in Fig. 4 was achieved with a band saw!

The purpose of this paper is to critically review the water jet techniques, currently in use or proposed, for medical applications, but most importantly, to emphasize the potential dangers of liquid jets to human body if strict adherence to safety regulations is not observed. Although some aspects of water jet injury have been taken into account in formulating safety codes (Refs. 2 to 5), the intensity or severity of the wound that an operator can sustain in case of an accident have not been emphasized in these codes. It is only recently that Summers and Viebrock (Ref. 6) have attempted to bring this home to the personnel involved, particularly in the field of water jet technology, by reviewing a number of cases reported in the medical and dental fields. This paper goes a step further in that while it describes the injuries reported in the literature by listing more than 100 related papers (by no means exhaustive), it stresses the other aspect of water jet technique viz., its excellent potential for novel medical applications, if used with proper precautions.

With regard to INJURY, it should be stated that not all the publications listed in the REFERENCES were examined, for the simple reason that while some of them were not available at the time of writing this paper, some others were brief clinical case reports without much new information. Most of the papers reviewed contained vivid photographs of the injured organs, showing the extent and the severity of the damage. Although a few of these photographs have been reproduced here to emphasize the intensity of the injury, the author strongly recommends that the reader, particularly those in supervisory positions, should study some of the publications listed to fully grasp the gravity of an accident, if it occurs, and how to cope with it. Medical or dental literature contain terms which are usually foreign to nonmedical personnel. Therefore, in order to facilitate comprehension of the medical terms used in the following sections a short glossary together with photographs of the human body (Fig. 4) are included in the paper.

2.0 FLUID JET INJURIES

The term "fluid" rather "water" jet is used here to stress the fact that any pressurized fluid is capable of inflicting damage to the tissue, should an accident occur. In fact, majority of the cases reported in the literature, involved injuries caused by a fluid other than water (Refs. 7 to 107; these references are listed chronologically to indicate that although injuries of this type have been dealt with for more than 50 years, not much progress has been made in understanding the mechanism of damage which might lead to improvements in the methods of treatment). This might at first appear as irrelevant to those involved in water jet technology, but on thorough examination of the injuries reported in the literature, it becomes clear that all high pressure injuries have certain features in common, for instance, they are considered as "SURGICAL EMERGENCIES" (Ref. 96), that it is important to be aware of them, irrespective of whether the operator or the supervisor is using that particular fluid or not. It is not possible, in this short paper, to give all the details found in the literature (a full report might appear in the near future). In

order to emphasize the gravity of the injury, however, complete details of a few of cases, taken from the first, Rees, 1937 (Ref. 7), and the most recent, Weltmer & Pack, 1988 (Ref. 106) publications are given here. Details of a severe abdominal injury caused by high pressure water jet, reported by Neill & George (Ref. 50), are reproduced here to underscore that soft tissues are highly susceptible to fluid jet injuries and the damage can be irreversible or even fatal. Following this, a brief description of the effect of the type of jet (continuous, pulsed, abrasive-entrained, etc.), pressure, power and the standoff distances on the wounds are given. Salient features of the injuries, taken from some of the references, are summarized in Table 1, together with some photographs (Figs. 5 to 13) to make the gravity of the injury visible to those who are unaware of it.

2.1 INJURIES OF ORGANS

2.11 Injury of the Hand

Rees (Ref. 7): A 47 year old motor mechanic was testing the jet of a Diesel engine. He was holding the nozzle which he had removed from a cylinder head, about 2.5 cm (1 inch) from the tip of his right middle finger when he tripped the valve. A jet of oil was forced into the finger which he estimated to be about 28 MPa (4000 psi). There was immediate slight bleeding from several points in the finger-tip and pain, which gradually became intense. When he was first seen by the physician 24 hours later, opiates were necessary to relieve the pain. At this time the finger and hand were edematous, swollen and tense (Figs. 5A & 5B), and the epitrochlear and axillary lymph nodes were enlarged and tender. A round area of epidermis about 1 cm in diameter at the end of the finger was loose and was removed. The tissue beneath the skin was dusky red. The patient was sent to the hospital, where the hand was elevated and hot compresses were applied. The pain in the finger and in a triangular area in the palm and dorsum of the hand (Fig. 5B) at the base of the middle finger persisted, but the pain and swelling in the remainder of the hand subsided somewhat. Within the next 24 hours the epidermis on the distal half of the finger loosened and was removed, and again a deep red colour in the underlying tissue was revealed. Dehydration of this area resulted in dry gangrene, which began at the tip of the finger and extended down to the first interphalangeal joint. The epidermal skin over the first phalanx and the base of the finger then loosened and the same dusky red that was seen at the tip of the finger before the onset of the gangrene was disclosed in the subjacent tissue. Involvement of the bone was not demonstrable on the x-ray taken seven days after the injury.

Exploratory incision over the first phalanx at this time showed that all the tissue in this area had undergone liquefaction necrosis with secondary infection. A thick creamy puss was present in which an occasional gram-positive coccus was found. The tissue of the palm and dorsum of the hand at the base of the finger was of the same dusky red previously noted in the finger. Bleeding was very slight. The pain was still severe. During this he had some fever. It was decided to amputate the finger and remove if possible all the involved tissue. Amputation was performed through a palmer and dorsal wedge-shaped incision over the metacarpal bone. Dusky and edematous tissue with small pockets of pus extended into the midpalmer region. The metacarpal bone was sectioned in its middle third. Only the lateral digital artery required ligation. The wound was left open on the dorsal side and was closed by loose silkworm sutures on the palmer side. The swelling and pain in the remainder of the hand subsided immediately. There was considerable suppuration in the area of amputation following operation, and it was not until **EIGHT WEEKS** later that healing was complete. When the patient was seen two years later after the accident, the function of the rest of the fingers was good. Based on this case Rees recommended early and liberal incisions over and into the affected area allowing the escape of the foreign material, relieving edema which is intense and may be destructive if allowed to persist.

2.12 Fluids

As indicated in Table 1, since the reporting of this first incident, the number of injuries caused by fluids such as grease (Refs. 9-11,13-15,17-23,26,29,30,35,44,48,51,64,68,73 & 88), paint (Refs. 25,32,34,35,39-43,45-48,54,55,59,63,65,66,73-78,80,90), fuel and hydraulic fluids (Refs. 8,12,24,27,28,35,74), molten plastics (Refs.16,33), cement (Ref. 49), water (Refs. 31,50,83-86,92,96,103,106) and other materials (Refs.62,69,70,71,72,82,95) have greatly increased in frequency. While water may not be as chemically irritant or toxic as other fluids, it can still cause serious infection depending on its quality. Frank (Ref. 99) has, for example, reported that favourable conditions exist for the multiplication of bacteria, microbial and macroscopic fungus growth in water reservoirs. Calder & Boustred (Ref. 93) have emphasized that sea water is often contaminated by micro-aerophilic bacteria from sewage, and any injury resulting in penetrating wounds require special treatment by surgery and antibiotics. Greenberg (Ref. 83) has reported a case of injury caused by high pressure (55.2 MPa) river water to a young man of age 22 years. The man reported to the emergency department 30 minutes after the accident. He had a laceration of the posterior-

lateral aspect of the right calf approximately 4 cm in length and 3 cm wide, extending into the deep fascia. There was no active bleeding present and no swelling of the calf. All motor, sensory and vascular aspects of the limb were intact. An x-ray film revealed air extending into the soft tissue about the knee and into the suprapatellar bursa as well. The wound was cleaned, debrided, and oral antibiotics administered. He returned seven days later and his leg showed evidence of diffuse cellulitis without abscess formation. He was admitted to the hospital and recovered uneventfully with intravenous antibiotics, warm soaks and elevation. Greenberg (Ref. 83) insists that water jet injury is a surgical emergency, as in other cases where materials such as paint or grease are involved. The river water (in field work, water is often taken from ponds, lakes, rivers, etc.) is a significant biological and chemical toxin because it is often contaminated by sewage and industrial wastes. Its irritative and infective potential is great and therefore immediate medical attention should be sought after the accident.

2.13 Responsibility

The cases reported by O'reilly and Blatt (Ref. 69) bring out several important points. The authors point out that high pressure soft tissue injury requires rapid and vigorous therapy. Physicians initially seeing these patients are often not aware that such injuries are serious, debilitating, and require immediate and specialized care. The purpose of the paper was to educate surgeons, radiologists, emergency room staff, industrial workers and supervisors and to emphasize that these injuries constitute a surgical emergency. Special attention should be paid to the following case:
An operator accidentally injured his middle finger of the right hand with paint at 20.7 MPa. He was refused permission by his supervisor for medical attention at the time of injury. The authors reiterate that this refusal of permission to seek medical attention immediately denotes a significant lack of understanding of this facet of industrial safety. Four hours elapsed before he was allowed to consult a physician. The result was the patient developed complications of secondary infection, with fever, lethargy and shock-like state. Delayed attention can also result in ischemia of the finger.

2.14 Mechanism of Damage & Other Factors

It is obvious from the list in Table 1, and the 'references', that adequate information now exists on high pressure fluid injury (albeit, a physician in attendance at the emergency department in the hospital may not be aware of it). However, there is a paucity of information on the mechanism of damage (histology, pathology, etc., and which may lead to better and quicker ways of treating the wounds), and on how the pressure, amount of fluid, the standoff distance, etc., influence the process and extent of damage. The information that is available, mostly in dental field (Refs. 52,56,97 & 107), is confined generally to low pressures and flows. Recently some attempts have been made in the high pressure area to understand the mechanism of tissue damage (Refs. 46,47,54,55,69,78,88,93,98 & 102). With regard to the dangers posed by the abrasive-entrained fluid jets, useful information can be extracted from the very limited studies reported, once again, in the dental field (Refs. 56,87,89,91,94,104,105 & 107). A brief description of some of these findings is given below (see Figs. 6 to 10):

The site of impact is usually small (Fig. 6 & 9A), often the cause for not reporting to the hospital immediately after the accident (Ref. 46). The symptoms can be divided into (a) Acute stage: immediate symptoms due to entry of foreign substance consisting of swelling and an increase in the interstitial pressure, accompanied by edema. Following the distension, the tissues become white and anaesthetic, due to interference of vascular supply, which may be due to thrombosis or compression of arteries, (b) Intermediate stage: this phase is characterized by the presence of oleogranulomas (may not be present in the case of water) which are nodular tumors, formed as a result of foreign-body tissue reaction. These may remain without any changes for a number of years, and (c) Late stage: eventually there is a breakdown of the oleomas close to the surface of the skin, associated with the appearance of widespread cutaneous and subcutaneous lesions. Malignancy may also result.

In order to determine the immediate physical damage and distribution of the injected material, Kaufman (Ref. 47) reproduced the injuries on cadaverous hands (Figs. 6,7 & 8) and Calder & Boustred (Ref. 93) on lower limbs (Fig. 9). Whereas the former used a mixture of white spirit and wax from a spray gun at 5.2 MPa, the latter used hydraulic oil (at 2 MPa?) from a gun fired by compressed air. Kaufman found that following the injection, the stream of wax travels through the various tissue layers in the line of its fire, until it hits a structure of sufficient resistance to deflect it. At this point, the wax spreads laterally within that tissue plane (Figs. 7 & 8). Therefore, different results will occur according to the site of injection. Similar observations were made by Calder & Boustred (Fig. 9B). They also showed that the amount of fluid entering the body was a strong function of the standoff distance. The degree of spread of the material in the tissue and the consequent

damage were found to depend on the kinetic energy of the jet. Katakura & Tsuji (Ref. 98) were the only authors who investigated systematically the effect of pressure (Max = 20 MPa), nozzle diameter (0.5 to 2 mm) and the standoff distance (0 to 120 cm) on dangers posed by fluid jets, by conducting tests, using hydraulic fluid, on raw skins of ox, believed to be similar to human skin. They also tested the effectiveness of transparent resin boards of PVC for protection against injury. Fig. 10, for example shows that a 2 mm jet at 15 MPa is capable of penetrating through the skin in 6 seconds (indicating that the time of exposure is very important) even at a standoff distance of 70 cm. The same jet can penetrate the skin in less than a second at a standoff distance of 5.5 cm. The authors conclude that PVC clothing may be useful, but there is no guarantee (see also Refs. 31 & 93), for protection against injury.

The effect of pressure is not clear. It probably depends on the site of impact (Figs. 11 & 12). In the case of the eyes (Ref. 92), a magnitude of pressure as low as 0.55 MPa (80 psi) was sufficient to cause severe damage to the eye lids (Fig. 11). The force of jet pushed the orbital tissues with great force resulting in compression of the blood vessels and rupture along anatomical seams. Edema of the lids was attributed to the powerful concussion caused by the water. Reddy and Kesavan (Ref. 97) have given a detailed account of damage mechanisms which could lead to tissue necrosis. These include, among others, pressure induced, diffusion mediated, deposition of bacteria and toxins through the sulcular epithelium into the underlying tissue, damage to the collagen network integrity in the tissue, damage to the blood and lymphatic microcirculation, and direct mechanical damage due to the abnormal shear forces induced by the jet, at pressures as low as 0.12 MPa.
O'reilly & Blatt (Ref. 69), on the other hand, argue that injury does not result from the high pressure itself. Pressure per se is important only as it is responsible for delivery and widespread distribution of the foreign substance in the body.

The release of gas (in the case of water, essentially air) along soft tissue plains (Fig. 12) can cause severe emphysema. According to Nichols & Smith (Ref. 77), gas induced infections can be fatal if not treated early by adequate surgical debridement.

2.15 Effect of Abrasives

There have been no reports of serious injuries caused by abrasive slurries. However, in dental practice, particularly in periodontics, air-water-powder abrasive systems (Prophy-Jets) have been used for removal of dental plaque, tooth associated stains and root preparations (Refs. 56,58,87,89,91,94,100,101,104,105 & 107). Beasley (Ref. 56), for instance used spherical polymer beads (specific gravity = 1.25; size = 10 to 70, mean = 24 microns; concentration = 5 gms of particles per 500 ml of tap water) to study the damaging effects of abrasive slurries, used in the pulsating jet devices, on oral mucosa (a soft tissue). Tests were conducted on adult albino rats and also included the effect of pressure. Fig. 13A shows a magnified specimen with intraepithelical inclusion of particles. Furthermore, as the pressure was increased from 345 to 414 kPa, the damage increased from epithelical disruption to epithelical tearing, fragmentation, vascular congestion and edema in the connective tissue (Fig. 13C). The author concluded that an increase in local tissue damage occurs when the particles are used in suspension as compared to tissues lavaged with tap water. The penetration of the particles was found only in the epithelical layers.

If the damage can occur with the abrasive jets at such a low pressure (621 kPa, 90 psi), one can very well imagine the severity of damage if impacted by a garnet (most commonly used abrasive in water jet technology) bearing water jet at 69 MPa (10000 psi)!

This section on the "INJURY" is concluded with a summary of two severe cases, one of them (Ref. 106) reported very recently in the literature, deliberately included to stress the point.

2.16 Injuries to Abdomen

Neill & George (Ref. 50) : Accident occurred to a man of 25 years of age when clearing a heat exchanger tube bundle. He was not wearing any protective clothing. The jet was accidentally directed towards his abdomen. He did not experience any immediate symptoms. He was seen half hour later at the hospital when he complained of a little right-handed pain and had vomited once. The only abnormalities were minimal tenderness and guarding in the right iliac fossa, and a semi-circle of 5 cm radius comprised of tiny pin-point puncture wounds of the skin low in the fossa, the appearance closely resembling a superficial abrasion. During the next 48 hours he vomited a small amount on several occasions and then began to complain of more severe generalized abdominal pain. Examination showed widespread tenderness and guarding and the absence of bowel sounds. X-ray examination showed distended loops of small bowel containing fluid levels. A diagnosis of perforated abdominal viscus producing generalized peritonitis was made, and after 48 hours after the injury the abdomen was

explored under general anaesthesia through a right paramedian incision. The findings were: (1) Fluid faeces in the peritoneal cavity, (2) two ragged holes in the ileum 1.0 cm in diameter and surrounded by many small perforations; the larger holes were situated 60 and 15 cm respectively from the ileocaecal junction, (3) Multiple small perforations of the cecum and (4) A shallow crater wound 4 cm in diameter on the peritoneal aspect of the anterior abdominal wall, which was deep and in communication with the external semi-circular wound. It was plugged with omentum.

The proximal 3 cm of the ascending colon, the cecum bearing the appendix and the distal 30 cm of ileum were resected and an end-to-end ileocolic anastomosis was fashioned. The more proximal ileal wound was treated by resection of 15 cm of bowel and end-to-end anastomosis. The peritoneal cavity was irrigated with saline. Two Ragnell drains were placed one through the entry wound and the other through a stab incision in the left iliac fossa. Post-operatively, the patient was given intramuscular cephaloridine and except for a wound abscess, made a straight forward recovery. He went home on the 22nd day after the operation.

In order to avoid such serious injuries, the authors recommended strict observation of comprehensive safety regulations, including the wearing of a full set of protective PVC clothing and the use of a fail-safe valve.

2.17 Injuries to the Extremities

Weltmer & Pack (Ref. 106): The authors reported evaluation of functional results in six patients who had high-pressure water-gun injection injuries to an extremity. Five of the injuries were to the foot and one was to the hand. All of the patients were followed to the time of complete recovery. The duration of the follow-up averaged 33.8 weeks (range: 3 to 110 weeks). Details were described for one patient. A 28 year old man shot the right foot with a water gun, at 48.3 MPa (7000psi) at a standoff distance of 30.5 cm. There were four puncture wounds on the dorsum of the right foot, beginning in the middle of the mid-part of the foot and progressing in a line to the second web space. The largest of these wounds was 5 mm in diameter. The patient had crepitation on motion of the ankle and on palpation of the dorsum of the foot to the ankle. Air in the soft tissues was seen on the x-rays (Fig. 12). Note that accumulation of gas in the tissues causes emphysema and infection (Ref. 77). Irrigation and debridement of the dorsal wound were performed, along with two longitudinal planar fasciotomies, five centimeters long, done as a precautionary measure. Several small (< 1 mm in diameter) fragments of his boot were found in the superficial part of the largest puncture site. The fasciotomies were closed after six days, and Cefadyl was administered intravenously for 8 days. No tetanus prophylaxis was needed. The patient started weight bearing at ten days, and the crepitation was gone at about three weeks. He had full recovery of function at one month.

Other patients had massive amount of subcutaneous emphysema and crepitation which may also be caused by clostridial and non-clostridial infections, injection of compressed air, etc. The wounds were clean, there was a minimum of foreign material and no evidence of massive soft tissue destruction. All of the wounds healed without complication. The authors recommended that such injuries should be treated with thorough irrigation and debridement, with fasciotomy only for patients who have symptoms of elevated compartment pressures. A broad-spectrum cephalosporin should be administered parenterally for two days, and then orally for a week.

2.18 Conclusions:

1. **Exercise extreme care in the use of high pressure equipment, including hoses.**
2. **Do not ignore water jet injury, in case of an accident, no matter how small it may appear at first sight.**
3. **Report immediately to the hospital and seek the attention of an experienced physician or surgeon, not the inexperienced interns or residents who are usually in attendance at the emergency departments.**

3.0 MEDICAL APPLICATIONS

3.1 General Remarks

Low pressure pulsating plain water and abrasive-entrained (Prophy Jet) jets have been in existence for a long time in the dental and the medical fields for cleaning, irrigating or debriding teeth, injuries or wounds etc (Refs. 36,37,38,52,53,56,57,58,60,61,81,87,89,91,94, 97,100,101,104,105 & 107). Investigators involved in these fields have not only given detailed descriptions of several types of instruments used in practice and their advantages compared to conventional techniques (e.g., Refs. 36,37 & 105), but have also thoroughly investigated the potential dangers, as stated in the paragraphs above, posed by these instruments to damaging soft tissues (e.g., Ref. 97). Briefly, the pulsating jets are

produced from pumps capable of generating pressures up to 1.4 MPa (200 psi), the pulsating rates varying any where from 100 to 2000 pulses per minute (Ref. 57). The amount of fluid can vary from 20 to 700 ml per pulse. Sohn & Weinstein (Ref. 81) found a pulsating device to be very useful for lavaging unhealed perineal wounds after proctectomy or proctocolectomy for inflammatory bowel disease or cancer. The application of the technique resulted in early discharge of the patient from the hospital. The technique has also been used successfully for lavaging contaminated and battle wounds (Refs. 57,60 & 61). Air-powder abrasive devices, which operate by directing fine particles of sodium bicarbonate through a stream of air surrounded by water, are becoming increasingly popular for cleaning and root preparation in periodontics. It is not the purpose of this paper to give details of these well established techniques. The purpose is to briefly describe novel applications, which appear to have great potential for regular use, with proper precautions, in the hospitals in the future. Some of these have already been tested clinically, while others either remain at developmental stage, or are undergoing in vitro experimentation. The description given below is by no means exhaustive.

3.2 Surgical Device for Eye Surgery (Ref. 108)

Wallach (Ref. 108) obtained a patent from the United States on this conceptual device for removing a defective or unwanted tissue, for example, from the lens of an eye, by directing a pulsating high velocity liquid jet onto the tissue to disintegrate it. The device incorporated a controlled suction conduit for sucking the liquid which entrained the disintegrated tissue. The inventor also claimed that salt crystals could be added to improve the cutting action of the jet. The pulse frequency could be varied from one in a few seconds to 333 pulses per second. The nozzle diameter and pressure could be varied within the range of 0.0254-0.254 mm and 0.1035-24.2 MPa respectively. Although several advantages for the device were claimed, it appears that it was never manufactured and tested on animals (it was particularly meant for animals) or humans. All attempts to contact the author or the firm to obtain further information on the device were futile. A literature search also failed to reveal any test results from this invention.

3.3 Stimulation of Acupuncture Points (Ref. 109)

According to the authors (Ref. 109), acupuncture implies treatment either by needles, electrostimuli via penetrated needles, or contact stimuli with surface electrodes, respectively. They, however, investigated a noninvasive water or air jet, naming it "fluidopuncture" for stimulating acupuncture points on the body. The first clinical testing of the concept was performed on a girl, 4 years and 9 months old. The girl had allergic manifestations on the skin which were visible as big, unevenly arranged, clearly delineated red spots all over the body, and were characterized by edema of the upper skin layers. The allergy point on the middle finger of both hands was treated for 2 minutes per point with a pulsed water jet. The jet frequency and the pressure were 18 Hz and 187 kPa (27 psi) respectively. Fifteen minutes after the treatment, the allergy traces withdrew completely. Twenty four hours later, the same manifestation returned with considerably smaller intensity. The same treatment was applied, after which the allergic manifestations disappeared. During the next 28 months of observation, no allergic symptoms were noted.

The authors also investigated air jets, believing that it is simpler to construct an air jet producing device. However, no tests results, clinical or otherwise, were given to compare air against water jet. The conclusion was that although the "fluidopuncture" apparatus may find its applications in all cases where contraindications or side effects from electric currents occur, further work is needed to fully establish its benefits.

3.4 Cutting or Fragmentation of Calculi & Ulcers (Refs. 110,112,114 & 117)

Jessen, et. al (Refs. 110 & 112) and Aeikens, et. al (Ref. 114) have investigated the feasibility of using high speed pulsed water jets for cracking gallstones (Refs. 110 & 112) and ureter calculi (Ref. 114). The investigations were undertaken because some of the existing techniques, such as endoscopic papillotomy, electrohydraulic lithotripsy or chemical stone dissolution are not satisfactory in nearly 15 to 20 percent of the cases. Tests were conducted, in vitro, on gallstones and ureter calculi previously extracted by other techniques. There were two kinds of gallstones, pigment stones and cholesterol stones, each type with differing internal structure and properties. In the first series of tests (Ref. 110), different sizes (diameters and weights ranging from 12.4-22.4 mm and 0.526-4.721 gm respectively) of stones were used to establish the operating parameters for cracking. Pulses of water were generated from a continuous jet by means of a magnetic valve. The nozzle diameter was 0.2 mm and the duration of the pulse was 0.25 seconds. The volume of water per pulse varied (from 1.10 to 1.90 ml) with the pressure (10 to 30 MPa). While some of the stones were smashed in one pulse, the others did not crack even after ten pulses. Apart

from the size, the type of stone dictated whether it could be cracked with the jet. For example, whereas dark pigment stones could be split at 15 MPa (2200 psi), the light coloured cholesterol stones were found to require pressures in excess of 20 MPa (2900 psi). Some of the cracked stones are illustrated in Fig. 14.

In the second investigation (Ref. 112), considerable attention was paid to aspects of system design, from the stand point of safety and reliability. The major concerns were (a) the fabrication of a small diameter flexible tubing of sufficient strength to withstand high pressures (Fig. 14), (b) accurate positioning of the nozzle against the stone, in order to avoid the damage to the surrounding soft tissue, and (c) design of a reliable, portable and disinfectable pump capable of producing high pressure pulses of varying durations.

The authors were successful in fabricating a small size (outer diameter = 2.0 mm, inner diameter = 0.6 mm) tube from PTFE, achieving a burst pressure of 45 MPa (6500 psi). Some in vitro tests were conducted under submerged conditions, simulating the bile duct, using a 0.2 mm nozzle at a maximum pressure of 25 MPa, the pulse duration being 200 ms. The splitting results were better than those obtained in air (Ref. 110). This observation is important from the stand point of safety, because the jet is now confined by the surrounding fluid, and will have less damaging effect on the adjacent tissues.

In the third investigation (Ref. 114), work was extended to cracking ureter calculi. Urolithiasis, the formation and growth of urinary calculi, appears to be world wide problem, which affects between 1 & 2 percent of the population. Most important types are renal calculi which can be as large as 30 mm in diameter and ureter calculi which can block the passage of urine. This can result in the build-up of back pressure and the failure of kidneys. All urinary calculi consist of quite hard crystalline material and an organic matrix of protein and uromucoide. As in the case of gallstones, some of the existing cracking techniques may not be suitable or satisfactory for some patients. Water jets, which can be used either for cracking the calculi into minute fragments in the ureter or pushing the calculus to the renal pelvis, where it can be cracked with the conventional techniques, might be considered as an alternative technique. However, the problems here are more severe than stated above. First, the nozzle and the flexible tubing have to be small enough to be inserted into the ureter, the diameter of which is of the order of 4 mm. Secondly, the ureter cannot take more than 1.0 ml of water per pulse, and this puts stringent constraints on the pressure, pulse length and the nozzle diameter. One of the tests indicated that a typical calculus required a pulse of 0.8 s duration at a pressure of 38.5 MPa (nozzle diameter = 0.18 mm) for fragmentation.

In all the investigations, no tests were conducted either on the animals or cadavers. Considering the immensity of the problems involved, it is fair to conclude that a great deal of developmental work is required before the technique can be put to work on the patients.

Recently, Sander et. al (Ref. 117) have reported (although not enough details were given) an interesting technique which combines a water jet with Nd-Yag laser for treating gastroduodenal ulcers with visible vascular stalks. A special method of water jet was developed to transport the laser beam. This method was compared with the traditional methods with endoscopy. Eleven patients, with comparable size ulcers, were treated with traditional endoscopy and non-contact laser (Group A) and nine patients with water jet laser (Group B). In group A, 6 patients developed severe bleeding during endoscopy; in two patients bleeding did not stop immediately and one patient started to bleed again later. Also only 4 out of 7 had reductions in size of the ulcer. In group B, bleeding stopped immediately and there was no bleeding after the surgery. Furthermore, 6 out of 7 patients had clearly small ulcers after 2 weeks. The authors concluded that water-jet-laser is a better method for treating ulcers with visible blood vessels.

3.5 Separation of the Tumor and Brain Surface (Refs. 115,120)

In all of the cases considered thus far, only one property of the pressurized fluid is used, viz., its cutting ability. Toth (Ref. 120) argues that there is another important property of pressurized fluids. Under appropriate conditions, the pressurized fluid can find its way through interspaces between adjoining bodies and can separate the boundaries if the pressure is greater than the force of adhesion. This is the principle behind the water jet technique developed by Toth and his co-workers (Ref. 115) for separating the tumor from the brain surface (Fig. 15). The benign tumors do not infiltrate the surrounding brain tissue and the surface of it is covered with connective tissue. Between the tumor surface and connective tissue shell there are spaces and adhesions, indicated by the arrows in Figs. 15A, B, C & D. The fluid can permeate these spaces and under an appropriate pressure can disintegrate the adhesions as well. In cases of meningiomass, the most important task is to separate the tumor from the brain surface,cranial nerves and vessels without damaging their function. With the fluid jet technique, this carried out by directing the jet (phys. NaCl) into the

tumor-arachnoidal space while the free edge of the tumor sheath is gently pulled (Fig. 15F). During this procedure, it is important to secure the outflow of the fluid. Otherwise, the pressure build-up will damage the brain tissue which is generally softer than the tumor. The jet was produced by an ordinary bulb syringe. The pressure in the direction of the flow, referred to as frontal pressure was between 3-10 kPa. The side pressure which separates the tumor from the brain surface was between 1-4 kPa.

The technique was clinically tested on 55 patients afflicted with meningiomas. A typical result is shown in Fig. 15E, where the uninjured brain tissue can be seen. Out of the 55 patients, 36 improved after the surgery, 14 remained unchanged (due to the complicated shape of the tumor, the technique was not effective), 2 got worse and 3 died. The authors concluded that although water jet technique appears promising, further work is required to develop more adaptable, more sophisticated and quantifiable pressure device for providing the jet.

3.6 Liver Resection (Refs. 111,113,116,118,119 & 122)

Hepatic resection, performed to remove damaged liver tissues due to various diseases such as metastatic liver cancer, is associated with substantial morbidity and an operative mortality rate of 5 to 20 percent (Ref. 118). Hemostasis can be difficult and many techniques have been used for the control of hemorrhage during the surgery. The main objective of the operation is to cut the parenchyma and to remove the affected tissue without impairing the intrahepatic fine vessels and biliary structures (Refs. 111,116 & 118). Papachristou and Barters (Ref. 111), by performing 45 lobectomies in dogs and four minor resections in patients with water jets, demonstrated that water jet technique was very effective in achieving hemostasis. Encouraged by these findings, perhaps, Nishisaka and Yonekawa (Ref. 113), developed a special water jet scalpel and by conducting tests on animals confirmed that water jets are indeed good for resection of the liver. Uchino, et. al (Ref. 116) and Une, et. al (119) extended the work further by conducting experimental work on pigs and clinical tests on human patients to establish the viability of the water jet technique compared to the conventional techniques. The optimum operating parameters, pressure, flow, etc., were obtained from the work on pigs. Hepatic resections were performed on 35 patients (26 male and 9 female, ages ranging from 8 to 76 years). The patients had various types of cancer and cirrhosis of the liver was associated with 10 of the 24 with hepatocellular carcinoma.

The apparatus used in the investigation is shown in Figs. 16A & B (Ref. 122). It consisted of a pressure generating unit (maximum pressure = 2.5 MPa, 362 psi) and a flexible hose connected to a hand piece (Fig. 16A). The nozzle fabricated from stainless steel was located at the tip of the hand piece which also incorporated an on/off micro-valve (Fig. 16B). The flexible hose was fabricated from hard rubber with a burst pressure of 5 MPa. In the clinical studies, a nozzle of 0.15 mm was used, with saline as the working fluid.

Fig. 16C illustrates a typical surgical procedure. Fragile hepatic parenchyma were washed out by the jet, while the intrahepatic vessels, capable of withstanding the jet pressures of 1.0 - 1.2 MPa, were left intact (Fig. 16D). In the case of chronic hepatitis or cirrhosis, in which the tissue becomes fibrotic, pressures as high as 1.8 MPa were not sufficient to cut the parenchyma. Pressures beyond 1.8 MPa posed a threat to the intrahepatic vessels.

Postoperative wound healing and regeneration of the operated area were found to be satisfactory. Histological examination revealed that the cut surface was smooth compared to that obtained with the conventional techniques. The main disadvantages of the technique were (a) difficult visualization of the operative field due to the formation of air bubbles, and (b) the splashing of the blood mixed with the fluid onto the faces of the operating personnel. Although the acrylic head attached to the suction device removed the air to some extent, it was not sufficient to improve the visibility. The major problem was the sterilization of the equipment (gas was employed to sterilize) because of its size. The authors felt that these problems could be solved by further development and concluded that the water jet technique is simpler, economical and better than the existing techniques.

Persson, et. al (Ref. 118) employed slightly smaller nozzle diameters (0.08 -0.10 mm) at higher pressures (1.5 - 5 MPa) to produce a coherent beam of jet (length = 10 cm) to improve the visibility during the surgery. They also added the drug, norepinephrine, to the saline solution and found that it reduced the oozing from the resection surface, but the blood loss was not sufficiently reduced. The technique was evaluated on 10 pigs all of which survived the resection. It was then used during hepatic resections upon six patients. The jet effectively washed away parenchymal tissue and displayed blood vessels and bile ducts. The authors stated that visualization of even minute vessels enabled a well controlled and safe resection. They concluded that although bleeding can be held at a minimum level even with

the standard blunt instruments, the main advantage of the jet technique is that it offers better control with less risk of troublesome bleeding. The addition of the drug was found to have no adverse effects on the humans.

3.7 Needleless Jet Injectors (Ref. 121)

Fig. 17 shows a typical injector, referred to as "needleless injector", which is a hand held unit for injection of medication (Ref. 121). The idea behind such systems is not new, although attempts to improve their performance and reliability are being made continually. The unit shown in Fig. 17 utilizes a disposable polycarbonate ampule to hold the medication. The CO_2 gas power source moves a piston which strikes the plunger of the ampule, creating an internal pressure within the ampule of about 41 MPa (6000 psi). This accelerates the medication out of the ampule at approximately 270 m/s through a very small orifice, creating a fine jet which penetrates the skin surface and is carried into the subcutaneous tissue. Depending upon the patient and the body site, intramuscular injection may also be possible. Schwartz (Ref. 121) states that the technique can be suitable for the non-particulate medications in dosages of 1.0 ml or less.

The advantages of the unit for medical injection are reduced pain and tissue trauma, a much shorter injection time (< 1/30 s) and the elimination of needle-stick cross-contamination risk for the health care worker. The problems encountered to date have centered around the high pressure created in the ampule and the need to contain that pressure within an inexpensive plastic to maintain disposability. Moulding techniques, such as ultrasonic welding are believed to solve this problem. However, problems related to shape of the tip and the optimum orifice size still remain. When the unit becomes available, some precautions are warranted. It may not be used on patients with fragile skin, minimum of adipose tissue, or those taking anti-coagulants or with coagulation abnormalities.

3.8 Conclusions

This brief review of the use of fluid jets for medical applications shows that while some are at the laboratory level (e.g., cracking gall stones), others are quite well advanced, with proven clinical results, to the point that they can be used in the hospitals on a regular basis. However, the technique calls for extreme caution, for any slight errors in the procedure or the parameters (e.g., pressure) can be fatal, as discussed in the section on 'injuries'. For some applications the technique may not even be suitable. For example, although considerable work has been done on cracking of gall stones and ureter calculi, the technique does not appear to be feasible. The same applies to amputation of large bones, unless one considers employing abrasive-entrained liquid jets. But then, what kind of abrasives and how about their undesirable effects on the tissue? Finally, the question of acceptability by the medical community needs to be addressed.

4.0 EPILOGUE

Why did the rabbits die in the amputation experiments in the laboratory? After this review, it seems reasonable to assume that they died due to (i) shock - because of the very high pressures, (ii) edema - too much water used during the surgery, (iii) emphysema - tap water contains abundant air, and probably (iv) infection - equipment was not sterilized. In all of the medical applications discussed above, generally low pressures and low flows were involved, indicating that the human body will not take excessively high pressures or large amounts of fluids, imposing a limitation on the uses!

5.0 ACKNOWLEDGMENTS

The author is thankful to publishers of the journals and the book from which the photographs reproduced in Figs. 4 to 13 were taken, and to Dr. H. Louis, University of Hannover, Germany, for the photograph shown in Fig. 14, Dr. S. Toth, Medical University of Debrecen, Hungary (Fig. 15), Dr. J. Uchino, School of Medicine, Hokkaido University, Japan (Fig. 16), and Mr. T.E. Schwartz, Bioject Medical Systems Ltd., Canada (Fig. 17) and also for their personal communications. It is a pleasure to acknowledge Dr. R.G. Williamson, Head, Gas Dynamics Laboratory for the encouragement to write this paper. Thanks are also due to Mrs. H. McDonald for typing the manuscript of this paper.

6.0 REFERENCES

1. Vijay, M.M., and Brierley, W.H.: Cutting Cleaning and Fragmentation of Materials with High Pressure Liquid Jets. Proc. 1st U.S. Water Jet Symposium. Golden. Colorado. 1981. pp. V-41-12.
2. Ward, G.M.: Safety Considerations Arising from Operational Experience with High Pressure Jet Cleaning. Paper F1. Proc. 1st International Symposium on Jet Cutting

Technology. BHRA. England. 1972. pp. 1-40.
3. Adaway,C.W., Hinrichs,J.F., and Frye, J.D.: Hydro-Blasting Safety. Proc. 2nd U.S. Water Jet Conference. Rolla. Missouri. 1983. pp.127-132.
4. Anon: Jetting Safety - A Special Supplement to Industrial Jetting Report. Industrial Jetting Report. No. 25. June 1985. BHRA. England. pp.1-8.
5. Anon.: Recommended Practices for the Use of Manually Operated High Pressure Water Jetting Equipment. Proc. 3rd U.S. WaterJet Conference. Pittsburgh. 1985. pp.63-79.
6. Summers,D.A., and Viebrock,J.: The Impact of Waterjets on Human Flesh. Paper H4. Proc. 9th International Symposium on Jet Cutting Technology. BHRA. England. 1988. pp.423-433.
7. Rees,C.E.: Penetration of Tissue by Fuel Oil Under High Pressure from Diesel Engine. Jour. A.M.A. V.109. No.11. 1937. pp.866-867.
8. Dial, D.E.: Hand Injuries Due to Injection of Oil at High Pressure. J. Am. Med. Assn. V.110. 1938. pp.1747-.
9. Brooke, R., and Rooke, C.J.: Two Cases of Grease-Gun Finger. British Med. J. V.2. 1939. pp.1186-.
10. Smith, F.H.: Penetration of Tissue by Grease under Pressure of 7000 Pounds. J. Am. Med. Assn. V.112. 1939. pp.907-908.
11. Mason, M.L., and Queen, F.B.: Grease Gun Injuries to the Hand. Quart. Bull. Northwestern Univ. Med. Sch. V.15. 1941. pp.122.132.
12. Hughes, J.E.: Penetration of Tissue by Diesel Oil Under Pressure. J. Am. Med. Assn. V.116. 1941. pp.2848-2849.
13. Byrne, J.J.: Grease-Gun Injuries. J. Am. Med. Assn. V.125. 1944. pp. 405-407.
14. Bell, R.C.: Grease-Gun Injuries. British J. Plast. Surg. V.5. 1952. pp.138-145
15. Tempest, M.N.: Grease-Gun Injuries. University Leeds Med. J. V.2. 1953. pp.125-129.
16. Baker, J.M.: Molten Plastic Injuries of the Hand. Plast. Reconstr. Surg. V.15. 1955. 233-240.
17. Vivian, D.N., and Christian, S.G.: Grease-Gun Injury. A Case Report. Indus. Med. V.24. 1956. pp.282-284.
18. Rains, A.J.H.: Grease-Gun Injury to the Hand. Value of Early Treatment. British Med. J. V.1. 1958. pp.625-626.
19. Innes,C.B.: Grease Gun Finger. New Zealand Med. J. V.58. 1959. pp.177-178.
20. Harrison, R.: Grease-Gun Injury. British. J. Surg. V.46. 1959. pp.514-515.
21. Milliken,T.W., and Weston,T.S.: Grease Gun Injuries. NZ Med. J. V.59. 1960. pp.413-416.
22. Osborne,J.C.: Grease Gun Injury. Canad. J. Surg. V.3. 1960. pp.339-340.
23. Stark,H.H., Wilson,J.N., and Boyles, J.H.: Grease-Gun Injuries of the Hand. The Journal of Bone and Joint Surgery. V.43A. No.4. 1961. pp.485-491.
24. Bottoms, R.W.A.: A Case of High Pressure Tool Injury to the Hand, Its Treatment Aided by Dexamenthasone and a Plea for Further Trial of This Substance. Med. J. Austral. V.2. 1962. pp.591-592.
25. Workman,C.E.: Power Paint Sprayer Injury to Hand. Missouri Med. V.60. 1963. pp.856-858.
26. Tanzer,R.C.: Grease-Gun Type Injuries of the Hand. Surg. Clin. North Am. V.43. 1963. pp.1277-1282.
27. Jones,J.B.: Gangrene of a Finger due to Hydraulic Fluid. Clin. Orthop. Rel. Res. V.32. 1964. pp.110-113.
28. Malherbe,W.D.F., and Heydenrych,J.J.: Hand Injuries Caused by Oil Injection Under Pressure. South Afr. Med. J. V.38. 1964. pp.844-847.
29. Smith,M.G.H.: Grease Gun Injury. Br. Med. J. V.2. 1964. pp.918-920.
30. Blue,A.I., and Dirstine,M.J.: Grease Gun Damage, Subcutaneous Injection of Paint, Grease, and Other Materials by Pressure Guns. Northwest Med. V.64. 1965. pp.342-344.
31. Gardner, A.W.: High Pressure Water Jet Injury. Trans. Soc. Occ. Medicine. V.16. 1966. pp.30.
32. Nahigan, S.H.: Airless Spray Gun, a New Hand Hazard. J. Am. Med. Assn. V.195. 1966. pp.688-691.
33. Flint, M.H.: Plastic Injection Moulding Injury. Br. J. Plast. Surg. V.19. No.1. 1966. pp.10-78.
34. Kaufman,H.D., and Williams, H.O.: Systemic Absorption from High-Pressure Spray Gun Injuries. Br. J. Surg. V.53. No.1. 1966. pp.57-58.
35. Editors: "Annotations" Section: Injection Accidents in Industry. Lancet. V.1. 1966. pp.37-38.
36. Berman, C.L.: Oral Hydrotherapy. Periodontal Abstract. V.14. 1966. pp.151-152
37. Karjewski, J.J., Rubach, W.C., and Higginbotham, T.L.: Current Status of Water Cleansing in Oral Hygiene. J. Calif. St. Dent. Ass. Nevada St. Dent. Ass. V.42. 1966. pp.433-435.
38. Sumner, C.F.: What is the Value of Water Spray Devices in Maintaining Adequate Oral

Hygiene? Periodont Abstract. V.14. 1966. pp.150-151.
39. Stark,H.H., Ashworth, C.R., and Boyles, J.H.: Paint Gun Injuries of the Hand. The Journal of Bone and Joint Surgery. V.49A. No.4. 1967. pp.637-647.
40. Waters, W.R., Penn, I., and Ross,H.M.: Airless Paint Gun Injuries of the Hand : A Clinical and Experimental Study. Plast Reconstr Surg. V.39. 1967. pp.613-618.
41. Weeks,P.M.: Airless Paint Gun Injuries of the Hand. J. Ky Med. Assoc. V.65. 1967. pp.1086.
42. Morley, R.: Injuries due to Accidental Injection of Paint from High-Pressure Paint Guns. Br. Med. J. V.1. 1967. pp.25-26.
43. Wofford,B.H.: Treatment of High Velocity Paint Gun Injury of the hand. Southern Med. V.66. No.3. 1967. pp.307 & 344.
44. Morley,R.: An Evaluation of the Safety of Shrouded Nozzles Used on High Pressure Greasing Equipment. Br. J. Indust. Med. V.24. 1967. pp.152-155.
45. Spak, I.: Finger Injury Caused by Paint Spray Gun : A Report of a Case. Acta Chir. Scand. V.133. 1967. pp.331-332.
46. Kaufman,H.D.: The Clinicopathological Correlation of High-Pressure Injection Injuries. Brit. J. Surg. V.55. No.3. 1968. pp. 214-218.
47. Kaufman,H.D.: The Anatomy of Experimentally Produced High-Pressure Injection Injuries of the Hand. Brit. J. Surg. V.55. No.5. 1968. pp.340-344.
48. Sharrard,J. Industrial Injection Injuries. The Journal of Bone and Joint Surgery. V.50. 1968. pp.1.
49. Hutchinson,C.H.: Hand Injuries Caused by Injection of Cement Under Pressure. The Journal of Bone and Joint Surgery. V. 50B. No.1. 1968. pp.131-133.
50. Neill, R.W.K., and George, B.: Penetrating Intra-Abdominal Injury Caused by High Pressure Water Jet. British Medical Journal. May 1969. pp. 357-358.
51. Benson,E.A.: Grease-Gun Injury. Br. J. Surg. V.56. 1969. pp. 397-399.
52. Seliger, W.G.: A Technique for Measuring the Penetration of Pulsating-Jet Oral Irrigators. Archs. Oral Biol. V.14. 1969. pp.435-436
53. Isshiki, Y.: Effect of Oral Cleansing in Cerebral Palsied Children - Application of a Water Jet Device. Bull. Tokyo Dent. Coll. V.11. No.2. 1970. pp.121-131.
54. Ramos,H.,Posch,J.L., and Lie,K.K.: High Pressure Injection Injuries of the Hand. Plastic & Reconstructive Surg. V.45. No.3. 1970. pp.221-226.
55. Kaufman, H.D.: High Pressure Injection Injuries. The Problems, Pathogenesis and Management. Hand. V.2. 1970. pp.63-73.
56. Beasley, J.D.: The Effect of Spherical Polymers and Water Jet Lavage on Oral Mucosa. Oral Surgery. V.32. No. 6. 1971. pp. 998-1007.
57. Bhaskar, S.N., Cutright,D.E., Hunsuck,E.E., and Gross, A.: Pulsating Water Jet Devices in Debridement of Combat Wounds. Military Medicine. March 1971. pp.264-266.
58. Bhaskar, S.N., Cutright,D.E., Gross,A., Frisch,J., Beasley,J.D., and Perez,B.: Water Jet Devices in Dental Practice. Journal Periodont. V.42. No.10. 1971. pp.658-664.
59. Walton, S.: Injection Gun Injury of the Hand with Anti-Corrosive Paint and Paint Solvent. Clin. Orthop. Related Research. V.74. 1971. pp.141-145.
60. Grower, M.F., and Bhaskar, S.N.: Effect of Pulsating Water Jet Lavage on Radioactive Contaminated Wounds. Wound Decontamination, V.51. No.2. 1972. pp.536-538.
61. Gross, A., Cutright, D.E., and Bhaskar, S.N.: Effectiveness of pulsating Water Jet Lavage in Treatment of Contaminated Crushed Wounds. The American Journal of Surgery. V.124. 1972. pp.373-377.
62. Albernethy, P.J., and Guy, J.G.: An unusual Injection Injury of the Thumb. Hand. V.4. 1972. pp.173-175.
63. Scher,C.,Schuh,F.D., and Harvin,J.S.: High Pressure Paint Gun Injuries of the Hand. A Report of Two Cases. Brit. J. Plastic Surg. V.26. 1973. pp.167-171.
64. Baylor, C.H., Samuelson, C.L., and Sinclaire, H.A.: Treatment of Grease Gun Injuries. J. Occup. Med. V.15. 1973. pp.799-800.
65. Burke, P.J., and Connoly, W.B.: Paint Gun Injection Injury of the Hand. A Surgical Emergency. Med. J. Austral. V.2. 1973. pp.276-278.
66. Gillespie,C.A.,Rodeheaver,G.T., Smith,S.,Edgerton,M.T., and Edlich, R.F.: Airless Paint Gun Injuries : Definition and Management. The American Journal of Surgery. V.128. 1974. pp.383-391.
67. Palmieri,T.J.: High Pressure Injection Injuries of the Hand-Treatment by Early Mobilization. Bull. Hosp. Joint Dis. V.35. 1974. pp.18-35.
68. Williams,C.S., and Riordan, D.C.: High Velocity Injection Injuries of the Hand. Southern Med. J. V.67. 1974. pp.295-302.
69. O'reilly, R.J., and Blatt,G.: Accidental High-Pressure Injection-Gun Injuries of the Hand. The Journal of Trauma. V.15. No.1. 1975. pp.24-31.
70. Apfelberg, D.B., Lash, H., Maser, M.R., et al.: High-Pressure Silicone Injection Injury of the Hand. J. Trauma. V.15. 1975. pp.922-925.
71. Gelberman,R.H., Madison,J.L., Posch,M.D., et al.: High Pressure Injection Injuries of the Hand. J. Bone Jt. Surg. V.57A. 1975. pp.935-937.
72. Kleinert,H.E., Bronson,J.L., and Thurston,J.B.: The Hand - High Pressure Injection Injuries. Res. Staff Phys. V.22. 1976. pp.110-.

73. Mann, R.J.: Paint and Grease Gun Injuries of the Hand. J.A.M.A. V.231. 1975. pp.933.
74. O'Reilly,R.J., and Blatt,G.: High Pressure Injection Injury. J.A.M.A. V.233. 1975. pp.533-534.
75. Parks,B.J., Horner,R.L., and Trimble,C.: Emergency Treatment of High Pressure Injection Injuries of the Hand. JACEP. V.4. 1975. pp. 216-217.
76. Lotem, M., and Conforty, B.: High Pressure Injection Injuries of the Hand. Harefuah, V.89. 1975. pp.213-.
77. Nichols, R.L., and Smith, J.W.: Gas in the Wound : What Does it Mean? Surgical Clinics of North America. V.55. No.6. 1975. pp.1289-1296.
78. Dickson,R.A.: High Pressure Injection Injuries of the Hand : A Clinical, Chemical and Histological Study. Hand. V.8. 1976. pp.189-193.
79. Phelps,D.B.,Hastings,H., and Boswick,J.A.,Jr.: Systemic Corti-costeroid Therapy for High-Pressure Injection Injuries of the Hand. J. Trauma. V.17. 1976. pp.206-210.
80. Silsby,J.J.: Pressure Gun Injection Injuries of the Hand. Western J. Med. V.125. 1976. pp.271-276.
81. Sohn, N., and Weinstein, M.A.: Unhealed Perineal Wound - Lavage with a Pulsating Water Jet. The American Journal of Surgery. V.137. 1977. pp.426-427.
82. Childress,M.H.: High Pressure Injection Injury of the Hand. J. Nat. Med. Ass. V.69. 1977. pp.663-664.
83. Greenberg, M.I.: High-Pressure Injection Injury with River Water. J. Am. Coll. Emerg. Phys. (JACEP). V.7. No.6. 1978. pp.241-242.
84. De Beaux, J.L.M.: High Pressure Water Jet Injury. British Medical Journal. V.280. 1980. pp.1417-1418.
85. Calder, I.M., and Boustred, D.: High Pressure Water Jet Injury. British Medical Journal. V.280. 1980. pp. 1620.
86. King, J.: High Pressure Water Jet Injury. British Medical Journal. July 1980. pp.232.
87. Gwinnett,J.S.: A Report on the Removal of Stain and Debris from Teeth Using the Prophy-Jet. Promotional Material. Cooper/Laser Sonics (Dentsply), Inc. Long Island City, NY. 1980.
88. Schoo,M.J., Scott,F.A., and Boswick, J.A.: High Pressure Injection Injuries of the Hand. The Journal of Trauma. V.20. No.3. 1980. pp. 229-238.
89. Willmann, D.E., Norling, B.K., and Johnson, W.N.: A New Prophylaxis Instrument: Effect on Enamel Alterations. J Am Dent Assoc. V.101. 1980. pp. 923.
90. Engel,J., Lin,E., and Tsur,H.: Neurovascular Island Flap Reconstruction Following High Pressure Injection Injuries of the Hand. Injury:the British J. Acc. Surg. V.13. No.3. 1981. pp.181-184.
91. Anon: Oral Prophylaxis: Prophy-Jet. Clinical Research Associates Newsletter. V.5. 1981. pp.1-.
92. Salminen, L., and Ranta, A.: Orbital Laceration Caused by a Blast of Water: Report of Two Cases. British Journal of Ophthalmology. V.67. 1983. pp. 840-841.
93. Calder J.M., and Boustred, D.: Experiments Using High Pressure Fluid Jets on Human Tissues. Forensic Science International. V.26. 1984. pp. 123-129.
94. Atkinson, D.R., Cobb, C.M., and Killoy, W.J.: The Effect of an Air-Powder Abrasive System on in Vitro Root Surfaces. J. Periodontol. V.55. 1984. pp.13-18.
95. Craig,E.V.: A New High Pressure Injection Injury of the Hand. J. Hand Surg. V.9A. 1984. pp.240-242.
96. Kon, M., and Sagi, A.: High-Pressure Water Jet Injury of the Hand. The Journal of Hand Surgery. V.10A. No.3. 1985. pp.412-414.
97. Reddy, N.P., and Kesavan, S.K.: Mechanisms of Tissue Damage Resulting from the Use of Oral Water Irrigation Devices. Medical Hypotheses. V.18. 1985. pp.417-423.
98. Katakura, H., and Tsuji, S.: A Study to Avoid the Dangers of High Speed Liquid Jets. Bulletin of JSME. V.28. No.238. 1985. pp.623-630.
99. Frank, H.K.: Mundduschen aus Kunststoffen als Oekosysteme fur aerobe Bakterien. In: Material und Organismen. Editors: Goronde M., and Kerner W. V.20. No.1. 1985. Duncker & Humblot, Berlin, Germany. pp. 1-9. In German (Translation available from the National Research Council of Canada).
100. Toevs, S.E.: Root Topography Following Instrumentation. Dent Hyg. V.59. 1985. pp.350.
101. Watts,E.A., and Newman,H.N.: Clinical Effects on Chronic Periodontitis of a Simplified System of Oral Hygiene Including Subgingival Pulsated Jet Irrigation with Chlorhexidine. J. Clin. Periodontol. V. 13. No.7. 1986. pp.666-670.
102. Yen,R.T., Fung,Y.C., Ho,H.H., and Butterman,G.: Speed of Stress Wave Propagation in Lung. J. Appl. Physiol. V.61. No.2. 1986. pp.701-705.
103. Facheson,J., Wong,D., and Chignell,A.H.: Eye Injuries Caused by Directed Jets of Water from a Fire Hose. British Medical Journal. V. 294. 1987. pp.481-482.
104. Berkstein,S., Reiff,R.L., McKinney,J.F., and Killoy,W.J.: Supragingival Root Surface Removal During Maintenance Procedures Utilizing an Air-Powder Abrasive System or Hand Scaling - An In Vitro Study. J. Periodontol. V. 58. 1987. pp.327-330.
105. Horning,G.M., Cobb,C.M., and Killoy,W.J.: Effect of an Air-Powder Abrasive System on

Root Surfaces in Periodontol Surgery. J. Clin Periodontol. V.14. 1987. pp.213-220.
106. Weltmer,J.B., Jr., and Pack,L.L.: High-Pressure Water-Gun Injection Injuries to the Extremities. The Journal of Bone and Joint Surgery. V.70-A. No.8. 1988. pp.1221-1223.
107. Pippin,D.J., Crooks,W.E.,Barker,B.F., Walters,P.L., and Killoy,W.J.: Effects of an Air-Powder Abrasive Device Used During Periodontal Flap Surgery in Dogs. J. Periodontol. V.59, No.9. 1988. pp.584-588.
108. Wallach,M.: Surgical Apparatus for Removal of Tissue. United States Patent No.3,930,505. January 6, 1976. pp.1-14.
109. Majic,V., Skokljev,A., Knezevic,D., and Bajc,P.: Air-and Water-Jet Stimulation of Acupuncture Points. Acupuncture & Electro-Therapeut. Res. Int. J. V.4. 1979. pp.17-21.
110. Jessen,K.,Philipp,J., Classen,M., Schikorr,W., and Louis,H.: Endoscopic Jet-Cutting - A New Method for Stone Destruction in the Common Bile Duct. Paper B1. Proc. 6th International Symposium on Jet Cutting Technology. BHRA. England. 1982. pp.39-52.
111. Papachristou,D., and Barters,R.: Resection of the Liver with a Water Jet. Br. J. Surg. V.69. 1982. pp.93-94.
112. Jessen,K., Classen,M., Leuschner,U., Haferkamp,H., Louis,H., and Schikorr,W.: Endoscopic Jet Cutting of Human Gallstones. Paper D4. Proc. 7th International Symposium on Jet Cutting Technology. BHRA. England. 1984. pp.211-220.
113. Nishisaka,T., and Yonekawa,M.: Development of the Water Jet Scalpel. Proc. International Symposium on Water Jet Technology. The Water Jet Technology Society of Japan. Tokyo. Japan. 1984. pp.49-61. In Japanese.
114. Aeikens,B., Decker,B., Haferkamp,H., and Louis,H.: Cracking of Ureter Calculi by High Speed Water Jet Pulses. Paper 15. Proc. 8th International Symposium on Jet Cutting Technology. BHRA. England. 1986. pp.157-166.
115. Toth,S., Vajda,J., Pasztor,E., and Toth,Z.: Separation of the Tumor and Brain Surface by "Water Jet" in Cases of Meningiomas. Journal of Neuro-Oncology. V.5. 1987. pp.117-124.
116. Uchino,J., Une,Y., Horie,T., Yonekawa,M., Kakita,A., and Sano,F.: Surgical Cutting of the Liver by Water Jet. Paper P2. Proc. 9th International Symposium on Jet Cutting Technology. BHRA. England. 1988. pp. 641-650.
117. Sander,R., Poesl,H., Zuern,W., and Spuhler,A.: The Water Jet Nd-Yag Laser, A New Tool for Treating Gastroduodenal Ulcers with Visible Vascular Stalks. Zeitschrift fur Gastroenterologie. V.26. N.9. 1988. pp.451.
118. Persson,B.G., Jeppsson,B., Thranberg,K.G., Roslund,K., and Bengmark S.: Transection of the Liver with a Water Jet. Surgery, Gynecology & Obstetrics. V.168. 1989. pp.267-268.
119. Une,Y., Uchino,J., Horie,T., Sato,Y., Ogasawara,K., Kakita,A., and Sano, F.: Liver Resection Using a Water Jet. Cancer Chemother Pharmacol. V.23 (Suppl). 1989. pp.74-77.
120. Toth,S.: Surgery Using Water Jet for Tumor-Brain Separation. Personal Communication. April 1989.
121. Schwartz,T.E.: The Biojector Needleless Jet Injection System. Personal Communication. March 1989.
122. Uchino,J.: Water Jet Cutting of Liver. Personal Communication. June 1989.
123. Miller,B.F., and Galton,L.: The Complete Medical Guide. Simon & Schuster, New York. U.S.A. 1978.

Table 1. A Brief Summary of the Injuries Reported in the Literature (mostly taken from Ref. 88)

Ref.	Pressure(MPa) & Material	Age & site of Injury	Treatment	Result	Remarks
7	27.6, Diesel fuel	47. Right long finger tip	Elevation; debridement at 7 days	Amputation	Loss of finger
10	48.3, Grease	31. Left index finger	Debridement within 24 hr	Amputation	Loss of finger
11	Grease	23. Palm	Debridement	Large oleoma excised at 8 months	

	Grease	26. Left index finger	No treatment	Large oleoma excised at 6 months	
12	Diesel Oil	31. Left long & ring fingers	Debridement at 6 hr.	Amputation at long & ring meta-carpals	
13	Grease	54. Left ring finger	Small incision	Amputation of finger tip	Discharged oleomas
14	Grease	Right long finger	Immediate antibiotics & debridement at 10 days	Prolonged drainage & oleomas	
	Grease	Right index finger	Poultices & debridement at 2 years	Chronic drainage & tenderness	Lost wages for one year!
18	Grease	36. Left palm	Debridement at 1 month	No functional loss	Cultures negative
24	Hydraulic fluid	34. Palm	Debridement of hand & wrist; dexa-methasone & antibiotic	Cosiderable disability	First to use steroid
25	0.55, Paint	52. Left index finger	Immediate debridement	Disarticu-lation at left index PIP	
27	20.7, Hydraulic Fluid	21. Left index finger	Debridement at 24 hr.	Amputation of left index ray	Fat necrosis evident; culture neg.; antibiot. no improvement
28	Diesel fuel	19. Right thumb	Small inci-sion at 1 week. Debri-dement at 9 months	Returned to work in 1 month	Pathology: granulomatous foreign body reaction
30	Paint	24. Left index finger	Primary amputation	Amputation of left index ray	
	Paint	20. Left index finger	Debridement at 12 hr.	Disarticu-lation through PIP joint	
	Hydraulic fluid	47. Left index finger	Immediate debridement	Severe loss of function	Amputation recommended
31	41, Sea Water	Lower abdominal wall	No details given	Skin healed in 29 days	Discharged and returned to work on the 32nd day

33	69, Molten Plastic	31. Left palm	Debridement	Left ring ray amputation required	
	69, Molten Plastic	30. Right palm	Debridement	Nonunion ring M.C. fix	Required skin &tendon graft
	Molten nylon	40. Right index finger	Debridement	Right index amputation	
39	13.8 to 20.7 Paint & Paint thinner	23 to 49. Left & right index fingers, thumbs & left palm	Debridements at verying times (2 hr to 4 days)	Varied from amputation to no amputation.	One case had severe inflammation and the other decreased flex/extension
40	Paint thinner	31. Left index finger	Debridement at 4 hr; steroids & stellate blocks	Amputation of index & long fingers	Abdominal flap required. Author felt steroids of no use
42	13.8 to 20.7 Paint	38 to 50. Left thumb tip, left palm & right long finger	Dressing & debridement	Loss of thumb tip pulp; Loss of palm tissue, index & long finger amputation & disarticulation of right long PIP	Accidents caused by (1)removal of safety nozzle (1) Failure of safety nozzle
49	20.7, Cement	25 & 30. Right thumb & index fingers	No treatment & debridement	Ulcer formation,decreased IP joint motion disarticulation at PIP & amputation	Localized and chronic inflammation and infection
50	41.4 to 48.3 Water	25. Abdomen	Irrigation with saline, followed by surgery & antibiotic	Good recovery	Had no protective clothing
59	0.41, Paint thinner	49. Left long finger	Immediate debridement	Amputation long finger	Chemical inflammationculture negative
62	Indium	23. Right thumb tip	Immediate debridement	Slight tenderness	Material is low toxicity
68	Grease	45. Left tnumb	Debridement antibiotics	No amputation	Decreased range of motion and sensation
	12.4, Hydraulic fluid	26. Left thumb	Debridement at 9 days	Healed with scar	

	Paint	33. Left palm	Debridement at 2 days	Amputation ring finger	Decreased sensation & flexion contractures of long & small
	41.4, Mud	49. Right 1st web	Debridement at 12 hr	Median & ulnar neuropathy	50% impairment; decreased range of motion
	Hydraulic fluid	54. Left long finger	Debridement at 2 weeks	Multiple oleoma formation	70% decreased motion of long finger
	Paint thinner	62. Left index finger	Debridement at 4 hr	Ampute left index	25% permanent loss
70	Silicone	20. Right long finger	Debridement	Skin & tendon loss	
78	20.7, Paint thinner	45. Left index finger	Debridement at 5 hr	Amputation left index finger	
79	12.4, Hydraulic fluid	48. Left palm	Debridement at 72 hr & steroids	Full function, normal range of motion	No clinical infection
83	55.2, Polluted river water	22. Laceration of right calf	Debridement antibiotics	Recovered uneventfully	Required intravenous antibiotics, warm soaks and elevation
84	Upto 100 MPa, Sea Water	32. Blow to the abdomen	No details given	Uneventful convalescence	Protective clothing minimized the seriousness of the injury
92	0.55, water	52. Left eye	Sutures & antibiotics	Blood in the vitreous disappeared within 10 days	Completely recovered after 10 days
96	34.5, water	32. Left thumb	Conservative initially. Later, antibiotics, etc.	Normal function of all fingers on the 10th day	There was swelling and severe tenderness on the palmer side of the wrist

APPENDIX : GLOSSARY

Abscess : Collection of puss accompanied by swelling
Adipose : Consisting of fat
Anastomosis : To unite by contact
Aponeurosis : An expanded tendon
Arachnoidal : Related to serous membrane enveloping the brain
Axillary : of or near the armpit
Biliary : of bile or carrying bile
Botulism : Poisoning caused by anaerobic (free of oxygen) bacteria
Bursa : Small fluid filled sac in the joints which helps cushion the bones against friction
Calculus : A stony mass in the gallbladder, kidney, or urinary bladder
Cecum : Sac of the large intestine located where the large and small intestines join

Cellulitis : Inflammation of cellular tissue
Cephalosporin : An antibiotic related to penicillin
Cirrhosis : A chronic disease of the liver characterized by degeneration of liver cells and hardening due to great increase of fibrous tissue on the liver
Clostridium : A type of bacteria, causing tetanus or botulism
Coagulation : Formation of a semisolid mass from a liquid, such as blood or lymph
Collagen : the protein substance in the fibres of connective tissue
Concussion : A sudden violent shaking or shock
Cortex : The layer of gray matter that covers most of the brain surface
Corticosteroid : Any one of a group of steroids produced by the adrenal cortex
Crepitation : Crackle or rattle
Debride (ment) : The cleansing of a wound by cutting away dead or infected tissue, foreign matter, etc,
Distension : Swelling by internal pressure
Dorsum : The back, or outer surface of an organ or part
Edema : Swelling of parts arising from water collection
Emphysema : Swelling of tissues from air or gas
Endoscopy : Examination of a hollow organ by an endoscope
Epidermis : Outer layer of the skin, composed of two to four layers
Epithelium : A thin layer of cells forming a tissue that covers surfaces of the body and lines hollow organs
Fascia : Thin band of connective tissue
Fossa : Elongated shallow cavity especially in a bone
Gangrene : Decay or death of tissue due to lack of blood
Gastroduodenal : Related to stomach and duodenum (small intestine nearest the stomach)
Gingiva : Flesh around the teeth; gum
Granulation : The formation of flesh on the surface of a wound
Granuloma : A tumor composed of granulated tissue
Hemostasis : The stopping of blood, as by tying an artery
Hepatic : Pertaining to the liver
Histology : Study of microscopic structure of tissues
Ileocaecal : Related to both the ileum and cecum
Ileum : The lowest portion of the small intestine
In vitro : Outside the living animal or plant
In vivo : Inside a living animal or plant
Ischemia : Deficiency of blood in a part
Laceration : A wound caused by the cutting or tearing of the tissue
Ligation : Tying of blood vessels to prevent bleeding
Lithotomy : Removing a stone by cutting through the bladder
Lobectomy : The removal of a lobe
Meningioma : A tumor situated in the meninges (the membranes covering the brain and spinal cord) that grows by expansion causing damage to the brain
Metacarpus : The part of the hand between the wrist and the fingers
Metastasis : The spread of disease from one part of the body to another
Microbe : Germ or bacteria
Mucosa : Tissues that secrete mucus
Necrosis : The death and breakdown of tissues which are surrounded by healthy tissues
Omentum : The fold of peritoneum which covers and connects the stomach and other abdominal organs
Palpation : Examination by touch
Parenchyma : The parts of an organ that are especially adapted for its function
Parenteral : Not into the intestine, intravenous
Pathology : Study of the changes in the body produced by disease
Periodontics : Dentistry concerned with the supporting tissues of the teeth
Peritoneum : The membrane which forms the lining of the abdominal cavity and covers the stomach, intestines, and other organs
Peritonitis : Inflammation of the peritoneum
Phalanx : Bone of the finger or toe, three in each digit
Poultice : Soft, moist mass, applied hot to the body
Prophylaxis : Prevention of disease
Renal : Pertaining to the kidney
Resection : Surgical removal of a part of an organ
Subcutaneous : Under the skin
Suppuration : Formation of puss
Suprapatellar : Above the kneecap
Tetanus : Disease caused by bacteria entering the body though wounds
Thrombosis : Formation of a blood clot blocking a blood vessel
Ulcer : An open sore other than a wound
Ureter : The tube through which urine passes from the kidney to the bladder
Vascular : Pertaining to or containing blood or other vessels

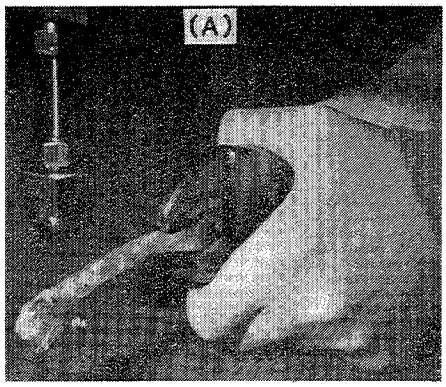

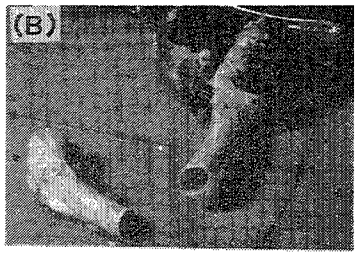

Fig. 1 Leg bone of a dead rabbit being tested for amputation (A) with high pressure water jets. Nozzle diameter = 0.127mm; Nozzle pressure = 172 MPa; Standoff distance = 6 mm. (B) Cross-section of the bone showing the clean cut.

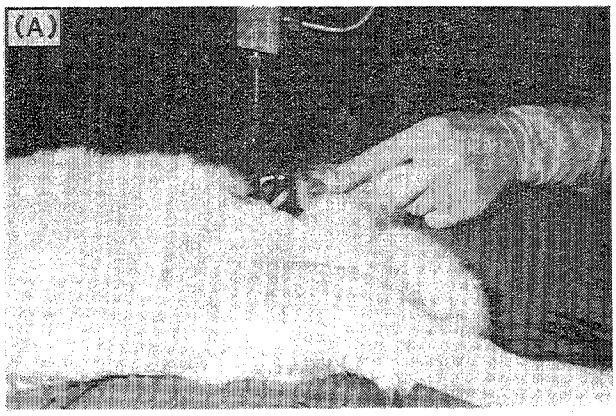

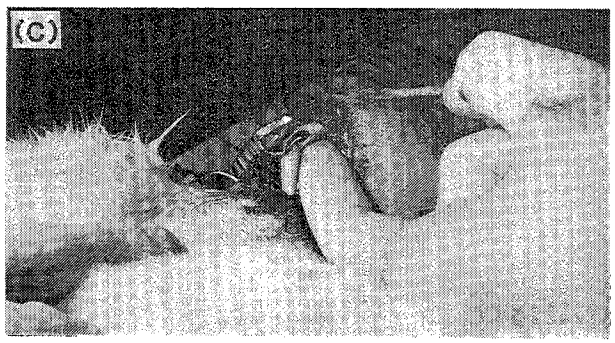

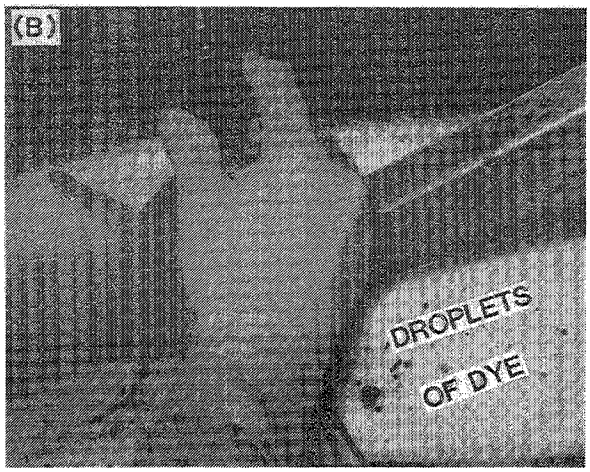

Fig. 2 Leg bone surgery tests of anaesthetized live rabbits with high pressure water jets at the same operating conditions as in Fig. 1. (A) Rabbit moving under a stationary nozzle. (B) Surgery performed by maneuvering the hand held nozzle; water stained with a blue dye. (C) Amputated leg bone.

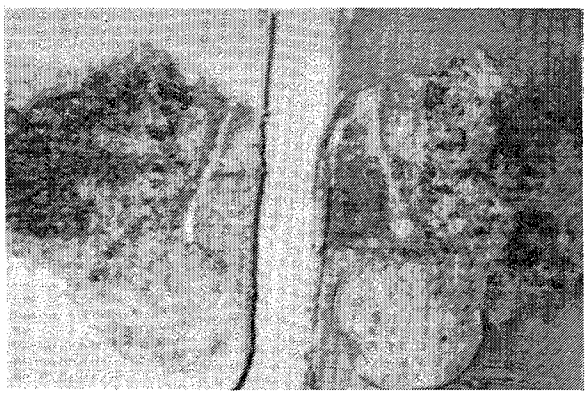

Fig. 3 Attempts were made to cut into thin sections a specimen of large human bone (equivalent dia > 5 cm) with high pressure water jets. The tests were not successful. Figure shows bone sectioned with a band saw.

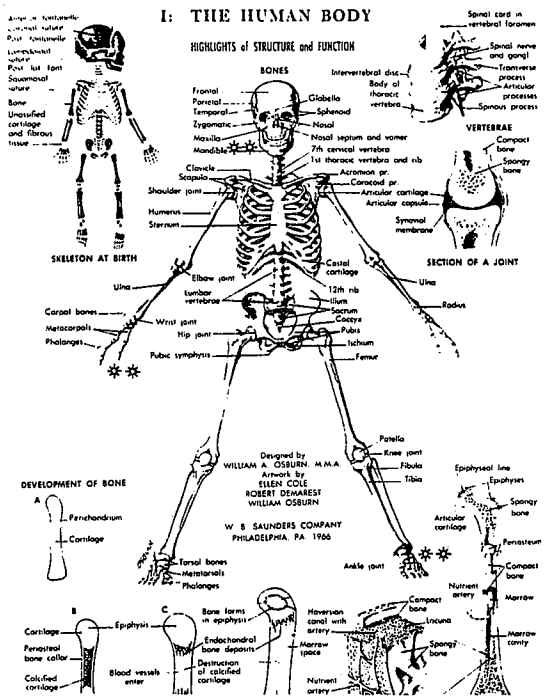

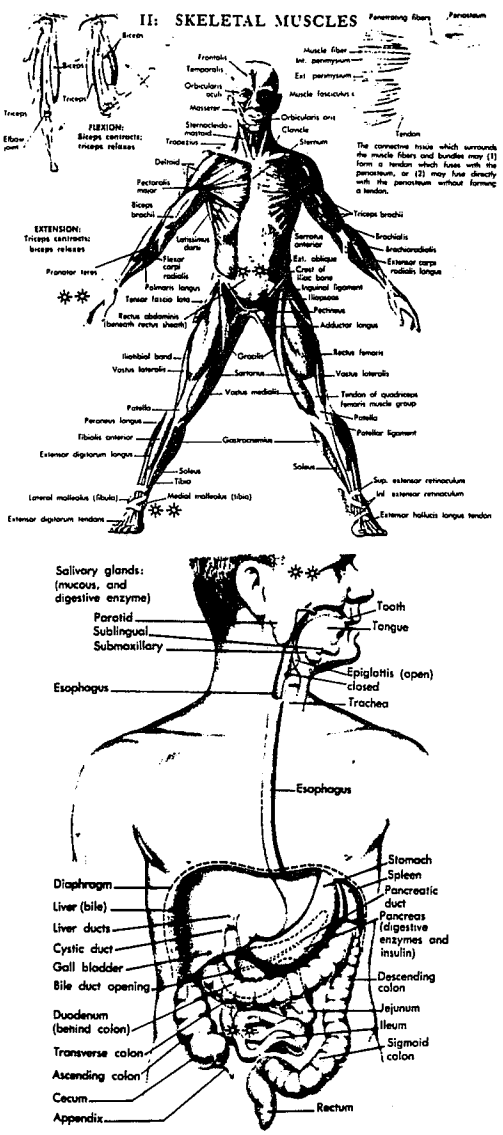

Fig. 4 Highlights of structure of the human body (Ref. 123), included for ease of understanding the medical terminology used in the paper. Asterisks (**) indicate the sites of injury reported in the literature.

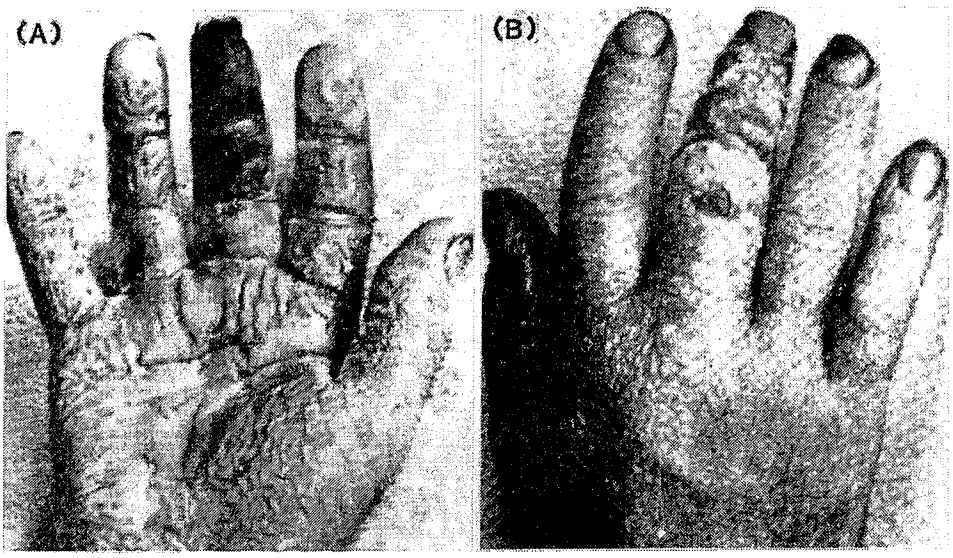

Fig. 5 Injury of the finger caused by the injection of fuel oil. (A) Epidermis of third finger denuded to first interphalangeal joint showing dry gangrene. Area of destructionextends to darkened area in midpalmar space. Macerationofremainder of hand due to wet packs. (B) Dorsal view. (Ref. 7).

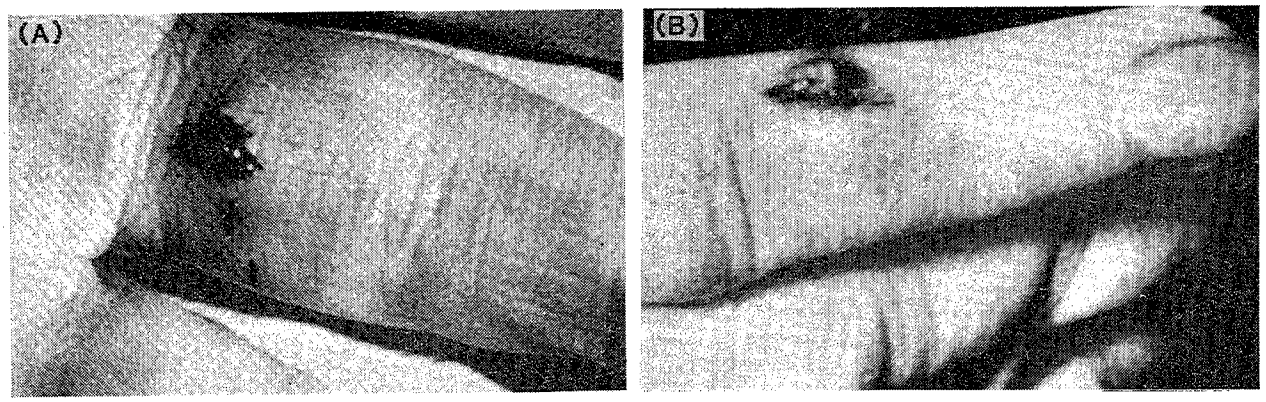

Fig. 6 Injection injury of the finger, showing the external appearance at the entrance (A) and the exit (B). Tests conducted on cadavers (Ref. 47).

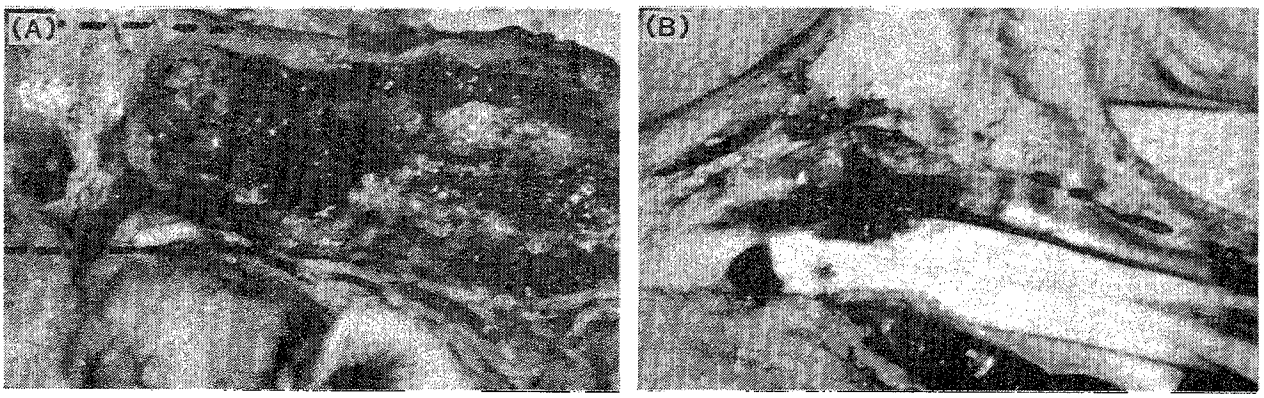

Fig. 7 Subcutaneous appearance of the injury. Spread of wax in the tissue (A) and tendon-sheath (B). Broken lines indicate digital nerves (Ref. 47).

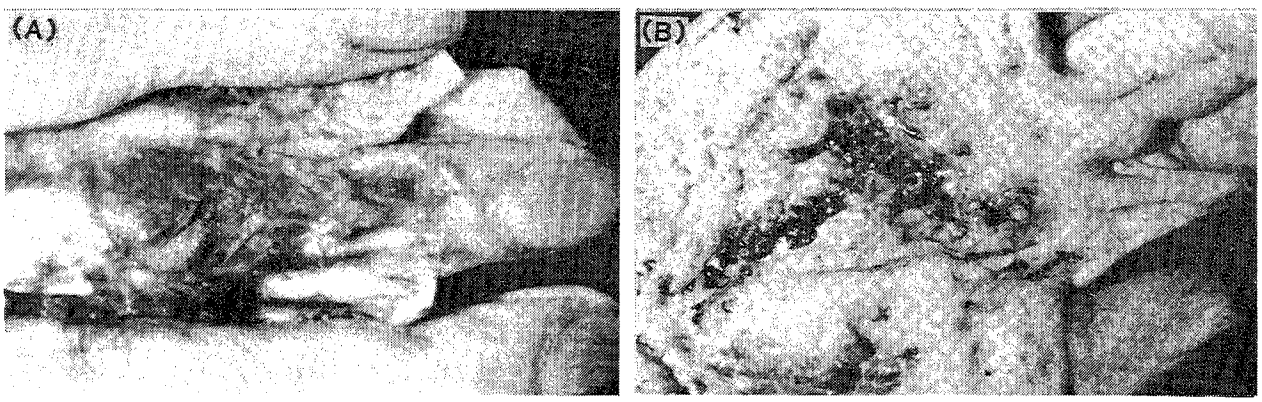

Fig. 8 Dorsal aspect of the finger (A) showing the extensor tendon being heavily surrounded by wax and (B) Spread of wax in the palm (Ref. 47).

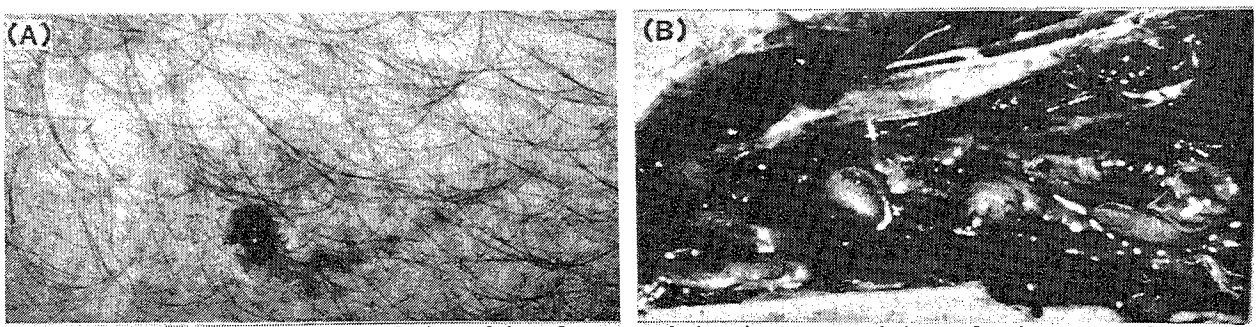

Fig. 9 Puncture wound in skin from a jet at 10 cm (A) and at very close distance (<2 cm) showing deep destruction of tissues, including periosteum (B). Tests conducted on cadaverous lower limbs with hydraulic oil (Ref. 93).

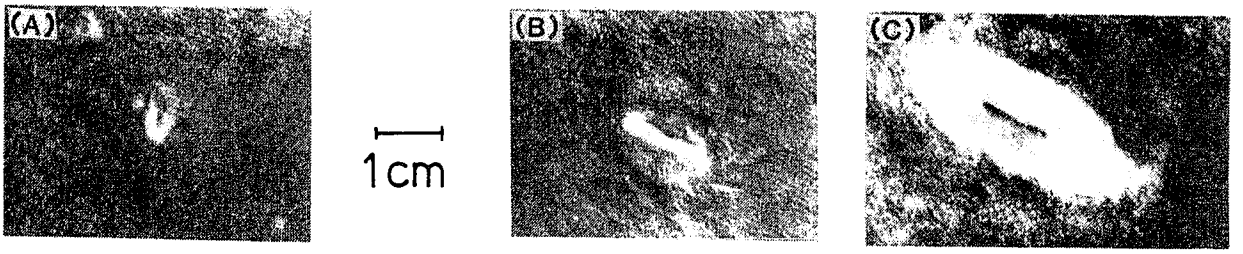

Fig. 10 Test results showing the time (T) taken for a jet of hydraulic fluid at 15 MPa (nozzle diameter = 2 mm) to penetrate through samples of skins of ox, believed to be similar to human skin, at various standoff distances (S.D). (A) S.D = 5.5 cm & T = 0.8 s, (B) S.D = 11.5 cm & T = 1.0 s, and (C) S.D = 70.5 cm & T = 6.0 s (Ref. 98).

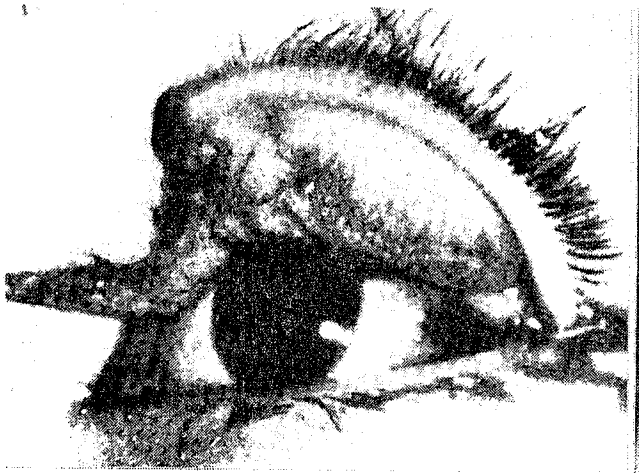

Fig. 11 Orbital laceration caused by a jet of water from a powerful agricultural irrigator. The rupture of the medial canthal tendon and the upper lid along the medial border of the superior tarsus (Ref. 92).

Fig. 12 High-pressure water-gun injection injury to the extremities. Anteroposterior and lateral roentgenograms of the foot showing extensive dissection of air along soft-tissue plains, causing emphysema; nozzle pressure = 48 MPa & S.D = 30.5 cm (Ref. 106).

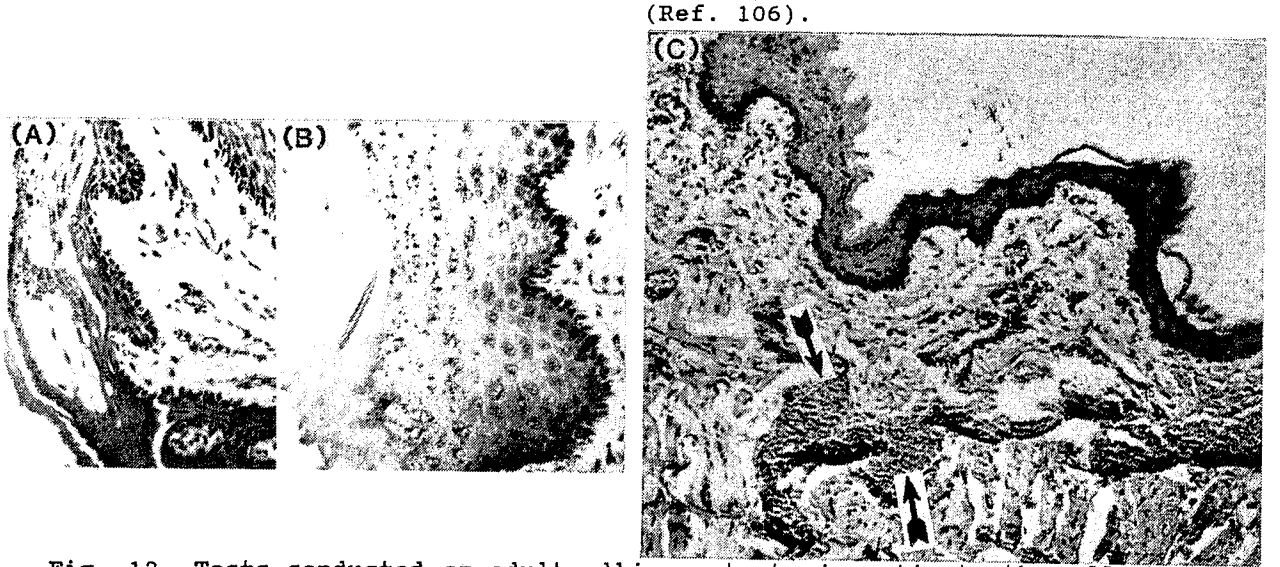

Fig. 13 Tests conducted on adult albino rats to investigate the effect of spherical polymer (abrasive) slurry and tap water jet lavage on oral mucosa. Increase in tissue damage with abrasives was observed. (A) Magnified (x225) specimen showing intraepithelical inclusion of particles. (B) Specimen lavaged with tap water showing swelling and slight discontinuity of the keratin layer of the epithelium. Nozzle pressure = 345 kPa. (C) Extravasation of red blood cells and vascular congestion (arrows) accompanied by edema in the connective tissue and skeletal muscle; pressure = 414 kPa (Ref. 56).

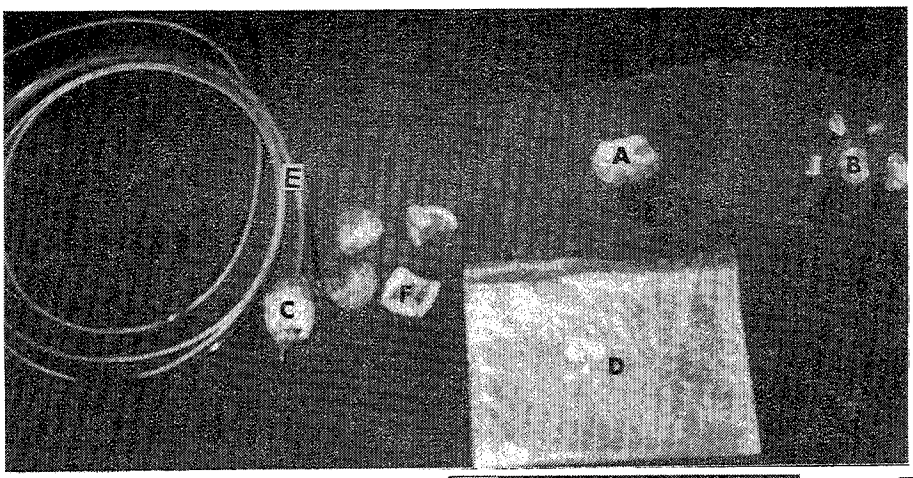

Fig. 14 Endoscopic jet cutting of human gallstones, and craking of ureter calculi by pulsed jets. (A) & (C) Calculus or stone before, and (B),(D) & (F) after cracking. (E) High pressure flexible tubing with the nozzle, not visible in the figure (Refs. 110, 112 & 114).

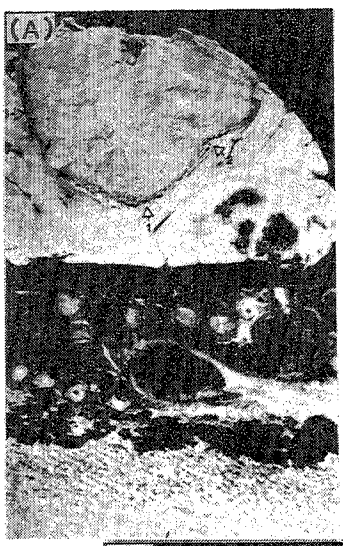

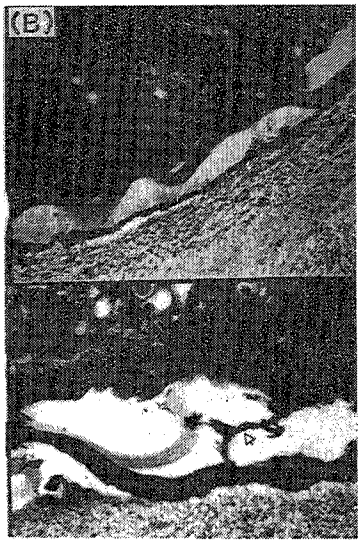

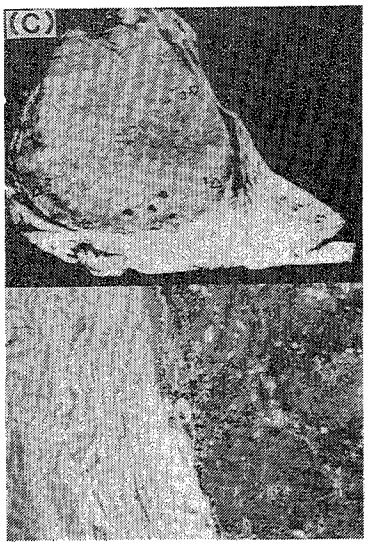

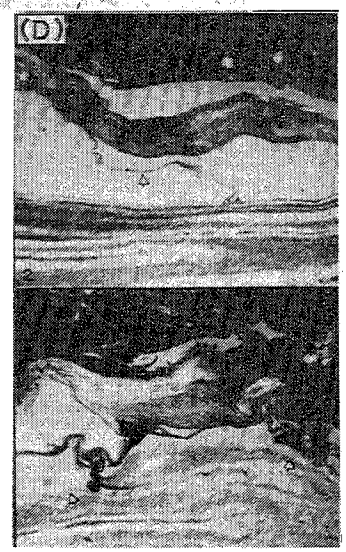

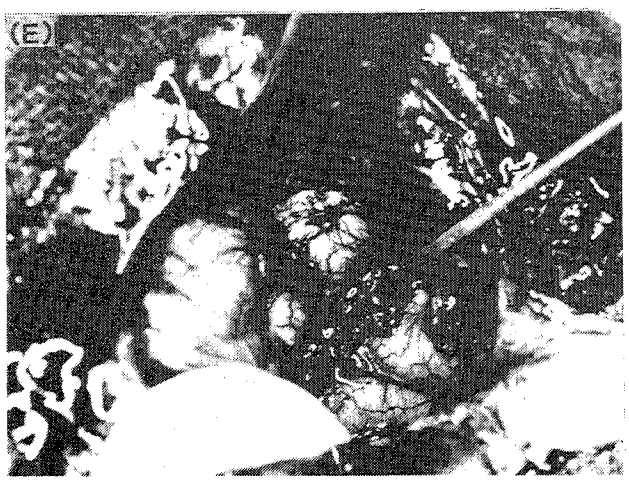

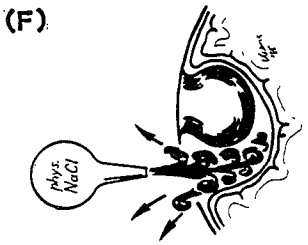

Fig. 15 Water jet technique for the separation of the tumor and brain surface in cases of meningiomas. (A), (B), (C), & (D) Meningiomas of the cerebellar and parietal convexity. Arrows show the space between the tumor and brain with adhesions. (E) The dissector is pointing to the lower part of the excised falx tumor. The intact surface of the brain is visible. (F) Water jet technique procedure (Refs. 115 & 120).

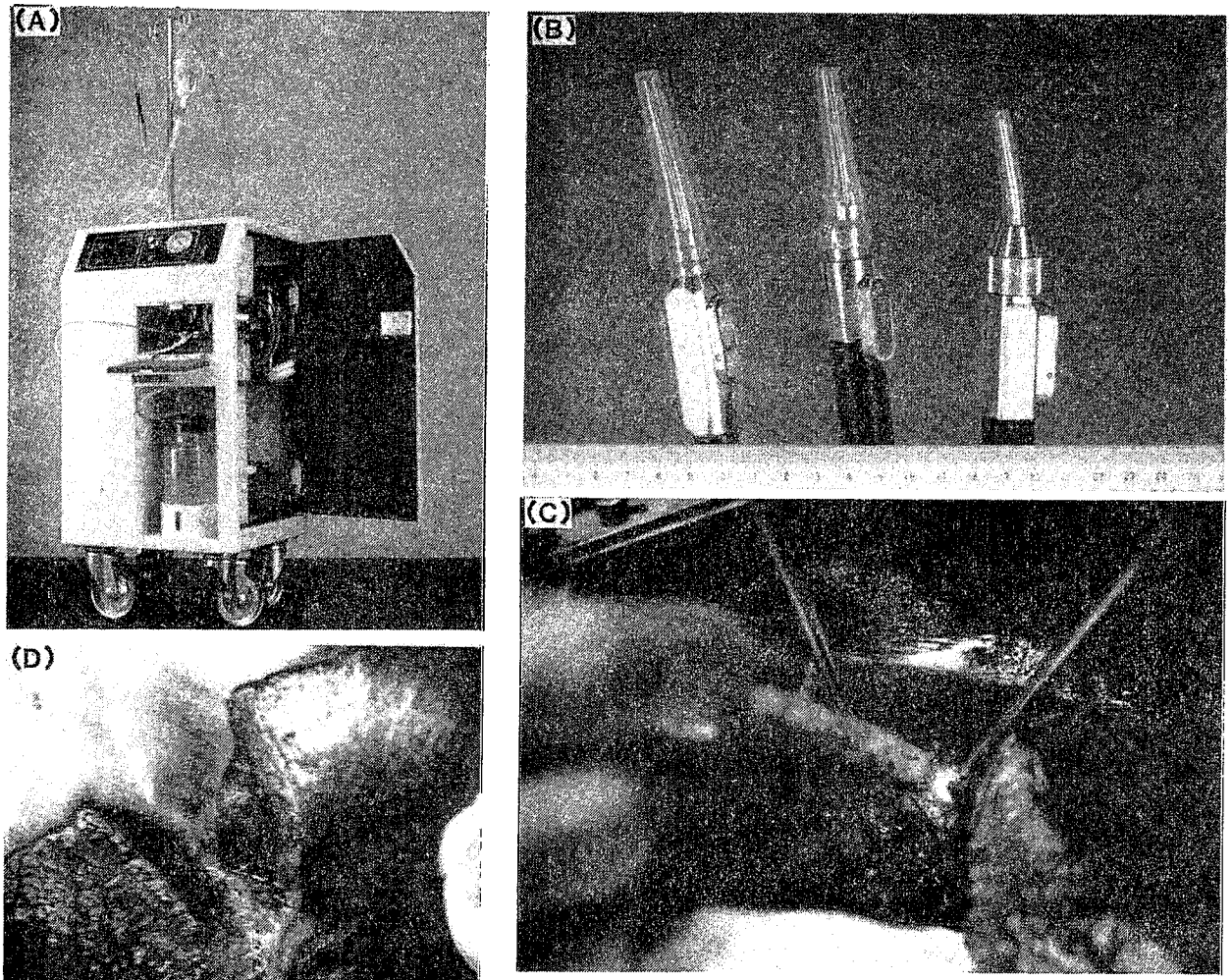

Fig. 16 Resection of the liver with a water jet. (A) Equipment showing high pressure pump (Maximum pressure = 2.5 MPa)and a flexible hose connected to a hand piece. (B) Tip of the hand piece consisting of a nozzle (diameter = 0.1 - 0.15 mm) and a microvalve to control the jet. (C) Right hepatic lobectomy using the jet, and (D) Hepatic parenchyma washed by the jet, leaving the intrahepatic vessels intact (Refs. 116, 119 & 122).

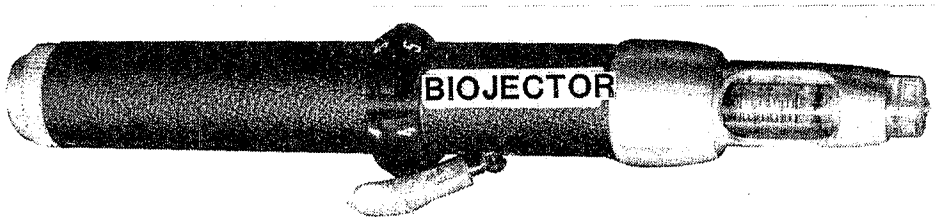

Fig. 17 Needleless jet injection system is a new hypodermic syringe designed to inject medication through a patient's skin without the traditional needle puncture, driven by a CO_2 gas cartridge (pressure = 41 MPa). The injection happens in 1/30 second (Ref. 121).

5th American Water Jet Conference
August 29 - 31, 1989: Toronto, Canada

Paper / Communication 43

DEVELOPMENT OF A 7,000 BAR HOSE

C. Raghavan AND J. Olsen
Pump and High Pressure Department
Flow International Corporation
Kent (Seattle), Washington 98032, USA

ABSTRACT: Development of a 7,000 Bar hose was started in 1985 by Flow Systems/ADMAC. Kevlar and steel reinforced hoses were designed, manufactured and tested until a 7,000 Bar burst pressure was obtained. The problems of design, manufacture, performance and safety are discussed in this paper.

RÉSUMÉ : La mise au point d'un boyau de 7 000 bars a été entreprise en 1985 par Flow Systems/ADMAC. Des boyaux renforcés de kevlar et d'acier ont été conçus, fabriqués et vérifiés jusqu'à une pression de rupture de 7 000 bars. Les problèmes de conception, de fabrication, de rendement et de sécurité sont analysés dans cette communication.

Organized and Sponsored by the National Research Council of Canada and the U.S. Water Jet Technology Association.

1.0 INTRODUCTION

With the development of reliable pumping equipment to produce high pressure water, and the discovery of new applications for this technology, it became apparent that further progress would be hampered by the performance of the high pressure hoses existing in the market. This technology could be shut out from entire sectors of the market because of the lack of a reliable high pressure hose. In factory applications, the location of the cutting system is fixed, and the points where cutting is performed are limited. Most waterjet cutting systems, operating in factories, are plumbed with high pressure tubing interconnected with swivels oriented so as to provide the required freedom of movement for the cutting head. These systems operate at 55,000 psi (3,741 Bar) and until now there have been no hoses capable of operating at this pressure. Hard plumbing has many disadvantages. It is cumbersome and expensive to install. The swivel bores are usually very small and produce considerable pressure losses. In dynamic applications, long tubes with swivel masses at the ends can cause vibration problems. They cannot be dragged around on the ground.

These disadvantages can prove fatal to waterjet cutting technology in field applications such as hydromilling, rock drilling, concrete dental work and ultrahigh pressure cleaning. We cannot use hard plumbing in these cases. The equipment has to be rugged and capable of withstanding physical abuse. Without a high pressure hose, there are almost no field applications for UHP waterjet cutting technology.

In the early eighties, we started using UHP hose manufactured by two companies in Western Germany. These hoses have burst pressures around 60,000 PSI (4,082 Bar). There was no possibility of using 55,000 PSI (3,741 Bar) equipment with these hoses. Therefore, for field applications, we built 35,000 PSI (2,381 Bar) systems so that these hoses could be used. But this was an uncomfortable situation to be in because of the low factor of safety. We therefore started the practice of installing a safety shield around every UHP hose so that any burst is contained. Safety aspects are discussed later on in this paper.

Our attempts to find a hose manufacturer who could develop reliable hoses, capable of operating at 55,000 PSI (3,741 Bar) were not successful. The state of the art in UHP hose technology appeared to be static. Most of the existing hoses, when pressurized, shrank and twisted a great deal. Their fatigue life varied considerably from sample to sample. Some hose liners examined under a microscope were found to have cracks. These problems were not getting resolved over a period of time. We therefore started a program to develop our own hose.

2.0 THE PROGRAM

The program to develop the hose had to integrate a wide spectrum of activities from the theoretical to the practical end. In view of the large number of variables in the problem, it was necessary to develop a theoretical model of stress distribution in the hose windings and validate the theory with experimental data. To obtain experimental data, it was necessary to set up a facility for manufacturing test hose specimens. To test the hose specimens, we had to develop end fittings that would survive the high pressures which we wanted the hose to experience. Finally, after obtaining the experimental data, it would usually turn out that it did not match the theory. Then we looked for flaws in the theory to explain these inconsistencies, designed another hose and continued. Today, we have a proprietary theoretical model, fully capable of predicting the burst pressures of new designs of steel and Kevlar reinforced hoses.

3.0 THE HOSE

Initial calculations indicated that it would be possible to make a hose with a bore of 3/16 inch (4.8 mm) that would have a burst pressure in excess of 100,000 PSI (7,000 Bar) by winding Kevlar filament on nylon tubing. The first few hoses burst at 30,000 PSI (2,041 Bar). Experimental study of the lateral compression of Kevlar led to the first breakthrough in our theoretical understanding, and this was closely followed by a hose which we tested in September of 1985, that had a burst pressure of 65,000 PSI (4,422 Bar). This is close to the limit that can be achieved with Kevlar. Therefore, to get to 100K (7,000 Bar) and beyond we had to find another way.

The existing UHP hoses in the market were reinforced with multiple wraps of steel wires having a circular cross-section, wound at approximately the same helical angle. Two round wires on adjacent layers, wound in alternating helical directions, have a point contact. When subjected to a compressive force laterally, the contact stresses are very high. This causes two problems. The stress riser here causes premature failure. The excessive stress also causes excessive radial strain, causing the inner layers to sink into the outer layers. This increases the circumferential strain which increases the tensile loading on the inner layers, aggravating the problem of premature failure. By using flat steel wire, the contact between wires on adjacent layers is over a surface and the problem is considerably improved.

Another feature of our hose is that the angles at which the reinforcement wires are wound varies from the inner to the outer layers. The existing UHP hoses in the market typically have the wires in all the layers wound at a constant helix angle of about 53 degrees in alternating directions. The helix angle is measured with respect to the longitudinal axis of the hose. The number of wires is increased from the inner to the outer layers so that this angle can be maintained without creating excessive gaps between the wires. It is obvious that a gap between wires creates a stress riser on the layer just below it, since the wires in that region are like a beam, supported at the ends and loaded along the span. The practice of winding all the layers at a uniform angle clearly does not take into consideration the radial stresses and strains mentioned earlier. Even with flat wire and the elimination of the Hertzian contact stresses, the radial stresses and strains are considerable.

Our theoretical model is used to optimize the helical angles of the different layers in order to obtain uniform load sharing. The internal pressure in the hose creates radial, circumferential and longitudinal loads on the hose. Most of the longitudinal load is taken up by the inner layers which are oriented at a shallow helix angle. Very little is taken up by the outer layers. The calculation of these loads is further complicated by having to consider the curvature of the hose when it is flexed, and the curvature of the wire itself as it is wrapped in a helix. In Table 1 below, the helix angle of the different layers is listed:

Layer	Wires	Helix Angle
1	20	39.0
2	20	44.8
3	20	48.9
4	20	51.6
5	10	73.2
6	10	75.2
7	5	82.1
8	5	83.5

Table 1 **Helix Angles**

The angles increase from the inner to the outer layers. The different layers numbered "L1" through "L8" are shown in Figure 1. The inner liner "12" in the hose functions as a flexible seal. With a modulus of elasticity of 400,000 PSI (27,200 Bar) compared to 30,000,000 PSI (2,000,000 Bar) for steel, its contribution to structural integrity is minimal. However, it provides a fairly rigid core on to which the reinforcement layers can be wound.

By December 1985 we had completed the development of this hose. It is currently being manufactured by Flow International Corporation and has a burst pressure that lies in a range of 103,000 to 105,000 PSI (7,008 Bar to 7,143 Bar) A U.S. patent was issued in 1987 (Reference 1). Foreign patents are pending.

We have continued our research effort and in Jan 1989, we tested a modified design with a burst pressure of 129,000 PSI (8,776 Bar). Our goal is 140,000 PSI (9,524 Bar) which will be 2.5 times the working pressure of 55,000 PSI (3,741 Bar). At this pressure, water at room temperature will be compressed to ice.

We have also continued work on larger diameter hoses reinforced with Kevlar and with steel, for use with our line of high flow rate pumps, developed for concrete hydromilling.

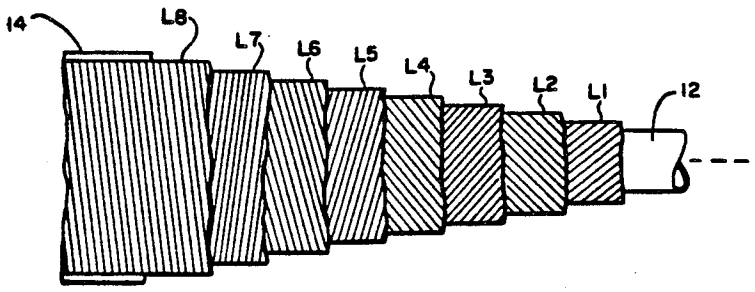

Figure 1 **Hose Reinforcement Layers**

3.1 Manufacture

During 1985, we were replacing a lot of burst hoses which had been purchased by us and which were covered by us under warranty to ensure equipment sales. These costs were mounting. After the development of the 100,000 PSI (7,000 Bar) hose, it was necessary to take it from the laboratory to the field in a hurry. During a six month period we designed, built and debugged a hose manufacturing system.

The manufacture of this hose requires a considerable degree of precision. A layout of the hose manufacturing system is shown in Figure 2. There is a continuous feed of the liner from the pay-out reel (16) into the system. Eight layers of flat steel wire are wrapped around it at winding stations 1 through 8. A thin layer of Kevlar is wound around the steel reinforcement layers at (18). This Kevlar layer provides little additional strength, but prevents the hose from springing apart when it is cut. The hose is kept moving by the Haul-off (20) and is then wound on to a take-up reel (24). The first layer that is adjacent to the liner is the most critical and difficult to wind. In the process of winding, if the outside diameter of the liner varies, the gaps between the wires vary. If the gaps exceed a few thousandths of an inch, the liner will extrude between the gaps at high pressure and the hose will fail. If the gap closes up too much, the flat wires will rise up on their edges and start overlapping which is also a defect. From the liner payout reel to the hose take-up reel at the other end, the hose string is like a rubber band in dynamic balance, held by the tension of a hundred and ten wires. Variations in tension in individual wires can cause longitudinal and torsional vibrations.

A nylon outer jacket is extruded over the hose. This protects the Kevlar winding securement from abrasion and the environment.

Our hose manufacturing system is capable of producing 1000 feet (305 meters) of hose in one eight hour run. To date, over a thousand hose assemblies have been manufactured and shipped out to customers. Their performance is evaluated below.

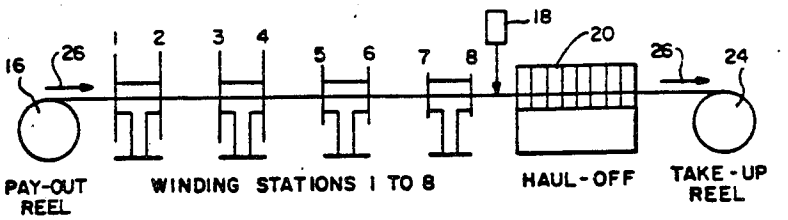

Figure 2 **UHP Hose Production System Layout**

3.2 Performance

Burst tests are periodically performed in the lab. The range of burst pressures is 103,000 to 108,000 PSI (7,007 Bar to 7,347 Bar). Samples are tested from each lot of hose for fatigue. In this test, the pressure is cycled from 0 to 55,000 PSI (3,741 Bar) and back at the rate of 15 cycles per minute. The range of fatigue life is 10,000 to 16,000 cycles. At 0 to 35,000 PSI (0 to 2,381 Bar) pressure cycling, the fatigue life is over 30,000 cycles.

Over 95% of the hose assemblies sent out to customers have been for field applications at 35,000 PSI (2,381 Bar). In this group, no fatigue failures have been reported. The predominant mode of failure is non-catastrophic fitting leaks caused by physical abuse of the hose. This group can be subdivided into two categories. Half the hoses are 15 feet (4.1 meter) to 100 feet (30.5 meters) UHP conduits. They are usually laid out to convey pressure from point to point and are subjected to very little physical abuse. These hoses last over 1000 hours at 35,000 PSI (2,381 Bar) without failing. In fact, there is very little failure data reported back from the field for this category and hardly any complaints from customers. The second category consists of "whip" hoses. These are 6 to 8 feet (1.8 to 2.4 meters) long. They are connected between the conduit and the cutting tool and are subjected to a great deal of flexing, twisting and jerking. The life of "whip" hoses depends on how it is used and is usually not as good as the life of hoses used as conduits. Strain reliefs at the end fittings have helped improve performance.

In the world of 55,000 PSI (3,741 Bar), our hoses have been used to plumb robots and X-Y tables at about a dozen installations. Typically, the hoses have lasted about 800 hours, and again the predominant mode of failure has been non-catastrophic fitting leaks. They have also been successfully used in the field for 55,000 PSI (3,741 Bar) concrete cutting.

The performance data of the hose including pressure drop at different flow rates is summarized in Table 2.

Flow Rate (gpm)	Fitting Pressure Drop (psi)	Hose Pressure Drop(psi/ft)
1	12	1.8
2	48	6.0
3	110	12.0
4	200	20.0
5	300	30.0
6	430	40.0

Dimensions 0.1860 in.(4.7 mm) I.D. 1.0625 in.(2.7 cm) O.D. (nominal)	Typical burst pressure 105,000 psi (7,143 bar)
Length to customer specifications- minimum 2 feet (61 cm)	Minimum burst pressure 95,000 psi (6,463 bar)
Weight (lbs/ft) Hose 0.35	Minimum fatigue life 0-55,000 psi (3,741 bar):10,000 cycles 0-35,000 psi (2,381 bar):30,000 cycles
Shield 0.36 (black)	Minimum bend radius 24 inc. (61 cm)

Table 2 **UHP Hose Specifications**

3.3 Safety

The general practice has been to use the ratio of minimum burst pressure to working pressure as an indicator of the safety and reliability of hoses. In the absence of an accurate theoretical model, this ratio is the best measure. It can be determined through tests. A better indicator is the minimum safety factor on the wires at the working pressure. This is the ratio of ultimate tensile stress of the wire to the maximum Von Mises stress on a wire at the working pressure.

Hoses can therefore be designed based on either one of these two criteria. Keeping the liner bore, O.D. and I.D. of the reinforcement constant, we can have two possible designs; one for maximum burst pressure and the other optimized for fatigue life at the working pressure.

However, from our experience with over 1000 assemblies, we find that the most important factor that affects hose life is the physical abuse it is subjected to, which leads to non-catastrophic fitting leaks. This is especially true of the "whip" hoses which are closest to the operating personnel. In effect, this feature is like a safety valve, forcing us to replace a hose before the end of its life.

Every hose assembly, including the ones for 35,000 PSI (2,381 Bar) applications, is subjected to 200 pressure cycles at 0 to 55,000 PSI (0 to 3,741 Bar) in order to ensure that no defective assemblies get sent to customers. After this test, a safety shield is placed over the hose from fitting to fitting. This shield fits loosely over the hose. It is a hydraulic hose with steel wire braids and its function is to contain hose bursts at 55,000 PSI (3,741 Bar), drain the leakage water away and prevent injury to personnel.

At 35,000 PSI (2,381 Bar), we have a 3:1 burst to working pressure ratio, a safety shield and a generally non-catastrophic mode of failure. Hand-tools, which bring the operator close to the hose, are generally operated at this pressure. The 55,000 PSI (3,741 Bar) systems are in general more remote from the operating personnel.

4.0 CONCLUSION

Developing an accurate theoretical model for ultrahigh pressure hoses has enabled us to develop hoses with burst pressures up to 129,000 PSI (8,776 Bar), which we believe are currently the highest performing hoses available on the market. We are also not aware of any other hoses available at present that can consistently last 10,000 to 15,000 full pressure cycles at 0 to 55,000 O PSI (0 to 3,741 Bar). We are pursuing the development of larger diameter hoses and more reliable fittings. The steps we have taken to ensure personnel safety have been expensive but in return the safety record of our hoses has been excellent. We intend to keep it that way.

REFERENCES

1. "Ultra High Pressure Hose Assembly", U.S. Patent No.4,649,963; Inventors: Chidambaram Raghavan and John Olsen; March 17, 1987.

5th American Water Jet Conference
August 29 - 31, 1989: Toronto, Canada

Paper / Communication 44

EYE AND RESPIRATORY PROTECTION DEVICES FOR USE IN WATER JETTING APPLICATIONS

S.P.D. Swan AND N.A. Johnson
S.P.D. Swan Consultants Limited
Ilkeston, UK

ABSTRACT: This paper describes the various devices worn in h.p. water jetting applications as eye protectors, including visors and anti-mist goggles. It summarizes work carried out by the authors investigating the use of different eye protectors currently commonly used in the water jetting industry in the UK. It describes tests carried out on these devices to determine a method for minimising wear and fouling and describes air curtain adaptation made to existing devices and outlines experiments with these devices to determine their efficiency against bacterial and chemical aerosols. The paper points possible ways forward and describes probable conclusions to field use of devices. The work is continuing.
This paper and the work it describes were funded by the Health and Safety Executive (HSE). Its contents, including any opinions and/or conclusions are those of the authors alone and do not necessarily reflect HSE policy.

RÉSUMÉ : La présente communication décrit les divers dispositifs portés dans des applications des jets d'eau h.p. pour protéger la vue, comme les visières et les lunettes anti-embrun. Elle résume les études effectuées par les auteurs sur l'utilisation actuellement répandue de différents dispositifs de protection de la vue dans l'industrie des jets d'eau au Royaume-Uni. Elle décrit les essais effectués sur ces dispositifs pour élaborer une méthode de minimisation de l'usure et de l'encrassement; comment des rideaux d'air ont été ajoutés dans des dispositifs existants; les expériences effectuées pour déterminer l'efficacité de ces dispositifs contre les aérosols bactériens et chimiques. Elle mentionne des orientations futures possibles et présente des conclusions probables découlant de l'utilisation de ces dispositifs sur le terrain. Les travaux se poursuivent.

Organized and Sponsored by the National Research Council of Canada and the U.S. Water Jet Technology Association.

1.0 INTRODUCTION

The vast preponderance of water jetting applications are still carried out manually and especially at the higher pressures and flows (about 700 bar and 50 l/min), visibility becomes a problem. In applications where surface cleaning is involved e.g. concrete cutting and removal, tube bundle shell side cleans and wet abrasive blasting, water spraying back from the work surface create an aerosol mist. The mist generated contains surface contaminants and abrasive or sticky particles. These particles are also contained in the water reflected from the work surface and can act synergistically with the water stream to cause reductior in visibility. In some of these activities visibility can reduced to unacceptably low levels in minutes. This visibility reduction can be largely attributed to wear at the surface of the eye protectors or, in the case of oil based products the material being thrown on to the visor and sticking to it causing fouling which in some cases can be extreme. In these circumstances much water jetting is carried out by replying on other senses than sight. Thus, a momentary loss of concentration in conditions of poor visibility can lead to an accident. In particular, accidents involving cuts across the top of the foot can often be attributed to this cause.

There is a requirement in law under UK regulations for the employer to provide suitable eye protectors and for the employee to wear them. As well as the accidents which have been reported where poor visibility has, almost certainly, played a part; anecdotal evidence has linked water jetting operations to increased levels of respiratory infection. This has led in at least one case (to the authors knowledge) of water jetting being discontinued as a maintenance procedure.

The series of experiments described below were directed towards optimising visibility during water jetting operations and continue work already carried out in this area by Harris and Shaw (1987)

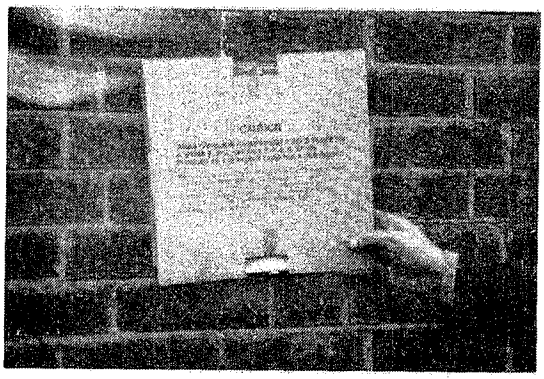

FIG 1 View through new visor BS1542 at 2 m from sign.

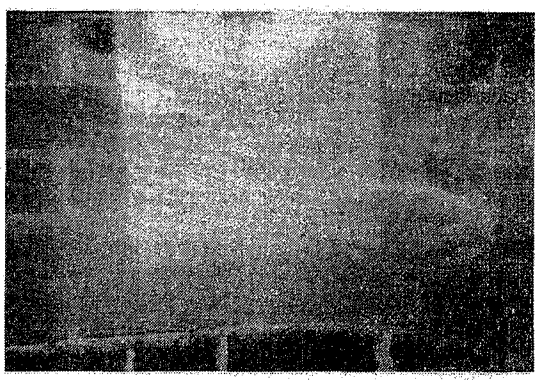

FIG 2 View through visor BS1542 at 2 m from sign after 10 mins concrete cutting at 700 bar and 60 l/m.

A review of equipment for eye protection was carried out and the main types currently in use in water jetting are discussed below.

2.0 EYE PROTECTORS USED IN WATER JETTING

Currently, a variety of equipment are used in Europe, and with the movement towards a single market in 1992, standards, in general, are being harmonised. However, to the authors knowledge there is no specific standard equipment for this application; the equipment described in this paper cover the ones in most common use in the UK.

2.1 GOGGLES

A range of standard goggles to BS2092 are available and, whilst widely used in the 1960s and 70s, these have largely been superseded because of problems with internal misting adding to the incipient problems or poor visibility caused by blow back. Harris (1987) described goggles which have vents to allow air flow and which in water jetting field testing were found not to mist or allow ingress of particles of aerosol droplets. These goggles were the subject of extensive laboratory and field testing and were the only goggles tested which consistently passed a misting test which is currently under consideration for adoption as a standard test. (Proctor, 1988).

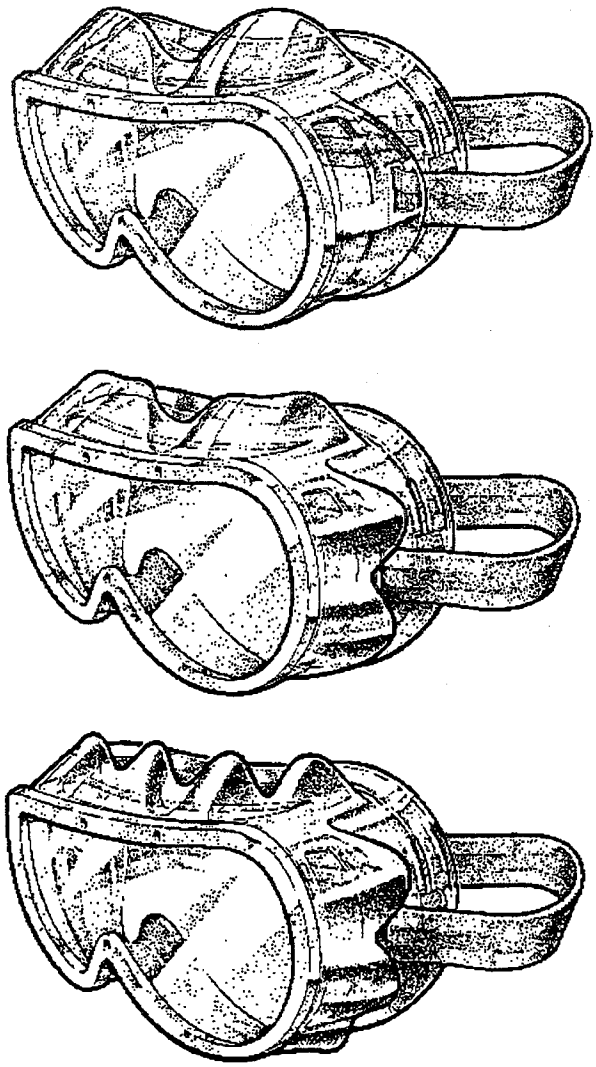

FIG 3 Diagram of anti-mist goggles, general configuration.

2.2 VISORS:

A series of visors are on the market to BS1542. In general these are of two main types:

- BS1542. VISOR WITHOUT CHINGUARD
- BS1542. VISOR WITH CHINGUARD.

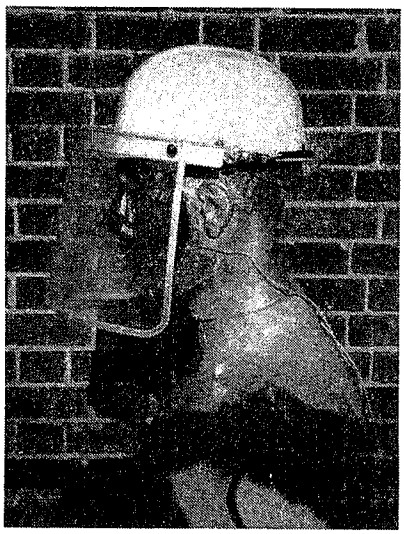

FIG 4 Dummy with BS1542 visor without chinguard.

This visor without chinguard is still commonly used, even though water and debris is carried up towards the operator's face underneath the front of the visor adding lack of comfort and exposure to potentially hazardous materials, to visibility problems.

The visor with the chinguard was developed as a result of work carried out by British Hydromechanical Research Association (BHRA) and largely solves the problem of ingress of debris and water but is still subject to wear and fouling. However, this visor is being used preferentially by experienced operators.

2.3 ENCLOSED HELMETS

The problem of water jetting operator eye and respiratory protection has been addressed by several users by the use of existing proprietary equipment, such as closed environment helmets. These helmets, often with their own enclosed air supply, are sometimes cumbersome, bulky and usually expensive. Since such helmets are designed to filter dust out they tend to be inefficient against water spray borne aerosols and they still do not solve the problem of maintaining good visibility.

Shot blast helmets have been adapted for use in water jetting and in particular an adaptation made by Harben Systems Ltd. (see Fig. 5) seemed to the authors to attempt to address the main problems encountered in practical on-site water jetting.

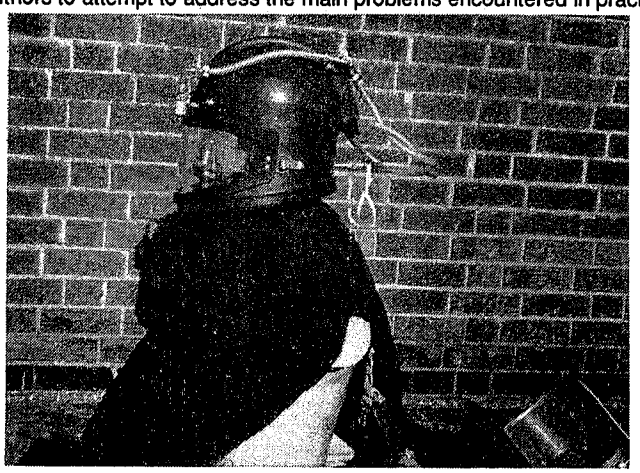

FIG 5 Shot blast helmet by Harben Systems Ltd for water jetting applications

3.0 TESTING

The main criteria in devising an eye protection device apart from the ingestion or inhalation of toxicants or potential pathogens in an aerosol by the operator were seen as:

- Extending the life of a current eye protector by deflecting material away from it.
- Making the device as robust as possible so as to endure life on site.
- Making the device as convenient as possible so that it would be worn preferentially.
- Making the device so that it could be realistically produced at an economical price.

Work already carried out by Harris and Shaw was taken as a starting point. In this study a device, working on the air curtain/ elutriator principle, had been designed and was the subject of some preliminary study for water jetting applications. This device which fitted on to the front of a standard visor had been shown in the laboratory to be capable of deflecting particles (Fig. 6). This was expected to give a consequent extended life to the visor.

On the basis of this work a series of tests were devised to investigate the various parameters outlined above.

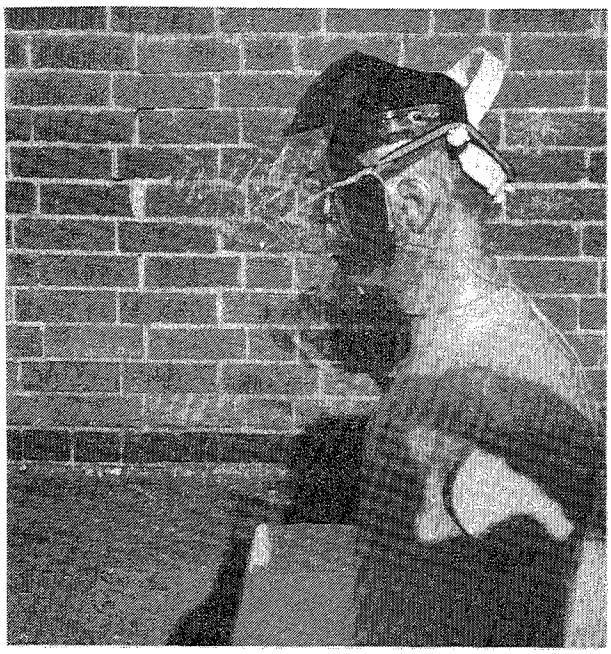

FIG. 6 Visor with air curtain/elutriator attachment after Harris and Shaw

The tests carried out were as follows:

1 LABORATORY TESTING OF UNMODIFIED VISOR BS1542 FOR ABRASION.

2 LABORATORY DEVELOPMENT AND TEST OF AIR-CURTAIN VISOR ATTACHMENT.

3 LABORATORY TEST OF AIR-CURTAIN VISOR ATTACHMENT FOR PROTECTION AGAINST CHEMICAL AND BACTERIAL AEROSOLS AND SPRAY BACK FROM THE WORK SURFACE.

4 FIELD TESTING OF AIR-CURTAIN VISOR AND ANTI-MIST GOGGLES.

METHODOLOGY:
In all laboratory test eye protectiors were mounted on a "breathing dummy" (developed by HSE) and at a distance of 1.5 m from the work surface (see fig 1). In early tests the jet was reflected back at the dummy from a steel wear plate set at 90 degrees to the jet. The dummy was set up in an enclosed cabinet and a pump operating at up to approximately 700 bar and 60 l/min with a 1.8 mm tungsten carbide nozzle of Cd 0.9 was used for tests involving HP water alone.

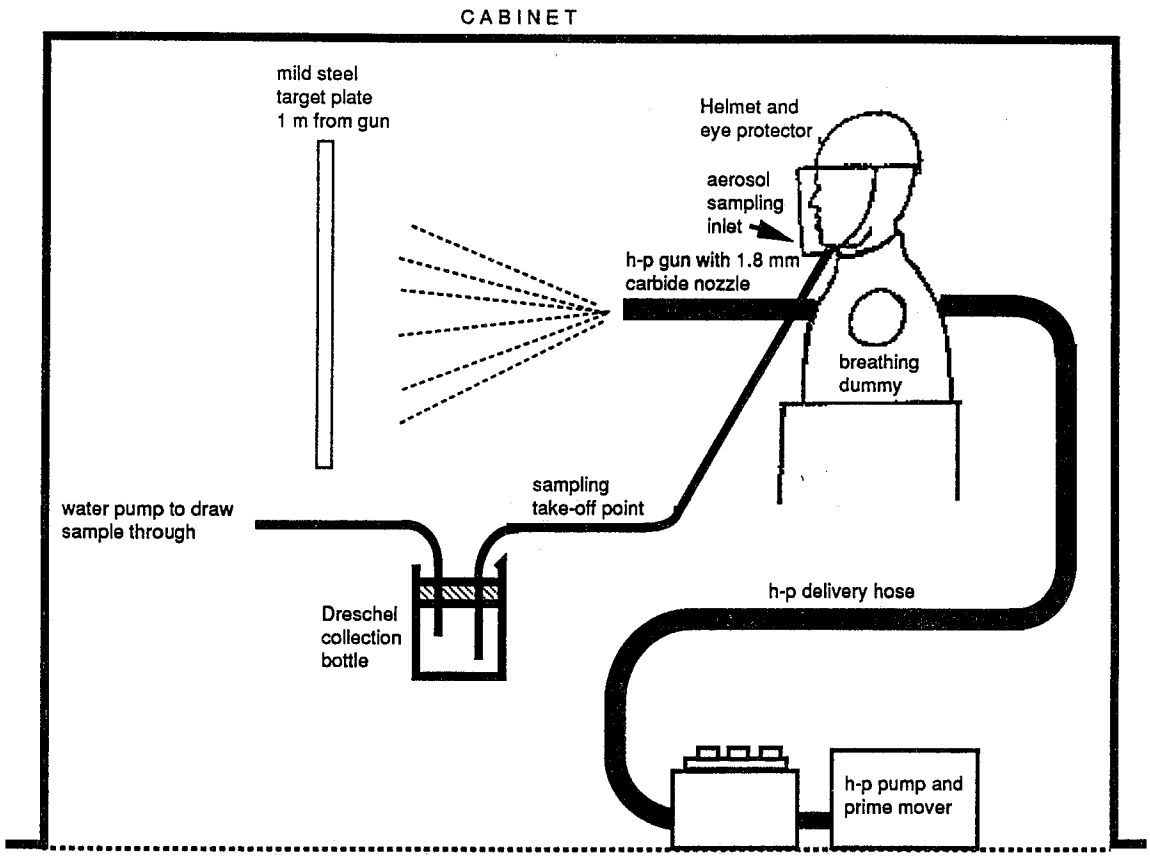

FIG. 7. Experimental set up with "breathing dummy".

Samples of aerosols and blasted back fluid were taken through the dummy using an air pump and chemical sample bottle containing 50 cm^3 of distilled water. The chemical used for aerosol generation was sodium chloride and the bacterium used was *Pseudomonas fluorescens.* The abrasive used in the tests was copper slag of maximum particle size 6 mm and minimum particle size 0.6 mm. The abrasive was delivered through an abrasive injector with nozzles chosen to keep the flow constant i.e. 60 l/m, and allow variation of pressure.

4.0 RESULTS

4.1 LABORATORY TESTING OF UNMODIFIED VISOR BS1542 FOR ABRASION
A BS1542 visor was tested using 5 kg of abrasive delivered to the target plate at 70 bar, 200 bar and 700 bar. The visor was covered by aluminium foil and the number of impinged particles measured for each minutes jetting. The number of particles were measured as a mean of three 10 mm square quadrats taken across the face of the visor.

TABLE 1. Number of abrasive particles
impinging per 10 mm square visor per minute mean over a minute test.

pressure (bar)	*abrasive particles (qty)*
70	78
200	142
700	217

These results were compared visually with samples of the same visor taken from site and it was calculated that the results obtained were equivalent to abrasion obtained in the field. Tests, which at the time of writing have not yet been concluded, are in hand to equate abrasion in the field with a standard test used for visibility index in motor cycle helmets.

The purpose of this test was to give a bench mark to allow progress in the second series of tests with the air-curtain visor, which aimed to reduce particle impingement.

4.2 LABORATORY DEVELOPMENT AND TEST OF AIR-CURTAIN VISOR ATTACHMENT.

METHODOLOGY:
Existing modified adaptions were tested in a live situation by an experienced operator. These included a Harben Systems helmet, but this was discarded because of its inherently fragile design characteristics.

It had been decided at an earlier point in the decision making process to use either an air or water curtain based on results achieved by Harris and Shaw and private correspondence with end users and colleagues (notably Barton at BHRA) who had already carried out some preliminary work. On the basis of these discussions and tests it was decided to design and build and adjustable nozzle carrier across the front of the visor which, similarly to the Harben helmet, could provide air-curtain and prevent particles reaching the visor.

On the basis of live testing an optimum appeared to be the provision of an air-curtain operating through 2 x 0.8 mm 90 degree fan jets set to provide an overlapping curtain. This curtain was arranged to cover the part of the visor directly in front of the eyes and driven by a compressor at approximately 3.5 bar and delivering 300 l/m air.

FIG. 8 Adapted visor with chinguard and air curtain produced by 2 x 0.8 mm jets.

A test was carried out in which abrasive (5 kg/min) was delivered to the workpiece at 350 bar and 60 l/m through a sand injector with 4 x 1.1 mm jets.

The air flow was modified at 350 bar and 60 l/m reflected back from the metal workpiece to visor with air curtain adaptor at various input air pressures from an approximately 2 kW compressor.

TABLE 2

air pressure (bar)	*abrasion particles per 10 mm²/min*
0.0	185
0.5	168
1.0	186
1.5	154
2.0	92
2.5	69
3.0	33
3.5	38

It would appear that all other things being equal an improvement in life, under fairly extreme jetting conditions of 4–5 times could be looked for i.e. from say 30 mins to 2–3 hours using such an adaptation. This accords with results obtained by Harris and Shaw and private correspondence with Bennie of Harben Systems Ltd.

4.3 LABORATORY TEST OF AIR-CURTAIN VISOR ATTACHMENT AGAINST CHEMICAL AND BACTERIAL AEROSOLS SPRAY BACK FROM THE WORK SURFACE.

METHODOLOGY:
The inhalation and ingestion of chemical and bacterial aerosols were investigated on the breathing dummy using a range of eye protectors. These included the following:-

- standard visor.
- visor with a chinguard.
- visor with a chinguard and an air-curtain external to the visor.
- visor with a chinguard and an air-curtain external and internal to the visor, (this was an adaptation of the existing system described previously with an extra 90 degree 0.8 mm fan jet fitted inside the visor and directly in front of the dummy's face).
- enclosed helmet (see Fig. 5).

The breathing dummy was set up 1 mm from the target plate and a stream of water was fired at the plate from a 1.8 mm jet at 350 bar and 50 l/m.

CHEMICAL TESTS:
The chemical used in these tests was sodium chloride which was made up as a standard solution of 1 kg in 500 litres of tap water. This was passed directly through the pump from a mixing tank and gave a conductance of approximately 14 mS/cm³.

Samples were taken from the mist using a water pump operating at about 1 bar and passing the sample through 50 cm³ of distilled water.

The build up of conductance was measured by a conductivity meter and the following results were obtained.

RESULTS:

TABLE 3 CHEMICAL TESTS Conductance μScm³

Time (min)	*without visor*	*with ordinary*	*with chinguard visor*	*with chinguard visor with external air*	*with chinguard visor with external and internal air*
0	7	7	7	7	7
2	8	7	16	7	7
4	14	9	21	8	8
6	29	29	22	9	9
8	85	46	23	10	10
10	134	50	25	11	11
12	138	51	26	12	11
14	139	82	27	13	11
Total build-up	**132**	**75**	**20**	**6**	**4**

BACTERIAL TESTS:

METHODOLOGY:
The bacterial pseudomonas fluorescens was chosen as being naturally occurring non pathogen. However, sterile procedures were observed and the tests were carried out in a jetting cabinet which could be evacuated through a biological filter by negative air pressure.

In preliminary tests a bacterial sample was introduced through an injector, so that bacteria were added to the jet AFTER it left the nozzle. In the test results recorded below the bacteria were added to a header tank and passed through the pump. The bacteria thus, have passed through a pump and out through the nozzle.
The samples were collected from the dummy through a Dreschel bottle with a water pump operating at 1 bar and after 10 minutes the bacterial population were measured by the surface plate count method using Kings medium. The colonies were identified by their bright yellow fluorescence under U.V. light.

RESULTS:

TABLE 4. Bacterial population Bacterial colonies discovered in samples drawn from breathing dummy.

reference sample	*colonies detected*
Ordinary visor	less than 10
Visor with a chinguard	less than 10
Visor with a chinguard and air curtain external to the visor	less than 10
Visor with a chinguard and air curtain external and internal to the visor	less than 10
Enclosed helmet.	no colonies detected

These results are not apparently significant in themselves but taken together with earlier results where up to 600,000 bacteria were discovered in samples where the bacteria were introduced after the nozzle, gave an indication that bacteria may actually be damaged in the pump or, by passing through the nozzle.

It was also interesting to note that once an aerosol had been established that no significant difference could be established, even in the sample with the enclosed helmet.

This work has given rise to an interesting line of study which may be reported in the future.

4.4 FIELD TESTING OF ADAPTED VISOR AND ANTI-MIST GOGGLES.
This work is continuing and is briefly described in the conclusions to this paper.

5.0 CONCLUSIONS

At the date of writing this paper field testing of the various devices referred to in the paper are proceeding. Initial tests of the anti-mist goggles showed that they were appropriate for water jetting applications probably and especially where, either lower pressures may be involved or in situations where a visor without a chinguard is used.

It is obvious that in water jetting applications, certainly in the UK, visors and specifically the visor with the chinguard have achieved common usage. Whilst this has solved the problem of water and debris spraying up under the visor these visors are still susceptible to abrasion.

Visors with air-curtain devices and with chinguards are a possible solution to visor abrasion caused by flying particles and fouling to the ingestion or inhalation of aerosols. The current plan is to build prototype helmets which have air connections and nozzles built in and replicate fairly closely the test model shown in Fig.8.These will have the advantage of allowing the fitting of the standard BS1542 chinguard visor and we hope will prove appropriate for field use especially in "heavy duty" manual applications.

6.0 BIBLIOGRAPHY

'New developments in testing and design of anti-mist goggles',
Proctor T.D., Harris G.W. and Gray M.I.
COPE 88 Toronto, Canada
31 October–2 November 1988

'A device for reducing water and dirt impacts on visors in water-jetting applications',
Harris G.W. and Shaw S.R.,
additional references to:
BS 1542; Equipment for eye, face and neck protection,
BS 2092; Eye protectors for industrial and non-industrial uses.
in HSE Research Laboratories Division, Report number IR L PE 87 10.

5th American Water Jet Conference
August 29 - 31, 1989: Toronto, Canada

Paper / Communication 45

HIGH PRESSURE WATER-ABRASIVE JET CUTTING FOR STEEL PIPES OF GAS WELL CASINGS

A. El-Saie
Consolidation Coal Company,
Research & Development,Library
Pennsylvania 15129, USA

ABSTRACT: Flame or other heat generating tools for cutting gas well casings are not allowed in underground coal mining. A cutting device is needed to cut the steel pipes of gas well casings. A preliminary test with a high pressure water-abrasive jet was successfully carried out by slotting a 6.4 mm thick steel plate. The high-pressure water-abrasive jet cut a 3.2 mm wide slot at a rate of 44.4 mm/min. with a flow rate of 19 L/min. at a pressure of 345 bar. A high pressure water-abrasive jet pipe-cutting device was fabricated. A high-pressure pump, hydraulic motor, and safety and measuring devices were assembled so that they could be used in underground situations. A test was conducted on 254 mm diameter, schedule 40 steel pipe. A pipe circumference cutting rate of 38.1 mm/min. was achieved during that test. The abrasive consumption rate was 1.1 kg/min.

RÉSUMÉ : La coupe des tubages des puits de gaz à la flamme ou avec d'autres outils chauffants est interdite dans l'exploitation souterraine du charbon. Un dispositif s'impose pour couper les tubages en acier des puits de gaz. Un essai préliminaire sur un jet eau-abrasif à haute pression a permis de pratiquer une fente dans une plaque d'acier de 6,4 mm d'épaisseur. Le jet eau-abrasif à haute pression a découpé une fente de 3,2 mm de large à une vitesse de 44,4 mm/min avec un débit de 19 L/min, à une pression de 345 bar. Un coupe-tuyau à jet eau-abrasif à haute pression a été fabriqué. Une pompe haute pression, un moteur hydraulique et des dispositifs de sécurité et de mesure ont été assemblés de façon à pouvoir être utilisés en milieu souterrain. Un essai a été effectué sur un tuyau en acier no 40 de 254 mm de diamètre. Une vitesse de coupe de la circonférence du tuyau de 38,1 mm/min a été atteinte au cours de cet essai. La consommation d'abrasif a été de 1,1 kg/min.

Organized and Sponsored by the National Research Council of Canada and the U.S. Water Jet Technology Association.

INTRODUCTION

The underground environment does not allow flame or heat generating tools to be used for cutting water and gas well casings usually encountered in underground mining. These casings have to be cut and removed before the mine face can advance. The use of the shearer or continuous miner to destroy the gas or water well casing is expensive and time consuming as well as a potential safety hazard. The well casings usually consist of 254 or 305 mm diameter steel pipe. The use of a high pressure water jet with entrained abrasives to cut the steel pipe casing was evaluated.

There are many constraints in designing the pipe cutting assembly. This assembly should have the following characteristics:

1. Easy to move underground.
2. Light weight.
3. Easily assembled and disassembled underground.
4. The operator should be away from the cutting nozzle.
5. Only hydraulic power should be used.

TEST SET-UP

The test set-up consisted of a high pressure triplex water pump (Figure 1) capable of producing a flow rate of 19 L/min. at a pressure of 345 bars. The water pump was driven by a hydraulic motor with a flow rate of 54 L/min. at a pressure of 138 bars. The hose used in these tests was a 12.7 mm diameter high pressure hydraulic hose with staple connections. The pump assembly consisted of oil pressure gages and flowmeters, a hydraulic valve to control the hydraulic motor speed, water pressure gage, water flowmeter, water bypass valve, and safety relief valve, which was set for 380 bars. The nozzle assembly used in these tests is shown in Figure 2. The nozzle assembly consisted of a water nozzle holder, water nozzle, abrasive feed line holder, suction chamber, water-abrasive nozzle, spacers, and a nut. The water nozzle has a flow conditioner to produce a coherent jet (Figure 3). The water nozzle had an orifice diameter of 1.19 mm, and the water-abrasive nozzle orifice diameter was 3.18 mm. The abrasive feeding arrangement is shown in Figure 4, which consisted of a small tank, and a 12.7 mm diameter hose with a ventilated connection.

PRELIMINARY TEST

Preliminary tests of high pressure water-abrasive jet cutting were successful. Figure 4 shows the preliminary test set-up. The test set-up consisted of 6.4 mm thick plate, a screw feed for nozzle traverse motion and a nozzle holder. The traverse motion of the nozzle was achieved by the motor assembly, which consisted of a small electric motor, gear reducer, and speed control (Figure 5).

A 3050 mm long flexible shaft was used to couple the screw to the electric gear reducer shaft, so that the motor assembly could be away from the test stand for safety. The test was conducted by slotting 6.4 mm thick steel plate with a high pressure water-abrasive jet with a water flow rate of 19 L/min. at a pressure of 345 bars. Different nozzle configurations and sizes were tested. The nozzle configuration which is shown in Figure 2 gave the best cutting performance. The water nozzle orifice used in these tests was 1.19 mm in diameter. The stand-off distance of 12.7 mm was proven during a preliminary test to be the optimum stand-off distance. The test result showed that a cutting rate of 44.4 mm/min. with a 3.2 mm slot width is achievable, as shown in Figure 6.

Different sizes of garnet (#16, 36, 50, and 60) were tested. A screen analysis was conducted on these sizes of garnet. Table 1 shows the results of this screen analysis. It was found that garnet #36 has the best feeding characteristics and cutting rate, while the other sizes caused plugging of the abrasive feeding line. The garnet feeding rate was 1.1 kg/min.

PIPE CUTTING TEST

Figure 7 shows the pipe cutting test setup. It consists of the water pump assembly, abrasive feeding tank assembly, traverse motion assembly, and pipe cutting device. Figure 8 shows the pipe cutting device, which consists of a modified torch cutting device. It enables the water-abrasive nozzle to rotate 360 degrees around the pipe circumference. It is clamped on the pipe by a saddle and chain arrangement as shown in Figure 8. Traverse motion is provided by a flexible shaft, which is connected to the electric motor gear case. The flexible shaft is 3050 mm long. This provides enough distance for the operator to be away from the cutting device for safety. The electric motor can be eliminated for underground application, and the traverse motion would be provided by turning the flexible shaft manually. The nozzle assembly is attached to the nozzle holder by a hose clamp. The standoff distance can be changed by sliding the nozzle assembly up and down on the nozzle holder. The standoff distance was kept at 12.7 mm during the test. The nozzle configuration is shown in Figure 2. The water nozzle orifice is 1.19 mm in diameter with a flow conditioner, and the abrasive nozzle orifice is 3.18 mm in diameter. The abrasive hose size is 12.7 mm and the high pressure hose is 12.7 mm with staple connections.

The test results show that a pipe circumference cutting rate of 38 mm/min. can be achieved with flow rate of 19 L/min. at 345 bars, at a stand-off distance of 12.7 mm, using garnet #36 at a consumption rate of 1.1 kg/min., the slot width was between 3.2 and 4.8 mm.

The device is light weight, can be moved easily underground, and can be assembled and disassembled underground. Hydraulic power is the only power used, and can be obtained from the shield support on the longwall face or from one of the other pieces of equipment used in underground mining.

SUMMARY AND CONCLUSIONS

A device was assembled and tested to cut the steel pipes of gas and water well casings in an underground situation. The tests showed that the device is capable of cutting along the circumference of schedule 40 steel pipe at a rate of 38 mm/min. with a flow rate of 19 L/min. at pressure of 345 bars with garnet #36 abrasive at a feeding rate of 1.1 kg/min.

This cutting device has many potential advantages for underground mining applications. The work described in this paper has identified the development needs for commercial use.

ACKNOWLEDGEMENT

The author wishes to express his sincere appreciation to the individuals who helped in this project. Special appreciation is extended to Eston Petry, Dr. Pramod Thakur, David McCain, David Campbell, Steve Lauer, and Thomas Miller of Consolidation Coal Company, Research & Development Department.

REFERENCES

1. El-Saie, A. A.: "Investigation of Rock Slotting by High Pressure Water Jet for Use in Tunneling." Ph.D. Thesis, University of Missouri-Rolla, 1977.

2. Roberts, Marion L.: "Erosion-Resistance Water and Grit Blasting Assembly." NASA Tech. Briefs, September 1988, pp 83-84.

3. Saunders, D. H.: "A Safe Method of Cutting Steel and Rock." 6th International Symposium on Jet Cutting Technology, April 1982.

4. Saunders, D. H., Griffith, N. J., and Moodie, K.: "Water Abrasive Cutting in Flammable Atmospheres." R. R. 1608, BHRA Fluid Engineering, Cranfield, June 1980.

TABLE 1: GARNET SCREEN ANALYSIS

SCREEN	GARNET NO.							
SIZE,	#16		#36		#50		#60	
mm	%	ACCUM.	%	ACCUM.	%	ACCUM.	%	ACCUM.
+2.000	0.0	0.0	0.0	0.0	0.0	0.0	0.0	0.0
2.000X1.000	94.5	94.5	1.5	1.5	0.0	0.0	0.0	0.0
1.000X0.500	5.4	99.9	96.2	97.7	1.5	1.5	0.1	0.1
0.500X0.025	0.1	100.0	1.9	99.6	97.6	99.1	69.3	69.4
0.025X0.125	0.0	100.0	0.2	99.8	0.7	99.8	30.4	99.8
0.125X0.063	0.0	100.0	0.1	99.9	0.1	99.9	0.1	99.9
-0.063	0.0	100.0	0.1	100.0	0.1	100.0	0.1	100.0

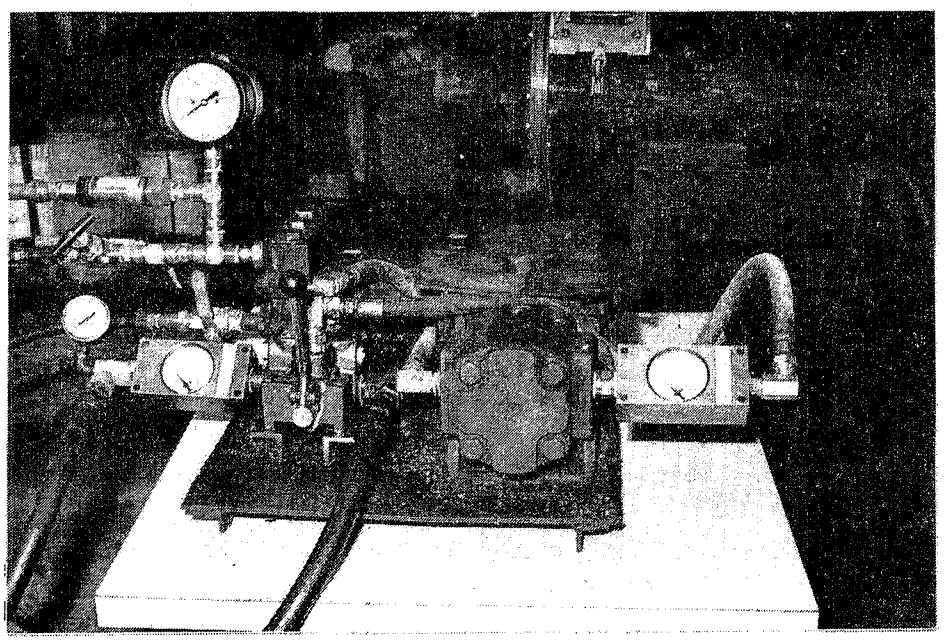

FIGURE 1: The High Pressure Water Pump

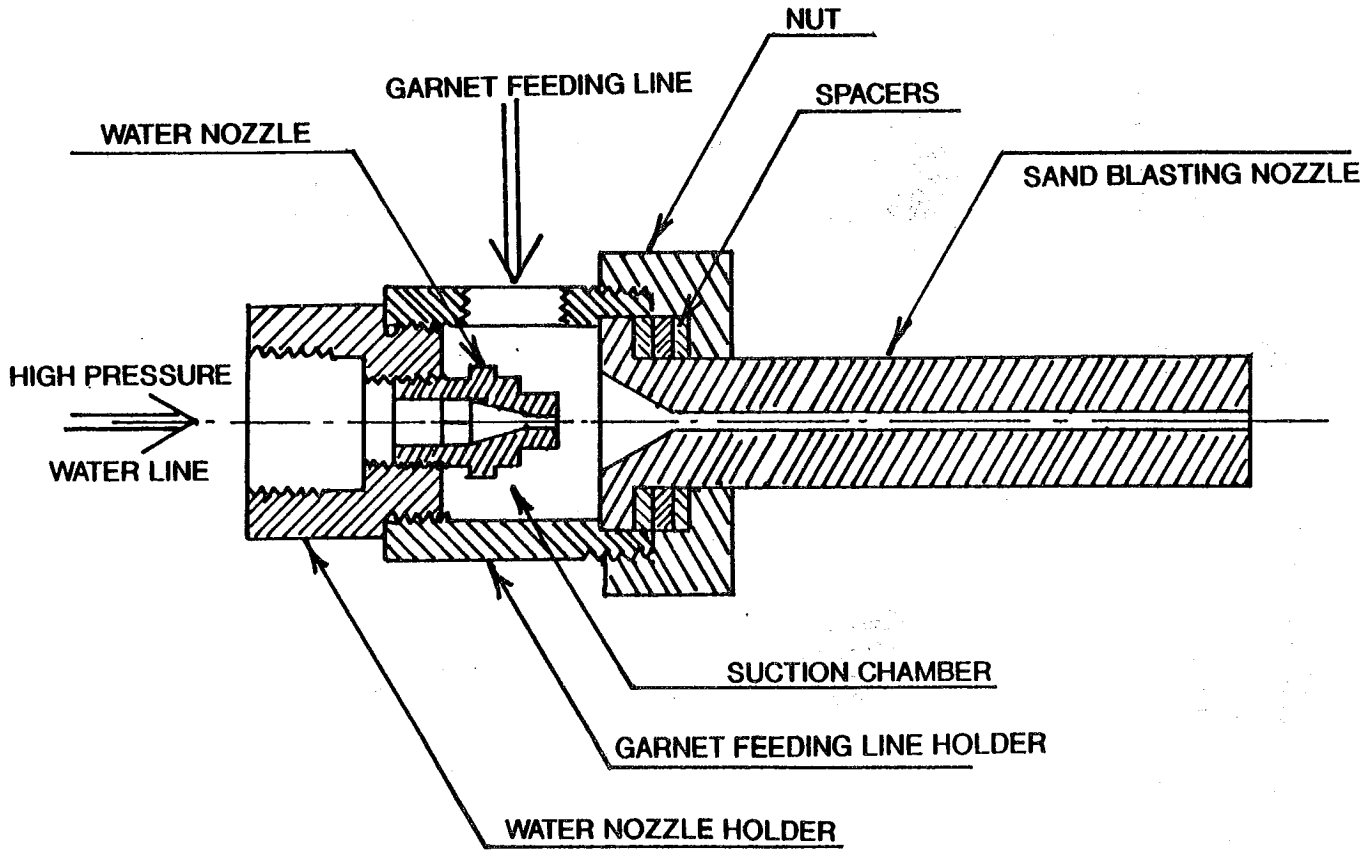

Figure 2. High Pressure Water Abrasives Nozzle

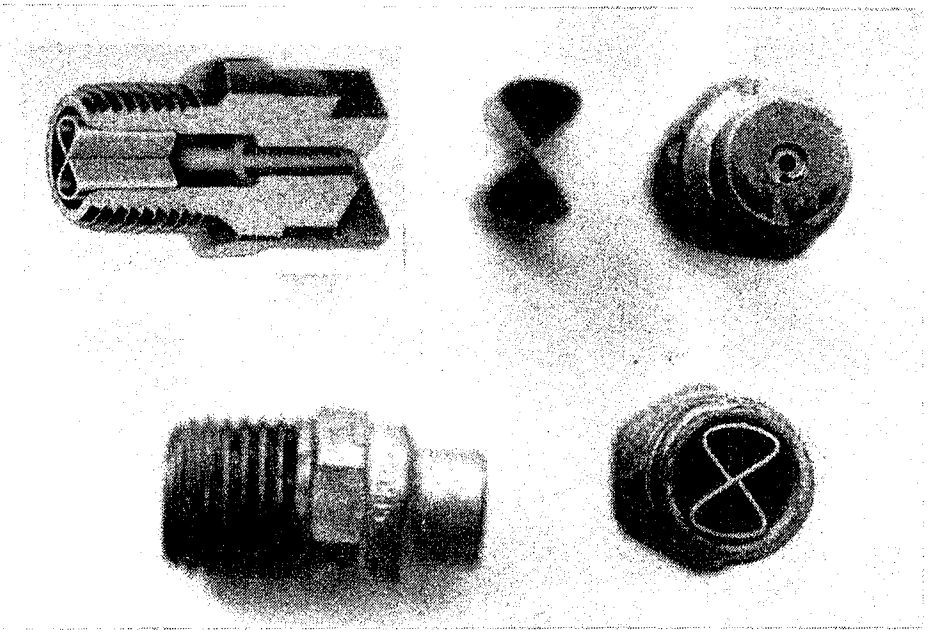

FIGURE 3: The Water Nozzle With Flow Conditioner

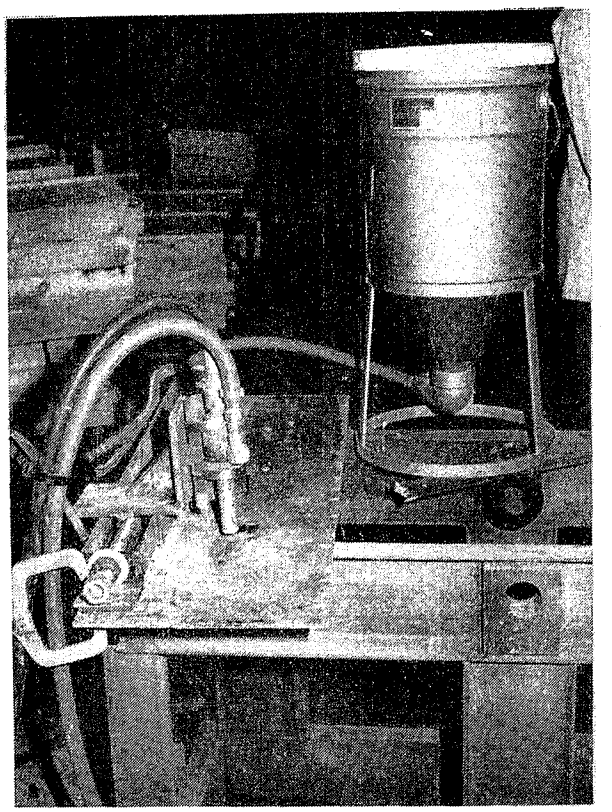

FIGURE 4: The Abrasive Feeding Arrangement and the Preliminary Test Set-Up

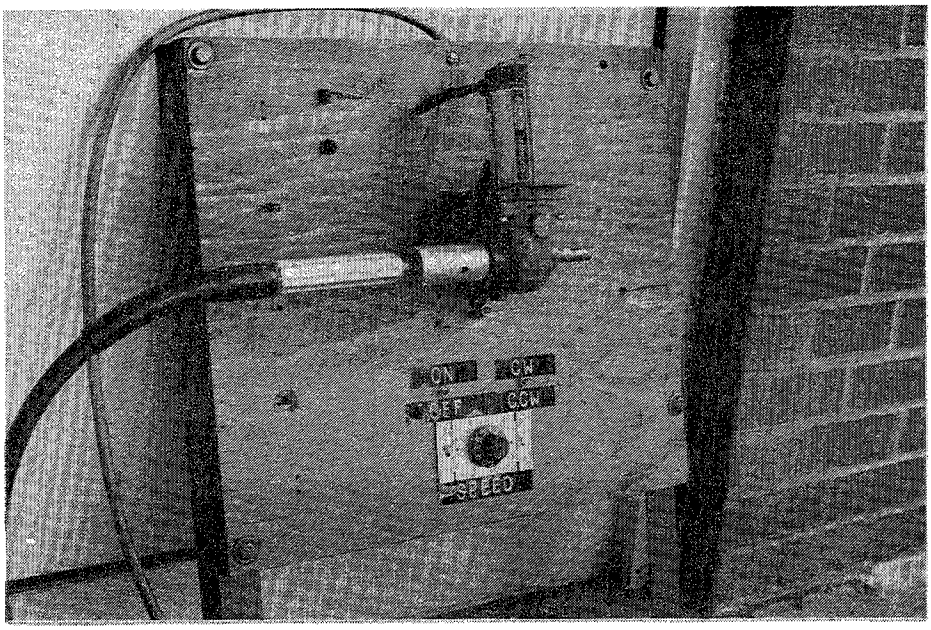

FIGURE 5: The Traverse Motion Control Assembly

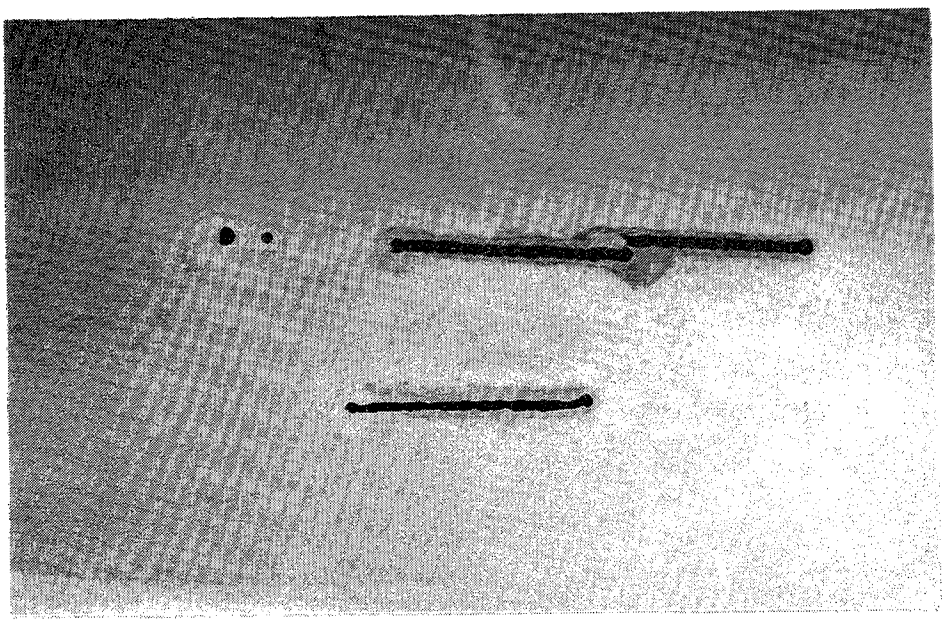

FIGURE 6: The Slots Achieved During the Preliminary Test

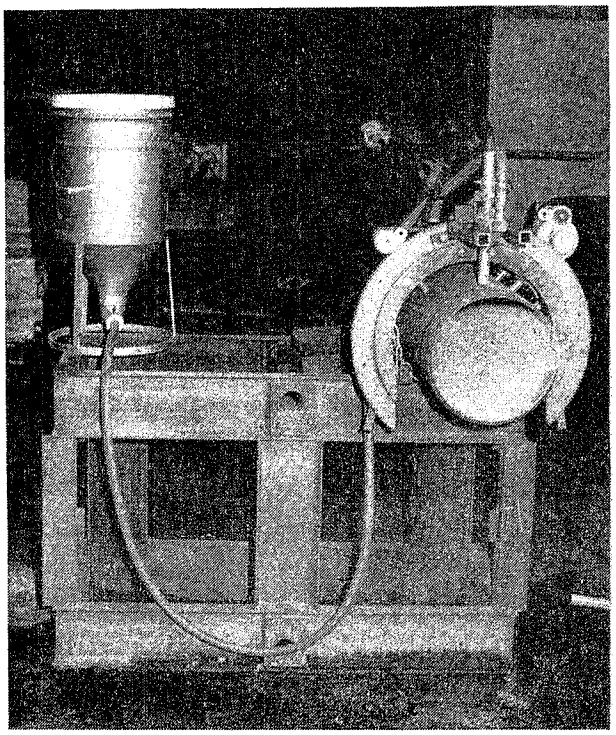

FIGURE 7: The Pipe Cutting Test Set-Up

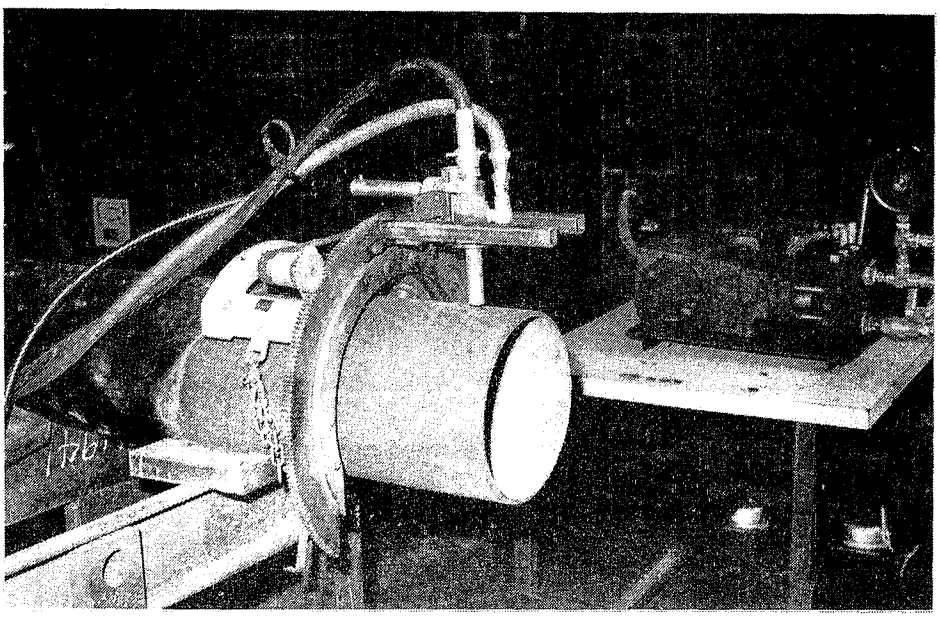

FIGURE 8: The Pipe Cutting Device

5th American Water Jet Conference
August 29 - 31, 1989: Toronto, Canada

Paper / Communication 46

ADVANCED ABRASIVE-WATERJET HARDWARE AND CUTTING PERFORMANCE

K. Zaring,
Flow International Corporation
Kent (Seattle), Washington 98032, USA

ABSTRACT: Continued research in abrasive waterjet technology has yielded many improvements in the components of Abrasive Waterjet (AWJ) Cutting Systems. These improvements have given AWJ's more reliability as a production line cutting tool for many different applications. Almost all system components have been upgraded, including the additions of compact point catchers and a very efficient vacuum system to evacuate those catchers. Improvements in abrasive flow rates and nozzle wear enable users to perform extended cuts without system downtime.

RÉSUMÉ : Des efforts constants de recherche en technologie des jets d'eau abrasifs ont mené à de nombreuses améliorations dans les éléments des systèmes de coupe par jets d'eau abrasifs (JEA). Ces améliorations ont rendu les JEA plus fiables comme outils de coupe industriels pour un grand nombre d'applications. Presque tous les éléments des systèmes ont été améliorés, y compris l'addition de prises ponctuelles compactes et d'un système d'évacuation de ces prises très efficace. Les améliorations apportées aux débits d'abrasifs et à l'usure de la buse permettent aux utilisateurs d'effectuer des coupes sans arrêter le système.

Organized and Sponsored by the National Research Council of Canada and the U.S. Water Jet Technology Association.

1. INTRODUCTION

An AWJ Cutting System combines a focused, high energy waterjet with granular abrasive to provide an extremely powerful means of cutting and piercing various metallic and non-metallic substances. Abrasivejet operation does not produce heat-affected zones in the material being processed. In addition, compared to conventional cutting and piercing tools, the abrasivejet subjects material to low cutting forces and is virtually vibration free.

Abrasivejet cutting is a technology that is continually evolving and improving. The AWJ System will run using abrasive mesh sizes of 60 to 120 mesh with abrasive flow rates of up to four pounds (1.8 kilogram) per minute depending on the combination of jewel and mixing tube being used. The abrasive used most frequently for cutting is garnet. The combinations of abrasive mesh size and flow rate, high pressure orifice size, water pressure and mixing tube size are determined by the particular cutting application and the results desired.

AWJ Cutting Systems can be installed on all types of motion control equipment to suit particular applications. The improvements to the AWJ System provide consistent, repeatable cutting without frequent operator attention. Cutting cell integration with AWJ Systems produces high quality results and greater productivity along with the ability to cut within tight tolerances.

The basic components of an AWJ Cutting System include the Abrasive Metering System and the Abrasive Cutting System (Figure 1.) To enhance the productivity of abrasivejet cutting, other system options/enhancements including catchers, a waste evacuation and disposal system, and several other options to automate the AWJ cutting process are also available. This paper will outline the improvements in AWJ that have allowed it to become a tool for high tolerance, repeatable part production.

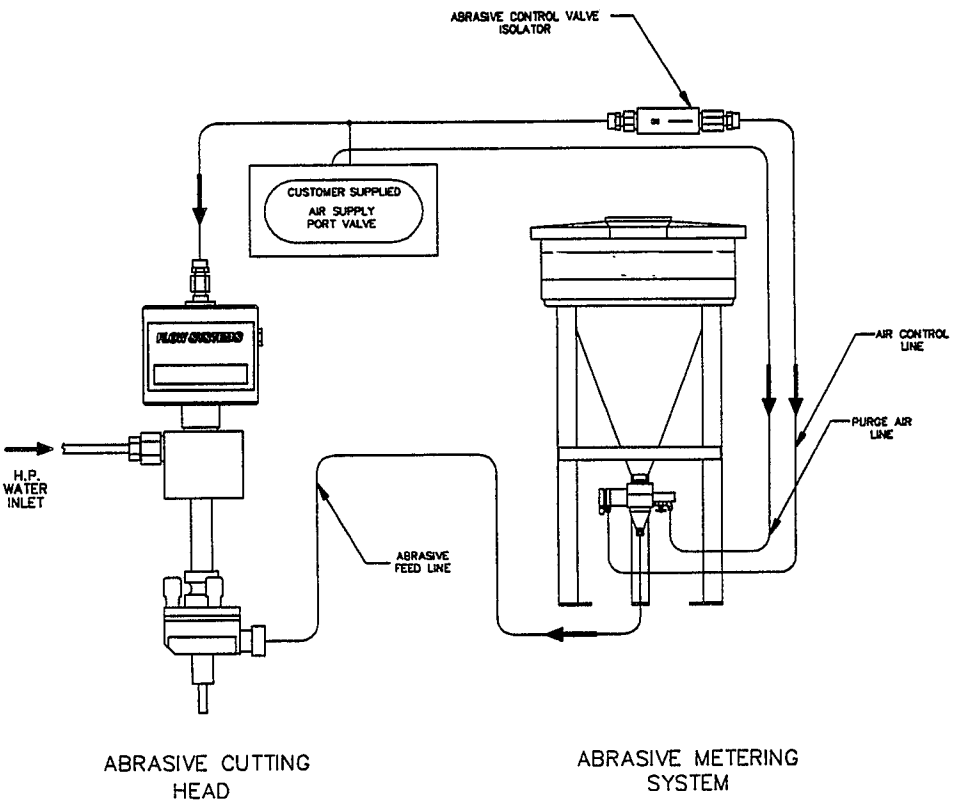

FIGURE 1 **System Package Abrasive Waterjet**

2. THE ABRASIVE METERING SYSTEM

The reliability and cutting efficiency of AWJ cutting is very dependent on the smooth operation of the abrasive metering system. The abrasive must be metered to the cutting head reliably and repeatedly. The abrasive metering system, as shown in Figure 2, consists of the following components: the abrasive hopper, the abrasive, the abrasive metering valve, and the abrasive delivery line. Recent improvements in the hopper, metering valve and delivery line have increased the reliability of AWJ cutting.

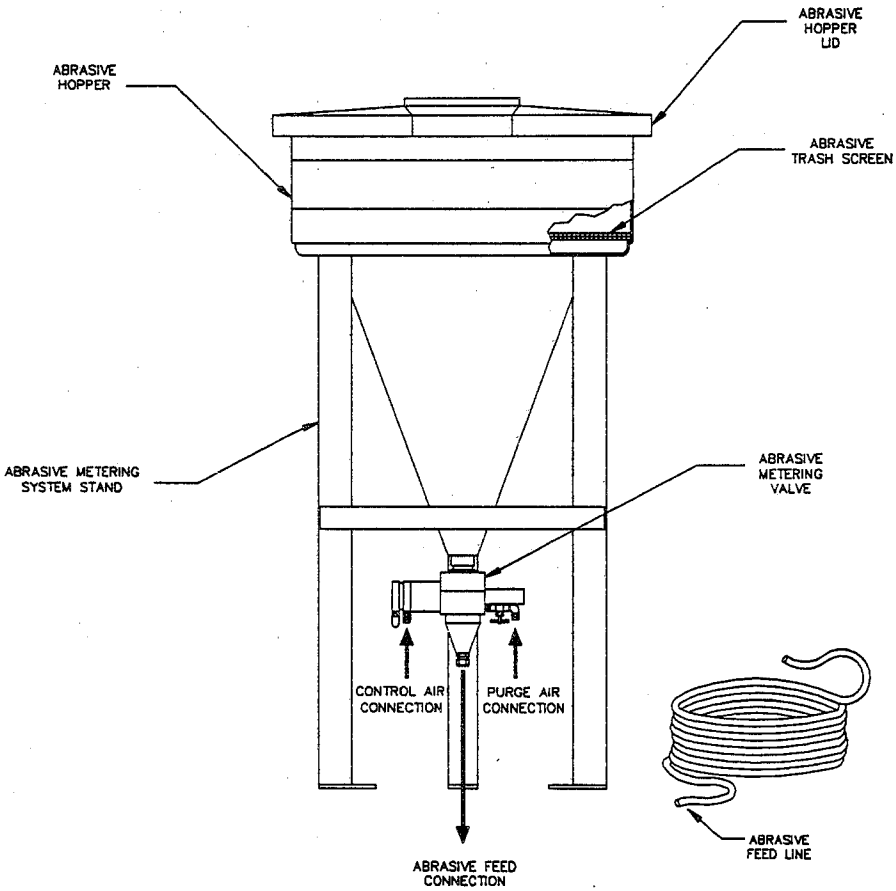

FIGURE 2 **Abrasivejet Metering System**

2.1 Abrasive Hopper

The abrasive delivery hopper is a rotomolded plastic container attached to a sturdy stand of steel tubing. The hopper has a capacity to hold 300 pounds (136 kilogram) of abrasives. The cone angle of the hopper is such that it eliminates "ratholing" of the abrasives as they are being used during abrasivejet cutting. A trash screen is part of the hopper assembly. This screen filters out any foreign material in the abrasive before it can be fed through the rest of the delivery system, thus eliminating any potential clogging problems. The lightweight lid is built in such a way that it does not allow stray water to leak into the hopper and render the abrasive useless for feeding. The hopper may be bolted to the floor using the bolt holes provided. Loading of the abrasive into the hopper is easy because of its convenient height and lightweight lid.

2.2 Metering Valve

Attached directly to the exit port of the hopper is the abrasive metering valve. Its function is to turn the flow of abrasive on and off, to meter the amount of abrasive used, and to purge the abrasive feed line of any transient water when the abrasivejet is not in use.

The on/off function of the metering valve is controlled by a sliding shutter which is actuated by an air cylinder. The metering valve is normally closed and is controlled with the use of a four-way, five-port pneumatic control valve. Any potential for jamming of the on/off shutter has been eliminated by the correct part tolerances and the use of materials that resist abrasive wear.

The metering mechanism consists of a manually adjustable digital micrometer used to set the flow rate of the abrasive for the required output. The micrometer head is attached to a sliding plate which is positioned such that it moves over a metered opening allowing the appropriate amount of abrasive flow. The micrometer reading corresponds to a flow rate shown on the rate of flow charts included with the valve. The metering mechanism of this valve is totally separate from its on/off mechanism. This separation is an improvement over previous valve designs. Separating the on/off and metering functions improves both the repeatability and accuracy of the valve because the metering setting is not disturbed each time the valve is turned on and off. The abrasive flow rate will vary slightly depending upon abrasive mesh size.

Unlike previous valve designs, the rate of abrasive flow through this metering valve is solely dependent on gravity. Previous valve designs have relied on the vacuum of the abrasive cutting head to pull the abrasive through the metering valve into the feed line and then to the cutting head. Since this valve does not rely on vacuum to pull the abrasives through the valve, its metering function is very repeatable. This valve design is easily calibrated for use with various abrasives should abrasive flow charts not be available.

A repeatable and reliable metering valve allows the AWJ user to use less abrasive to achieve their desired cut speed. Use of less abrasive will save considerably in system operating costs as abrasive is the highest cost consumable item in the system.

The third function of the abrasive metering valve is the line purge. The purge is integrated into the metering valve and consists of a needle valve coupled with a piece of tubing installed in the outlet cone of the valve which directs air through the abrasive line and out through the cutting head. The line purge should be activated only when the abrasive is not being fed to the cutting head as its purpose is to keep the feed line and mixing chamber free of any transient water which may foul the system when it is not operating and cause an interruption of abrasive flow on start up. The line purge provides a simple, reliable way to prevent water from entering the delivery line.

2.3 Abrasive Feed Line

Another component of the Abrasive Metering System is the abrasive feed line. It is always recommended that the shortest possible distance be maintained between the abrasive hopper and the cutting head for optimum cutting results, but if physical circumstances do not permit a short run, an appropriate abrasive feed line is available.

There are two types of feed line available for AWJ systems. One line is meant for transporting abrasive to the cutting head in line runs of 25 feet (7.6 meters) or less. An alternate feed line demonstrates significantly better abrasive transport capability for abrasive line runs of distances over 25 feet (7.6 meters).

3. ABRASIVE CUTTING SYSTEM

Working in conjunction with the Abrasive Metering System is the Abrasive Cutting System (Figure 3.) The cutting system consists of the Abrasivejet cutting head including the abrasive mixing chamber, the high pressure valve actuator, valve body, nozzle body and mixing tube. The cutting head is pneumatically operated with its operation tied into that of the abrasive metering valve i.e. when the cutting head is activated, the metering valve is opened to allow abrasive flow.

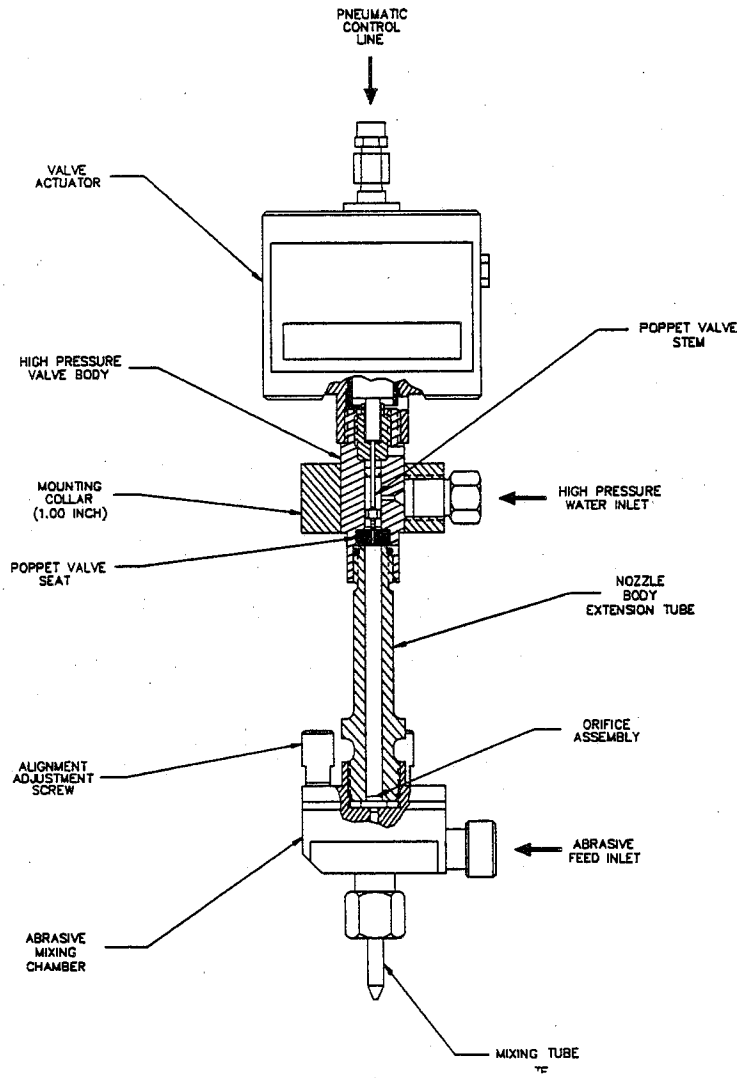

FIGURE 3 **Abrasivejet Cutting Head**

When the Abrasive Cutting System is actuated, high pressure water flows through the orifice into the mixing chamber. As the water enters the mixing chamber, it creates an area of partial vacuum, which induces the metered flow of abrasive particles through the abrasive feed line. The abrasive combines with the waterjet stream to create the high energy abrasivejet cutting stream. This stream exits the cutting head through the mixing tube.

The high pressure valve actuator and valve body are light- weight and reliable components designed for long life at ultrahigh pressures. In addition, leakage of water at the high pressure nozzle outlet has been virtually eliminated with this cutting head design. This light- weight valve coupled with the long life mixing tubes allows abrasivejet technology to be used in many robotic and limited clearance applications.

Improvements in the rate of wear of the consumable materials of the abrasivejet cutting head have enhanced its use for continuous cutting and tight tolerance applications. Previous cutting head technology required the replacement of wear parts and realignment of the cutting head generally every one to two hours depending on the application and accuracy required. This frequent changing of components required constant operator attention to the system. Now the greatly extended mixing tube life permits parts which are produced at the end of a shift to be within several thousandths of an inch tolerance to those produced at the start of the shift, without resetting the machine tool for kerf compensation or numerous replacements of mixing tubes as was previously required.

Mixing tube sizing has also been optimized for various inside diameters versus lengths. This optimization creates a more coherent focused cutting stream.

4. SYSTEM OPTIONS/ENHANCEMENTS

4.1 Catchers

Abrasivejet cutting develops a large amount of energy (up to 50 HP/52 HP Metric) at the cutting nozzle. As much as 75% of that energy may be retained in the stream after it has passed through a cut. Three basic types of catchers are available to accommodate various industrial needs of the abrasivejet. These catcher types are room catchers, tank catchers and compact catchers. Each catcher dissipates the remaining energy of the abrasivejet stream and collects and disposes of the spent abrasives and kerf material.

A room catcher is simply a room or compartment of the facility which has been prepared as an operating area for abrasivejet multi-axis cutting. In these applications, the room itself is designed to both contain the residual abrasive stream and separate the process waste. The floor of the room catcher contains a settling tank or other process waste separation system, and the waste is drained directly from the room catcher by gravity.

A tank catcher is a large steel container permanently positioned beneath the work surface. The actual configuration and capacity of water tank catchers are determined by the specific application of the system. Tank catchers are supplied for applications where the workpiece is stationary and the end effector is mobile and capable of vertical or near vertical cuts only.

Tank catchers are filled with at least 20 inches (50.8 cm) of water to absorb residual energy. Tank catchers can also be filled with other energy absorbing media in addition to the water. The typical energy absorbing media used for these catchers are stainless steel balls or pea gravel. This combination of an energy absorbing media and water is preferred over only water in installations where quieter operation is required.

The spent abrasives and kerf material can be handled in a number of ways when using a tank catcher. The solids may settle out of the flow and remain in the tank, and the water will drain to an appropriate drain if a water only tank catcher is used. When using a tank catcher filled with other energy absorbing media, flush water is employed to flush the solids and spent water out of the tank to an adjoining weir tank where the solids will settle out and be disposed of.

A compact catcher (Figure 4) is a small container filled with energy absorbing media, typically stainless steel balls. After the abrasivejet stream passes through the workpiece, it enters the container and strikes the balls, sending them into motion. The continuous collision and agitation of the balls effectively absorbs and dissipates residual abrasivejet energy. The catcher bodies are not wear items, but the stainless steel balls they contain are consumable at a predictable rate and must be replenished periodically. Compact catchers have a limited capacity for both catcher balls and waste. Therefore, the catcher balls must be periodically replenished and the process waste must be continuously evacuated or the catcher quickly becomes unserviceable.

Catcher ball replenishment is typically performed manually by either filling an external reservoir or removing the catcher lid and pouring the balls in. The process waste is continuously evacuated by means of a specially designed vacuum (see Section 4.2) and passed on to a waste separation and disposal system for treatment.

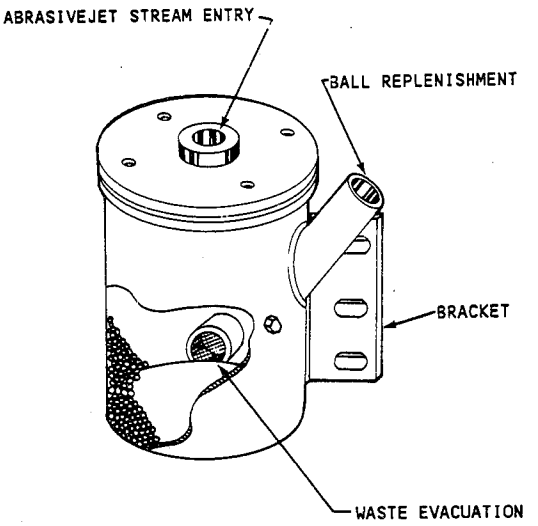

FIGURE 4 Compact Catcher

Compact catcher bodies are designed as small as possible in order to function in tight spaces. Compact catchers are ideally suited for robotic applications where a low profile cutting head is necessary. Following special operating procedures also allows use of compact catchers in non-vertical cutting applications.

4.2 Waste Evacuation and Disposal System

The process waste produced by AWJ cutting is a slurry consisting of water and solid sediments, which are minute particles of abrasive grit , kerf material and catcher ball fragments. To prevent the slurry from separating and settling in compact catchers, a vacuum system is required to constantly evacuate process waste and transfer it to a waste separation and disposal system. This system is shown in Figure 5.

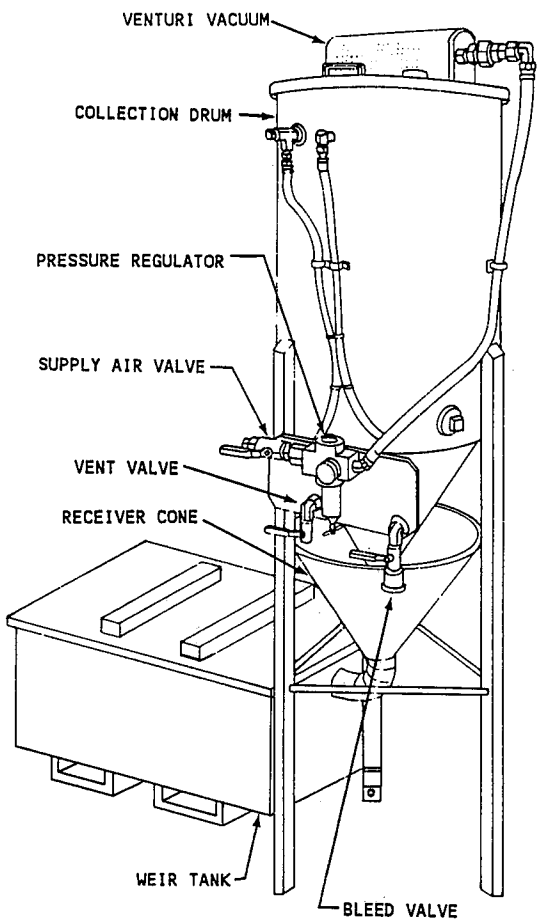

FIGURE 5 **Waste Evacuation and Disposal System**

The abrasivejet vacuum constantly evacuates waste from compact catchers. It consists of an air powered venturi-type vacuum unit which sits atop a collection drum. The drum has a conical bottom with a drain port. A receiver cone is located directly below the drain port and its outlet is connected by hose to a settling tank. The vacuum unit is connected to the evacuation outlet of the catcher with a hose. Supply air flowing through the venturi creates a vacuum inside the collection drum which closes a check valve at the drain port, and induces an air flow through the catcher and evacuation hose. The process waste is entrained in this air flow and deposited into the collection drum.

The waste separation device provided with the vacuum system is a weir tank design. Two vertical baffles of unequal height separate a large, rectangular holding tank into three compartments of graduated depths. The vacuum drum drains by hose into the deepest compartment of the weir tank. The solids settle out as the slurry proceeds through the compartments and the remaining waste water drains from the tank. When all compartments of the weir tank become filled with waste solids, the tank will cease to function and must be emptied.

5. OTHER ENHANCEMENTS

Two other system enhancements are available for use with the AWJ cutting system. One is an automated abrasive metering valve. This valve serves the same purpose in the system as the manual metering valve in that it repeatedly and reliably meters abrasives to the cutting head. Instead of using a digital micrometer, the flow is adjusted with the use of a servo- driven motor that is set from a control box. This automated valve may then be tied into the control system of the cutting module for an automated cutting cell.

Another enhancement for automation is the abrasive loss of flow switch. This component is a feedback device that will indicate when the abrasive flow has dropped below a pre-determined set point. When the abrasive flow is lost, the system can be shut down automatically, so that any parts being cut will not be damaged.

5th American Water Jet Conference
August 29 - 31, 1989: Toronto, Canada

Paper / Communication 47

ROBOTIC WATERJET APPLICATIONS AND RELATED TOOLING

D. LeBlanc
ASI Robotic Systems
Clawson, Michigan, USA

ABSTRACT: ASI has integrated the Waterjet Cutting Process into over 200 installations. The following information is based on the outcome of the various applications and their related tooling concerns.

RÉSUMÉ : ASI a intégré la méthode de coupe par jets d'eau dans plus de 200 installations. L'information présentée est basée sur les résultats de diverses applications et les problèmes d'outillage connexes.

Organized and Sponsored by the National Research Council of Canada and the U.S. Water Jet Technology Association.

As a Gantry manufacturer, we have been involved with many applications involving the waterjet cutting process.

I would like to cover some of the applications and highlight the approaches we have taken to tooling the parts.

In addition to the types of tools we have used, I will explain how the tools play a major role in the area of noise abatement. With the stream velocity approaching mach 3, the noise is well above acceptable decibel readings as called out in OSHA Standards. But, if properly "deflected", the DB ratings are well within the range of acceptability.

Designed into our tools are what we call "deflectors." Once the jet stream passes through the material, it then is met by our deflector shield which abates the noise and also aids in keeping the water routed in the direction desired. The deflectors are made up utilizing D2 Tool Steel, through hardened to Rockwell 60.

Depending on the type of use the tool sees, number of shifts, days and what pressure, the deflectors will eventually wear. We have seen the high usage shields, lasting as long as one year. The shields themselves are made to easily be unbolted, removed and replaced with a minimal amount of replacement time.

Instrument Panels:

The I/P tooling that we have supplied has varied. We began with trying a complete mold of the inter substrate, but due to the sometimes multiple molds they were formed in this proved to be providing too much contact.

We have since gone to what we term a "Multiple Point Contact" fixture. With this type, we nest the part in the most rigid and accessible points within the inside of the part. We then design in as high as five (5) clamps to hold the part in place once nested.

Also, built into the tool, are several part in place switches. The operator knows prior to pressing his palm buttons that all switches are made by indicator lights on his consolette.

Headliners - Carpets:

With the less rigid parts, such as headliners and carpets, an Epoxy or fiberglass female mold is most commonly used. Vacuum is sometimes used depending on the size and the availability of manufacturing holes to aid in locating and nesting. The vacuum we have used when needed has been most commonly a squirrel cage type. We drill in the mold itself, multiple small diameter holes that pull and hold the part in place for the cutting operation. Where the trim line is required, a small slot is cut through the nest to allow the jet stream to pass into the inner cavity of the mold. Once the stream has passed through the material and nest, we then design in the deflectors for noise abatement and water routing.

Door Panels:

Similar to the Instrument Panel fixtures, is the approach we have taken on door panel tools. Multipoint contact, with the noise abatement deflectors and part in place switches.

Abrasive Cutting:

I will discuss the two approaches we have taken on applications we have supplied to the aerospace industry.

A: C-Frame Type Catcher:

The C-Frame is mounted to our six-axis gantry and has a designed throat of 24" or 36". It is adjustable in depth from 2" to 8".

The abrasive material and the kerf is caught directly underneath the nozzle itself and captured within the C-Frame canister. It is broken up by stainless steel balls that disburse the jet stream and serve the purpose of noise abatement.

The waste handling system is connected to the C-Frame Catcher. It is a venturi type, where vacuum is formed within the drum tank to capture and suspend the waste material. When the vacuum unit is turned off, the material then flows to the settling tank and the solid materials are no longer suspended. The water itself is then drained out the side of the settling tank into a proper drain.

B: Abrasive Tank Catcher:

For other applications, we have utilized the tank design. A steel tank is constructed and the bottom of the tank is covered with gravel; about 5" deep. We then fill the tank with water to aid in noise abatement.

The part to be trimmed is set on a steel grate that is know to be sacrificial. The part is located and clamped in a suitable area.

On some applications the use of plywood between the grate and part is used so there is no splash-back up and into the part.

If parts are not susceptible to water, it can be submerged below water level to aid in noise abatement.

Types of Systems:

- Gantry Style Design
- Accu-Cell Gantry
- Low Rail Gantry
- Cantilever Style

5th American Water Jet Conference
August 29 - 31, 1989: Toronto, Canada

Paper / Communication 48

INDUSTRIAL APPLICATIONS FOR ROTATING NOZZLE TECHNOLOGY

M.T. Gracey
NLB CORPORATION
Wixom, Michigan 48096, USA

ABSTRACT: High pressure water jet users, manufacturing companies and research facilities have been attempting to develop nozzle systems that improve cleaning and cutting while maintaining or reducing horsepower requirements. NLB CORPORATION has developed rotating nozzle systems to enable high pressure water to work more efficiently. This paper will include application examples, recently developed nozzles, tests, and a glimpse into future developments in the water jet industry.

RÉSUMÉ : Les utilisateurs et les fabricants de jets d'eau ainsi que les organismes de recherche dans le domaine ont tenté de mettre au point des systèmes d'ajutage pour améliorer le nettoyage et la coupe tout en maintenant ou en diminuant les impératifs de puissance. NLB Corporation a mis au point des systèmes de buses rotatives permettant d'augmenter le rendement des jets d'eau à haute pression. La présente communication décrit des exemples d'applications, de nouvelles buses, des essais et des projets d'avenir dans l'industrie des jets d'eau.

Organized and Sponsored by the National Research Council of Canada and the U.S. Water Jet Technology Association.

1.0 INTRODUCTION

Rotating high pressure water jet nozzles have been in development for many years and it is not over yet. Rotation of a nozzle system is an attempt to cover a larger area while moving the surface to be cleaned or moving the nozzle system.

Several types of rotating nozzle systems will be examined in this report including self-rotating, power rotating and self-propelled nozzles as shown in Figure 1.

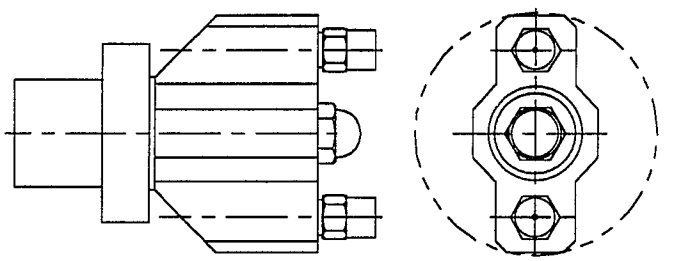

(A) SELF ROTATING

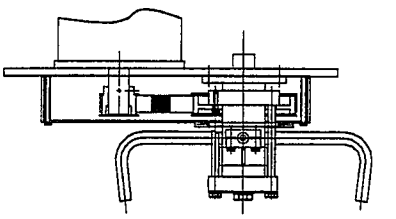

(B) POWER ROTATING

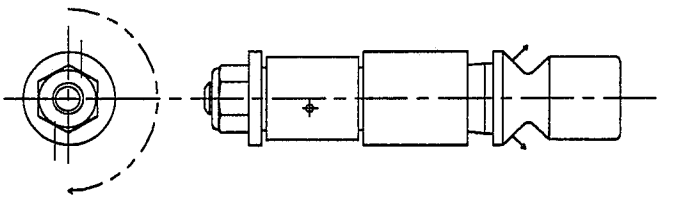

(C) SELF ROTATING
SELF PROPELLED

FIGURE 1 - THREE TYPES OF ROTATING NOZZLE SYSTEMS

2.0 SELF-ROTATING NOZZLE SYSTEM

There are several nozzle system applications using the advantage of self-rotation to reduce equipment cost, hardware size/weight and system complexity. Figure 2 shows examples of self-rotating nozzles used in various cleaning systems in the petrochemical industry and by water blasting contractors.

The principles used in the self-rotating nozzles rely on part of the thrust of the water jet to cause rotation or spinning of the orifices. The thrust or reaction force (R.F.) of a water jet can be calculated by multiply the volume of water times the velocity;

R.F. = 1.95 x cu. ft./sec. x velocity (fps) and can be reduced to: Thrust(lbs) = .05266 $Q\sqrt{\Delta P}$ where Q = flow in gallons per min. and ΔP = pressure in pounds per square inch.

If one orifice is sized for 5 gpm at 10,000 psi, thrust would be approximately 26 lbs (11.8 kg) Using vector algebra, the amount of rotational thrust can be controlled. Figure 3 shows the amount of turning moment generated by a total of 10 gpm (37.8 lpm) at 10,000 psi (68.9 MPa) and a 1" (2.5 cm) offset.

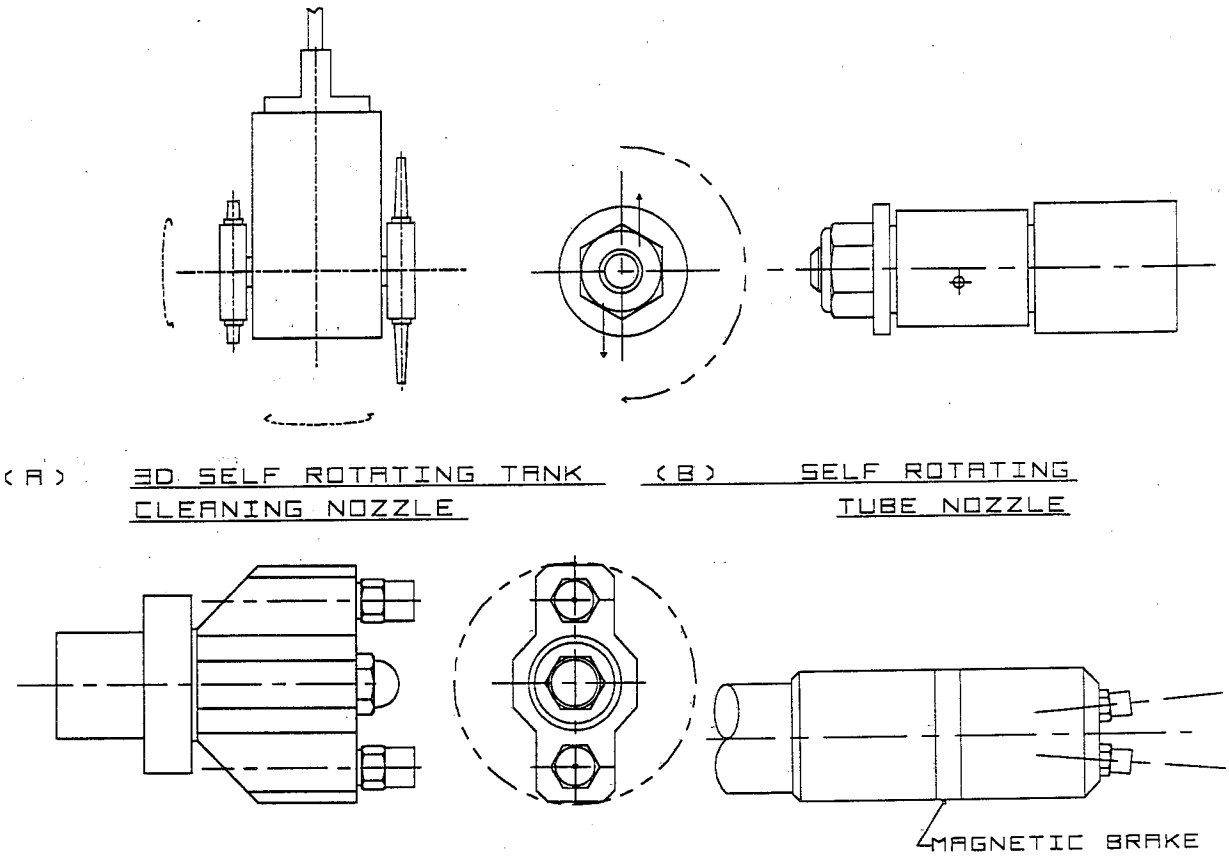

FIGURE 2 - EXAMPLES OF SELF-ROTATING NOZZLES

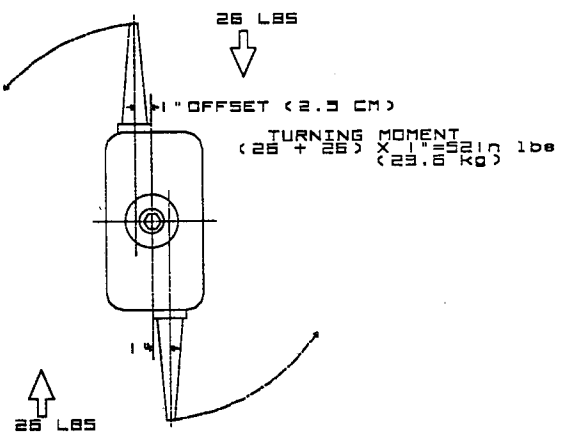

FIGURE 3 TURNING MOMENT FOR OFFSET NOZZLES

The disadvantges of self-rotating nozzles include a speed fluctuations due to changes in pressure and flow, that part of the energy is used in the rotational process and that setting desired speed can be difficult. Notice on Figure 3 that speed controls or breaks are used on some nozzles to control rotational speed.

Self-rotating Spin-Nozzles®, as shown in Figure 1c, are working well on hand lances (guns) to increase the effective cleaning rate, and have been adapted to Robotic cleaning systems. Self-rotating Spin Jets®, as shown in Figure 1e, are being developed for use in industrial applications.

3.0 POWER ROTATING NOZZLE SYSTEM

Pneumatically, hydraulically and small engine powered rotating nozzle systems are the present state-of-the-art hardware being used in many water jet systems. One of the most widely used adaptations for a Spin Jet® is a floor or grate cleaner "lawn mower", as shown in Figure 4. Other rotating nozzle systems for cleaning process equipment are responsible for much of the advancements in the rotating technology field.

A simple system is shown in Figure 5 for using high pressure water to remove build-up of product on customer's hardware. The newest developments using the latest technology incorporates robotic cleaning with rotating water jets as shown in Figure 6. The cost of a robotic system is usually much greater than other systems, but offers an advantage if areas to be clean are hard to reach or if a number of cleaning patterns are needed to do the desired job. In reference (1), a system is discussed for cutting a circular plug of payment to be removed for servicing utilities such as gas, electricity and pipe buried under streets.

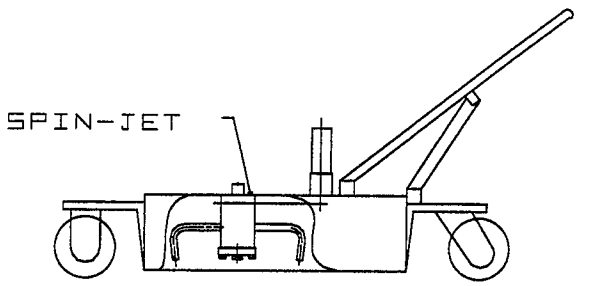

FIGURE 4 FLOOR OR GRATE CLEANER

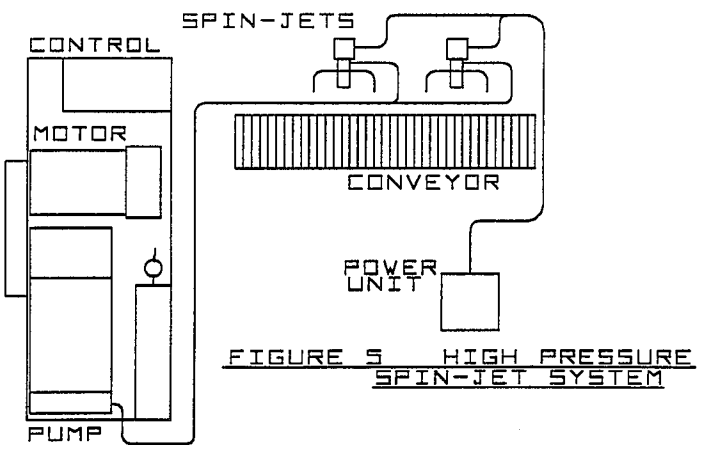

FIGURE 5 HIGH PRESSURE SPIN-JET SYSTEM

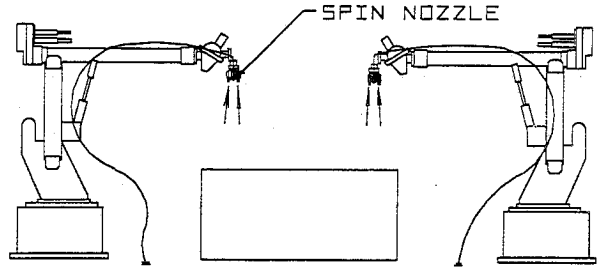

FIGURE 6 ROBOTIC SPIN NOZZLE SYSTEM

The experimental cutter used 20 to 30 gpm (75 to 113 lpm) at 10,000 psi (68.9 MPa) to cut 1.5 to 4 feet (.5 to 1.2 meters) diameter plugs that could be replaced after repair work is completed. This is an example of rotating a nozzle for cutting material and there are many more examples of rotating water used in concrete removal. A study made in 1985 estimated that 140,000 bridges in the U.S. out of 573,000 are classified as structurally deficient. The concrete bridge decks on many of these bridges need repair and high pressure water jets have proven effective in removing deteriorated concrete without damaging the reinforcing grid. In one system, a rotating nozzle is moved across the surface in a programmed pattern to blast away unsound concrete.

The powered rotation of nozzles is used to clean exteriors and interiors of stacks, vessels, pipe and tubulars. Figure 7 shows two types of nozzle systems used to clean the internal diameters of stacks and pipe.

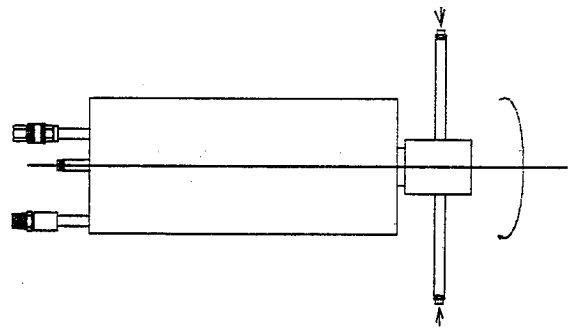

(A) STACK AND PIPE CLEANER

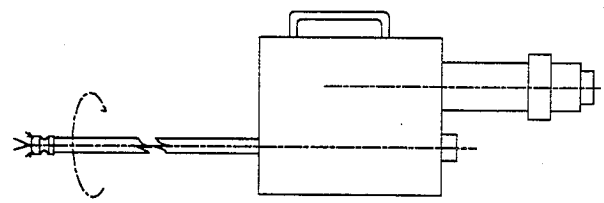

(B) ROTATING LANCE

FIGURE 7 - POWER ROTATED INTERNAL DIAMETER NOZZLES

4.0 SELF PROPELLED, SELF-ROTATING NOZZLES SYSTEMS

Vessels, large pipe, stacks and tubulars are also a good area to use self-rotating nozzles. Figure 1c shows a self-rotating, self propelled nozzle that can polish the internal diameter of tubulars while pulling itself along. Systems as shown in Figure 7a can be fitted with wheels and angled nozzles to enable it to rotate and self-propel itself along the inside of large pipe. Water motors recently developed for the U.S. Navy may find their way into high pressure water blasting; their use might enable rotation, propulsion and high pressure jetting supplied by the pump unit.

5.0 DESIGN CONSIDERATIONS

In addition to the method of rotation, other design considerations must be taken into account. The rotational speed (RPM) and the nozzle arm length (L) effect the nozzle tip speed (V_1). Using the formula $2 L \pi \times RPM = V_1$ it is possible to calculate the velocity at which the nozzle will move. Experience or testing will determine the cleaning effectiveness of the nozzle velocity.

Coverage being a prime reason for rotating nozzles, the movement of the system or work piece must be considered for desired area of cleaning. If this movement rate (V_2) is too great, striping will be apparent. The sincronizing of the rotating nozzle and movement rate follow the formula: Path width (PW) x rotational speed (RPM) = V_2 and is shown in Figure 8.

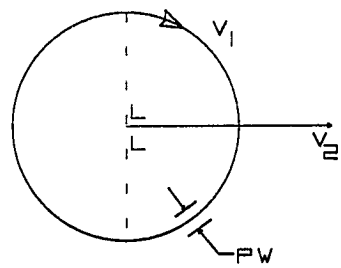

FIGURE 8 - NOZZLE SYSTEM MOVEMENT

If PW = .25" and RPM = 120, V_2 = 30"/min. (75 cm/min.). Once the effective tip velocity has been determined along with the effective pressure and flow, adding nozzles will allow V_2 to be increased. If one nozzle allows 30"/min. travel, then two nozzles will allow 60"/min. (150 cm/min) travel. The formula is then n (PW x RPM) = V_2 where n is the number of nozzles. Horsepower must also be added to the system to maintain the cleaning effectiveness of the increased travel speed. Horsepower (H.P.) $= \frac{Q \times P}{1714}$ where Q is flow in GPM and P is pressure in psi. As nozzles are added the horse power needed is H.P. = $\frac{Q \times P}{1714}$ n Nozzle arm angle, number of nozzles and desired cleaning results are part of the skill used in designing an effective system.

6.0 FUTURE DEVELOPMENTS

Self rotating nozzles and systems are being developed for special purposes along with improvements to existing designs. In reference (2) nozzle technology is discussed as used for material testing. These nozzles used by the Tennessee Valley Authority to test weld metals, repairs and pipe material use cavitation to erode metal faster than other methods tried by TVA. Reference (3) discusses the use of cavitating nozzles in research facilities. The future developments in high pressure water jetting may include special nozzles and their adaptation to rotating nozzle technology. The goal is to produce more effective coverage of high pressure water jets.

7.0 CONCLUSIONS

In reference (4), a discussion meeting was held where the effect of nozzle diameter on traverse rate was a topic. It was suggested that there is a trend to rotate at high velocity and higher pressures, but that larger diameter nozzles are more effective. Rotating of the nozzle is the easiest way to reducing the number of nozzles in the system, therefore, allowing the nozzle diameter to increase. Rotating nozzle technology is already used in many high pressure water jetting applications and has a bright future.

8.0 ACKNOWLEDGEMENTS

The author wants to thank employees of NLB CORPORATION Mrs. Debbie Kelbert and Mr. Troy Aldea for helping with typing and illustration.

9.0 REFERENCES

1. Conn A.F., Gracey M.T., Rosenburg "Development of Cavitating Jet Equipment for Pavement Cutting", 4th. U.S. Water Jet Conference Berkely, California August 26-28, 1987.

2. March P.A., "Cavitating Jet Facility For Cavitation Erosion Research", Proceedings of the ASME International Symposium on Cavitation Research Facilities and Techniques, "Boston, Massachusetts, December 13-18, 1987.

3. Gracey M.T., Conn A.F., "Research Facilities Using Cavitating Water Jet Techniques to Test Materials, "Proceeding of the ASME International Symposium of Cavitation Research Facilities and Techniques" Boston Massachusetts, December 13-18, 1987.

4. Summers, D.A. The Effect of Nozzle Diameter on Traverse Rate, 3rd. BHRA Water Jetting Discussion Meeting, Stratford-Upon-Avon, February 13-14, 1985

5th American Water Jet Conference
August 29 - 31, 1989: Toronto, Canada

Paper / Communication 49

IMPROVEMENTS IN HIGH PRESSURE WATER COMPONENTS FOR FIELD USE

O. L. Tremoulet AND S. Sisson
Pump and High Pressure Development Department
Flow International Corporation
Kent (Seattle), Washington 98032, USA

ABSTRACT: High pressure water (above 30,000 psi/2,004 bar) can be used in a broader range of field applications due to recent improvements in components such as swivels, valves, hoses and nozzles.
This paper will discuss some of the tools and applications affected by these advances. In particular, lightweight hand-held tools, concrete surface cleaners and heat exchanger tube cleaners will be discussed.

RÉSUMÉ : Les jets d'eau à haute pression (plus de 2 004 bars) trouvent des applications dans un nombre croissant de domaines à cause des améliorations apportées à divers éléments tels que pivots, robinets, boyaux et buses.
La communication traite de quelques outils et quelques applications touchés par ces améliorations, notamment d'outils manuels légers, de nettoyeurs de surfaces bétonnées et de nettoyeurs à tubes à échange de chaleur.

Organized and Sponsored by the National Research Council of Canada and the U.S. Water Jet Technology Association.

1.0 INTRODUCTION

Research has shown that a high pressure waterjet (above 30,000 psi/2,041 bar) can be very effective at removing coatings from surfaces if the jet is not allowed to dwell longer than is necessary to remove the coating. Excessive dwell time may result in damage to the surface being cleaned. This suggests that a rapidly traversing waterjet may be an effective surface cleaner.

As high pressure waterjet applications were identified in areas such as concrete surface cleaning, paint removal, heat exchanger tube cleaning, etc., the need for high speed rotation, flexible hoses, reliable valves and small nozzle assemblies was recognized as essential for the development of effective tools for these applications. The small nozzle mount would allow several nozzles to be mounted in a close packed array while the rotating swivel spins the nozzles at high traverse speeds. This, combined with a flexible hose and a reliable on/off valve would give the needed maneuverability and safety required for the development of manually operated, hand-held tools.

It was also recognized that the use of very high pressures, in addition to being more effective at cleaning, also reduces the amount of waste water at a given power level. Further, the higher pressure reduces the jet reaction forces which is particularly advantageous on hand-held tools.

2.0 COMPONENTS AND HOW THEY IMPROVE THE TOOLS

2.1 Swivel

High traverse speeds are more easily obtained by using rotary motion than translating motion. The development of a reliable high speed swivel made high traverse speeds easy to obtain.

A typical swivel and its operating characteristics is shown below in Figure 1.

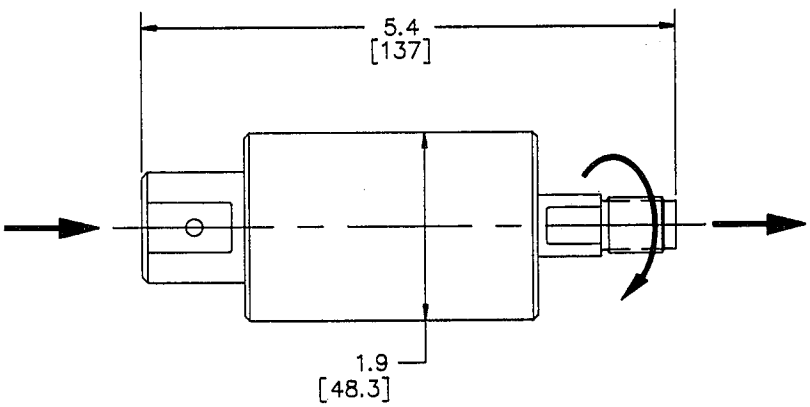

Figure 1 **High Pressure Swivel**

Life @ 35,000 psi (2,381 bar) & 2,000 rpm: 300 hrs
Flow Rate: up to 5.6 gpm (.35 l/sec)
Weight: 2.3 lbs.(1 kg)

2.2 Valves

The main contribution of better on/off valves has been in improved tool control and safety. High pressure systems cannot use a bypass valve like low pressure systems do. If 35,000 psi (2,381 bar) water is allowed to bleed past a throttling valve, for even a short time, the valve seat will be quickly destroyed. Without an on/off valve the operator must depend on controlling the pump itself (which may be some distance away) to turn the water off or on.

The development of reliable hand and hydraulically actuated valves allows the operator to directly control the tool in his hands or hydraulically control a tool that is being operated remotely. The safety implications of good valves are very obvious. The stream of water can be immediately shut off if there is any danger to the operators or the equipment. Two typical valves are shown below in Figure 2 and 3.

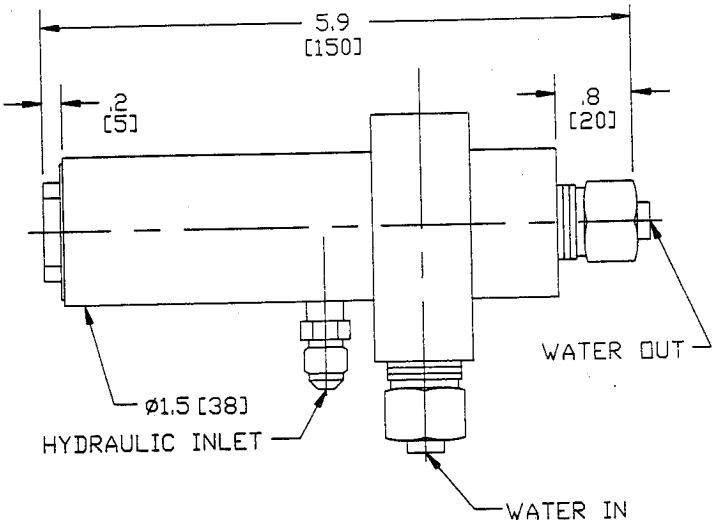

Figure 2 **High Pressure Valve**
(hydraulic actuated)

Flow Rate: 5.6 gpm(.35 l/sec)
Operating Pressure: 35,000 psi(2,381 bar)

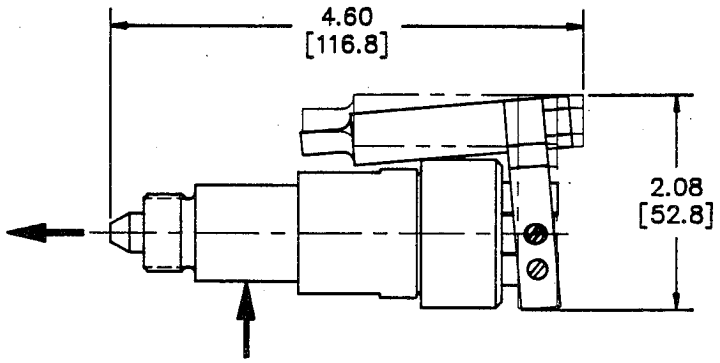

Figure 3 **High Pressure Valve**
(manually actuated)

Flow Rate: 5.6 gpm(.35 l/sec)
Operating Pressure: 35,000 psi(2,381 bar)

2.3 Hose

Before the development of a reliable high pressure hose it was very difficult and cumbersome to move a waterjet around. High pressure tubing was the only way to conduct water from the pump to the nozzle. Lengths of tubing would be connected together with swivels to allow the nozzles some limited freedom of movement. Another way to allow some movement of the nozzle was to bend the tubing in a multiple turn coil. Only small displacements could be handled with this setup. These problems do not exist now that reliable hose is available. The hose must not be bent too sharply or carry any torsional loads but getting high pressure water from pump to nozzle is a relatively simple task. The specifications of a high pressure hose are shown in Figure 4 below. Hose installations are also less expensive than comparable tube installations.

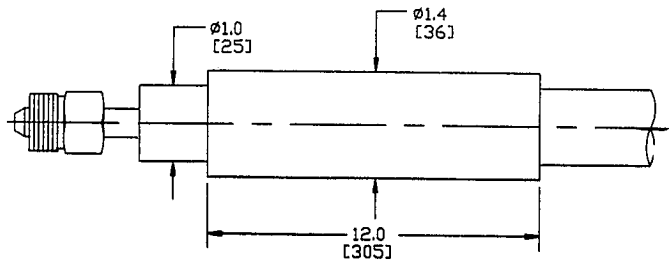

Flow Rate (gpm)	Fitting Pressure Drop (psi)	Hose Pressure Drop(psi/ft)
1	12	1.8
2	48	6.0
3	110	12.0
4	200	20.0
5	300	30.0
6	430	40.0

Dimensions 0.1860 in.(4.7 mm) I.D.
1.0625 in.(2.7 cm) O.D.
(nominal)

Length to customer specifications-
minimum 2 feet (61 cm)

Weight (lbs/ft)
Hose 0.35

Shield 0.36 (black)

Typical burst pressure
105,000 psi (7,143 bar)

Minimum burst pressure
95,000 psi (6,463 bar)

Minimum fatigue life
0-55,000 psi (3,741 bar):10,000 cycles
0-35,000 psi (2,381 bar):30,000 cycles

Minimum bend radius
24 inc. (61 cm)

Figure 4 **High Pressure Hose Specifications**

2.4 Set Screw Nozzles

A single jet is best for cutting, but for cleaning, closely spaced multiple jets are needed. Closely spaced multiple jets cover a larger area than a single jet and since they are smaller, they will clean instead of cutting. The development of set screw nozzles allowed smaller jets to be spaced fairly close together so that the power is spread over a large area. Now the jets clean instead of cutting. A typical set screw nozzle is shown below in Figure 5.

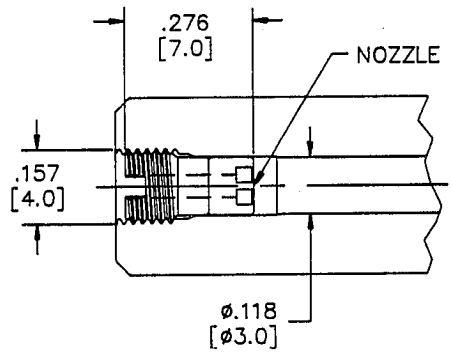

Figure 5 **Set Screw Nozzle**

Available Sizes: .002" to .040"(.05 mm to 1 mm)
Maximum pressure: 55,000 psi(3,741 bar)

Each of these components by itself makes a significant contribution to improved cleaning but together they do even more. Hoses and valves allow almost complete portability and mobility. Hand-held tools would be terribly cumbersome without these components. Swivels that allow high surface speeds combined with nozzles than can be closely spaced, disperse the energy sufficiently so the surface is cleaned instead of being cut. Because the jets may make several passes over a particular area, only part of the material needs to be removed with each pass. This prevents damage to the underlying surfaces. All of these features make the tools easier and more efficient to use. High pressure water can be used in situations now that would have been impossible before the development of these components.

3.0 DESCRIPTION OF TOOLS AND APPLICATIONS

3.1 Heat Exchanger Tube Cleaner

One place that high pressure water has been especially effective is in cleaning the tubes of oil refinery and chemical plant heat exchangers. The tube bore and tube sheets can be cleaned to like new thermal efficiency without damaging the exchanger. Even plugged exchangers that would normally have to be scrapped can be returned to service.

The heat exchanger cleaning tool is a good example of how improved components are combined into a useful tool. Figure 6 shows this tool and how it conducts the high pressure water to clean the surface. A cleaning tip that will hold 1 to 5 set screw nozzles is attached to an appropriate length of high pressure tubing. A hydraulic motor rotates the high pressure tube while a high pressure swivel supplies water to the tube. The swivel is mounted to a carriage that moves back and forth on a track. The track can be adjusted vertically and horizontally so the cleaning tube can index to the exchanger tubes. Another swivel and a length of high pressure hose conduct water to the carriage as it moves back and forth to clean the tubes. A high pressure on/off valve is also on the carriage so that the water can be shut off when the cleaning tip is withdrawn from the heat exchanger. The operator controls the rotation, advance/retract, and on/off functions from a remote hydraulic control stand. Figure 7 (Photo) shows before and after pictures of a heat exchanger tube sheet.

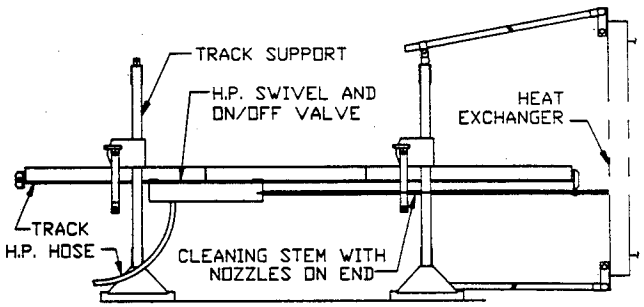

Figure 6 **Heat Exchanger Tube Cleaner**

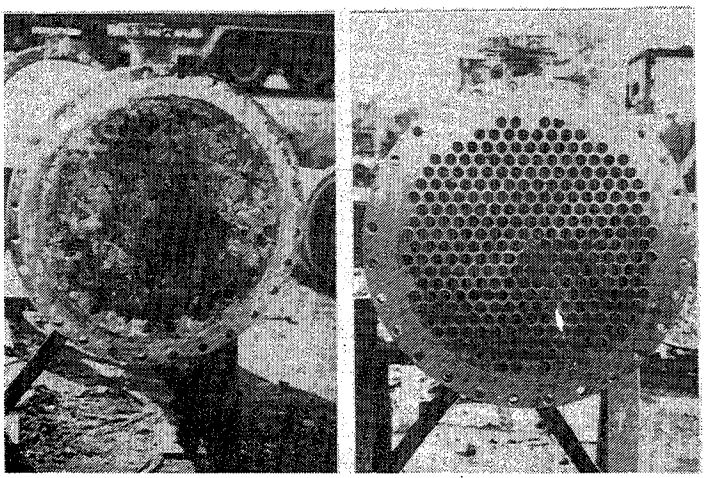

Figure 7 **Photo "Before and After Cleaning with Heat Exchanger Tube Cleaner"**

3.2 Hand-held Tools

Figure 8 shows an effective application of a flexible high pressure hose and an on/off valve assembled with a trigger mechanism for operating the valve. A swivel is connected between the hose and valve to prevent twisting loads from damaging the end connection on the high pressure hose.

The trigger mechanism is designed to snap the valve open under full pressure. This snap action is intended to prevent the valve from opening partially, causing destructive erosion of the valve poppet and seat. The valve is held closed by a stiff spring and opened by a trigger mechanism that reduces the hand force required to hold the valve open. This feature reduces operator fatigue when the valve is held open for long periods of time.

A single jet nozzle is usually used with this non-rotating design. Some typical applications for this tool are:

1. Concrete removal where detail is important in a small space and where deep penetration is required.

2. Dry dock work on ship bottoms.

3. With abrasives entrained in the jet, the tool becomes very effective at cutting rock, steel, concrete, and other hard materials.

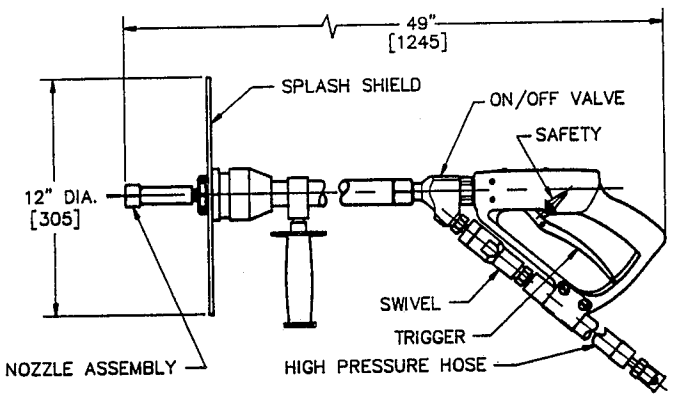

Figure 8 **Non-rotating Jetwand Assembly**

Figure 9 shows the same handle/valve assembly connected to an offset drive, where the swivel is driven through a gearbox by a small lightweight hydraulic motor. An assortment of attachments are then assembled to the end of the gearbox and swivel. The nozzle assembly may contain up to eight jet orifices than can spin at speeds up to 2,000 rpm while operating at 35,000 psi (2,381 bar). This effectively directs a cone of high pressure, fast moving waterjets to the surface being cleaned.

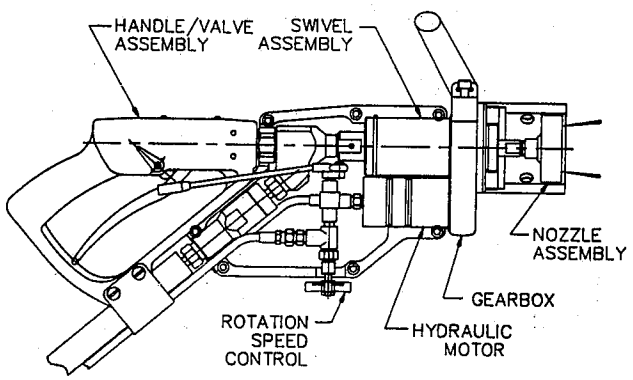

Figure 9 **Rotating Jetlance Assembly**

Figure 10 shows the Jetlance assembled with an extended rotary lance that can be fitted with a variety of nozzle assemblies. The drawing shows one version that has several nozzles mounted at an angle to the centerline. This is particularly useful for reaching into tight corners and pockets.

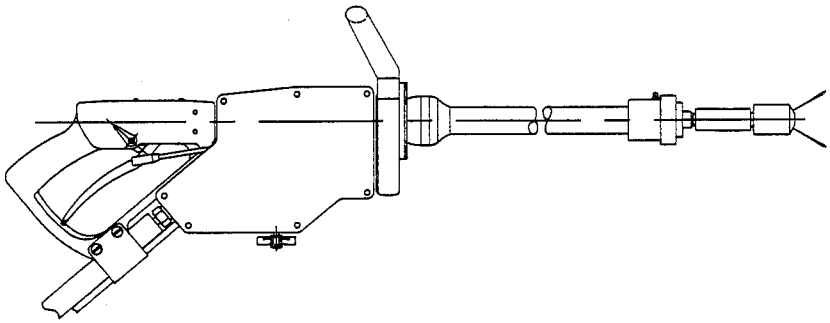

Figure 10 **Rotating Jetlance Assembly with extension**

3.3 Airport Runway Cleaner

A runway cleaner has been developed to remove aircraft tire rubber from the grooved concrete surfaces of airport runways. Tests have been conducted at many military and commercial airports around the United States. The results indicate that high pressure water at 35,000 psi (2,381 bar) selectively removes the rubber and paint from the harder underlying surface without harming the surface. New cleanliness standards are being set by the airport regulating agencies as a result of using the higher pressures. The high pressure, fast traversing waterjet removes the difficult to reach paint and rubber down in the grooves very effectively with no harm done to the concrete.

Figure 11 shows how the high pressure swivel and hose are integrated into the design of the runway cleaner. The jet manifold spins at 2,500 rpm while operating continuously at 35,000 psi (2,381 bar). The unit rides on five wheels to accurately control the jet stand-off distance.

The entire assembly is attached to the power supply truck that rides down the runway at a speed of 100 feet/minute (30.5 meters/minute). The truck supplies the high pressure water and hydraulic power for rotating the manifold.

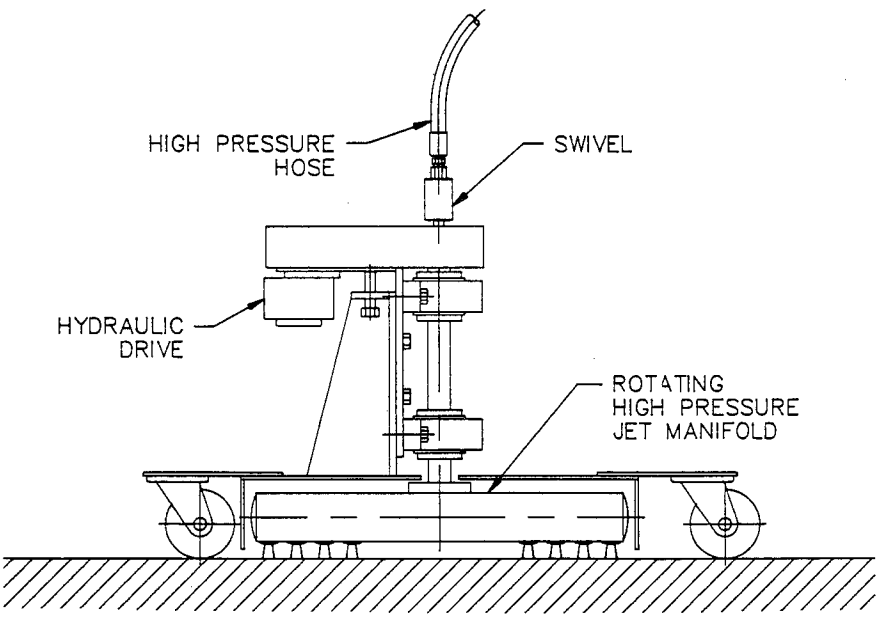

Figure 11 **Runway Cleaner**

The photograph in Figure 12 shows the effectiveness of the runway cleaner at removing painted runway numbers, which is more difficult to accomplish than the rubber removal.

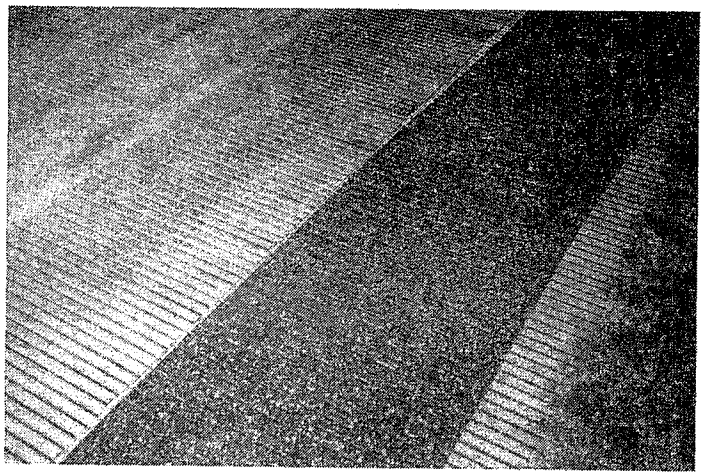

Figure 12 **Photo "Showing effectiveness of runway cleaner in removal of painted runway numbers"**

INDEX OF AUTHORS

INDEX DES AUTEURS